frontiers | Research Topics

Recent advances in energy systems for sustainable development

Edited by
Sunday Olayinka Oyedepo, Abimbola Patricia Popoola, Mufutau Adekojo Waheed, Tosin Somorin and Oluseyi Olanrewaju Ajayi

Published in
Frontiers in Energy Research

ISSN 1664-8714
ISBN 978-2-8325-7353-2
DOI 10.3389/978-2-8325-7353-2

Generative AI statement
Any alternative text (Alt text) provided alongside figures in the articles in this ebook has been generated by Frontiers with the support of artificial intelligence and reasonable efforts have been made to ensure accuracy, including review by the authors wherever possible. If you identify any issues, please contact us.

About Frontiers

Frontiers is more than just an open access publisher of scholarly articles: it is a pioneering approach to the world of academia, radically improving the way scholarly research is managed. The grand vision of Frontiers is a world where all people have an equal opportunity to seek, share and generate knowledge. Frontiers provides immediate and permanent online open access to all its publications, but this alone is not enough to realize our grand goals.

Frontiers journal series

The Frontiers journal series is a multi-tier and interdisciplinary set of open-access, online journals, promising a paradigm shift from the current review, selection and dissemination processes in academic publishing. All Frontiers journals are driven by researchers for researchers; therefore, they constitute a service to the scholarly community. At the same time, the *Frontiers journal series* operates on a revolutionary invention, the tiered publishing system, initially addressing specific communities of scholars, and gradually climbing up to broader public understanding, thus serving the interests of the lay society, too.

Dedication to quality

Each Frontiers article is a landmark of the highest quality, thanks to genuinely collaborative interactions between authors and review editors, who include some of the world's best academicians. Research must be certified by peers before entering a stream of knowledge that may eventually reach the public - and shape society; therefore, Frontiers only applies the most rigorous and unbiased reviews. Frontiers revolutionizes research publishing by freely delivering the most outstanding research, evaluated with no bias from both the academic and social point of view. By applying the most advanced information technologies, Frontiers is catapulting scholarly publishing into a new generation.

What are Frontiers Research Topics?

Frontiers Research Topics are very popular trademarks of the *Frontiers journals series*: they are collections of at least ten articles, all centered on a particular subject. With their unique mix of varied contributions from Original Research to Review Articles, Frontiers Research Topics unify the most influential researchers, the latest key findings and historical advances in a hot research area.

Find out more on how to host your own Frontiers Research Topic or contribute to one as an author by contacting the Frontiers editorial office: frontiersin.org/about/contact

Recent advances in energy systems for sustainable development

Topic editors

Sunday Olayinka Oyedepo — Bells University of Technology, Nigeria
Abimbola Patricia Popoola — Tshwane University of Technology, South Africa
Mufutau Adekojo Waheed — Federal University of Agriculture, Abeokuta, Nigeria
Tosin Somorin — University of Strathclyde, United Kingdom
Oluseyi Olanrewaju Ajayi — Covenant University, Nigeria

Citation

Oyedepo, S. O., Popoola, A. P., Waheed, M. A., Somorin, T., Ajayi, O. O., eds. (2026). *Recent advances in energy systems for sustainable development*. Lausanne: Frontiers Media SA. doi: 10.3389/978-2-8325-7353-2

Table of contents

frontiers | Frontiers in Energy Research

TYPE Editorial
PUBLISHED 02 January 2026
DOI 10.3389/fenrg.2025.1760863

OPEN ACCESS

EDITED AND REVIEWED BY
Michael Carbajales-Dale,
Clemson University, United States

*CORRESPONDENCE
Sunday O. Oyedepo,
sooyedepo@bellsuniversity.edu.ng

RECEIVED 04 December 2025
REVISED 13 December 2025
ACCEPTED 15 December 2025
PUBLISHED 02 January 2026

CITATION
Oyedepo SO, Ajayi OO, Adekojo WM, Popoola API and Somorin T (2026) Editorial: Recent advances in energy systems for sustainable development.
Front. Energy Res. 13:1760863.
doi: 10.3389/fenrg.2025.1760863

Editorial: Recent advances in energy systems for sustainable development

Sunday O. Oyedepo[1]*, Oluseyi O. Ajayi[2], Waheed M. Adekojo[3], Abimbola P. I. Popoola[4] and Tosin Somorin[5,6]

[1]Department of Mechanical/Biomedical Engineering, Bells University of Technology, Ota, Nigeria, [2]Department of Mechanical Engineering, Covenant University, Ota, Nigeria, [3]Department of Mechanical Engineering, Federal University of Agriculture, Abeokuta, Nigeria, [4]Department of Chemical and Metallurgical Engineering, Tshwane University of Technology, Pretoria, South Africa, [5]Department of Chemical and Process Engineering, University of Strathclyde, Glasgow, United Kingdom, [6]International Water Management Institute, Accra, Ghana

KEYWORDS

energy conservation, energy systems optimization, renewable systems design, sustainable development, sustainable energy

Editorial on the Research Topic
Recent advances in energy systems for sustainable development

Being the primary engine of global economic activity, energy obtained from non-renewable sources also plays a large role in environmental damage. In order to move toward clean and green energy and achieve net-zero carbon emissions, it is crucial to develop reliable and sustainable alternatives to fossil fuels as well as smart and sustainable energy technology. The seventh Sustainable Development Goal (SDG 7) aims to ensure that everyone has access to modern, dependable, cheap energy. Unfortunately, developing countries are currently experiencing an energy crisis. This challenge requires innovative and transformative solutions; hence a variety of methodologies and technologies are required. These include advancing cleaner and more cost-effective fossil fuel technology as well as moving toward cleaner power generation based on effective energy management strategies and policies that minimize energy waste and consumption. We also require radical adjustments in the way we use and provide energy services if we are to adapt to the shifting global energy landscape. The fundamental tenet of conserving our limited resources, which are required for the needs of future generations, is known as sustainable development.

The increasing recognition that we must transition away from fossil fuel dependence and towards a sustainable energy future makes this Research Topic both timely and relevant. Moreover, considering continued development and application of energy as essential to the sustainable advancement of society, all aspects of the energy options, including performance against known criteria, efficiency, processing and utilization requirements are essential for critical examination. Based on the above, the Frontiers in Energy Research Journal agreed to host a Research Topic about Recent Advances in Energy Systems for Sustainable Development. This Special Research Topic focuses on the practical issues surrounding energy efficiency, energy conservation & management and renewable energy concepts and systems in achieving sustainable development. Nearly 28 papers have been submitted to this Research Topic, and 12 have been finally accepted, including 7 original research papers, 4 review papers and 1 correction paper. This Research Topic received very positive and supportive responses from various stakeholders globally. Since it began

in 2023, there were 41,010 total views; 24,356 article views; 7,613 article downloads and 16,654 Research Topic views as of 24 November 2025. Twelve articles published within this Research Topic can be found at: https://www.frontiersin.org/research-topics/56757/recent-advances-in-energy-systems-for-sustainable-development/articles.

The paper "Should energy efficiency be improved? The impact of energy efficiency improvements on green economic growth—evidence from China" by Wu et al. evaluates energy efficiency with the Sustainable Business Model (SBM) and constructs a system of green economic growth index, and verifies the relationship between energy efficiency improvement and green economic growth with an econometric model using China as case study. The following findings are reached in this study: 1) On the whole, energy efficiency improvement is currently inhibiting the growth of its green economy. However, as the energy efficiency level increases, the inhibitory effect gradually weakens, showing a non-linear trajectory of "inhibition—weakening inhibition". 2) In the short term, China is still in the expansion stage of energy consumption, and the development of its green economy is thus limited to a certain extent. 3) The expansion of the nation's industrial sectors will intensify resource consumption and pollutant emissions, while technological innovation and urbanization levels can ease the current strenuous status of energy rebound.

In their study on "Promoting the use of bioenergy in developing nations: a CDM route to sustainable development", Dirisu et al. (2024) review strategies to promote the use of bioenergy in developing nations via a clean development mechanism (CDM) route. The study focuses on a forensic assessment of bioenergy utilization in developing countries, emphasizing how to improve bioenergy resources for a sustainable economy and development.

The paper "Experimental evaluation of the performance and power output enhancement of a divergent solar chimney power plant by increasing the chimney height" by Prasad and Ahmed experimentally evaluates the performance and power output enhancement of a divergent solar chimney power plant by increasing the chimney height. The study shows that: 1) the temperature rise in the collector is the highest for the 4 m tall solar chimney power plant (SCPP) with an exit temperature of 50.8 °C and the smallest for the 8m SCPP with an exit temperature of 43.6 °C due to the shorter stay of air in the taller chimney. 2) the temperature drops along the chimney height was the maximum for the 8 m SCPP and minimum for the 4 m SCPP. 3) the air velocity at the turbine section increased with chimney height for all solar insolation and a maximum air velocity of 8.29 m/s was recorded for the 8 m SCPP; it was observed that the increase in the maximum air velocity is not linear but tends to be logarithmic. 4) the maximum turbine output power for the 8m tall SCPP increased by 252% compared to the 4m tall SCPP indicating that significant improvement in the power output can be achieved by increasing the height of a divergent chimney SCPP.

The study on "Enhancing the biomethane yield of groundnut shells using deep eutectic solvents for sustainable energy production" by Olatunji and Madyira investigates the deep eutectic solvent (DES) pretreatment of groundnut shells using choline chloride and ethyl glycerol at different solid: liquid ratios and temperatures to enhance biomethane yield for sustainable energy production. Results of the study reveal that a solid: liquid ratio of 1:2 at 100 °C produced the optimum biomethane yield. This study concludes that, DES pretreatment using choline chloride and ethyl glycerol is a bright, low-cost pretreatment method for enhancing the biomethane yield of lignocellulose feedstocks.

The article on "Control strategies in enhanced stand-alone mini-grid operations for the NESI–an overview" by Balogun et al. reviews control strategies in enhanced stand-alone mini-grid operations for the Nigerian electricity supply industry (NESI). The study shows that the power infrastructure layouts in various climes investigated are identified to have common control objectives, such as efficiency optimization. What really differs in all of the climes was in the availability of resources for distributed generation. Usually, technical, economical, and environmental factors dictated the choice of suitable technological outlay for stand-alone distribution grids. Therefore, the applicable control strategies in this reviewed paper can be adopted in the NESI to enhance mini-grid operations and promote green energy generation and utilization.

Modelling and optimization of operating parameters for improved steam energy production in the food and beverage industry in a developing country was carried out by Olusanya et al. This study focused on refining operational parameters in a steam production plant to maximize steam energy output. It utilized mathematical models and optimization tools to identify ideal operational conditions and investigate extreme scenarios. Design-Expert version 13.0 statistical software and Response Surface Methodology (RSM) via Centre Composite Design (CCD) were employed to create a comprehensive design matrix encompassing key variables like time, pressure levels, temperature, mass flow rate, and steam energy production across three experimental levels. The study shows that increased pressure and time significantly boosted steam energy production by leveraging water's energy content rise under initial conditions, thus improving efficiency by reducing required water mass circulation. A corrigendum to this paper that addresses minor correction to the paper is also included in the Research Topic.

In "The role of product market competition and analyst attention in modulating the link between equity pledges and classification shifting", Xue and Lu investigate the association between equity pledges and classification shifting earnings management in Chinese listed firms, spanning the period from 2016 to 2022. The study further explores the moderating influence of product market competition (PMC) and analyst attention on this relationship. Results of the study demonstrate a positive moderating effect of PMC on the relationship between equity pledges and classification shifting, with an interaction coefficient of 0.0165 ($p < 0.01$).

"Progress in green hydrogen adoption in the African context" is authored by Obanor et al. The study explores the influence of policy frameworks, technological innovations, and market forces in promoting green hydrogen adoption across Africa. The study concludes that to speed up the shift towards a sustainable hydrogen economy in Africa, strategic investments and collaborative efforts are essential. Beside these, by harnessing its renewable energy potential and establishing strong policy frameworks, Africa can not only fulfill its energy requirements but also support global initiatives to mitigate climate change and achieve sustainable development objectives.

Shanmugam and Sharmila present "An intelligent adaptive neuro-fuzzy based control for multiport DC-AC converter with differential power processing converter for hybrid renewable power generation systems". The study shows that the proposed system demonstrates an efficiency of 99.45% and achieves stability in just 0.02 s. Compared to conventional algorithms, the approach adopted in the study shows superior performance across multiple metrics.

In "A critical review on enhancement and sustainability of energy systems: perspectives on thermo-economic and thermo-environmental analysis", Oyedepo et al. critically review new techniques–known as thermo-economic and thermo-environmental analyses for the evaluation and optimization of energy conversion processes, from the perspectives of thermodynamics, economics, and the environment. The outcome of the study shows that (i) the sustainability of energy conversion systems can be enhanced with the use of exergy techniques assessment; (ii) by reducing energy losses, exergy efficiency initiatives can lessen their adverse effects on the environment; and (iii) the best methods for efficient use of energy resources, low energy production costs, and less environmental impact can be provided by hybrid energy systems.

The paper on "Advancing sustainable mobility in India with electric vehicles: market trends and machine learning insights" is authored by Devarasan et al. The authors present an in-depth analysis of India's Electric Vehicle (EV) market dynamics from FY 2014 to February 2024, utilizing machine learning techniques to identify sales trends, regional disparities, and adoption drivers. The outcome of the study shows a consistent rise in EV sales in India from FY 2014 to 2024, driven by factors like environmental awareness, technological advancements in EV, and government incentives.

In summary, the collective knowledge and research on this Research Topic provide valuable insights and motivation for ongoing endeavours toward a more sustainable and energy-efficient future.

Author contributions

SO: Conceptualization, Investigation, Methodology, Supervision, Writing – original draft, Writing – review and editing. OA: Investigation, Methodology, Writing – review and editing. WA: Investigation, Methodology, Writing – review and editing. AP: Conceptualization, Methodology, Supervision, Writing – review and editing. TS: Investigation, Methodology, Writing – review and editing.

Funding

The author(s) declared that financial support was not received for this work and/or its publication.

Conflict of interest

The author(s) declared that this work was conducted in the absence of any commercial or financial relationships that could be construed as a potential conflict of interest.

Generative AI statement

The author(s) declared that generative AI was not used in the creation of this manuscript.

Any alternative text (alt text) provided alongside figures in this article has been generated by Frontiers with the support of artificial intelligence and reasonable efforts have been made to ensure accuracy, including review by the authors wherever possible. If you identify any issues, please contact us.

Publisher's note

Reference

Dirisu, J. O., Salawu, E. Y., Ekpe, I. C., Udoye, N. E., Falodun, O. E., Oyedepo, S. O., et al. (2024). Promoting the use of bioenergy in developing nations: a CDM route to sustainable development. *Front. Energy Res.* 11, 1184348. doi:10.3389/fenrg.2023.1184348

frontiers | Frontiers in Energy Research

TYPE Original Research
PUBLISHED 02 October 2023
DOI 10.3389/fenrg.2023.1249092

OPEN ACCESS

EDITED BY
Sunday Olayinka Oyedepo,
Covenant University, Nigeria

REVIEWED BY
Moses Omolayo Petinrin,
University of Ibadan, Nigeria
Elizabeth Oses Amuta,
Covenant University, Nigeria

*CORRESPONDENCE
Guonian Wang,
bobbywang@cug.edu.cn

RECEIVED 28 June 2023
ACCEPTED 19 September 2023
PUBLISHED 02 October 2023

CITATION
Wu L, Zhu C, Cheng M, Dai W and Wang G (2023), Should energy efficiency be improved? the impact of energy efficiency improvements on green economic growth—evidence from China. *Front. Energy Res.* 11:1249092. doi: 10.3389/fenrg.2023.1249092

Should energy efficiency be improved? the impact of energy efficiency improvements on green economic growth—evidence from China

Lei Wu[1,2], Chengao Zhu[1], Mengxuan Cheng[1], Wen Dai[1] and Guonian Wang[3]*

[1]School of Economics and Management, China University of Geosciences, Wuhan, China, [2]Hubei Green Finance and Resource Environment Innovation Research Base, Wuhan, China, [3]School of Foreign Languages, China University of Geosciences, Wuhan, China

Green economic growth is the main direction of China's future economic development, while energy efficiency improvement—an important prerequisite for promoting the nation's sustainable development—is a necessary way to guarantee its economic transformation and development. It is thus of great practical significance to study the relationship between energy efficiency improvement and green economic development. On the basis of analyzing the mechanism and how energy efficiency improvement influences green economic growth, this paper measures energy efficiency with the SBM model and constructs a system of green economic growth index, and verifies the relationship between energy efficiency improvement and green economic growth with an econometric model empirical analysis. It is found that, on the whole, the improvement of energy efficiency at this stage in China inhibits green economic growth. However, with the improvement of energy efficiency level, the inhibition effect gradually weakens, showing a non-linear trajectory of "inhibition–inhibition weakening". At present, China's energy rebound effect is still on the rise in the short term, and green economic development is restrained to a certain extent. The current expansion of the industrial sector will exacerbate resource consumption and pollutant emissions, while technological innovation and urbanization levels will alleviate the current energy rebound tension. The paper concludes with recommendations from the perspectives of the government, R&D institutions and personnel, the power sector, and urbanization.

KEYWORDS

energy efficiency, green economic growth, energy rebound, technological innovation, industrial structure, urbanization

1 Introduction

With more than 40 years of the implementation of the reform and opening-up policy, China's economy has witnessed a significantly steady development, creating a miracle of growth in the history of world economy. However, the traditional crude economic development approach has brought about certain consequences like high energy consumption and serious pollution, which are imposing considerable pressure on the nation's natural resources and ecological environment. In order to achieve sustainable

socio-economic development in China, a low-carbon green transformation of the economy is an inevitable choice. In 2020, China made a commitment to the world at the United Nations General Assembly that it would "peak at 2030 and become carbon neutral in 2060"; in 2021, China clearly proposed in its 14th Five-Year Plan that it would adhere to the path of green and sustainable development; and in 2022, China further emphasized the need to implement high-quality development, to unswervingly follow the ecological priority, green and low-carbon high-quality development path, and to make efforts to promote the comprehensive green transformation of economic and social development.

Energy utilization efficiency is one of the significant factors to measure the quality of contemporary economic development and an important means to achieve green economic growth. From the perspective of resource sustainability, Huang et al. (2023) pointed out that energy efficiency improvement could largely reduce the waste of resources, alleviate the contradiction triggered by resource allocation, and contribute to sustainable socio-economic development. From the perspective of environment, energy efficiency improvement can reduce pollutant emissions to the environment through energy-saving and carbon emission cuts. From the perspective of economic output, energy efficiency boost can lead to improved production efficiency and stimulate the increase of gross national product (GNP). From the perspective of international economic competition, an effective increase in energy efficiency can generate low-cost advantages for local manufacturing industries and enhance international market competitiveness. However, from the perspective of the whole economic system, energy efficiency improvement may also produce a series of negative impacts. For example, Li (2021) suggested that the energy rebound effect, which would render the potential goals of energy conservation and emission reduction unattainable, could result in the failure of environmental policies and thus hinder the prospect of green economic growth. At the same time, Zhang and Guo, (2023) found that the action mechanism of energy efficiency was also likely to be inhibited or exacerbated by other socio-economic development factors, such as the level of industrial structure, urbanization level, and technological level. Therefore, it has become urgent to explore the impact of energy efficiency improvement on green economic growth.

Earlier scholars believed that the path of economic growth was rather fixed and the main driving force came from traditional factors of production such as technology, capital and labor. The introduction of the concept of green growth has provided scholars with new research ideas, and at the same time, they pointed out the direction for optimizing economic growth. Green economic growth is influenced by a variety of factors, and is mostly analyzed from the perspectives of environmental policy, technological innovation and resource utilization on the basis of connotations. The mainstream view is that environmental policy, technological innovation and resource utilization all have positive effects on green economic growth. Wang and Liu (2015), by exploring whether energy conservation and emission reduction policies would impact green productivity from the perspective of total factor productivity (TFP), found that policies of energy conservation and emission reduction could significantly promote green economic growth and they achieved this mainly through technological progress. Zhang and Bai (2016), by including such green growth indices as technological gap, technological introduction and independent R&D in the measurement model, analyzed the green economic growth of Chinese industries, and finally found that the green economic growth in regions of high-tech levels mainly relied on independent R&D, and areas with medium and low levels of technology chiefly depended on technological introduction, while the technological gap between regions could contribute to green economic development. Li (2019) studied the levels and influencing factors of green economic growth based on data from Japan, and eventually found that technological innovation and the importance of basic education are the main drivers of green economic growth.

As a key part of resources, energy has both economic and environmental attributes, and the impact of its utilization on green economic growth has received much attention from the academic community. Current research mainly focuses on clean energy, energy consumption and energy efficiency. Regarding the greening process of energy use and green economic development, Wang and Li (2021) concluded that there was a two-way causal relationship between clean energy and green economic growth, and the positive effect of clean energy on green economic growth outweighed the negative effect. Shobande et al. (2023) argued that the development of renewable energy is important for reducing carbon emissions. Wan (2022) empirically demonstrated by the VAR model[1] that the contribution of clean energy to green economic development is higher than that of other energy sources.

Differences, however, also exist in academic views on the relationship between energy consumption and economic growth. Han et al. (2004) argued that there is a two-way causal relationship between energy consumption and economic development, i.e., an increase in energy consumption can promote economic development, and economic development can also generate an increased demand for energy consumption. Another scholar Wang (2020) believed that economic growth is a one-way cause of the greening transition in energy use. In addition, some other scholars focus on energy efficiency. By definition, the increase in energy efficiency itself includes the economic benefits of energy conservation. However, quite some scholars have found through their research that this is not the case. After a study using the DSGE[2] model, Wu et al. (2022) found that energy efficiency improvements can indirectly weaken economic growth through energy prices and environmental expenditures. Some scholars observed, by means of the energy rebound effect, the negative impact of energy efficiency improvement. For example, Zhang and Zhang (2014), after measuring the energy rebound, found that energy efficiency boost had generated unsatisfactory energy savings, and energy consumption had little impact on economic growth. Lin and Zhou (2022) found no significant improvement in the quality of economic growth by energy efficiency, but there was a significant

1 VAR model(Vector Autoregressive Model) is a model of unstructured system of equations used to estimate the dynamic relationship between multiple variables.

2 DSGE (Dynamic Stochastic General Equilibrium) model is an equation for the optimal behavior of each economic agent in the face of a variety of different environmental constraints, coupled with market conditions, before obtaining the final equation for the overall economic satisfaction in the uncertain environment.

U-shaped relationship between energy efficiency and the quality of economic growth. Hu et al. (2019) found that energy rebound existed in more than 60% of Chinese cities—with those in east and central China recording more obvious rebounds—and the energy rebound effect was more pronounced when technological progress improved energy efficiency. Xu et al. (2022) reported that technological progress has continuously exacerbated energy rebound in recent years, and the positive effect brought about by technological progress mainly flows to high energy-consuming sectors, making energy consumption intensity remain at a high level amidst economic growth, and virtually reaching a dilemma of low-level or inefficient energy conservation. Jia et al. (2022) analyzed carbon energy consumption and found that the carbon energy rebound effect lingered within a high rebound interval. Except for the period of relevant policy adjustment, the carbon energy rebound has shown an increasing trend for most of the time.

Although the research work on the factors influencing green economic growth is relatively mature, there is less literature directly linking energy efficiency with green economic growth. Therefore, based on the principle that the improvement of energy efficiency will bring about resource saving and new energy demand, this paper will sort out the channels and paths through which energy efficiency acts on green economic growth. It aims to measure the total factor energy efficiency and green economy level with the DEA method[3] and entropy method, and to answer the question of whether energy efficiency can promote green economic growth through econometric models. The study is intended to fill the gap in research related to the role of energy efficiency in green economic growth.

2 Theoretical analysis

2.1 Relationship between energy efficiency and green economic growth

Green economic growth is an economic development that integrates the concept of green development into economic growth while effectively combining resources and environment with economy. The improvement of energy efficiency demonstrates both positive and negative influencing mechanisms on green economic growth.

The mechanism of positive influence of energy efficiency improvement on green economic growth is manifested as follows. Firstly, there is the resource allocation effect. The improvement of energy efficiency can largely facilitate the reallocation of resources, reduce the possibility of resource mismatch and avoid the waste of resources. Wei and Li (2017) noted that the rational allocation of resources can effectively alleviate the pressure of resource shortage in the process of late-stage industrial development, thus improving output efficiency, maintaining sustainable economic development, and promoting green economic growth. Secondly, there is the effect of energy saving and carbon emission reduction. The improvement of energy efficiency can effectively relieve energy pressure, cut energy consumption and reduce pollutant emissions; the upgrading of energy technology can also play a positive role in combating pollution and improving the environment; while energy saving and emission reduction can effectively facilitate the development of green economy. Thirdly, increased energy efficiency promotes green energy consumption. The key to energy efficiency is to promote the development of green and clean energy technology, and the popularity of such technology can largely and widely expand the demand for new and green energy consumption, which in turn will speed up the development of green economy. Fourthly, energy efficiency boost contributes to the optimization of energy structure. Zheng et al. (2021) stated that one manifestation of lifted energy efficiency was the optimized energy structure. It can further enhance the effect of energy saving and emission reduction, and also accelerate the effect of resource allocation, thus further promoting the development of green economy.

Conversely, the mechanism of negative impact of energy efficiency improvement on green economic growth is demonstrated as follows. Firstly, it may lead to the excess of resource factors. Ji (2020) pointed out that energy efficiency enhancement could render the resource factors redundant, and the excess and underutilization of resource factors would, to a certain extent, hold back the development of green economy. Secondly, better energy efficiency may lead to an increase in energy consumption. Han et al. (2017) suggested that the improvement in energy efficiency had proved to produce the "energy rebound" effect. Amidst energy efficiency boost, energy prices may fall, thus stimulating consumption of more energy. Producers, on the other hand, tend to obtain more profits and expand production, resulting in more energy demand and eventually pumping up energy consumption. While the gross national product (GNP) has increased, the development of green economy has stalled. Thirdly, it could worsen environmental pollution. The increase in energy consumption stimulated by the boost in energy efficiency has churned out more greenhouse gases and pollutant emissions, a sudden increase in the pressure on environmental protection. With a considerable portion of resources invested in environmental conservation, the green economy is unavoidably hampered to some extent.

2.2 Relationship between energy efficiency and green economic growth under different mechanisms of action

2.2.1 Action mechanism of technological innovation: energy efficiency and green economic growth

In the context of open innovation, be it external technology acquisition or independent technology development, Shan (2018) pointed out that there would be an obvious time lag between technological innovation and its performance in the development of social economy. Technological innovation is one of the main influencing factors for energy efficiency improvement. When the

3 DEA method(Data envelopment analysis)is expressed as a ratio of outputs to inputs. It is primarily a quantitative analysis method for evaluating the relative effectiveness of comparable units of the same type on the basis of multiple input indicators and multiple output indicators, utilizing the method of linear programming.

level of technological innovation is relatively low at the early stage of its development, energy efficiency can be effectively improved to promote the growth of green economy through energy saving and emission reduction. However, Wang (2020) stated that if compared with the capital cost, human cost and even energy consumption already invested in the early stage of its R&D, the improvement of energy efficiency usually failed to compensate for these resource investments, and thus the growth of green economy was inhibited. As technological innovation constantly develops, the innovative level keeps rising and the technology continues to mature, the positive externalities thus brought about not only help improve the efficiency of energy, reducing production costs, but they also yield high returns and low pollution. In addition, secondary innovation is a probable result of high-end technological development through the clustering effect of innovation factors. Liu and Sun (2008) pointed out—through an empirical study on the relationship between technological innovation, industrial structure and energy consumption—that technological innovation could also promote the upgrading of industrial structure and reduce resource mismatch, so as to increase gross national product (GNP).

2.2.2 Action mechanism of industrial structure: energy efficiency and green economic growth

Zhang and Cheng (2020) indicated that a proper industrial structure usually generated a significant influence on energy efficiency and green economic development. As the pillar of China's economy, the secondary industry has been the main force of economic development. On the one hand, when the secondary industry accounts for a larger share of the economic structure, an improved economic level helps to increase the capital investment in the innovation of energy technology, facilitate the improvement of energy efficiency, reduce energy consumption for industries, and lower the intensity of carbon emissions. On the other hand, however, the expansion of traditional industrial sectors has brought about a huge increase in energy consumption, which has led to a relative decrease in energy efficiency. In general, due to the high pollution and high emission characteristics of the secondary industry, energy efficiency improvement can boost economic growth but ignore the green development of the economy, and instead, energy efficiency improvement actually hinders the growth of green economy. Compared with the secondary industry, the tertiary industry is less intensive in energy consumption and environmental pollution. When the proportion of tertiary industry increases in the economic structure, the investment increase in innovation elements like high technology can provide a better innovative environment for economic development and promote technological progress while improving energy efficiency. In addition, the rapid expansion and development of the tertiary sector can directly contribute to green economic growth by resolving social conflicts such as unemployment and community welfare through spillover effects and scale effects of population.

2.2.3 Action mechanism of urbanization: energy efficiency and green economic growth

The urbanization process is an indicator reflecting the level of socio-economic development. At a low level of urbanization with a small urban population, the improvement of energy efficiency can lead to lower energy prices and reduce pollution emissions in production, but it cannot effectively stimulate the increase of consumption and production expansion, and the cost investment to improve energy efficiency may lead to lower enterprise performance and inhibit economic growth. When the urban population gradually increases, Wu (2020) argued that the effects of resource agglomeration, knowledge spillover and economies of scale would come into play, which on the one hand might stimulate competition, accelerate technological innovation, reduce resource mismatch, produce effective improvement of energy efficiency, promote industrial structure upgrading and increase output value. On the other hand, Li et al. (2021) indicated that as the economic level of urban areas improved, *per capita* income would go up and residents' awareness of environmental protection increases, green consumption were likely to grow and ecological environment would improve. The above changes will generally promote energy efficiency, optimize the energy consumption structure, and reduce the pressure on resources and environment, thus effectively promoting green economic growth.

Based on the above theoretical analysis, the impact transmission mechanism of energy efficiency affecting green economic growth in this paper can be derived, as shown in Figure 1.

3 Model setting

3.1 Econometric model setting

Based on the previous analysis, and in order to explore the impact of energy efficiency on green economic growth in China, the following benchmark model is constructed, with reference to Chen et al. (2020), for this paper:

$$Gree_{it} = \alpha_0 + \alpha_1 Effi_{it} + \alpha_2 X_{it} + u_{it} + \varepsilon_{it} \quad (1)$$

Where i and t represent the province and year, respectively; $Gree_{it}$ is green economic growth; $Effi_{it}$ is energy efficiency; X_{it} represents a series of control variables, including Urbn, FDI, Disp, Huma, Envi, Stru, Gove and Tech; u_{it} represents the fixed effects of the province and year, and ε_{it} is a random error term. (See Section 3.2; Table 2 for specific variable names and abbreviations).

Considering the possible non-linear effect of energy efficiency on green economic growth, this paper introduces the threshold model proposed by Hansen (1999). The model is constructed as follows:

$$Gree_{it} = \rho_0 + \rho_1 Effi_{it} \times I(Effi_{it} \le \theta) + \rho_2 Effi_{it} \times I(Effi_{it} > \theta) + \rho_3 X_{it} + \mu_i + \varepsilon_{it} \quad (2)$$

Where the threshold variable is the energy efficiency, and I is an indicator function that takes 0 or 1. It takes the value 1 if the conditions in brackets are met; otherwise it takes 0. Eq. 2 is a single-threshold model, which can be changed to a multi-threshold form according to the actual demand and the threshold significance test.

In order to further test the possible mechanisms of the roles of industrial structure, technological innovation and urbanization level in the relationship between energy efficiency and green economic growth, with reference to Ye and Wen (2013), the moderating model

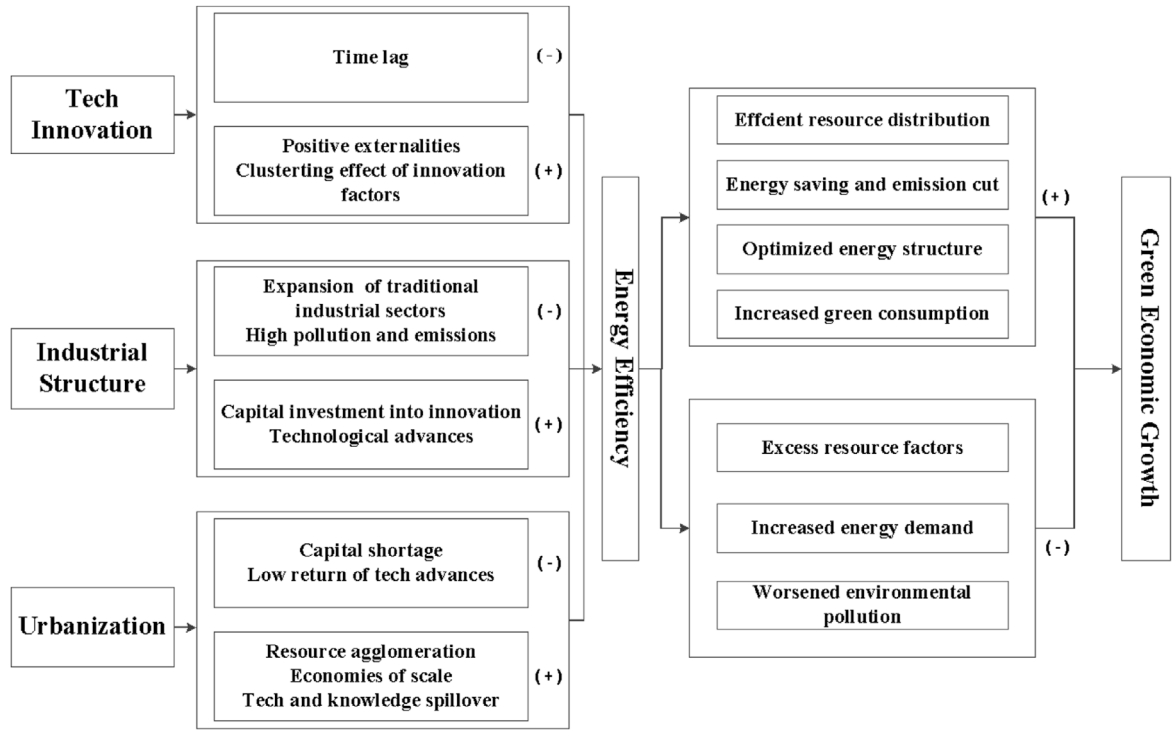

FIGURE 1
Transmission mechanism of energy efficiency affecting green economic growth.

is selected for mechanism testing in this paper, and the model is set below:

$$Gree_{it} = \alpha_0 + \alpha_1 Effi_{it} + \alpha_2 Effi_{it} \times B_{it} + \alpha_3 X_{it} + u_{it} + \varepsilon_{it} \quad (3)$$

Where B_{it} denotes the moderators, which include Stru, Tech and Urbn, respectively. The positive or negative properties of the estimated coefficients α_1 and α_2, as well as their significance levels, are used to determine whether Stru, Tech and Urbn play a moderating role in the relationship between energy efficiency and green economic growth.

Considering that the effect of energy efficiency on green economic growth may be differentially influenced by Stru, Tech and Urbn, the following model is thus set in this paper:

$$Gree_{it} = \rho_0 + \rho_1 Effi_{it} \times I(B_{it} \le \theta) + \rho_2 Effi_{it} \times I(B_{it} > \theta) + \rho_3 X_{it} + \mu_i + \varepsilon_{it} \quad (4)$$

Where B_{it} represents the threshold variables, including Stru, Tech and Urbn. The threshold setting of the model is determined according to the test.

3.2 Selection and description of variables

3.2.1 Dependent variable

Level of green economic growth (Gree). When scholars at home and abroad measure the index of green economic development level, most of them measure it from such three levels as economy, ecology and society. The Asian Development Bank (ADB) selected a total of 28 indicators to construct an inclusive measurement system of green growth index around three themes: economic growth, social equity and environmental sustainability; Gu (2022) selected 18 specific secondary indicators from the three dimensions of economic efficiency, social foundation and green environment. Geng and Huang (2022) subdivided the social perspective into hard conditions and soft guarantees to illustrate in more detail the degree of contribution of social development to green economic growth. Yang et al. (2022) and others introduced the government factor on the basis of the above two scholars, adding the indicator of government support; and at the second level indicators they roughly categorized the resource environment into resource consumption and environmental protection, while further subdividing social development into four categories: science and technology, education, innovation, and services.

According to the connotation of green economic growth and the actual situation of each province in China, and with reference to the relevant literature, we finally constructed a development measurement and evaluation index system for green economy consisting of three primary indicators—economic efficiency, resource environment, and society and livelihood—and 12 secondary indicators. Under the principles of scientificalness, factuality, data validity and accessibility, all the index data in this paper are selected from the National Bureau of Statistics of China (NBSC), the National Food and Strategic Reserves Administration of China (NFSRAC), the Ecology and Environment of China (MEEC), and the Ministry of Agriculture Rural Affairs of China (MARAC). The data of all the indicators are retrieved from the

TABLE 1 Measurement index system of development level for green economy.

Primary indicators	Secondary indicators	Properties	Unit
Economic efficiency	Value-added of tertiary industry	Positive	Hundred million yuan
	Consumer Price Index (CPI)	Positive	Previous year = 100
	Per capita GDP	Positive	yuan
	Internet broadband access users	Positive	10,000 households
Resource Environment	Operating costs for industrial waste gas treatment facilities	Negative	Ten thousand yuan
	Average amount of water used per person	Positive	m3/person
	Electricity consumption	Negative	Hundred million kWh
	Forest coverage rate	Positive	%
Society and People's Livelihood	Income ratio of urban to rural residents (rural residents = 1)	Negative	yuan/person
	Average number of college students currently on campus	Positive	People
	Number of primary healthcare facilities	Positive	Sites
	Urban registered unemployment rate	Negative	%

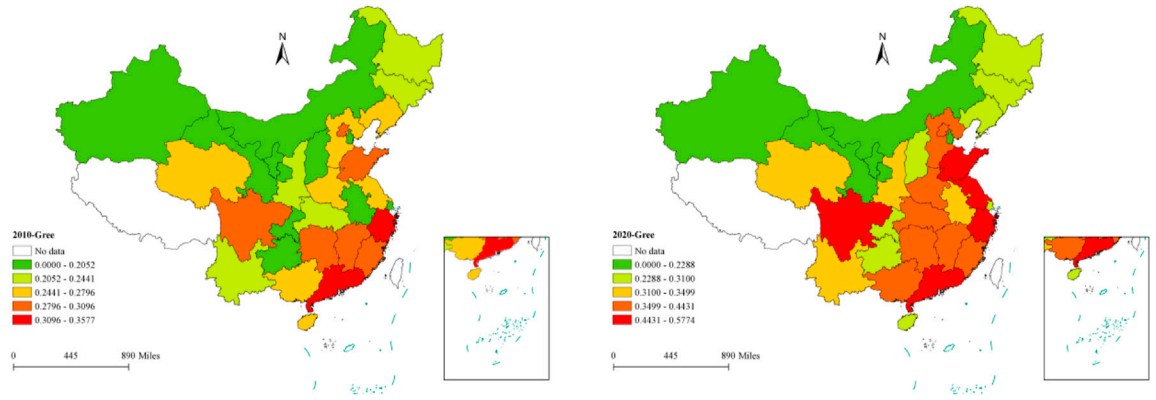

FIGURE 2
Regional differences of the level of green economic growth among 30 Chinese provinces, 2010-2020.

relevant databanks of NBSC, NFSRAC and MEEC between 2010 and 2020. The specific index system is shown in Table 1.

The results of the provincial measures of China's green economy growth are shown in Figure 2. There are large differences in the growth level of green economy among the nation's provinces both in time and space. From the geographical point of view, the high level of green economic growth is mostly concentrated in the eastern and southern regions, while the western and northern regions are generally at a lower level, showing the geographical distribution pattern of "strong in the east and south, weak in the west and north"; and the majority of the high-level regions are concentrated in the economically developed coastal areas, indicating that the level of green economic growth is influenced by the level of local economic development. From the perspective of time dimension, the growth of green economy in each province shows a general trend of "the east in the lead and the middle and west on the rise". Additionally, the green growth rate in the eastern region is still progressing in the fast lane, and some provinces in the western region have also realized a gradient leap.

3.2.2 Key explanatory variable

Energy efficiency (Effi). Energy efficiency is a comprehensive indicator reflecting the efficiency of energy consumption and energy utilization, thus the measure of economic efficiency from the input and output of energy factors alone does not fully reflect the energy utilization rate and high-quality economic development. Considering that the current energy efficiency is also influenced by other factors of production such as capital and labor, as well as the possible pollutant emissions brought about by energy consumption, this paper chooses the green total factor productivity—which allows for multifactor inputs and pollutant emissions—to measure the energy efficiency. Meanwhile, we make measurements of China's provincial energy efficiency by drawing on Wang and Lu, (2021) practice of utilizing a super-efficiency SBM model with undesirable outputs. (See the appendix for the specific calculation process).

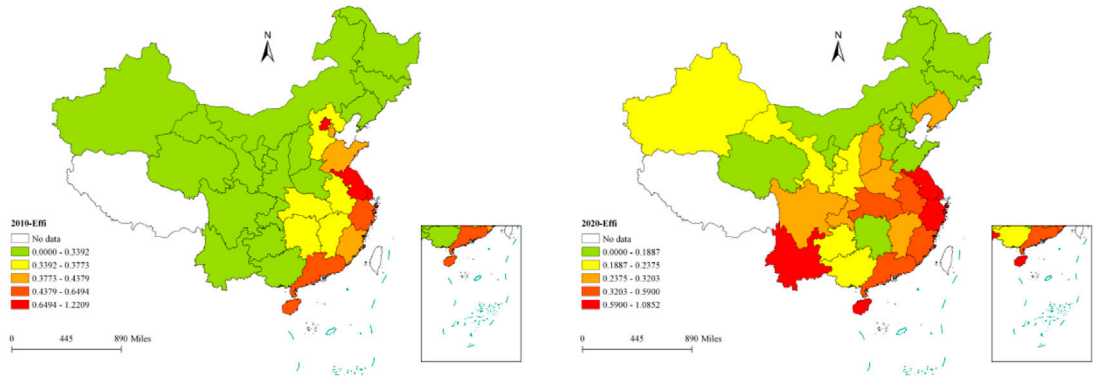

FIGURE 3
Regional differences of energy efficiency levels among 30 Chinese provinces, 2010-2020.

The input factors selected in this paper include capital, labor and energy consumption. Among them, capital is expressed with total social fixed asset investment. By referring to the study of Zhang et al. (2004), this paper adopts 2006 as the base period and estimates the capital stock with the perpetual inventory method. In the formula $K_{it} = I_{it} + (1 - \delta)K_{it-1}$, the depreciation rate $\delta = 10.96\%$, and the fixed asset price index is adopted for deflating. The labor force is expressed with the number of employees at the end of the year. Considering the existing energy consumption structure of China, coal is still used as the main supply of energy, and coal consumption also serves as an important criterion to measure the greening level of the region, thus the consumption of coal is used as the input variable of energy consumption in this paper. The regional GDP of the province is used as the desired output; industrial sulfur dioxide emissions, industrial wastewater emissions and industrial soot emissions are used as the undesirable output.

Figure 3 shows the results of provincial measures of energy efficiency. It can be seen that the overall energy efficiency level of most provinces is low, and only some provinces show a more prominent level of energy efficiency. Over time, the southern and central provinces of China have experienced a rapid increase in energy efficiency, while the northern provinces are all at low levels of energy efficiency, with the gap in energy efficiency levels widening. The fact that there are quite some provinces with boosted gradients indicates that energy efficiency as a whole has been partially improved, showing a distribution pattern of "central and southern regions leading, and northern regions lagging behind".

3.2.3 Control variables

Urbanization level (Urbn): The promotion of urbanization can accelerate the intensive use of resources and the improvement of industrialization level, which is a general rule of socio-economic development. Generally speaking, urbanization level is closely related to both energy efficiency and green economic growth, and the level of urbanization affects energy efficiency and directly contributes to green economic growth. In this paper, we adopt the urbanization rate suggested by Hu et al. (2018) to demonstrate the level of urbanization.

Foreign direct investment (FDI): As a factor of capital production, direct investment by multinational companies also enables the transfer of technology and environmental costs, so FDI can significantly act on industries that require bulky capital and technological inputs, and eventually affect the industrial structure of China. Therefore, this paper will refer to Yuan and Xie (2014) and utilize the FDI index.

Disposable income of urban residents (Disp): Considering that disposable income of urban residents can directly affect the development of green economy and energy consumption demand of urban residents, their disposable income (its logarithm value) is used to express this control variable.

Human capital (Huma): With the gradual massification of higher education in China, human capital shows a more significant correlation with graduates bearing a bachelor's degree, and college graduates can increasingly represent the quality level of human capital.

Environmental regulation (Envi): Standards, institutions and market incentives for the purposes of environmental protection can significantly influence the development of regional green economies, and the related expenditure on environmental protection needs to be borne by the whole society. Therefore, this paper presents, by drawing on the practice of Tao and Zhou (2015), the level of environmental regulation with the intensity of environmental regulation, which is measured by the ratio of completed investment in industrial pollution control to the added-value of the secondary industry.

Industrial structure (Stru): The secondary industry, as the largest energy-consuming sector, is the mainstay of resource consumption and environmental pollution. Therefore, this paper draws on the practice of Duan and Du, (2022) and uses the proportion of secondary industry (percentage) to measure the change in regional industrial structure.

Level of governmental financial support (Gove): The development of green economy cannot be separated from the support and guidance of the government and market managers, so this paper follows the same approach as Yang et al. (2023) and employs the proportion of financial expenditure to GDP in expressing the level of financial support.

Level of technological innovation (Tech): Scientific and technological innovation can develop synergistically with energy efficiency, and green economic development is also inseparable from the support of green innovative technology. Therefore, this paper draws on the practice of Wang et al. (2023) to interpret the level of technological innovation by the logarithm of the number of patent applications granted.

TABLE 2 Statistical description of the variables.

Variables	Observations	Average value	Standard deviation	Maximum value	Minimum value
Gree	330	0.2897	0.0812	0.5813	0.1021
Effi	330	0.4304	0.2751	1.2818	0.0000
Urbn	330	0.5836	0.1252	0.8960	0.3381
FDI	330	81.0060	79.0744	357.5956	0.0446
Huma	330	8.9325	6.9087	43.8000	2.1629
Disp	330	9.9231	0.3153	10.8536	9.2049
Envi	330	0.0029	0.0028	0.0245	0.0000
Stru	330	43.6717	8.8125	59.0000	15.8000
Gove	330	26.1611	11.3986	75.8292	11.2987
Tech	330	10.0157	1.4679	13.4726	5.5759

3.2.4 Threshold variables (moderating variables)

In this paper, Stru, Tech and Urbn are used as threshold variables, with the selection of specific measurement indicators already shown in the above Section: Control variables.

3.3 Data sources

Considering that since 2010, the Chinese government has gradually introduced policies to start phasing out backward production capacities and increasing investment in clean energy, China's domestic energy and environmental policies have been significantly modified. To ensure the completeness of the panel data and the robustness of the regression results, this paper selects data between 2010 and 2020 from 30 provinces (municipalities) in China to conduct the study, and after data processing, 330 data samples are obtained as province-year observations. The data used for the study in this paper are mainly from the EPS database, Wind database and the *Chinese City Statistical Yearbook* of the 11 years Table 2 shows the results of descriptive statistics of the variables in this paper. The results show that the mean value of Gree is 0.2897, with the maximum value at 0.5813, the minimum at 0.1021, and the standard deviation at 0.0812, indicating that there are large differences in green economic growth levels among different provinces and municipalities. The mean value of Effi is 0.4304, with the maximum value at 1.2818, the minimum value at 0.0000, and the standard deviation at 0.2751, indicating that there is a large difference in energy efficiency between different places. The rest control variables also have significant variability among different provinces.

4 Empirical conclusion and analysis

4.1 Analysis of benchmark regression results

In this paper, the software Stata 17.0 and a benchmark regression model are applied to the selected full sample data of 30 provinces (municipalities) across China from 2010 to 2020. Meanwhile, in order to further explore the different impacts of energy efficiency improvement on green economic growth in different regions of China, this paper, referring to Liu et al. (2022), divides the selected Chinese provinces into three sub-regions, i.e., eastern, central and western regions, to probe the characteristics of the spatial distribution in different sub-regions regarding the impacts of energy efficiency on green economic growth. The results are shown in Table 3.

Table 3 above reports the results of the benchmark regression model for the impact of energy efficiency improvement on green economic growth in China. In Column (1) of the table, the estimated coefficient of the core explanatory variable, energy efficiency (Effi), is significantly negative, indicating that the higher the energy efficiency, the lower the level of green economic growth. In other words, the increase in energy efficiency inhibits the green economic growth in China at this stage. The reason for this could be that China is still in the rising period of energy "rebound effect", and the increase of energy efficiency level further increases the consumption of energy, which in turn hinders the green economic growth. Among the remaining control variables, urbanization level and FDI show a significant positive effect on green economic growth, while technological innovation, government financial support and urban disposable income show a significant inhibitory effect on green economic growth, with human capital having no effect on green economic growth.

The regression results in Columns (2)–(4) of Table 3 reflect different coefficients of energy efficiency (Effi) in relation to green economic performance in the three sub-regions. The coefficient of energy efficiency improvement on green economic growth in the eastern region is −0.0260, significant at a 1% level of significance, i.e., energy efficiency in the eastern provinces inhibits the growth of their green economies. The coefficient of the central region is 0.0513, significant at 5%, i.e., increases in energy efficiency in the middle part of China promote regional development of green economy. The coefficient of the western sub-region, however, is 0.0420, not significant, suggesting that energy efficiency boost and green economic growth there do not show a strong correlation. Generally, the eastern, central and western regions show a spatial pattern of "inhibiting—promoting—not significant". Given the actual situation, the eastern region has a developed economy, strong technological innovation capability, advanced production technologies, and high efficiency of resource utilization, and the

TABLE 3 Spatial distribution of energy efficiency Impacts on green economic growth.

Variables	(1)	(2)	(3)	(4)
	National	Eastern	Central	Western
Effi	−0.0177*** (−2.73)	−0.0260*** (−3.63)	0.0513** (2.34)	0.0420 (1.53)
Urbn	0.3278*** (3.36)	0.5559*** (3.58)	0.6954*** (3.48)	0.9516*** (2.66)
FDI	0.0002*** (5.94)	0.0001** (2.54)	0.0004*** (4.98)	−0.0001 (−0.29)
Huma	−0.0004 (−0.43)	0.0001 (0.07)	−0.0081*** (−3.43)	−0.0026 (−1.07)
Disp	−0.2009*** (−5.57)	−0.2437*** (−4.18)	−0.0915* (−1.70)	−0.1445* (−1.81)
Envi	1.6419** (2.57)	4.7493*** (2.89)	1.2117 (1.31)	0.2649 (0.32)
Stru	0.0018*** (3.68)	0.0035*** (3.30)	0.0007 (1.46)	−0.0022** (−2.22)
Gove	−0.0016*** (−2.79)	0.0008 (0.49)	−0.0001 (−0.16)	−0.0012 (−1.55)
Tech	−0.0385*** (−6.87)	−0.0651*** (−5.75)	−0.0304*** (−4.60)	−0.0282*** (−2.91)
Cons	2.2941*** (6.69)	2.7860*** (4.49)	1.4547*** (3.97)	1.5449** (2.07)
N	330	132	99	99
R^2	0.7967	0.8531	0.9389	0.7912

1) The figures in brackets refer to the Z statistics of the coefficients; 2) *, ** and *** refer to the significant results at the significance levels of 10%, 5% and 1%, respectively. The same rule applies hereinafter.

rebound effect there is dominant. The central region, where energy efficiency is low, however, has not reached, or incompletely reached, the rebound stage of energy efficiency improvement, and is currently in the partial rebound stages according to Hu et al. (2019). The effect of energy saving and production expansion generated by energy efficiency improvement is greater than that of increased resource consumption brought about by energy rebound, as is reflected in promoting the development of green economy. At this stage, energy efficiency improvement can reduce energy consumption, which in turn promotes the development of green economy. As for the western sub-region, the effect of energy efficiency increase on green economic growth has not been reflected yet, probably because the western provinces are rich in fossil energy resources and located in less developed areas, and thus the economic development thereof does not heavily rely on energy. Furthermore, the western region is mostly an environmental protection zone—which attaches more importance to environmental conservation than the eastern and central sub-regions—so energy efficiency improvement and green economic development are not directly interrelated.

4.2 Analysis of heterogeneous regression results of energy efficiency

Before estimating the threshold model, a test for the existence of the panel threshold is conducted based on Hansen, (1999) method. After 300 iterations of Bootstrap self-sustaining sampling, the results show that in the threshold model test with energy efficiency as the explanatory variable, the energy efficiency level threshold significantly passes the single threshold but fails the double and triple threshold tests. Therefore, the regression model with a single threshold is set on this basis, and the regression results are obtained as shown in Table 4.

TABLE 4 Results of energy efficiency threshold.

Effi	
Threshold	0.2406
95% confidence interval	[0.2388, 0.2424]
Effi (Effi ≤0.2406)	−0.1719*** (−5.83)
Effi (Effi >0.2406)	−0.0203** (−2.53)
Cons	0.7652*** (3.11)
N	330
R^2	0.6753

The results in Table 4 show that with the increase of energy efficiency, the impact of energy efficiency on China's green economic growth shows different degrees of inhibition, i.e., the impact of energy efficiency on green economic growth has a non-linear trajectory of "inhibition—weakening inhibition". Specifically, when the threshold energy efficiency is lower than 0.2406, the coefficient of energy efficiency on green economic growth is −0.1719, which means that energy efficiency at a low level hinders the development of green economy as a whole; when energy efficiency is equal to or higher than 0.2406, the coefficient of energy efficiency on green economic growth is −0.0203, and the coefficient of energy efficiency on green economic growth is still negative, but the inhibitory effect is gradually weakening. Furthermore, as China is currently in a critical period of industrial structure upgrading and energy structure transformation, the engine of the old economic growth mode has been slightly weak and worn out; the driving power of the new economic growth mode, however, has not been fully incubated, and the economic growth is therefore lacking in strength. Moreover, the

TABLE 5 Results of mechanism test.

Variable	(1)	(2)	(3)
	Stru	Tech	Urbn
Effi	0.0082 (0.47)	−0.1206** (−2.32)	−0.1061*** (−3.32)
Effi × Stru	−0.0008 (−1.59)		
Effi × Tech		0.0093** (2.00)	
Effi × Urbn			0.1330*** (2.38)
Cons	2.1925*** (0.3478)	2.3961*** (6.95)	2.2333*** (6.58)
N	330	330	330
R^2	0.7986	0.7996	0.8024

TABLE 6 Results of Industrial structure threshold.

Stru	
Threshold	44.6000
95% confidence interval	[44.4324, 44.7348]
Effi (Stru ≤44.6)	0.0047 (0.57)
Effi (Stru >44.6)	−0.0656*** (−6.56)
Cons	0.5332** (2.25)
N	330
R^2	0.7003

coal-based energy structure hardly fits into the current environment of green economic growth, and the rebound effect from energy efficiency improvement has not yet reached its peak, resulting in the fact that at this stage China's green economic growth is blocked with great resistance.

4.3 Analysis of mechanism test results

It is found, on the basis of the preceding theoretical analysis, that Stru, Tech and Urbn all play a role in the influence of energy efficiency on the level of green economic growth. In order to verify this theoretical hypothesis, the moderating model is selected for empirical testing in this paper, and the regression results are shown in Table 5.

In Column (1), the coefficients of Effi and Effi × Stru as moderating variables do not show significance, indicating that industrial structure does not have a moderating effect on the relationship between energy efficiency and green economic growth. In reality, China's industrial structure is in a period of transformation and upgrading, with advanced manufacturing and backward production capacity co-existing, and with an insignificant energy rebound effect caused by industrial structure fluctuations. The Effi coefficient in Column (2) is significantly negative, while the Effi × Tech coefficient is significantly positive. This indicates that, from a practical point of view, the effects of lower energy consumption and higher output brought about by the increased level of technological innovation have sufficiently ameliorated the situation that energy efficiency improvement inhibits green economic growth, with technological innovation playing a positive moderating effect. The coefficient of Urbn in Column (3) is significantly negative, and that of Effi × Urbn is significantly positive. This indicates that—due to the positive moderating effect of the increased urbanization level—the agglomeration effect of resources, knowledge spillover effect and effect of economies of scale have effectively improved the situation that the increase of energy efficiency inhibits the growth of green economy.

4.4 Analysis of threshold effect

4.4.1 Threshold effect of industrial structure

To verify the above analysis of the moderating mechanism, this paper explores the threshold effect of industrial structure to test whether the rationalization of industrial structure contributes to green economic growth. By testing the existence of the panel threshold, it is found that the industrial structure threshold does not pass the double threshold and triple threshold tests, and there is a nonlinear single threshold relationship. Therefore, the regression model of a single threshold is set on this basis, and the regression results are obtained as shown in Table 6.

As shown in Table 6, the effect of energy efficiency on green economic growth shows a non-linear relationship of "insignificant—inhibition" with the increase of the proportion of secondary industry in the industrial structure observations. When Stru ≤44.6, the coefficient of energy efficiency on green economic growth is 0.0047, but the *p*-value is not significant, which indicates that when the proportion of the secondary industry is low, the effect of energy efficiency improvement on green economic growth is not significant; when Stru >44.6, the coefficient is −0.0656, and energy efficiency significantly inhibits green economic development at the 1% level, which suggests that when the proportion of industrial manufacturing is too large, energy efficiency improvement hinders green economic development instead. The fact suggests that a large share of the secondary sectors means that most of the production factors such as technology and capital are flowing to the energy-intensive industrial manufacturing sectors. The expansion of the industrial sectors will intensify resource consumption, increase energy consumption and pollutant emissions, and thus reduce the level of green economic growth.

4.4.2 Threshold effect of technological innovation

This paper explores the threshold effect of technological innovation to test whether technological innovation contributes to green economic growth. By testing the existence of the panel threshold, it is found that the threshold of technological innovation fails the dual-threshold and triple-threshold tests, and there is a nonlinear single-threshold relationship. Therefore, the regression model of a single threshold was set on this basis, and the regression results were obtained as in Table 7.

As shown in Table 7, the effect of energy efficiency on green economic growth shows a non-linear relationship of "inhibiting—promoting" as the level of technological innovation increases. When Tech ≤12.5060, energy efficiency improvement significantly inhibits the growth of green economy, and when Tech >12.5060, energy efficiency increase significantly promotes the growth of green economy. To start with, in light of the characteristics of technological innovation, the effectiveness of

TABLE 7 Results of technological innovation level threshold.

Tech	
Threshold	12.5060
95% confidence interva	[12.4647, 12.5589]
Effi (Tech ≤12.5060)	−0.0329*** (−4.09)
Effi (Tech >12.5060)	0.0479*** (3.98)
Cons	0.7160*** (3.01)
N	330
R^2	0.6961

TABLE 8 Results of urbanization level threshold.

Urbn	
Threshold	0.6951, 0.8470
95% confidence interval	[0.6921, 0.7002], [0.8360, 0.8596]
Effi (Urbn ≤0.6951)	−0.0317*** (−3.36)
Effi (0.6591 < Urbn ≤0.8470)	0.0709*** (5.63)
Effi (Urbn >0.8470)	−0.0291** (−1.99)
Cons	0.8527*** (3.68)
N	330
R^2	0.7251

technological innovation has a time lag. At the initial low level of technological innovation, in order to achieve the progress of sci-tech innovation, the demand for energy resources in enterprises increases, and a large amount of capital, manpower, resources and other innovation factors are invested, only to obtain a small increase in energy efficiency. The effect of energy saving and emission reduction at this stage is not noticeable, with the effective growth of the green economy inhibited. Next, the improvement of technological innovation level will stimulate industrial production and increase energy demand, while the boost of energy efficiency is limited by the bottleneck of technological innovation, and the overall downward trend of green economic development level is observed when comparing the two. In the later stage, with the continuous level improvement of technological innovation, the industrial structure is optimized, the energy efficiency improvement effect is prominent, and the green and low-carbon technology is continuously moving towards maturity and application, which will further benefit the green economic growth.

4.4.3 Threshold effect of urbanization level

This paper explores the threshold effect of technological innovation to test whether the level of urbanization contributes to green economic growth. By testing the existence of the panel threshold, it is found that the threshold of urbanization level fails the triple-threshold test, while the double thresholds pass the significance test with a nonlinear double-threshold relationship. Therefore, the regression model of the double thresholds is set on this basis, and the regression results are obtained as shown in Table 8.

The regression results of the double panel thresholds are shown in the above table. The results indicate that there is a significant double-threshold effect of urbanization between energy efficiency and green economic growth, showing an inverse "N-type" nonlinear effect. When Urbn ≤0.6951, energy efficiency improvement shows a significant negative effect on green economic growth. When 0.6951 < Urbn <0.8470, energy efficiency increases, making a significant contribution to green economic growth. When Urbn >0.8470, energy efficiency enhancement significantly inhibits the green economic growth in China.

In light of the actual analysis, when the level of urbanization is low, the economic growth rate and range are restricted, green technologies are developed to some extent but incompletely, energy efficiency enhancement is limited, and the high cost of putting green low-carbon technologies into use may lead to the closure or bankruptcy crisis of small- and medium-sized enterprises. As urbanization deepens, the *per capita* income of residents increases, and public awareness of environmental protection strengthens, and the consumption structure can be effectively influenced. This, in turn, drives the product structure toward high-tech and green directions, and improves the energy efficiency in line with the demand for green development. Resources are effectively allocated, pollution emissions are reduced, and production efficiency is improved, jointly promoting the green and quality growth of the national economy. However, when urbanization develops faster than necessary, urban diseases emerge. For example, energy efficiency improvement stimulates residents' energy consumption, more energy will be consumed. Population concentration also leads to lower urban operation efficiency and increases energy consumption, both of which exacerbate the pressure on resource supply and inhibit the development of green economy.

5 Robustness tests

As there may be some bias in the previous regression results, this paper further employs endogeneity tests and sample subintervals for the following robustness tests.

5.1 Endogeneity test

A key point of empirical research is to address the endogeneity issue. As for the research content of this paper, there may be reverse causality between energy efficiency and green economic growth, which could influence each other. On the other hand, there are plentiful exogenous factors affecting green economic growth, and some influencing variables are likely to have been omitted. As the systematic GMM method[4] is an important method to test the endogeneity issue, this paper constructs a two-step systematic

4 GMM (Generalized Method of Moment) is a model that explains economic phenomena based on a finite number of mathematical parameters. It uses optimal estimation techniques to fit large amounts of data to predict and analyze the patterns hidden behind them.

TABLE 9 Endogeneity test results.

Variables	Gree
L. Gree	0.8345*** (9.96)
Effi	−0.0638** (−2.22)
Cons	−0.3021 (−0.86)
N	300
AR (1)–P value	−3.48 (0.001)
AR (2)–P value	1.05 (0.292)
Hansen–P value	28.09 (0.107)
chi2	14,210.84
Number of instrumental variables	31

GMM method for endogeneity test to deal with the possible endogeneity slip in order to ensure the reliability of the empirical results. The model setup is shown as follows:

$$Gree_{it} = \alpha_0 + \alpha_1 Gree_{it-1} + \alpha_2 Effi_{it} + \alpha_3 X_{it} + u_{it} + \varepsilon_{it} \quad (5)$$

Where $Grir_{it-1}$ represents the green economy growth lagged by one order. To avoid the autocorrelation likelihood of the perturbation term ε_{it}, the Arellano-Bond test for autocorrelation is introduced. In addition, the dependent variables, namely, the second- and third-order lag terms of energy efficiency are selected as instrumental variables in this paper, and the Hansen test is introduced to identify the validity of the instrumental variables. The results of the systematic GMM model are shown in Table 9 below.

The Arellano-Bond test results in Table 9 show that AR (1) passes the 1% significance level test and AR (2) fails the significance test. It suggests that there is first-order autocorrelation in the differences of the model perturbation terms, which do not pass second-order autocorrelation, i.e., the perturbation terms are not auto-correlated, and thus estimation with the systematic GMM model is feasible. Additionally, the results of Hansen's test show that the original hypothesis cannot be rejected, indicating the validity of all instrumental variables. Therefore, all the instrumental variables selected in this paper are rational and valid.

The coefficient of L. Gree is positive and significant at the 1% level of significance, indicating that green economic growth in the previous period is highly positively correlated with that in the current period, and that green economic growth is fairly persistent over time. The coefficient of Effi is significantly negative, indicating that the energy efficiency has a dampening effect on green economic growth, a result that remains largely consistent with the regression results of the benchmark model, confirming the robustness of the conclusions in the paper.

5.2 Sample subinterval estimation

As the COVID-19 pandemic has imposed a lingering negative impact on the energy industry and green sectors, as well as on many others, this paper draws on Duan and Zhuang, (2021) practice, and chooses to exclude the sample data for 2019 and 2020, the early stage of the pandemic, to further examine the model's estimation results for the sample subintervals. The results are shown in Table 10.

TABLE 10 Model estimation results for sample subintervals.

Variables	Gree
Effi	−0.0350*** (−4.11)
Urbn	0.2443** (2.48)
FDI	0.0001*** (3.98)
Disp	−0.0003 (−0.34)
Huma	−0.1872*** (−5.79)
Envi	0.4303 (0.79)
Stru	0.0018*** (3.73)
Gove	−0.0010* (−1.86)
Tech	−0.0326*** (−5.93)
Cons	2.1550*** (6.98)
N	270
R2	0.7341

The estimation results of the sample subintervals in Table 10 show that the energy efficiency continues to exert a significant negative effect on China's green economic growth, and the remaining control variables stay largely consistent, indicating the validity of the theoretical hypotheses in this paper and further confirming the robustness of the benchmark regression results.

6 Conclusion and policy implications

This paper, by constructing an analysis of the impact mechanism of energy efficiency improvement on green economic growth, has explained the linear as well as nonlinear effects between them, and studied the impact of energy efficiency improvement on green economic growth from different perspectives such as technological innovation, industrial structure and urbanization level, before empirically verifying the relevant theories based on provincial-level regional panel data in China. Three major findings are reached. 1) On the whole, energy efficiency improvement is currently inhibiting the growth of its green economy. However, as the energy efficiency level increases, the inhibitory effect gradually weakens, showing a non-linear trajectory of "inhibition—weakening inhibition". 2) In the short term, China is still in the expansion stage of energy consumption, and the development of its green economy is thus limited to a certain extent. 3) The expansion of the nation's industrial sectors will intensify resource consumption and pollutant emissions, while technological innovation and urbanization levels can ease the current strenuous status of energy rebound.

Based on the aforementioned research findings, this paper presents the following policy implications. Firstly, with regard to the government, there is a need to intensify efforts towards energy structure reform while concurrently promoting energy efficiency. Given the presence of the energy rebound effect, it is crucial to adjust

the energy consumption structure based on the specific attributes of various energy sources and the distinct characteristics exhibited by different regions. In alignment with such adjustments, it becomes essential to optimize emission reduction strategies. Furthermore, there exists an opportunity to pursue the enhancement of efficiency by utilizing non-renewable conventional energy sources, including coal, charcoal, and oil. Simultaneously, endeavors to broaden the scope and utilization of cleaner energy sources, such as hydropower and solar energy, should be undertaken. With a combination of measures such as energy pricing, taxation, and subsidies, certain regions can employ administrative and market mechanisms to alleviate their reliance on traditional energy consumption patterns.

Secondly, in order to foster a greater inclination among R&D institutions and personnel to enhance their investments in eco-friendly innovation technologies, it is imperative for research organizations to augment their financial commitments towards green technologies. At the same time, they should introduce novel technological advancements and innovative management approaches while effectuating institutional reforms. Concurrently, it is imperative to prioritize the cultivation of relevant technical expertise and foster the intra-regional mobility of proficient practitioners, thus resulting in a synergistic confluence of industry, academia, and research. This shall afford a heightened fluidity to the process of industrializing green innovation technology. Additionally, magnifying collaborations with green innovation enterprises shall effectively mitigate the barriers constraining enterprises' endeavors in embracing eco-friendly transformations.

Thirdly, for the electricity industry, it is crucial to prioritize the feedback effect of industrial and technological structure, thereby avoiding the energy-saving trap caused by an excessive concentration of production factors in high energy-consuming sectors. By employing market mechanisms to eliminate outdated capacity and reorganize surplus productivity in high energy-consuming sectors, we can guide advanced technologies and supportive policies towards low energy-consuming sectors, thus reducing the counteractive rebound effect of energy consumption. Furthermore, enhancing the deep integration of the manufacturing industry and the modern service sector can effectively reduce resource waste and energy consumption, thereby offering greater development opportunities for environmentally friendly industries like renewable energy.

Lastly, it is imperative to maintain an appropriate level of urbanization. High-quality urban development should be firmly grounded in reality, avoiding the pitfalls of urbanization that are detached from industrial and agricultural foundations or overly inflated by the tertiary sector. By intensifying the efficient use of resources through urban economics, it is possible to facilitate the optimization of industrial structures, as well as the concentration of human and financial capital. This not only enhances energy efficiency but also augments the potential for regional green growth. Strengthening the provision of public services in cities can mitigate social inequities that may otherwise obstruct the process of sustainable growth.

Data availability statement

Publicly available datasets were analyzed in this study. This data can be found here: EPS database, Wind database and the Chinese City Statistical Yearbook.

Author contributions

LW: Conceptualization; Investigation; Project administration; Formal analysis; Resources; Supervision; Methodology; Writing–original draft; Writing–review and editing. CZ: Conceptualization; Investigation; Data curation; Methodology; Software; Formal analysis; Writing–original draft; Writing–review and editing. MC: Supervision; Methodology; Formal analysis; Writing–review and editing. WD: Supervision; Methodology; Formal analysis; Writing–review and editing. GW: Supervision; Formal analysis; Writing–original draft; Writing–review and editing. All authors contributed to the article and approved the submitted version.

Funding

This work was supported by a grant of the general program from Hubei Research Center for Eco-Civilization (grant numbers STZK 2023Y05) and the soft science research base of regional innovation capability monitoring and analysis in Hubei Province (grant numbers HBQY 2023z02).

Acknowledgments

This paper benefited from years of thinking about these issues and the discussion with many colleagues related to energy economics at that time.

Conflict of interest

The authors declare that the research was conducted in the absence of any commercial or financial relationships that could be construed as a potential conflict of interest.

Publisher's note

References

Chen, Q. Y., Lin, S. T., and Zhang, X. (2020). The effect of China's incentive policies for technological innovation: incentivizing quantity or quality. *China Ind. Econ.* 385 (4), 79–96. doi:10.19581/j.cnki.ciejournal.2020.04.004

Duan, D. Z., and Du, D. B. (2022). Spatial and temporal distribution characteristics and influencing factors of green technology innovation in Chinese cities. *Acta Geogr. Sin.* 77 (12), 3125–3145. doi:10.11821/dlxb202212012

Duan, J. S., and Zhuang, X. D. (2021). Financial investment behavior and enterprise technological innovation—Motivation analysis and empirical evidence. *China Ind. Econ.* 394 (01), 155–173. doi:10.19581/j.cnki.ciejournal.2021.01.009

Geng, J., and Huang, P. P. (2022). Measurement and spatial variability analysis of provincial green economy development in China. *Invest. Entrepreneursh.* 33 (21), 33–36.

Gu, S. T. (2022). A study on the measurement and spatial and temporal evolution of green economy development in China: A TOPSIS evaluation model based on mahalanobis distance. *China Price* 402 (10), 3–7.

Han, Y., Zhai, J. L., and Shi, J. H. (2017). "Research on provincial energy rebound effect in China," in Proceedings of the 2017 2nd International Conference on Civil, Transportation and Environmental Engineering (ICCTE 2017) (Atlantis Press).

Han, Z. Y., Wei, Y. M., Jiao, J. L., et al. (2004). On the co-integration and causality between Chinese GDP and energy consumption. *Syst. Eng.* 22 (12), 17–21.

Hansen, B. E. (1999). Threshold effects in non-dynamic panels: estimation, testing, and inference. *J. Econ.* 93 (02), 345–368. doi:10.1016/S0304-4076(99)00025-1

Hu, A. J., Guo, A. J., Zhong, F. L., et al. (2018). Can the high-tech industrial agglomeration improve the green economic efficiency of the region? China population. *Resour. Environ.* 28 (09), 93–101. doi:10.12062/cpre.20180404

Hu, D. L., Shen, H., and Liu, Z. (2019). Study on the spatial-temporal evolution and formation mechanism of energy rebound effect in Chinese cities. *China Soft Sci.* 347 (11), 96–108.

Huang, Y. H., Cu, J. B., and Lin, S. (2023). Green technology innovation under China's new development concept: the effects of policy-push and demand-pull on renewable energy innovation. *Soc. Sci. China* 44 (1), 158–180. doi:10.1080/02529203.2023.2192093

Ji, Z. (2020). Does factor market distortion affect industrial pollution intensity? Evidence from China. *J. Clean. Produc-tion* 267, 122136. doi:10.1016/j.jclepro.2020.122136

Jia, R. N., Shao, S., Du, K. R., et al. (2022). Spatial-temporal pattern, dynamic evolution, and driving factors of carbon rebound effect in China:based on improved stochastic frontier model of carbon emission. *China Soft Sci.* 384 (12), 23–34.

Li, X. L. (2019). Regional green growth: measurement, decomposition and driving factor. *J. Hebei Univ. Econ. Bus.* 40 (5), 24–34. doi:10.14178/j.cnki.issn1007-2101.2019.05.004

Li, X. Y. (2021). Study on the impact of energy rebound effect on carbon emission reduction at different stages of urbanization in China. *Ecol. Indic.* 120 (7), 106983. doi:10.1016/j.ecolind.2020.106983

Li, X. Y., Zhang, D. Y., and Zhang, T. (2021). Awareness, energy consumption and pro-environmental choices of Chinese households. *J. Clean. Prod.* 279 (5), 123734. doi:10.1016/j.jclepro.2020.123734

Lin, B. Q., and Zhou, Y. C. (2022). Does energy efficiency make sense in China? Based on the perspective of economic growth quality. *Sci. Total Environ.* 804, 149895. doi:10.1016/j.scitotenv.2021.149895

Liu, F. Z., and Sun, Y. T. (2008). Effect of innovation' industrial change on energy consumption. *China Popul. Resour.*

Liu, M. L., Huang, X., and Sun, J. (2022). Impact of digital finance on China's green development and its mechanism. *China Popul. Resour. Environ.* 32 (06), 113–122. doi:10.12062/cpre20220426

Shan, Y. (2018). "The impact of technological innovation on China's economic level," in Proceedings of the 2018 International Symposium on Humanities and Social Sciences, Management and Education Engineering (HSSMEE 2018) (Atlantis Press).

Shobande, O. A., Ogbeifun, L., and Tiwari, A. K. (2023). Re-Evaluating the impacts of green innovations and renewable energy on carbon neutrality: does social inclusiveness really matters? *J. Environ. Manag.* 336, 117670. doi:10.1016/j.jenvman.2023.117670

Tao, C. Q., and Zhou, X. (2015). Effect analysis of industrial structure optimization and upgrading—Empirical research on coupling of information industry and manufacturing. *Industrial Econ. Res.* 76 (03), 21–31+110. doi:10.13269/j.cnki.ier.2015.03.003

Wan, Y. Y. (2022). Green economic development, clean energy consumption and carbon dioxide emissions. *Ecol. Econ.* 38 (05), 40–46.

Wang, B., and Liu, G. T. (2015). Energy conservation and emission reduction and China's green economic growth—Based on a total factor productivity perspective. *China Ind. Econ.* 326 (5), 57–69. doi:10.19581/j.cnki.ciejournal.2015.05.006

Wang, L., Xiao, Q., and Deng, F. F. (2023). The impact of artificial intelligence on innovation in Chinese manufacturing: evidence from the adoption of robots. *Collect. Essays Finance Econ.*, 1–14. doi:10.13762/j.cnki.cjlc.20230227.001

Wang, Q. Y., and Lu, F. Z. (2021). Economic effects of high-speed rail: emission reduction and efficiency enhancement. *Stat. Res.* 38 (2), 29–44. doi:10.19343/j.cnki.11-1302/c.2021.02.003

Wang, S., Zhou, S. Y., Xie, X. Y., Zhao, L., Fu, Y., Cai, G. Z., et al. (2020). Comparison of the acute toxicity, analgesic and anti-inflammatory activities and chemical composition changes in Rhizoma anemones Raddeanae caused by vinegar processing. *Soft Sci.* 34 (10), 7–11+24. doi:10.1186/s12906-019-2785-0

Wang, Y. B., and Li, A. H. (2021). Research on the dynamic relationship between clean energy and green economic growth in hubei province-based on VAR model. *Spec. Zone Econ.* 390 (07), 71–76.

WangYuLiu, J. Y. S. A. T. S. (2021). A theoretical analysis of the direct rebound effect caused by energy efficiency improvement of private consumers. *Econ. Analysis Policy* 69, 171–181. doi:10.1016/j.eap.2020.12.002

Wei, C., and Li, C. Z. (2017). Resource misallocation in Chinese manufacturing enterprises: evidence from firm-level data. *J. Clean. Prod.* 142, 837–845. doi:10.1016/j.jclepro.2016.04.083

Wu, X. L., Wang, D., and Chao, J. F. (2022). Energy use efficiency, economic growth and ecological environmental quality: based on the DSGE model containing carbon emissions. *J. Tech. Econ. Manag.* 315 (10), 28–33.

Wu, Z. H. (2020). Urbanization, human capital agglomeration and industrial structure adjustment. *Reform Econ. Syst.* (1), 59–65.

Xu, G. Q., Zhang, W. D., and Chen, X. Y. (2022). Estimation of macro energy rebound effects considering technological progress and structural change. *Econ. Theory Bus. Manag.* 42 (11), 26–41.

Yang, D. Y., Zhang, H., Miao, C. H., et al. (2023). Study on eco-efficiency and the driving effects of industrial structure transformation in the Yellow River basin. *J. Henan Normal Univ. Nat. Sci. Ed.* 51 (01), 1–11+171. doi:10.16366/j.cnki.1000-2367.2023.01.001

Yang, Q., Zhao, Y., Zhang, R. G., et al. (2022). Government innovation preference, industrial structure optimization and green economy development level. *Statistics Decis.* 38 (19), 169–173. doi:10.13546/j.cnki.tjyjc.2022.19.034

Ye, B. J., and Wen, Z. L. (2013). A discussion on testing methods for mediated moderation models: discrimination and integration. *Acta Psychol. Sin.* 45 (9), 1050–1060. doi:10.3724/SP.J.1041.2013.01050

Yuan, Y. J., and Xie, R. H. (2014). Research on effect of the environmental regulations to industrial restructuring-empirical test based on provincial panel data of China. *China Ind. Econ.* 317 (08), 57–69. doi:10.19581/j.cnki.ciejournal.2014.08.005

Zhang, D. M., and Bai, X. Y. (2016). Technology gap, technology introduction and green economic growth of Chinese industry. *Soc. Sci. Guangxi* 247 (1), 71–76. doi:10.3969/j.issn.1004-6917.2016.01.014

Zhang, J., and Guo, L. F. (2023). Study on the impact of digital economy on regional total factor energy efficiency. *Coal Econ. Res.* 43 (3), 4–12. doi:10.13202/j.cnki.cer.2023.03.015

Zhang, J., Wu, G. Y., and Zhang, J. P. (2004). The estimation of China's provincial capital stock:1952—2000. *Econ. Res. J.* 10 (10), 35–44. http://CNKI:SUN:JJYJ.0.2004-10-004

Zhang, J. Q., and Cheng, Q. (2020). The research on the impact of industrial structure upgrading on energy efficiency in the yangtze river economic Belt. *J. Industrial Technol. Econ.* 39 (1), 129–135. doi:10.3969/j.issn.1004-910X.2020.01.015

Zhang, J. S., and Zhang, X. K. (2014). Technological progress, energy efficiency and rebound effect-empirical estimation based on China's provincial panel data. *J. Shanxi Univ. Finance Econ.* 36 (11), 50–59. doi:10.13781/j.cnki.1007-9556.2014.11.003

Zheng, C., Zhang, Y. F., and Long, L. J. (2021). When MARCH family proteins meet viral infections. *Coal Geol. China* 33 (S1), 49–51. doi:10.1186/s12985-021-01520-4

frontiers | Frontiers in Energy Research

TYPE Original Research
PUBLISHED 08 January 2024
DOI 10.3389/fenrg.2023.1283818

OPEN ACCESS

EDITED BY
Sunday Olayinka Oyedepo,
Covenant University, Nigeria

REVIEWED BY
Agnimitra Biswas,
National Institute of Technology, Silchar, India
Anthony Onokwai,
Bells University of Technology, Nigeria

*CORRESPONDENCE
M. Rafiuddin Ahmed,
ahmed_r@usp.ac.fj

RECEIVED 27 August 2023
ACCEPTED 18 December 2023
PUBLISHED 08 January 2024

CITATION
Prasad R and Ahmed MR (2024), Experimental evaluation of the performance and power output enhancement of a divergent solar chimney power plant by increasing the chimney height.
Front. Energy Res. 11:1283818.
doi: 10.3389/fenrg.2023.1283818

Experimental evaluation of the performance and power output enhancement of a divergent solar chimney power plant by increasing the chimney height

Reemal Prasad and M. Rafiuddin Ahmed*

Division of Mechanical Engineering, The University of the South Pacific, Suva, Fiji

Solar energy is an attractive renewable energy option for countries located in the tropical region. Harvesting this energy using simple yet innovative technologies such as solar chimney power plants (SCPP) will help the developing countries in meeting their sustainable development goals. In an SCPP, air is heated under a greenhouse collector and the hot air is passed to a chimney, where it drives a turbine while rising up. Research efforts have been directed in the past at improving the performance and power output of an SCPP by varying its geometric parameters. The chimney height of a previously optimized solar chimney power plant, having a divergent chimney, was increased from 4 to 6 m and then to 8 m in this first experimental work of this kind. The temperature variations inside the collector, along the chimney height, the velocity at the turbine section, the power available and the output power of an air turbine, estimated by applying mechanical load, are compared for the three chimney heights. The temperature rise of the air inside the collector was the highest for the 4 m tall SCPP and reduced as the chimney height was increased to 6 and 8 m due to the lower time of stay of air in the collector for greater chimney heights. Along the height of the divergent chimney, the temperature dropped with the maximum drop occurring for the 8 m tall SCPP indicating a lower enthalpy loss at the chimney exit. The air velocity at the turbine section was found to increase with chimney height for given solar insolation/time of the day due to the higher driving force which is the buoyancy effect produced by the hot air. The maximum turbine output power for the 8 m tall SCPP increased by 252% compared to the 4 m tall SCPP indicating that significant improvement in the power output can be achieved by increasing the height of a divergent chimney SCPP. An average power of about 40 kW will be available for a chimney height of 100 m which will be extremely beneficial for the sustainable development of small islands.

KEYWORDS

solar chimney power plant, solar collector, experimental testing, air turbine, power output

1 Introduction

The Pacific Islanders have a strong relationship with their ocean and their land. Any changes in climate directly impact their livelihood, culture, and customs (Hennessy et al., 2011). Climate change is caused mainly by burning fossil fuels such as oil and coal which release harmful gases to the environment. The impact of climate change on the environment includes cyclones, droughts, rising sea levels, extreme heat waves, bushfires, ocean acidification, and many more (Casule, 2020). An example of these impacts is the cyclone Winston that affected Fiji in 2016. Cyclone Winston was one of the strongest cyclones in the recorded history of the southern hemisphere which caused $470 million worth of damage to Fiji (Casule, 2020). To mitigate such issues, the energy sector over the last decade has been focusing on moving to renewable sources of energy including wind, solar, hydro, geothermal, biomass, etc. The consumption of renewable energy is now showing an increasing trend compared to all other sources with solar energy being one of the largest contributors in 2020 (Looney, 2021).

About 174 PW worth of solar energy falls onto the earth's atmosphere which is 10,000 times the total energy consumed by humans on earth (Rhodes, 2010). Solar energy, being the largest source of energy available, can be directly used for processes like cooking, water and space heating, and agricultural dryers or it can be converted to electrical energy using a system such as a photovoltaic cell (Al Qubeissi and El-Kharouf, 2020).

One of the popular technologies for harvesting solar energy is a solar chimney power plant (SCPP). An SCPP is a very innovative yet simple technology comprising of three key components: the collector, the chimney and a power conversion unit which consists of the turbine-generator unit (Cao et al., 2018). The radiation from the Sun penetrates the collector cover which is transparent and heats up the air and the ground under the collector. Due to the greenhouse effect, the air in the collector becomes warmer, while the ambient temperature at the exit of the chimney is significantly lower. This temperature difference between the collector and the chimney exit causes the air in the collector to rise upwards in the chimney. This rising airflow is used to drive a turbine-generator unit which is usually located near the base of the chimney. Air moving out of the collector is replaced by the ambient air from the outside due to natural convection. This cycle continues as long as a sufficient temperature difference exists between the collector and the chimney exit. The SCPP does not require any fuel or cooling water and has a very simple operating principle; it does not require sophisticated and expensive materials for construction or maintenance, can be constructed in any geographic location if good amount of solar radiation is available and has a long operating life (Ming, 2016). Another major advantage of SCPPs is that they can be constructed on a smaller land area compared to PV panels; this is a very important factor in countries where land is not easily available. It can help in the sustainable development of Pacific Island countries and meet their sustainable development goals especially SDG 7. Regardless of its low efficiency, the advantages it offers has motivated several investigators to carry out further research on the SCPP.

2 Background

The first ever prototype of a solar chimney power plant (SCPP) was proposed and fabricated by Schlaich and his colleagues in 1981 in Manzanares, Spain (Haaf et al., 1983; Haaf, 1984) with a height of 194.6 m, a radius of 5.08 m and a collector radius of 133 m. The characteristics of this SCPP and the technical issues are reported by Schlaich et al. (2005). The viability of SCPPs for rural areas was investigated by Padki et al. (1989). To investigate the theoretical and experimental performance characteristics of SCPPs, Pasumarthi and Sherif. (1998a) proposed a mathematical model and studied the effect of different geometric parameters on the temperature, velocity and power output of the plant. In a subsequent work, Pasumarthi and Sherif. (1998b) made further modifications to their plant and reported better performance. The collector radius and chimney height of their demonstration model were 9.15 and 7.92 m respectively. A model to evaluate the performance of SCPPs was developed by Ming et al. (2006). In a subsequent work, Ming et al. (2008) studied the heat storage characteristics of an energy storage layer under different solar insolations.

Esmail et al. (2021) identified the need for design theories for the SCPP turbine because existing design theories being utilized were initially formulated for gas and steam turbines. Operating gas and steam turbines under the operating conditions of an SCPP adversely affected the overall performance of an SCPP. Kasaeian et al. (2017) carried out CFD simulation to understand the effect of the number of turbine blades, rotational speed of the turbine, chimney height and collector diameter on the performance of the SCPP. A three-bladed turbine was reported to show the highest mass flow rate, whereas a five-blade turbine produced the maximum power. The study also reported that increasing the collector diameter while keeping the turbine rotational speed fixed, directly increased the air velocity, turbine torque and the output power. An axisymmetric mathematical model using the continuity equation, Navier-Stokes equations and the energy equation was developed by Xu et al. (2011). After validating their results, they presented results of static pressure, velocity, and temperature distributions for two turbine pressure drops. The effect of solar radiation was also studied in their work.

Experimental work under controlled conditions at three heat fluxes was carried out by Li and Liu (2014) with the use of a phase change material for energy storage and release. A CFD analysis of an SCPP of 10 m height with a divergent chimney was carried out by Patel et al. (2014), in which the effects of collector inlet opening, outlet height, outlet diameter, the chimney divergence angle, chimney inlet opening, and chimney diameter were studied in detail. Optimum values of these parameters were obtained and a chimney divergence angle of 2° (each side) was found to give the best performance. Ahmed and Patel (2017) reported results from further detailed experiments on a 4 m tall SCPP that was designed based on the findings of the previous optimization work carried out using CFD, including the temperature variations in the collector and the chimney, and the velocity of air at the turbine section at different solar insolations and at different times of the day. Similar to the findings of Patel et al. (2014), Motoyama et al. (2014) found that a diffuser tower gives higher velocity in the chimney from their experimental work on a 4 m high SCPP. An indoor SCPP was

built by Guo et al. (2016) which was used to study the air temperature and velocity for different solar insolations and heights of the chimney. For a constant solar insolation, they reported an increasing air velocity in the chimney with a trend matching their theoretical results of velocity being proportional to 1/3 power of chimney height; however, the rate of increase of air velocity reduced with increasing chimney height. This was attributed to the heat losses through the chimney walls as well as the flow losses. Based on their findings, they suggested that there has to be an upper limit for the chimney height above which the air velocity does not increase much.

Singh et al. (2021) proposed the novel concept of a bell-mouth shaped collector inlet in a converging-diverging SCPP. They reported that an efficient bell-mouth shaped collector inlet can improve the air velocity by up to 270%. The improvement in air velocity was because of high or uniform static pressure recovery in the chimney which does not occur in a conventional system. Faisal et al. (2023) used ANSYS Fluent software to minimize flow losses by modifying the chimney inlet. The connection at the collector outlet and the chimney inlet was modified by rounding it rather than having a sharp bend. The available power improved by 55% when the ratio between the curvature radius and the chimney diameter was 0.45.

Habibollahzade et al. (2021) proposed a modified theoretical model which could be used to realistically simulate solar chimneys incorporating wind turbine power curves. It was concluded by these researchers that increasing the chimney height and collector radius to very high values can adversely affect the system performance. The multi-objective grey wolf optimization technique employed by them provided a range of most suitable design parameters for the locations studied. Patil et al. (2023) developed a machine learning model which could be used to vary dimensional parameters of the SCPP and understand their effect on the power output. They reported that increasing the chimney height and collector radius enhances the power production of an SCPP. Azad et al. (2021) also used multi-objective optimization to obtain the best design parameters by changing the geometric parameters such as collector diameter, collector height, chimney diameter, chimney height and the chimney wall curvature to achieve balance between power and water production for an SCPP combined with a water desalination plant. Considering the design parameters, chimney height and the collector diameter were identified as the most influential parameters. Cottam et al. (2019) developed a thermo-fluid based numerical model first presented by Cottam et al. (2016) to optimize the performance of solar chimney power plants by dimension matching. Optimum pressure drop in the system was found to be dependent on the collector and chimney radius only. Power output was seen to linearly increase before reaching a maximum by varying the collector and chimney radius. However, increasing the chimney height increased the power output quadratically. A simple cost model coupled with the thermodynamic model indicated that multiple plants with an optimum collector radius would be better compared to a single large power plant. Larger solar chimney power plants can be economical until the cost of the chimney increases more than quadratically with height.

Nia and Ghazikhani (2023) carried out experimental and numerical studies on an SCPP which had a chimney height of 4 m and a collector diameter of 5 m. Various parameters such as the collector height, collector radius and the chimney height were varied to optimize the power output of the SCPP. Maximum available power of 1.74 W was reported for the SCPP with the optimized parameters. Mandal et al. (2021) carried out a numerical study by varying the height of the collector inlet. They reported that reducing the collector inlet height from 10 cm to 5 cm increases the velocity of the air at the chimney inlet from 1.5 m/s to around 5.5 m/s which significantly improves the power generation of the SCPP. Cuce et al. (2020) analyzed the effect of chimney height on the various performance parameters of an SCPP using 3D axisymmetric CFD modelling. The mass flow rate of the air increased when the chimney height was increased. Similar to the findings of Guo et al. (2016), they concluded that there should be an optimum chimney height. Another important parameter studied was the temperature rise in the collector. It was found that increasing the chimney height reduced the air temperature in the collector. When the chimney height was increased 5 times, the temperature in the collector dropped by about 3°. Najm and Shaaban (2018) conducted numerical simulation and optimization of the SCPP performance with different geometric and operating conditions. The solar chimney height was increased keeping the solar insolation and the optimum collector radius fixed. Increasing the chimney height increased the turbine power. Shirvan et al. (2017) carried out 2D axisymmetric numerical simulation and sensitivity analysis on a prototype SCPP in Zanjan, Iran to determine the potential maximum power output. They concluded that the maximum power output reduces when the entrance gap of the collector is increased and increases when the chimney height and diameter are increased. Kebabsa et al. (2020) carried out a numerical investigation using 2D axisymmetric chimney model to investigate the effect of collector inlet geometry. Weli et al. (2021) studied the effect of ground slope, collector tilt angle and the collector inlet height using CFD simulations. They studied the above parameters against the temperature of the air at the chimney inlet, air velocity and pressure variations. They reported an optimum ground slope of 35° which enables the collector span to be reduced by 18% and chimney height by 36% having the same system volume as the flat ground collector.

In other studies, Mandal et al. (2023) used ANSYS Fluent to carry out a 3D study to understand the effect of modifying the absorber surface. Biswas et al. (2023) also used ANSYS Fluent to carry out 3D study by modifying the absorber surface. Guo et al. (2019) carried out a detailed review by focusing on the current understanding of the SCPPs in terms of the optimal arrangement of geometric parameters, effect of climate conditions, role of radiation heat transfer, maximizing power production, scaling of laboratory results to commercial plants, lack of large-scale power plants and current innovations in this area. Guo et al. (2017) carried out an economic analysis considering parameters such as the cost advantage of materials in China, low loan rates and low maintenance and operating cost. They reported that the levelized cost of electricity (LCOE) for a 10 MW SCPP in Yinchuan, China was 0.4174 Yuan/kWh. The LCOE is reported to be comparable with wind power and solar PV in China.

A 6 m tall SCPP was designed, fabricated and experimented upon by Balijepalli et al. (2020). They reported the absorber plate temperature, collector cover surface temperature and air temperature from 6.00 a.m. to 6.00 p.m. They reported a

FIGURE 1
A photograph of the 8 m tall SCPP (inset: a photograph of the 4 m tall SCPP).

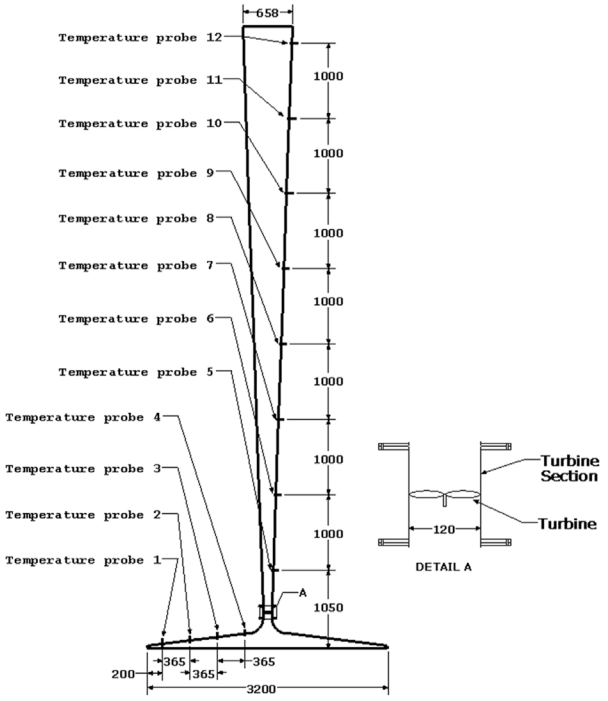

FIGURE 2
Locations of the temperature sensors and turbine on the 8 m tall SCPP.

maximum air velocity of 4.7 m/s and 5.5 m/s before and after the turbine, respectively (the velocity before the turbine was measured in the collector). The theoretical power output of the SCPP was reported to be 1.37 W whereas the actual power output was reported to be 0.82 W. Bansod (2020) varied the chimney height from 0.5 to 2.0 m in an experimental SCPP with a collector diameter of 1.8 m and a constant chimney diameter of 38 mm. It was reported that the maximum air velocity increases from 0.953 to 1.645 m/s when the chimney height is increased from 0.5 to 1.5 m and then reduces slightly to 1.641 m/s when the height is further increased to 2.0 m. Ghalamchi et al. (2016) from their research concluded that, of the three chimney heights of 2, 3, and 4 m, the height of 3 m is optimum and gives the maximum air velocity in the chimney. It should, however, be noted that in some of these works, temperature inversion effect was observed. An experimental SCPP with a chimney height of 6 m and a collector diameter of 2.5 m was built and tested for performance by Mandal et al. (2022). For a maximum solar radiation of 750 W/m^2, they reported a maximum velocity of 1.5 m/s. They performed a computational study and found that the air velocity increases to 2.7 m/s if the chimney height is increased to 8 m for the same collector diameter for a solar insolation of 600 W/m^2. Das and Chandramohan (2019a) reported from their computational work that as the height of the constant diameter chimney is increased from 3 to 8 m, the air velocity increased up to 44%.

It can be seen that while some researchers, e.g., Cottam et al. (2019) and Pradhan et al. (2021) concluded that the dimensions of the main components of an SCPP should be matched well for optimum performance, other researchers such as Sivaram et al. (2018), Bansod (2020), Belkhode et al. (2020) and Mandal et al. (2022) concluded that the chimney height has a direct effect on the pressure difference and that the exit air velocity increases with chimney height. They argued that an SCPP with a smaller collector area and a greater chimney height could produce higher velocity and better efficiency compared to an SCPP with higher collector area. Some other researchers concluded that there will be an optimum chimney height above which the air velocity does not increase (Kasaeian et al., 2014; Ghalamchi et al., 2016). However, these works were carried out on constant diameter chimneys. In view of the above, the present work is intended to study the effect of chimney height on the performance characteristics of an SCPP having a divergent chimney by keeping the collector area constant.

In the present work, the effect of chimney height on the performance enhancement of an SCPP having a divergent chimney is experimentally investigated. A 4 m tall SCPP was initially fabricated and tested for performance by Ahmed and Patel (2017); two sections of 2 m each were then added to this SCPP one after the other to obtain total chimney heights of 6 m and 8 m and experiments were carried out under different conditions to investigate the effect of chimney height on the performance of the plant. No such experimental work on the effect of chimney height of a divergent chimney on the performance of an SCPP has been reported till now. The results of temperature distributions across the collector and along the chimney height, the air velocity at the turbine section, the available power and the turbine power recorded and estimated hourly at different solar insolations throughout a day are presented. As the experiments were performed up to solar insolations of 1,000 W/m^2, the present work is expected to enhance the existing state of knowledge and understanding of the effect of chimney height on the SCPP performance. Moreover, the turbine power was directly measured by loading the air turbine mechanically at different solar insolations for the three chimney

heights. Direct power measurements of an SCPP have not been reported in the literature so far.

3 Experimental setup

An existing solar chimney power plant initially constructed for experimentation with a total height of 4 m (Ahmed and Patel, 2017) was refurbished and used for the present experimental work. Figure 1 shows the newer, completed 8 m tall SCPP while a photograph of the 4 m tall SCPP is shown in the inset. The collector diameter was 3.2 m. Further details on the dimensions of the SCPP are available in the work reported by Ahmed and Patel (2017).

The footing of the SCPP consisted of a 1,000 mm deep foundation to hold the solar chimney structure in place. The absorber around the foundation was created by pouring concrete and making a flat surface of 50 mm thickness. The area of the absorber was slightly larger than the diameter of the collector cover. The concrete was painted with black paint to improve the absorption capacity. A chimney bell-mouth was constructed to connect the solar collector to the solar chimney. The chimney bell-mouth acts as a nozzle accelerating the flow towards the turbine section, hence the inner surface was smoothened using Bondo body filler. The bell-mouth housing was 200 mm in height and 700 mm in diameter.

The construction details and a schematic of the 4 m tall SCPP used for experimentation earlier are reported in detail in ref. (Ahmed and Patel, 2017). For the present work, the SCPP height was firstly increased to 6 m and then finally another detachable 2 m unit was constructed to increase the SCPP height to 8 m above the ground. The detailed dimensions are shown in Figure 2. The ratio of chimney height to the collector diameter in the present experimental work ranged from 1.25 to 2.5 which is well within the acceptable range of 0.8–5.0 (Pasumarthi and Sherif, 1998a; Zhou et al., 2007a).

A turbine housing unit was constructed and installed in between the solar chimney and the bell housing. An axial flow turbine was placed in the turbine section of the chimney. An inspection glass was provided on the housing to allow for shaft rotational speed and power measurement.

The 4 m tall SCPP was initially tested in 2016 (Ahmed and Patel, 2017) for temperature and velocity variations whereas the 6 m and 8 m tall SCPPs were tested in 2022. The turbine installation and the associated measurements were carried out in 2022 as well.

PT-100 K type temperature sensors were placed across the radius of the collector and along the height of the chimney. The temperature sensors have a measurement range, resolution and accuracy of 0°C–700°C, 0.1°C, and ±0.5%, respectively. The locations of the temperature sensors are shown in Figure 2.

The temperature readings were logged onto a 16 port CR-1000 series data-logger with an accuracy of ±0.06% of the reading for the temperature range of 0°C–40°C, ±0.12% of the reading for the temperature range of -25°C–50°C and ±0.18% of the reading for the temperature range of -55°C–85°C. The data-logger has an external keyboard for taking instantaneous measurements. The data-logger requires a 12 V DC battery and suspends measurements when the voltage drops below 9.6 V. The temperature measurements were recorded onto the in-built 4 MB memory card of the data-logger from which a dongle was used to retrieve the data.

A pitot-static tube was fitted at the turbine location to measure the air velocity. The pitot-static tube was aligned perfectly parallel to the airflow to ensure that accurate velocity measurements were recorded. A Furness Controls (model FCO510) digital micromanometer was connected to the pitot-static tube to measure the dynamic pressure readings. The micromanometer has a range of −2,000 to + 2,000 mm of water and an accuracy of ±0.25%. The maximum error in the estimation of velocity was found to be 4.9% (Ahmed and Patel, 2017).

A Licor LI200S Pyranometer was used to measure the solar insolation. The absolute maximum error in the measurements of solar insolation was ±5% with a typical error of ±3%.

A photo-tachometer (model: DT-2234B) was used to measure the turbine rpm. The tachometer has a range of 0–99,999 rpm. The tachometer has a resolution of 0.1 rpm for measurements less than 1,000 rpm and a resolution of 1 rpm for measurements above 1,000 rpm. The accuracy of the Tachometer is ±0.05%.

The torque of the turbine was measured using a mass and string system along with a spring balance as shown in Figure 3. The string's one end was loaded with a mass via a pulley and the other end was attached to a spring balance. For all the experiments, the spring balance did not show any deflection, but it was kept in place throughout the torque measurements to ensure that the shaft of the turbine did not bend. The mass on the other side was gradually varied and the rpm was noted. The torque was obtained by multiplying the net force with the radius. The torque was multiplied with the angular velocity to get the power output of the turbine. The maximum error in the estimation of power output was estimated to be 2.7% following the procedure described by Moffat (1988).

Figure 4 shows a photograph of the turbine housing and the turbine inside the housing (A) along with the instrumentation and the box containing the data acquisition system (B). The constant diameter turbine section between the two flanges can be seen in the figure.

4 Results and discussion

To compare the present results with the previously reported results by Ahmed and Patel (2017), solar insolations and ambient temperatures over three typical days in February 2016 and February 2022 were measured. The solar insolations and ambient temperatures showed similar trends for 2016 and 2022. The solar insolation peaked at 1.00 p.m. with values of about 1000 W/m^2 for both the years. The maximum deviation in the solar insolation trends was seen at 10.00 a.m. where the solar insolation for 2022 was 133 W/m^2 higher than that of the year 2016. The ambient air temperature for both the years peaked at 3.00 p.m. even though the peak solar insolations were measured at 1.00 p.m. The ambient air temperatures for 2022 throughout the day, however, were slightly higher than that of 2016 with the greatest difference of 0.8°C recorded at 2.00 p.m. (31.94°C in 2022 and 31.13°C in 2016). A similar trend of ambient temperature peaking at 3.00 p.m. while the solar insolation peaking at 1.00 p.m. was reported by Mekhail et al. (2017).

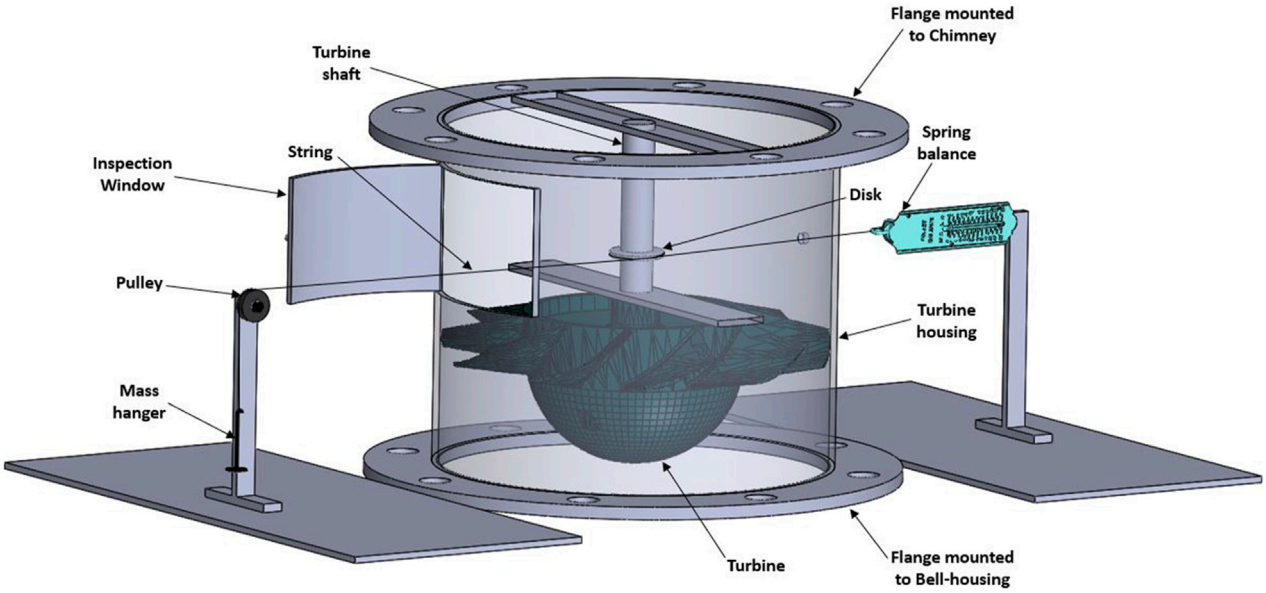

FIGURE 3
Torque measurement setup.

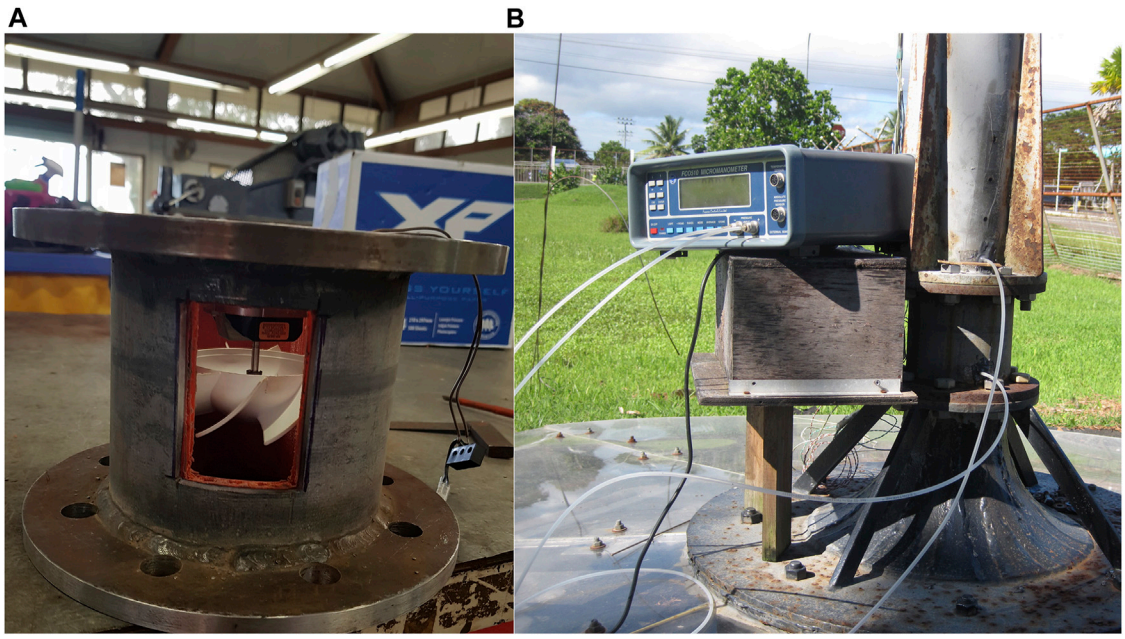

FIGURE 4
A photograph of the turbine placed inside the turbine housing **(A)** and set-up for measurements in the turbine section **(B)**.

They attributed it to the time it takes for the heat to be absorbed by the ground and then transferring it to the air.

Variation of ground temperature at different solar insolations was also compared for the years 2016 and 2022. The maximum ground temperature for 2016 was recorded to be 68.75°C whereas the maximum ground temperature for 2022 was recorded to be 72.26°C. The variation of ground temperature with solar insolation was seen to be linear for both the years. A best fit straight line was drawn by Ahmed and Patel (2017) for the variation of ground temperature with solar insolation for 2016 and its equation was reported. The results presented in this work are based on the measurements performed in the months of January to April, during which the ambient temperatures varied between 27°C and 33°C. As Fiji is a tropical country, there are very little variations in

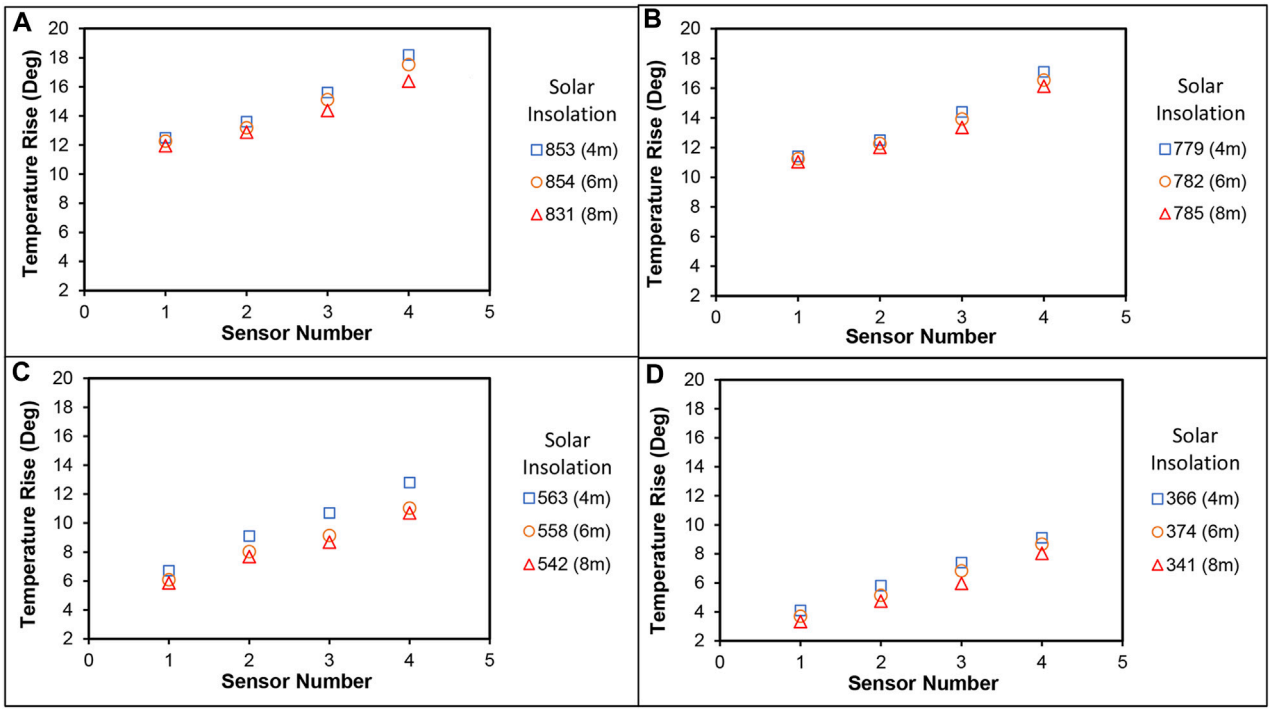

FIGURE 5
Temperature rise in the collector at solar insolation of: **(A)** 831–855 W/m^2. **(B)** 779–785 W/m^2. **(C)** 542–563 W/m^2. **(D)** 341–374 W/m^2.

the daytime temperature. The average temperatures in Fiji remain relatively constant throughout the year (World Bank, 2021).

The temperature rise in the collector for days which had relatively similar solar insolations was compared for the three chimney heights and the results are shown in Figure 5. A very interesting trend is observed in the temperature rise with solar insolation. The temperature rise in the collector is found to reduce as the chimney height is increased. The reduction in the temperature rise is apparently due to the increase in the air velocity with chimney height which shortens the time for which the air stays in the collector. Similar results were reported by Cuce et al. (2020) and Sivaram et al. (2018). At the (average) higher solar insolation of 846 W/m^2 shown in Figure 5A, the average of the maximum temperature rise for the 4 m, 6 m and 8 m tall solar chimneys are recorded to be 18°, 17.5° and 16.4°, respectively. As the solar insolation reduces (shown in Figures 5B–D), the temperature rise in the collector also shows a reducing trend; however, the trend of lower temperature rise from collector inlet to outlet with increasing chimney height can be seen for all the solar insolations.

The rise in the air temperature inside the collector from sensor 1 to sensor 4 for days which had relatively similar solar insolations was also compared from 9.00 a.m. to 9.00 p.m. for the three SCPP heights and the results are presented in Figure 6. At 9.00 a.m., the temperature rise in the collector from sensor 1 to sensor 4 for the three chimney heights is almost similar. There is a noticeable difference in the temperature rise between the three chimney heights from 11.00 a.m. onwards. The temperature rise peaked at 1.00 p.m., along with the solar insolation. Despite the solar insolation peaking at 1.00 p.m., the degree of temperature rise in the collector from sensor 1 to sensor 4 for the three

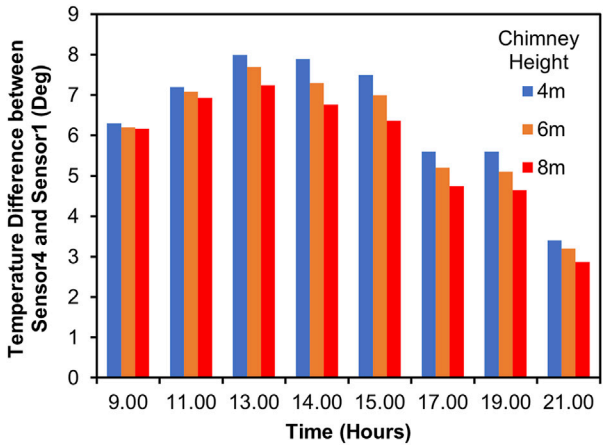

FIGURE 6
Temperature rise from sensor1 to sensor4 in the collector from 9.00 a.m. to 9.00 p.m. for the three chimney heights.

chimney heights was the greatest at 2.00 p.m. This is due to the fact that it takes some time for the ground to absorb the solar heat, get heated up and then transfer the heat to the air that is entering the collector by convection and radiation. The difference (rise) in temperatures between sensor 1 and sensor 4 for the three chimney heights was also the highest at 2.00 p.m. followed by 3.00 p.m. At 9.00 p.m., the difference in the temperature rise reduces considerably between the three chimney heights although the effect of the heated ground is still felt with the air in the collector still at a higher temperature compared to the

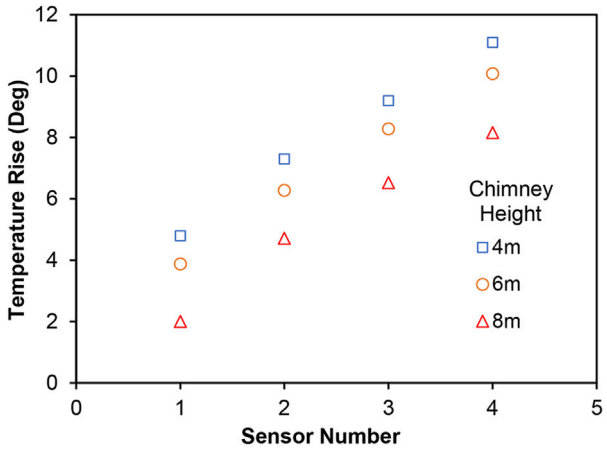

FIGURE 7
Temperature rise in the collector at 9.00 a.m. for the three chimney heights.

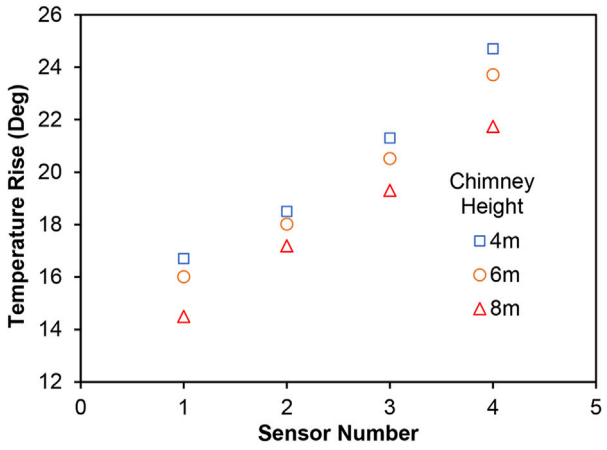

FIGURE 8
Temperature rise in the collector at 1.00 p.m. for the three chimney heights.

ground temperature thus causing an upward flow of air as can be seen in the variation of air velocity (Figure 13).

The temperature rise recorded by the 4 sensors placed across the collector (from inlet to outlet) at 9.00 a.m. on different days with similar solar insolations is shown in Figure 7, noting that the temperature rise right at the collector inlet would be zero. The temperatures gradually rise from the collector inlet to the outlet for all the three chimney heights. For the chimney height of 4 m, the temperature rise was found to be the highest, while it was the lowest for the maximum chimney height of 8 m.

The temperature rise measured by the 4 sensors placed across the collector at 1.00 p.m. at relatively similar solar insolations is shown in Figure 8. The temperature rise at 1.00 p.m. is considerably higher due to the high solar insolation at this time of the day which was about 1,000 W/m^2 during these days. The 4 m tall SCPP showed the highest temperature rise with the first sensor recording a

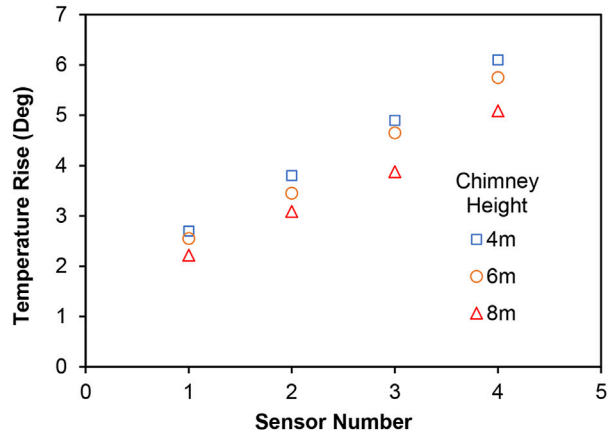

FIGURE 9
Temperature rise in the collector at 9.00 p.m. for the three chimney heights.

temperature rise of 16.7° and the last sensor close to the collector exit showed a temperature rise of 24.7°. The temperature rise was lower for the greatest chimney height of 8 m with the first sensor recording a temperature rise of 14.5° and the last sensor showing a rise of 21.74°. Similar trends were observed by Rishak et al. (2021) who reported the maximum temperature rise at 1.00 p.m. for two chimney heights of 3.3 and 4.5 m. Cuce et al. (2020) reported a reduction in the temperature rise in the collector as the chimney height is increased. Due to the increased velocity of air through the SCPP for greater chimney height, the air stays for less time inside the collector and hence absorbs less heat, which is the reason for lower temperature at the collector outlet for greater chimney height.

Figure 9 shows the temperature rise measured by the 4 sensors placed across the collector at 9.00 p.m. for the three chimney heights. All the three heights showed gradual increase at 9.00 p.m. and the temperature rise was the least compared to morning and afternoon times. The maximum temperature rise of 6.1° was recorded for the 4 m tall SCPP by sensor number 4 located close to the collector exit. At this time, the solar insolation is zero; however, the ground remains heated due to absorption of heat the whole day and transfers that heat to the air that enters the collector. The temperature of the air gradually rises till the exit of the collector. Due to the lower air velocities at this time (shown in Figure 13), the time for which air remains in the collector is longer causing the air to get heated; however, the temperature rise is significantly less compared to the rise at 1.00 p.m., as can be seen from a comparison of Figures 8, 9. Similar observations were made by Rishak et al. (2021) who recorded a reducing temperature difference after 1.00 p.m. Their last measurement was performed at 5.00 p.m. when a temperature rise of about 8° was recorded for a chimney height of 4.5 m.

The variations of the air temperature at the collector outlet were also plotted at different solar insolations and the results are shown in Figure 10. The exit air temperature is found to increase linearly as the solar insolation increased for all the three chimney heights. The outlet air temperatures for all the three chimney heights were

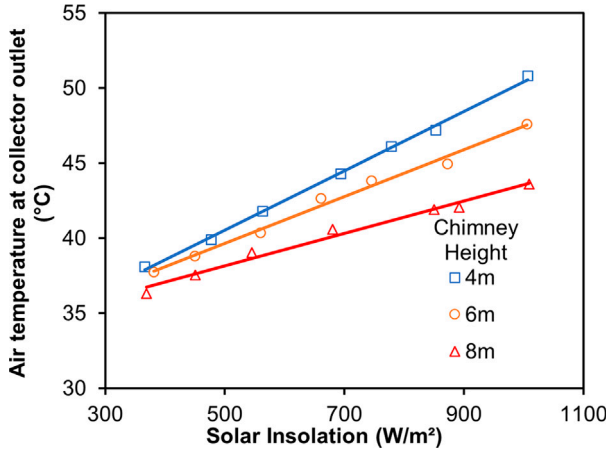

FIGURE 10
Variation of air temperature at the collector outlet with solar insolation for the three chimney heights.

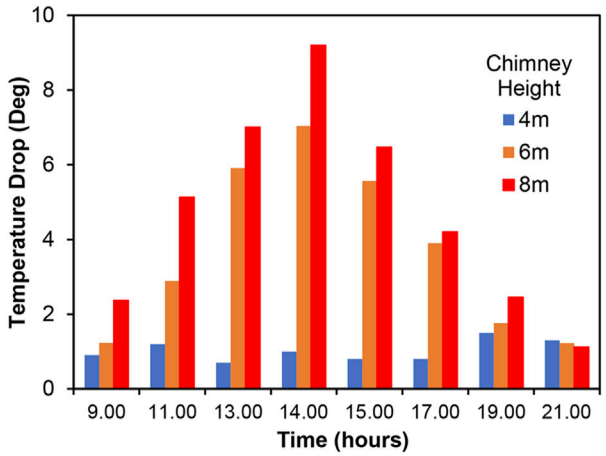

FIGURE 11
Temperature drop of air along the chimney height for the three chimney heights measured from 9.00 a.m. to 9.00 p.m.

measured to be almost identical at lower solar insolations of less than 300 W/m^2. Similar trends were also reported by Sivaram et al. (2018). Zhou et al. (2007b) argued that this is due to the temperature inversion effect which starts clearing as the area close to the ground heats up with rising ambient temperature or solar insolation. At the insolation of about 360 W/m^2, the difference in the collector outlet air temperature between the three chimney heights was recorded to be 1.8° which is very small. The difference starts to increase with increasing solar insolation, and at the highest insolation of about 1000 W/m^2, the difference between the collector outlet temperatures was recorded to be 7.2° between the 4 m tall SCPP and the 8 m tall SCPP. As discussed earlier, the lower temperature for the 8 m tall SCPP is due to the smaller duration of time for which the air stays in the collector due to higher velocity, as will be shown later.

Figure 11 shows the temperature drop along the chimney for the three chimney heights from 9.00 a.m. to 9.00 p.m. for days which had relatively similar solar insolations. This is the difference in air temperature between the chimney inlet and the outlet. As the air enters the chimney from the collector, the air pressure reduces while the velocity increases due to a reduction in area and the flow becoming predominantly uni-directional. As the air passes over the turbine blades, it transfers energy to the blades causing them to rotate. It was reported by Huang et al. (2007) that the temperature difference inside the collector as well as the pressure reduction during transition from the collector to the chimney increase with increasing solar insolation. The drop in temperature along the chimney height is due to the conversion of the enthalpy of air and the kinetic energy into pressure energy with the increasing area facilitating the pressure recovery from suction to atmospheric pressure at the chimney exit. The air velocity increases from zero at the collector inlet to its maximum at the location of minimum area in the chimney (Ming, 2016). The temperature drop in the 4 m tall chimney remained below 1.5° at all the times measurements were performed. The previous work also had similar trends (Ahmed and Patel, 2017). For the 6 m tall chimney, an increasing temperature drop from 9.00 a.m. to 2.00 p.m. was recorded along the chimney height, after which the drop reduced until 9.00 p.m. Similar trend was also observed for the 8 m tall chimney. The 8 m tall chimney produced the largest temperature drop of 9.2° at 2.00 p.m. The largest temperature drop for this case indicates a greater conversion of energy; at the same time, it also means that there is minimum loss of energy from the chimney outlet (loss of air enthalpy) as the temperature of air at the collector outlet (chimney inlet) was the lowest for this case. Das and Chandramohan (2019b) also reported the lowest air temperature at the chimney exit (maximum temperature drop) for the maximum chimney height of 8 m from their work on a constant diameter chimney. A similar level of temperature drop was also reported by Zhou et al. (2007a) for a chimney height of about 8 m although the solar insolations were not recorded in their work. Rishak et al. (2021) reported a temperature drop of about 8° at 12.00 p.m. and a drop of about 6° at about 2.00 p.m. for a chimney height of 3.3 m.

The effect of chimney height on the air velocity was studied by plotting the variation of the air velocity at the turbine section at different solar insolations for the three chimney heights as shown in Figure 12. The air velocities were estimated on typical days with relatively similar solar insolations. The air velocities linearly increase for all the three chimney heights as the solar insolation increases. The air velocity increases with increasing chimney height because of the larger driving force which is the buoyancy effect due to the vertical column of hot air which has to link with the outside ambient air of the same height and lower temperature (Koonsrisuk et al., 2010; Ming, 2016). Thus, there is a larger pressure difference between the air entering the collector and the air entering the chimney for larger chimney height. Effect of changing the chimney height on the air velocity was also reported by Ghalamchi et al. (2016), Cuce et al. (2020), Sivaram et al. (2018) and Rishak et al. (2021) where similar trends were presented. Best fit straight lines are drawn to see the effect of chimney height on the air velocity more clearly. It can be seen from Figure 12 that the velocities for the lowest chimney height

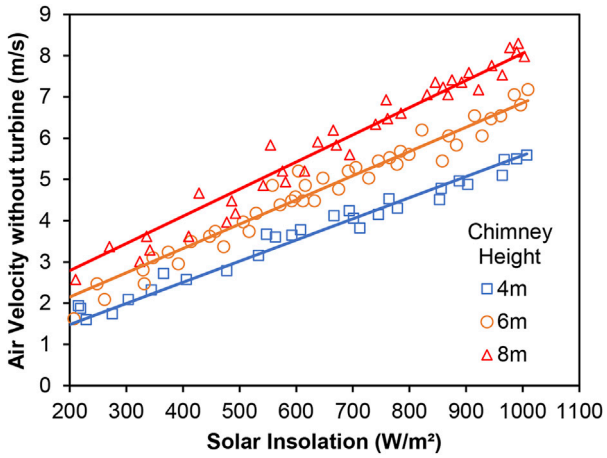

FIGURE 12
Variation of air velocity at the turbine section with solar insolation for the three chimney heights.

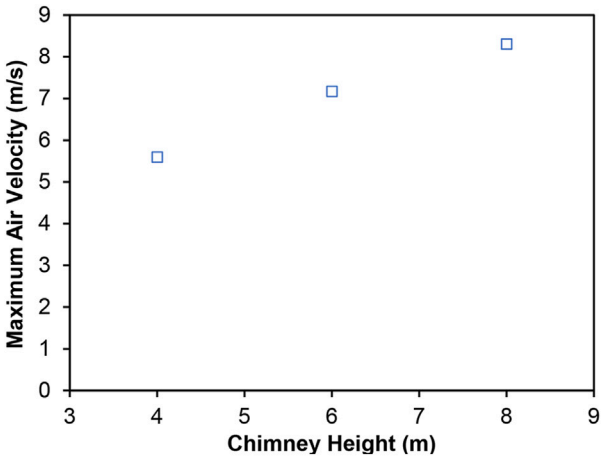

FIGURE 14
Maximum air velocity at the turbine section with increasing chimney height.

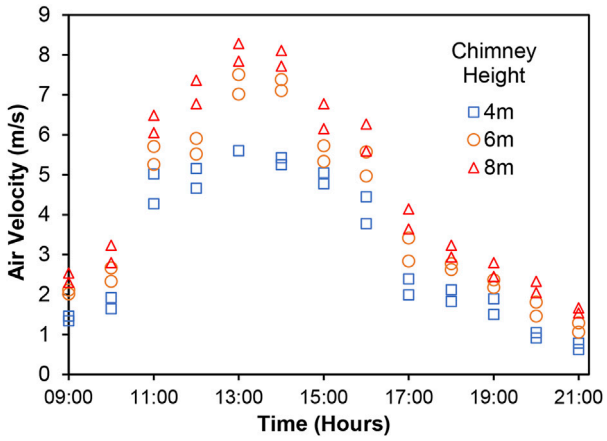

FIGURE 13
Variation of air velocity at the turbine section from 9.00 a.m. to 9.00 p.m. for the three chimney heights for typical days.

are lower and the difference between the velocities for 4 m and 6 m chimneys is larger than that between 6 m and 8 m chimney heights, indicating that after an optimum height, they may not be a significant increase in the air velocity. Some other researchers also made a conclusion that there will be an optimum chimney height above which the air velocity does not increase (Kasaeian et al., 2014; Ghalamchi et al., 2016). An optimization work by Dos Santos et al. (2017) based on constructal theory showed that there is an intermediate ratio of the chimney diameter at the exit and the chimney height that relates to the best performance of the device. In the present work, the loss due to friction in the chimney will be reduced as the velocity decreases in the divergent chimney. There is also a greater utilization of the enthalpy of air due to higher temperature drop along the chimney height. Ming. (2016) mentioned that the energy loss from the chimney outlet is the most significant loss and research efforts should be directed at reducing this loss. The present results show that the energy loss can be reduced by employing a divergent chimney and a suitable chimney height.

Figure 13 shows the variation of air velocity at the turbine section from 9.00 a.m. to 9.00 p.m. recorded on typical days with relatively similar solar insolations for the three chimney heights. The velocity trends for all the three chimney heights were similar. The air velocities were below 3 m/s for 9.00 a.m. and 10.00 a.m. for the three chimney heights. A substantial increase was observed from 10.00 a.m. until 1.00 p.m. for all the three heights. This correlates well with the significant increase in solar insolations during that time. Rishak et al. (2021) also reported the maximum air velocity at 1.00 p.m. for the two chimney heights of 3.3 and 4.5 m. The air velocities showed a decreasing trend from 1.00 p.m. to 4.00 p.m. The air velocities significantly reduced at 5.00 p.m. This is because the solar insolation at 5.00 p.m. starts to reduce significantly. From 5.00 p.m. to 9.00 p.m., the air velocities show a steady decline for all the three chimney heights. The air velocities for all the three chimney heights peaked at 1.00 p.m. with the 8 m tall chimney recording the highest velocity of 7.64 m/s corresponding to a solar insolation of about 1000 W/m^2. The increments in air velocities as the chimney height increases are significant. The air velocity improves by 27% at the peak time when the chimney height is increased from 4 m to 6 m and further increases by 10% when the chimney height is increased to 8 m. Similar findings were reported by Al-Kayiem et al. (2014) who reported enhancement of velocity by 23% when the solar chimney height was increased from 5 m to 15 m. Das and Chandramohan (2019a) also studied the effect of solar chimney height on the air velocity and reported a 33% increase in air velocity when the chimney height was increased from 3 m to 8 m.

Figure 14 shows the maximum recorded air velocity at the turbine section as a function of chimney height. The maximum recorded air velocity was found to increase logarithmically as the chimney height is increased. This indicates that there exists a maximum chimney height after which the air velocity will not

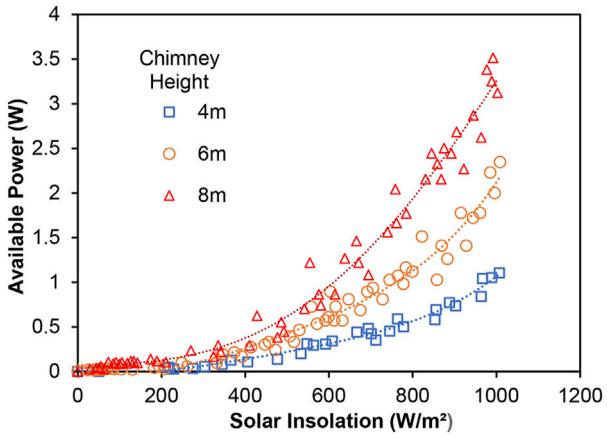

FIGURE 15
Variation of power available to the turbine with solar insolation for the three chimney heights.

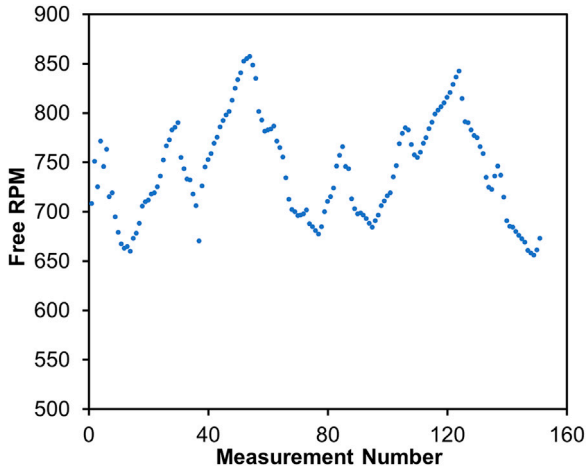

FIGURE 16
The free rpm of the turbine at a solar insolation of 800 W/m^2.

increase much. A very similar trend of air velocity increase was reported by Das and Chandramohan (2019b) when the chimney height was increased from 3m to 8 m. For a collector height of 50 mm, Rishak et al. (2021) reported an increase of 8.7% in the air velocity when the chimney height was increased from 3.3 to 4.5 m. Cuce et al. (2020) carried out performance studies taking into consideration geometrical parameters of the Manzanares pilot plant and reported the results. They also found that the maximum velocity tends to rise to a maximum. They presented a regression model which could be used to determine the optimum solar chimney height. Habibollahzade et al. (2021) also carried out parametric studies on the effect of geometric parameters on the performance of an SCPP and concluded that extreme values of collector diameter and chimney height reduce the power output of an SCPP. The findings of the present work support the above-mentioned findings.

The power available to the turbine at different solar insolations for the three chimney heights recorded on typical days with relatively similar solar insolations is shown in Figure 15. The power available was estimated using Eq. (1)

$$P_{available} = 0.5\rho AV^3 \quad (1)$$

For an SCPP of 6 m height with a constant diameter chimney, Mekhail et al. (2017) reported an available power of 3 W, while in the present work, it is 2.35 W. The power available at the turbine section at the solar insolation of 1000 W/m^2 increased by 112% when the chimney height was increased from 4 m to 6 m and increased by 49% when the chimney height was increased from 6 m to 8 m, again indicating that the power will not keep increasing at the same rate with height. At the solar insolation of 1000 W/m^2, the power available to the turbine for the 8 m tall SCPP is estimated to be about 3.5 W. For a collector height of 50 mm, Rishak et al. (2021) reported an increase of 25.2% in the available power when the constant diameter chimney height was increased from 3.3 to 4.5 m.

Figure 16 shows the free rpm of the turbine at a nearly constant solar insolation of 800 W/m^2. About 150 measurements were taken within a short span of time during which the solar insolation did not change much. It can be seen that the free rotational speed varies between 650 rpm and 850 rpm. The free rpm of the turbine was found to generally increase with the solar insolation (not shown). The free rpm of a turbine is a direct indication of the energy transferred from the fluid to the rotor. Balijepalli et al. (2020) reported a speed range of 140–320 rpm from their SCPP of 6 m height and constant diameter chimney. Noting that the maximum air velocity in their case was 4.7 m/s, the lower range of rpm is expected as the lower air velocity results in lower transfer of energy to the turbine.

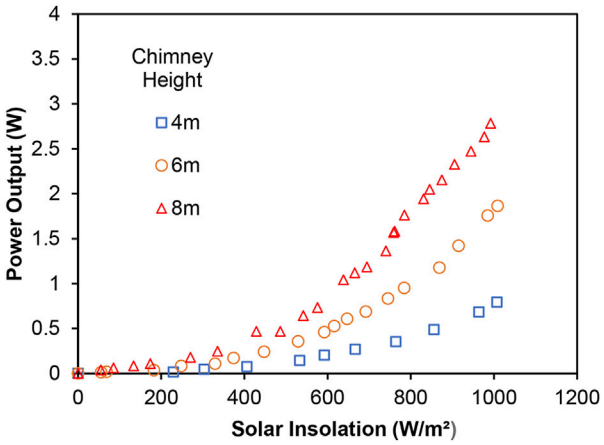

FIGURE 17
Power output from the turbine for the three chimney heights at different solar insolations.

Figure 17 shows the power output from the turbine with respect to solar insolation for the three chimney heights. The turbine power output followed a trend similar to that of the available power at the turbine section for all the three cases. However, it is always lower than the available power due to the efficiency of the turbine which is lower at lower solar insolations

due to the low air velocities. It should be noted that the power was measured fewer times compared to the velocity. The maximum measured powers for the 4 m, 6 m and 8 m tall SCPP are 0.79, 1.86, and 2.78 W, respectively. In the present work, the maximum power output increased by 135% when the SCPP height was increased from 4 m to 6 m and by 49% when the SCPP height was increased from 6 m to 8 m. For a chimney height of 6 m, Balijepalli et al. (2020) reported a theoretical power output of 1.37 W, which is lower than the power estimated in the present work. The higher power in the present work is due to the divergent chimney and a higher solar insolation. For a constant diameter chimney height increase of 33.3% (from 3.6 to 4.8 m), Belkhode et al. (2020) reported an electrical power output increase of 38.46%. Cuce et al. (2020) and Zhou et al. (2007b) presented a linear relationship between power output and solar chimney height. Li et al. (2012) however, reported a logarithmic trend between power output and chimney height. They suggested that as the chimney height increases, buoyancy weakens and the flow losses increase. They also suggested that there should be a maximum chimney height after which the power output will not increase much. It was reported from our previous work (Ahmed and Patel, 2017) that an average power of about 40 kW will be available for a chimney height of 100 m at a solar insolation of 800 W/m^2 which will be extremely beneficial for meeting the energy needs of small islands.

5 Conclusion

The height of a solar chimney power plant having a divergent chimney was increased from 4 m to 6 m and then to 8 m in this experimental work. For all the three heights, the temperature variations inside the collector and along the chimney height, the air velocity at the turbine section, the power available and the power output from an axial flow turbine were measured/estimated. The main conclusions of the present work are:

- the temperature rise in the collector is the highest for the 4 m tall SCPP with an exit temperature of 50.8°C and the smallest for the 8 m SCPP with an exit temperature of 43.6°C due to the shorter stay of air in the taller chimney because of larger driving force and higher velocity in the chimney.
- the temperature drop along the chimney height was the maximum for the 8 m SCPP and minimum for the 4 m SCPP. The largest temperature drop for the 8 m SCPP indicates a lesser loss of energy from the chimney outlet.
- the air velocity at the turbine section increased with chimney height for all solar insolations and a maximum air velocity of 8.29 m/s was recorded for the 8 m SCPP; it was observed that the increase in the maximum air velocity is not linear but tends to be logarithmic.
- the free rpm of the turbine was measured to be in the range of 650 rpm–850 rpm at a solar insolation of 800 W/m^2.
- the power output from the turbine was estimated by loading the turbine mechanically; the maximum power output increased from 0.79 W for the 4 m tall SCPP to 2.78 W for the 8 m SCPP at a solar insolation of 1000 W/m^2, which is an increase of 252%.
- the output of the SCPP can be further enhanced by increasing the chimney height and a power of about 40 kW will be available at a solar insolation of about 800 W/m^2.

Data availability statement

The original contributions presented in the study are included in the article/Supplementary Material, further inquiries can be directed to the corresponding author.

Author contributions

RP: Data curation, Formal Analysis, Investigation, Methodology, Writing–original draft. MRA: Conceptualization, Funding acquisition, Project administration, Supervision, Writing–review and editing.

Funding

The author(s) declare financial support was received for the research, authorship, and/or publication of this article. The student was provided funding from the University for his research work.

Conflict of interest

The authors declare that the research was conducted in the absence of any commercial or financial relationships that could be construed as a potential conflict of interest.

Publisher's note

Supplementary material

The Supplementary Material for this article can be found online at: https://www.frontiersin.org/articles/10.3389/fenrg.2023.1283818/full#supplementary-material

References

Ahmed, M. R., and Patel, S. K. (2017). Computational and experimental studies on solar chimney power plants for power generation in Pacific Island countries. *Energy Convers. Manag.* 149, 61–78. doi:10.1016/j.enconman.2017.07.009

Al-Kayiem, H. H., Sreejaya, K., and Gilani, S. I. U. H. (2014). Mathematical analysis of the influence of the chimney height and collector area on the performance of a roof top solar chimney. *Energy Build.* 68, 305–311. doi:10.1016/j.enbuild.2013.09.021

Al Qubeissi, M., and El-Kharouf, A. (2020). *Renewable energy: resources, challenges and applications*. London, United Kingdom: InTechOpen.

Azad, A., Aghaei, E., Jalali, A., and Ahmadi, P. (2021). Multi-objective optimization of a solar chimney for power generation and water desalination using neural network. *Energy Convers. Manag.* 238, 114152. doi:10.1016/j.enconman.2021.114152

Balijepalli, R., Chandramohan, V., and Kirankumar, K. (2020). Development of a small scale plant for a solar chimney power plant (SCPP): a detailed fabrication procedure, experiments and performance parameters evaluation. *Renew. Energy* 148, 247–260. doi:10.1016/j.renene.2019.12.001

Bansod, P. J. (2020). "Determination of optimum height of small prototype model of chimney operated solar power plant," in *Proceedings of ICRRM 2019 – system reliability, quality control, safety, maintenance and management* (Singapore: Springer).

Belkhode, P., Sakhale, C., and Bejalwar, A. (2020). Evaluation of the experimental data to determine the performance of a solar chimney power plant. *Mater. Today Proc.* 27, 102–106. doi:10.1016/j.matpr.2019.09.006

Biswas, N., Mandal, D. K., Manna, N. K., and Benim, A. C. (2023). Novel stair-shaped ground absorber for performance enhancement of solar chimney power plant. *Appl. Therm. Eng.* 227, 120466. doi:10.1016/j.applthermaleng.2023.120466

Cao, F., Liu, Q., Yang, T., Zhu, T., Bai, J., and Zhao, L. (2018). Full-year simulation of solar chimney power plants in Northwest China. *Renew. energy* 119, 421–428. doi:10.1016/j.renene.2017.12.022

Casule, N. (2020). The state of the climate in the Pacific. Available at: https://apo.org.au/sites/default/files/resource-files/2020-12/apo-nid309955.pdf (Accessed July 22, 2023).

Cottam, P., Duffour, P., Lindstrand, P., and Fromme, P. (2016). Effect of canopy profile on solar thermal chimney performance. *Sol. Energy* 129, 286–296. doi:10.1016/j.solener.2016.01.052

Cottam, P., Duffour, P., Lindstrand, P., and Fromme, P. (2019). Solar chimney power plants–Dimension matching for optimum performance. *Energy Convers. Manag.* 194, 112–123. doi:10.1016/j.enconman.2019.04.074

Cuce, E., Sen, H., and Cuce, P. M. (2020). Numerical performance modelling of solar chimney power plants: influence of chimney height for a pilot plant in Manzanares, Spain. *Sustain. Energy Technol. Assessments* 39, 100704. doi:10.1016/j.seta.2020.100704

Das, P., and Chandramohan, V. (2019a). Computational study on the effect of collector cover inclination angle, absorber plate diameter and chimney height on flow and performance parameters of solar updraft tower (SUT) plant. *Energy* 172, 366–379. doi:10.1016/j.energy.2019.01.128

Das, P., and Chandramohan, V. (2019b). Effect of chimney height and collector roof angle on flow parameters of solar updraft tower (SUT) plant. *J. Therm. Analysis Calorim.* 136 (1), 133–145. doi:10.1007/s10973-018-7749-y

Dos Santos, E. D., Isoldi, L. A., Gomes, M. D. N., and Rocha, L. A. (2017). "The constructal design applied to renewable energy systems," in *Sustainable energy technologies*. Editors E. Rincón-Mejía and A. De Las Heras (Florida, United States: CRC Press), 55–61.

Esmail, M. F., A-Elmagid, W., Mekhail, T., Al-Helal, I., and Shady, M. (2021). A numerical comparative study of axial flow turbines for solar chimney power plant. *Case Stud. Therm. Eng.* 26, 101046. doi:10.1016/j.csite.2021.101046

Faisal, S. H., Aziz, B. S., Jabbar, T. A., and Hameed, R. S. (2023). Hydrodynamic study of a solar chimney power plant for better power production. *Therm. Sci.* 00, 42. doi:10.2298/TSCI220819042F

Ghalamchi, M., Kasaeian, A., Ghalamchi, M., and Mirzahosseini, A. H. (2016). An experimental study on the thermal performance of a solar chimney with different dimensional parameters. *Renew. Energy* 91, 477–483. doi:10.1016/j.renene.2016.01.091

Guo, P., Li, T., Xu, B., Xu, X., and Li, J. (2019). Questions and current understanding about solar chimney power plant: a review. *Energy Convers. Manag.* 182, 21–33. doi:10.1016/j.enconman.2018.12.063

Guo, P., Wang, Y., Meng, Q., and Li, J. (2016). Experimental study on an indoor scale solar chimney setup in an artificial environment simulation laboratory. *Appl. Therm. Eng.* 107, 818–826. doi:10.1016/j.applthermaleng.2016.07.025

Guo, P., Zhai, Y., Xu, X., and Li, J. (2017). Assessment of levelized cost of electricity for a 10-MW solar chimney power plant in Yinchuan China. *Energy Convers. Manag.* 152, 176–185. doi:10.1016/j.enconman.2017.09.055

Haaf, W. (1984). Solar chimneys: part ii: preliminary test results from the Manzanares pilot plant. *Int. J. Sustain. Energy* 2 (2), 141–161. doi:10.1080/01425918408909921

Haaf, W., Friedrich, K., Mayr, G., and Schlaich, J. (1983). Solar chimneys part I: principle and construction of the pilot plant in Manzanares. *Int. J. Sol. Energy* 2 (1), 3–20. doi:10.1080/01425918308909911

Habibollahzade, A., Fakhari, I., Mohsenian, S., Aberoumand, H., and Taylor, R. A. (2021). Multi-objective grey wolf optimization of solar chimneys based on an improved model incorporating a wind turbine power curve. *Energy Convers. Manag.* 239, 114231. doi:10.1016/j.enconman.2021.114231

Hennessy, K., Power, S., and Cambers, G. (2011). *Climate change in the pacific: scientific assessment and new research. Volume 1*. Canberra, Australia: Regional Overview.

Huang, H., Zhang, H., Huang, Y., and Lu, F. (2007). "Simulation calculation on solar chimney power plant system," in *Challenges of power engineering and environment* (Hangzhou, China: Spinger), 1158–1161.

Kasaeian, A., Ghalamchi, M., and Ghalamchi, M. (2014). Simulation and optimization of geometric parameters of a solar chimney in Tehran. *Energy Convers. Manag.* 83, 28–34. doi:10.1016/j.enconman.2014.03.042

Kasaeian, A., Mahmoudi, A. R., Astaraei, F. R., and Hejab, A. (2017). 3D simulation of solar chimney power plant considering turbine blades. *Energy Convers. Manag.* 147, 55–65. doi:10.1016/j.enconman.2017.05.029

Kebabsa, H., Lounici, M. S., Lebbi, M., and Daimallah, A. (2020). Thermo-hydrodynamic behavior of an innovative solar chimney. *Renew. Energy* 145, 2074–2090. doi:10.1016/j.renene.2019.07.121

Koonsrisuk, A., Lorente, S., and Bejan, A. (2010). Constructal solar chimney configuration. *Int. J. Heat Mass Transf.* 53 (1-3), 327–333. doi:10.1016/j.ijheatmasstransfer.2009.09.026

Li, J. Y., Guo, P. H., and Wang, Y. (2012). Effects of collector radius and chimney height on power output of a solar chimney power plant with turbines. *Renew. Energy* 47, 21–28. doi:10.1016/j.renene.2012.03.018

Li, Y., and Liu, S. (2014). Experimental study on thermal performance of a solar chimney combined with PCM. *Appl. Energy* 114, 172–178. doi:10.1016/j.apenergy.2013.09.022

Looney, B. (2021). Statistical review of world energy. *Bp*. 70th Edn, 58. Available at: https://www.bp.com/content/dam/bp/business-sites/en/global/corporate/pdfs/energy-economics/statistical-review/bp-stats-review-2021-full-report.pdf

Mandal, D., Goswami, P., Pradhan, S., Chakraborty, R., Khan, N., and Bose, P. (2021). A Numerical experimentation on fluid flow and heat transfer in a SCPP. *IOP Conf. Ser. Mater. Sci. Eng.* 1080, 012027. doi:10.1088/1757-899X/1080/1/012027

Mandal, D. K., Biswas, N., Barman, A., Chakraborty, R., and Manna, N. K. (2023). A novel design of absorber surface of solar chimney power plant (SCPP): thermal assessment, exergy and regression analysis. *Sustain. Energy Technol. Assessments* 56, 103039. doi:10.1016/j.seta.2023.103039

Mandal, D. K., Pradhan, S., Chakraborty, R., Barman, A., and Biswas, N. (2022). Experimental investigation of a solar chimney power plant and its numerical verification of thermo-physical flow parameters for performance enhancement. *Sustain. Energy Technol. Assessments* 50, 101786. doi:10.1016/j.seta.2021.101786

Mekhail, T., Rekaby, A., Fathy, M., Bassily, M., and Harte, R. (2017). Experimental and theoretical performance of mini solar chimney power plant. *J. Clean Energy Technol.* 5 (4), 294–298. doi:10.18178/jocet.2017.5.4.386

Ming, T. (2016). *Solar chimney power plant generating technology*. Academic Press, 147–162.

Ming, T., Liu, W., Pan, Y., and Xu, G. (2008). Numerical analysis of flow and heat transfer characteristics in solar chimney power plants with energy storage layer. *Energy Convers. Manag.* 49 (10), 2872–2879. doi:10.1016/j.enconman.2008.03.004

Ming, T., Liu, W., and Xu, G. (2006). Analytical and numerical investigation of the solar chimney power plant systems. *Int. J. Energy Res.* 30 (11), 861–873. doi:10.1002/er.1191

Moffat, R. J. (1988). Describing the uncertainties in experimental results. *Exp. Therm. Fluid Sci.* 1, 3–17. doi:10.1016/0894-1777(88)90043-x

Motoyama, M., Sugitani, K., Ohya, Y., Karasudani, T., Nagai, T., and Okada, S. (2014). Improving the power generation performance of a solar tower using thermal updraft wind. *energy power Eng.* 6 (11), 362–370. doi:10.4236/epe.2014.611031

Najm, O. A., and Shaaban, S. (2018). Numerical investigation and optimization of the solar chimney collector performance and power density. *Energy Convers. Manag.* 168, 150–161. doi:10.1016/j.enconman.2018.04.089

Nia, E. S., and Ghazikhani, M. (2023). Dimensional investigation of solar chimney power plant based on numerical and experimental results. *Therm. Sci. Eng. Prog.* 37, 101548. doi:10.1016/j.tsep.2022.101548

Padki, M., Sherif, S., and Chan, A. (1989). "Solar chimney for power generation in rural areas," in *Seminar on energy conservation and generation through renewable resources* (Ranchi, India: Spinger).

Pasumarthi, N., and Sherif, S. (1998a). Experimental and theoretical performance of a demonstration solar chimney model—Part I: mathematical model development. *Int. J. Energy Res.* 22 (3), 277–288. doi:10.1002/(sici)1099-114x(19980310)22:3<277::aid-er380>3.0.co;2-r

Pasumarthi, N., and Sherif, S. (1998b). Experimental and theoretical performance of a demonstration solar chimney model—Part II: experimental and theoretical results and economic analysis. *Int. J. energy Res.* 22 (5), 443–461. doi:10.1002/(sici)1099-114x(199804)22:5<443::aid-er381>3.0.co;2-v

Patel, S. K., Prasad, D., and Ahmed, M. R. (2014). Computational studies on the effect of geometric parameters on the performance of a solar chimney power plant. *Energy Convers. Manag.* 77, 424–431. doi:10.1016/j.enconman.2013.09.056

Patil, S., Dhoble, A., Sathe, T., and Thawkar, V. (2023). Predicting performance of solar updraught tower using machine learning regression model. *Aust. J. Mech. Eng.* 2023, 1–19. doi:10.1080/14484846.2023.2179134

Pradhan, S., Chakraborty, R., Mandal, D., Barman, A., and Bose, P. (2021). Design and performance analysis of solar chimney power plant (SCPP): a review. *Sustain. Energy Technol. Assessments* 47, 101411. doi:10.1016/j.seta.2021.101411

Rhodes, C. J. (2010). Solar energy: principles and possibilities. *Sci. Prog.* 93 (1), 37–112. doi:10.3184/003685010x12626410325807

Rishak, Q. A., Sultan, H. S., and Jawad, I. N. (2021). Experimental study of the performance of a solar chimney power plant model in Basrah city. *J. Mech. Eng. Res. Dev.* 44 (7), 340–351.

Schlaich, J. R., Bergermann, R., Schiel, W., and Weinrebe, G. (2005). Design of commercial solar updraft tower systems—utilization of solar induced convective flows for power generation. *J. Sol. Energy Eng.* 127 (1), 117–124. doi:10.1115/1.1823493

Shirvan, K. M., Mirzakhanlari, S., Mamourian, M., and Abu-Hamdeh, N. (2017). Numerical investigation and sensitivity analysis of effective parameters to obtain potential maximum power output: a case study on Zanjan prototype solar chimney power plant. *Energy Convers. Manag.* 136, 350–360. doi:10.1016/j.enconman.2016.12.081

Singh, A. P., Kumar, A., and Singh, O. (2021). A novel concept of integrating bell-mouth inlet in converging-diverging solar chimney power plant. *Renew. Energy* 169, 318–334. doi:10.1016/j.renene.2020.12.120

Sivaram, P. M., Harish, S., Premlatha, M., and Arunagiri, A. (2018). Performance analysis of solar chimney using mathematical and experimental approaches. *Int. J. Energy Res.* 42 (7), 2373–2385. doi:10.1002/er.4007

Weli, R. B., Atrooshi, S. A., and Schwarze, R. (2021). Investigation of the performance parameters of a sloped collector solar chimney model–An adaptation for the North of Iraq. *Renew. Energy* 176, 504–519. doi:10.1016/j.renene.2021.05.075

World Bank (2021). Fiji's current Climatology. Available at: https://climateknowledgeportal.worldbank.org/country/fiji/ (Accessed November 30, 2023).

Xu, G., Ming, T., Pan, Y., Meng, F., and Zhou, C. (2011). Numerical analysis on the performance of solar chimney power plant system. *Energy Convers. Manag.* 52 (2), 876–883. doi:10.1016/j.enconman.2010.08.014

Zhou, X., Yang, J., Xiao, B., and Hou, G. (2007a). Experimental study of temperature field in a solar chimney power setup. *Appl. Therm. Eng.* 27 (11-12), 2044–2050. doi:10.1016/j.applthermaleng.2006.12.007

Zhou, X., Yang, J., Xiao, B., and Hou, G. (2007b). Simulation of a pilot solar chimney thermal power generating equipment. *Renew. Energy* 32 (10), 1637–1644. doi:10.1016/j.renene.2006.07.008

frontiers | Frontiers in Energy Research

TYPE Original Research
PUBLISHED 19 February 2024
DOI 10.3389/fenrg.2024.1346764

OPEN ACCESS

EDITED BY
Sunday Olayinka Oyedepo,
Bells University of Technology, Nigeria

REVIEWED BY
Joseph Oyebanji,
Bells University of Technology, Nigeria
Augustine Omoniyi Ayeni,
Covenant University, Nigeria

*CORRESPONDENCE
Kehinde O. Olatunji,
olaoladoke293@gmail.com

RECEIVED 29 November 2023
ACCEPTED 29 January 2024
PUBLISHED 19 February 2024

CITATION
Olatunji KO and Madyira DM (2024), Enhancing the biomethane yield of groundnut shells using deep eutectic solvents for sustainable energy production.
Front. Energy Res. 12:1346764.
doi: 10.3389/fenrg.2024.1346764

Enhancing the biomethane yield of groundnut shells using deep eutectic solvents for sustainable energy production

Kehinde O. Olatunji* and Daniel M. Madyira

Department of Mechanical Engineering Science, Faculty of Engineering and the Built Environment, University of Johannesburg, Johannesburg, South Africa

This study examined the influence of DES pretreatment using choline chloride and ethyl glycerol with the molar ratio of 1: 1 at different solid:liquid ratios and temperatures on groundnut shells' microstructural arrangement and biomethane yield. Scanning electron microscopy (SEM), X-ray diffraction (XRD), and Fourier-transform infrared spectroscopy (FTIR) were used to study the effects of pretreatment on microstructural arrangements, and the pretreated substrate was digested at mesophilic temperature to determine its biomethane potential. The result of SEM analysis indicated that DES pretreatment alters the microstructural arrangement of groundnut shells, and XRD analysis showed an optimum crystallinity index of 20.71% when the substrate with a solid:liquid ratio of 1:2 was experimented at 80°C. The highest theoretical biomethane yield of 486.81 mL CH_4/gVS_{added} was recorded when the substrate with a 1:4 solid:liquid ratio was investigated at 100°C, and the highest biodegradability rate (84.87%) was observed from the substrate treated with a 1:2 solid:liquid ratio at 100°C. The optimum biomethane yield of 365.70 mL CH_4/gVS_{added}, representing a 226.05% increase, was observed from 1:2 of solid:liquid ratios at 100°C. Therefore, DES pretreatment using choline chloride and ethyl glycerol is a bright, low-cost pretreatment method for enhancing the biomethane yield of lignocellulose feedstocks.

KEYWORDS

lignocellulose feedstocks, groundnut shells, pretreatment, deep eutectic solvents, microstructural arrangements, biomethane

1 Introduction

Sustainable, affordable, and reliable energy, as well as appropriate waste management systems, support sustainable development (Olatunji and Madyira, 2023a). Energy is crucial to social and economic development; however, the primary source of world energy is fossil fuels that burn with harmful effects on the environment (Yildiz, 2018). Energy resources have improved living and working conditions, boosted economic expansion, allowed comfort and movement, and made necessities accessible. Energy-driven technologies replaced manual, labor-intensive jobs during the Industrial Revolution, when energy supplies were abundant, and there was little worry about their usage and availability; however, this is no longer the case. The difference between the supply and demand of energy has widened significantly. This imbalance may be caused by several factors, including population growth, rising living standards, careless use, and technical breakthroughs (Gautam et al., 2019). Most energy mix projections indicate that the present and

predicted future energy sources are unsustainable. Despite projecting serious improvements in energy supply, it has been observed that long projection of energy demand globally will rise drastically, with a major increase to be experienced in developing countries. These trends suggest that a decoupling of economic activity from the use of fossil fuels, the primary source of energy, is important to meet the requirements for the three elements of sustainability (economic, environmental, and social) regarding energy production and consumption (Oyedepo, 2012). Fossil fuels are not renewable and are depleted faster than the rate at which they are being replenished. Another challenge of relying majorly on fossil fuels is the release of carbon dioxide during combustion, which is valued at approximately 21.3 billion tons per annum. It was observed that carbon dioxide released from fossil fuels and industries in 2016 was nearly stable, approximately 0.2%, as against the projected value of 2.2% (2017 UN Climate Change Conference in Bonn, Germany (COP23)—Wednesday, 4 October 2017, n.d.). This is not only because of reductions in fossil fuel consumption but also due to energy efficiency techniques and the production of renewable energy.

Renewable energy will play a significant role in supplying future energy requirements and the remediation of the ecosystem. Renewable energy is the energy source replenished through natural processes with limitless supply and can operate without pollution. This includes energy from the Sun, geothermal sources, biomass, wind, ocean waves and tides, and rivers. Renewable energy technologies (RETs), commonly known as "clean technologies" or "green energy," are technologies that have been created to utilize these forms of renewable energy. Because of their unlimited supply, their supply is secure compared to that of fossil fuels, which is determined by national and international market situations (Oyedepo, 2012). Developing and applying renewable energy systems needs special attention, particularly in awareness of the harmful effects of fossil fuel usage. Globally, there has been a growing increase in the development of sustainable energy sources in recent years. The general acceptability of renewable energy is crucial to the development of sustainable energy in developing and developed countries. When renewable resources are used wisely for the benefit of current and future generations, they should be used at a reasonable pace that is neither too fast nor too slow. This ensures that the natural wealth they symbolize is transformed into long-term wealth as they are used (Taiwo, 2009). Although there are significant disparities in the objectives and accomplishments of different countries in the energy transition, it is undeniable that they are at a pivotal point in the process. Indeed, the energy transition needs to be established while fossil fuel prices are low and are expected to remain that way for the foreseeable future to prevent the irreversible effects of climate change caused by greenhouse gas emissions through fossil fuel burning. Major advantages and drawbacks are associated with consolidating the transition from fossil fuels to clean energy, and energy policies must be designed to handle these challenges appropriately (Arezki and Matsumoto, 2017).

Solid waste generation and management continue to be major social and political issues, especially in cities where waste generation outpaces available space and there is a rapid rise in population. Several worldwide development agendas, charters, and visions emphasize solid waste management's role in attaining sustainable development. For instance, appropriate and sustainable waste management can assist in achieving some of the United Nations' Sustainable Development Goals (SDGs), such as goals 2, 3, 6, 7, 9, 13, and 15 (Chowdhury et al., 2022). Additionally, it supports the development of a circular urban economy that minimizes the use of finite resources, encourages the reuse and recycling of materials to reduce waste, pollution, and costs, and promotes green growth. In a more sustainable waste management approach, techniques such as reduction in production, waste classification, reuse, recycling, and energy recovery are given priority over open dumps, landfilling, and open incineration (Yang et al., 2018; Kabera and Nishimwe, 2019). Energy recovery from waste is getting better attention globally because of its inclusivity, environment-friendly nature, and minimal harmful impact on human health and the environment (Rimi Abubakar and Aina, 2016). Waste-to-energy (WTE) technology not only produces clean energy but also offers an environmentally beneficial waste disposal option. Waste is converted into energy using WTE techniques. The kind of waste, the plant's performance, and the method or path taken for energy recovery all affect how much energy can be recovered (Okedu et al., 2022). The most promising solution to the energy dilemma appears to be converting waste into energy, which can be accomplished through various technological means. The feasibility of these WTE solutions is determined by several parameters, including the energy content, the desired final energy form, the nature and composition of waste, the chemical and thermodynamic conditions, and the overall energy efficiency. Waste-to-energy technologies include biochemical conversion, thermal conversion, landfill with gas capture, chemical conversion (esterification), microbial fuel cell, and hydrothermal carbonization (Gautam et al., 2019).

Biochemical conversion techniques use microbial processes to transform organic waste into energy. The biodegradable portion of municipal solid wastes, wastewater sludge, agricultural residues, energy grasses, etc., are some of the bright feedstocks for these techniques (Olatunji et al., 2023a). Waste-to-energy biochemical conversion is divided into two processes, which are fermentation and anaerobic digestion. Fermentation is the process of converting organic waste into alcohol or acid (ethanol, lactic acid, etc.) and residue that is rich in nutrients in the absence of oxygen (Cai et al., 2016). Bioethanol is a clean fuel that can be produced from a pure culture of specific yeast strains (Orozco-González et al., 2022). The microbial breakdown of organic waste in the absence of oxygen is known as anaerobic digestion, producing biogas (methane and carbon dioxide) digestate (fertilizer). Biogas released from tightly closed tanks (digester) can be used to generate electricity or heat as renewable energy (Olatunji et al., 2022a). Anaerobic digestion has four stages: hydrolysis, acidogenesis, acetogenesis, and methanogenesis (Raja and Wazir, 2017). Biogas can be generated from different organic wastes, such as corn cob, groundnut shells, wastewater sludge, cow dung, *Jatropha* cake, macroalgae and microalgae, poultry droppings, and duck waste (Ogunkunle et al., 2018; Venturin et al., 2018; Olatunji and Madyira, 2023b). Utilization of lignocellulose biomass for biogas production has been encouraged because of its environment-friendly nature and role as an economically sustainability source of feedstock. It is regarded as an eco-friendly second-generation technology for energy generation. Methane production from lignocellulose is an

efficient technique for energy recovery from biomass compared to other techniques that require a higher energy input/output ratio (Monlau et al., 2013). Lignocellulose feedstocks are identified as an abundant and renewable feedstock for biogas production. The global production is approximately 120×10^9 annually, equivalent to 2.2×10^{21} J, approximately 300 times higher than the present global energy demand (Guo et al., 2015). One of the largest sources of lignocellulose materials is the crop residues from agricultural activities; most of them do not have other uses. The unused agricultural residues on the field can release greenhouse gases or cause serious environmental pollution when burned openly. These residues have been reported to have high biogas production potential that can be annexed as renewable energy sources (Rabemanolontsoa and Saka, 2016; Xu et al., 2019; Podgorbunskikh et al., 2020). However, lignocellulose feedstocks are recalcitrant, inhibiting the anaerobic digestion process and limiting their biogas production potential (Madyira and Olatunji, 2023). Therefore, pretreatment is required to convert lignocellulose feedstocks into biogas and other value-added products efficiently. Pretreatment aimed to break down the strong microstructural arrangement of the lignocellulose by altering the lignin and hemicellulose arrangement, thereby improving the porosity and reducing the cellulose crystallinity and polymerization level (Patowary and Baruah, 2018). Different pretreatment techniques have been investigated on lignocellulose, and recently, several studies have examined these techniques for improving the digestion process and enhancing biogas release from lignocellulose feedstock. These techniques are categorized as biological, thermal, mechanical/physical, chemical, nanoparticle additives, and combined pretreatment (Olatunji et al., 2021). A comprehensive review of the application of pretreatment techniques on lignocellulose feedstock before biogas and methane production has been published (Millati et al., 2011; Zhang et al., 2016; Brémond et al., 2018; Olatunji et al., 2021; 2023b). Different methods have been experimented with on various lignocellulose feedstocks, but their efficiency depends on the microstructural arrangement, treatment type, temperature, etc., making comparing the pretreatment techniques difficult.

Deep eutectic solvents (DESs) are a chemical pretreatment technique that has been regarded as one of the most acceptable green solvents of the 21st century. DESs are gaining attention in studies due to their biodegradability, low cost, ease of recycling, high solubility, non-flammability, and environment-friendly nature (Smith et al., 2014). DESs are defined as the combination of two or more components that can be liquid or solid, and the specific resulting mixture has a high melting point but becomes liquid at room temperature. Common DESs are choline chloride, succinic acid, citric acid, glycerol, urea, etc. (Paiva et al., 2014). Compared to other chemical and ionic liquids, the application of DESs has been limited to enzyme reactions (Gorke et al., 2008), organic reactions (Gore et al., 2011), electrochemistry (Jhong et al., 2009), and organic extractions (Abbott et al., 2009). Because of their biodegradable characteristics and acceptable toxicity, they have been considered an ideal candidate for feedstock pretreatment (Dai et al., 2013). Pretreatment with DESs improves the surface area and cellulose crystallinity, enhancing digestion. It also eliminates hemicellulose by altering the glycosidic bonds (C–O–C) to produce monosaccharides (Xu et al., 2020). Furthermore, DESs can selectively destroy the higher percentage of lignin by primarily splitting the aryl ether bond (β-O-4) within the feedstock (Alvarez-Vasco et al., 2016; Shen et al., 2020). The efficiency of DES pretreatment depends on the strength of the selected DESs to separate carbon–carbon linkages and aryl ether linkages in the feedstock's microstructural arrangement (Xu et al., 2020).

Groundnut shells are one of the most abundant lignocellulose materials with biogas production potential (Olatunji et al., 2022c). Being a lignocellulose feedstock, the anaerobic digestion of this feedstock is ineffective without pretreatment. Some studies have examined the influence of different pretreatment techniques to enhance the biogas yield of groundnut shells (Dahunsi et al., 2017; Jekayinfa et al., 2020; Olatunji and Madyira, 2023b). Their findings indicate that pretreatment methods improve the biogas and methane yield of groundnut shells, but their degree of effectiveness differs. It was further reported that there is still a need for more research in the pretreatment of this economical feedstock to establish the most economical means of optimum recovery of renewable energy from groundnut shells. Therefore, this study examines the effects of DES pretreatment on the microstructural arrangement, crystallinity, functional groups, and biomethane yield of groundnut shells. Groundnut shells are mostly left on the farm/processing area after harvesting and are usually burnt off, posing health and fire-related hazards, promoting pathogen growth, and contributing to greenhouse gas emissions. The literature on the DES pretreatment technique is limited, and we aim to establish the potential of DESs on the structural arrangement and biomethane yield of groundnut shells. The study used scanning electron microscopy (SEM), X-ray diffraction (XRD), and Fourier-transform infrared spectroscopy (FTIR) to investigate the effects of DES pretreatment on surface changes and interior arrangement to provide the theoretical interpretation of the method. Finally, the pretreated and untreated feedstocks were subjected to an anaerobic digestion process to ascertain the influence of the method on biomethane yield. The result from this study is expected to provide baseline information for future studies on lignocellulose pretreatment for enhancing biomethane yield.

2 Materials and methods

2.1 Materials

Groundnut shells were sourced locally from a groundnut farm at Mogwase, Rustenburg, North West Province, South Africa (GPS: −25.2621, 27.27336), after harvesting and processing. The sample was then reduced to a particle size of between 2 and 4 mm using a hammer mill. Inoculum was collected from a recently terminated digester, whereby wastewater was digested at mesophilic temperature (35 ± 2). The pH value of the inoculum was observed to be 7.2. The substrate and inoculum were stored at 4°C in the laboratory before pretreatment, laboratory analysis, and anaerobic digestion. Choline chloride and ethyl glycerol were procured from Sigma-Aldrich (Darmstadt, Germany) for pretreatment.

2.2 Deep eutectic solvent preparation

The deep eutectic solvent was prepared from the combination of choline chloride and ethyl glycerol, as reported by Smith et al.

TABLE 1 NADES pretreatment conditions.

Treatments	Choline chloride:ethyl glycerol (w/w)	Solid:liquid (w/w)	Temperature (°C)
A	1:1	1:2	80
B	1:1	1:4	80
C	1:1	1:2	100
D	1:1	1:4	100
E	Untreated	Untreated	Untreated

(2014), with a pH value of 6.7 (presented in Table 1). The choline chloride and ethyl glycerol ratios were measured using a 1: 1 M ratio. A mixture of 1: 1 was selected because they are both hydrogen-bond donor and acceptors, which is the basis for the complexation of solid-producing liquids with a supramolecular arrangement (Dai et al., 2013). The mixture of choline chloride and ethyl glycerol in the beaker was heated at different temperatures, as shown in Table 1, on a magnetic stirrer at 500 rpm for 1 hour until a clear homogenous solution was achieved (Olugbemide et al., 2021).

2.3 Substrate pretreatment with DES

Groundnut shells were pretreated with the prepared DES using different solid:liquid ratios and temperatures. The calculated quantity of groundnut shells was added to the DES using the solid:liquid ratio presented in Table 1 and heated at temperatures specified in Table 1 for 1 hour as recommended (Olugbemide et al., 2021). Pretreated samples were allowed to cool down to room temperature and washed with running water until a neutral pH (7) was achieved. The cleaned feedstock was oven-dried at 70°C for 1 h and kept in a zip-lock plastic before being stored at 4°C in the laboratory for physicochemical property analysis, structural analysis, and the biomethane potential test.

2.4 Substrate characterization

2.4.1 Physicochemical property analysis

To determine the compositional level of the substrate and inoculum, their physicochemical properties were examined. Total solids (TSs), moisture content, percentage ash, and volatile solids (VSs) were examined using the established procedures of the Association of Official Analytical Chemists (AOAC) (Official Methods of Analysis, 21st Edition (2019)—AOAC INTERNATIONAL, n.d.). Lignin, hemicellulose, and cellulose percentage were analyzed as prescribed by Van Soest et al. (1991). The nitrogen, carbon, and hydrogen percentages were determined using an elemental analyzer (Vario El cube, Germany), and the percentage of oxygen was calculated with the assumption that C + N + H + O = 99.50% (Rincón et al., 2012).

2.4.2 Microstructural characterization

The impacts of different solid:liquid ratios and temperatures of DES pretreatment on the microstructural arrangement of groundnut shells were studied using a scanning electron microscope (VEGA3 TESCAN X-Max, Czech Republic). The analysis was duplicated, and the images were picked at different magnifications before selecting the most explicit image. X-ray diffraction (D-8 Advance, Indiana, USA) was used to study the degree of cellulose crystallinity of groundnut shells before and after DES pretreatment. This investigation was carried out at 5°C–35°C with 5°C/min speed at 2Θ as the diffraction angle. Equation 1 was used to calculate the crystallinity index (I_c) of the pretreated and untreated substrates using the empirical data from the XRD analysis (Atalla and VanderHart, 1999). The influence of DES pretreatment on the functional group of the substrate was investigated under Fourier-transform infrared spectroscopy (SHIMADZU IRAfinity-1, Japan). This was considered under the wavelengths of 500 and 4,000 cm^{-1}, and the changes in the absorbent ratio of the substrates were determined from the FTIR data using Eq. 2 (Dahunsi et al., 2019).

$$I_c = \frac{I_{max} - I_x}{I_{max}} \quad X\,100. \tag{1}$$

Here, I_c is the crystallinity index, I_{max} is the highest diffraction at peak position at 2Θ = 22°, and I_x is the intensity at 2Θ = 18°.

2.5 Anaerobic digestion

The experiment to examine the influence of the DES pretreatment method on groundnut shells was conducted in a batch digester in the laboratory following the VDI 4630 standard (organischer Stoffe Substratcharakterisierung, 2016). The experiment was set up at mesophilic temperature using the Automatic Methane Potential Test System II (AMPTS II). AMPTS II reactor bottles of 10–500 mL were preloaded with 400 g of stabled inoculum as recommended by VDI 4630 (organischer Substratcharakterisierung, 2016). The quantity of substrate added to the inoculum was determined using Eq. 2, considering the volatile solids of the substrate and inoculum. Reactors were loaded at a 2:1 ratio of substrate:inoculum, and the AMPTS II water bath was maintained at 37°C ± 2 throughout the digestion process. The calculated quantity of DES-pretreated and untreated substrates was charged in each digester, as given in Table 1, and the experiment was replicated twice as recommended (Caillet et al., 2019). Two reactors with only stabilized inoculum were run as a parallel experiment to ascertain the exact volume of biomethane released. The biomethane yield released from the parallel experiment was used as a head-space correction for the reactors with both substrate and inoculum. In the AMPTS II programming, the mixing time was set as 60 s with 60 s off time. The agitation speed adjustment was maintained at 80%, and the carbon dioxide flush gas had a concentration of 10%. The reactor head-space

was kept at 100 mL, and 60% methane content was presumed (Brennan and Owende, 2010). Nitrogen baseline gas was used to flush out the oxygen in the reactors to set an anaerobic condition. Screw cap bottles of 100 mL were filled with NaOH (3M NaOH) at the carbon dioxide removal section to eliminate the carbon dioxide in the gas released. The reactor bottles were linked with the carbon dioxide removal bottles using silicon tubes. The carbon dioxide removal unit was also connected to the third unit with another silicon tube, where the quantity of biomethane generated was rerecorded. Gas chromatography installed with the system was used to analyze the gas released to understand the quality of the gas. When it was observed that the daily biomethane released was below 1% of the cumulative biomethane released by day 35, the experiment was terminated.

$$M_s = \frac{M_i C_i}{2C_S}. \quad (2)$$

Here, M_s is the mass of the substrate (g), M_i is the mass of the inoculum (g), C_s is the concentration of the substrate (%), and C_i is the concentration of the inoculum (%) (organischer Substratcharakterisierung, 2016).

2.6 Theoretical methane yield and biodegradable rate (B_d)

The biomethane potential of the pretreated and untreated substrates was determined through theoretical yield using the result of the elemental analysis with Eqs 3, 4 (Buswell and Mueller, 2002). The biodegradability percentage of the digestion process was calculated using the experimental methane yield (EMY) and theoretical methane yield (TMY), as shown in Eq. 5 and reported by Elbeshbishy et al. (2012).

$$C_aH_xO_yN_z + \left(a - \frac{x}{4} - \frac{y}{2} - \frac{3z}{4}\right)H_2O \rightarrow \left(\frac{a}{2} + \frac{x}{8} - \frac{y}{4} - \frac{3z}{8}\right)CH_4 + \left(\frac{a}{2} - \frac{x}{8} + \frac{y}{4} + \frac{3z}{8}\right)CO_2 + zNH_3, \quad (3)$$

$$TMY\left(\frac{mLCH_4}{gVS}\right) = \frac{22.4\,X\,1000\,X\left(a/2 + x/8 - y/4 - 3z/8\right)}{12a + x + 16y + 14z}, \quad (4)$$

where a, x, y, and z are the stoichiometry ratios of carbon, hydrogen, oxygen, and nitrogen, respectively.

$$B_d\,(\%) = \frac{EMY}{TMY}\,X\,100. \quad (5)$$

3 Results and discussion

3.1 Effects of DES pretreatment on the structural arrangements of groundnut shell

3.1.1 Effects of pretreatment on microstructural arrangements

The influence of different DES pretreatment conditions on the microstructural arrangement of groundnut shells was investigated with scanning electron microscopy, and the result is presented with the images in Figure 1. It was observed from the figure that DES pretreatment significantly impacts the microstructural arrangement of the substrate when images in Figures 1A–D are compared to Figure 1E. The images showed that different pretreatment conditions produce varying effects on the substrate. The effects of DES pretreatment on the groundnut shells can be traced to the biocatalysis characteristics of the solvents (Paiva et al., 2014). Figure 1E presents a more intertwined and smoother arrangement with several fiber layers that can inhibit the activities of microorganisms during digestion. Figures 1A–E indicate that the DES alters the lignin arrangement of the substrate with variation in the influence based on solid:liquid ratios and treatment temperatures. It was observed that the cell walls were broken down, and the initial compact and fine surface were loosened and fragmented, as can be observed in the morphological images shown in Figures 1A–E. It was observed from the images that the varying conditions (solid:liquid ratios and temperature) influenced the defibrillation and coarseness of the substrate. This result agrees with the previous report that indicated that pretreatment techniques significantly influence the structural arrangement of lignocellulose feedstocks. Still, the severity level depends on the microstructural arrangement of the feedstock and pretreatment conditions (Olatunji et al., 2021).

The image in Figure 1A presents more damage to the lignin portion of the feedstock, which is swollen and has higher degrees of surface fragmentation with internal tissue exposure. It shows some tendency for methanogenic bacteria activities to have more accessible space during anaerobic digestion. On the other hand, the image in Figure 1B shows a collapsed structure with pores and cracks. It was observed that the internal tissue exposure was limited compared to other pretreated substrates, which can minimize the accessibility of anaerobic digestion bacteria during digestion. Comparing images picked for treatments A and B, it is evident that the selected solid:liquid ratio significantly influences the impacts of DES pretreatment on the microstructural arrangements of groundnut shells, which agrees with the previous study (Olugbemide et al., 2021). Figures 1C, D depict a significant effect of DES pretreatment on groundnut shells. There is a sign of lignin removal/redistribution, which enhances the accessibility to cellulose and hemicellulose. However, this is more pronounced in Figure 1D than in Figure 1C, which indicates that the solid:liquid ratio is important to the effect of DES pretreatment. These images indicate better availability for methanogenic bacteria, which is expected to improve the biomethane yield, provided the level of inhibitory compounds generated is minimal. Compared to other chemical pretreatment of groundnut shells, DES pretreatment's influence on the microstructural arrangements of groundnut shells is not as severe as that of alkali and acidic pretreatment (Madyira and Olatunji, 2023). This could be due to the strength of the other chemicals, although it is presumed that DES will produce fewer inhibitory compounds, which could be advantageous to biomethane release.

3.1.2 Effects of DES pretreatment on crystallinity

Lignocellulose feedstocks have been observed to consist of both crystalline and non-crystalline microstructures, whereby the cellulose portion is identified as a crystalline structure, while hemicellulose and lignin are reported to be amorphous structures

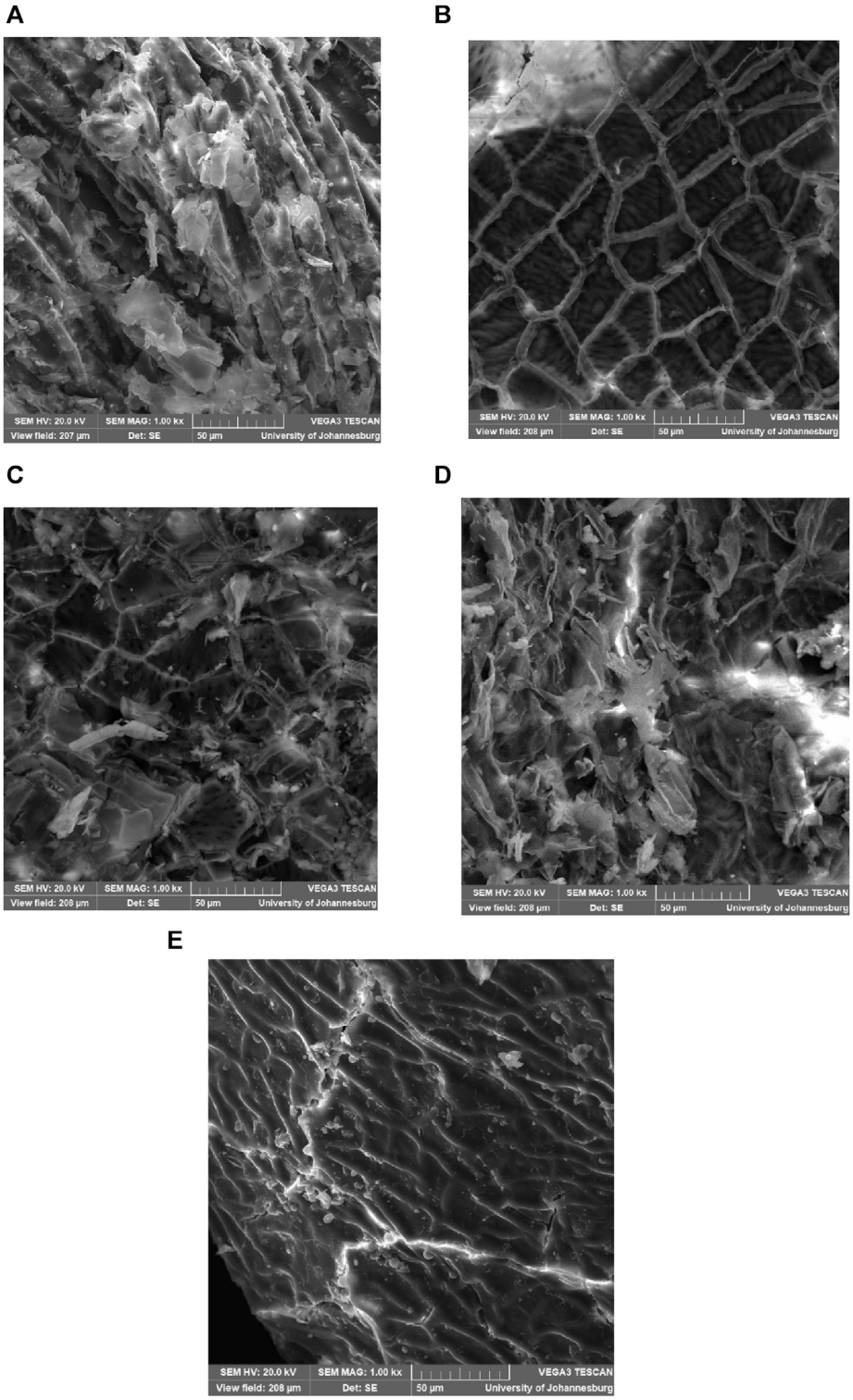

FIGURE 1
SEM images of DES-pretreated **(A)** 1:2 at 80°C, **(B)** 1:4 at 80°C, **(C)** 1:2 at 100°C, 1:4 at 100°C, and untreated groundnut shells.

(Kim and Holtzapple, 2006; Sarbishei et al., 2021). DES-pretreated and untreated groundnut shells were investigated by XRD; the result is illustrated in Figure 2. It was inferred that untreated samples produce seven different distinctive peaks, which is a characteristic of cellulose materials (Olugbemide et al., 2021). It was observed that the peak of the pretreated substrate begins to flatten out at 18°, indicating crystalline reduction and cellulose transformation. There are no significant differences in the intensity of the pretreated samples, meaning that the cellulose did not undergo structural change during pretreatment. No noticeable difference exists

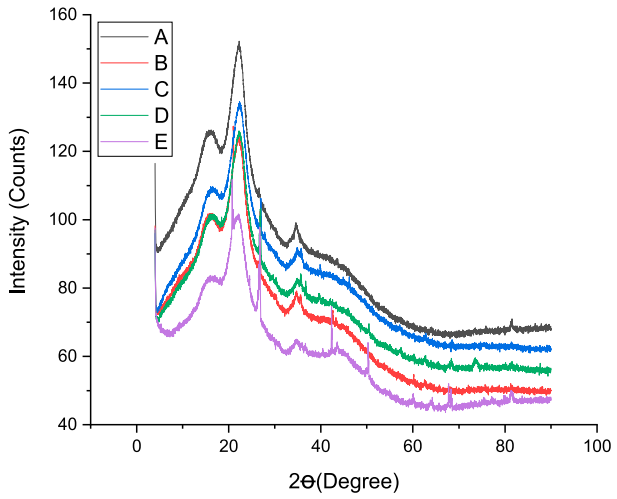

FIGURE 2
XRD analysis of DES-pretreated and untreated groundnut shells.

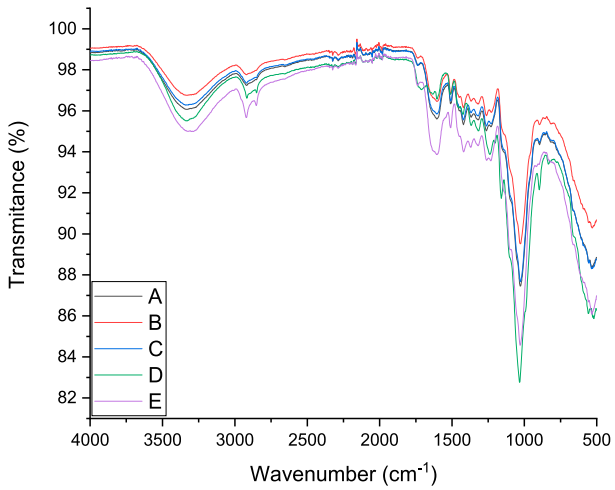

FIGURE 3
FTIR spectra image.

TABLE 2 Crystallinity index of DES-pretreated and untreated groundnut shells

Pretreatment	I_{min} (2Θ = 18°)	I_{max} (2Θ = 22°)	I_c (%)
A	112.04	141.30	20.71
B	107.46	132.96	19.18
C	102.84	129.26	20.44
D	103.11	127.57	19.17
E	94.25	112.90	16.52

between the peaks of the pretreated feedstocks, indicating cellulose transition during dissolution (Moyer et al., 2018).

Table 2 presents the crystallinity index (I_c) of pretreated and untreated substrates. It was observed that the I_c of the samples is 20.71, 19.18, 20.44, 19.17, and 16.52 for treatments A, B, C, D, and E, respectively. It was observed from the table that DES pretreatment significantly influences the I_c of groundnut shells. Compared to the untreated substrate, the I_c was improved by 25.36, 16.10, 23.55, and 16.04% for treatments A, B, C, and D, respectively. It was observed that the solid:liquid ratio plays a more significant role in the I_c than the temperature. A solid:liquid ratio of 1:2 showed better I_c improvement than 1:4, but temperatures did not have any significant impact. This result agrees with other literature works that pretreatment methods influence the I_c of lignocellulose feedstocks. Compared to other studies, this research produced a lower I_c than other pretreatment techniques on the same substrate (Madyira and Olatunji, 2023). The lower I_c recorded in this study can be traced to the reduction in cellulose content, which implies that the DES molar ratio is considered, the solid:liquid ratio is reduced, and the temperature reduces the I_c of groundnut shells. Furthermore, the lower I_c in this study means an increase in the diffraction intensity observed in the amorphous region, which can be linked to the properties of the DES used to recrystallize the cellulose crystal region (Olugbemide et al., 2021). It was also observed that the DES composition partially reduces the amorphous portion, like hemicellulose and lignin. It has been reported that crystalline cellulose restricts microbial activities more than amorphous cellulose (Zhao et al., 2012). Findings from this study support previous investigations on the influence of DES pretreatment techniques on lignocellulose feedstocks (Procentese and Rehmann, 2018). It is difficult to compare the effects of the pretreatment techniques because the impact of pretreatment depends on the structural arrangement of the feedstocks, which varies from one to another (Olatunji et al., 2021). Different studies have investigated the influence of crystallinity on enzymatic hydrolysis, but there is no concrete agreement because other factors involved in the process are more important or the same. When dilute acidic pretreatment of lignocellulose materials was considered, it was observed that the I_c did not directly relate to enzymatic hydrolysis (Moutta et al., 2014).

On the other hand, a significant relationship between the I_c and enzymatic hydrolysis at high enzyme loading was observed to be negative. The investigation also opined that the influence of the I_c on enzymatic hydrolysis needs to be examined without enzymes being a hindrance parameter (Li et al., 2014). The result of I_c values from this investigation showed an improved crystallinity compared to untreated substrate, and it is expected to enhance biomethane yield provided other factors (inhibitory compounds, pH, temperature, etc.) are within the acceptable range.

3.1.3 Functional group analysis

The impact of DES pretreatment on the functional group characteristics of groundnut shells and untreated feedstock was examined under FTIR spectra. Figure 3 illustrates the detailed characterization and spectra images, while Table 3 presents the spectrum assignment as observed by Shahid et al. (2020). The samples followed the same pattern until 3,329 cm^{-1} wavenumber was reached, as shown in Figure 3. The O–H straining in the untreated groundnut shells is responsible for the vibration intensity detected at 3,329 cm^{-1}, which decreased with DES treatment. This suggests that both intramolecular and extramolecular hydrogen bonds in the cellulose were broken down, which facilitates better cellulose digestion because the dissolution of hydrogen bonds can modify how

TABLE 3 FTIR spectrum peak assignments of groundnut shells pretreated with DES at varying conditions.

Number	Wavenumber (cm^{-1})	Functional group	Assignment
1	3,329	O–H stretching vibration	Hydrogen cellulose connection bond
2	2,921	CH and CH_2 up stretching vibration	Methyl/methylene cellulose
3	2,624	C=O asymmetric bending vibration of xylan	Hemicellulose and lignin removal
4	1,992	C=C straining vibration of the aromatic ring	Lignin removal
5	1,792	C=C vibrating of the aromatic ring	Changes in lignin structure
6	1,509	C–O–C straining vibration	Acetyl–lignin group cleavage
7	1,262	C–O straining vibration	Hemicellulose and cellulose
8	1,027		
9	896	-CH bending vibration in the plane	Amorphous cellulose

groundnut hells are arranged and increase the amount of cellulose available for anaerobic digestion. Similar straining vibrations for –CH and $–CH_2$ were revealed by the vibration detected at 2,921 cm^{-1}. This indicates a partial breakdown of the carbon chain following DES pretreatment, which results in the alteration in the cellulose structure. Carbonyl bands are apparent at approximately 2,624 cm^{-1} and are associated with the hydroxyl C=O straining vibration. These are the ester functional groups connected to ketones, carboxylic compounds, celluloses, and hemicelluloses (Heredia-Guerrero et al., 2014). This feature is readily discernible in the untreated substrate, and it was observed that it gradually vanished in all the treated specimens. The extinction of the carbonyl might be connected to the removal of a significant amount of lignin. The C=C aromatic structural vibration in lignin and the C=C straining of the aromatic ring are responsible for the strength of vibrations at 1,992 cm^{-1} and 1,792 cm^{-1}, respectively. The strength of the substrate samples was lowered at different points following the DES pretreatment. As the solid:liquid ratio and temperature increased, the vibration strength at 1,509 cm^{-1} indicated that the C–O–C stretching vibration was less prominent in the untreated substrate, confirming lignin removal.

However, the C–O stretching vibration in cellulose and hemicellulose is represented by the vibration strength at 1,262 cm^{-1}. The strength was moderately reduced, suggesting that the DES pretreatment fractured the hemicellulose and cellulose parts. There was no discernible difference in treatments A and C and the peak at 896 cm^{-1} except for treatments B and D. This section displays the C–H bending vibration in the cellulose's plane, and the 1:2 solid:liquid ratio has the most impact on it.

3.2 Effect of DES on the physicochemical properties of groundnut shells

The AOAC standard procedure was used to determine the TS and VS of the DES-pretreated and untreated groundnut shells (Official Methods of Analysis, 21st Edition (2019)—AOAC INTERNATIONAL, 2019). It was noticed that the TS value was 85.00, 78.63, 100, 98.64, and 100% for treatments A, B, C, D, and E, respectively. Likewise, the VS values of 97.00, 97.00, 98.50, 99.00, and 94.00 were observed for treatments A, B, C, D, and E, respectively. It was noticed that DES pretreatment influenced the TS and VS of groundnut shells. The VS values of pretreated groundnut shells were improved compared to those of the untreated substrate. This can be linked to the strength of the pretreatment technique to remove/redistribute the lignin portion and expose the cellulose, the major content for biomethane production. This indicates that the pretreated substrate's biomethane potential is high since the VS represents the percentage of substrate available for biogas production. This result corroborates previous studies on the influence of pretreatment on the VS of lignocellulose materials (Olatunji and Madyira, 2023c). It was noticed that the solid:liquid ratio does not significantly impact the VS of the substrate, but temperature variation does. EDS pretreatment was discovered to influence the elemental composition of groundnut shells. The analysis shows that DES pretreatment increases the percentage of the carbon content but reduces the nitrogen content. The increase in carbon content indicates food availability for methanogenic activities during biomethane production and determines the quantity and quality of biomethane released (Khayum et al., 2020). This may be because some nitrogen content was used or released during pretreatment. This has a significant influence on the C/N ratio of the substrate. It was noticed that the C/N ratios were 48.37, 47.29, 52.95, 66.93, and 27.63 for treatments A, B, C, D, and E, respectively. It has been observed that a C/N ratio of 20–30 is the most productive for biomethane production (Kainthola et al., 2020). This implies that only the untreated substrate falls within the range. An inoculum high in nitrogen content will be ideal for effectively digesting the pretreated substrate. DES pretreatment affected the values of hydrogen and oxygen content, as shown in Table 4. This result agreed with previous studies on the impact of DES pretreatment on the physicochemical characteristics of lignocellulose feedstocks (Dai et al., 2013; Smith et al., 2014; Procentese et al., 2015).

3.3 Effect of DES pretreatment on biomethane yield

3.3.1 Daily biomethane yield

The daily biomethane yield generated from the DES-pretreated and untreated groundnut shells is illustrated in Figure 4. It was observed that biomethane release began from all digesters on day 2,

TABLE 4 Physicochemical characteristics of pretreated and untreated groundnut shells (%wt).

Treatments	TS (%)	VS (%)	C (%)	N (%)	H (%)	O (%)	C/N
A	85.00	97.00	43.53	0.90	6.06	49.01	48.37
B	78.63	97.00	47.29	1.00	5.80	45.71	47.29
C	100.00	98.50	46.60	0.88	5.73	46.29	52.95
D	98.64	99.00	50.87	0.76	5.73	42.14	66.93
E	100.00	94.00	44.21	1.60	5.68	48.01	27.63

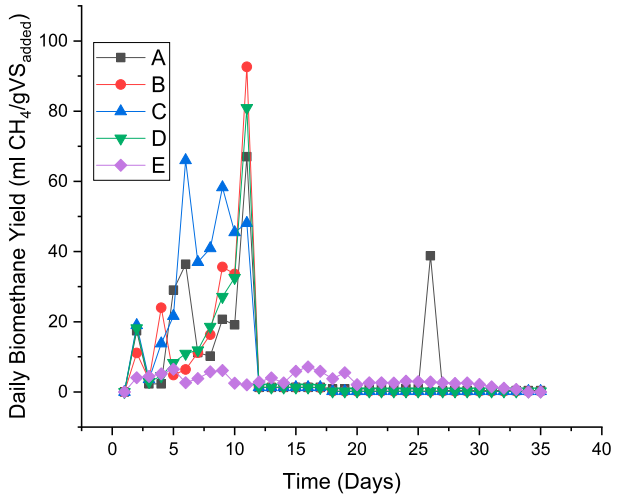

FIGURE 4
Daily biomethane yield of DES-pretreated and untreated groundnut shells.

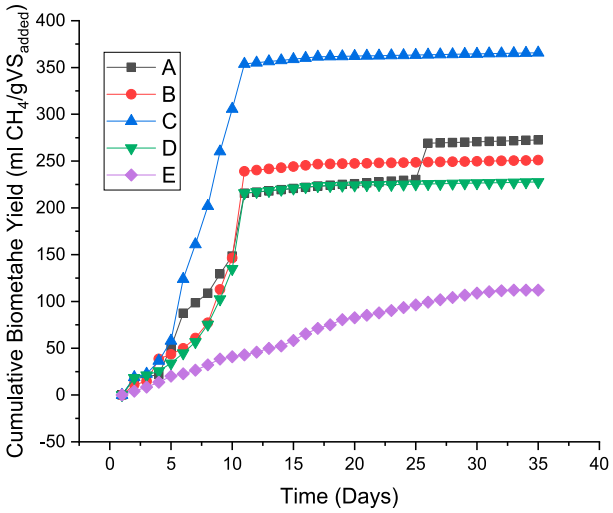

FIGURE 5
Cumulative biomethane yield of DES-pretreated and untreated groundnut shells.

although at a different rate. The result indicates that biomethane yield from DES-pretreated samples declines after day 2 before it peaks up later during digestion. The daily biomethane yield was observed to be improved by DES pretreatment when compared to the untreated substrate. The optimum daily biomethane yield of 92.60 mL CH_4/gVS_{added} was recorded on day 11, while the least biomethane yield from the DES-pretreated substrate was observed from treatment A on day 6. The optimum daily biomethane released was recorded between days 6 and 11 for pretreated substrates, whereas the optimum daily biomethane yield from untreated substrates was recorded on day 16. This result further established the previous findings that pretreatment methods influence the daily biomethane yield of lignocellulose feedstocks (Olatunji and Madyira, 2023d). This indicates that DES pretreatment significantly affects the daily biomethane yield and reduces the retention time of the process. Optimum daily biomethane concentrations of 36.40, 92.60, 66.00, 80.90, and 7.12 mL CH_4/gVS_{added} were reported for treatments A, B, C, D, and E at days 6, 11, 6, 11, and 16, respectively. It was noticed that the solid:liquid ratio plays a major role in the daily yield more than the temperature. A solid:liquid ratio of 1:4 produced the highest daily biomethane yield at the temperature ranges considered. This can be linked with the strength of the DES to remove/redistribute the lignin portion of the substrate, thereby making the cellulose accessible for methanogenic bacteria. Treatment B was observed to produce a spike on day 26 after flattening for some days, while all other treatments continued with their flattening curve. It can be inferred from this study that DES pretreatment under all the conditions experimented to improve the daily biomethane yield of groundnut shells. This investigation agreed with previous studies that concluded that pretreatment at appropriate levels could enhance the daily biomethane yield of lignocellulose feedstocks (Almomani et al., 2019; Olatunji et al., 2021).

3.3.2 Cumulative biomethane yield

DES-pretreated and untreated groundnut shells were subjected to anaerobic digestion for 35 days in a laboratory batch reactor at mesophilic conditions, and the biomethane yield is presented in Figure 5. The total biomethane yield of 272.50, 251.00, 365.70, 227.70, and 112.16 mL CH_4/gVS_{added} was recorded for treatments A, B, C, D, and E, respectively. Compared to the untreated substrate, it was observed that the biomethane yield was improved by 142.96, 123.79, 226.05, and 103.01% for treatments A, B, C, and D, respectively. It was deduced from the result that all the pretreatment conditions of DES considered in this study enhance the biomethane yield but at different percentages. This agreed with previous studies that observed pretreatment techniques improve the biomethane yield of lignocellulose feedstocks (Olugbemide et al.,

TABLE 5 elemental formula, theoretical and experimental biomethane potential, and biodegradability of groundnut shells.

Treatment	Elemental formula (N)	TMY (ml CH_4/gVS_{added})	EMY (ml CH_4/gVS_{added})	BD (%)
A	$C_{60.5}H_{101}O_{51}$	402.17	272.50	67.76
B	$C_{56.29}H_{82.86}O_{40.86}$	438.39	251.00	57.25
C	$C_{64.67}H_{95.5}O_{48.17}$	430.89	365.70	84.87
D	$C_{84.8}H_{114.6}O_{52.6}$	486.81	227.70	46.77
E	$C_{33.45}H_{51.64}O_{27.27}$	396.62	112.16	28.28

TMY, theoretical methane yield; EMY, experimental methane yield; BD, biodegradability.

2021; Dasgupta et al., 2022; Olatunji et al., 2023b). It was observed from Figure 5 that there was a slow biomethane enhancement from all the pretreated samples at the beginning of the digestion. Still, a significant increase was experienced within the first 11 days of the retention period before it flattened around the middle of the retention period. It was inferred that the DES pretreatment method reduces the retention period of the digestion process. The influence of the solid:liquid ratio is more pronounced than that of the temperature. The result indicates that a 1:2 ratio of solid: liquid produces better biomethane yield at the different temperatures. The optimum cumulative biomethane yield of 365.70 mL CH_4/gVS_{added} was observed from treatment C (1:2 of solid:liquid at 100°C). The least liquid ratio produced the best result because of fewer inhibitory compounds due to less liquid available for pretreatment. It was inferred from the effect that a higher solid: liquid ratio with a high temperature generates the least yield besides the untreated feedstock. This could be linked to the ability of the chemical and temperature to release inhibitory compounds during the pretreatment process. Another reason for the lower yield could be cellulose loss during pretreatment. When the biomethane yields are compared to the effect of pretreatment on the microstructural arrangement using SEM, it was noticed that the most affected samples release the highest biomethane yield. This indicates a significant correlation between microstructural arrangements and methane yield. This supports the previous studies that considered the influence of pretreatment methods on microstructural arrangements and biomethane yield (Olatunji et al., 2022a). The variation in the percentage of biomethane yield corresponding to the crystallinity index results in a slight difference. It can be established from this study that crystallinity plays a significant role in biomethane yield.

Compared with other chemical pretreatment methods of groundnut shells, it was observed that DES pretreatment produces a better yield. The methane yield of groundnut shells was enhanced by 69.79% when 3% NaOH was used for 15 min at 90°C (Olatunji et al., 2022c). Thermal pretreatment with conventional heating produces a 23.96% increase in biomethane yield, and it was observed that the low improvement could be traced to the release of inhibitory compounds during pretreatment (Olatunji et al., 2022a). A 178% increase in methane yield released was reported when acidic pretreatment of groundnut shells was considered (Olatunji and Madyira, 2023b). It can be observed that among some of the pretreatment techniques experimented with on groundnut shells, DES pretreatment produced the most significant improvement except when combined pretreatment (particle size reduction and Fe_3O_4 additive) was investigated (Olatunji et al., 2022b). However, it has been reported that combined pretreatment increases the cost of production compared to single pretreatment, which could present DES pretreatment as the most efficient method. When DES pretreatment was investigated on corn stover, it was noticed that biomethane yield was improved by 48% (Olugbemide et al., 2021), which is lower than the improvement achieved in this study. Although there are few studies available on DES pretreatment for biogas production, there are few that focus on other end products. Corn cob was pretreated with DES before saccharification, and an approximately 76% increase in yield was observed (Procentese et al., 2015). Enzymatic hydrolysis of oil palm trunk pretreated with DES for 24 h at 50°C produces an optimum glucose yield of 74% (Zulkefli et al., 2017). Compared with other chemical pretreatment techniques on other lignocellulose materials, it can be observed that DES pretreatment on groundnut shells is more efficient in yield. Sweet sorghum was pretreated with different techniques, and it was noticed that pretreatment with NaOH produced the highest gas, followed by oxidative pretreatment. The result showed a 90.9% rise in hydrolysis with a 19.1% increase in total sugar (Cao et al., 2012). It has been discovered that the oxidative pretreatment of rice straw increases the biogas yield; when the biogas yield and process economy are considered, the efficiency is 3% (Song et al., 2012). Anaerobic digestion of sunflower stalks produced 33% more biogas when applying oxidative pretreatment (Monlau et al., 2012). When the results of this study are compared to those of the previous investigation, it becomes evident that the lignocellulose feedstocks' efficiency varies. Differences in the DES composition, temperature, time, and the microstructural arrangement of groundnut shells may cause this fluctuation. It can be shown from the findings that none of the lignocellulose feedstocks reviewed generates more efficient outcomes than the one found in this study when treated chemically. It is also more successful than some of the results in the literature. Since the lignocellulosic arrangement and pretreatment circumstances differ, it is difficult to conclude that this chemical pretreatment is superior to other findings.

3.3.3 Biodegradability rate

Equations 4, 5 were used to calculate the theoretical methane yield and biodegradability rate of the pretreated and untreated groundnut shells, and the result is presented in Table 5. The result indicates that DES pretreatment influenced the elemental composition of the substrate, theoretical methane yield, experimental methane yield, and biodegradability rate. The result indicates that DES pretreatment improves the biomethane potential of groundnut shells. Despite DES pretreatment, it was observed that only 67.76, 57.26, 84.87, and 46.77% of the theoretical methane yield was released while only 28.28% of the theoretical methane yield of

the untreated substrate was released. It was noticed that a lower solid:liquid ratio (1:2) with a lower temperature (80°C) has a higher biodegradability rate (84.87%). At either temperature considered, it was discovered that a lower temperature with a lower solid:liquid ratio produced the best biodegradability rate. The lower biodegradability of a higher solid:liquid ratio and temperature could be linked to the release of inhibitory compounds produced during pretreatment from both chemical and heat used. This agreed with earlier reports on the ability of thermal and chemical pretreatment to generate inhibitory compounds at higher temperatures and chemical concentrations (Zhang et al., 2011; Bolado-Rodríguez et al., 2016; Dumlu et al., 2017; Şenol, 2021). Considering the percentage of degradation, the addition of another pretreatment method could improve the yield further.

4 Conclusion

The deep eutectic solvent pretreatment of groundnut shells using choline chloride and ethyl glycerol at different solid:liquid ratios and temperatures was studied. The pretreatment method was observed to be efficient for lignocellulose material in terms of microstructural arrangement and biomethane yield. The microstructural analysis of the pretreated substrate indicates that DES pretreatment alters the substrate's structural arrangement, improving the enzymatic hydrolysis, biodegradability, and biomethane yield of groundnut shells. Biomethane yield was increased from 112.16 to 365.70 mL CH_4/gVS_{added}, and it was discovered that a solid:liquid ratio of 1:2 at 100°C produced the optimum biomethane yield. Results from this investigation are comparable with existing studies where lignocellulose pretreatment improves the enzymatic hydrolysis and methane yield. This study produced a further step toward establishing baselines for optimum pretreatment conditions for the DES pretreatment of lignocellulose feedstocks.

Data availability statement

The raw data supporting the conclusion of this article will be made available by the authors, without undue reservation.

Author contributions

KO: conceptualization, investigation, methodology, and writing–original draft. DM: conceptualization, investigation, project administration, supervision, and writing–review and editing.

Funding

The authors declare that no financial support was received for the research, authorship, and/or publication of this article.

Conflict of interest

The authors declare that the research was conducted in the absence of any commercial or financial relationships that could be construed as a potential conflict of interest.

Publisher's note

References

Abbott, A. P., Collins, J., Dalrymple, I., Harris, R. C., Mistry, R., Qiu, A. F., et al. (2009). Processing of electric arc furnace dust using deep eutectic solvents. *Aust. J. Chem.* 62, 341–347. doi:10.1071/CH08476

Almomani, F., Bhosale, R. R., Khraisheh, M. A. M., and Shawaqfah, M. (2019). Enhancement of biogas production from agricultural wastes via pre-treatment with advanced oxidation processes. *Fuel* 253, 964–974. doi:10.1016/J.FUEL.2019.05.057

Alvarez-Vasco, C., Ma, R., Quintero, M., Guo, M., Geleynse, S., Ramasamy, K. K., et al. (2016). Unique low-molecular-weight lignin with high purity extracted from wood by deep eutectic solvents (DES): a source of lignin for valorization. *Green Chem.* 18, 5133–5141. doi:10.1039/C6GC01007E

AOAC INTERNATIONAL (2019). *Official methods of analysis*. 21st Edition. Available at: https://www.aoac.org/official-methods-of-analysis-21st-edition-2019/ (Accessed October 15, 2021).

Arezki, R., and Matsumoto, A. (2017). Chapter 4. The energy transition in an era of low fossil fuel prices. *Int. Monet. Fund.* Available at: https://www.elibrary.imf.org/display/book/9781484310328/ch004.xml (Accessed November 3, 2023).

Atalla, R. H., and VanderHart, D. L. (1999). The role of solid state NMR spectroscopy in studies of the nature of native celluloses. *Solid State Nucl. Magn. Reson* 15, 1–19. doi:10.1016/S0926-2040(99)00042-9

Bolado-Rodríguez, S., Toquero, C., Martín-Juárez, J., Travaini, R., and García-Encina, P. A. (2016). Effect of thermal, acid, alkaline and alkaline-peroxide pretreatments on the biochemical methane potential and kinetics of the anaerobic digestion of wheat straw and sugarcane bagasse. *Bioresour. Technol.* 201, 182–190. doi:10.1016/j.biortech.2015.11.047

Brémond, U., de Buyer, R., Steyer, J. P., Bernet, N., and Carrere, H. (2018). Biological pretreatments of biomass for improving biogas production: an overview from lab scale to full-scale. *Renew. Sustain. Energy Rev.* 90, 583–604. doi:10.1016/j.rser.2018.03.103

Brennan, L., and Owende, P. (2010). Biofuels from microalgae-A review of technologies for production, processing, and extractions of biofuels and co-products. *Renew. Sustain. Energy Rev.* 14, 557–577. doi:10.1016/j.rser.2009.10.009

Buswell, A. M., and Mueller, H. F. (2002). Mechanism of methane fermentation. *Ind. Eng. Chem.* 44, 550–552. doi:10.1021/IE50507A033

Cai, D., Li, P., Chen, C., Wang, Y., Hu, S., Cui, C., et al. (2016). Effect of chemical pretreatments on corn stalk bagasse as immobilizing carrier of Clostridium acetobutylicum in the performance of a fermentation-pervaporation coupled system. *Bioresour. Technol.* 220, 68–75. doi:10.1016/J.BIORTECH.2016.08.049

Caillet, H., Lebon, E., Akinlabi, E., Madyira, D., and Adelard, L. (2019). Influence of inoculum to substrate ratio on methane production in Biochemical Methane Potential (BMP) tests of sugarcane distillery waste water. *Procedia Manuf.* 35, 259–264. doi:10.1016/J.PROMFG.2019.05.037

Cao, W., Sun, C., Liu, R., Yin, R., and Wu, X. (2012). Comparison of the effects of five pretreatment methods on enhancing the enzymatic digestibility and ethanol production from sweet sorghum bagasse. *Bioresour. Technol.* 111, 215–221. doi:10.1016/j.biortech.2012.02.034

Chowdhury, H., Chowdhury, T., Sharifi, A., Corkish, R., and Sait, S. M. (2022). Role of biogas in achieving sustainable development goals in Rohingya refugee camps in Bangladesh. *Sustain. Switz.* 14, 11842. doi:10.3390/su141911842

Dahunsi, S. O., Adesulu-Dahunsi, A. T., Osueke, C. O., Lawal, A. I., Olayanju, T. M. A., Ojediran, J. O., et al. (2019). Biogas generation from Sorghum bicolor stalk: effect of pretreatment methods and economic feasibility. *Energy Rep.* 5, 584–593. doi:10.1016/j.egyr.2019.04.002

Dahunsi, S. O., Oranusi, S., and Efeovbokhan, V. E. (2017). Optimization of pretreatment, process performance, mass and energy balance in the anaerobic

digestion of *Arachis hypogaea* (Peanut) hull. *Energy Convers. Manag.* 139, 260–275. doi:10.1016/J.ENCONMAN.2017.02.063

Dai, Y., van Spronsen, J., Witkamp, G. J., Verpoorte, R., and Choi, Y. H. (2013). Natural deep eutectic solvents as new potential media for green technology. *Anal. Chim. Acta* 766, 61–68. doi:10.1016/j.aca.2012.12.019

Dasgupta, S., Li, J., Chikani-Cabrera, K. D., Machado, P., Fernandes, B., Tapia-Tussell, R., et al. (2022). Improvement in methane production from pelagic *sargassum* using combined pretreatments. *Life (Basel)* 12, 1214. doi:10.3390/LIFE12081214

Dumlu, L., Gunerhan, U., Us, E., Yilmaz, V., Carrère, H., Perendeci, A., et al. (2017). Effects of thermal-HCl pretreatment process on biogas production from greenhouse residues Effects of thermal-HCl pretreatment process on biogas production from greenhouse residues Effects of thermal-HCl pretreatment process on biogas production from greenhouse residues No.IWA-503590 METHODS towards a more sustainable world INTRODUCTION. Available at: http://www.AD15.org.cn.

Elbeshbishy, E., Nakhla, G., and Hafez, H. (2012). Biochemical methane potential (BMP) of food waste and primary sludge: influence of inoculum pre-incubation and inoculum source. *Bioresour. Technol.* 110, 18–25. doi:10.1016/J.BIORTECH.2012.01.025

European Parliament (2017). Texts adopted - 2017 UN climate change conference in Bonn, Germany (COP23) - Wednesday. Available at: https://www.europarl.europa.eu/doceo/document/TA-8-2017-0380_EN.html (Accessed November 3, 2023).

Gautam, P., Kumar, S., and Lokhandwala, S. (2019). "Energy-aware intelligence in megacities," in *Current developments in biotechnology and bioengineering: waste treatment processes for energy generation*, 211–238. doi:10.1016/B978-0-444-64083-3.00011-7

Gore, S., Baskaran, S., and Koenig, B. (2011). Efficient synthesis of 3,4-dihydropyrimidin-2-ones in low melting tartaric acid–urea mixtures. *Green Chem.* 13, 1009–1013. doi:10.1039/C1GC00009H

Gorke, J. T., Srienc, F., and Kazlauskas, R. J. (2008). Hydrolase-catalyzed biotransformations in deep eutectic solvents. *Chem. Commun.*, 1235–1237. doi:10.1039/B716317G

Guo, M., Song, W., and Buhain, J. (2015). Bioenergy and biofuels: history, status, and perspective. *Renew. Sustain. Energy Rev.* 42, 712–725. doi:10.1016/J.RSER.2014.10.013

Heredia-Guerrero, J. A., Benítez, J. J., Domínguez, E., Bayer, I. S., Cingolani, R., Athanassiou, A., et al. (2014). Infrared and Raman spectroscopic features of plant cuticles: a review. *Front. Plant Sci.* 5, 305. doi:10.3389/FPLS.2014.00305

Jekayinfa, S. O., Adebayo, A. O., Oniya, O. O., and Olatunji, K. O. (2020). Comparative analysis of biogas and methane yields from different sizes of groundnut shell in a batch reactor at mesophilic temperature. *J. Energy Res. Rev.* 5, 34–44. doi:10.9734/jenrr/2020/v5i130140

Jhong, H. R., Wong, D. S. H., Wan, C. C., Wang, Y. Y., and Wei, T. C. (2009). A novel deep eutectic solvent-based ionic liquid used as electrolyte for dye-sensitized solar cells. *Electrochem Commun.* 11, 209–211. doi:10.1016/J.ELECOM.2008.11.001

Kabera, T., and Nishimwe, H. (2019). Systems analysis of municipal solid waste management and recycling system in east Africa: benchmarking performance in Kigali city, Rwanda. *E3S Web Conf.* 80, 03004. doi:10.1051/E3SCONF/20198003004

Kainthola, J., Kalamdhad, A. S., and Goud, V. V. (2020). Optimization of process parameters for accelerated methane yield from anaerobic co-digestion of rice straw and food waste. *Renew. Energy* 149, 1352–1359. doi:10.1016/J.RENENE.2019.10.124

Khayum, N., Rout, A., Deepak, B. B. V. L., Anbarasu, S., and Murugan, S. (2020). Application of fuzzy regression analysis in predicting the performance of the anaerobic reactor Co-digesting spent tea waste with cow manure. *Waste Biomass Valorization* 11, 5665–5678. doi:10.1007/s12649-019-00874-9

Kim, S., and Holtzapple, M. T. (2006). Effect of structural features on enzyme digestibility of corn stover. *Bioresour. Technol.* 97, 583–591. doi:10.1016/J.BIORTECH.2005.03.040

Li, L., Zhou, W., Wu, H., Yu, Y., Liu, F., and Zhu, D. (2014). Relationship between crystallinity index and enzymatic hydrolysis performance of celluloses separated from aquatic and terrestrial plant materials. *Bioresources* 9, 3993–4005. doi:10.15376/BIORES.9.3.3993-4005

Madyira, D. M., and Olatunji, K. O. (2023). Investigating the influence of different pretreatment methods on the morphological structure of Arachis hypogea shells. *Mater Today Proc.* doi:10.1016/J.MATPR.2023.07.289

Millati, R., Syamsiah, S., Niklasson, C., Nur Cahyanto, M., Lundquist, K., and Taherzadeh, M. J. (2011). *Biological pretreatment: review*.

Monlau, F., Barakat, A., Steyer, J. P., and Carrere, H. (2012). Comparison of seven types of thermo-chemical pretreatments on the structural features and anaerobic digestion of sunflower stalks. *Bioresour. Technol.* 120, 241–247. doi:10.1016/J.BIORTECH.2012.06.040

Monlau, F., Barakat, A., Trably, E., Dumas, C., Steyer, J. P., and Carrère, H. (2013). Lignocellulosic materials into biohydrogen and biomethane: impact of structural features and pretreatment. *Crit. Rev. Environ. Sci. Technol.* 43, 260–322. doi:10.1080/10643389.2011.604258

Moutta, R. D. O., Ferreira-Leitão, V. S., and Bon, E. P. D. S. (2014). Enzymatic hydrolysis of sugarcane bagasse and straw mixtures pretreated with diluted acid. *Biocatal. Biotransformation* 32, 93–100. doi:10.3109/10242422.2013.873795

Moyer, P., Kim, K., Abdoulmoumine, N., Chmely, S. C., Long, B. K., Carrier, D. J., et al. (2018). Structural changes in lignocellulosic biomass during activation with ionic liquids comprising 3-methylimidazolium cations and carboxylate anions 03 Chemical Sciences 0306 Physical Chemistry (incl. Structural). *Biotechnol. Biofuels* 11, 1–13. doi:10.1186/S13068-018-1263-0/FIGURES/7

Ogunkunle, O., Olatunji, K. O., and Jo, A. (2018). Comparative analysis of Co-digestion of cow dung and jatropha cake at ambient temperature. *Res. Article.* doi:10.4172/2090-4541.1000271

Okedu, K. E., Barghash, H. F., and Al Nadabi, H. A. (2022). Sustainable waste management strategies for effective energy utilization in Oman: a review. *Front. Bioeng. Biotechnol.* 10, 825728. doi:10.3389/fbioe.2022.825728

Olatunji, K. O., Ahmed, N. A., and Ogunkunle, O. (2021). Optimization of biogas yield from lignocellulosic materials with different pretreatment methods: a review. *Biotechnol. Biofuels* 14, 159. doi:10.1186/s13068-021-02012-x

Olatunji, K. O., and Madyira, D. M. (2023a). Anaerobic co-digestion of alkali-pretreated groundnut shells and duck waste for methane yield optimization and sustainable environment. *E3S Web Conf.* 433, 02005. doi:10.1051/E3SCONF/202343302005

Olatunji, K. O., and Madyira, D. M. (2023b). Effect of acidic pretreatment on the microstructural arrangement and anaerobic digestion of Arachis hypogea shells; and process parameters optimization using response surface methodology. *Heliyon* 9, e15145. doi:10.1016/j.heliyon.2023.e15145

Olatunji, K. O., and Madyira, D. M. (2023c). Effect of acidic pretreatment on the microstructural arrangement and anaerobic digestion of Arachis hypogea shells; and process parameters optimization using response surface methodology. *Heliyon* 9, e15145. doi:10.1016/J.HELIYON.2023.E15145

Olatunji, K. O., and Madyira, D. M. (2023d). Optimization of biomethane yield of xyris capensis grass using oxidative pretreatment. *Energies 2023* 16, 3977. *Page 3977* 16. doi:10.3390/EN16103977

Olatunji, K. O., Madyira, D. M., and Adeleke, O. (2023a). Optimizing anaerobic co-digestion of Xyris capensis and duck waste using neuro-fuzzy model and response surface methodology. *Fuel* 354, 129334. doi:10.1016/J.FUEL.2023.129334

Olatunji, K. O., Madyira, D. M., Ahmed, N. A., and Ogunkunle, O. (2022a). Biomethane production from Arachis hypogea shells: effect of thermal pretreatment on substrate structure and yield. *Biomass Convers. Biorefin.* doi:10.1007/s13399-022-02731-7

Olatunji, K. O., Madyira, D. M., Ahmed, N. A., and Ogunkunle, O. (2022b). Effect of combined particle size reduction and Fe_3O_4 additives on biogas and methane yields of Arachis hypogea shells at mesophilic temperature. *Energies (Basel)* 15, 3983. doi:10.3390/en15113983

Olatunji, K. O., Madyira, D. M., Ahmed, N. A., and Ogunkunle, O. (2022c). Influence of alkali pretreatment on morphological structure and methane yield of Arachis hypogea shells. *Biomass Convers. Biorefin.* doi:10.1007/s13399-022-03271-w

Olatunji, K. O., Madyira, D. M., and Amos, J. O. (2023b). Sustainable enhancement of biogas and methane yield of macroalgae biomass using different pretreatment techniques: a mini-review. *Energy Environ.* doi:10.1177/0958305X231193869

Olugbemide, A. D., Oberlintner, A., Novak, U., and Likozar, B. (2021). Lignocellulosic corn stover biomass pre-treatment by deep eutectic solvents (DES) for biomethane production process by bioresource anaerobic digestion. *Sustain. 2021* 13 10504 13, 10504. doi:10.3390/su131910504

Orozco-González, J. G., Amador-Castro, F., Gordillo-Sierra, A. R., García-Cayuela, T., Alper, H. S., and Carrillo-Nieves, D. (2022). Opportunities surrounding the use of sargassum biomass as precursor of biogas, bioethanol, and biodiesel production. *Front. Mar. Sci.* 8, 2066. doi:10.3389/fmars.2021.791054

Oyedepo, S. O. (2012). On energy for sustainable development in Nigeria. *Renew. Sustain. Energy Rev.* 16, 2583–2598. doi:10.1016/J.RSER.2012.02.010

Paiva, A., Craveiro, R., Aroso, I., Martins, M., Reis, R. L., and Duarte, A. R. C. (2014). Natural deep eutectic solvents - solvents for the 21st century. *ACS Sustain Chem. Eng.* 2, 1063–1071. doi:10.1021/sc500096j

Patowary, D., and Baruah, D. C. (2018). Effect of combined chemical and thermal pretreatments on biogas production from lignocellulosic biomasses. *Ind. Crops Prod.* 124, 735–746. doi:10.1016/J.INDCROP.2018.08.055

Podgorbunskikh, E. M., Bychkov, A. L., Ryabchikova, E. I., and Lomovsky, O. I. (2020). The effect of thermomechanical pretreatment on the structure and properties of lignin-rich plant biomass. *Molecules* 25, 995. doi:10.3390/MOLECULES25040995

Procentese, A., Johnson, E., Orr, V., Garruto Campanile, A., Wood, J. A., Marzocchella, A., et al. (2015). Deep eutectic solvent pretreatment and subsequent saccharification of corncob. *Bioresour. Technol.* 192, 31–36. doi:10.1016/J.BIORTECH.2015.05.053

Procentese, A., and Rehmann, L. (2018). Fermentable sugar production from a coffee processing by-product after deep eutectic solvent pretreatment. *Bioresour. Technol. Rep.* 4, 174–180. doi:10.1016/J.BITEB.2018.10.012

Rabemanolontsoa, H., and Saka, S. (2016). Various pretreatments of lignocellulosics. *Bioresour. Technol.* 199, 83–91. doi:10.1016/j.biortech.2015.08.029

Raja, I. A., and Wazir, S. (2017). Biogas production: the fundamental processes. *Univers. J. Eng. Sci.* 5, 29–37. doi:10.13189/ujes.2017.050202

Rimi Abubakar, I., and Aina, Y. (2016). "Achieving sustainable cities in Saudi arabia: juggling the competing urbanization challenges," in *Population growth and rapid urbanization in the developing world*, 43–64. doi:10.4018/978-1-5225-0187-9.ch003

Rincón, B., Heaven, S., Banks, C. J., and Zhang, Y. (2012). Anaerobic digestion of whole-crop winter wheat silage for renewable energy production. *Energy Fuels* 26, 2357–2364. doi:10.1021/EF201985X

Sarbishei, S., Goshadrou, A., and Hatamipour, M. S. (2021). Mild sodium hydroxide pretreatment of tobacco product waste to enable efficient bioethanol production by separate hydrolysis and fermentation. *Biomass Convers. Biorefin* 11, 2963–2973. doi:10.1007/S13399-020-00644-X

Şenol, H. (2021). Effects of NaOH, thermal, and combined NaOH-thermal pretreatments on the biomethane yields from the anaerobic digestion of walnut shells. *Environ. Sci. Pollut. Res. 2021* 28, 21661–21673. 1728. doi:10.1007/S11356-020-11984-6

Shahid, M. K., Kashif, A., Rout, P. R., Aslam, M., Fuwad, A., Choi, Y., et al. (2020). A brief review of anaerobic membrane bioreactors emphasizing recent advancements, fouling issues and future perspectives. *J. Environ. Manage* 270, 110909. doi:10.1016/J.JENVMAN.2020.110909

Shen, X. J., Chen, T., Wang, H. M., Mei, Q., Yue, F., Sun, S., et al. (2020). Structural and morphological transformations of lignin macromolecules during bio-based deep eutectic solvent (DES) pretreatment. *ACS Sustain Chem. Eng.* 8, 2130–2137. doi:10.1021/acssuschemeng.9b05106

Smith, E. L., Abbott, A. P., and Ryder, K. S. (2014). Deep eutectic solvents (DESs) and their applications. *Chem. Rev.* 114, 11060–11082. doi:10.1021/cr300162p

Song, Z., Yang, G., Guo, Y., and Zhang, T. (2012). Comparison of two chemical pretreatments of rice straw for biogas production by anaerobic digestion. *Bioresources* 7, 3223–3236. doi:10.15376/biores.7.3.3223-3236

Substratcharakterisierung, V. (2016). Verein deutscher ingenieure characterisation of the substrate, sampling, collection of material data, fermentation tests vdi 4630 vdi-richtlinien. Available at: www.vdi.de/richtlinien.

Taiwo, A. (2009). Waste management towards sustainable development in Nigeria: a case study of Lagos state. *Int. NGO J.* 4, 173–179. Available at: http://www.academicjournals.org/INGOJ (Accessed November 3, 2023).

Van Soest, P. J., Robertson, J. B., and Lewis, B. A. (1991). Methods for dietary fiber, neutral detergent fiber, and nonstarch polysaccharides in relation to animal nutrition. *J. Dairy Sci.* 74, 3583–3597. doi:10.3168/JDS.S0022-0302(91)78551-2

Venturin, B., Frumi Camargo, A., Scapini, T., Mulinari, J., Bonatto, C., Bazoti, S., et al. (2018). Effect of pretreatments on corn stalk chemical properties for biogas production purposes. *Bioresour. Technol.* 266, 116–124. doi:10.1016/j.biortech.2018.06.069

Xu, H., Peng, J., Kong, Y., Liu, Y., Su, Z., Li, B., et al. (2020). Key process parameters for deep eutectic solvents pretreatment of lignocellulosic biomass materials: a review. *Bioresour. Technol.* 310, 123416. doi:10.1016/J.BIORTECH.2020.123416

Xu, N., Liu, S., Xin, F., Zhou, J., Jia, H., Xu, J., et al. (2019). Biomethane production from lignocellulose: biomass recalcitrance and its impacts on anaerobic digestion. *Front. Bioeng. Biotechnol.* 7, 191. doi:10.3389/fbioe.2019.00191

Yang, Q., Fu, L., Liu, X., and Cheng, M. (2018). Evaluating the efficiency of municipal solid waste management in China. *Int. J. Environ. Res. Public Health* 15, 2448. doi:10.3390/IJERPH15112448

Yildiz, L. (2018). 1.12 fossil fuels. *Compr. Energy Syst.* 1–5, 521–567. doi:10.1016/B978-0-12-809597-3.00111-5

Zhang, H., Zhang, P., Ye, J., Wu, Y., Fang, W., Gou, X., et al. (2016). Improvement of methane production from rice straw with rumen fluid pretreatment: a feasibility study. *Int. Biodeterior. Biodegrad.* 113, 9–16. doi:10.1016/j.ibiod.2016.03.022

Zhang, Q., Tang, L., Zhang, J., Mao, Z., and Jiang, L. (2011). Optimization of thermal-dilute sulfuric acid pretreatment for enhancement of methane production from cassava residues. *Bioresour. Technol.* 102, 3958–3965. doi:10.1016/J.BIORTECH.2010.12.031

Zhao, X., Zhang, L., and Liu, D. (2012). Biomass recalcitrance. Part I: the chemical compositions and physical structures affecting the enzymatic hydrolysis of lignocellulose. *Biofuels, Bioprod. Biorefining* 6, 465–482. doi:10.1002/BBB.1331

Zulkefli, S., Abdulmalek, E., and Abdul Rahman, M. B. (2017). Pretreatment of oil palm trunk in deep eutectic solvent and optimization of enzymatic hydrolysis of pretreated oil palm trunk. *Renew. Energy* 107, 36–41. doi:10.1016/J.RENENE.2017.01.037

frontiers | Frontiers in Energy Research

TYPE Review
PUBLISHED 13 June 2024
DOI 10.3389/fenrg.2024.1397482

OPEN ACCESS

EDITED BY
Mufutau Adekojo Waheed,
Federal University of Agriculture, Nigeria

REVIEWED BY
Kenneth E. Okedu,
Melbourne Institute of Technology, Australia
Leo Raju,
SSN College of Engineering, India

*CORRESPONDENCE
Ayokunle Awelewa,
ayokunle.awelewa@covenantuniversity.edu.ng

RECEIVED 07 March 2024
ACCEPTED 10 May 2024
PUBLISHED 13 June 2024

CITATION
Balogun A, Olajube A, Awelewa A, Agoro S, Okafor F, Sanni T, Samuel I and Ajilore A (2024), Control strategies in enhanced stand-alone mini-grid operations for the NESI–an overview. *Front. Energy Res.* 12:1397482. doi: 10.3389/fenrg.2024.1397482

Control strategies in enhanced stand-alone mini-grid operations for the NESI–an overview

Adeola Balogun[1], Ayobami Olajube[2], Ayokunle Awelewa[3]*, Sodiq Agoro[4], Frank Okafor[1], Timilehin Sanni[3], Isaac Samuel[3] and Adejumoke Ajilore[3]

[1]Department of Electrical and Electronics Engineering, University of Lagos, Lagos, Nigeria, [2]Department of Electrical and Computer Engineering, Florida State University, Tallahassee, FL, United States, [3]Department of Electrical and Information Engineering, Covenant University, Ota, Ogun, Nigeria, [4]Department of Electrical and Computer Engineering, North Carolina State University, Raleigh, NC, United States

Diverse control strategies for enhancing operations of isolated distribution grids are reviewed. Such distribution grids are called mini-grids or micro-grids, depending on their power flow capabilities. Robust control schemes identified in other climates for mini-grid and micro-grid operations are yet to be fully explored in the Nigerian electricity supply industry (NESI). Sustainable control strategies suitable for isolated distribution grids in the NESI predicate on capabilities for diverse objectives, such as energy conservation, affordability, efficient power throughput, and utilization, for enhanced resiliency and reliability. Consequently, the distributed control system in hierarchical layers is identified as a suitable choice for mini-grid operations in Nigeria because of its robustness in scalability and in energy conservation. However, the model predictive control (MPC) scheme is observed to be uniquely applicable in all of the hierarchical control layers. Therefore, a cascade-free MPC with improved robustness against sensitivity to system parameter variation is presented at the primary control layer for an H8 voltage source inverter (VSI) used for grid integration of the solar photovoltaic (PV) system. The H8 inverter gives more promising mitigation strategies against common-mode voltage and leakage current. Moreover, the control of DC link voltage for maximum power point tracking (MPPT) is achieved by the H8 inverter, thereby eliminating the need for a separate converter for MPPT. Thus, sustainability is achieved.

KEYWORDS

distributed control system, hierarchical control system, model predictive control, H8 2-level voltage source inverter, stand-alone mini-grid

1 Introduction

Expansion of the legacy electric power grids in most emerging economies is increasingly becoming unsustainable. The Nigerian electricity supply industry (NESI), in particular, suffers from investment neglect over the last 3 decades. Therefore, the possibility of availability of electric power to every household through national grids in Nigeria has been heavily degraded.

The concept of a much smaller power grid structure trends globally as a viable alternative to the legacy national grids (Xin et al., 2011; Bhandari et al., 2014; Bidram et al., 2014; Cai et al., 2016; Golsorkhi et al., 2017; Shafiee et al., 2018; Wu et al., 2018). Such

grids are termed mini- or micro-grids (Bidram et al., 2014; Cai et al., 2016; Golsorkhi et al., 2017; Shafiee et al., 2018; Wu et al., 2018; Pedrasa et al., 2006; Guerrero et al., 2013a; Guerrero et al., 2013b; Che et al., 2014; Amoateng et al., 2018), with the propensity for more flexibility in configuration (Qu et al., 2008; Arnold, 2011; Aziz et al., 2013; Li et al., 2016; Chen et al., 2017; Chu and Iu, 2017; Sahoo et al., 2017; Morstyn et al., 2018; Arfeen et al., 2019; Lai et al., 2019; Narang et al., 2020) and easier in scalability and deployment, as indicated in the following studies (Bidram et al., 2013; Liu et al., 2014a; Chen et al., 2015; Guo et al., 2015; Moayedi and Davoudi, 2016; Zuo et al., 2016; Dehkordi et al., 2017a; Antoniadou-Plytaria et al., 2017; Wu and Shen, 2017; Kumar et al., 2018; Meng et al., 2018; Dehkordi et al., 2019). Moreover, with the proliferation of renewable energy sources (RESs) in the energy mix because of near zero carbon footprints, micro-/mini-grids are becoming more competitive and attractive for investors than legacy grids. The reason for such competitiveness is partly because most RESs are usually integrated at the distribution buses (Arfeen et al., 2019), which will not require huge capital investment on equipment and manpower because of lower voltage levels of integration (Lovejoy, 1992; Bidram and Davoudi, 2012; Hazelton et al., 2014; Mipoung et al., 2014; Dang et al., 2015; Singh et al., 2015; Unamuno and Barrena, 2015; Nasirian et al., 2016; Dehkordi et al., 2017b; Arcos-Aviles et al., 2018; Castilla et al., 2019; Flowers, 1997; Lasseter, 2002; Lasseter and Paigi, 2004; Lasseter, 2011; Olivares et al., 2014; Tahir and Mazumder, 2015; Chen et al., 2016; Fioriti et al., 2017; Li et al., 2017; Moayedi and Davoudi, 2017; Chen et al., 2018; Sen and Kumar, 2018; Xu et al., 2019; Jumani et al., 2020; Mujtaba et al., 2020; Shrestha et al., 2020; Abdulkareem et al., 2022; Anand et al., 2013; Awelewa et al., 2016; Awelewa et al., 2020; Buja and Kazmierkowski, 2004; Concari et al., 2016; De Carne et al., 2015; De Carne et al., 2018; Faisal et al., 2018; Gao et al., 2017; Holmes and Lipo, 2003; Josep, 2017; Maes and Melkebeek, 2000; Nasirian et al., 2014; Nik Idris and Mohamed Yatim, 2004; Ojo and Kshirsagar, 2003; Perlack et al., 1988; Poddar and Ranganathan, 2004; Surprenant et al., 2011; Vasquez et al., 2012; Xiang et al., 2019; Zhi and Xu, 2007). Such distribution buses with power generation sources when disconnected from the national grid can operate as stand-alone grids in the islanding mode (Chen et al., 2016; Li et al., 2017, Fioriti et al., 2017; Xu et al., 2019, Flowers, 1997; Chen et al., 2018) and can be constituted as the mini- or micro-grids. Power generation systems on such grids are termed distributed generation (DG) (Arfeen et al., 2019; Mujtaba et al., 2020) or embedded generation alternatively. Such micro-/mini-grids are promising power solutions much easier to deploy to remotely off-grid sites and regions severely affected by natural disasters that have been cut off from the main grid.

Since power synchronization with the main grid is completely lost in the islanding mode, the need arises to create references for control of voltage magnitude, frequency, phase angle, and phase sequence in such mini-grids with embedded generation systems. Some other control objectives are quite essential for enhancing the flexibility, functionality, and reliability of such isolated distribution grids (Bhandari et al., 2014; Xin et al., 2011; Pedrasa et al., 2006; Guerrero et al., 2013a). As such, concepts of centralized and decentralized (Li et al., 2016; Liu et al., 2014a) control systems emerged as applicable control schemes to mini-grids and micro-grids. There has not been a generally acceptable defined demarcation between a micro-grid and a mini-grid. In some literature, the quantum of power in a micro-grid is specified to be in the range of tens of kW to hundreds of kW, while the quantity of power flow in a mini-grid could be in the range of tens of MW. In Worldbank (2024), mini-grids were defined as small, privately owned and operated systems with generating up to 10 MW (MW) capacity and a network that distributes power to several customers, which will be adopted herein. However, in (NERC, 2024) a mini-grid was defined as an integrated local generation and distribution system with installed capacity below 1 MW, capable of serving numerous end-users independent of the national grid.

In this paper, therefore, the distribution networks that constitute a mini-grid with diverse distributed generation systems such as fossil fuel-based generating systems, solar photovoltaic (PV) power plant, battery storage system, and mini-hydro systems are methodologically investigated. The power electronics converter topologies utilized for integration and primary control on such a distribution grid are reviewed, as well as the applicable control architecture, strategies, and objectives. Specific examples of efficient control strategies given by power converters are 1) maximum power point tracking (MPPT); 2) charging of batteries; 3) discharging of batteries; 4) specifying (*forming*) of the grid's voltage magnitude, frequency, and phasors; 5) synchronization of the RES for power evacuation into grids. The power generation resources making up the distributed generation systems are suggested to be diversified as a technical solution for improving resiliency and reliability in the mini-grid. Critical loads are suggested to be well-placed in buses that can be constantly supplied with steady electric power. Consequently, sustainable control strategies for mini-grids in the NESI are suggested. Furthermore, a health monitoring and control scheme for all the control layers in mini-grids in the NESI is proposed.

2 Electric power distribution grid: mini-grid

The concepts of small autonomous grids have existed for decades in communities that are off-grid due to economic and/or technical factors (Olivares et al., 2014). In recent times, the terms "mini-grid" and "micro-grid" have been used to characterize such small grids with increased resources, functionalities, and flexibilities. The use of the term "mini-grids" on power networks can be found in literature as far back as the 1980s (Perlack et al., 1988; Faisal et al., 2018), which predates the term "micro-grids" that was introduced in the late 1990s and early 2000s by Lasseter and Paigi (2004); Lasseter (2002). Going by the terms, it is intuitive that a mini-grid must have greater power flow capability than a micro-grid. Since there is no generally acceptable range in literature that uniquely defines lower and upper boundaries for power flow within a mini-grid or a micro-grid, the lower power range within mini-grids overlap the upper power range boundaries for micro-grids. With such an overlap, the control and protection schemes that are applicable to micro-grids are equally applicable to mini-grids. The only difference would only be in the power capacities in the control and protective devices, which would be much higher for mini-grids. Moreover, more power buses will constitute a mini-grid than a micro-grid. Another significant difference could be in the voltage levels, where the voltage level in a mini-grid would be preferable at a much higher medium level for loss reduction, while the voltage level of smaller

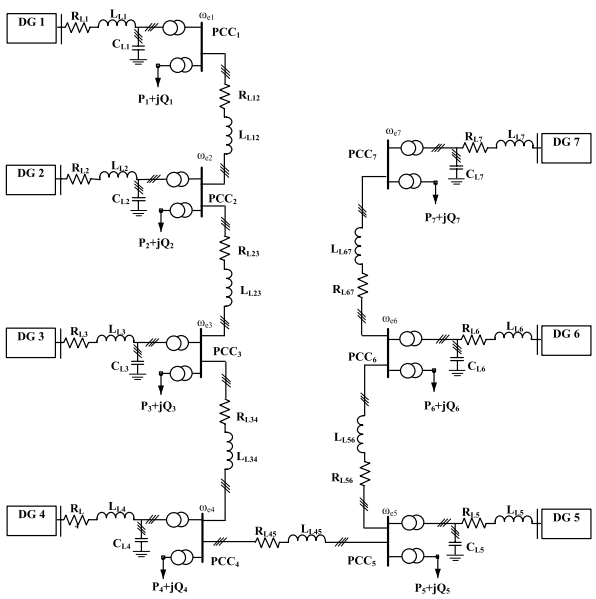

FIGURE 1
An illustration of a hypothetical AC mini-grid.

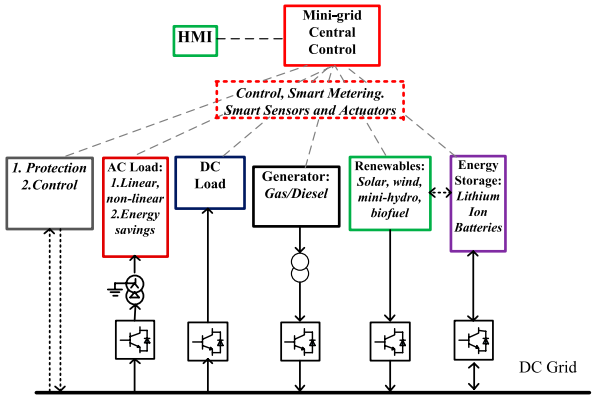

FIGURE 2
A block model illustration of a DC mini-grid.

micro-grids could be more sustainable at the low voltage. In Nigeria, for example, a mini-grid can be created at the 11 kV or 33 kV bus voltage level, while a small micro-grid (or nano-grid) could be constituted at the 400 V (line–line). Therefore, a mini-grid could be a collection of buses with DERs and load units that can operate in the islanding mode autonomously and in the grid-connected mode.

Typical examples of mini-grids existing in Nigeria are found in large universities campuses; administrative estates owned by state governments with larger economic powers, such as Lagos; and estates owned by multinational organizations. On the other hand, smaller micro- and nano-grids are commonly deployed in serviced residential estates all across the nation. Most of such grids are being powered by fossil fuel-based generators, which are not sustainable for carbon footprint mitigation. Though Nigeria has vast potential for renewable power generation, investment in renewable energy-fed grids is still significantly low. Investors are usually discouraged due to inefficient energy conversion technology and lack of enough seasoned manpower. With a population of 206.14 million that is about the size of Brazil (209.3 million), Nigeria, a tropical country located close to the equator with abundant solar potentials, still suffers from not meeting its electricity demand. Though Nigeria in 2019 achieved a power generation capacity of 12,522 MW (10,142 MW from fossil fuels and 2,380 MW from hydroelectric power), only an average 4,000 MW is available for distribution with a peak of 5,222 MW. The electricity per person in Nigeria is 128 kWh/person, while that of Brazil is 2,500 kWh/person. Therefore, increase in investments in renewable energy-fed mini-grids is justified as a more sustainable path to scale up kWh/person in Nigeria.

2.1 AC mini-grid

Medium- and heavy-power household and industrial equipment are usually developed for AC power applications because of the initial advantage AC power had over DC power in voltage conversion from one level to the other. The invention of power transformers in the 19th century was the game changer in voltage step-up and step-down from one level to the other. However, this advantage is fast fading away since the advent of power semiconductors (power electronics) in the 1960s and subsequent ingenuities and developments in power converters. As such, DC power transmission and distribution had since become a competitive alternative to AC power transmission and distribution.

A typical AC mini-grid is illustrated in Figure 1. The mini-grid is a 7-bus system at a medium voltage level of 11 kV or 33 kV with connected distributed energy resources (DERs) and loads. The DERs in a hybrid mini-grid are made up of RESs, battery storage systems, and fossil fuel-based generation systems. Therefore, the 7-bus mini-grid may be principally fed by solar PV renewable energy resources as the distributed generations embedded in the buses of the mini-grid. Lithium ion batteries and lead acid batteries can be introduced as storage systems in the network to also serve as DERs and equally serve to smoothen the intermittency in power flow that may arise from RESs. Other DERs such as fossil fuel-based generation and wind/hydro can be introduced as embedded generations.

Electric power injection by each of the DER into a mini-grid must be adequately synchronized to the grid's bus voltage and frequency references that must be preselected and regulated for system stability. Conventionally, a synchroscope synchronizes an AC generator into a grid's bus, but lately phase-locked loops (PLLs) (Chung, 2000; Sheikh et al., 2017, Surprenant et al., 2011; Rasheduzzaman and Kimball, 2019) achieve such synchronization for a grid-following inverter-based RES (Kumar et al., 2017). The real power flow and reactive power flow control, load sharing control, and other control objectives in mini-grids are regulated by either centralized or decentralized control systems or combination of both in form of a hierarchical control strategy. Further discussions and illustrations on centralized, decentralized, distributed, and hierarchical control systems are given subsequently.

2.2 DC mini-grid

AC generators can inject DC power into a DC grid by connecting a rectifier of the right power capability and control.

Likewise, DC power of a voltage level can be injected into a DC mini-grid of another level through DC–DC converters, such as the push–pull converters or flyback converters.

In general, the control objectives of a DC mini-grid differ from those of an AC mini-grid. Some complex control strategies in AC mini-grids do not apply to DC mini-grids. For example, a DC mini-grid will neither require frequency control nor reactive power control. Grid synchronization will also not be required. However, protection systems in DC mini-grids are more complicated because of no zero crossing point in DC currents. In addition, flow of real power without reactive power flow will degrade voltage stability. Figure 2 illustrates a DC mini-grid. Other merits and limitations of DC grids are given in (Rocabert et al., 2012; Josep, 2017, Anand et al., 2013; Nasirian et al., 2014; Wang et al., 2020).

2.3 Hybrid AC/DC mini-grid

A hybrid AC/DC mini-grid topology consists of the dual layout and configurations of both AC and DC mini-grids, making its control strategies more complicated. Some bus sections of such hybrid mini-grids are usually dedicated DC bus systems, while other sections constitute the AC bus systems (Rocabert et al., 2012; Lu et al., 2013).

3 Mini-grid control architecture

Solar power and other RESs are very attractive electric power solutions in Nigeria and sustainable alternatives to fossil fuel-based generation, which must be encouraged into the energy mix and made more affordable. Renewables generally are intermittent sources of energy and must be controlled to have good conversion efficiencies that can yield excellent returns on investment. Since the distributed generations (DGs) in mini-grids usually comprise the hybrid renewable energy system (HRES) that is made up of the RES, energy storage system (ESS) such as battery storage system (BSS) or flywheel system, fossil fuel-fed generators and the likes, and the control architecture in a mini-grid must be a multi-task/multi-objective multi-variable control structure. Therefore, the generalized functionalities of the controllers for a stand-alone mini-grid must be responsible for the following:

1) Voltage magnitude and frequency regulation.
2) Active and reactive power flow/sharing control.
3) Load-sharing capabilities.
4) Improve efficiency in energy conversion and utilization.
5) Reduce environmental impacts of electricity supply.
6) Power supply to remote communities.
7) Improve reliability and power quality.
8) Enhance availability of steady power supply for critical loads.
9) Capability for black start during voltage collapse.

As such, the overall control architecture in a mini-grid is generally classified as follows:

1) Centralized control system
2) Decentralized control system
3) Distributed control system
4) Hierarchical control system.

The distributed control system is sometimes considered synonymously with the decentralized control system in some literature (Liu et al., 2014b), while other literature differentiates between the two (Yazdanian et al., 2014; Meng et al., 2017).

3.1 Centralized control system

The philosophy of the centralized control system in mini-grids emanates from the configuration in which most legacy national grids were structured. In the legacy grid, usually, a central control station exists where coordinated control of power flow and power injection into the grid takes place. The control stations of legacy grids coordinate stiffness of the grid in terms of ensuring operations at constant voltage magnitudes and constant frequency. The stability profile of the legacy grid is also enhanced to prevent occurrence of unhealthy situations like voltage collapse. In the same vein, a centralized control system in a mini-grid coordinates and stabilizes power flow from every DER into load units. However, if unchecked, the point of common coupling (PCC) at which DERs are integrated into mini-grids suffers from more deviations in the voltage magnitudes and frequency, than obtained in PCCs of legacy national grids. The reason for such deviations could be derived from asymmetrical loadings on the individual phases and nonlinear loads, which are typical of distribution grids. Though the centralized control infrastructures of a mini-grid are not as huge and elaborate as those of a typical national grid, they must be able to deal with the emanating peculiarities of embedded generations. A centralized control system for a mini-grid is illustrated in Figure 2, which is equally applicable to AC grids. A major disadvantage of the centralized control system is that a single point of fault on the master control may paralyze the entire control structure. An overview of the merits and disadvantages of centralized control system are given in Yazdanian et al. (2014).

3.2 Decentralized *versus* distributed control systems

The decentralized control system does not require a central control unit. The entire control architecture is decentralized on the local controllers, which takes action by some preset or dynamic conditions in real-time. The decentralized control is differentiated from distributed control in Yazdanian et al. (2014); Morstyn et al. (2016). As such, a decentralized control method is a non-centralized control technique that assumes a negligible interaction between neighboring subsystems. In Energy (2004); Yazdanian et al. (2014), the widespread blackout of August 2003 in North America was stated as the consequence of the disadvantages of such non-centralized control. Contrarily, the distributed control system stated in Yazdanian et al. (2014) considers the interactions between control units of neighboring subsystems via communication means such as consensus-based communication links and multi-agent-based communication links. However, in Liu et al. (2014b), a decentralized control system was considered

equivalent to a distributed control system. The same philosophy of multi-agent control strategies stated in Yazdanian et al. (2014) as being peculiar to the distributed control system was also attributed as decentralized multi-agent control strategies in Liu et al. (2014b). Technically, the classical decentralized control techniques, which have negligible interactions with neighboring control subsystems, evolved into more intelligent and smarter decentralized control methods, subsequently called distributed control systems.

3.3 Hierarchical control system

In hierarchical control schemes, the control architecture in isolated distribution grids such as mini-grids is clearly classified into three layers, namely: 1) primary control; 2) secondary control; and 3) tertiary control. Hierarchical control strategies are well-illustrated in Zhao et al. (2016); Lu et al. (2013). The local controllers of the DERs and load distribution units are grouped under primary control, which may be completely stand-alone or have some limited interactions with neighboring local controllers. The secondary and tertiary control levels are higher-order controllers that can be responsible for higher reliability, security (e.g., cybersecurity), and situational awareness (Yazdanian et al., 2014). In Olivares et al. (2014), the hierarchical control classification was applied to both centralized and decentralized/distributed control strategies. In Shrestha et al. (2020); Rocabert et al. (2012); Hatziargyriou et al. (2006) the centralized control methodology was broken down into hierarchical classification, while in Yazdanian et al. (2014) the hierarchical classification was extensively adapted to a distributed control system. In Yazdanian et al. (2014) the tertiary control was considered the highest and slowest level of control and sets long-term set points based on the status of the DER units, market signals, and other system requirements.

A typical centralized control architecture can comprise a three-level hierarchical structure (Shrestha et al., 2020; Rocabert et al., 2012; Hatziargyriou et al., 2006), namely:

1) Local controllers, which are the local controllers on each of the DERs and load units.
2) Mini-grid central controller.
3) Distributed management system (DMS), which comprises controllers at the distribution network operator (DNO) and market operator (MO) level at medium and low voltages.

4 Distributed secondary control system

The distributed control systems for grid applications have been more flexible in design and implementation and very competitive. A distributed control architecture is illustrated in Figure 3. The droop controllers for regulating voltage magnitude and frequency are implemented at the primary control hierarchy level in distributed control systems. Examples of droop controllers in the primary level are given in Bidram et al. (2013); Meng et al., (2018). The local inverters on the DERs are responsible to implement the droop action and receive their reference command for frequency and voltage magnitude from phase-locked loop (PLL) (Li et al., 2017) (Hiskens and Fleming, 2008; Laaksonen et al., 2005) or more recently from frequency-locked loop (FLL) controllers (Sun et al., 2016) on distributed secondary control (DSC) levels in the hierarchy. Therefore, the dynamics of the DSC should be much slower than that of the primary control level (Golsorkhi et al., 2017). In a battery storage system, for example, state of charge (SoC) balancing may be required on the secondary level, but the dynamics of the DSC must be much faster than the rate of change of SoCs (Golsorkhi et al., 2017).

4.1 Communication layer on secondary control system level

Communication networks are essential for the distributed control systems. Without such communication networks, control interactions between neighboring controllers becomes impossible. In Lu et al. (2018), a micro-grid was considered a multi-agent system, which is equally applicable to mini-grids. As such, each distributed generation (DG) is a follower–agent and receives instructions from a tertiary unit that is a virtual leader–agent. In general, a multi-agent in a distributed control system improves scalability by ensuring that each agent interacts with a few neighboring agents (and not all agents) through a sparse cyber-communication network to reduce communication infrastructure cost (Wang et al., 2020). The communication network in Lu et al. (2018) was modeled by a digraph G (V, E, A) with a node set $V = \{V1, V2, \cdots, VN\}$, a communication link set $E \subseteq V \times V$, and a weighted adjacency matrix $A = (aij)N\times N$, where $aii = 0$, $aij \geq 0$, and $aij > 0$ if and only if the link $(Vi, Vj) \in E$ (Morstyn et al., 2018; Haimo, 1986).

4.2 Compensation control generation from secondary control system level

Beyond implementing the generation of the reference frequency and voltage magnitude control, other compensation control strategies can also be implemented at the distributed secondary control level. The issue of unbalanced phase voltages is a common phenomenon with distribution grids that constitute mini-grids. Such an unbalanced set of phase voltages is not particularly healthy for some loads such as induction motors. The doubly fed induction generator (DFIG), which is apparently the most versatile wind generator because of its smaller converter ratings, will give rise to a negative sequence voltage that spins at a negative synchronous frequency when connected to such a mini-grid. The effect of such negative sequence voltage is that the electromagnetic torque and stator power of the DFIG will have second harmonic pulsations at twice the fundamental frequency that must be mitigated for improved quality of power flow into the grid (Balogun et al., 2015). Control compensation strategies have been implemented for such voltage unbalance in Bidram et al. (2013); Wu et al. (2018) under distributed cooperative control at the secondary level. In Wu et al. (2018), an N+1 agent communication contingency plan was implemented in the communication network at the secondary layer called distributed voltage unbalanced compensation (VUC), where N is the number of agents in the grid. The cyber network discharges the global

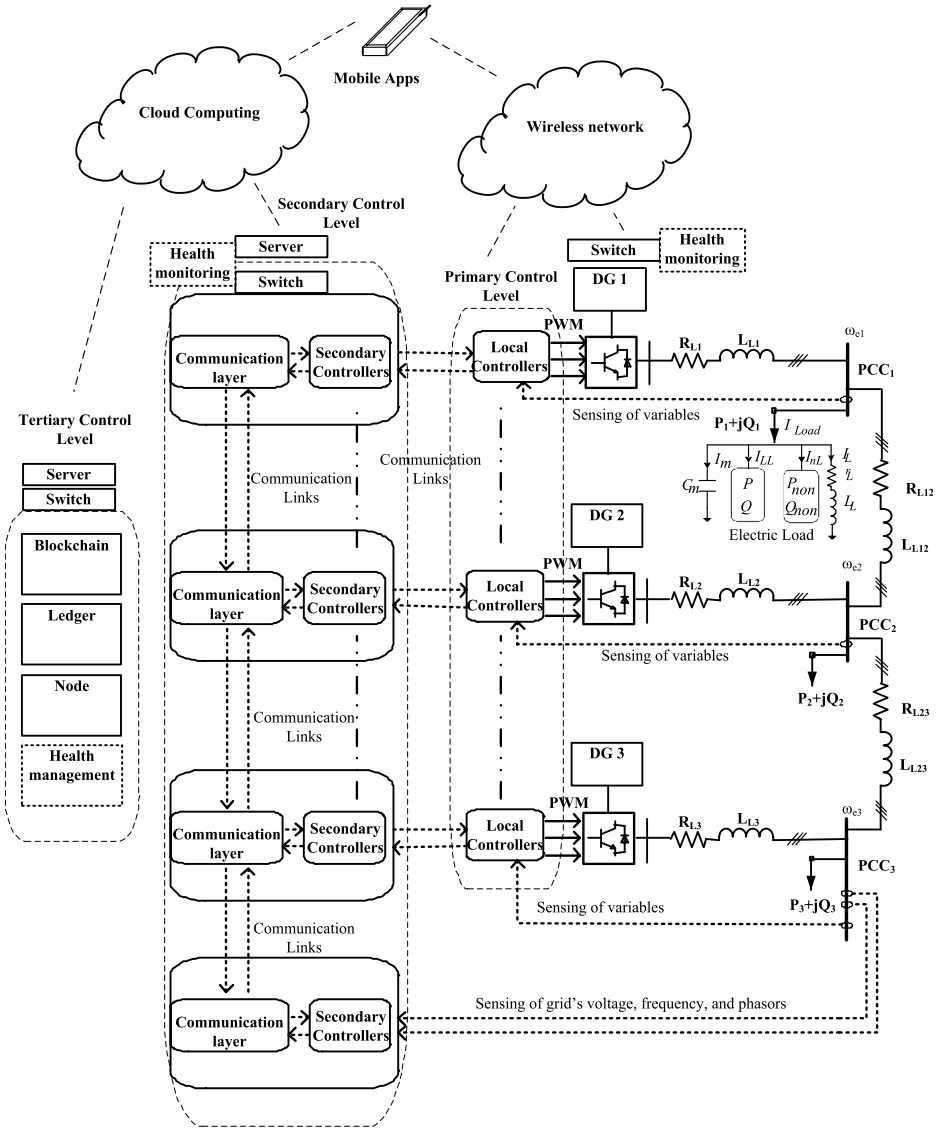

FIGURE 3
An illustration of a health management scheme on distributed control architecture showing hierarchical control with its communication layers in tertiary, secondary, and primary levels of a 3-bus mini-grid.

distributed secondary control objective as a reference to the local primary controllers on the DER for enhancing the grid's voltage magnitudes. The control infrastructure, in general, may require bandwidth for wireless communication resources that may be internet of things (IoT)-enabled. Therefore, efficient bandwidth management will be crucial for effective transmission and reception of control and monitoring signals for system devices.

4.3 Health management system and monitoring control

A healthy mini-grid must be able to ensure steady flow of demanded power at good quality that must be free of the following:

1) Harmonics (including inter-harmonics)
2) Flickers–rapid changes in voltage magnitude
3) Voltage dips and swells
4) Complete voltage collapse
5) Frequency deviations
6) Resonance in current and voltage
7) Cyber-attacks.

A way of determining or identifying the sources of degrading power quality in a grid network is by metering the distributed generations' points of injection and the points of load connections for power off-takers in the grid. The meters must be smart and IoT-enabled for remote monitoring and management. Moreover, the smart meters must be able to measure power in KVAhr and not only in kWhr for

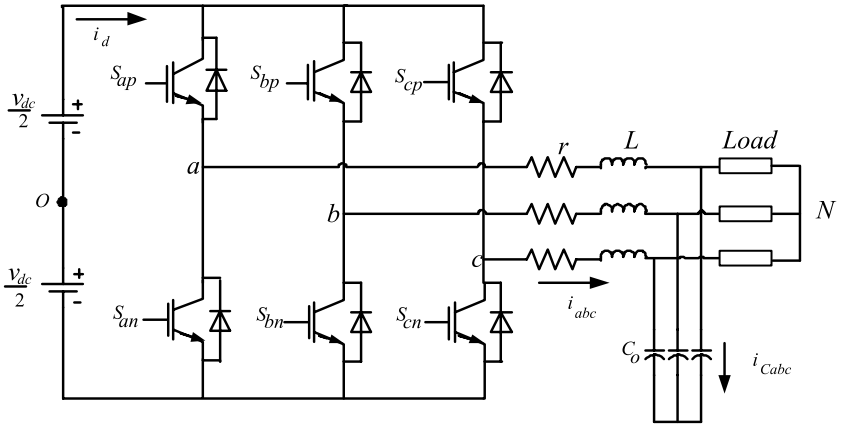

FIGURE 4
Three-phase 2-level inverter system.

determining the reactive power consumption by the customers. The functionalities of the smart meters should be of those of power analyzers that can determine harmonic frequency pollutions and identify sources of harmonics.

The health monitoring and management schemes should be deployed at the three hierarchical control layers, which will be incorporated into the protection system of the grid system. At the primary control levels on the outputs of the DERs and the points of taking off-loads, the quality of the voltage, current, and power will be observed by monitoring smart meters to comply to IEEE Std 519-2014. The grid-forming inverters and grid-following inverters for grid integration are usually equipped with output filter networks which combine with the inverters for providing active filtering capabilities and compensation. Therefore, the health monitoring on the primary control initiates dynamic responses of the secondary level control to generate appropriate references for the primary control unit to adjust accordingly. The automation involved is closed loop with potentials for open-loop in case of emergencies. The secondary distribution control is illustrated in Figure 3.

The tertiary level of control and some aspects of the secondary level of control will be blockchain-enabled for keeping record of the activities of the mini-grid. The blockchain can also be used at the tertiary level of control for resolving financial billing issues by the parties involved in power generation, distribution, and consumption by the system operators. On the generation, distribution, and power off-takes, any violation of IEEE Std 519-2014 will lead to penalties, financial, or other means, that will be generated with the aid of cloud computing at the tertiary level of control and transmitted to the offending parties.

Mobile apps for remote monitoring are encouraged for mobility in health monitoring and management by the system operators (SOs). Such mobile resources will be SIM card-enabled that can use the data resources of any of the private GSM or data providers in Nigeria. The wireless communication system utilized for control and monitoring are low bandwidth resources. An illustration of a health management scheme on distributed control architecture showing hierarchical control with its communication layers in tertiary, secondary, and primary levels of a 3-bus mini-grid is shown in Figure 3.

5 Trends and applications of power converters in grid integration

Without converters from power electronics, achieving optimal power extractions from renewables becomes practically almost impossible. As such, power converters dictate the optimal regimes for frequency, rotor speed adjustment, and output voltage in electric machines applied in small hydro-energy and wind energy conversion systems. A unidirectional back-to-back connected converter, having a rectifier's output tied to the input of an inverter via a DC-link capacitor, is applicable to deliver AC power from squirrel cage induction generators, wound field synchronous generators, permanent magnet synchronous generator, or synchronous reluctance generators. Those types of back-to-back converters must be rated in full capacity of such machines. It is only in DFIGs that converters are fractionally rated at 30% of machine ratings. The reason for the fractional rating is because the converters are usually connected to the rotor terminals of DFIGs, while the stator terminals do not usually require a converter interface to grids in the conventional configuration. However, the back-to-back converters can be replaced by matrix converters, which eliminate the requirement for a DC-link.

In addition, in solar power plants, maximum power point tracking (MPPT) is heavily dependent on the choice and control of the right type of converters. Equally, in the battery storage system (BSS), such as bank of lithium ion batteries, power converters are used for effective charging to maximum SoC and regulated discharge to a minimum of about 20% depth of discharge (DoD). By regulated charge and discharge, lithium ion batteries can deliver at their full cycle life. Although interests and competitiveness in use of lithium ion batteries for grid energy storage have increased in the last 2 decades because of high power densities, they are still quite expensive and require quite complex charging and discharge control strategies. Constant current charging, cell balancing, and constant voltage charging are stages that must be achieved for effective charging of lithium ion batteries. Without power converters, such charging stages cannot be achieved and consequently degrade the battery's benefits. DC–DC converters are applicable to charging

from DC mini-grids and solar power sources, while rectifiers are applicable to charging from AC mini-grids. Examples of basic DC–DC converters are buck converters, boost converters, buck–boost converters, SEPIC converters, etc. Other DC–DC converters in the form of DC power sources with electrical isolation but magnetic coupling are push–pull converters, forward converters, and flyback converters.

5.1 The three-phase voltage source inverter (VSI)

Three-phase voltage source inverters are frequently used by the RES for integration into AC grids via shunt injection transformers. The inverters are referred to as VSI because their input DC voltages are maintained steady via input polarized capacitors. A current source inverter (CSI), which has input current (DC) maintained as steady as possible via an inductor, exist also, but not as widely applied in the grid's DER. The integrated RES may be solar PV modules in DC or wind/mini-hydro generators in three-phase or multi-phase (5-phase, 7-phase etc.) outputs. Multi-phase machines have been promoted in the literature because of their better resilience against open-phase faults. For example, if a three-phase generator has an open-phase fault, it can never be started up with the two remaining phases, but if a five-phase generator loses two phases, it can still be started up with the remaining three phases. As such, multi-phase generators have greater reliabilities than 3-phase generators, but their power outputs must be converted back to 3-phase via a multi-phase rectifier tied back-to-back to three-phase voltage source inverters for grid integration. The three-phase system still remains the generally acceptable standard for grid systems globally.

In grid integration application, therefore, power inverters are usually classified as *grid-forming* or *grid-following*. In the *grid-forming* inverter, the voltage magnitude, frequency, and phasors of the grid are fixed/determined by droop controllers (Wang et al., 2020). However, in *grid-following* inverters, information on the grid's voltage magnitude, frequency, and phasors can be obtained from phase-locked loop (PLL) tied to the grid (Chung, 2000; Sheikh et al., 2017, Surprenant et al., 2011; Kumar et al., 2017; Rasheduzzaman and Kimball, 2019), which will consequently be used for generating the modulation frequency in pulse width modulation (PWM) strategies for inverters. The synchronous reference frame PLL (SRF-PLL) given in Chung (2000) is a classic PLL which is suitable for stiff grids where the phase voltages are balanced. The SRF-PLL consists of a phase detector (PD), a loop filter (LF), and a voltage-controlled oscillator (VCO).

The common modulation techniques are the carrier-based PWM(CB-PWM), the space vector PWM (SVM), and discontinuous PWM (DPWM). Other PWM schemes are given in (Hava et al., 1999; Holmes and Lipo, 2003; Ojo and Kshirsagar, 2003). Modulation schemes enable sequential turn-on and turn-off of the semiconductor devices of converters for effective operation. Analytically, modulation schemes can be embedded into the voltage equations of the inverter's power model by the use of switching functions. In such an approach, switching functions are assigned to indicate the switching states of power semiconductor devices of the converter. The respective switching function is assigned either logic *'1'*, when the switching device (e.g. *IGBT* and *MOSFET*) is turned on, or logic *'0'*, when switched off. For a three-phase inverter system, the switching functions of the upper devices are represented by S_{ip} and the lower devices by S_{in}, where the subscript i represents the respective phase, subscript p represents a positive voltage switching device, and subscript n represents a negative voltage switching device (Hava et al., 1999). By Kirchhoff's Voltage Law (*KVL*), the voltage equations of the inverter in Figure 4 are as follows:

$$v_{aO} = v_{aN} + v_{NO} = Lpi_a + ri_a + v_{Ca} + v_{NO}, \quad (1)$$

$$v_{bO} = v_{bN} + v_{NO} = Lpi_b + ri_b + v_{Cb} + v_{NO}, \quad (2)$$

$$v_{cO} = v_{cN} + v_{NO} = Lpi_c + ri_c + v_{Cc} + v_{NO}. \quad (3)$$

In terms of switch function:

$$\frac{v_{dc}}{2}\left(2S_{ap} - 1\right) = Lpi_a + ri_a + v_{Ca} + v_{NO}, \quad (4)$$

$$\frac{v_{dc}}{2}\left(2S_{bp} - 1\right) = Lpi_b + ri_b + v_{Cb} + v_{NO,} \quad (5)$$

$$\frac{v_{dc}}{2}\left(2S_{cp} - 1\right) = Lpi_c + ri_c + v_{Cc} + v_{NO}, \quad (6)$$

where

$$S_{in} = 1 - S_{ip},\ i = a, b, c \quad (7)$$

Although power converters have tremendously changed the dynamics in electric power engineering, they also pollute power networks by injecting harmonics when adequate filters are not incorporated. Common power filter configurations include C, L, RL, LC, and LCL. C stands for capacitor; L for inductor; and R for resistor. In all the configurations, the presence of little or more resistive composition is common for stability improvement. The LCL filter network is presented in Liserre et al. (2001) to give an optimal performance.

Other phenomena emanating from power converters that could degrade their applications for power integration include common-mode voltages and common-mode currents. As such, the interests in mitigating common-mode voltage by reduction or complete elimination have increased over the last 2 decades. In (Concari et al., 2016; Rahimi et al., 2018; Xiang et al., 2019), common-mode currents were seen to severely degrade power conversion from solar photovoltaic (PV) modules. In Karugaba et al. (2012), common-mode voltage was indicated to induce bearing currents in electric machines. The common-mode voltage for the inverter in Figure 4 is given as follows:

$$v_{NO} = \frac{(v_{aO} + v_{bO} + v_{cO})}{3}. \quad (8)$$

5.2 Three-phase H8 2-level VSI

A new H8 2-level inverter was proposed in (Concari et al., 2016; Rahimi et al., 2018; Xiang et al., 2019) to have a reduced common-mode current level than conventional two-level inverters. The name 2-level is derived from switching at + V_{dc} (voltage of DC input) and–V_{dc}. In the H8 converter, two additional power semiconductor devices are introduced with each connected at the input positive and negative terminals, as

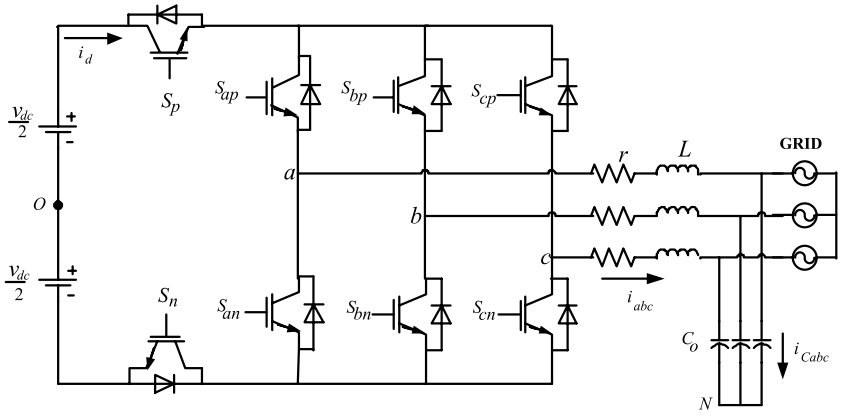

FIGURE 5
H8 2-level voltage source inverter.

illustrated in Figure 5. In Rahimi et al. (2018), the power semiconductor at the positive (+) terminal is switched on by the output of a NAND gate fed with the switching pulses of the three upper leg positive switching devices, while the negative (−) terminal is switched on by a NAND gate fed by three lower leg negative switching devices. Therefore, the sequential switching of the new semiconductors effectively cuts off the DC input power source during the null states ('000' and '111' states), thereby reducing the magnitude of the common-mode voltage and consequently minimizing the level of common-mode current flow back.

5.3 Multilevel inverters

VSI outputs are characterized by their voltage levels which determine them to be either two-level inverters or multilevel inverters. The multilevel inverter was first introduced in 1981 (Nabae et al., 1981). However, it gained more interests in the last 2 decades about the same time window when interests in the distributed grid system sprung up. The multilevel inverter introduced in Nabae et al. (1981) was a three-level neutral point clamped (NPC) inverter that switches at + V_{dc}, 0, $-V_{dc}$, which was unlike the 2-level NPC that switches at + V_{dc} and $-V_{dc}$. Subsequently, the 4-level flying capacitor (FC) and the 5-level Cascaded-H Bridge (CHB) multilevel inverters were introduced. The NPC is also known as the diode clamped because it uses diodes for clamping voltage poles. On the other hand, the FC multilevel utilizes the capacitor for its clamping, while the 5-level CHB connects VSI in series to achieve its multilevel of $+2V_{dc}$, V_{dc}, 0, $-V_{dc}$, $-2V_{dc}$ stepping. The NPC, FC, and CHB are the classical multilevel inverters, but several other topologies are available in literature (Loh et al., 2002; Celanovic and Boroyevich, 2001; Yao et al., 2008). The modulation schemes for multilevel inverters are well-articulated in Boonchiam and Mithulananthan (2008) as phase disposition (PD), phase opposition disposition (POD), and alternate phase opposition disposition (APOD). The unique advantage of stepping up voltage in multilevel inverters and rectifiers makes them attractive for solid-state transformers (SSTs), smart transformers (STs), and other distribution grid applications.

5.4 Multistring multilevel inverters

Multistring multilevel inverters (Liao and Lai, 2011; Angirekula and Ojo, 2014; Rahim and Selvaraj, 2010) are even better replacements for CHB multilevel inverters because of their unique advantage of reduced number of power electronics devices (Agoro et al., 2018a). As such, they have lower switching losses and reduced total harmonic distortions (THDs) and consequently lower electromagnetic interference (EMI) (Angirekula and Ojo, 2014). The same multistring inverters can be switched as multistring rectifiers that can enable bi-direction flow of power. Such reverse-flow switching is also applicable to multilevel CHB inverters. Capability for bi-directional power flow gives such multilevel converters more flexibility in SST applications.

A proposed three-phase five-level multistring inverter in Agoro et al. (2018a); Balogun et al. (2019) connected to the grid through an R-L filter is shown in Figure 6A. In each phase, two PV strings are connected to six power switches through DC capacitors. The connection of these switches is such that on each side of each phase-leg, similar terminals of the switch are connected. Each PV string incorporates a MPPT control scheme that provides the appropriate reference for maximum power output.

5.5 Solid-state transformer and smart transformer

Interests have sprung up in the last decade on developing SSTs (She et al., 2014) and consequently smart transformers (STs) (De Carne et al., 2015; Gao et al., 2017; De Carne et al., 2018) for grid integration. Though a ST is of a much higher order of control intelligence than an SST, both are made from topologies of back-to-back connected group of converters in two or three layers for power conversion with a high frequency magnetic core isolation. With converters involved, dynamic control of real power and reactive power control becomes possible with the SST and ST. Other control objectives include harmonic elimination and power quality improvement. In Figure 6B, a smart transformer layout developed from a three-phase multistring inverter is presented.

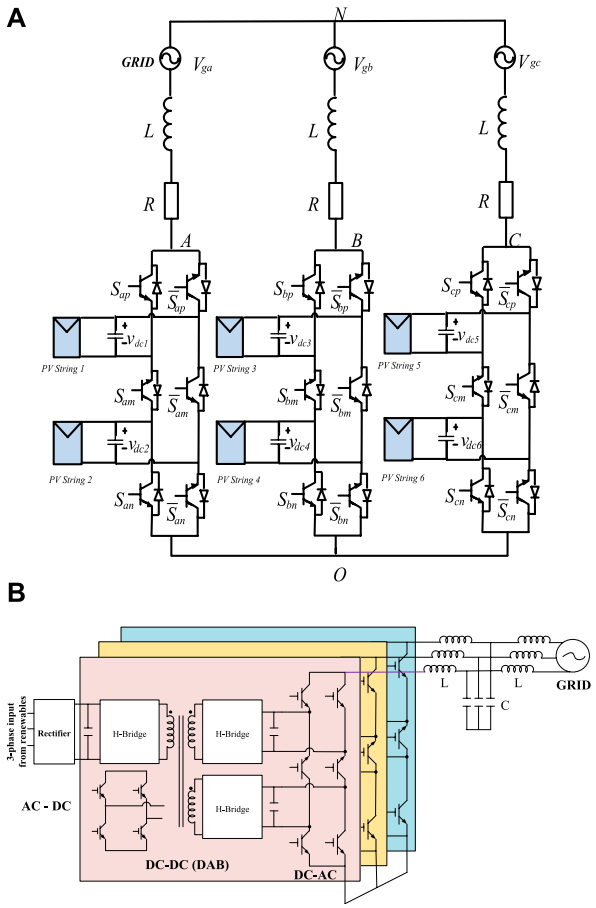

FIGURE 6
(A) A three-phase topology of the proposed five-level multistring inverter connected to the grid (Agoro et al., 2018a; Balogun et al., 2019). **(B)** A smart transformer layout developed from a three-phase five-level multistring multilevel inverter.

The ST has got three stages of power conversion: AC to DC rectifier, DC to DC double active bridge (DAB) converter via high frequency core (transformer), and three-phase 5-level multistring multilevel inverter. Some other STs could be arranged for a two-stage power conversion that could be applicable to directly integrate renewable into an AC grid.

6 Grid integration and modeling

Power injection into the grid network is mostly conducted in shunt (parallel) formation, whereby current is injected into the grid. Though series injection methods exist whereby series voltage is injected via special transformers, they are more complicated, which makes them not as competitive as shunt injection. A typical example depicting the two methods of injection can be found in unified power flow controllers (UPFCs). One end of the UPFC uses the series integration, while the other end utilizes the shunt injection strategy.

The voltage magnitude, frequency, and phasors in mini-grids and micro-grids must be preselected, and all connected distributed generation systems must synchronize to such. Assume that a distribution grid's voltage equations can be given "*a-b-c*" reference frame as follows:

$$v_{ag} = v_{m1}\,Cos\left(\theta_e + \gamma\right), \tag{9}$$

$$v_{bg} = v_{m2}\,Cos\left(\theta_e + \gamma - \beta\right), \tag{10}$$

$$v_{cg} = v_{m3}\,Cos\left(\theta_e + \gamma + \beta\right), \tag{11}$$

where $\theta_e = 2\pi f_e$, $\beta = 2\pi/3$, γ = phase angle, and f_e = grid's frequency (50 Hz in Nigeria; 60 Hz in USA). In a stiff grid like the standard legacy grid the voltage magnitude is fixed at a magnitude v_m. Therefore, $v_m = v_{m1} = v_{m2} = v_{m3,}$ and deviations in f_e must be negligible. Fossil fuel-based generation responds dynamically to mitigate deviations from such conditionality because its output terminals are synchronized directly to the grid. Real power is released to mitigate frequency deviation, while reactive power flow is adjusted to enhance the stability of voltage magnitudes. However, the conditionality of electrical stiffness in grids may be difficult for a mini-grid or micro-grid to accomplish because the loading units across all phases cannot be perfectly balanced. In addition, combined nonlinear load units could influence deviation of frequency from the set point. Unlike the fossil fuel generating units, the RES and ESS in distribution grids will not directly mitigate deviations from the conditionality of stiffness unless told by some inertia emulation control. The operational frequencies of the electric machine-based RES and ESS (such as wind generators and flywheels, respectively) are completely decoupled from the grid's frequency by the coupling inverters. Invariably, such electric machines are allowed to operate at variable speed principally for loss minimization and consequently efficiency improvement. Therefore, it is only via actuated control such as inertia emulation control that the RES and ESS can change the flow of real and reactive power for frequency and voltage magnitude control. Consequently, the SRF-PLL will be heavily degraded from predicting the grid's frequency once $v_{m1} \neq v_{m2} \neq v_{m3}$ in (9) to (11). Transformations of the unbalanced phase voltages into qd-reference and αβ-reference frames become riddled with harmonics and DC offsets. As such, a more robust PLL will be applicable for such a distorted grid. A method of improving the SRF-PLL is by introducing filters into the phase detection (PD stage, such that the positive and negative sequence components of the unbalanced phase voltages can be extracted. Dual second-order generalized integrator (DSOGI) is an example of the pre-filter that is applicable for such extraction (Sheikh et al., 2017; Rasheduzzaman and Kimball, 2019).

The formulation of the model for distribution grids with DER in the "*a-b-c*" reference frame is quite complex because of the cosines or sines in the voltage and current equations. Therefore, transformation from "*a-b-c*" to "*q-d-0*" reference frames becomes essential to ease computations because "*q-d-0*" eliminates such cosines or sines in variables and system parameters.

6.1 Solar PV power integration

Therefore, KVL and KCL are used to model integration of solar PV power to a distribution grid. The solar PV inverter arrangement is shown in Figure 7 for storage-less topology. The voltage potentials and the nodal currents in "a-b-c" reference frames are given in Eqs 12–(14), and after transformation into "q-d" frames Eqs 15–(17)

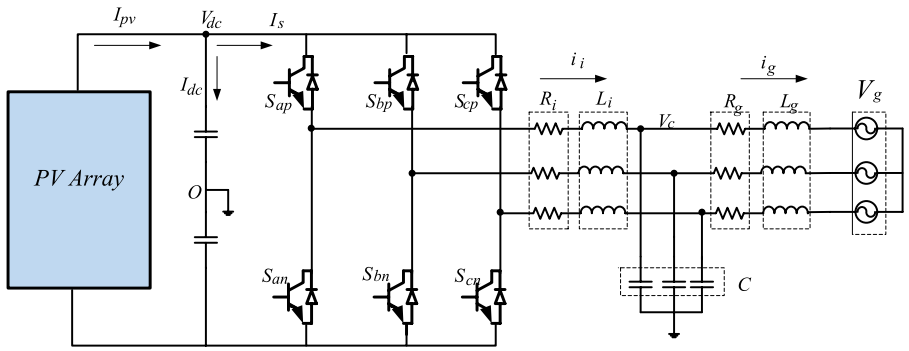

FIGURE 7
Topology of the storage-free grid connected PV system (Agoro et al., 2018b).

evolve. KCL is established at the DC-link by (18). At steady state, Eq. 19 gives the power balance between the inverter and the solar PV DC power. Furthermore, in Eq. 15, the inverter's output voltage is modeled for space vector modulation (SVM) and also expressed in terms of the q-d modulation index of the inverter for a carrier-based pulse width modulation (CB-PWM). Therefore, the power being injected from the solar PV via inverter is given in Eq. 20, while the reactive power is given in Eq. 21, which can be used in load flow studies.

$$v_{i_{abc}} = R_i i_{i_{abc}} + L_i \frac{di_{i_{abc}}}{dt} + v_{c_{abc}}, \tag{12}$$

$$i_{i_{abc}} = C \frac{dv_{c_{abc}}}{dt} + i_{g_{abc}}, \tag{13}$$

$$v_{c_{abc}} = R_g i_{g_{abc}} + L_g \frac{di_{g_{abc}}}{dt} + v_{g_{abc}}, \tag{14}$$

$$v_{i_{dq}} = R_i i_{i_{dq}} + L_i \frac{di_{i_{dq}}}{dt} - j\omega L_i i_{i_{dq}} + v_{c_{dq}}, \tag{15}$$

$$i_{i_{dq}} = C \frac{dv_{c_{dq}}}{dt} - j\omega C v_{c_{dq}} + i_{g_{dq}}, \tag{16}$$

$$v_{c_{dq}} = R_g i_{g_{dq}} + L_g \frac{di_{g_{dq}}}{dt} - j\omega L_g i_{g_{dq}} + v_{g_{dq}}, \tag{17}$$

$$I_{pv} = C_{dc} \frac{dV_{dc}}{dt} + I_s, \tag{18}$$

$$P_{inv} = \frac{3}{2}\left(v_{i_q} i_{i_q} + v_{i_d} i_{i_d}\right) = \frac{3V_{dc}}{4}\left(m_{i_q} i_{i_q} + m_{i_d} i_{i_d}\right) = V_{dc} I_{pv}, \tag{19}$$

$$P_{inj} = \frac{3}{2}\left(v_{g_q} i_{g_q} + v_{g_d} i_{g_d}\right), = \frac{3V_{dc}}{4}\left(m_{i_q} i_{i_q} + m_{i_d} i_{i_d}\right) - 3R_i\left({i_{i_q}}^2 + {i_{i_d}}^2\right) - 3R_g\left({i_{g_q}}^2 + {i_{g_d}}^2\right) \tag{20}$$

$$Q_{inj} = \frac{3}{2}\left(v_{g_d} i_{g_q} - v_{g_q} i_{g_d}\right). \tag{21}$$

6.2 System bifurcation

The dynamic model given in (15) to (17) could yield a non-linear system, particularly when frequency deviation occurs. Therefore, a Jacobi expansion or performing small perturbation on (15) to (17) changes the entire nonlinear dynamics into linear dynamics. If a small perturbation is performed on the model by setting the state variables $x = x_o + \Delta x$ about an equilibrium state x_o, and then a linear small signal model emerges when higher-order terms are neglected. The small signal model given in Eq. 22 represents the state dynamics in (15) to (17). The matrix A gives the characteristic equation in (23), which predicts the regions of stability and instability. Solving (23) gives loci of eigenvalues at a given operating condition. The root loci of the eigenvalues in Eq. 23 must be restrained to the left hand plane to ensure system stability.

$$p\Delta x = A\Delta x + B\Delta u, \tag{22}$$

$$|\lambda I - A| = 0. \tag{23}$$

7 Primary level dynamic control schemes on the RES

There are various types of linear, non-linear, and predictive control schemes available in literature for grid applications with different control objectives but with a commonality in efficiency optimization. In the RES that utilizes electric machines such as wind and hydro-energy conversion systems, variable-frequency variable-voltage control by its local controllers is essential for variable speed control. The volt per Hertz control is the simplest control strategy that can deliver variable-frequency variable-voltage regulation but at a lower efficiency than the vector control schemes. The volt per Hertz is a scalar control scheme.

7.1 Vector control scheme

In vector control, alignment of variables is usually done to achieve control schemes similar to DC controllers. Vector control is the favorite control strategies by many for industrial drive applications, and it is usually a cascade of inner-loop and outer-loop controllers. However, the inner-loop current controllers are more significant in dictating the stability of the entire control structure (Ali et al., 2020). Vector control is also applicable on grid-side converters (GSCs) by alignment of magnitude of voltage or current along the q or d axis. A vector control scheme for a grid-side converter is illustrated in Figure 8

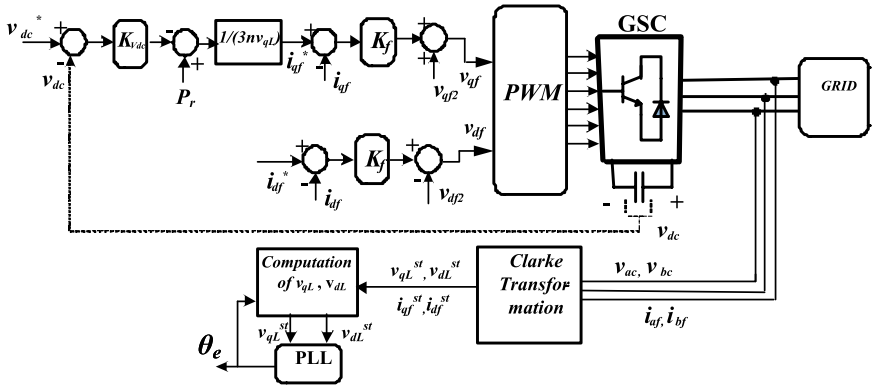

FIGURE 8
A vector control scheme for grid-side converters (Balogun et al., 2021).

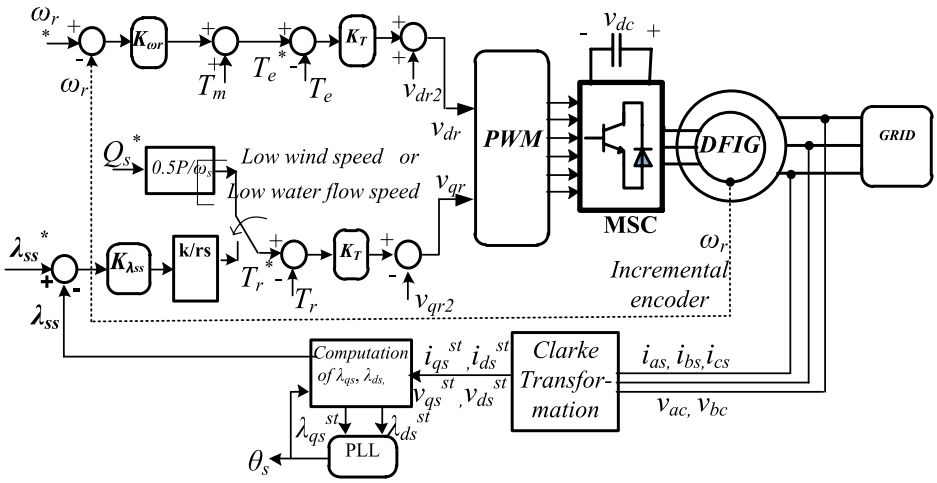

FIGURE 9
A direct torque control scheme with symmetrical switching for a DFIG (Balogun et al., 2013).

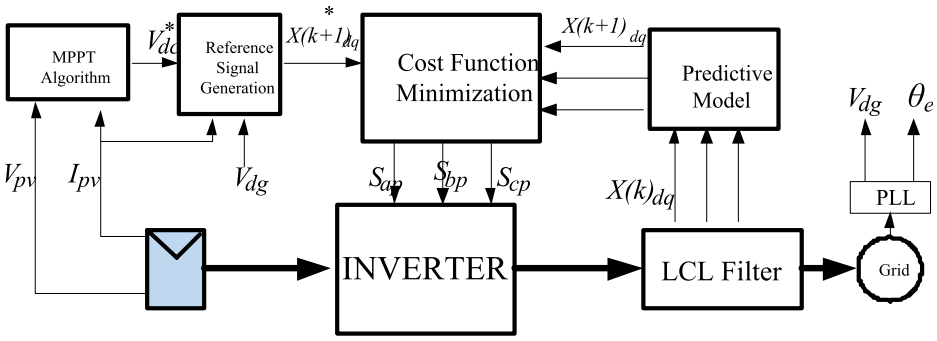

FIGURE 10
Block diagram of the model predictive control scheme for the storage-free grid connected PV system.

(Balogun et al., 2021) with the magnitude of the grid's voltage aligned along the q-axis. Orientation of variable's magnitude along an axis usually gives a linear relationship between the controlled variable and control input. Both volt per Hertz and vector control schemes are classified under linear control systems.

7.2 Direct scalar control scheme

In vector control, alignment of variables is usually done to achieve control schemes. Direct scalar control schemes such as direct torque control (DTC) and direct power control (DPC) are non-linear control schemes that are applicable to DERs. DTC strategies are applicable to machine-based RES, while DPC strategies are applicable to both machine-based RES and GSC for integrating solar PV and battery storage systems. No inner-loop current regulation is required in both DTC and DPC, which makes it less sensitive to system parameter variations, i.e., they are more robust against system parameter mismatch. Classical DTC and DPC are achieved by non-linear hysteresis controllers (Maes and Melkebeek, 2000; Buja and Kazmierkowski, 2004; Poddar and Ranganathan, 2004) with an asymmetrical switching frequency dependent on the load, but interest in symmetrical switching in DTC and DPC have yielded promising results via feedback linearization techniques and proportional plus integral (PI) controllers (Nik Idris and Mohamed Yatim, 2004; Zhi and Xu, 2007, Balogun et al., 2013; Awelewa et al., 2020, Awelewa et al., 2016; Abdulkareem et al., 2022). A DTC for a DFIG that is applicable to both wind and small hydroenergy conversion systems is illustrated in Figure 9 with symmetrical switching frequency. Similar to vector control, the direct scalar control schemes are local control strategies at the primary control level.

8 Predictive control

In grid power integration, predictive control schemes have significantly gained interests lately, principally because of their applications at all three layers of control (primary, secondary, and tertiary) (Arfeen et al., 2019). Usually, predictive control schemes are less sensitive to system parameter mismatch.

8.1 Model predictive control

An example of such predictive control is the model predictive control (MPC) where the state space model in continuous time (CT) of the entire system is discretized into discrete time (DT) by the forward Euler's approximation given as

$$\frac{dx}{dt} \approx \frac{x(k+1) - x(k)}{T_s}. \tag{24}$$

The obtained discrete time model is used in deriving the predictors which are compared to preselected or dynamically obtained references in one or two cost (or objective) function(s). Classical MPC was used in chemical engineering plants, but lately, it has found interesting applications in power electronic converters. In finite set MPC, each error between a reference and a predictor in the objective function in MPC is usually characterized by a weight gain to aid the derivation of the voltage set that gives the least cost function in a prediction horizon. The conventional MPC in power converters is usually applied to the inner-loop current control, while outer loops maintain the use of PI controllers. However, a direct MPC was introduced in Agoro et al. (2018b) whereby the need for a PI outer-loop control does not arise for storage-less solar PV power conversion. The cascade of outer and inner loops was completely eliminated by ensuring that the cost function comprises desired control loops. The direct MPC scheme developed in Agoro et al. (2018b) is illustrated in Figure 10 for grid integration of storage-less PV systems.

8.2 Model predictive control on H8 VSI

Consequently, the direct MPC scheme developed in Agoro et al. (2018b) for an *H6 VSI* is adopted in this sub-section for an *H8 VSI*. As such, applying (24) to the CT state space model of *q-d* expansions of (15) to (17) in Sub-Section VI *A* gives the predictive model in (25), which is used for closed loop predictive control.

$$\begin{bmatrix} i_{i_d}(k+1) \\ i_{i_q}(k+1) \\ i_{g_d}(k+1) \\ i_{g_q}(k+1) \\ v_{c_d}(k+1) \\ v_{c_q}(k+1) \end{bmatrix} = [\Phi]*\begin{bmatrix} i_{i_d}(k) \\ i_{i_q}(k) \\ i_{g_d}(k) \\ i_{g_q}(k) \\ v_{c_d}(k) \\ v_{c_q}(k) \end{bmatrix} + [\Psi]*\begin{bmatrix} v_{i_d}(k) \\ v_{i_q}(k) \end{bmatrix} + [\mathrm{H}]*\begin{bmatrix} v_{g_d}(k) \\ v_{g_q}(k) \end{bmatrix}, \tag{25}$$

where

$$[\Phi] = \begin{bmatrix} 1-\frac{R_i T_s}{L_i} & \omega(k)T_s & 0 & 0 & \frac{-T_s}{L_i} & 0 \\ -\omega(k)T_s & 1-\frac{R_i T_s}{L_i} & 0 & 0 & 0 & -\frac{T_s}{L_i} \\ 0 & 0 & 1-\frac{R_g T_s}{L_g} & \omega(k)T_s & \frac{T_s}{L_g} & 0 \\ 0 & 0 & -\omega(k)T_s & 1-\frac{R_g T_s}{L_g} & 0 & \frac{T_s}{L_g} \\ \frac{T_s}{C} & 0 & -\frac{T_s}{C} & 0 & 0 & \omega(k)T_s \\ 0 & \frac{T_s}{C} & & -\frac{T_s}{C} & -\omega(k)T_s & 0 \end{bmatrix},$$

$$[\Psi] = \begin{bmatrix} \frac{T_s}{L_i} & 0 \\ 0 & \frac{T_s}{L_i} \\ 0 & 0 \\ 0 & 0 \\ 0 & 0 \\ 0 & 0 \end{bmatrix}, \text{and } [\mathrm{H}] = \begin{bmatrix} 0 & 0 \\ 0 & 0 \\ -\frac{T_s}{L_g} & 0 \\ 0 & -\frac{T_s}{L_g} \\ 0 & 0 \\ 0 & 0 \end{bmatrix}$$

As indicated in (115), in developing the dynamics of model predictive control of the DC-link voltage, the CT model of (18) is discretized by (24) to obtain (26). If it is assumed that the resistance of the filter is considered negligible, then the grid voltage, $v_{g_d}(k)$ is considered approximately equal to the converter voltage, $v_{i_d}(k)$. As such, the dynamics of the input capacitor voltage are captured in the converter's voltage selection when included in the cost function.

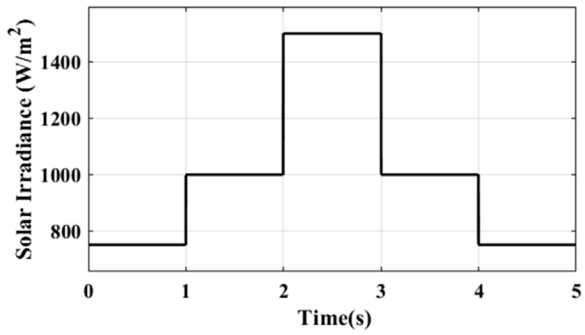

FIGURE 11
Solar irradiance.

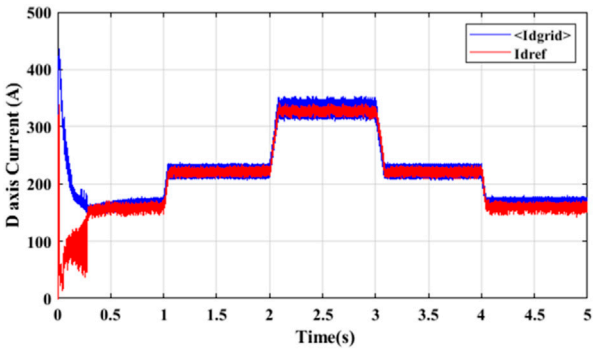

FIGURE 14
d-axis current into the grid from Figure 7.

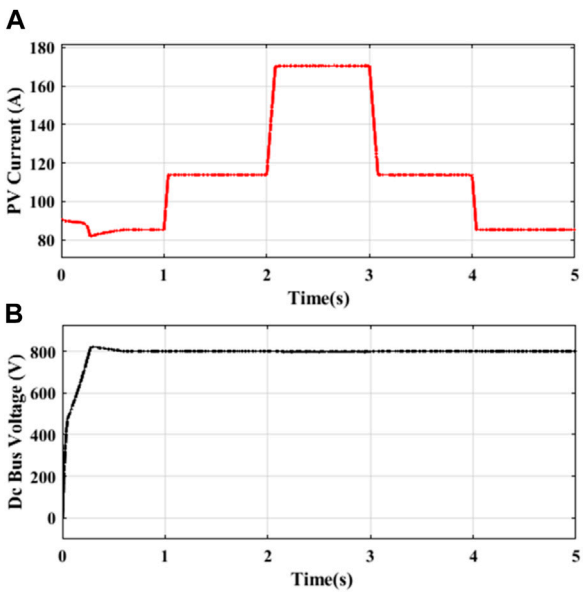

FIGURE 12
(A) PV current. **(B)** DC bus voltage.

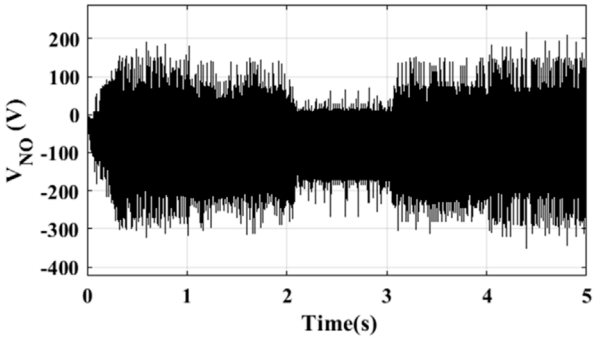

FIGURE 15
Common-mode voltage from Figure 7.

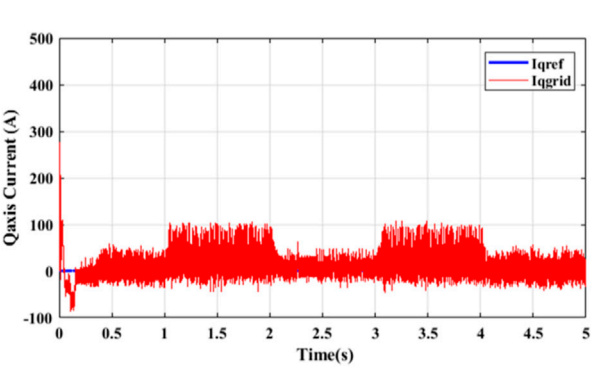

FIGURE 13
q-axis current into the grid from Figure 7.

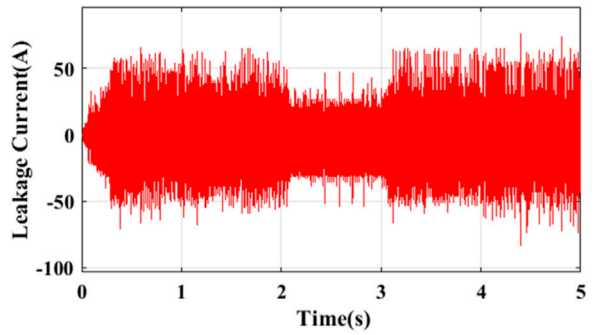

FIGURE 16
Common-mode leakage current from Figure 7.

This method eliminates the need for an outer-loop cascade PI controller for regulating the DC-link voltage.

$$V_{dc}(k+1) = V_{dc}(k) + \frac{T_s}{C}\left(I_{pv}(k) - \frac{3}{2V_{dc}}\left(v_{id}(k) i_{gd}(k)\right)\right). \quad (26)$$

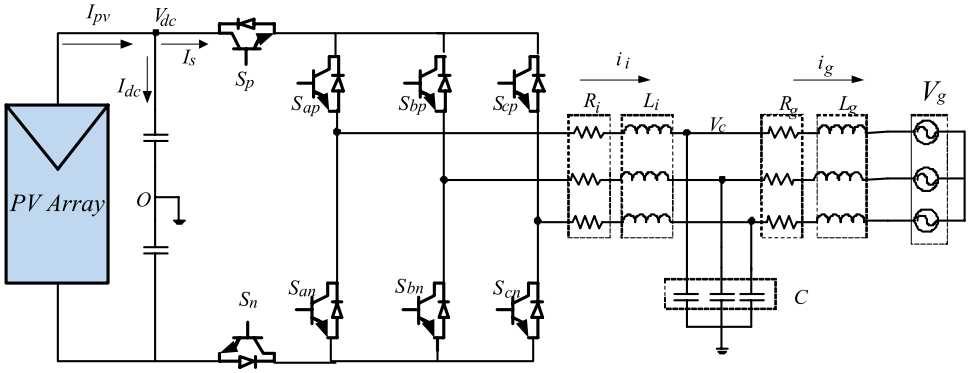

FIGURE 17
PV H8 inverter system.

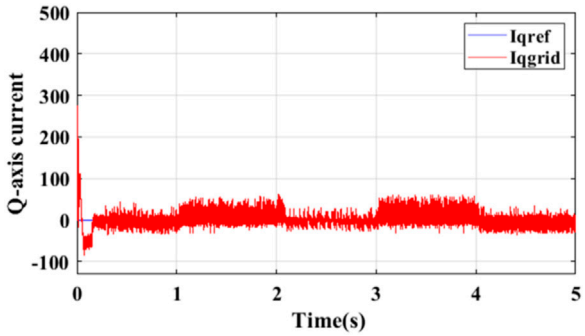

FIGURE 18
q-axis current into the grid from Figure 11.

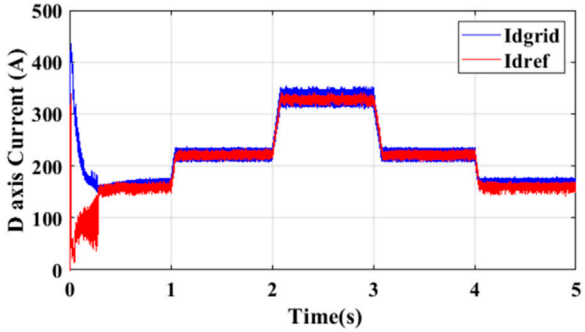

FIGURE 19
d-axis current into the grid from Figure 11.

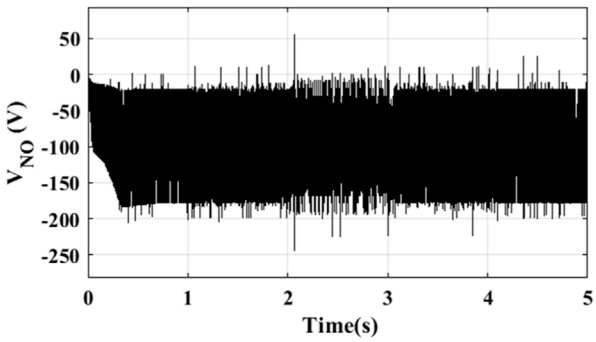

FIGURE 20
Common-mode voltage from Figure 11.

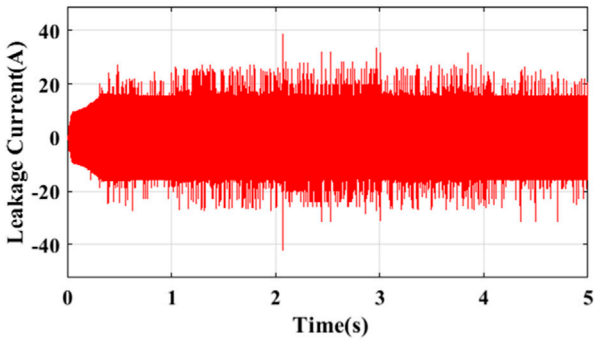

FIGURE 21
Common-mode leakage current from Figure 11.

Furthermore, in MPC, it is essential that the cost function(s) is (are) carefully selected. Therefore, in this sub-section, the primary control objectives of *H8 VSI* are to control the inverter side and grid side inductor current, regulate the filter capacitor voltage, and ensure a maximum power point tracking (MPPT) operation via DC-link voltage control. A secondary control objective can be set to maintain reduced switching losses during operation. Therefore, the compact control cost function used for the overall control scheme is given in (27).

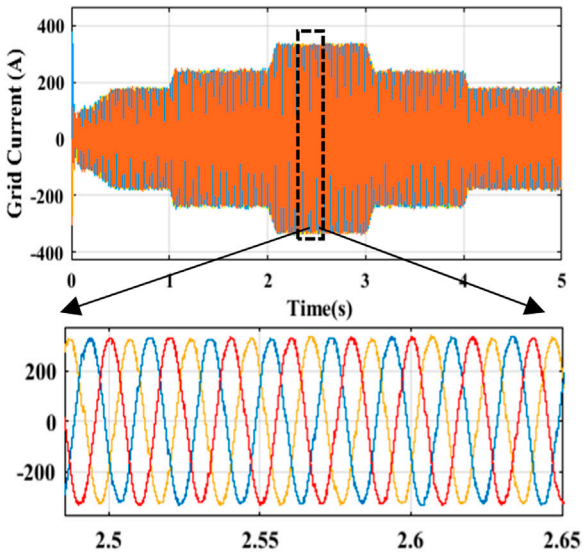

FIGURE 22
Three-phase current injection into the grid.

$$\zeta = \lambda_i\left|i^*_{i_d}(k+1) - i_{i_d}(k+1)\right| + \lambda_i\left|i^*_{i_q}(k+1) - i_{i_q}(k+1)\right| + \lambda_g\left|i^*_{g_d}(k+1) - i_{g_d}(k+1)\right| + \lambda_g\left|i^*_{g_q}(k+1) - i_{g_q}(k+1)\right| + \lambda_{Vc}\left|v^*_{c_d}(k+1) - v_{c_d}(k+1)\right| + \lambda_{Vc}\left|v^*_{c_q}(k+1) - v_{c_q}(k+1)\right| + \lambda_{Vdc}\left|V^*_{dc}(k+1) - V_{dc}(k+1)\right| \quad (27)$$

The variables with '*' index are the dynamically generated reference signals. The cost function contains seven different terms with four weights, which are λ_i, λ_g, $\lambda_{Vc,}$ and λ_{Vdc}. The weights are carefully selected to be larger than 0 to ensure operation stability of the dynamic predictive control system.

8.3 Simulation of model predictive control on H8 VSI

The direct MPC in the previous sub-section was simulated in the MATLAB/Simulink environment for two different categories. In the first category, the MPC was deployed on the *H6* PV inverter system in Figure 7, and the results obtained are presented in Figures 11–16. The entire simulation was performed for a solar irradiance shown in Figure 11. The PV current in Figure 12A is seen to follow the path of the irradiance in Figure 11 and peaked at about 170 A. In Figure 12B, the DC-link voltage was maintained steady at 800 V. The q-axis and d-axis currents injected into the grid are shown in Figures 13, 14, respectively. The common-mode voltage and common-mode leakage current are shown in Figures 15, 16, respectively.

Under the second category, the MPC was deployed on an *H8* PV inverter system (Figure 17), and similar results obtained are presented in Figure 18–21. However, comparing previous Figures 16, 17 reveals significant reduction in the magnitudes of the common-mode voltage and common-mode leakage current. This is seen translating into improved quality of grid currents, as evident in q-axis current of Figure 18 with lower ripples than shown in Figure 14. Therefore, the inverse transformation of the q-d currents

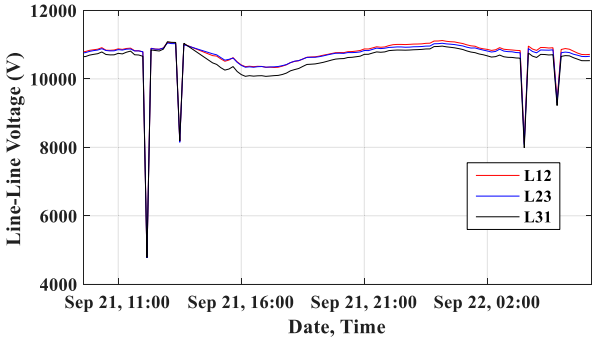

FIGURE 23
An 11-kV distribution grid in the NESI.

in Figures 18, 19, respectively, to the "a-b-c" reference frame as shown in Figure 22 reveals balanced three-phase current injection into the grid with negligible distortions.

9 contingency structure

In Figure 23, the profile of line-to-line voltages in an 11-kV distribution grid in Nigeria with a steel mill connected at its PCC is shown. The steel mill uses both induction and arc furnaces. Evident in Figure 23 is the profound levels and frequency of voltage dip occurrence at such a distribution grid. If a similar load in the distribution grid exists in the 7-bus mini-grid given in Figure 1 and a stable voltage profile is desired, then robust contingency must be in place to support compensation whenever required. The 7-bus mini-grid may be modeled in ETAP as given in Figure 24. A fundamental technical solution for improved resiliency in such an isolated distribution grid is diversifying the power generation resources making up the distributed generation. This is evident in Figure 24 whereby the distributed generations (DGs) in Figure 1 are diversified as follows:

DG1–Wind or mini-hydro or bio-fuel-based energy resources without storage.

DG2–Fossil fuel-based generation (*spinning reserve*).

DG3–Battery storage systems.

DG4–Fossil fuel-based generation.

DG5–Solar PV system with storage.

DG6–Wind or mini-hydro or bio-fuel based energy resources with storage.

DG7–Solar PV system without storage.

The nomenclature of the buses in the ETAP model of Figure 24 when compared to the hypothetical model in Figure 1 is given in Table 1.

In Figure 24, the classical contingency strategy of *N-1* is fulfilled by ensuring that fossil fuel-based generation is set aside as a spinning reserve for redundancy. Therefore, the fossil fuel-based generation does not always inject power into grid except when called upon for contingency. The other renewable energy resources are solar PV systems, wind, and/or mini-hydro energy resources. Battery storage systems are also connected to smoothen the intermittencies that may result from the renewable energy resources. Furthermore, critical loads are connected where steady power can always be guaranteed, such as buses 112 and 106. Buses 2 and 120 would not be considered for critical loads because whenever a fault

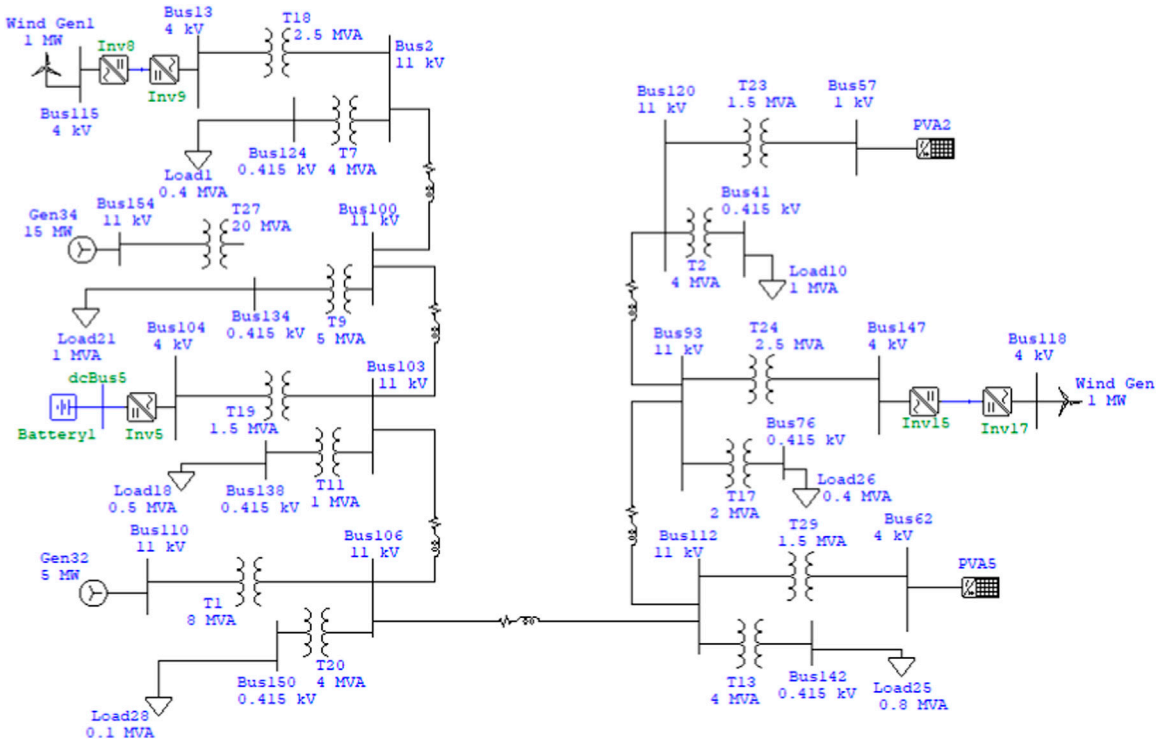

FIGURE 24
7-bus mini-grid in ETAP.

TABLE 1 Nomenclature of buses.

Hypothetical (Figure 1)	ETAP (Figure 24)
PCC_1	Bus 2
PCC_2	Bus 100
PCC_3	Bus 103
PCC_4	Bus 106
PCC_5	Bus 112
PCC_6	Bus 93
PCC_7	Bus 120

occurs that isolates those buses, then the load connected gets completely isolated. However, a more comprehensive selection of buses suitable for steady power supply can be achieved via power flow studies. Moreover, the health management in sub-Section 4.3 will entail monitoring and management at the utilization/demand side to promote efficient and responsible utilization by power off-takers.

10 Conclusion

Control structures and strategies of autonomous distribution grids with embedded generation systems have been reviewed. The papers reviewed are from diverse climes of the world. The power infrastructure layouts in the papers are identified to have common control objectives, such as efficiency optimization. What really differs in all of the climes was in the availability of resources for distributed generation. Usually, technical, economical, and environmental factors dictated the choice of suitable technological outlay for stand-alone distribution grids. Therefore, the applicable control strategies reviewed can be adopted in the NESI to enhance mini-grid operations and promote green energy generation and utilization.

The distributed control system in hierarchical layers was observed to be generally preferred because of its robustness and easier scalability. MPC was seen to be applicable at the three hierarchical control layers. MPC on the PV H8 inverter system at the primary control layer was simulated, and the results revealed more reduction in common mode voltage and common mode leakage current than the conventional 2-level inverter.

Author contributions

AB: conceptualization and writing–original draft. AO: investigation, software, and writing–review and editing. AW: funding acquisition, investigation, and writing–review and editing. SA: conceptualization, methodology, and writing–review and editing. FO: project administration, supervision, and writing–review and editing. TS: funding acquisition, investigation, and writing–review and editing. IS: funding acquisition, investigation, and writing–review and editing. AA: funding acquisition, software, and writing–review and editing.

Funding

The author(s) declare that no financial support was received for the research, authorship, and/or publication of this article.

Acknowledgments

The authors acknowledge and appreciate the financial sponsorship and technical support given to this project by the Nigerian Electricity Regulatory Commission (NERC) and the University of Lagos. The authors deeply recognize the assistance given by Covenant University in all aspects of this research, especially the payment of the publication charges.

Conflict of interest

The authors declare that the research was conducted in the absence of any commercial or financial relationships that could be construed as a potential conflict of interest.

Publisher's note

All claims expressed in this article are solely those of the authors and do not necessarily represent those of their affiliated organizations, or those of the publisher, the editors, and the reviewers. Any product that may be evaluated in this article, or claim that may be made by its manufacturer, is not guaranteed or endorsed by the publisher.

References

Abdulkareem, A., Oguntosin, V., Popoola, O., and Idowu, A. (2022). Modeling and nonlinear control of a quadcopter for stabilization and trajectory tracking. *Hindawi J. Eng.* 2022, 1–19. doi:10.1155/2022/2449901

Agoro, S., Balogun, A., Ojo, O., and Okafor, F. (2018a). "Control of a three-phase multi-string five-level inverter for grid integration of PV systems with unbalanced DC-link voltage," in Proceedings for the 6th International Symposium on Power Electronics and Distributed Generation (PEDG) Systems, Charlotte North Carolina, USA, June 25–28, 2018.

Agoro, S., Balogun, A., Ojo, O., and Okafor, F. (2018b). "Direct model-based predictive control of a three-phase grid connected VSI for photovoltaic power evacuation," in 2018 9th IEEE Int. Symp. Power Electron. Distrib. Gener. Syst. PEDG 2018, vol. 2, 1–6.

Ali, M. T., Zhou, D., Song, Y., Ghandhari, M., Harnefors, L., and Blaabjerg, F. (2020). Analysis and mitigation of SSCI in DFIG systems with experimental validation. *IEEE Trans. Energy Convers.* 35 (2), 714–723. doi:10.1109/tec.2019.2953976

Amoateng, D. O., Al Hosani, M., Elmoursi, M. S., Turitsyn, K., and Kirtley, J. L. (2018). Adaptive voltage and frequency control of islanded multi-microgrids. *IEEE Trans. Power Syst.* 33 (4), 4454–4465. doi:10.1109/tpwrs.2017.2780986

Anand, S., Fernandes, B. G., and Guerrero, J. M. (2013). Distributed control to ensure proportional load sharing and improve voltage regulation in low-voltage DC microgrids. *IEEE Trans. Power Electron.* 28 (4), 1900–1913. doi:10.1109/tpel.2012.2215055

Angirekula, B. N. V., and Ojo, O. (2014). "A Karnaugh mapping technique for the modeling of single phase multi string multilevel inverter," in Applied Power Electronics Conference and Exposition (APEC), 2014 Twenty-Ninth Annual IEEE (IEEE).

Antoniadou-Plytaria, K. E., Kouveliotis-Lysikatos, I. N., Georgilakis, P. S., and Hatziargyriou, N. D. (2017). Distributed and decentralized voltage control of smart distribution networks: models, methods, and future research. *IEEE Trans. Smart Grid* 8 (6), 2999–3008. doi:10.1109/tsg.2017.2679238

Arcos-Aviles, D., Pascual, J., Marroyo, L., Sanchis, P., and Guinjoan, F. (2018). Fuzzy logic-based energy management system design for residential grid-connected microgrids. *IEEE Trans. Smart Grid* 9 (2), 530–543. doi:10.1109/tsg.2016.2555245

Arfeen, Z. A., Khairuddin, A. B., Larik, R. M., and Saeed, M. S. (2019). Control of distributed generation systems for microgrid applications: a technological review. *Int. Trans. Electr. Energy Syst.* 29 (9), 1–26. doi:10.1002/2050-7038.12072

Arnold, G. W. (2011). Challenges and opportunities in smart grid: a position article. *Proc. IEEE* 99 (6), 922–927. doi:10.1109/jproc.2011.2125930

Awelewa, A., Awosope, C. O. A., Abdulkareem, A., and Samuel, I. (2016). Nonlinear excitation control laws for electric power system stabilization. *J. Eng. Appl. Sci.* 11 (7), 1525–1531.

Awelewa, A., Popoola, O., Samuel, I., and Olajube, A. (2020). Comparison of nonlinear excitation controllers for power system stabilization. *Int. J. Eng. Res. Technol.* 13 (2), 320–333. doi:10.37624/ijert/13.2.2020.320-333

Aziz, T., Mhaskar, U. P., Saha, T. K., and Mithulananthan, N. (2013). An index for STATCOM placement to facilitate grid integration of der. *IEEE Trans. Sustain. Energy* 4 (2), 451–460. doi:10.1109/tste.2012.2227517

Balogun, A., Agoro, S., Okafor, F., Adetona, S., and Ojo, O. (2019). Common-mode voltage reduction and elimination in a space vector modulated three-phase five-level multistring inverter. *IEEE PES/IAS PowerAfrica Conf. Power Econ. Energy Innov. Afr. Power Afr.*, 672–676. doi:10.1109/powerafrica.2019.8928909

Balogun, A., Ojo, O., and Okafor, F. (2015). "Compensation control of doubly-fed induction generator for wind energy conversion," in IEEE International Electric Machines and Drives Conference (IEMDC), Coeur d'Alene, Idaho, USA, May 10–13, 2015, 1526–1531.

Balogun, A., Ojo, O., and Okafor, F. (2021). Efficiency optimization control of doubly-fed induction generator transitioning into shorted-stator mode for extended low wind speed application. *IEEE Trans. Industrial Electron.* 68 (12), 12218–12228. doi:10.1109/tie.2020.3037990

Balogun, A., Ojo, O., and Okafor, F. (2013). Decoupled direct control of natural and power variables of doubly-fed induction generator for extended wind speed range using feedback linearization. *IEEE J. Emerg. Sel. Top. Power Electron. (JESTPE)* 1 (4), 226–237. doi:10.1109/jestpe.2013.2283149

Bhandari, B., Lee, K. T., Lee, C. S., Song, C. K., Maskey, R. K., and Ahn, S. H. (2014). A novel off-grid hybrid power system comprised of solar photovoltaic, wind, and hydro energy sources. *Appl. Energy* 133, 236–242. doi:10.1016/j.apenergy.2014.07.033

Bidram, A., and Davoudi, A. (2012). Hierarchical structure of microgrids control system. *IEEE Trans. Smart Grid* 3 (4), 1963–1976. doi:10.1109/tsg.2012.2197425

Bidram, A., Davoudi, A., and Lewis, F. L. (2014). A multiobjective distributed control framework for islanded AC microgrids. *IEEE Trans. Ind. Inf.* 10 (3), 1785–1798. doi:10.1109/tii.2014.2326917

Bidram, A., Davoudi, A., Lewis, F. L., and Guerrero, J. M. (2013). Distributed cooperative secondary control of microgrids using feedback linearization. *IEEE Trans. Power Syst.* 28 (3), 3462–3470. doi:10.1109/tpwrs.2013.2247071

Boonchiam, P., and Mithulananthan, N. (2008). Diode-clamped multilevel voltage source converter based on medium voltage DVR. *Int. J. power energy Syst. Eng.* 1 (2), 62–67.

Buja, G. S., and Kazmierkowski, M. P. (2004). Direct torque control of PWM inverter-fed AC motors—a survey. *IEEE Trans. Industrial Electron.* 51 (4), 744–757. doi:10.1109/tie.2004.831717

Cai, H., Hu, G., Lewis, F. L., and Davoudi, A. (2016). A distributed feedforward approach to cooperative control of AC microgrids. *IEEE Trans. Power Syst.* 31 (5), 4057–4067. doi:10.1109/tpwrs.2015.2507199

Castilla, M., de Vicuña, L. G., and Miret, J. (2019). "Control of power converters in AC microgrids," in *n Microgrids design and implementation* (Cham: Springer), 139–170.

Celanovic, N., and Boroyevich, D. (2001). A fast space-vector modulation algorithm for multilevel three-phase converters. *IEEE Trans. industry Appl.* 37 (2), 637–641. doi:10.1109/28.913731

Che, L., Khodayar, M. E., and Shahidehpour, M. (2014). Adaptive protection system for microgrids: protection practices of a functional microgrid system. *IEEE Electrif. Mag.* 2 (1), 66–80. doi:10.1109/mele.2013.2297031

Chen, F., Chen, M., Li, Q., Meng, K., Guerrero, J. M., and Abbott, D. (2016). Multiagent-based reactive power sharing and control model for islanded microgrids. *IEEE Trans. Sustain. Energy* 7 (3), 1232–1244. doi:10.1109/tste.2016.2539213

Chen, F., Chen, M., Li, Q., Meng, K., Zheng, Y., Guerrero, J. M., et al. (2017). Cost-based droop schemes for economic dispatch in islanded microgrids. *IEEE Trans. Smart Grid* 8 (1), 63–74. doi:10.1109/tsg.2016.2581488

Chen, G., Lewis, F. L., Feng, E. N., and Song, Y. (2015). Distributed optimal active power control of multiple generation systems. *IEEE Trans. Ind. Electron.* 62 (11), 7079–7090. doi:10.1109/tie.2015.2431631

Chen, M., Xiao, X., and Guerrero, J. M. (2018). Secondary restoration control of islanded microgrids with a decentralized event-triggered strategy. *IEEE Trans. Ind. Inf.* 14 (9), 3870–3880. doi:10.1109/tii.2017.2784561

Chu, C. C., and Iu, H. H. C. (2017). Complex networks theory for modern smart grid applications: a survey. *IEEE J. Emerg. Sel. Top. Circuits Syst.* 7 (2), 177–191. doi:10.1109/jetcas.2017.2692243

Chung, S. K. (2000). A phase tracking system for three phase utility interface inverters. *IEEE Trans. Power Electron.* 15 (3), 431–438. doi:10.1109/63.844502

Concari, L., Barater, D., Buticchi, G., Concari, C., and Liserre, M. (2016). H8 inverter for common-mode voltage reduction in electric drives. *IEEE Trans. Ind. Appl.* 52 (5), 4010–4019. doi:10.1109/tia.2016.2581763

Dang, D. Q., Choi, Y. S., Choi, H. H., and Jung, J. W. (2015). Experimental validation of a fuzzy adaptive voltage controller for three-phase PWM inverter of a standalone DG unit. *IEEE Trans. Ind. Inf.* 11 (3), 632–641. doi:10.1109/tii.2015.2416981

De Carne, G., Buticchi, G., Liserre, M., and Vournas, C. (2015). "Frequency-based overload control of smart transformers," in 2015 IEEE Eindhoven PowerTech, Eindhoven, Netherlands, 1–5.

De Carne, G., Buticchi, G., Liserre, M., and Vournas, C. (2018). Load control using sensitivity identification by means of smart transformer. *IEEE Trans. Smart Grid* 9 (4), 2606–2615. doi:10.1109/tsg.2016.2614846

Dehkordi, N. M., Baghaee, H. R., Sadati, N., and Guerrero, J. M. (2019). Distributed noise-resilient secondary voltage and frequency control for islanded microgrids. *IEEE Trans. Smart Grid* 10 (4), 3780–3790. doi:10.1109/tsg.2018.2834951

Dehkordi, N. M., Sadati, N., and Hamzeh, M. (2017a). Distributed robust finite-time secondary voltage and frequency control of islanded microgrids. *IEEE Trans. Power Syst.* 32 (5), 3648–3659. doi:10.1109/tpwrs.2016.2634085

Dehkordi, N. M., Sadati, N., and Hamzeh, M. (2017b). Fully distributed cooperative secondary frequency and voltage control of islanded microgrids. *IEEE Trans. Energy Convers.* 32 (2), 675–685. doi:10.1109/tec.2016.2638858

Energy (2004). "Final report on the August 14, 2003 blackout in the United States and Canada: causes and recommendations," in *U.S.-Canada power system outage task force, tech. Rep*. Available at: http://energy.gov/sites/prod/files/oeprod/DocumentsandMedia/BlackoutFinal-Web.pdf.

Faisal, M., Hannan, M. A., Ker, P. J., Hussain, A., Mansor, M. B., and Blaabjerg, F. (2018). Review of energy storage system technologies in microgrid applications: issues and challenges. *IEEE Access* 6, 35143–35164. doi:10.1109/access.2018.2841407

Fioriti, D., Giglioli, R., Poli, D., Lutzemberger, G., Vanni, A., and Salza, P. (2017). "Optimal sizing of a hybrid mini-grid considering the fuel procurement and a rolling horizon system operation," in Conf. Proc. - 2017 17th IEEE Int. Conf. Environ. Electr. Eng. 2017 1st IEEE Ind. Commer. Power Syst. Eur. EEEIC/I CPS Eur. 2017.

Flowers, L. (1997). Renewables for sustainable village power. *Natl. Renew. Energy Lab*.

Gao, X., De Carne, G., Liserre, M., and Vournas, C. (2017). "Voltage control by means of smart transformer in medium voltage feeder with distribution generation," in 2017 IEEE Manchester PowerTech, Manchester, 1–6.

Golsorkhi, M. S., Shafiee, Q., Lu, D. D. C., and Guerrero, J. M. (2017). A distributed control framework for integrated photovoltaic-battery-based islanded microgrids. *IEEE Trans. Smart Grid* 8 (6), 2837–2848. doi:10.1109/tsg.2016.2593030

Guerrero, J. M., Chandorkar, M., Lee, T. L., and Loh, P. C. (2013a). Advanced control architectures for intelligent microgridspart i: decentralized and hierarchical control. *IEEE Trans. Ind. Electron.* 60 (4), 1254–1262. doi:10.1109/tie.2012.2194969

Guerrero, J. M., Loh, P. C., Lee, T. L., and Chandorkar, M. (2013b). Advanced control architectures for intelligent microgridsPart II: power quality, energy storage, and AC/DC microgrids. *IEEE Trans. Ind. Electron.* 60 (4), 1263–1270. doi:10.1109/tie.2012.2196889

Guo, F., Wen, C., Mao, J., Chen, J., and Song, Y. D. (2015). Distributed cooperative secondary control for voltage unbalance compensation in an islanded microgrid. *IEEE Trans. Ind. Inf.* 11 (5), 1078–1088. doi:10.1109/tii.2015.2462773

Haimo, V. (1986). Finite-time controllers. *SIAM J. Contr. Optim.* 24 (4), 760–770. doi:10.1137/0324047

Hatziargyriou, N. D., Jenkins, N., and Strbac, G. (2006). Microgrids-large scale integration of microgeneration to low voltage grids. *CIGRE* C6-309, 1–8.

Hava, A. M., Kerkman, R. J., and Lipo, T. A. (1999). Simple analytical and graphical methods for carrier-based PWM-VSI drives. *IEEE Trans. Power Electron.* 14 (1), 49–61. doi:10.1109/63.737592

Hazelton, J., Bruce, A., and MacGill, I. (2014). A review of the potential benefits and risks of photovoltaic hybrid mini-grid systems. *Renew. Energy* 67, 222–229. doi:10.1016/j.renene.2013.11.026

Hiskens, I. A., and Fleming, E. M. (2008). Control of inverter-connected sources in autonomous microgrids. *Proc. Am. Control Conf.*, 586–590. doi:10.1109/acc.2008.4586555

Holmes, D. G., and Lipo, T. A. (2003) *Pulse width modulation for power converters: principles and practice*. IEEE Press, Wiley-Interscience, John Wiley and Sons, Inc.

Josep, M. (2017). Review on control of DC microgrids and multiple microgrid clusters aalborg universitet review on control of DC microgrids and multiple microgrid clusters. *IEEE J. Emerg. Sel. Top. Power Electron.* 5 (3), 928–948.

Jumani, T. A., Mustafa, M. W., Alghamdi, A. S., Rasid, M. M., Alamgir, A., and Awan, A. B. (2020). Swarm intelligence-based optimization techniques for dynamic response and power quality enhancement of AC microgrids: a comprehensive review. *IEEE Access* 8, 75986–76001. doi:10.1109/access.2020.2989133

Karugaba, S., Muetze, A., and Ojo, O. (2012). On the common-mode voltage in multilevel multiphase single-and double-ended diode-clamped voltage-source inverter systems. *IEEE Trans. Ind. Appl.* 48 (6), 2079–2091. doi:10.1109/tia.2012.2226223

Kumar, R., Ghatikar, G., Seethapathy, R., Sonavane, V. L., Khaparde, S. A., Yemula, P. K., et al. (2018). "Compendium of technical papers," in 4th International Conference and Exhibition on Smart Grids and Smart Cities, Berlin, Germany, 20-24 May 2018.

Kumar, S., Verma, A. K., Hussain, I., Singh, B., and Jain, C. (2017). Better control for a solar energy system: using improved enhanced phase-locked loop-based control under variable solar intensity. *IEEE Ind. Appl. Mag.* 23 (2), 24–36. doi:10.1109/mias.2016.2600730

Laaksonen, H., Saari, P., and Komulainen, R. (2005). Voltage and frequency control of inverter based weak LV network microgrid. *2005 Int. Conf. Futur. Power Syst.* 2005 (2), 6–11. doi:10.1109/fps.2005.204293

Lai, J., Lu, X., Yu, X., and Monti, A. (2019). Cluster-oriented distributed cooperative control for multiple AC microgrids. *IEEE Trans. Ind. Inf.* 15 (11), 5906–5918. doi:10.1109/tii.2019.2908666

Lasseter, R. H. (2002). "MicroGrids: a conceptual solution," in 2002 IEEE Power Eng. Soc. Winter Meet. Conf. Proc. (Cat. No.02CH37309), vol. 1, New York, NY, USA, 27-31 January, 2002, 305–308.

Lasseter, R. H. (2011). Smart distribution: coupled microgrids. *Proc. IEEE* 99 (6), 1074–1082. doi:10.1109/jproc.2011.2114630

Lasseter, R. H., and Paigi, P. (2004). "Microgrid: a conceptual solution," in 2004 IEEE 35th Annual Power Electronics Specialists Conference (IEEE Cat. No.04CH37551) 6, Aachen, Germany, 20-25 June 2004, 4285–4290.

Li, Q., Chen, F., Chen, M., Guerrero, J. M., and Abbott, D. (2016). Agent-based decentralized control method for islanded microgrids. *IEEE Trans. Smart Grid* 7 (2), 637–649.

Li, Q., Peng, C., Chen, M., Chen, F., Kang, W., Guerrero, J. M., et al. (2017). Networked and distributed control method with optimal power dispatch for islanded microgrids. *IEEE Trans. Ind. Electron.* 64 (1), 493–504. doi:10.1109/tie.2016.2598799

Liao, Y. H., and Lai, C. M. (2011). Newly-constructed simplified single-phase multistring multilevel inverter topology for distributed energy resources. *IEEE Trans. Power Electron.* 26 (9), 2386–2392. doi:10.1109/tpel.2011.2157526

Liserre, M., Blaabjerg, F., and Hansen, S. (2001). Design and control of an LCL-filter based three-phase active rectifier. *Conf. Rec. - IAS Annu. Meet. IEEE Ind. Appl. Soc.* 1 (C), 299–307.

Liu, W., Gu, W., Sheng, W., Meng, X., Wu, Z., and Chen, W. (2014a). Decentralized multi-agent system-based cooperative frequency control for autonomous microgrids with communication constraints. *IEEE Trans. Sustain. Energy* 5 (2), 446–456. doi:10.1109/tste.2013.2293148

Liu, W., Member, S., Gu, W., Sheng, W., Meng, X., and Chen, W. (2014b). Decentralized multi-agent system-based cooperative frequency control for autonomous microgrids with communication constraints. *IEEE Trans. Sustain. Energy* 5 (2 April), 446–456. doi:10.1109/tste.2013.2293148

Loh, P. C., Holmes, D. G., Fukuta, Y., and Lipo, T. A. (2002). "Reduced common mode carrier-based modulation strategies for cascaded multilevel inverters," in Industry Applications Conference, 2002. 37th IAS Annual Meeting. Conference Record of the, vol. 3, Pittsburgh, Pennsylvania, USA, 13-18 October 2002 (IEEE).

Lovejoy, D. (1992). Electrification of rural areas by solar PV. *Nat. Resour. Forum* 16 (2), 102–110. doi:10.1111/j.1477-8947.1992.tb00555.x

Lu, X., Guerrero, J. M., Sun, K., Vasquez, J. C., Teodorescu, R., and Huang, L. (2013). Hierarchical control of parallel AC-DC converter interfaces for hybrid microgrids. *IEEE Trans. Smart Grid* 5 (2), 683–692. doi:10.1109/tsg.2013.2272327

Lu, X., Yu, X., Lai, J., Wang, Y., and Guerrero, J. M. (2018). A novel distributed secondary coordination control approach for islanded microgrids. *IEEE Trans. Smart Grid* 9 (4), 2726–2740. doi:10.1109/tsg.2016.2618120

Maes, J., and Melkebeek, J. A. (2000). Speed–sensorless direct torque control of induction motors using an adaptive flux observer. *IEEE Trans. Industry Appl.* 36 (3), 778–785. doi:10.1109/28.845053

Meng, L., Shafiee, Q., Member, S., and Trecate, G. F. (2017). Review on control of DC microgrids. *IEEE J. Emerg. Sel. Top. Power Electron.* 5 (3), 928–948.

Meng, W., Wang, X., and Liu, S. (2018). Distributed load sharing of an inverter-based microgrid with reduced communication. *IEEE Trans. Smart Grid* 9 (2), 1354–1364. doi:10.1109/tsg.2016.2587685

Mipoung, O. D., Lopes, L. A. C., and Pillay, P. (2014). Frequency support from a fixed-pitch type-2 wind turbine in a diesel hybrid mini-grid. *IEEE Trans. Sustain. Energy* 5 (1), 110–118. doi:10.1109/tste.2013.2273944

Moayedi, S., and Davoudi, A. (2016). Distributed tertiary control of DC microgrid clusters. *IEEE Trans. Power Electron.* 31 (2), 1717–1733. doi:10.1109/tpel.2015.2424672

Moayedi, S., and Davoudi, A. (2017). Unifying distributed dynamic optimization and control of islanded DC microgrids. *IEEE Trans. Power Electron.* 32 (3), 2329–2346. doi:10.1109/tpel.2016.2565517

Morstyn, T., Hredzak, B., and Agelidis, V. G. (2018). Control strategies for microgrids with distributed energy storage systems: an overview. *IEEE Trans. Smart Grid* 9 (4), 3652–3666. doi:10.1109/tsg.2016.2637958

Morstyn, T., Member, S., Hredzak, B., and Member, S. (2016). Control strategies for microgrids with distributed energy storage systems: an overview. *IEEE Trans. Smart Grid* 9 (4), 3652–3666. doi:10.1109/tsg.2016.2637958

Mujtaba, G., Rashid, Z., Umer, F., Baloch, S. K., Hussain, G. A., and Haider, M. U. (2020). Implementation of distributed generation with solar plants in a 132 kV grid station at layyah using ETAP. *Int. J. Photoenergy* 2020, 1–14. doi:10.1155/2020/6574659

Nabae, A., Takahashi, I., and Akagi, H. (1981). A new neutral-point-clamped PWM inverter. *IEEE Trans. Ind. Appl.* 1A-17 (5), 518–523. doi:10.1109/tia.1981.4503992

Narang, D., Ingram, M., Hoke, A., Narang, D., Ingram, M., and Hoke, A. (2020) *Clause-by-Clause summary of requirements in IEEE standard 1547- 2018*. Golden, CO (United States): National Renewable Energy Lab.NREL. (No. NREL/TP-5D00-75184).

Nasirian, V., Member, S., Moayedi, S., Member, S., and Davoudi, A. (2014). Distributed cooperative control of DC microgrids. *IEEE Trans. Power Electron.* 30 (4), 2288–2303. doi:10.1109/tpel.2014.2324579

Nasirian, V., Shafiee, Q., Guerrero, J. M., Lewis, F. L., and Davoudi, A. (2016). Droop-free distributed control for AC microgrids. *IEEE Trans. Power Electron.* 31 (2), 1600–1617. doi:10.1109/tpel.2015.2414457

NERC (2024). Niegerian electricity regulatory commission. Available at: www.nerc.gov.ng.

Nik Idris, N. R., and Mohamed Yatim, A. H. (2004). Direct torque control of induction machines with constant switching frequency and reduced torque ripple. *IEEE Trans. Power Electron.* 51 (4), 758–767. doi:10.1109/tie.2004.831718

Ojo, O., and Kshirsagar, P. (2003). The generalized discontinuous PWM modulation scheme for three-phase voltage source inverters. *IECON Proc. Ind. Electron. Conf.* 2, 1629–1636.

Olivares, D. E., Mehrizi-Sani, A., Etemadi, A. H., Canizares, C. A., Iravani, R., Kazerani, M., et al. (2014). Trends in microgrid control. *IEEE Trans. Smart Grid* 5 (4), 1905–1919. doi:10.1109/tsg.2013.2295514

Pedrasa, M. A., Spooner, T., Pedrasa, M. A., and Spooner, T. (2006). A survey of techniques used to control microgrid generation and storage during island operation. *AUPEC* 1, 15.

Perlack, R. D., Petrich, C. H., and Schweitzer, S. (1988). A comparison of decentralized minigrids and dispersed diesels for irrigation pumping in sahelian africa. *Nat. Resour. Forum* 12 (3), 235–242. doi:10.1111/j.1477-8947.1988.tb00823.x

Poddar, G., and Ranganathan, V. T. (2004). Direct torque and frequency control of double-inverter-fed slip-ring induction motor drive. *IEEE Trans. Industrial Electron.* 51 (6), 1329–1337. doi:10.1109/tie.2004.837897

Qu, Z., Wang, J., and Hull, R. A. (2008). Cooperative control of dynamical systems with application to autonomous vehicles. *IEEE Trans. Autom. Contr.* 53 (4), 894–911. doi:10.1109/tac.2008.920232

Rahim, N. A., and Selvaraj, J. (2010). Multistring five-level inverter with novel PWM control scheme for PV application. *IEEE Trans. industrial Electron.* 57 (6), 2111–2123. doi:10.1109/tie.2009.2034683

Rahimi, R., Farhangi, S., Farhangi, B., Moradi, G. R., Afshari, E., and Blaabjerg, F. (2018). H8 inverter to reduce leakage current in transformerless three-phase grid-connected photovoltaic systems. *IEEE J. Emerg. Sel. Top. Power Electron.* 6 (2), 910–918. doi:10.1109/jestpe.2017.2743527

Rasheduzzaman, M., and Kimball, J. W. (2019). Modeling and tuning of an improved delayed-signal-cancellation PLL for microgrid application. *IEEE Trans. Energy Convers.* 34 (2), 712–721. doi:10.1109/tec.2018.2880610

Rocabert, J., Luna, A., Blaabjerg, F., and Rodriguez, P. (2012). Control of power converters in AC microgrids. *IEEE Trans. power Electron.* 27 (11), 4734–4749. doi:10.1109/tpel.2012.2199334

Sahoo, S. K., Member, S., and Sinha, A. K. (2017). Control techniques in AC, dc, and hybrid AC–DC microgrid: a review. *IEEE J. Emerg. Sel. Top. Power Electron.* 6 (2), 738–759. doi:10.1109/jestpe.2017.2786588

Sen, S., and Kumar, V. (2018). Microgrid control: a comprehensive survey. *Annu. Rev. Control* 45, 118–151. doi:10.1016/j.arcontrol.2018.04.012

Shafiee, Q., Nasirian, V., Vasquez, J. C., Guerrero, J. M., and Davoudi, A. (2018). A multi-functional fully distributed control framework for AC microgrids. *IEEE Trans. Smart Grid* 9 (4), 3247–3258. doi:10.1109/tsg.2016.2628785

She, X., Yu, X., Wang, F., and Huang, A. Q. (2014). Design and demonstration of a 3.6kV-120V/10KVA solid state transformer for smart grid application. *Conf. Proc. - IEEE Appl. Power Electron. Conf. Expo.-APEC* 29 (8), 3982–3996. doi:10.1109/tpel.2013.2293471

Sheikh, A., Youssef, T., and Mohammed, O. (2017). "AC microgrid control using adaptive synchronous reference frame PLL," in *IEEE green technol. Conf.*, 46–51.

Shrestha, A., Rajbhandari, Y., Khadka, N., Bista, A., Marahatta, A., Dahal, R., et al. (2020). Status of micro/mini-grid systems in a himalayan nation: a comprehensive review. *IEEE Access* 8, 120983–120998. doi:10.1109/access.2020.3006912

Singh, M., Lopes, L. A. C., and Ninad, N. A. (2015). Grid forming Battery Energy Storage System (BESS) for a highly unbalanced hybrid mini-grid. *Electr. Power Syst. Res.* 127, 126–133. doi:10.1016/j.epsr.2015.05.013

Sun, Q., Guerrero, J. M., Jing, T., Quintero, R., and Yang, J. C. V. (2016). An islanding detection method by using frequency positive feedback based on FLL for single-phase microgrid. *IEEE Trans. Smart Grid* 8 (4), 1821–1830. doi:10.1109/tsg.2015.2508813

Surprenant, M., Hiskens, I., and Venkataramanan, G. (2011). "Phase locked loop control of inverters in a microgrid," in IEEE Energy Convers. Congr. Expo. Energy Convers. Innov. a Clean Energy Futur. ECCE 2011, Proc., September, 2011, 667–672. doi:10.1109/ecce.2011.6063833

Tahir, M., and Mazumder, S. K. (2015). Self-Triggered communication enabled control of distributed generation in microgrids. *IEEE Trans. Ind. Inf.* 11 (2), 441–449.

Unamuno, E., and Barrena, J. A. (2015). Hybrid ac/dc microgrids - Part II: review and classification of control strategies. *Renew. Sustain. Energy Rev.* 52, 1123–1134. doi:10.1016/j.rser.2015.07.186

Vasquez, J. C., Guerrero, J. M., Savaghebi, M., and Teodorescu, R. (2012). Modeling, analysis, and design of stationary reference frame droop controlled parallel three-phase voltage source inverters. *IEEE Trans. Industrial Electron.* 60 (4), 1271–1280. doi:10.1109/tie.2012.2194951

Wang, X., Taul, M. G., Wu, H., Liao, Y., Blaabjerg, F., and Harnefors, L. (2020). Grid-synchronization stability of converter-based resources—an overview. *IEEE Open J. Industry Appl.* 1, 115–134. doi:10.1109/ojia.2020.3020392

Worldbank (2024). openknowledge. Available at: www.openknowledge.worldbank.org.

Wu, X., and Shen, C. (2017). Distributed optimal control for stability enhancement of microgrids with multiple distributed generators. *IEEE Trans. Power Syst.* 32 (5), 4045–4059. doi:10.1109/tpwrs.2017.2651412

Wu, X., Shen, C., and Iravani, R. (2018). A distributed, cooperative frequency and voltage control for microgrids. *IEEE Trans. Smart Grid* 9 (4), 2764–2776. doi:10.1109/tsg.2016.2619486

Xiang, Y., Pei, X., Wang, M., Shi, P., and Kang, Y. (2019). An improved H8 topology for common-mode voltage reduction. *IEEE Trans. Power Electron.* 34 (6), 5352–5361. doi:10.1109/tpel.2018.2870039

Xin, H., Qu, Z., Seuss, J., and Maknouninejad, A. (2011). A self-organizing strategy for power flow control of photovoltaic generators in a distribution network. *IEEE Trans. Power Syst.* 26 (3), 1462–1473. doi:10.1109/tpwrs.2010.2080292

Xu, Y., Sun, H., Gu, W., Xu, Y., and Li, Z. (2019). Optimal distributed control for secondary frequency and voltage regulation in an islanded microgrid. *IEEE Trans. Ind. Inf.* 15 (1), 225–235. doi:10.1109/tii.2018.2795584

Yao, W., Hu, H., and Lu, Z. (2008). Comparisons of space-vector modulation and carrier-based modulation of multilevel inverter. *IEEE Trans. Power Electron.* 23 (1), 45–51. doi:10.1109/tpel.2007.911865

Yazdanian, M., Member, G. S., and Mehrizi-sani, A. (2014). Distributed control techniques in microgrids. *IEEE Trans. Smart Grid* 5 (6), 2901–2909. doi:10.1109/tsg.2014.2337838

Zhao, Z., Yang, P., Guerrero, J. M., Xu, Z., and Green, T. C. (2016). Multiple-time-scales hierarchical frequency stability control strategy of medium-voltage isolated microgrid. *IEEE Trans. Power Electron.* 31 (8), 5974–5991. doi:10.1109/tpel.2015.2496869

Zhi, D., and Xu, L. (2007). Direct power control of DFIG with constant switching frequency and improved transient performance. *IEEE Trans. Energy Convers.* 22 (1), 110–118. doi:10.1109/tec.2006.889549

Zuo, S., Davoudi, A., Song, Y., and Lewis, F. L. (2016). Distributed finite-time voltage and frequency restoration in islanded AC microgrids. *IEEE Trans. Ind. Electron.* 63 (10), 5988–5997. doi:10.1109/tie.2016.2577542

frontiers | Frontiers in Energy Research

TYPE Original Research
PUBLISHED 04 July 2024
DOI 10.3389/fenrg.2024.1417031

OPEN ACCESS

EDITED BY
Mufutau Adekojo Waheed,
Federal University of Agriculture, Abeokuta, Nigeria

REVIEWED BY
Collins Nwaokocha,
Olabisi Onabanjo University, Nigeria
Olufemi Babalola,
Covenant University, Nigeria
Olawale Olaluyi,
Bamidele Olumilua University of Education, Science and Technology, Nigeria

*CORRESPONDENCE
Olamide O. Olusanya,
ooolusanya@bellsuniversity.edu.ng
Anthony O. Onokwai,
onokwaianthony@gmail.com
Benjamin E. Anyaegbuna,
banyaegbuna@pau.edu.ng

RECEIVED 13 April 2024
ACCEPTED 06 June 2024
PUBLISHED 04 July 2024

CITATION
Olusanya OO, Onokwai AO, Anyaegbuna BE, Iweriolor S and Omoniyi EB (2024), Modelling and optimization of operating parameters for improved steam energy production in the food and beverage industry in a developing country. *Front. Energy Res.* 12:1417031. doi: 10.3389/fenrg.2024.1417031

Modelling and optimization of operating parameters for improved steam energy production in the food and beverage industry in a developing country

Olamide O. Olusanya[1,2]*, Anthony O. Onokwai[2,3]*, Benjamin E. Anyaegbuna[2]*, Sunday Iweriolor[4] and Ezekiel B. Omoniyi[5]

[1]Department of Computer Engineering, Bells University of Technology, Ota, Nigeria, [2]Department of Mechanical Engineering, Pan-Atlantic University, Lekki, Nigeria, [3]Department of Mechatronics Engineering, Bowen University, Iwo, Nigeria, [4]Department of Mechanical Engineering, University of Delta, Agbor, Nigeria, [5]Department of Mechanical Engineering, Bells University of Technology, Ota, Nigeria

Efficient steam energy production was essential for reducing energy consumption and operational costs while enhancing productivity, particularly in industrial settings prone to explosions due to boiler parameter control issues. This challenge was especially acute in the food and beverage industry amid rising energy costs and stricter environmental regulations, highlighting the importance of optimizing steam energy production. This study focused on refining operational parameters in a steam production plant to maximize steam energy output. It utilized mathematical models and optimization tools to identify ideal operational conditions and investigate extreme scenarios. Design-Expert version 13.0 statistical software and Response Surface Methodology (RSM) via Centre Composite Design (CCD) were employed to create a comprehensive design matrix encompassing key variables like time, pressure levels, temperature, mass flow rate, and steam energy production across three experimental levels. The research revealed that increased pressure and time significantly boosted steam energy production by leveraging water's energy content rise under initial conditions, thus improving efficiency by reducing required water mass circulation. Moreover, elevated temperature and extended operation enhanced economizer efficiency, leading to increased heat recovery and reduced steam generation. Steam generation also increased with temperature and time due to the pressure rise during boiling, necessitating more energy for steam conversion. An optimum yield of steam energy of 620 Cal was attained at a time, pressure, temperature, and mass flow rate of 1 h, 16.97 MPa, 249.5°C, and 59.85 kg/s, respectively. The mathematical model developed is accurate, reliable, responsive, and can replicate the experimental data due to the high F-value (24.48), low CV (0.94) low p-value (< 0.005), and high R^2 (0.9821) value close to 1.

This research promises to enhance the efficiency of steam energy production in the food and beverage industry by reducing the need for resource-intensive experimental procedures, thus lowering costs and resource consumption.

KEYWORDS

steam energy generation, response surface methodology, mathematical modelling, optimization, boiler efficiency

1 Introduction

In today's industrial landscape, where energy costs are rising, and environmental regulations are becoming more stringent, enhancing steam energy production has become a critical priority for many industries (Kumar et al., 2020; Onokwai et al., 2023a; Olusanya et al., 2023; Efetobor et al., 2024). Efficient steam energy production can lead to reduced energy consumption, increased productivity, and lower operating costs (Dieckhoffff et al., 2014). However, achieving optimal steam energy production requires attention to various operating factors. Ensuring proper regulation of a boiler's operational parameters is crucial, given the significant risks of explosion associated with high working pressures and temperatures (Guo et al., 2017). Additionally, the financial implications of boiler operation and maintenance, including the expenses related to construction and fuel consumption, should not be overlooked (Dieckhoffff et al., 2014; Ahmadi and Dincer, 2018).

Plant steam also referred to as industrial steam, is utilized in the processing of food and beverages. This type of steam is generated by treating softened water, de-alkalized water, or reverse osmosis water with pre-heating and chemical treatment to prevent the formation of corrosion and scale in the system (Onokwai et al., 2023b). While steam is generally perceived as a clean and sanitary energy source that can be utilized in various applications, including heat exchangers, boiling systems, and hot water generation, it may also be used in direct contact with the process or product (Osueke et al., 2015a; Osueke et al., 2015b; Onokpite et al., 2023). In such cases, it is crucial to ensure the steam's quality and purity to prevent any potential contamination that could compromise human health or the final product's quality (Guo et al., 2017).

In the food and beverage sector, manufacturers must ensure the safety and quality of their products by identifying potential hazards and implementing control measures (Akinbami et al., 2002). Studies (Wang et al., 2023; Pealy, 2024) showed how the food and beverage industry is constantly working to maintain product safety and quality by implementing strict control procedures and cutting-edge technologies. During steam energy generation, potential sources of contamination include the boiler feed water, the steam distribution system, and any equipment or materials that interface with the steam.

To prevent contamination, manufacturers may implement measures such as using high-quality feed water, regularly cleaning and sanitizing the steam system, and using appropriate materials and design features to prevent the buildup of contaminants (Egeonu et al., 2015; As'ad et al., 2019). In modern industrial settings, steam energy production plays a crucial role in powering various processes and operations. As a result, the efficiency and reliability of steam plants are essential factors that directly impact overall energy consumption and productivity. In this regard, the design and operation of steam boilers represent a critical area of focus for maximizing steam energy production (Singha and Forcinito, 2018; Salahi et al., 2023).

Boiler efficiency is influenced by several factors, including the selection of appropriate boiler designs, fuel types, and combustion systems. For instance, a poorly designed or operated boiler can result in decreased efficiency, increased fuel consumption, and higher emissions. Therefore, it is crucial to select the right boiler design and fuel type based on the specific needs of the industrial process. Moreover, the quality of feedwater and its treatment can also impact boiler efficiency and lifespan. High-quality feed water can help minimize corrosion, scale formation, and other forms of damage that can affect the lifespan of boilers. Therefore, implementing proper water treatment measures and ensuring the quality of feedwater is essential for maintaining boiler efficiency and extending the lifespan of steam generation equipment (Szymon et al., 2016; Albana and Dahdah, 2023).

Researchers have investigated different approaches to enhance steam generation. Madu (2018) examined crucial factors that affect the variables for achieving effective operation of a typical steam power plant. The study yielded a specific work output of 854.65 kJ/kg at turbine pressures of 20 bar and 2 bar, and the plant's thermal efficiency was 26.08%, while the rate of heat loss by the condenser and heat generation were 4114.55 and 5027.74 J/s, respectively.

The results showed wet steam at points 4 and 6s, but superheated steam at points 3 and 5. The study recommended optimizing the enthalpy values at points 3 and 5 to enhance the plant's thermal efficiency. Egeonu et al. (2015) presented a successful application of genetic algorithms to optimize the performance of a power plant boiler, which has practical significance for improving the efficiency and cost-effectiveness of power generation. The results showed that the application of genetic algorithms in the thermodynamic optimization of the Egbin power plant boiler leads to a 4.76% and 3.89% increase in thermal efficiency.

Podlasek et al. (2016) applied a PLC control system to automatically adjust the pressure and temperature of the generated steam, which is necessary to ensure the optimal performance of the steam engines under varying load conditions. In a study on a boiler in a petrochemical company, Khoshhal et al. (2010) used numerical simulation to show that NOx emissions were consistent with measured values, indicating that NOx emissions are highly dependent on temperature and oxygen concentration. Similarly, Thornock et al. (2014) used numerical simulation, and large Eddy Dissipation (LES), to predict NOx formation in a steam generator, and proposed a burner design that resulted in lower NOx values. In their study on fuel-staged Low-NOx Burners (LNB), Liu et al. (2016) predicted flow field, temperature, OH molar fraction,

and NO distribution, concluding that the number of staged guns had a significant effect on OH distribution but a negligible impact on the flow field and NO emission. In the study by Ye et al. (2017), a 3-D computational fluid dynamics (CFD) model to scrutinize the fluid dynamics inside an OTSG was created, and evaluated the impact of various structural configurations on coolant flow parameters.

Additionally, Liu et al. (2017) utilized numerical simulations to optimize the position and angle of staged gun injection for reducing NO pollutants and confirmed their findings with experiments. Ensuring effective control of a boiler's operational conditions is crucial due to the potential hazards posed by high working pressures and temperatures, such as the risk of explosion. In addition to construction costs, there are high operating costs (due to significant fuel consumption) and maintenance expenses associated with these conditions. However, finding and maintaining optimal operating conditions for a steam boiler is challenging due to the complexity and inter-relatedness of all variables. Direct testing on a boiler is difficult and dangerous, as it involves manipulating operating conditions and requires significant time and money. Therefore, simulation may be a viable alternative method of analysis (Díaz, 2001).

Researchers have explored the intricacies of optimizing the operating conditions of a steam boiler, considering factors such as safety risks, operational costs, and the intricate interactions of multiple variables (Zhang et al., 2014; Varganova et al., 2023). Nevertheless, there is a lack of information in the literature regarding the optimization of more than three operating factors such as time, pressure, temperature, and mass flow rate using response surface methodology (RSM) to enhance steam energy production. RSM combines statistics and numerical optimization to generate empirical equations that clarify condition-response relationships. RSM combines statistical and numerical optimization techniques to generate empirical equations and determine the impact of specific conditions on targeted responses (Meshalkin et al., 2017; Onokwai et al., 2023c).

In RSM, the input variables are independent conditions, and the performance measures are considered responses (Laouge et al., 2020). During RSM, numerical optimization capabilities are embedded in Design-Expert version 13, allowing for the extraction of optimal numerical solutions (best values) from a given set of input factors and responses within the software (Maddah et al., 2019). Previous research by Onokwai et al. (2019) also implemented RSM to optimize the energy and exergy efficiency of a parabolic dish cooker and found that solar irradiances and temperature had a significant impact on efficiency. Similarly, pyrolysis operating parameters were optimized using RSM to enhanced the yield of pyrolysis products (Hassan et al., 2017).

The focus of this study was to utilize RSM to improve the operational factors of a steam production plant by modeling and optimizing these factors. The main goal was to understand the relationship between operating conditions and steam generation and to identify the optimal process conditions using RSM to optimized steam production. In this study, four steam energy generation operating factors such as time, pressure level, temperature, and mass flow rate. The influence of individual and two most important interactive factors on steam energy generation was investigated using RSM. The essence is to reduce the bottleneck in performing rigorous experimental runs and enhance the efficiency of steam energy production in the food and beverage industry by reducing costs and materials.

2 Methodology

2.1 Research design

This study employed the central composite design (CCD) as the experimental framework for optimizing the steam energy production process systematically. Utilizing response surface methodology (RSM) in conjunction with CCD, facilitated by Design-Expert version 13.0 statistical software (as detailed in Table 1), was the chosen approach. While methods such as Central Composite Design (CCD) and Box-Behnken Design (BBD) are commonly used for RSM, CCD was specifically selected in this investigation. The rationale behind this choice lies in CCD being a widely accepted statistical method for fitting second-order models and optimizing operational factors in steam energy production, as highlighted by previous research (Park et al., 2008; Martin et al., 2020; Yahya et al., 2021; Nainggolan et al., 2023; Umelo-Ibemere, 2023). The study by (Szpisják-Gulyás et al., 2023) further demonstrates how flexible and efficient CCD is in fitting second-order models to optimize a wide range of processes, especially when it comes to the production of steam energy and related fields. CCD stands out for its reliability, time and resource efficiency, ability to deduce regression model equations from pertinent experiments, exploration of interactions among independent factors influencing steam energy production, and efficiency in suggesting the minimum number of test runs when considering the effects of various operating conditions on the final output (Maddah et al., 2019). Given that this study involves four operating parameters with one response variable (steam energy), RSM proves invaluable in reducing analysis time. This is achieved through enhanced computational capabilities, converting numerical data into coded parameters within its black box, and subsequently recalculating it back to numerical data. Additionally, RSM facilitates the grouping of analyses for multi-objective functions (Akhtar et al., 2023). RSM aids in statistical judgments, considering factors such as *p*-values and F-values, guiding decisions on whether to adopt fractional factorial design for 1st-degree polynomial relationships or central composite design for 2nd-degree polynomial relationships for all independent factors and the response variable (Szpisják-Gulyás et al., 2023). Intriguingly, RSM also facilitates the exploration of interactions between independent parameters and the response variable, allowing for maximization, minimization, or specific target setting (Hossain et al., 2017). Since the interactions are limited to the 2nd order, the central composite design (CCD) proves to be highly effective in this context (Kumar et al., 2019). Furthermore, RSM investigates the influence of individual factors, the square of individual factors, and the interaction between two factors on steam energy production as shown in Eq. 1. This study employed key operational factors, specifically time (ranging from 1 to 5 h), pressure levels (ranging between 5 and 20 MPa), temperatures spanning from 100°C to 300°C, and mass flow rates ranging from 50 to 100 kg/s. Each factor was systematically varied at three levels throughout the experimental runs.

TABLE 1 Experimental design matrix and the corresponding Steam energy production.

Std	Run	Factor 1	Factor 2	Factor 3	Factor 4	Response 1
		A:Time (hr)	B: Pressure (Mpa)	C: Temperature (oC) (kg/s)	D: Mass Flow rate	Steam Energy Production
17	1	1	12.5	200	75	604
16	2	5	20	300	100	573
1	3	1	5	100	75	621
18	4	5	12.5	200	75	601
12	5	5	20	100	100	548
9	6	1	5	100	100	540
14	7	5	5	300	100	523
13	8	1	5	300	100	548
3	9	1	20	100	50	595
2	10	5	5	100	50	554
24	11	3	12.5	200	100	569
19	12	3	5	200	75	599
30	13	3	12.5	200	75	602
26	14	3	12.5	200	75	603
23	15	3	12.5	200	25	598
11	16	1	20	100	100	592
29	17	3	12.5	200	75	602
22	18	3	12.5	300	75	503
28	19	3	12.5	200	75	601
7	20	1	20	300	50	589
20	21	3	20	200	75	630
27	22	3	12.5	200	75	603
8	23	5	20	300	50	546
15	24	1	20	300	100	579
21	25	3	12.5	100	75	567
25	26	3	12.5	200	75	601
10	27	5	5	100	100	602
4	28	5	20	100	50	567
5	29	1	5	300	50	563
6	30	5	5	300	50	528

These factors were carefully chosen due to the influence on the quality and quantity of steam energy production as postulated by Chien and Schrodt (1995); Bouamama et al. (2006); Stanley and Pedrosa (2011); Bouamama et al. (2015); Qi et al. (2015). A mathematical expression (Eq. 1) was derived to depict the relationship between these operating factors and the response variable, steam energy production. Subsequently, the constant, linear, quadratic, and interactive coefficients were computed. The optimization of these operating factors aimed to enhance steam energy yield. The statistical model's accuracy and significance were assessed through various criteria, including probability (p-value), lack-of-fit, Fisher (F) value, coefficient of variation (CV), coefficient of determination (R^2), and the comparison between the adjusted and predicted R^2 values (Ehsan et al., 2019; Okokpujie et al., 2023). This rigorous evaluation ensures the robustness and reliability of the mathematical model.

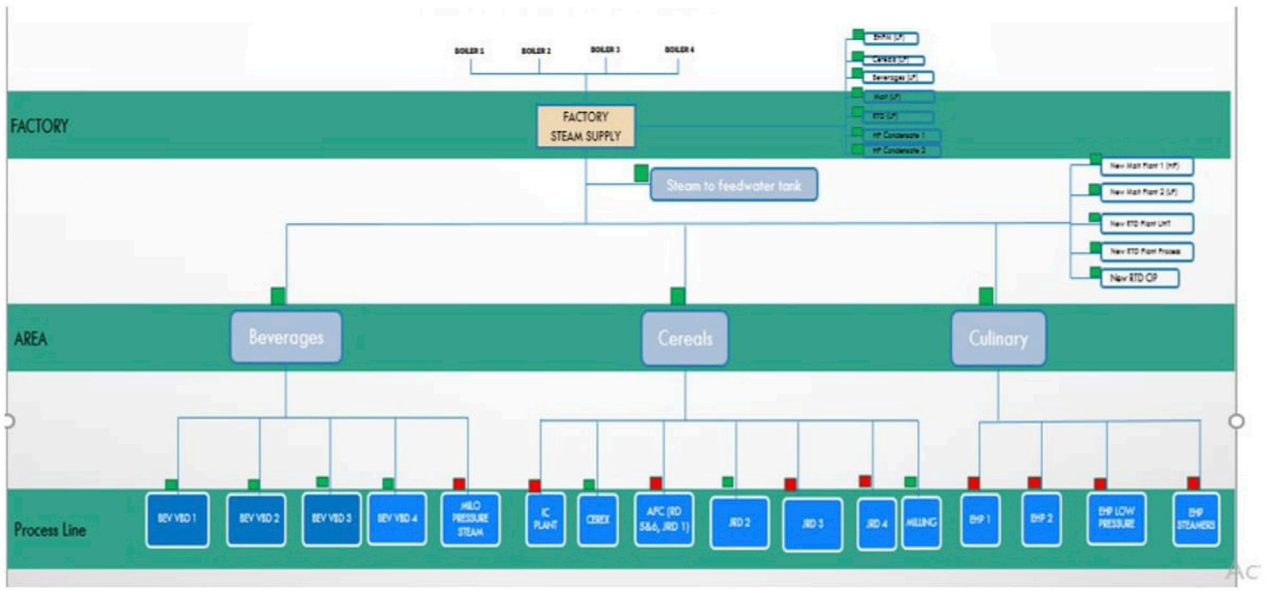

FIGURE 1
Steam flow meter mapping.

$$y = \beta_0 + \sum_{i=1}^{k}\beta_i x_i + \sum_{i=1}^{k}\beta_{ii} x_i^2 + \sum_{i=1}^{k}\sum_{j>1}^{k}\beta_{ij} x_i x_j + \varepsilon_i \quad (1)$$

Where, x_i and x_j are coded independent factors, y is a response of the steam energy production, while β_i, β_{jj} and β_{ij} are the coefficients for linear, quadratic, and interaction effects respectively and k represents the number of operating factors, lastly, ε_i represents the random error in the experiment.

Thirty (30) experimental runs were generated from the Design Expert version 13.0 software statistical software and validated using Eq. 2.

$$N = 2^k + 2k + n_c = 2^4 + 2(4) + 5 = 30 \quad (2)$$

Where N is the actual experimental runs, k is the number of operating factors and n_c = 5 is the repeated number of identical runs at the centre points of the centre composite design.

2.2 Data collection

The steam energy production was generated from Boilers 1 to 4 as shown in Figure 1, while a digitized electronic flow meter with HTML5 and C# was utilized to record the quantity of steam energy production from the beverages industry, Nigeria was utilized due to its ease of configuration and sustainable system maintenance.

3 Results and discussion

Table 1 shows the experimental design matrix and the corresponding steam energy production obtained at different operational factors such as time, pressure, temperature, and mass flow rate. These factors were utilized each at three levels of experimental runs. The maximum steam energy production of 625 was achieved with specific operating conditions: a time (T) of 5 h, a pressure level (P) of 20 MPa, a temperature (θ) of 300°C, and a mass flow rate (M) of 50 kg/s.

3.1 Statistical analysis model for steam energy production

The coded mathematical model that was utilized to predict the steam production in a Nigerian beverage industry is shown in Eq. 3, while Table 2, depicts the summary of the outcome obtained from the Analysis of Variance (ANOVA) which assesses the influence of individual and interactive factors on steam energy production was conducted to validate the mathematical model's accuracy in predicting steam energy production.

$$\begin{aligned} SEP = {} & 596.22 - 10.50A + 7.83B - 13.00C - 4.83D + 8.58A^2 \\ & + 20.588.58B^2 - 58.928.58C^2 - 3.50AB + 10.00AD \\ & + 8.75BC + 8.75CD \end{aligned} \quad (3)$$

Where, SEP denotes steam energy production, while A, B, C, D, and E represent the coded values for time (h), pressure level (MPa), temperature (°C), and mass flow rate (kg/s), respectively. In the mathematical model, a positive (+) sign signifies a synergistic effect, while a negative (−) sign indicates antagonistic effects on steam energy production.

The Fischer test (F-value) and probability value (*p*-value) emerged as acceptable parameters for scrutinizing regression models, as highlighted in studies by Bensouici et al. (2023) and Okokpujie et al. (2023). The F-value compares the mean square value of the residuals and the mean square value of the developed regression model. A higher F-value signifies a more accurate, reliable, responsive, and reproductive regression model.

TABLE 2 Analysis of variance (ANOVA) for the production of steam energy.

Source	Sum of squares	df	Mean square	F-value	*p*-value	Remarks
Model	9058.68	13	696.82	24.48	< 0.0001	Significant
A-Time	760.50	1	760.50	26.71	< 0.0001	Significant
B-Pressure	1682.00	1	1682.00	59.08	< 0.0001	Significant
C-Temperature	1880.89	1	1880.89	66.07	< 0.0001	Significant
D-Mass Flowrate	1334.72	1	1334.72	46.88	< 0.0001	Significant
AB	172.25	1	172.25	6.08	0.0228	Significant
AC	202.25	1	202.25	8.43	0.0112	Significant
BC	202.25	1	202.25	8.43	0.0112	Significant
BD	30.25	1	30.25	1.06	0.3180	Not Significant
CD	240.25	1	240.25	9.3113	0.0091	Significant
A^2	85.27	1	85.27	3.00	0.1027	Not significant
B^2	175.78	1	175.78	6.17	0.0244	Significant
C^2	71.05	1	71.05	2.50	0.1337	Not significant
D^2	58.13	1	58.13	2.04	0.1722	Not significant
Residual	455.49	16	28.47			
Lack of Fit	448.66	11	70.79	2.47	0.1463	Not significant
Pure Error	6.83	5	1.37			
Cor Total	9514.17	29				
Std Dev = 5.34			R^2 = 0.9821			
Mean = 565.83			Adjusted R^2 = 0.9132			
C.V% = 0.9430			Predicted R^2 = 0.7968			
			Adeq Precision = 19.2050			

Additionally, for a model to carry higher significance, the *p*-value should be low, as emphasized by Kumar et al. (2019) and Laouge et al. (2020). The ANOVA analysis showed a high F-value of 24.48 and a low *p*-value of 0.0001 ($p < 0.05$), signifying the high significance and precision of the developed regression model. The likelihood of a model F-value of this magnitude occurring solely due to noise is highly implausible, with a minimal chance (0.01%), as emphasized by Onokwai et al. (2022).

Results indicated that time (A), pressure (B), temperature (C), mass flow rate (D), quadratic of A (A^2), the interaction between time (A) and pressure (B), the interaction between time (A) and temperature (C), the interaction of pressure (B) and temperature (C), the combination of temperature (C) and mass flow rate (D), are significance terms. Consequently, enhancing steam energy production is positively influenced by these significant terms, while insignificant terms do not contribute meaningfully to the improvement of steam energy production. The lack of fit of 0.1463 indicates the suitability of the developed mathematical model, as suggested by Tripathi et al. (2020), as capable of accurately predicting and reproducing the experimental data.

The metric for measuring the dispersion of values in the dataset relative is referred to as the coefficient of variation (%). A small CV value (CV < 10%) is indicative of the high reliability, consistency, reproducibility, and accuracy of the models. In the current study, the calculated CV% value of 0.9843 is relatively low. This low CV% suggests a high level of reproducibility and reliability in the conducted experiments and the investigated model (Kumar et al., 2019).

The R^2 value quantifies the proportion of the variation in the dependent variable explained by all the independent factors incorporated into the model. This metric operates under the assumption that each independent variable in the model contributes to explaining variations in the dependent variable. It acts as the coefficient of determination for the regression model and is expected to be close to 1, aligning with the standards for a robust model (Akhtar et al., 2023). Specifically, the R^2 value of 0.982 is approaching 1. This value affirms the goodness of the mathematical model under scrutiny, signifying its ability to accurately replicate the experimental data. The adjusted R^2 value quantifies the fraction of variation elucidated solely by those independent factors that genuinely contribute to explaining the dependent variables

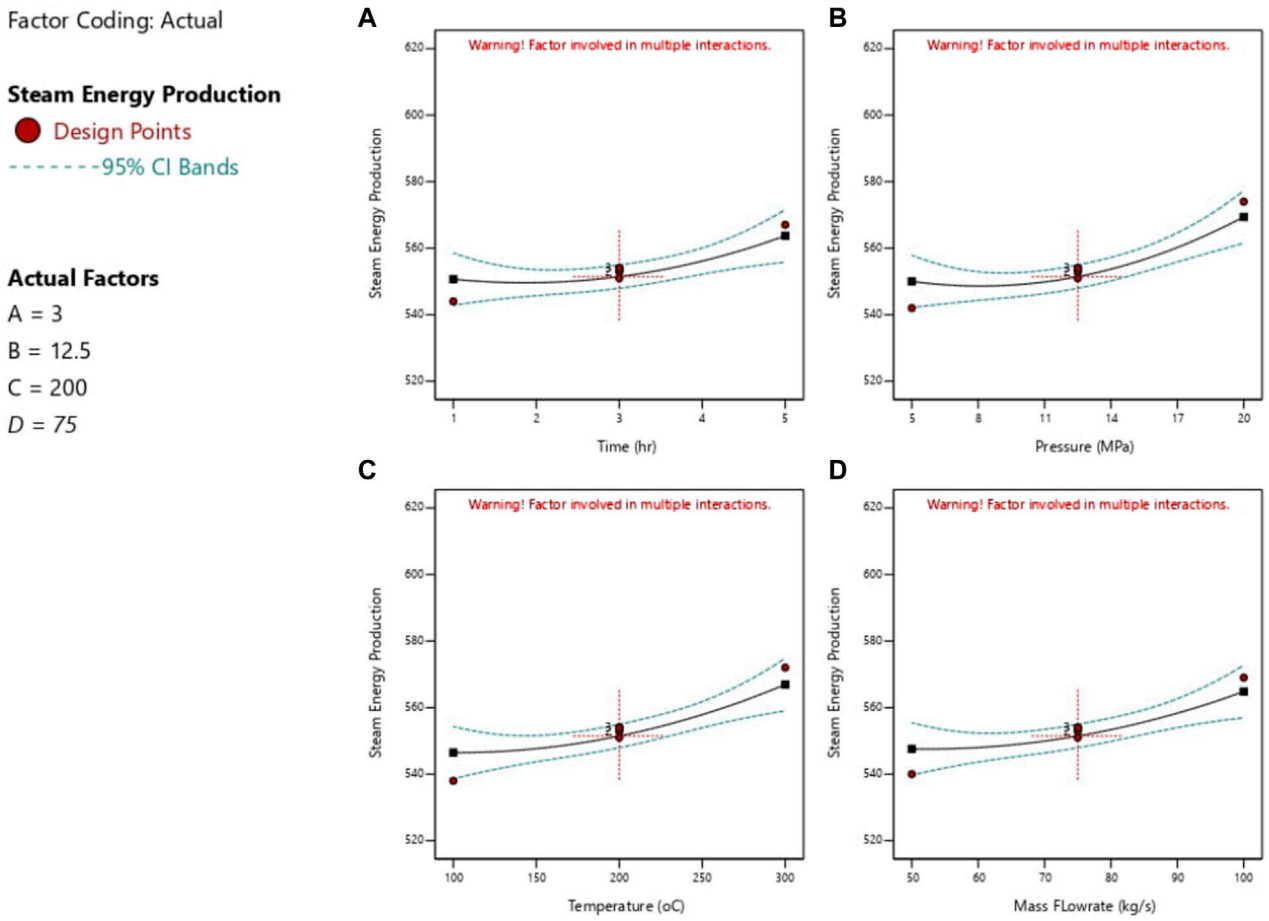

FIGURE 2
Influence of individual factors on steam energy production.

(responses) in the regression model. On the other hand, the predicted R^2 value gauges the extent to which the model explains variation in new data. Generally, a reasonable agreement between the adjusted and predicted R^2 values is indicated when the difference is approximately within 0.2 (Onokwai et al., 2023a). The predicted R^2 (0.7968) is in reasonable consonance (difference of 0.1164) with the adjusted R^2 of 0.9132. Thus, the mathematical model closely aligns with the predicted values, indicating that the model can replicate the data obtained from the beverage industry.

3.2 Influence of individual factors on the steam energy production

Figures 2A–D depicts the influence of individual factors on steam energy production. The combination of higher pressure, simultaneous temperature elevation, and increased mass flow rate (ranging from 50 to 75 kg/s) enhances steam energy production as time increases. However, a reduction in steam energy was observed due to entropy inherent in the steam exchanger, resulting from losses related to initial thermal effects, minimized empty space, and overheating (Nadir et al., 2016).

3.3 Influence of two most significant factors on operating factors on the steam energy production

The 3D response surface and 2D contour plots (Figures 3–6) demonstrate how two key factors significantly influence steam energy production, based on the experimental conditions from Design expert version 13.0 software. Figure 4 depicts the combined effect of pressure level and time on steam energy production, shown through 3D response surface and 2D contour plots. The maximum steam energy production (574 Cal) was attained at a constant temperature (200°C) and mass flow rate (75 kg/s). Increasing pressure coupled with time (h) increased steam energy production, attributed to the increase in energy content of the mass of water under initial conditions, which decreased circulation of mass of water required for energy generation (Figures 3A, B), thereby improving steam energy production efficiency. However, increasing temperature (from 100°C to 200°C) and extending operational time enhanced economizer efficiency, leading to higher heat recovery at the steam generation outlet and consequently reducing steam energy generation (Hasananto et al., 2021).

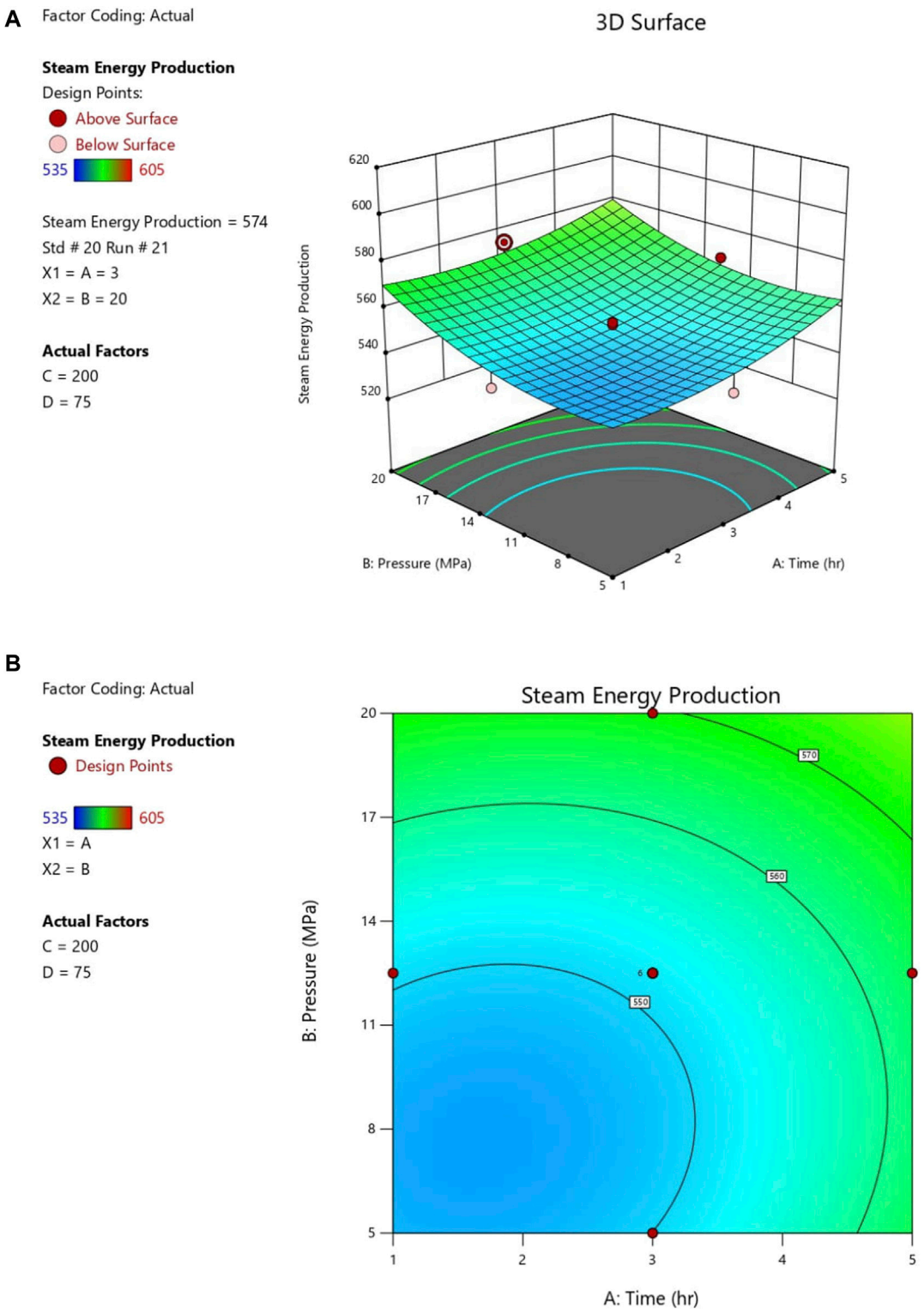

FIGURE 3
(A) 3D response surface plot showing the effect of pressure level and time on steam energy production at a constant 200°C of temperature and 75 kg/s of mass flow rate. **(B)** 2D contour plot showing the effect of pressure level and time on steam energy production at constant 200°C of temperature and 75 kg/s of mass flow rate.

Similarly, steam energy generation rose with increasing temperature and time (Figures 4A, B) due to increased pressure on boiling water, requiring more energy to convert water into steam. Optimal steam energy (572 Cal) was observed at a pressure of 12.5 MPa and 3-h operation. Figures 5A, B depicts the pressure-temperature relationship on steam

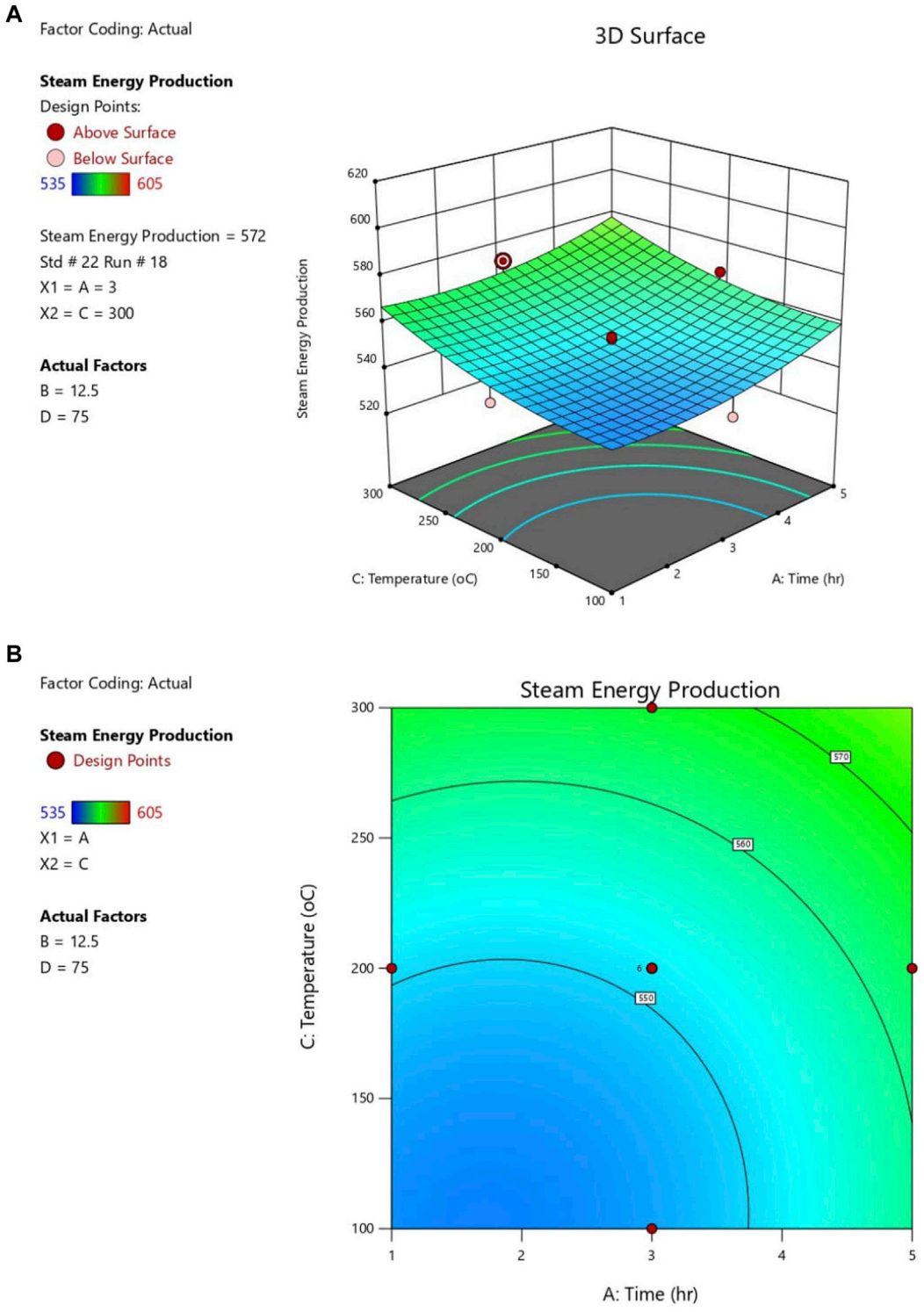

FIGURE 4
(A) 3D response surface plot showing the effect of time and temperature on steam energy production at a constant 12.5 MPa of pressure and 75 kg/s of mass flow rate. **(B)** 2D contour plot showing the effect of time and temperature on steam energy production at a constant 12.5 MPa of pressure and 75 kg/s of mass flow rate.

energy production. Simultaneous increases in temperature and pressure elevated energy transfer (enthalpy) in heat exchangers at higher levels, enhancing energy generation efficiency. Optimal steam energy (572 Cal) occurred at 12.5 Mpa pressure and 300°C temperature, with constant time and mass flow rate. Regarding temperature and mass flow rate interaction (Figures 6A, B), it was

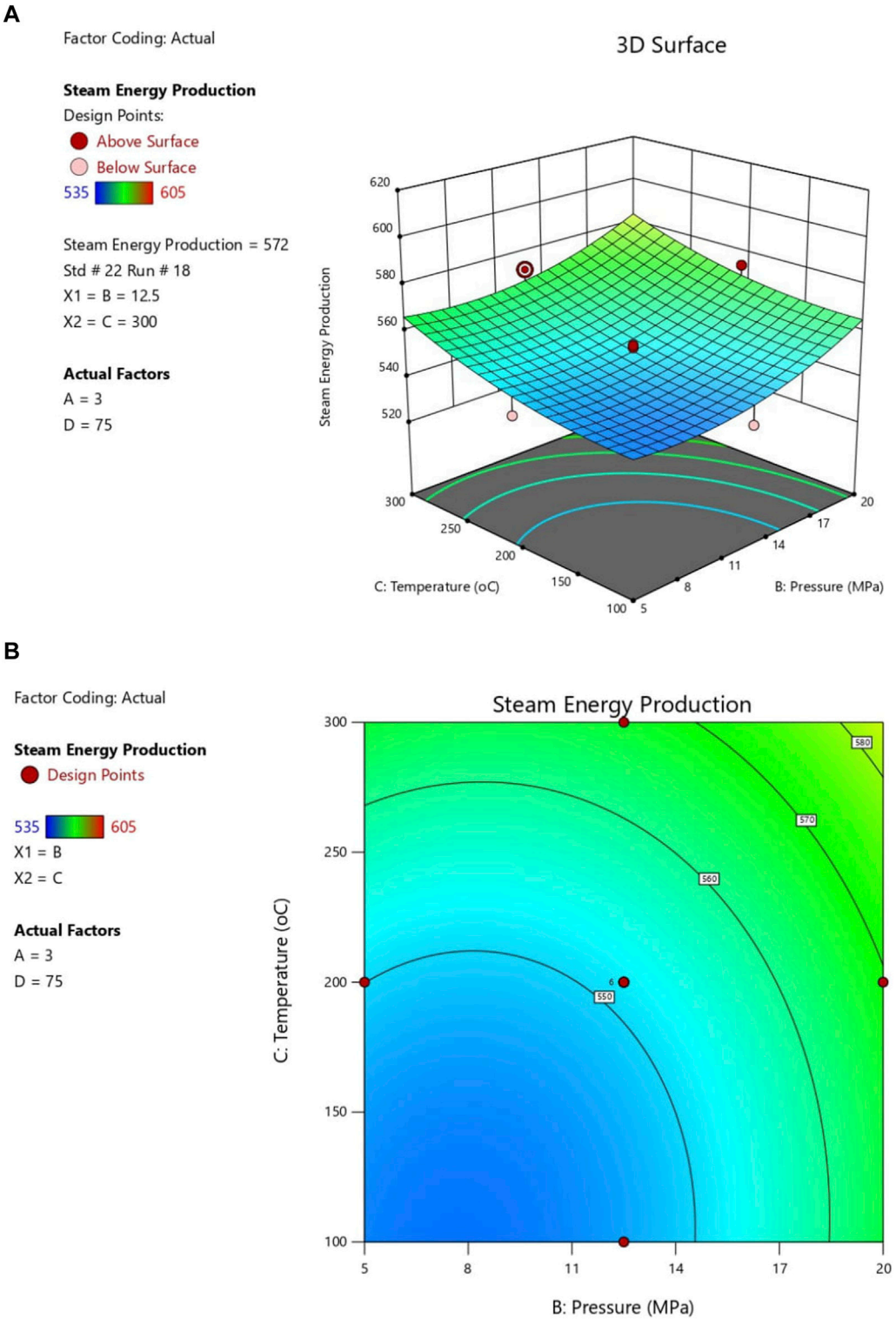

FIGURE 5
(A) 3D response surface plot showing the effect of temperature and pressure level on steam energy production at constant 3 h of time and 75 kg/s of mass flow rate. **(B)** 2D contour plot showing the effect of temperature and pressure level on steam energy production at constant 3 h of time and 75 kg/s of mass flow rate.

found that simultaneous increases enhanced steam velocities entering heat exchangers and water boiling point pressure, augmenting heat energy transfer to fluids and overall efficiency (Vargas et al., 2000). Maximum steam energy (569 Cal) was recorded at 3-h operation and 12.5 Mpa pressure, with constant temperature.

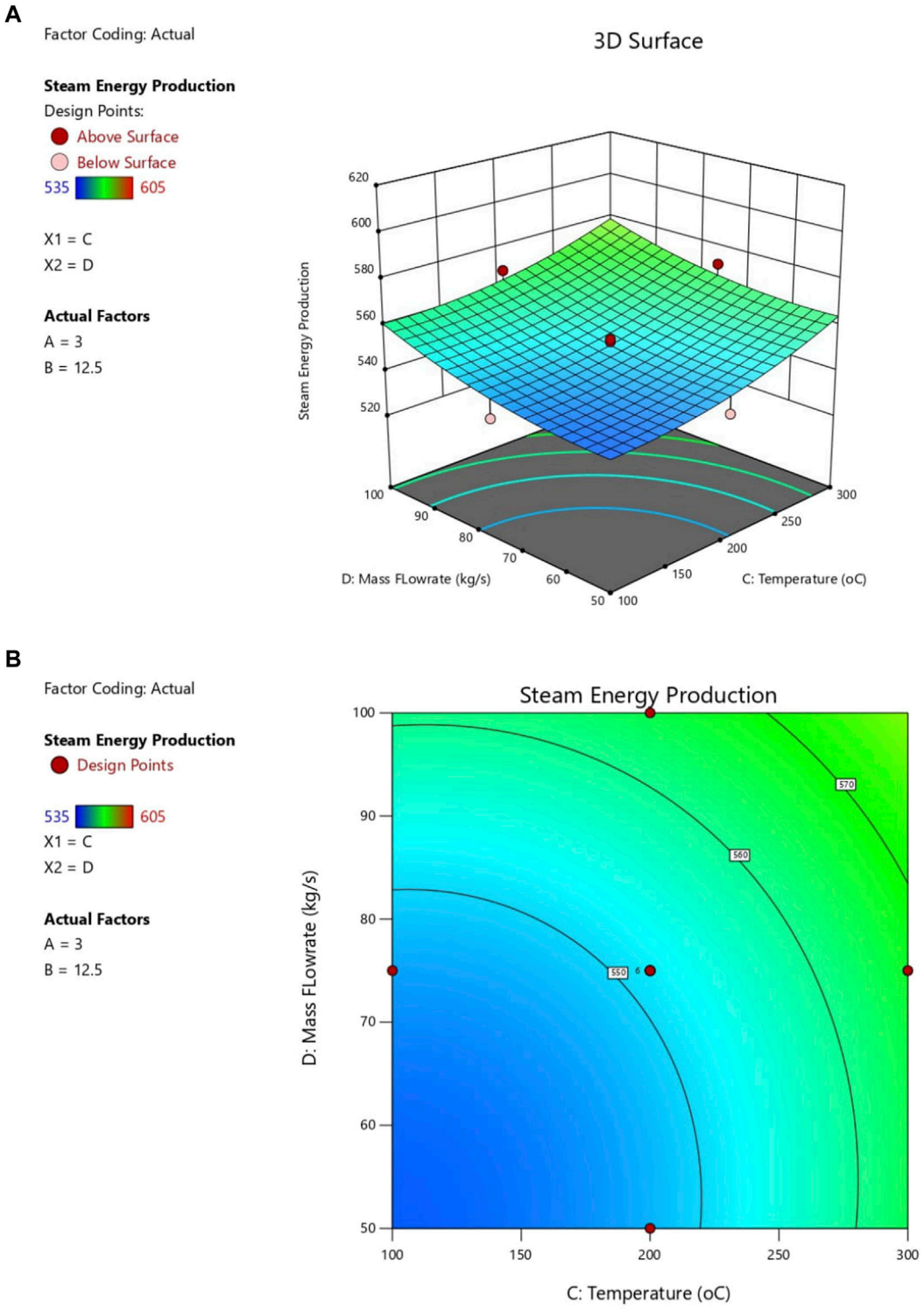

FIGURE 6
(A) 3D response surface plot showing the effect of temperature and mass flow rate on steam energy production at constant 3 h of time and 12.5 MPa of pressure level. **(B)** 2D contour plot showing the effect of temperature and mass flow rate on steam energy production at constant 3 h of time and 12.5 MPa of pressure level.

3.4 Optimum conditions of operating parameters

The optimal values of operating factors that enhance steam energy generation are shown in Figure 7. An optimum yield of steam energy (620 Cal) was attained at a time, pressure, temperature, and mass flow rate of 1 h, 16.97 MPa, 249.5°C, and 59.85 kg/s, respectively (Figure 8). Any value of the operating factors above or below these optimal values would lead to a reduction in steam energy generation. The ANOVA result

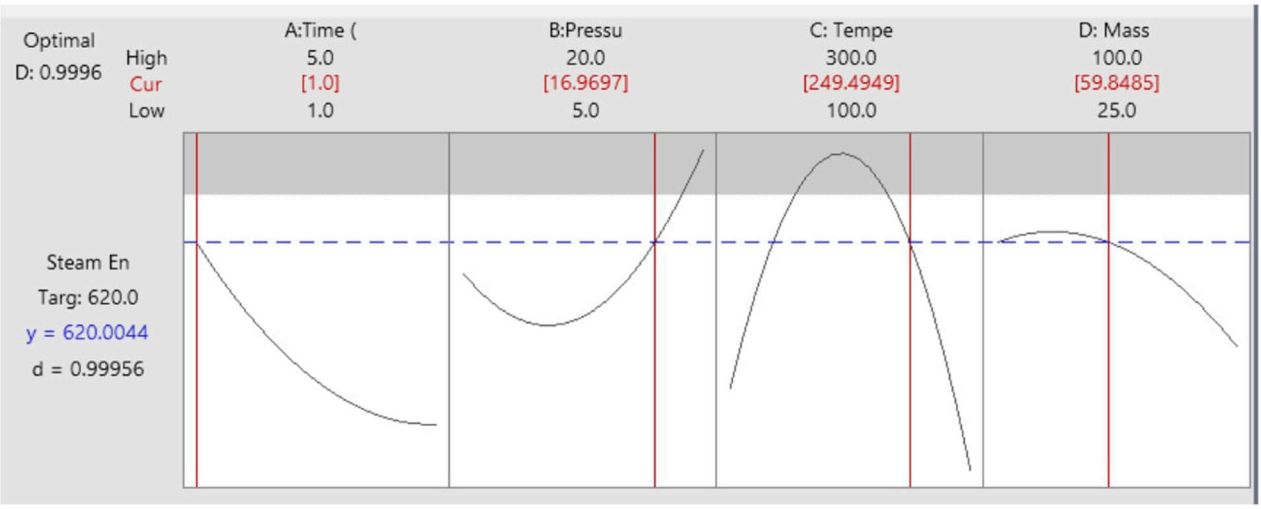

FIGURE 7
Optimization plot.

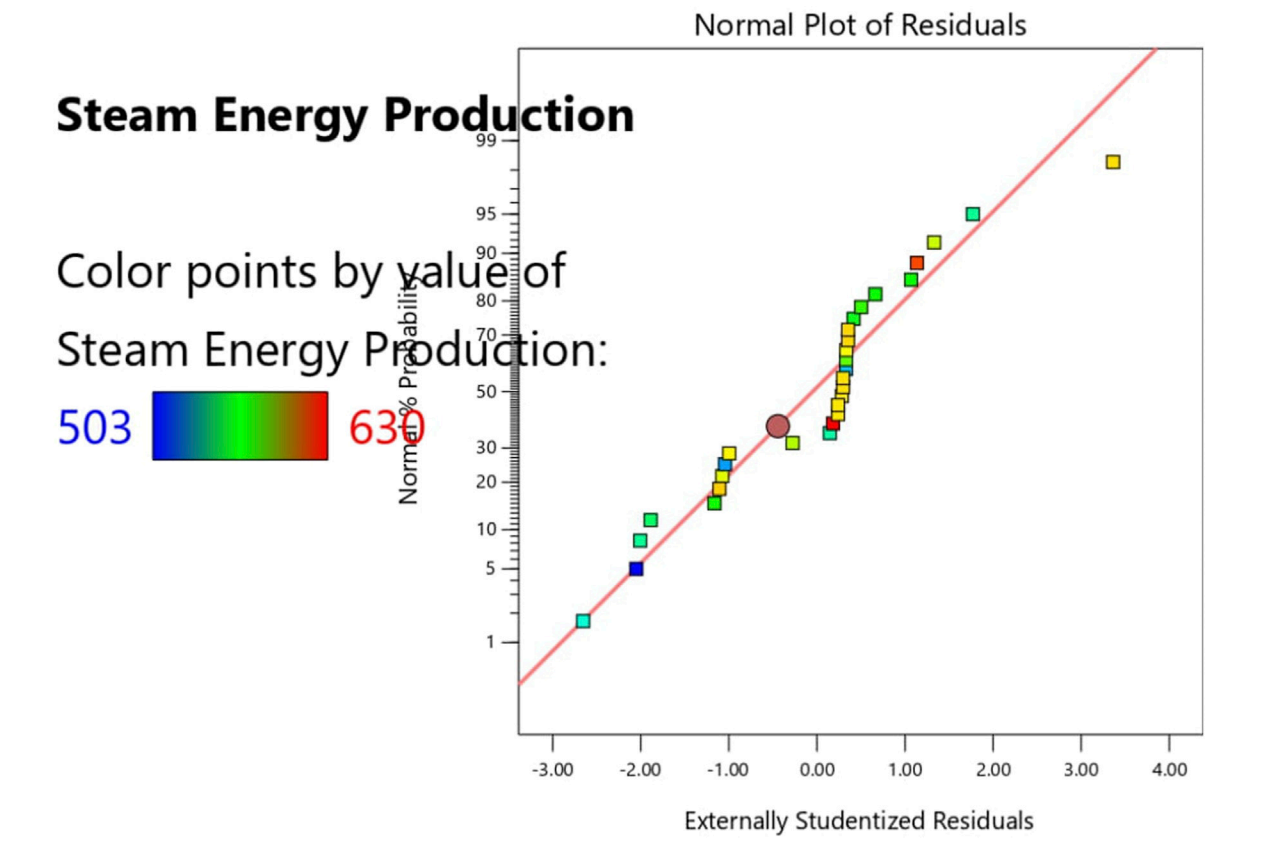

FIGURE 8
Model validation.

(Table 3) obtained showed that the p-value is (> 0.05), Consequently, the established mathematical model stands as a reliable and practical tool for forecasting the steam energy production.

3.5 Validations of results

Tables 3, 4 revealed good agreement between the predicted and actual data. The variances were similar, suggesting comparable

TABLE 3 Validation of experimental and predicted steam energy production.

Run order	Actual value	Predicted value	Residual	Leverage	Internally studentized residuals	Externally studentized residuals	Cook's distance	Influence on fitted value dffits	Standard order
1	544.00	550.70	−6.70	0.485	−1.751	−1.886	0.207	−1.831	17
2	605.00	604.54	0.4627	0.596	0.136	0.132	0.002	0.161	16
3	535.00	534.54	0.4627	0.596	0.136	0.132	0.002	0.161	1
4	567.00	563.70	3.30	0.485	0.862	0.854	0.050	0.830	18
5	585.00	589.84	−4.84	0.596	−1.428	−1.480	0.215	−1.799	12
6	559.00	556.76	2.24	0.596	0.661	0.649	0.046	0.788	9
7	587.00	592.95	−5.95	0.596	−1.756	−1.892	0.325	−2.299[1]	14
8	581.00	578.45	2.55	0.596	0.751	0.740	0.059	0.899	13
9	564.00	561.62	2.38	0.596	0.702	0.690	0.052	0.838	3
10	555.00	552.54	2.46	0.596	0.726	0.715	0.056	0.869	2
11	569.00	564.81	4.19	0.485	1.094	1.101	0.081	1.069	24
12	542.00	550.04	−8.04	0.485	−2.099	−2.388	0.297	−2.319[1]	19
13	554.00	551.46	2.54	0.096	0.500	0.488	0.002	0.159	30
14	551.00	551.46	−0.4649	0.096	−0.092	−0.089	0.000	−0.029	26
15	540.00	547.59	−7.59	0.485	−1.983	−2.211	0.265	−2.147[1]	23
16	580.00	578.34	1.66	0.596	0.489	0.477	0.025	0.579	11
17	553.00	551.46	1.54	0.096	0.303	0.294	0.001	0.096	29
18	572.00	566.92	5.08	0.485	1.326	1.361	0.118	1.322	22
19	554.00	551.46	2.54	0.096	0.500	0.488	0.002	0.159	28
20	583.00	584.32	−1.32	0.596	−0.388	−0.377	0.016	−0.458	7
21	574.00	569.37	4.63	0.485	1.210	1.229	0.099	1.194	20
22	553.00	551.46	1.54	0.096	0.303	0.294	0.001	0.096	27
23	590.00	592.32	−2.32	0.596	−0.683	−0.671	0.049	−0.815	8
24	594.00	596.54	−2.54	0.596	−0.748	−0.738	0.059	−0.896	15
25	538.00	546.48	−8.48	0.485	−2.215	−2.576	0.331	−2.502[1]	21
26	554.00	551.46	2.54	0.096	0.500	0.488	0.002	0.159	25
27	577.00	574.76	2.24	0.596	0.661	0.649	0.046	0.788	10
28	575.00	573.12	1.88	0.596	0.554	0.542	0.032	0.658	4
29	562.00	560.73	1.27	0.596	0.374	0.364	0.015	0.442	5
30	578.00	575.23	2.77	0.596	0.816	0.807	0.070	0.981	6

variability patterns (Table 3). Additionally, a strong positive linear association between the two variables was evident from the high correlation coefficient near 1. Furthermore, the very low t-statistic (0.000216) indicated a minimal difference between the predicted and actual values. The *p*-values, exceeding 0.05 for both one-tailed (0.4999) and two-tailed (0.9998) tests (Table 4), suggested a lack of statistically significant difference between the predicted and actual values. In other words, we failed to reject the null hypothesis, implying no meaningful difference in means exists. Similarly, the t-statistic being significantly lower than critical values reinforces the conclusion that the observed difference is likely due to random chance rather than a true discrepancy between the actual and predicted data. The *t*-test results and *p*-values thus support the interpretation that any observed variations are attributable to random fluctuations rather than reflecting a substantial difference between the predicted and actual values. Furthermore, the predicted values are in close proximity with the actual values as their values align along the regression line

TABLE 4 *t*-test: two-sample assuming equal variances.

	Variable 1	*Variable* 2
Mean	565.8333	565.8323
Variance	328.0747	312.396
Observations	30	30
Pooled Variance	320.2353	
Hypothesized Mean Difference	0	
df	58	
t Stat	0.000216	
P (T ≤ t) one-tail	0.499914	
t Critical one-tail	1.671553	
P (T ≤ t) two-tail	0.999828	
t Critical two-tail	2.001717	

(Figure 8), thereby confirming the model's efficacy. Hence, the mathematical model can replicate the experimental data accurately.

4 Conclusion

Steam energy plays a vital role in the food and beverage industry's production, processing, handling, and packaging, such as cooking, sterilization, drying, humidification, etc,. The study utilized response surface methodology (RSM) based on centre composite design (CCD) to develop an experimental design matrix using four operating factors names time ranging from 1 to 5 h, pressure level (5–20 Mpa), temperature (100°C–300°C), and mass flow rate ranged between 50–100 kg/s, each varies at three levels of experimental runs. The response (steam energy production) and the operational factors were input into the Design-Expert version 13.0 software to generate a mathematical model, which was utilized for predicting and optimizing steam energy production. Increasing pressure and time significantly boosted steam energy production by elevating the water's energy content, thereby reducing the required water mass circulation and enhancing steam energy production efficiency. Conversely, elevated temperature and extended operational time improved economizer efficiency, leading to higher heat recovery at the steam generation outlet, resulting in reduced steam energy generation. Similarly, steam energy generation increased with rising temperature and time due to the heightened pressure on boiling water, necessitating more energy for water-to-steam conversion. An optimal steam energy yield of 620 calories was achieved at specific conditions: 1 h time, 16.97 MPa pressure, 249.5°C temperature, and a mass flow rate of 59.85 kg/s. The ANOVA analysis showed that the mathematical model was significant, reliable, and responsive due to the high F-value (24.48), low CV (0.943) and low *p*-value (< 0.005). The predicted values correlate very well with the experimental values, confirming the model's capability to reproduce the experimental data. It was observed that the R^2 value (0.9821) is close to 1 and the difference between the adjusted (0.9132) and predicted R^2 value (0.7968) falls within the recommended range of 0.1164. Hence, the mathematical model accurately predicts the experimental data. This study contributes to predicting future steam energy production for industrial usage and reduces the bottle in performing rigorous experimental runs.

Data availability statement

The original contributions presented in the study are included in the article/Supplementary Material, further inquiries can be directed to the corresponding authors.

Author contributions

OO: Conceptualization, Data curation, Formal Analysis, Methodology, Resources, Software, Validation, Writing–original draft, Writing–review and editing. AO: Conceptualization, Data curation, Formal Analysis, Investigation, Methodology, Software, Supervision, Validation, Visualization, Writing–original draft, Writing–review and editing. BA: Funding acquisition, Investigation, Methodology, Project administration, Software, Supervision, Writing–original draft, Writing–review and editing. SI: Conceptualization, Funding acquisition, Investigation, Methodology, Resources, Supervision, Validation, Writing–original draft, Writing–review and editing. EO: Data curation, Funding acquisition, Investigation, Methodology, Resources, Software, Visualization, Writing–original draft, Writing–review and editing.

Funding

The author(s) declare that no financial support was received for the research, authorship, and/or publication of this article.

Acknowledgments

The Authors appreciate the Management of Pan-Atlantic University, Lekki, Nigeria for their immense contributions to the success of the study.

Conflict of interest

The authors declare that the research was conducted in the absence of any commercial or financial relationships that could be construed as a potential conflict of interest.

Publisher's note

All claims expressed in this article are solely those of the authors and do not necessarily represent those of their affiliated organizations, or those of the publisher, the editors and the reviewers. Any product that may be evaluated in this article, or claim that may be made by its manufacturer, is not guaranteed or endorsed by the publisher.

References

Ahmadi, P., and Dincer, I. (2018). 1.28 energy optimization. *Compr. Energy Syst.* 1, 1085–1143. doi:10.1016/B978-0-12-809597-3.00135-8

Akhtar, M., Shankarampeta, A., Gupta, V., Patil, A., Cocarascu, O., and Simperl, E. (2023) "Exploring the numerical reasoning capabilities of language models: a comprehensive analysis on tabular data," in *Computer science > computation and language*. Cornell University.

Akinbami, J., Ilori, M. O., and Sanni, A. A. (2002). Improving energy use efficiency in Nigeria's industrial sector: a case study of a beverage plant. *Int. J. Glob. Energy Issues* 18, 239. doi:10.1504/IJGEI.2002.000962

Albana, A., and Dahdah, S. S. (2023). Improving the quality of boiler feed water based on the PDCA cycle by integrating seven tools. *Daengku Journal of Humanities and Social Sciences Innovation*, 3 (6), 907–915. doi:10.35877/454RI.daengku2113

As'ad, R., Alkhati, O., and Alkhatib, O. (2019). Two-stage closed-loop supply chain models under consignment stock agreement and different procurement strategies. *Appl. Math. Model.* 65 (2019), 164–186. doi:10.1016/j.apm.2018.08.007

Bensouici, M., Azizi, M. W., and Bensouici, F. Z. (2023). Performance analysis and optimization of regenerative gas turbine power plant using RSM. *Int. J. Automot. Mech. Eng.* 20 (3), 10671–10683. doi:10.15282/ijame.20.3.2023.10.0824

Bouamama, B. O., Medjahera, K., Samantaray, A. K., and Staroswiecki, M. (2006). Supervision of an industrial steam generator. Part I: bond graph modelling. *Control Eng. Pract.* 14 (2006), 71–83. doi:10.1016/j.conengprac.2005.01.004

Bouamama, B. O., Staroswiecki, M., Riera, B., and Cheri, E. (2015). Multi-modelling of an industrial steam generator. *Control Eng. Pract.* 8 (2000), 1249–1260. doi:10.1016/s0967-0661(00)00018-6

Chien, S., and Schrodt, J. L. G. (1995). Determination of steam quality and flow rate using pressure data from an orifice meter and a critical flowmeter. *E&P Technol. Dept* 10, 76–81. doi:10.2118/24832-pa

Della, A. (2021). How to improve feedwater quality to prevent boiler corrosion. *CorrosionPedia*.

Díaz, S. P. (2001). "Modelling and simulation of an industrial steam boiler with Ecosimpro," in *1st meeting of EcosimPro users* (Madrid: UNED), 1–10.

Dieckhoffff, C., Appelrath, H. J., Fischedick, M., Grunwald, A., and Höfflflfflfler, F. (2014). *Interpretation of energy scenarios, Mai 2014.* München: acatech-Deutsche Akademie der Technikwissenschaften, 2014. (in German).

Efetobor, U. J., Onokwai, A. O., Onokpite, E., and Okonkwo, U. C. (2024). Response surface methodology application for the optimization of biogas yield from an anaerobic Co-digestion process. *Port. Electrochem. Acta* 42, 205–221. (Scopus Indexed). doi:10.4152/pea.2024420304

Egeonu, D., Oluah, C., Okolo, P., and Njoku, H. (2015). Thermodynamic optimization of steam boiler parameter using genetic algorithm. *Innovative Syst. Des. Eng.* 6 (11), 53–64.

Ehsan, A., Mahsa, M., and Omid, F. V. (2019). A novel model for optimization of logistics and manufacturing operation service composition in Cloud manufacturing system focusing on cloud-entropy. *Int. J. Prod. Res.* 58 (10), 1–29.

Guo, S., Liu, D., Chen, X., Chu, Y., Xu, C., Liu, Q., et al. (2017). Model and control scheme for recirculation mode direct steam generation, parabolic trough solar power plants. *Appl. Energy* 202, 700–714. doi:10.1016/j.apenergy.2017.05.127

Hasananto, N., Darmadi, D. B., and Yuliati, L. (2021). Modelling of load variation effect on the steam power plant heat rate and performance using Gatecycle. *IOP Conf. Ser. Mater. Sci. Eng.* 1034, 012048. IOP Publishing. doi:10.1088/1757-899X/1034/1/012048

Hassan, S. N. A., Ishak, M. A., and Ismail, K. (2017). Optimizing the physical parameters to achieve maximum products from co-liquefaction using response surface methodology. *Fuel* 207 (2017), 102–108. doi:10.1016/j.fuel.2017.06.077

Hossain, A., Ganesan, P., Laxmi, J., and Chinna, K. (2017). Optimization of process parameters for microwave pyrolysis of oil palm fiber (OPF) for hydrogen and biochar production. *Energy Convers. Manag.* 133 (2017), 3 49–362. doi:10.1016/j.enconman.2016.10.046

Khoshhal, A., Rahimi, M., and Alsairafifi, A. A. (2010). The CFD modeling of NOx emission, HiTAC, and heat transfer in an industrial boiler. *Numer. Heat. Transf. Part A Appl.* 58, 295–312. doi:10.1080/10407782.2010.505156

Kumar, G., Kim, S. H., Lay, C. H., and Ponnusamy, V. K. (2020). Recent developments on alternative fuels, energy and environment for sustainability. *Bioresour. Technol.* 317, 124010. doi:10.1016/j.biortech.2020.124010

Kumar, M., Mishra, P. K., and Upadhyay, S. N. (2019). Pyrolysis of Saccharum munja: optimization of process parameters using response surface methodology (RSM) and evaluation of kinetic parameters. *Bioresour. Technol. Rep.* 8 (2019), 100332. doi:10.1016/j.biteb.2019.100332

Laouge, Z. B., Çığgın, A. S., and Merdun, H. (2020). Optimization and characterization of bio-oil from fast pyrolysis of Pearl Millet and Sida cordifolia L. by using response surface methodology. *Fuel* 274, 117842. doi:10.1016/j.fuel.2020.117842

Liu, B., Bao, B., Wang, Y., and Xu, H. (2017). Numerical simulation of flow, combustion and NO emission of a fuel-staged industrial gas burner. *J. Energy Inst.* 90, 441–451. doi:10.1016/j.joei.2016.03.005

Liu, B., Wang, Y.-H., and Xu, H. (2016). Numerical study of the effect of staged gun and quarl on the performance of low-NOx burners. *J. Energy Eng.* 142, 04015040. doi:10.1061/(asce)ey.1943-7897.0000296

Maddah, H., Sadeghzadeh, M., Ahmadi, H., Kumar, R., and Shamshirband, S. (2019). Modeling and efficiency optimization of steam boilers by employing neural networks and response-surface method (RSM). *Mathematics* 7 (7), 629. doi:10.3390/math7070629

Madu, K. (2018). Performance analysis of a steam power plant operating under superheated and isentropic conditions. *Equat. J. Eng.* 2018, 22–28.

Martin, M., Kasina, K. J., and Mutiso, J. (2020). Application of central composite design to optimize spawns propagation. *Open J. Optim.* 9 (3), 2020.

Meshalkin, V. P., Bobkov, V. I., Maksim, D., and Khodchenko, S. M. (2017). Optimizing the energy efficiency of the chemical and energy engineering process of drying of a moving dense multilayer mass of phosphorite pellets. *Dokl. Chem.* 477 (2), 286–289. doi:10.1134/s0012500817120059

Nadir, M., Ghenaiet, A., and Carcasci, C. (2016). Thermo-economic optimization of heat recovery steam generator for a range of gas turbine exhaust temperatures. *Appl. Therm. Eng.* 106, 811–826. doi:10.1016/j.applthermaleng.2016.06.035

Nainggolan, E. A., Banout, J., and Urbanova, K. (2023). Application of central composite design and superimposition approach for optimization of drying parameters of pretreated cassava flour. *Foods* 12, 2101. doi:10.3390/foods12112101

Okokpujie, I. P., Onokwai, A. O., Onokpite, E., Babaremu, K., Ajisegiri, E. S. A., Osueke, C. O., et al. (2023). Modelling and optimisation of intermediate pyrolysis synthesis of bio-oil production from palm kernel shell. *Clean. Eng. Technol.* 16 (2023), 100672. doi:10.1016/j.clet.2023.100672

Olusanya, O. O., Olabode, E., Olakunle, K., Onokwai, O. A., Omoniyi, E. B., and Olakunle, A. J. (2023). "Application of programmable electronic flow meter for enhanced data capturing: a case study of the beverage industry in ogun state, Nigeria," in International conference on science, engineering and business for sustainable development goals (SEB-SDG), Omu-Aran, Nigeria, 05-07 April 2023 (IEEE), 57117–57123. doi:10.1109/SEB-SDG57117.2023.10124623

Onokpite, E., Balogun, A. O., Onokwai, A. O., Oki, M., Olabisi, S. A., and Oyebanji, J. O. (2023). Preliminary characterization of woody and non-woody biomass samples based on physicochemical, structural composition and thermal analyses for improving bio-oil yield quality. *Port. Electrochem. Acta* 42, 285–298. doi:10.4152/pea.2024420404

Onokwai, A. O., Ajisegiri, S. A. E., Omoniyi, E. B., Aliyu, J. S., Ibikunle, A. R., Onokpite, E., et al. (2023a). "Optimization of process parameters for intermediate pyrolysis of sugarcane bagasse for biochar production using response surface methodology," in International conference on science, engineering and business for sustainable development goals (SEB-SDG), Omu-Aran, Nigeria, 05-07 April 2023 (IEEE). doi:10.1109/SEB-SDG57117.2023.10124642

Onokwai, A. O., Okokpujie, I. P., Ajisegiri, E. S. A., Nnodim, C. T., Kayode, J. F., and Tartibu, L. K. (2023b). Application of response surface methodology for the modelling and optimisation of bio-oil yield via intermediate pyrolysis process of sugarcane bagasse. *Adv. Mater. Process. Technol.*, 1–19. doi:10.1080/2374068X.2023.2193310

Onokwai, A. O., Okokpujie, I. P., Onokpite, E., Ajisegiri, E. S. A., Oki, M., Onokpite, E., et al. (2023c). Optimization of pyrolysis operating parameters for biochar production from palm kernel shell using response surface methodology. *Math. Model. Eng. Problems* 10 (3), 757–766. doi:10.18280/mmep.100304

Onokwai, A. O., Okonkwo, U. C., Osueke, C. O., Okafor, C. O., Olayanju, T. M. A., and Dahunsi, S. O. (2019). Design, modelling, energy and exergy analysis of a parabolic cooker. *Renew. Energy* 142 (2019), 497–510. doi:10.1016/j.renene.2019.04.028

Onokwai, A. O., Owamah, H. I., Ibiwoye, M., Ayuba, G., and Olayemi, O. A. (2022). Application of response surface methodology (RSM) for the optimization of energy generation from jebba hydro-power plant, Nigeria. *ISH J. Hydraulic Eng.* 28 (1), 1–9. doi:10.1080/09715010.2020.1806120

Osueke, C. O., Onokwai, A. O., and Adeoye, A. O. (2015b). Energy and exergy analysis of a 75MW steam power plant in sapele (Nigeria). *Int. J. Innovative Res. Adv. Eng. (IJIRAE)* 11 (2), 169–179. Available at: http://www.ijirae.com/volumes/Vol2/iss6/26.JNAE10124.pdf.

Osueke, C. O., Onokwai, A. O., Adeoye, A. O., and Ezugwu, C. A. K. (2015a). Enhancing the performance of 75MW steam power plant with second law efficiency, condenser pressure, and rankine cycle. *Int. J. Eng. Sci. (IJES)* 10 (9), 18–29. Available at: http://www.theijes.com/papers/v4-i9/Version-2/C0492018029.pdf.

Park, S. H., Kim, H. J., and Cho, J. I. (2008). Optimal central composite designs for fitting second order response surface linear regression models. *Physica-Verlag* HD, 323–339. doi:10.1007/978-3-7908-2064-5_17

Pealy, H. (2024). Safety and security: the top 10 APAC food and beverage industry food safety and security stories from 2023. *FoodNavigator Asia*.

Podlasek, S., Lalik, K., Filipowicz, M., Sornek, K., Kupski, R., and Raś, A. (2016). Mathematical modeling of control system for the experimental steam generator. *EPJ Web Conf.* 114, 02151. doi:10.1051/epjconf/201611402151

Qi, F., Shukeir, E., and Kadali, R. (2015). Model predictive control of once through steam generator steam quality. *IFAC-PapersOnLine* 48-8, 716–721. doi:10.1016/j.ifacol.2015.09.053

Salahi, F., Zarei-Jelyani, F., and Rahimpour, M. R. (2023). Optimization of hydrogen production by steam methane reforming over Y-promoted Ni/Al2O3 catalyst using response surface methodology. *J. Energy Inst.* 108 (2023), 101208. doi:10.1016/j.joei.2023.101208

Singha, A., and Forcinito, M. (2018) "Emission characteristic map and optimization of NOx in 100 MW staged combustion once-through steam-generator (OTSG)," in Proceedings of the AFRC Industrial Combustion Symposium, Salt Lake City, UT, USA, 17–19.

Stanley, R., and Pedrosa, F. (2011). *Managing steam quality in food and beverage processing*. UK: Spirax Sarco Ltd.

Szpisják-Gulyás, N., Al-Tayawi, A. N., Horváth, Z. H., László, Z., Kertész, S., and Hodúr, C. (2023). Methods for experimental design, central composite design and the Box–Behnken design, to optimise operational parameters: a review. *Acta Aliment.* 52 (4), 521–537. doi:10.1556/066.2023.00235

Szymon, K. L., Filipowicz, M., Sornek, K., Kupski, R., and Ra, A. (2016). *Mathematical modeling of a control system for the experimental steam generator EPJ Web of Conferences 114*. doi:10.1051/epjconf/2016110

Thornock, J. N., Spinti, J. P., and Hradisky, M. (2014). Evaluating the NOx performance of a steam generator for heavy oil production. *Am. Flame Res. Comm. Houst. TX, USA*.

Tripathi, M., Bhatnagar, A., Mubarak, N. M., Sahu, J. N., and Ganesan, P. (2020). RSM optimization of microwave pyrolysis parameters to produce OPS char with high yield and large BET surface area. *Fuel* 225, 118184. doi:10.1016/j.fuel.2020.118184

Umelo-Ibemere, N. C. (2023). Extended central composite designs for second-order model: a performance comparison. *Asian J. Pure Appl. Math.* 5 (1), 98–111. Available at: https://globalpresshub.com/index.php/AJPAM/article/view/1798.

Varganova, A. V., Khramshin, V., and Radionov, A. A. (2023). Operating modes optimization for the boiler units of industrial steam plants. *Energies* 16 (6), 2596. doi:10.3390/en16062596

Vargas, J. V. C., Benjan, O. A., and Bejan, A. (2000). Power extraction from a hot stream in the presence of phase change. *Int. J. Heat Mass Transf.* 43 (2000), 191–201. doi:10.1016/s0017-9310(99)00146-5

Wang, Y., Jin, X., Yang, L., He, X., and Wang, X. (2023). Predictive modeling analysis for the quality indicators of matsutake mushrooms in different transport environments. *Foods* 12, 3372. doi:10.3390/foods12183372

Yahya, H. S. M., Abbas, T., and Amin, N. A. S. (2021). Optimization of hydrogen production via toluene steam reforming over Ni–Co supported modified-activated carbon using ANN coupled GA and RSM. *Int. J. Hydrogen Energy* 46 (48), 24632–24651. doi:10.1016/j.ijhydene.2020.05.033

Zhang, B., Li, Y., and Liu, M. (2014). "Case study: optimization of an industrial steam boiler system operation," in Conference: 2014 ASHRAE annual conference, Seattle, WA, June 28 - July 2, 2014.

frontiers | Frontiers in Energy Research

TYPE Correction
PUBLISHED 18 October 2024
DOI 10.3389/fenrg.2024.1506146

OPEN ACCESS

APPROVED BY
Frontiers Editorial Office,
Frontiers Media SA, Switzerland

*CORRESPONDENCE
Olamide O. Olusanya,
ooolusanya@bellsuniversity.edu.ng
Anthony O. Onokwai,
onokwaianthony@gmail.com
Benjamin E. Anyaegbuna,
banyaegbuna@pau.edu.ng

RECEIVED 04 October 2024
ACCEPTED 08 October 2024
PUBLISHED 18 October 2024

CITATION
Olusanya OO, Onokwai AO, Anyaegbuna BE, Iweriolor S and Omoniyi EB (2024) Corrigendum: Modelling and optimization of operating parameters for improved steam energy production in the food and beverage industry in a developing country. *Front. Energy Res.* 12:1506146. doi: 10.3389/fenrg.2024.1506146

Corrigendum: Modelling and optimization of operating parameters for improved steam energy production in the food and beverage industry in a developing country

Olamide O. Olusanya[1,2]*, Anthony O. Onokwai[2,3]*, Benjamin E. Anyaegbuna[2]*, Sunday Iweriolor[4] and Ezekiel B. Omoniyi[5]

[1]Department of Computer Engineering, Bells University of Technology, Ota, Nigeria, [2]Department of Mechanical Engineering, Pan-Atlantic University, Lekki, Nigeria, [3]Department of Mechatronics Engineering, Bowen University, Iwo, Nigeria, [4]Department of Mechanical Engineering, University of Delta, Agbor, Nigeria, [5]Department of Mechanical Engineering, Bells University of Technology, Ota, Nigeria

KEYWORDS

steam energy generation, response surface methodology, mathematical modelling, optimization, boiler efficiency

A Corrigendum on
Modelling and optimization of operating parameters for improved steam energy production in the food and beverage industry in a developing country

by Olusanya OO, Onokwai AO, Anyaegbuna BE, Iweriolor S and Omoniyi EB (2024). Front. Energy Res. 12:1417031. doi: 10.3389/fenrg.2024.1417031

In the published article, there was an error in Affiliation(s) Anthony O. Onokwai[3,4] * . Instead of "[3]Department of Mechatronics Engineering, Bowen University, Iwo, Nigeria [4]Department of Mechanical Engineering, Bells University of Technology, Ota, Nigeria", it should be "[2]Department of Mechanical Engineering, Pan-Atlantic University, Lekki, Nigeria [3]Department of Mechatronics Engineering, Bowen University, Iwo, Nigeria."

In the published article, there was an error in Affiliation(s) Ezekiel B. Omoniyi[3]. Instead of "[3]Department of Mechatronics Engineering, Bowen University, Iwo, Nigeria it should be "[5]Department of Mechanical Engineering, Bells University of Technology, Ota, Nigeria."

The authors apologize for this error and state that this does not change the scientific conclusions of the article in any way. The original article has been updated.

Publisher's note

frontiers | Frontiers in Energy Research

TYPE Review
PUBLISHED 23 August 2024
DOI 10.3389/fenrg.2024.1429118

OPEN ACCESS

EDITED BY
Sunday Olayinka Oyedepo,
Bells University of Technology, Nigeria

REVIEWED BY
Solomon Giwa,
Olabisi Onabanjo University, Nigeria
Lindley Andres Maxwell,
Universidad de Antofagasta, Chile

*CORRESPONDENCE
Enoch I. Obanor,
enoch.obanorpgs@stu.cu.edu.ng
Enesi Y. Salawu,
enesi.salawu@covenantuniversity.edu.ng
Oluseyi O. Ajayi,
oluseyi.ajayi@covenantuniversit.edu.ng

RECEIVED 07 May 2024
ACCEPTED 06 August 2024
PUBLISHED 23 August 2024

CITATION
Obanor EI, Dirisu JO, Kilanko OO, Salawu EY and Ajayi OO (2024) Progress in green hydrogen adoption in the African context. *Front. Energy Res.* 12:1429118. doi: 10.3389/fenrg.2024.1429118

Progress in green hydrogen adoption in the African context

Enoch I. Obanor*, Joseph O. Dirisu, Oluwaseun O. Kilanko, Enesi Y. Salawu* and Oluseyi O. Ajayi*

Department of Mechanical Engineering, Covenant University, Ota, Nigeria

Hydrogen is an abundant element and a flexible energy carrier, offering substantial potential as an environmentally friendly energy source to tackle global energy issues. When used as a fuel, hydrogen generates only water vapor upon combustion or in fuel cells, presenting a means to reduce carbon emissions in various sectors, including transportation, industry, and power generation. Nevertheless, conventional hydrogen production methods often depend on fossil fuels, leading to carbon emissions unless integrated with carbon capture and storage solutions. Conversely, green hydrogen is generated through electrolysis powered by renewable energy sources like solar and wind energy. This production method guarantees zero carbon emissions throughout the hydrogen's lifecycle, positioning it as a critical component of global sustainable energy transitions. In Africa, where there are extensive renewable energy resources such as solar and wind power, green hydrogen is emerging as a viable solution to sustainably address the increasing energy demands. This research explores the influence of policy frameworks, technological innovations, and market forces in promoting green hydrogen adoption across Africa. Despite growing investments and favorable policies, challenges such as high production costs and inadequate infrastructure significantly hinder widespread adoption. To overcome these challenges and speed up the shift towards a sustainable hydrogen economy in Africa, strategic investments and collaborative efforts are essential. By harnessing its renewable energy potential and establishing strong policy frameworks, Africa can not only fulfill its energy requirements but also support global initiatives to mitigate climate change and achieve sustainable development objectives.

KEYWORDS

green hydrogen, renewable energy, energy transition, energy availability, Africa

1 Introduction

Energy is vital for daily life, powering numerous aspects of our existence. Historically, Africa has primarily depended on fossil fuels for its energy needs. However, the prolonged use of fossil fuels has highlighted significant drawbacks, such as the substantial emission of greenhouse gases, as illustrated in Figure 1. These disadvantages have led to a growing imperative to seek alternative energy sources (Ajayi et al., 2016). The urgent need to combat climate change and cut greenhouse gas emissions has driven the global energy sector towards cleaner and more sustainable options. Within this framework, hydrogen, especially green hydrogen produced from renewable energy, has emerged as a viable solution for reducing carbon emissions in various sectors, including industry, transportation, and power generation (Ewing et al., 2020). With its abundant renewable energy resources, Africa is well-positioned to play a crucial role in the global hydrogen economy.

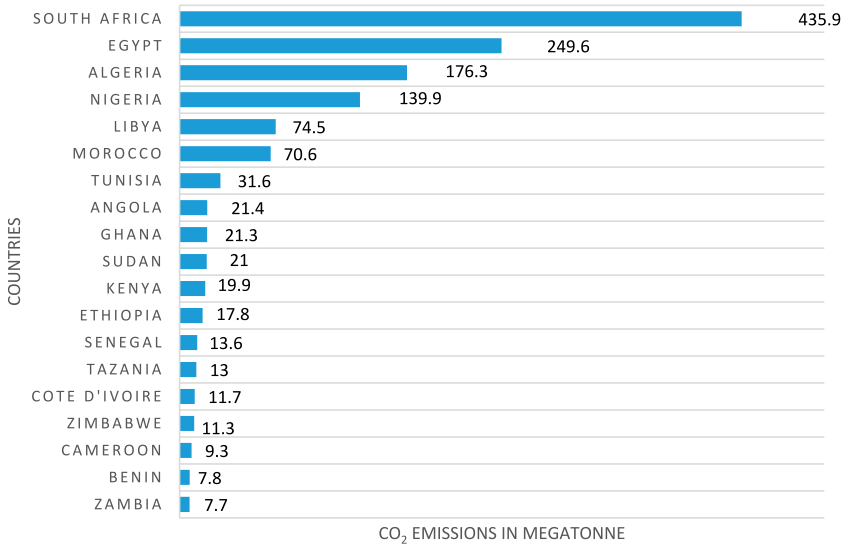

FIGURE 1
Production-based carbon dioxide (CO_2) emissions in Africa in 2021 in mega metric tons (Global Carbon Budget, 2021). https://ourworldindata.org/co2-and-greenhouse-gas-emissions.

1.1 Renewable energy progress in Africa

Africa's renewable energy landscape has seen remarkable advancements over the past decade. Countries across the continent have been harnessing their abundant natural resources which include solar, wind, and hydro in order to build a more sustainable and resilient energy system (Dirisu et al., 2024). According to the International Renewable Energy Agency (IRENA), the installed capacity for renewable energy in Africa grew by over 24% between 2010 and 2020, reaching approximately 56 GW (GW) by the end of 2020 and as at 2023, the total renewable energy capacity in Africa reached about 62 GW as depicted in Figure 2.

- Solar Energy: Africa's solar energy potential is immense, with several regions receiving over 2,000 kWh/m² of solar irradiance annually (Ogunniyi and Pienaar, 2019). Countries such as Egypt, Morocco, and South Africa have made significant strides in solar power generation. South Africa had the largest solar energy capacity in Africa as of 2023, reaching over 6 GW (Pourasl et al., 2023). According to the International Energy Agency (IEA, 2023), Egypt recorded the second biggest capacity, at approximately 1.9 GW while Morocco followed with 934 MW of solar energy capacity. The Noor Ouarzazate Solar Complex in Morocco, one of the world's largest concentrated solar power plants, exemplifies the continent's capability in harnessing solar energy (Bakhti, 2024).
- Wind Energy: Wind power is another critical component of Africa's renewable energy mix. Coastal regions and highland areas, particularly in countries like Kenya and South Africa, offer excellent wind resources (Ajayi et al., 2016; Merem et al., 2022). The Lake Turkana Wind Power project in Kenya, the largest wind farm in Africa, has an installed

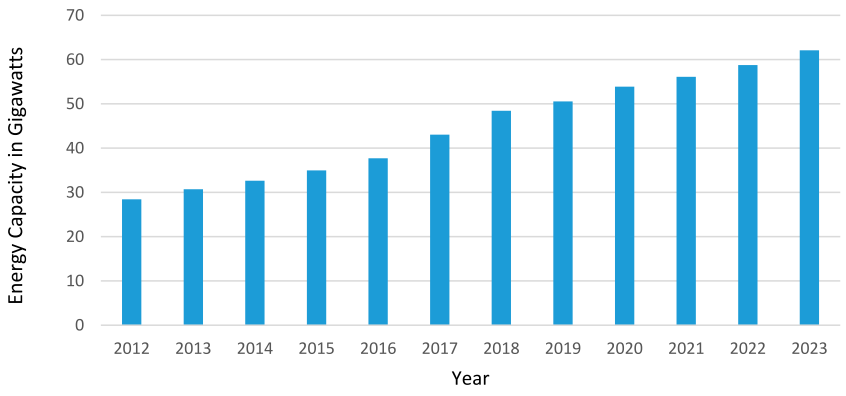

FIGURE 2
Renewable energy capacity in Africa (IRENA, 2024).

capacity of 310 MW (MW) and is a testament to the continent's wind energy potential (Ogeya et al., 2021).

- Hydropower: Hydropower remains the most established renewable energy source in Africa, contributing significantly to the electricity supply in countries like Ethiopia, the Democratic Republic of Congo, Nigeria, and Zambia (Ohunakin et al., 2011; Tiruye et al., 2021). In 2023, 2 GW of hydropower capacity was installed which contributed in increasing the continent's total energy capacity (Bamisile et al., 2023). The Grand Ethiopian Renaissance Dam (GERD), once fully operational, will be Africa's largest hydroelectric power plant, significantly boosting the region's renewable energy capacity (Tiruye et al., 2021).

While the progress in renewable energy adoption in Africa is increasing, the emergence of hydrogen as a viable alternative to fossil fuels can also be adopted to aid the diversification of energy sources in Africa.

1.2 Hydrogen as a viable energy source

Hydrogen is gaining traction as a potential replacement for fossil fuels due to increasing concerns about their environmental and financial drawbacks (Mustafa et al., 2020; Pastore et al., 2022). Bhagwat and Olczak (2020) highlight hydrogen's significant potential in various sectors, such as transportation, power generation, and industrial processes, with global production reaching around 120 million tonnes annually. In contrast, the continuous consumption of fossil fuels releases large amounts of CO_2, exacerbating global warming, and depletes energy resources (Mustafa et al., 2020). Currently, China leads the world in hydrogen production and consumption, using approximately 23.9 million metric tons in 2020. The United States follows, with 11.3 million metric tons of global hydrogen consumption (Kumar et al., 2024).

Hydrogen's appeal lies in its storage capabilities, efficiency, cleanliness, and compatibility with renewable energy sources (Qian et al., 2023). Consequently, hydrogen is crucial in decarbonizing various sectors and mitigating climate change, particularly in transportation and steel manufacturing (Banava, 2023). However, it is important to recognize that while burning hydrogen only emits water vapor, producing it from fossil fuels can still result in CO_2 emissions. To achieve truly emission-free hydrogen production, dependence on renewable energy sources is essential (Stavroulakis et al., 2023). According to Liu et al. (2023), green hydrogen is expected to replace fossil fuels in the near future. Table 1 illustrates the colour classification of hydrogen, the energy sources, and the production methods used.

Hydrogen, the simplest element, consistently yields a carbon-free molecule regardless of its production method (Van Hoecke et al., 2021). However, the methods used to produce hydrogen vary widely, influencing greenhouse gas emissions such as carbon dioxide (CO_2) and methane (CH_4) (Sánchez-Bastardo et al., 2021). Green hydrogen, produced from renewable sources like wind, solar, and hydropower, is viewed as a clean alternative to fossil-derived hydrogen (Kakoulaki et al., 2021). Its production represents a significant step toward achieving a carbon-neutral future, with applications spanning transportation, power generation, and industrial sectors (Kovač et al., 2021).

The process of electrolysis can be represented by the chemical equation:

$$2H_2O + \text{electricity} \rightarrow 2H_2 + O_2$$

Electrolytic hydrogen generation ensures purity levels exceeding 99.95%, free from hydrocarbon contamination (Burton et al., 2021; Newborough and Cooley, 2020). Electrolytic hydrogen production, unless powered by electricity from fossil fuel stations, is not associated with CO_2 or methane emissions, thereby obviating the necessity for carbon capture and storage.

The growing demand for hydrogen across sectors such as transportation, power generation, and manufacturing underscores the urgency of producing hydrogen from renewable energy sources (Ahmed et al., 2023). The potential for green hydrogen to decarbonize hard to abate sectors like heavy industry such as cement production, steel manufacturing, and chemical processing, and shipping and aviation has made it a crucial component of the energy transition (Harichandan et al., 2023) however, several factors need to be considered when producing green hydrogen using renewable energy sources.

TABLE 1 Showing the colour scheme of hydrogen (Ajanovic et al., 2022; Khan and Al-Ghamdi, 2023).

Source	Method of production	Colour
Renewable Energy	Water electrolysis using electricity generated from renewable energy sources	Green Hydrogen
Fossil fuels	Partial oxidation causing CO emissions in the process	Grey Hydrogen
Natural gas	Natural gas reforming	Grey Hydrogen
Methane	Pyrolysis where the by-product is solid carbon	Torquoise Hydrogen
Mixed grid electricity	Water electrolysis using grid electricity	Yellow Hydrogen
Nuclear Energy	Water electrolysis using electricity from Nuclear power plants	Pink Hydrogen
Black Coal	Gasification	Black Hydrogen
Lignite	Gasification	Brown Hydrogen

1.3 Factors considered when producing green hydrogen

Green hydrogen production hinges fundamentally on several key factors, each crucial for its economic viability, environmental sustainability, and widespread adoption as a clean energy solution.

1.3.1 Renewable energy availability

The production of green hydrogen is fundamentally anchored on the disposal and accessibility of renewable energy sources (Sarker et al., 2023). These sources, primarily solar, wind, and hydroelectric power, are pivotal in the electrolysis process that splits water into hydrogen and oxygen, producing green hydrogen. Regions endowed with a consistent and substantial supply of these renewable resources are naturally poised to become leaders in green hydrogen production, capitalizing on their sustainability and reduced environmental footprint compared to fossil fuel-based methods (Osman et al., 2023). As at 2018 however, Renewable energy sources was the least used in hydrogen production globally as depicted in Figure 3.

The variability and intermittency inherent in renewable energy sources present unique challenges to green hydrogen production (Coban et al., 2023). Fluctuations in solar irradiation, wind speeds, or water flow rates can impact the efficiency and reliability of electrolysis processes (Kojima et al., 2023). As such, integrating advanced energy storage systems and smart grid technologies becomes imperative. These systems can store excess energy during peak production periods and release it during low or no production periods, ensuring a continuous and reliable energy supply for hydrogen production.

While some regions may have abundant solar resources, they may lack sufficient wind or hydroelectric power. This disparity necessitates a multifaceted approach to green hydrogen production, incorporating a mix of renewable energy sources to optimize production efficiency and reliability. Strategic planning and investment in interconnected energy grids and cross-regional energy trading can facilitate the seamless integration and distribution of diverse renewable energy sources, bolstering the feasibility and scalability of green hydrogen production initiatives (Okolie et al., 2021; Raman et al., 2022).

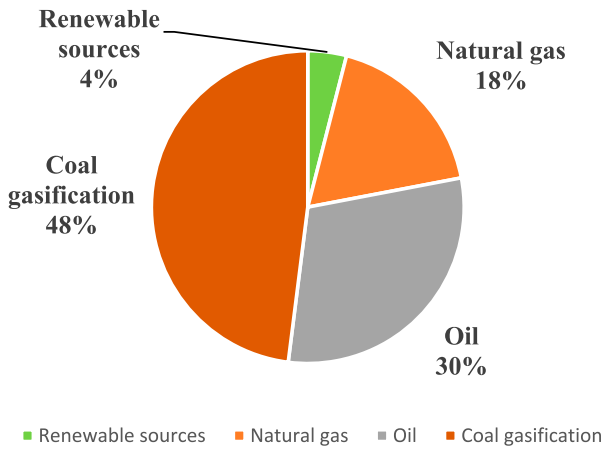

FIGURE 3
Global Hydrogen production by main source in 2018 (IRENA, 2018; Patonia and Poudineh, 2022).

1.3.2 Electrolysis efficiency

According to Hassan et al. (2023a), Electrolysis efficiency stands as a pivotal factor influencing the economic viability and scalability of green hydrogen production. Electrolysis is the process through which water is split into hydrogen and oxygen using an electric current. The efficiency of this process determines the amount of electrical energy required to produce a given quantity of hydrogen, directly impacting production costs and overall competitiveness of green hydrogen against conventional hydrogen production methods (Orjuela-Abril. et al., 2023).

Advancements in electrolysis technology have led to improvements in efficiency and reduced energy consumption over recent years. Traditional alkaline electrolysis, although mature and well-established, typically exhibits lower efficiency rates compared to proton exchange membrane (PEM) and solid oxide electrolysis technologies (Li and Baek, 2021). PEM electrolysis according to Zhang et al. (2022) has garnered significant attention due to its higher efficiency, rapid response times, and scalability, making it particularly suitable for decentralized green hydrogen production applications. However, PEM is also associated with high costs and the need for rare and expensive materials (Wappler et al., 2022). Table 2 shows the characteristics of Alkaline, PEM and Solid Oxide (SOE) Electrolysers.

Factors influencing electrolysis efficiency extend beyond technological advancements to include operational parameters and system design (Agyekum et al., 2022). Optimizing operating conditions, such as electrolyte concentration, temperature, and pressure, can significantly enhance electrolysis efficiency. Additionally, the integration of renewable energy sources with electrolysis systems, leveraging peak renewable energy production periods, can further improve overall system efficiency and reduce energy costs.

Moreover, according to Jiao et al. (2021), electrolysis efficiency is intrinsically linked to the quality and purity of the produced hydrogen. High-efficiency electrolysis processes typically yield hydrogen with lower impurity levels, meeting stringent quality requirements for various applications, from fuel cells to industrial processes. As such, continuous research and development efforts are focused on enhancing electrolysis efficiency, reducing energy consumption, and improving hydrogen purity to drive down production costs and enhance the competitiveness of green hydrogen.

1.3.3 Scale of production

The gauge of production is another significant factor to consider as it is crucial in the deployment and widespread adoption of green hydrogen technologies (Li et al., 2023). As with many industrial processes, economies of scale can significantly influence the cost-effectiveness and commercial viability of green hydrogen production. Large-scale production facilities can benefit from bulk purchasing, streamlined operations, and optimized supply chains, leading to reduced production costs per unit of hydrogen (Lagioia et al., 2023). The hydrogen production landscape has been dominated by large centralized production facilities, leveraging economies of scale to produce hydrogen from fossil fuel-based feedstocks (Jiao et al., 2021). However, the transition to green

TABLE 2 Characteristics of Different types of electrolyser technologies (Conte et al., 2009).

	Alkaline	PEM	SOE
Electrolyte	Aqueous potassium hydroxide	PFSA membranes (e.g., Nafion)	Yttria Stabilises Zirconia (YSZ)
Cathode	Nickel, Nickel-Molybdenum alloy	Platinum-Palladium alloy	Nickel/YSZ
Anode	Nickel-Cobalt alloys	Ruthenium oxide	YSZ
Operating Temperature (^{O}C)	60–80	50–80	500–850
Operating Pressure (Bar)	30	70	1–25
Stack Lifetimes	60–100 k	20–60 k	Less than 10 k
Technology Readiness	Matured	Commercialised	Demonstration
Efficiency (%)	50–70	60–80	80–95

hydrogen necessitates a shift towards decentralized and distributed production models, leveraging renewable energy sources and modular electrolysis systems. These smaller-scale production facilities can be strategically located closer to renewable energy generation sites, reducing transmission losses and infrastructure costs while enhancing system efficiency (Osman et al., 2023).

The cost of hydrogen production varies significantly depending on the type of hydrogen, production technique, and the source of electricity (Ishaq et al., 2022). Grey hydrogen, produced from natural gas through steam methane reforming, is currently the cheapest option but is associated with high carbon emissions. Blue hydrogen, which incorporates carbon capture and storage (CCS) with steam methane reforming, has a higher cost due to the additional CCS processes but results in lower emissions (Oni et al., 2022). Green hydrogen, produced via electrolysis using renewable electricity, is the most environmentally friendly option but is also the most expensive. The cost of green hydrogen is heavily influenced by the price of renewable electricity and the efficiency of the electrolysis process. PEM electrolysis, for example, offers higher efficiency and rapid response times but comes with higher costs due to the need for rare and expensive materials (Zhang et al., 2022). Alkaline electrolysis is generally cheaper but less efficient and slower in response (Santos et al., 2021).

Ultimately, the choice of production technique and the type of hydrogen produced will depend on the specific economic and environmental priorities, as well as the availability of renewable energy sources. The push towards decentralized production models aims to optimize these factors by situating hydrogen production closer to renewable energy generation, thereby minimizing costs and maximizing system efficiency. Advancements in electrolysis technology and the decreasing costs of renewable energy sources, such as solar and wind power, are facilitating the development of larger-scale green hydrogen production facilities. The integration of renewable energy with electrolysis systems at scale can result in significant reductions in greenhouse gas emissions and enhance the overall sustainability credentials of green hydrogen (Zhang et al., 2022).

1.3.4 Infrastructure and logistics

The infrastructure and logistics required for producing and distributing green hydrogen are also important factors to consider according to Kumar et al. (2023). This includes the availability of water and renewable energy sources, as well as the transportation and storage of hydrogen. Various hydrogen storage techniques play a crucial role in this process, ensuring that hydrogen can be efficiently stored and readily available when needed (Liu et al., 2023). They include:

- Compressed Gas Storage: This is the most common method, where hydrogen is stored under high pressure in specially designed tanks. Compressed gas storage is relatively straightforward and widely used, especially in the transportation sector. However, it requires robust and heavy containers to withstand high pressures, which can impact efficiency and cost (Orlova et al., 2023).
- Liquid Hydrogen Storage: In this method, hydrogen is cooled to cryogenic temperatures (−253°C) and stored as a liquid. Liquid hydrogen has a higher energy density compared to compressed gas, allowing for more hydrogen to be stored in a given volume. However, the liquefaction process is energy-intensive and requires significant cooling infrastructure, making it costly (Aziz, 2021).
- Metal Hydride Storage: Hydrogen can be stored in metal hydrides, which are compounds formed by the reaction of hydrogen with metals or alloys. Metal hydride storage systems have high energy densities and can operate at lower pressures compared to compressed gas storage. However, they are often heavy and can be expensive due to the materials used (Klopčič et al., 2023).
- Chemical Storage: Hydrogen can be stored in chemical compounds such as ammonia, formic acid, or liquid organic hydrogen carriers (LOHCs). These chemicals can release hydrogen upon demand through chemical reactions. Chemical storage offers the advantage of high energy density and ease of transport but requires additional processes to release the stored hydrogen, which can impact efficiency (Carmo and Stolten, 2022).
- Underground Storage: Large-scale storage of hydrogen can be achieved in underground geological formations such as salt caverns, depleted oil and gas fields, or aquifers. Underground storage can handle large quantities of hydrogen and is suitable for long-term storage. However, it requires suitable geological conditions and significant infrastructure investments (Tarkowski and Uliasz-Misiak, 2022).

Developing an efficient and cost-effective infrastructure for the production and distribution of green hydrogen is critical to the success of the technology (Morlanés et al., 2021).

Countries that have launched National initiatives to promote the deployment of green hydrogen across different sectors include Germany, Japan, South Korea and others. In Europe, the European Union recently launched Hydrogen strategy aim to establish a hydrogen economy that is competitive, sustainable and able to drive long-term economic growth (Khan and Al-Ghamdi, 2023).

The estimation of the green hydrogen (H_2) production potential represents the initial stage on the road to integrating the Hydrogen Economy into the energy systems of a country or region (Posso et al., 2023). Fuel cells and other hydrogen-based technologies are increasingly seen as a key pillar of global decarbonization efforts (Lindner, 2023).

Once hydrogen is generated and stored for future use, the focus shifts to methods of converting it into energy. The primary approach involves using hydrogen in fuel cells, which are electrochemical devices that convert chemical energy directly into electrical energy (Rai et al., 2022). Unlike batteries and other energy storage systems that rely on stored energy, fuel cells can continuously supply electricity as long as fuel is provided, offering uninterrupted power (Felseghi et al., 2019).

The cost-effectiveness of hydrogen production through electrolysis primarily hinges on the cost of electricity used in the process and the efficiency of electrolyzers (Martinez de Leon et al., 2023). This underscores the importance of optimizing electrolysis processes to enhance the economic viability of hydrogen as an energy carrier.

2 Applications of green hydrogen

One major advantage of green hydrogen is its environmental cleanliness. Unlike other types of hydrogen, green hydrogen is produced using renewable energy sources, resulting in zero carbon emissions. It can be used in a wide range of applications across various industries, including transportation, power generation, and industrial processes, offering a sustainable and carbon-free alternative.

2.1 Transportation

According to Pasini et al. (2023), green hydrogen can be used for transportation and is considered as one of the most promising options for decarbonizing the different modes of transportation, including cars, buses, trucks, trains, and airplanes as depicted in Figure 4.

Green hydrogen can be used as a fuel for hydrogen fuel cell vehicles. These vehicles use a fuel cell to convert hydrogen into electricity, which then powers an electric motor (Inci et al., 2021). The only emission from a hydrogen fuel cell vehicle is water vapor, making it a zero-emission vehicle. The use of green hydrogen as a fuel for transportation can help to reduce greenhouse gas emissions and improve air quality (Vardhan et al., 2022).

Green hydrogen may also be used as a fuel for waterborne transport, such as ships and boats (Jie et al., 2023). Hydrogen fuel cell vessels are becoming increasingly popular, especially for ferries and small inland waterway ships (Chatelier, 2023).

2.2 Power generation

Green hydrogen can also be used to generate electricity in fuel cells or through combustion in a gas turbine (Hwang et al., 2023). Green hydrogen can be used as a fuel in fuel cells, which convert the chemical energy of hydrogen and oxygen into electrical energy, water and heat (Liu et al., 2023). Fuel cells are highly efficient and emit only water vapour, making them a sustainable alternative to traditional fossil fuel power plants (Azni et al., 2023).

This can be particularly useful in remote locations or off-grid settings, where traditional power sources may not be available. The use of green hydrogen for power generation can help to reduce greenhouse gas emissions and improve energy security. Green hydrogen can be used in fuel cells (an electrochemical device that converts the chemical energy of green hydrogen and oxygen into electricity) to produce electricity (Yu et al., 2023). Fuel cells have high efficiency and emit only water and heat as byproducts.

Green hydrogen can also be burned in combustion engines to generate electricity (Teoh et al., 2023), similar to burning natural gas, except that the only emission is water vapor. It can also be used in specially designed gas turbines to generate electricity (Hassan et al., 2023a). However, it is important to note that green hydrogen, like other forms of hydrogen, cannot be used in conventional gas turbines without modifications (Bothien et al., 2019). The development of specific turbines capable of efficiently burning hydrogen is an area of active research. Additionally, natural gas-hydrogen blends can be used for electricity generation via modified gas turbines, providing a transitional solution towards cleaner energy. Similarly, green ammonia produced from hydrogen can also be used for electricity generation in gas turbines, offering another pathway to leverage hydrogen for sustainable energy production (Ağbulut et al., 2023).

2.3 Industrial processes

Green hydrogen can also be used in a variety of industrial processes, such as refining, chemical production, and steel production (Genovese et al., 2023). The global transition to climate neutrality will necessitate not only renewable power but also climate-neutral energy carriers such as hydrogen and its derivatives (Runge et al., 2023). These processes typically require large amounts of energy and produce significant greenhouse gas emissions. The use of green hydrogen as a feedstock or fuel for these processes can help to reduce greenhouse gas emissions and improve the sustainability of these industries.

Considering the factors that need to be considered when producing green hydrogen from renewable energy sources, this paper will be able to determine the prospects for the development of green hydrogen in Africa as a continent and also identify the various challenges that may be able to further delay or even hinder the development of green hydrogen in Africa.

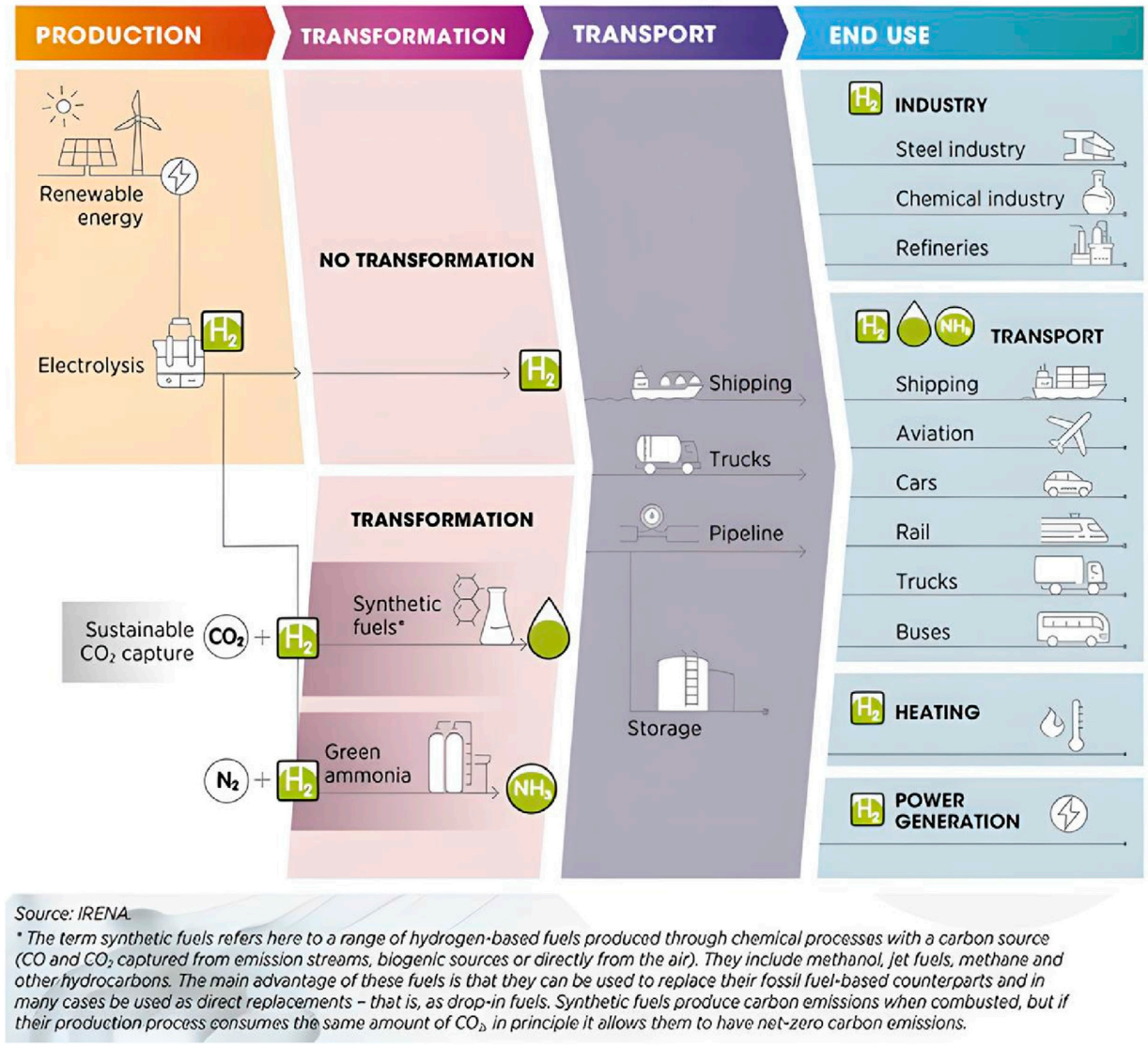

FIGURE 4
Process of Green hydrogen production to application (IRENA, 2020; Pachencko et al., 2023).

3 Prospects for the adoption of green hydrogen for africa

Africa has the potential to become a significant producer and exporter of green hydrogen due to its extensive renewable energy supplies (Panchenko et al., 2023). Green hydrogen adoption prospects in Africa are highly promising, and there are various elements that make this a potentially appealing alternative for the continent some of which are stated below.

3.1 Abundant renewable energy resources

As mentioned earlier, Africa has some of the world's largest renewable energy resources. Africa has not fully tapped into its abundant renewable energy potential. Estimates indicate that the continent's total renewable energy resources far exceed current and future energy requirements (Sohani et al., 2023). This underscores the immense opportunity for Africa to harness renewable sources to meet its energy demands sustainably and contribute significantly to global renewable energy goals. The continent has vast solar, wind, and hydropower potential, which make it an ideal location for the production of green hydrogen. With an abundance of renewable energy sources, African countries can produce green hydrogen in a sustainable and environmentally friendly way.

The continent is blessed with vast areas of land and water bodies that receive huge amounts of solar radiation, wind and hydrological resources. Solar energy is especially abundant in Africa, with large areas of the continent receiving high levels of sunlight throughout the year. Wind energy is also abundant in many parts of Africa, especially along the coasts and in high altitude areas. These resources could provide Africa with more energy than it could ever need and pave the way for the continent to become self-sufficient, environmentally sustainable, and economically prosperous.

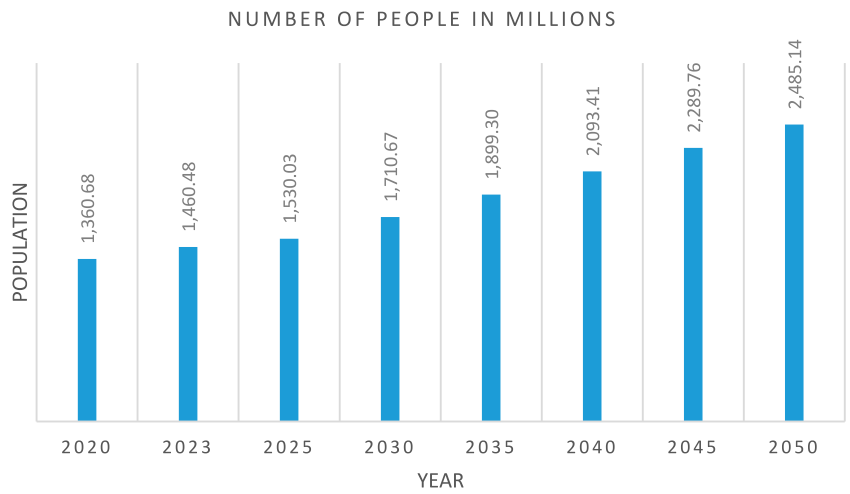

FIGURE 5
Forecast of the total population of Africa from 2020 to 2050 (Statista, 2024).

3.2 Growing demand for energy

According to global demographics, Africa's population was projected to grow by 2.37 percent in 2022 compared to the previous year. Since 2000, the continent has consistently experienced population growth rates exceeding 2.45 percent, reaching a peak of 2.59 percent between 2012 and 2013. Despite a slight slowdown in recent years, Africa's population is expected to continue increasing significantly in the foreseeable future, as illustrated in Figure 5 (Saifaddin Galal, 2023).

This demand is likely to rise more in the future years, and green hydrogen can assist supply it in a sustainable manner. Due to this demand, there is increasing international support and investment in green hydrogen development in Africa. The European Union, for instance, has identified Africa as a key partner for its green hydrogen strategy and has committed to supporting the adoption and development of green hydrogen in the continent (Sadik-Zada, 2021). Other countries, such as Japan and Australia, have also expressed interest in investing in green hydrogen projects in Africa (Kar et al., 2023).

3.3 Potential for export

Africa has the potential to become a significant producer and exporter of green hydrogen due to its extensive renewable energy supplies (Razi, Faran et al., 2022). With a growing emphasis on decarbonization and the need to transition towards clean and sustainable energy sources, green hydrogen presents a significant opportunity for African nations to drive economic growth while addressing environmental challenges.

According to Agyekum (2024), Africa's strategic geographic location offers access to key global markets, positioning the continent as a crucial player in the emerging hydrogen economy. With proximity to Europe, Asia, and the Middle East, African nations have the opportunity to export green hydrogen to regions seeking to reduce their carbon footprint and meet their renewable energy targets. This not only drives economic growth and job creation but also strengthens Africa's position as a reliable supplier of clean energy to the world.

Furthermore, Africa's dedication to sustainable development and climate action strengthens its potential for exporting green hydrogen (Bouchene et al., 2021). Embracing clean energy technologies and reducing reliance on fossil fuels enables African nations to lead in mitigating climate change and promoting environmental stewardship. Exporting green hydrogen not only supports global efforts towards achieving net-zero emissions but also unlocks new economic opportunities and fosters inclusive growth throughout the continent (Nwokolo et al., 2023). This dual benefit of environmental leadership and economic advancement positions Africa strategically in the global energy transition.

4 Advantages of green hydrogen adoption in African countries

Green hydrogen development and adoption in Africa has its benefits to the people, the continent and even the world at large. The adoption of Green hydrogen in African countries can also aid in the transition from polluted energy sources to clean and renewable energy sources.

4.1 Energy security

The potential for solar and wind energy in Africa is very high, with the region having some of the best solar and wind resources globally. According to IRENA (2020), Africa receives about 325 days of bright sunshine annually in many regions, particularly in North Africa and the Sahel region. This high solar irradiance makes these areas ideal for solar energy development (Chun et al., 2022). Additionally, IRENA reports that Africa has an estimated wind energy potential of over 1800 GW, particularly along coastal regions and in high-altitude areas such as the Ethiopian Highlands. The

production of green hydrogen using these renewable resources can contribute towards energy security for Africa, particularly in remote areas where grid infrastructure is not readily available (Bhandari, 2022). The development of green hydrogen can provide energy security to African countries in several ways.

By developing the capacity for green hydrogen production, these countries can diversify their energy sources and reduce their dependence on fossil fuels (Szemat-Vielma et al., 2023). This can make them less subject to price fluctuations in fossil fuels for their energy demands. Green hydrogen production, on the other hand, can diversify their energy mix by using renewable energy sources such as solar, wind, and hydro power. This can drastically reduce their reliance on fossil fuels, which are volatile in price and vulnerable to supply disruptions. With a more diversified energy mix, African countries can enhance their energy security and increase their resilience to external shocks (Chu, 2023).

Also, most African countries are net energy importers, which makes them vulnerable to fluctuations in global oil and gas prices (Galimova et al., 2023). Developing their own green hydrogen production capabilities can help them become more energy independent and reduce their dependence on imported fuel (Müller et al., 2023). This can ensure a consistent and predictable energy supply, improve their balance of payments, and improve their overall energy security.

4.2 Economic growth and employment opportunities

The adoption of green hydrogen in Africa can accelerate economic growth and create employment opportunities (Bhagwat and Olczak, 2020). The establishment of the green hydrogen industry can create job opportunities from manufacturing, installation, and maintenance of green hydrogen facilities to the production of green hydrogen fuel cells. The sector can also provide an opportunity for African countries to diversify their economies and reduce their reliance on fossil fuels.

The development of green hydrogen technology can generate economic growth in African countries by creating new job opportunities, developing local industries, and attracting foreign investments. Countries such as Morocco, Egypt, and South Africa have already started investing in this technology (Agyekum et al., 2023), and this could significantly reduce their dependence on fossil fuels and strengthen their energy security.

Green hydrogen production can support sustainable development in African countries by providing a clean and renewable source of energy. The development of a green hydrogen economy can also lead to the creation of new job possibilities, the expansion of local economies, and the development of new industries.

4.3 Reduction of greenhouse gas emissions and dependence on fossil fuels

Green hydrogen offers substantial benefits for Africa, including the potential to reduce global and local greenhouse gas emissions (Li et al., 2023). In Africa, where fossil fuels dominate the energy landscape and contribute significantly to greenhouse gas emissions, green hydrogen can serve as a cleaner alternative in sectors like transportation, power generation, and industry, fostering a more sustainable future. By generating green hydrogen from renewable sources, African countries can advance sustainable development goals, improving air quality and promoting environmental sustainability.

Adopting green hydrogen also holds promise for reducing Africa's reliance on imported fossil fuels, which exposes the region to volatility in global oil prices and supply disruptions (Odoom et al., 2023). Instead, green hydrogen production offers a stable and locally sourced energy option, enhancing energy security across the continent. Furthermore, embracing green hydrogen technology presents Africa with an opportunity to lead the global transition to renewable energy, a role that has often been overlooked in past energy revolutions (Panchencko et al., 2023).

The adoption of green hydrogen stands to benefit Africa through enhanced energy security, job creation, reduced dependence on imported fossil fuels, and leadership in renewable energy innovation. It is crucial for African governments and stakeholders to prioritize the development of green hydrogen infrastructure, supported by robust policies and regulations that facilitate its widespread adoption across the region.

5 Challenges in the development and adoption of green hydrogen

While the prospects for green hydrogen development in Africa are quite promising, there are several challenges that will need to be addressed in order to make it a viable option for the continent. Lack of infrastructure, high cost of production and limited technical expertise are challenges in the development of green hydrogen.

5.1 Lack of infrastructure

Developing green hydrogen in Africa faces significant challenges, primarily due to inadequate infrastructure (Sadik-Zada, 2021). The production, storage, and transportation of green hydrogen necessitate substantial investments in facilities such as production plants, pipelines, storage tanks, and refueling stations (Schaffert, 2022; Hassan et al., 2023b). Without proper infrastructure, the cost and feasibility of generating and distributing hydrogen could become prohibitively high (Azadnia et al., 2023).

Moreover, the lack of infrastructure poses a barrier to the adoption of hydrogen fuel cell vehicles, as the availability of refueling stations is crucial for their practical use (Geçici et al., 2023; Latapi et al., 2023). This limited accessibility may deter potential consumers from embracing hydrogen technology. Furthermore, insufficient infrastructure could restrict access to the renewable energy sources required for green hydrogen production (Nemmour et al., 2023). In regions lacking adequate renewable energy capacity, the potential for producing green hydrogen may be constrained, hindering the development of a hydrogen-based economy (Khan and Al-Ghamdi, 2023).

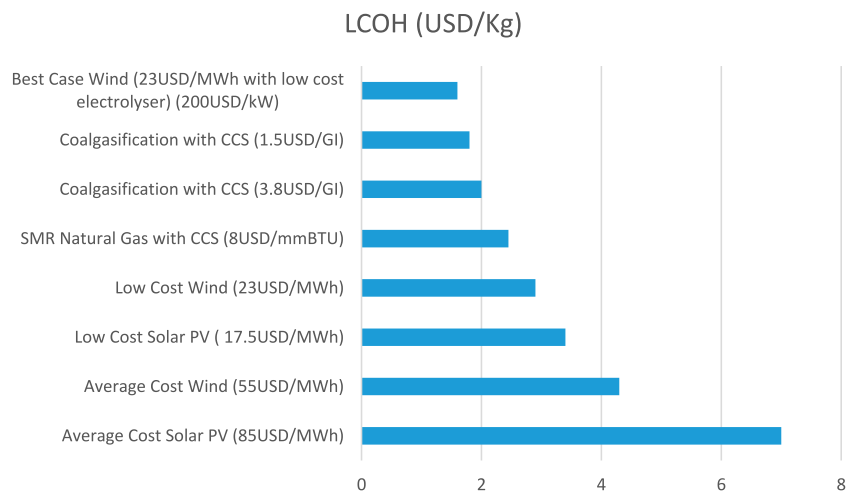

FIGURE 6
Hydrogen production cost by renewable and non-renewable energies in 2019 (IRENA, 2020).

Overall, the expansion and widespread adoption of green hydrogen as a sustainable energy solution in Africa hinge significantly on substantial investments in infrastructure. Addressing these infrastructure gaps is crucial to unlocking the full potential of green hydrogen in the region.

5.2 High costs of production

Developing green hydrogen in Africa faces a significant hurdle due to its high production costs (Sontakke, Ujwal, and Santosh Jaju, 2021). While the costs of renewable energy technologies have decreased recently, producing green hydrogen remains more expensive than traditional fossil fuels as shown in Figure 6 (Dong et al., 2022). Green hydrogen production involves electrolyzing water using renewable energy sources like wind and solar power, which adds to its cost compared to hydrogen derived from fossil fuels (Schnuelle et al., 2022).

This higher production cost poses several challenges for green hydrogen development. Firstly, it limits the competitiveness of green hydrogen against cheaper energy sources such as natural gas or gasoline (Kendall Kelvin, 2022). Without substantial government subsidies or incentives, green hydrogen may struggle to penetrate the market (Kar et al., 2023). Despite efforts to reduce electrolyzer technology costs since 2020 (Newborough and Cooley, 2020), the costs remain relatively high. For African countries, which often have limited financial resources, the high cost of green hydrogen production further complicates investment in its development. Addressing these cost barriers is crucial to making green hydrogen a viable and widespread energy solution in the region.

Secondly, the high cost of production could limit the availability of green hydrogen (Terlouw, et al., 2022). If the cost of creating green hydrogen is too high, it may be difficult to scale up production to meet demand, limiting the technology's potential for widespread adoption. Even with the current subsidy removal which has rapidly increased the price of diesel, gasoline, kerosene and other fuels in Nigeria, the most populated country in Africa, the cost of the conventional fuels will still not match up to that of the production and development of green hydrogen.

The high cost of production could also slow down innovation and research in green hydrogen development (Jilani et al., 2023). If the cost of manufacturing green hydrogen is too expensive, it may be more difficult to invest in more research and development to enhance efficiency and lower the cost of the technology. The average price of producing hydrogen by solar PV and wind energy is much higher than that of fossil fuel, while the decrease in the price of solar PV and wind energy is considered competitive. The International Renewable Energy Agency (IRENA) is expecting that the cost of hydrogen production via renewable energies will fall and become even cheaper than fossil fuel in 2050 (International Renewable Energy Agency, 2020)

5.3 Limited technical/qualified expertise

Developing green hydrogen requires technical expertise in areas such as renewable energy, chemistry, and engineering. Africa as a continent has a lot of academic potential but many African countries have limited qualified expertise to develop and maintain green hydrogen infrastructure (Mneimneh et al., 2023), while some of the personnel that may have the skills and are qualified to develop and maintain green hydrogen infrastructure end up migrating to other countries due to the high rate of unemployment (Rufus et al., 2022). The select few that remain may end up becoming entrepreneurs and having their own personal businesses which may be different from their area of specialization because of the need to generate funds for personal use. This can make it difficult to design and operate green hydrogen production facilities, as well as maintain and repair them over time (Mali et al., 2021).

It will be challenging to develop new procedures and technologies for manufacturing green hydrogen without technical competence. This may limit the ability of the required technical

expertise, and the development of green hydrogen technology may be slowed or hampered by concerns about safety, efficiency, and cost-effectiveness.

Green hydrogen production from renewable sources such as solar and wind, for example, necessitates extensive knowledge of electrolysis technology and the materials used in electrolysis cells. There is a danger of errors in the design and execution of the electrolysis process if technical expertise is absent or lacking, which could result in decreased efficiency or even safety issues.

Furthermore, technical skill is required for the transportation and storage of hydrogen (Sun et al., 2023). Hydrogen is a highly combustible gas that must be handled with care to ensure safe transit and storage (Tang Dan et al., 2023). Also, the storage of hydrogen necessitates sophisticated and advanced knowledge of materials science in order to design efficient and cost-effective storage solutions (Singh et al., 2023).

5.4 Policy and regulatory framework

The lack of clear policy and regulatory frameworks is another challenge facing green hydrogen development in Africa (Ballo et al., 2022). In many cases, there is a lack of clarity around the legal and regulatory frameworks that govern the production, distribution, and use of green hydrogen (Chege, 2023; Gordon et al., 2023). This can generate uncertainty for investors and make it difficult to obtain the necessary funds to promote green hydrogen development in developing countries. (Hassan et al., 2023b).

5.5 Competing priorities

Although electrolyser technology is currently being upscaled and cost-reduced in preparation for volume production (Kampouta, 2022), some African countries would still be unable to make it a top priority because it is still very expensive. For example, according to Gigastack phase 1 report 1, 2020, the price of a 100 MW PEM electrolyser system from ITM Power is expected to fall to $530 per kW by 2024, but many African countries may not still be able to concentrate on this as they have other competing priorities which would also involve a large amount of investment and financial assistance (Gigastack, 2020). These African countries face competing priorities and basic needs, such as addressing poverty and improving access to healthcare and education (Ayoo, 2022). These priorities can make it even more difficult to prioritize investment in green hydrogen development, which may be viewed as a longer-term priority in comparison to other more pressing demands.

Also, some governments and businesses may prioritize renewable energy sources like wind and solar power over green hydrogen (Munim et al., 2023), while others may prioritize energy storage technologies like batteries. Competing priorities might be a big obstacle for green hydrogen development. It is possible however to find areas of common ground and work toward a shared vision for the development of a sustainable hydrogen economy through good communication and collaboration among stakeholders.

5.6 Research development and innovation

Research, development, and innovation (RDI) are pivotal in advancing green hydrogen technologies, addressing technical challenges, and enhancing competitiveness in the energy sector. Efforts in RDI focus on several critical areas to accelerate the adoption and scale-up of green hydrogen (Heilala et al., 2022).

In electrolysis efficiency, ongoing research aims to improve the performance of electrolyzers, which convert water into hydrogen and oxygen using electricity. Innovations in materials and catalysts are crucial for enhancing electrolyzer efficiency and durability, reducing energy consumption, and lowering production costs (Burton et al., 2021). Additionally, advancements in storage and transportation technologies are essential. Researchers are exploring novel storage materials and infrastructure solutions to safely and efficiently store and transport hydrogen, ensuring its availability as a reliable energy carrier (Ahmad et al., 2021). Integrating green hydrogen production with renewable energy sources, such as solar and wind power, is another key area. Innovations in grid integration technologies help optimise the use of fluctuating renewable energy outputs, ensuring continuous and efficient hydrogen production (Zachary et al., 2022).

Scaling up production processes for electrolyzers and other hydrogen technologies is critical to achieve economies of scale and reduce costs. Strategic investments in RDI foster collaboration between academia, industry, and government, driving breakthroughs that accelerate the commercialisation of green hydrogen technologies globally.

5.7 Hydrogen standardisation and safety

Hydrogen standardisation and safety are paramount to ensure the reliability, interoperability, and public acceptance of hydrogen technologies. Establishing international standards is crucial for harmonising technical specifications across hydrogen production, storage, transportation, and utilisation. Standardisation efforts aim to facilitate global trade in hydrogen and hydrogen-based products while ensuring compatibility and reliability of equipment and infrastructure (Kumar et al., 2024). Safety regulations play a vital role in mitigating risks associated with hydrogen handling, storage, and utilisation (Li et al., 2022). Developing robust safety standards and certification processes ensures the protection of workers, communities, and the environment. Certification and testing protocols verify compliance with safety standards, promoting confidence in hydrogen technologies among stakeholders.

Public awareness and education initiatives are essential to increase understanding of hydrogen safety principles and practices. Educating stakeholders including industry professionals, policymakers, emergency responders, and the public on safe hydrogen handling and usage fosters a supportive regulatory environment and encourages responsible deployment of hydrogen technologies (Tchouvelev et al., 2019).

By prioritising hydrogen standardisation and safety alongside RDI, stakeholders can pave the way for the widespread adoption of green hydrogen as a clean and sustainable energy solution. These efforts contribute to achieving global energy transition goals and addressing climate challenges effectively.

6 Efforts of African countries in adopting green hydrogen

Green hydrogen is rapidly gaining popularity amongst African countries and the efforts of some of the countries in the adoption of green hydrogen cannot be overlooked. Both South Africa and Morocco are making significant efforts in order to position themselves as leaders in the adoption of green hydrogen in Africa (Pinto and Chege, 2024).

6.1 South Africa's green hydrogen initiatives

South Africa, with its significant renewable energy resources and industrial capabilities, has emerged as a key player in the development and adoption of green hydrogen (Pinto and Chege, 2024). Recognizing the potential of green hydrogen to transform its energy landscape, reduce carbon emissions, and create economic opportunities, South Africa has launched several initiatives aimed at positioning itself as a leader in the global hydrogen economy. South Africa's vast renewable energy resources are central to its green hydrogen strategy. The country enjoys abundant solar and wind resources, particularly in the Northern Cape region, which is one of the sunniest places on earth. This makes it an ideal location for large-scale solar photovoltaic (PV) and concentrated solar power (CSP) projects. Additionally, the coastal regions are well-suited for wind energy projects, further enhancing the country's renewable energy potential (Gaeatlholwe, 2021). Some of South Africa's initiatives regarding green hydrogen include:

- Hydrogen South Africa (HySA) Programme Launched in 2008 by the Department of Science and Innovation (DSI) which aims to develop and guide innovation along the hydrogen and fuel cell technology value chain (Roos and Wright, 2020). The programme focuses on developing efficient and cost-effective methods for hydrogen production, primarily through water electrolysis using renewable energy, and establishing infrastructure for storage and distribution (Roos, 2021), advancing fuel cell technologies for various applications, including transportation, stationary power generation, and portable power and demonstrating integrated hydrogen systems in real-world applications to showcase their feasibility and benefits.
- Hydrogen Valley Initiative The Hydrogen Valley Initiative, a collaborative effort between the DSI, Anglo American, Bambili Energy, and Engie, aims to create a hydrogen corridor linking the country's industrial hubs (Grobbelaar and Ngubevana, 2022). Similar to the HySA programme, it seeks to develop a hydrogen production and distribution network along the corridor, promote the use of hydrogen in various sectors, including mining, transportation, and manufacturing and attract investment and create jobs in the emerging hydrogen economy.

There are also renewable hydrogen production projects that South Africa has initiated aimed at producing green hydrogen using renewable energy. They include projects like the Boegoebbai hydrogen project and the Prieska Power reserve project (Kneebone, 2022; Kritzinger and Snyman, 2022).

To support the development of the hydrogen economy, the South African government has introduced the National Hydrogen strategy. The strategy outlines the country's vision for becoming a leading producer and exporter of green hydrogen and its derivatives. It emphasizes the development of domestic hydrogen markets, international partnerships, and the establishment of a conducive regulatory environment. Incentives and Funding: The government has introduced incentives and funding mechanisms to encourage investment in hydrogen technologies and infrastructure. These include tax breaks, grants, and low-interest loans for hydrogen projects (Bessarabov et al., 2012; Bessarabov and Pollet, 2022).

6.1.1 International collaboration

South Africa actively seeks international partnerships to advance its hydrogen agenda. Key collaborations include the agreements with Germany to develop green hydrogen projects, focusing on technology transfer, capacity building, and market development (Brauner et al., 2023). South Africa also partnered with Japanese companies and research institutions aim to advance hydrogen production technologies and explore potential markets for South African green hydrogen (Patel, 2020).

6.1.2 Challenges and opportunities

While South Africa's green hydrogen initiatives hold great promise, several challenges need to be addressed:

- Significant investment is required to develop the necessary infrastructure for hydrogen production, storage, and distribution (Ayodele and Munda, 2019).
- Reducing the cost of green hydrogen production to make it competitive with fossil fuels remains a key challenge.
- Establishing a clear and supportive regulatory framework is essential to attract investment and ensure the safe and efficient development of the hydrogen economy.

Despite these challenges, the opportunities for South Africa are substantial. By leveraging its renewable energy resources, industrial capabilities, and strategic location, South Africa can become a major player in the global green hydrogen market. The country's initiatives not only aim to reduce carbon emissions and enhance energy security but also to create economic growth and job opportunities in the emerging hydrogen sector.

6.2 Morocco's green hydrogen strategy

Morocco has emerged as a leader in green hydrogen within Africa, establishing the National Hydrogen Commission in 2019 to formulate a comprehensive strategy for green hydrogen production and use. Leveraging its renewable energy capacity, Morocco aims to play a significant role in the global green hydrogen market (van Wijk et al., 2019). The country's robust renewable energy infrastructure, including projects like the Noor Ouarzazate Solar Complex and Tarfaya Wind Farm, provides a reliable and scalable energy source for green hydrogen production (Bibih et al., 2024; Gawusu and Ahmed, 2024). These initiatives underscore Morocco's strong

commitment to advancing green hydrogen technologies. Additionally, through projects like Green H2A, in collaboration with international partners, Morocco plans to produce green hydrogen for domestic consumption and export, supported by agreements with European nations such as Germany to develop production facilities and export routes (Weko et al., 2024).

6.3 Key projects in African green hydrogen development

In the framework of green hydrogen adoption in Africa, ongoing projects are pivotal in shaping the region's energy landscape. One notable initiative is the Sahara Green Hydrogen Project, spearheaded by a consortium of international and local partners. This project aims to harness the vast solar energy potential of North Africa, particularly in Morocco and Algeria, to produce green hydrogen for domestic use and export (Tiar et al., 2024). Another significant project is the Hydrogen Initiative in Egypt, which focuses on utilizing renewable energy sources along the Nile Delta region. This initiative aims to establish a sustainable hydrogen economy by leveraging both solar and wind resources abundant in the area and also make the country a potential supplier of low-carbon hydrogen for Europe owing to its proximity and its large renewable energy potential (Ruseckas, 2022). The initiative not only aims at domestic energy security but also positions Egypt as a key player in the international green hydrogen market, catering to Europe's increasing demand for clean energy.

These ongoing projects underscore the growing momentum towards green hydrogen adoption in Africa, highlighting strategic investments and collaborative efforts aimed at achieving energy security and sustainability goals.

7 Conclusion

The adoption of green hydrogen in Africa offers promising prospects for a sustainable and low-carbon future especially due to the rapid increase in population which automatically increases the energy demand in the continent. Green hydrogen would be advantageous to African countries in several sectors and would be a better fuel compared to conventional fuels. Despite the abundance of renewable energy resources, the continent still faces challenges in harnessing them. Lack of infrastructure, financing, and political issues will have all hindered the growth of renewable energy in Africa. Additionally, many African countries still rely heavily on fossil fuels for their energy needs. However, recent years have seen a growing focus on renewable energy in Africa, with increased investments and policy support aimed at unlocking the vast potential of renewable energy resources on the continent. Addressing these challenges will require collaboration and support from international partners, as well as a commitment from African governments to prioritize and invest in green hydrogen development.

South Africa and Morocco's efforts in adopting green hydrogen demonstrate their commitment to sustainable energy and climate action. Through strategic policies, investments in renewable energy, and international collaborations, these countries are paving the way for a green hydrogen economy. Their initiatives serve as a model for other African nations and highlight the continent's potential to contribute significantly to the global green hydrogen landscape. Although it may take some time due to the basic amenities and immediate requirements that African countries must address first, tackling each of these difficulties will be advantageous to the continent and its residents in the long term. African countries may use these chances to establish a sustainable and low-carbon economy with the correct policies, investments, and technical knowledge.

In so doing, green hydrogen may be developed in Africa and could also be used as a substitute for fossil fuels thus reducing the emission of greenhouse gases which causes the depletion of the ozone layer and which may in turn reduce global warming in general.

Author contributions

EO: Conceptualization, Writing–original draft, Writing–review and editing. JD: Methodology, Supervision, Writing–original draft, Writing–review and editing. OK: Methodology, Supervision, Writing–review and editing. ES: Investigation, Methodology, Supervision, Writing–review and editing. OA: Conceptualization, Investigation, Methodology, Project administration, Supervision, Visualization, Writing–review and editing.

Funding

The author(s) declare that no financial support was received for the research, authorship, and/or publication of this article.

Acknowledgments

The Authors want to express their gratitude to Covenant University's administration and CUCRID Directorate for their support.

Conflict of interest

The authors declare that the research was conducted in the absence of any commercial or financial relationships that could be construed as a potential conflict of interest.

Publisher's note

References

Ağbulut, Ü., Yıldız, G., Bakır, H., Polat, F., Biçen, Y., Ergün, A., et al. (2023). Current practices, potentials, challenges, future opportunities, environmental and economic assumptions for Türkiye's clean and sustainable energy policy: a comprehensive assessment. *Sustain. Energy Technol. Assessments* 56, 103019. doi:10.1016/j.seta.2023.103019

Agyekum, E. B. (2024). Is Africa ready for green hydrogen energy takeoff? A multi-criteria analysis approach to the opportunities and barriers of hydrogen production on the continent. *Int. J. Hydrogen Energy* 49, 219–233. doi:10.1016/j.ijhydene.2023.07.229

Agyekum, E. B., Ampah, J. D., Uhunamure, S. E., Shale, K., Onyenegecha, I. P., and Velkin, V. I. (2023). Can africa serve Europe with hydrogen energy from its renewables? assessing the economics of shipping hydrogen and hydrogen carriers to Europe from different parts of the continent. *Sustainability* 15 (8), 6509. doi:10.3390/su15086509

Agyekum, E. B., Nutakor, C., Agwa, A. M., and Kamel, S. (2022). A critical review of renewable hydrogen production methods: factors affecting their scale-up and its role in future energy generation. *Membranes* 12 (2), 173. doi:10.3390/membranes12020173

Ahmad, F., Khalid, M., and Panigrahi, B. K. (2021). Development in energy storage system for electric transportation: a comprehensive review. *J. Energy Storage* 43, 103153. doi:10.1016/j.est.2021.103153

Ahmed, M. R., Barua, T., and Das, B. K. (2023). A comprehensive review on techno-environmental analysis of state-of-the-art production and storage of hydrogen energy: challenges and way forward. *Energy Sources, Part A Recovery, Util. Environ. Eff.* 45 (2), 5905–5937. doi:10.1080/15567036.2023.2211029

Ajanovic, A., Sayer, M., and Haas, R. (2022). The economics and the environmental benignity of different colors of hydrogen. *Int. J. Hydrogen Energy* 47 (Issue 57), 24136–24154. doi:10.1016/j.ijhydene.2022.02.094

Ajayi, O. O., Ohijeagbon, O. D., Mercy, O., and Ameh, A. (2016). Potential and econometrics analysis of standalone RE facility for rural community utilization and embedded generation in North-East, Nigeria. *Sustain. Cities Soc.* 21, 66–77. doi:10.1016/j.scs.2016.01.003

Ayodele, T. R., and Munda, J. L. (2019). The potential role of green hydrogen production in the South Africa energy mix. *J. Renew. Sustain. Energy* 11 (4), 044301. doi:10.1063/1.5089958

Ayoo, C. (2022). Poverty reduction strategies in developing countries. *Rural. Development-Education, Sustain. Multifunct*.

Azadnia, A. H., McDaid, C., Amin, M. A., and Seyed, E. H. (2023). Green hydrogen supply chain risk analysis: a european hard-to-abate sectors perspective. *Renew. Sustain. Energy Rev.* 182, 113371. doi:10.1016/j.rser.2023.113371

Aziz, M. (2021). Liquid hydrogen: a review on liquefaction, storage, transportation, and safety. *Energies* 14 (18), 5917. doi:10.3390/en14185917

Azni, M. A., Khalid, R.Md, Hasran, U. A., and Kamarudin, S. K. (2023). Review of the effects of fossil fuels and the need for a hydrogen fuel cell policy in Malaysia. *Sustainability* 15 (5), 4033. doi:10.3390/su15054033

Bakhti, H. (2024). *Model-based design of solar thermal power plants*. Hamburg, Germany: Universitätsbibliothek Hamburg.

Ballo, A., Valentin, K. K., Korgo, B., Ogunjobi, K. O., Agbo, S. N., Kone, D., et al. (2022). Law and policy review on green hydrogen potential in ECOWAS countries. *Energies* 15 (7), 2304. doi:10.3390/en15072304

Bamisile, O., Dongsheng, C., Li, J., Adun, H., Olukoya, R., Bamisile, O., et al. (2023). Renewable energy and electricity incapacitation in sub-Sahara Africa: analysis of a 100% renewable electrification in Chad. *Energy Rep.* 9, 1–12. doi:10.1016/j.egyr.2023.05.049

Banava, A. (2023). *The EU Green Deal for climate neutrality by 2050-The European energy and environmental policy for climate change*. Greece: European Parliament.

Bessarabov, D., and Pollet, B. G. (2022). "Hydrogen (H2) technologies in the republic of South Africa," in *Hydrogen in an international context* (New York, NY: River Publishers), 203–228.

Bessarabov, D., van Niekerk, F., van der Merwe, F., Vosloo, M., North, B., and Mathe, M. (2012). Hydrogen infrastructure within HySA national program in South Africa: road map and specific needs. *Energy Procedia* 29, 42–52. doi:10.1016/j.egypro.2012.09.007

Bhagwat, S., and Olczak, M. (2020). *Green hydrogen: bridging the energy transition in Africa and Europe*. Italy: European University Institute.

Bhandari, R. (2022). Green hydrogen production potential in west africa–case of Niger. *Renew. Energy* 196, 800–811. doi:10.1016/j.renene.2022.07.052

Bibih, M., Choukri, K., El Khaili, M., Babkrani, Y., and Chakir, H. (2024). "Renewable energy integration and green hydrogen prospects in Morocco: a comprehensive analysis of energy transition dynamics," in 2024 4th International Conference on Innovative Research in Applied Science, Engineering and Technology (IRASET), FEZ, Morocco, 16-17 May, 2024 (IEEE), 1–7.

Bothien, M. R., Ciani, A., Wood, J. P., and Fruechtel, G. (2019). Toward decarbonized power generation with gas turbines by using sequential combustion for burning hydrogen. *J. Eng. Gas Turbines Power* 141 (12), 121013. doi:10.1115/1.4045256

Bouchene, L., Cassim, Z., Engel, H., Jayaram, K., and Kendall, A. (2021). Green Africa: a growth and resilience agenda for the continent. *McKinsey Sustain.* 28, 28.

Brauner, S., Lahnaoui, A., Agbo, S., Böschen, S., and Kuckshinrichs, W. (2023). Towards green hydrogen? A comparison of German and African visions and expectations in the context of the H2Atlas-Africa project. *Energy Strategy Rev.* 50, 101204. doi:10.1016/j.esr.2023.101204

Burton, N. A., Padilla, R. V., Rose, A., and Habibullah, H. (2021). Increasing the efficiency of hydrogen production from solar powered water electrolysis. *Renew. Sustain. Energy Rev.* 135, 110255. doi:10.1016/j.rser.2020.110255

Carmo, M., and Stolten, D. (2019). "Energy storage using hydrogen produced from excess renewable electricity: power to hydrogen," in *Science and engineering of hydrogen-based energy technologies* (Academic Press), 165–199.

Chatelier, J. M. (2023). Entering a new era for electrical vessel on inland waterways. *Ship Science and Technology.* 16 (32), 21–32.

Chege, K. (2023) "Legal/policy tools and strategies for hydrogen in the low-carbon transition," in *Handbook of energy law in the low-carbon transition*, 217.

Chu, L. K. (2023). The role of energy security and economic complexity in renewable energy development: evidence from G7 countries. *Environ. Sci. Pollut. Res.* 30 (19), 56073–56093. doi:10.1007/s11356-023-26208-w

Chun, G., Days, J., Hwangbo, J., Ismatullayeva, Y., Kamb, E., Kobayashi, C., et al. (2022). *Global trends in energy and emissions: key points for policy decision-making*.

Coban, H. H., Lewicki, W., Miśkiewicz, R., and Drożdż, W. (2023). The economic dimension of using the integration of highway sound screens with solar panels in the process of generating green energy. *Energies* 16 (1), 178. doi:10.3390/en16010178

Conte, M., Di Mario, F., Iacobazzi, A., Mattucci, A., Moreno, A., and Ronchetti, M. (2009). Hydrogen as future energy carrier: the ENEA point of view on technology and application prospects. *Energies* 2 (1), 150–179. doi:10.3390/en20100150

Dirisu, J. O., Salawu, E. Y., Ekpe, I. C., Udoye, N. E., Falodun, O. E., Oyedepo, S. O., et al. (2024). Promoting the use of bioenergy in developing nations: a CDM route to sustainable development. *Front. Energy Res.* 11, 1184348. doi:10.3389/fenrg.2023.1184348

Dong, Z. Y., Yang, J., Yu, Li, Daiyan, R., and Rose, A. (2022). A green hydrogen credit framework for international green hydrogen trading towards a carbon neutral future. *Int. J. Hydrogen Energy* 47 (2), 728–734. doi:10.1016/j.ijhydene.2021.10.084

Ewing, M., Israel, B., Jutt, T., Talebian, H., and Stepanik, L. (2020). *Hydrogen on the path to net-zero emissions*. Calgary, AB, Canada: PEMBINA Institute.

Felseghi, R. A., Carcadea, E., Raboaca, M. S., Trufin, C. N., and Filote, C. (2019). Hydrogen fuel cell technology for the sustainable future of stationary applications. *Energies* 12 (23), 4593. doi:10.3390/en12234593

Gaeatlholwe, V. T. (2021). *A GIS-based approach for the evaluation of the land-use impact of future energy scenarios in South Africa for 2050*. Johannesburg (South Africa): University of.

Galal, S. (2023). 'Population growth rate in Africa from 2000 to 2030. *Stastita*, 1224179.

Galimova, T., Ram, M., Bogdanov, D., Fasihi, M., Gulagi, A., Khalili, S., et al. (2023). Global trading of renewable electricity-based fuels and chemicals to enhance the energy transition across all sectors towards sustainability. *Renew. Sustain. Energy Rev.* 183, 113420. doi:10.1016/j.rser.2023.113420

Gawusu, S., and Ahmed, A. (2024). "Africa's transition to cleaner energy: regulatory imperatives and governance dynamics," in *Energy regulation in Africa: dynamics, challenges, and opportunities* (Cham: Springer Nature Switzerland), 25–51.

Geçici, E., Güler, M. G., and Bilgiç, T. (2022). Multi-period planning of hydrogen refuelling stations using flow data: a case study for Istanbul. *Int. J. Hydrogen Energy* 47 (95), 40138–40155. doi:10.1016/j.ijhydene.2022.08.068

Genovese, M., Schlüter, A., Scionti, E., Piraino, F., Corigliano, O., and Fragiacomo, P. (2023). Power-to-hydrogen and hydrogen-to-X energy systems for the industry of the future in Europe. *Int. J. Hydrogen Energy* 48, 16545–16568. doi:10.1016/j.ijhydene.2023.01.194

Gigastack (2020). Gigastack: bulk supply of renewable hydrogen. *Phase 1 Rep. BEIS, Elem. Energy*.

Global Carbon Budget (2021). Global carbon Budget. Available at: https://ourworldindata.org/co2-and-greenhouse-gas-emissions.

Gordon, J. A., Balta-Ozkan, N., and Ali Nabavi, S. (2023). Socio-technical barriers to domestic hydrogen futures: repurposing pipelines, policies, and public perceptions. *Appl. Energy* 336, 120850. doi:10.1016/j.apenergy.2023.120850

Grobbelaar, N., and Ngubevana, L. (2022). Ensuring a just energy transition through hydrogen: how the G20 can support Africa. *South Afr. Inst. Int. Aff.*, 1–19.

Harichandan, S., Kar, S. K., and Rai, P. K. (2023). A systematic and critical review of green hydrogen economy in India. *Int. J. Hydrogen Energy* 48, 31425–31442. doi:10.1016/j.ijhydene.2023.04.316

Hassan, Q., Abdulateef, A. M., Abdul Hafedh, S., Al-samari, A., Abdulateef, J., Sameen, A. Z., et al. (2023a). Renewable energy-to-green hydrogen: a review of main resources routes, processes and evaluation. *Int. J. Hydrogen Energy* 48, 17383–17408. doi:10.1016/j.ijhydene.2023.01.175

Hassan, Q., Sameen, A. Z., Salman, H. M., and Jaszczur, M. (2023b). A roadmap with strategic policy toward green hydrogen production: the case of Iraq. *Sustainability* 15 (6), 5258. doi:10.3390/su15065258

Heilala, J., Paasi, J., Lanz, M., Aho, M., Salminen, K., and Kutvonen, A. (2022). *Sustainable industry X research ecosystem (SIRE): strategic research and innovation agenda SRIA 2022: project deliverable december 2022*.

Hwang, J., Maharjan, K., and Cho, H. (2023). A review of hydrogen utilization in power generation and transportation sectors: achievements and future challenges. *Int. J. hydrogen energy* 48 (74), 28629–28648. doi:10.1016/j.ijhydene.2023.04.024

IEA (2023). *Global hydrogen reviews*.

Inci, M., Büyük, M., Demir, M. H., and İlbey, G. (2021). A review and research on fuel cell electric vehicles: topologies, power electronic converters, energy management methods, technical challenges, marketing and future aspects. *Renew. Sustain. Energy Rev.* 137, 110648. doi:10.1016/j.rser.2020.110648

International Renewable Energy Agency (2020). *Green Hydrogen: a guide to policy making*, 52. Abu Dhabi: International Renewable Energy Agency. Available at: https://www.irena.org/-/media/Files/IRENA/Agency/Publication/2020/Nov/IRENA_Green_hydrogen_policy_2020.pdf (Accessed November 20, 2023).

IRENA (2018). Hydrogen from renewable power. Technology outlook for the energy transition. Available at: https://www.irena.org//media/Files/IRENA/Agency/Publication/2018/Sep/IRENA_Hydrogen_from_renewable_power_2018.pdf (Accessed May 20, 2024).

IRENA (2020). Green hydrogen cost reduction. Scaling up electrolysers to meet the 1.5oC climate goal. Available at: https://www.irena.org/-/media/Files/IRENA/Agency/Publication/2020/Dec/IRENA_Green_hydrogen_cost_2020.pdf (Accessed June 19, 2024).

IRENA (2024). *Renewable energy statistics*.

Ishaq, H., Dincer, I., and Crawford, C. (2022). A review on hydrogen production and utilization: challenges and opportunities. *Int. J. Hydrogen Energy* 47 (62), 26238–26264. doi:10.1016/j.ijhydene.2021.11.149

Jiao, S., Fu, X., Wang, S., and Zhao, Y. (2021). Perfecting electrocatalysts via imperfections: towards the large-scale deployment of water electrolysis technology. *Energy and Environ. Sci.* 14 (4), 1722–1770. doi:10.1039/d0ee03635h

Jie, S., Zhu, Y., Feng, Y., Yang, J., and Xia, C. (2023). A prompt decarbonization pathway for shipping: green hydrogen, ammonia, and methanol production and utilization in marine engines. *Atmosphere* 14 (3), 584. doi:10.3390/atmos14030584

Jilani, A., Hussain, S. Z., Melaibari, A. A., and Abu-Hamdeh, N. H. (2022). Development and mechanistic studies of ternary nanocomposites for hydrogen production from water splitting to yield sustainable/green energy and environmental remediation. *Polymers* 14 (7), 1290. doi:10.3390/polym14071290

Kakoulaki, G., Kougias, I., Taylor, N., Dolci, F., Moya, J., and Jäger-Waldau, A. (2021). Green hydrogen in Europe – a regional assessment: substituting existing production with electrolysis powered by renewables. *Energy Convers. Manag.* 228, 113649. doi:10.1016/j.enconman.2020.113649

Kampouta, D. (2022). Hydrogen economy-legislative framework and current status. *PhD diss., Univ. Piraeus (Greece)*.

Kar, S. K., Kumar Sinha, A. S., Bansal, R., Shabani, B., and Harichandan, S. (2023). Overview of hydrogen economy in Australia. *Wiley Interdiscip. Rev. Energy Environ.* 12 (1), e457. doi:10.1002/wene.457

Kendall, K. (2022). Green hydrogen in the UK: progress and prospects. *Clean. Technol.* 4 (2), 345–355. doi:10.3390/cleantechnol4020020

Khan, M. I., and Al-Ghamdi, S. G. (2023). Hydrogen economy for sustainable development in GCC countries: a SWOT analysis considering current situation, challenges, and prospects. *Int. J. Hydrogen Energy* 48 (28), 10315–10344. doi:10.1016/j.ijhydene.2022.12.033

Klopčič, N., Grimmer, I., Winkler, F., Sartory, M., and Trattner, A. (2023). A review on metal hydride materials for hydrogen storage. *J. Energy Storage* 72, 108456. doi:10.1016/j.est.2023.108456

Kneebone, J. (2022). *Redrawing the EU's energy relations: getting it right with African renewable hydrogen*.

Kojima, H., Nagasawa, K., Todoroki, N., Ito, Y., Matsui, T., and Nakajima, R. (2023). Influence of renewable energy power fluctuations on water electrolysis for green hydrogen production. *Int. J. hydrogen energy* 48 (12), 4572–4593. doi:10.1016/j.ijhydene.2022.11.018

Kovač, A., Paranos, M., and Marciuš, D. (2021). Hydrogen in energy transition: a review. *Int. J. Hydrogen Energy* 46 (16), 10016–10035. doi:10.1016/j.ijhydene.2020.11.256

Kritzinger, A., and Snyman, I. (2022). Socio-economic impact assessment report for the Prieska power reserve solar PV plant and wind energy facility phase 1. *Prieska, North. Cape*.

Kumar, S., Arzaghi, E., Baalisampang, T., Garaniya, V., and Abbassi, R. (2023). Insights into decision-making for offshore green hydrogen infrastructure developments. *Process Saf. Environ. Prot.* 174, 805–817. doi:10.1016/j.psep.2023.04.042

Kumar, S., Nanan-Surujbally, A., Sharma, D. P., and Pathak, D. (2024). "Hydrogen safety/standards (national and international document standards on hydrogen energy and fuel cell)," in *Towards hydrogen infrastructure* (Elsevier), 315–346.

Lagioia, G., Spinelli, M. P., and Vera, A. (2023). Blue and green hydrogen energy to meet European Union decarbonisation objectives. An overview of perspectives and the current state of affairs. *Int. J. Hydrogen Energy* 48 (4), 1304–1322. doi:10.1016/j.ijhydene.2022.10.044

Latapí, M., Davíðsdóttir, B., and Jóhannsdóttir, L. (2023). Drivers and barriers for the large-scale adoption of hydrogen fuel cells by Nordic shipping companies. *Int. J. Hydrogen Energy* 48 (15), 6099–6119. doi:10.1016/j.ijhydene.2022.11.108

Li, C., and Baek, J. B. (2021). The promise of hydrogen production from alkaline anion exchange membrane electrolyzers. *Nano Energy* 87, 106162. doi:10.1016/j.nanoen.2021.106162

Li, H., Cao, X., Liu, Y., Shao, Y., Nan, Z., Teng, L., et al. (2022). Safety of hydrogen storage and transportation: an overview on mechanisms, techniques, and challenges. *Energy Rep.* 8, 6258–6269. doi:10.1016/j.egyr.2022.04.067

Li, X., Raorane, C. J., Xia, C., Wu, Y., Tran, T. K. N., and Khademi, T. (2023). Latest approaches on green hydrogen as a potential source of renewable energy towards sustainable energy: spotlighting of recent innovations, challenges, and future insights. *Fuel* 334, 126684. doi:10.1016/j.fuel.2022.126684

Lindner, R. (2023). Green hydrogen partnerships with the Global South. Advancing an energy justice perspective on "tomorrow's oil". *Sustain. Dev.* 31 (2), 1038–1053. doi:10.1002/sd.2439

Liu, H., Zhang, J., Sun, P., Zhou, C., Liu, Y., and Fang, Z. Z. (2023a). An overview of TiFe alloys for hydrogen storage: structure, processes, properties, and applications. *J. Energy Storage* 68, 107772. doi:10.1016/j.est.2023.107772

Liu, L., Zhai, R., and Hu, Y. (2023b). Performance evaluation of wind-solar-hydrogen system for renewable energy generation and green hydrogen generation and storage: energy, exergy, economic, and enviroeconomic. *Energy* 276, 127386. doi:10.1016/j.energy.2023.127386

Mali, B., Niraula, D., Kafle, R., and Bhusal, A. (2021) "Green hydrogen: production methodology, applications and challenges in Nepal," in In2021 7th International Conference on Engineering, Applied Sciences and Technology (ICEAST). IEEE, 68–76.

Martinez de Leon, C., Ríos, C., and Brey, J. J. (2023). Cost of green hydrogen: limitations of production from a stand-alone photovoltaic system. *Int. J. Hydrogen Energy* 48 (32), 11885–11898. doi:10.1016/j.ijhydene.2022.05.090

Merem, E. C., Twumasi, Y., Wesley, J., Olagbegi, D., Crisler, M., Romorno, C., et al. (2022). The evaluation of wind energy potentials in South Africa. *Energy Power* 12 (1), 9–25. doi:10.5923/j.ep.20221201.02

Mneimneh, F., Ghazzawi, H., Abu Hejjeh, M., Manganelli, M., and Ramakrishna, S. (2023). Roadmap to achieving sustainable development via green hydrogen. *Energies* 16 (3), 1368. doi:10.3390/en16031368

Morlanés, N., Katikaneni, S. P., Paglieri, S. N., Harale, A., Solami, B., Mani Sarathy, S., et al. (2021). A technological roadmap to the ammonia energy economy: current state and missing technologies. *Chem. Eng. J.* 408, 127310. doi:10.1016/j.cej.2020.127310

Müller, L. A., Leonard, A., Trotter, P. A., and Stephanie, H. (2023). Green hydrogen production and use in low-and middle-income countries: a least-cost geospatial modelling approach applied to Kenya. *Appl. Energy* 343, 121219. doi:10.1016/j.apenergy.2023.121219

Munim, Z. H., Chowdhury, M. M. H., Tusher, H. M., and Notteboom, T. (2023). Towards a prioritization of alternative energy sources for sustainable shipping. *Mar. Policy* 152, 105579. doi:10.1016/j.marpol.2023.105579

Mustafa, A., Lougou, B. G., Shuai, Y., Wang, Z., and Tan, H. (2020). Current technology development for CO2 utilization into solar fuels and chemicals: a review. *J. Energy Chem.* 49, 96–123. doi:10.1016/j.jechem.2020.01.023

Nemmour, A., Inayat, A., Janajreh, I., and Ghenai, C. (2023). Green hydrogen-based E-fuels (E-methane, E-methanol, E-ammonia) to support clean energy transition: a literature review. *Int. J. Hydrogen Energy* 48 (75), 29011–29033. doi:10.1016/j.ijhydene.2023.03.240

Newborough, M., and Cooley, G. (2020). Developments in the global hydrogen market: the spectrum of hydrogen colours. *Fuel Cells Bull.* 2020 (11), 16–22. doi:10.1016/s1464-2859(20)30546-0

Nwokolo, S. C., Singh, R., Khan, S., Kumar, A., and Luthra, S. (2023). "Technological pathways to net-zero goals in africa," in *Africa's path to net-zero: exploring scenarios for a sustainable energy transition* (Cham: Springer Nature Switzerland), 93–210.

Odoom, R., Brännlund, R., Amin, K., and Nanzoninge, J. (2023). Oil and gas energy security. *Econ. Oil Gas Industry Emerg. Mark. Dev. Econ.*, 5.

Ogeya, M. C., Osano, P., Kingiri, A., and Okemwa, J. M. (2021). Challenges and opportunities for the expansion of renewable electrification in Kenya. *Youba Sokona, Vice-Chair Intergov. Panel Clim. Change (IPCC)* 46, 46–70. doi:10.4324/9781003054665-3

Ogunniyi, E., and Pienaar, C. (2019). "Paradox of Africa's renewable energy potentials and quest towards powering africa," in *2019 IEEE PES/IAS PowerAfrica* (IEEE), 556–562.

Ohunakin, O. S., Ojolo, S. J., and Ajayi, O. O. (2011). Small hydropower (SHP) development in Nigeria: an assessment. *Renew. Sustain. Energy Rev.* 15 (4), 2006–2013. doi:10.1016/j.rser.2011.01.003

Okolie, J. A., Patra, B. R., Mukherjee, A., Nanda, S., Dalai, A. K., and Kozinski, J. A. (2021). Futuristic applications of hydrogen in energy, biorefining, aerospace,

pharmaceuticals and metallurgy. *Int. J. hydrogen energy* 46 (13), 8885–8905. doi:10.1016/j.ijhydene.2021.01.014

Oni, A. O., Anaya, K., Giwa, T., Di Lullo, G., and Kumar, A. (2022). Comparative assessment of blue hydrogen from steam methane reforming, autothermal reforming, and natural gas decomposition technologies for natural gas-producing regions. *Energy Convers. Manag.* 254, 115245. doi:10.1016/j.enconman.2022.115245

Orjuela-Abril, S., Torregroza-Espinosa, A., and Duarte-Forero, J. (2023). Innovative technology strategies for the sustainable development of self-produced energy in the Colombian industry. *Sustainability* 15 (7), 5720. doi:10.3390/su15075720

Orlova, S., Mezeckis, N., and Vasudev, V. P. K. (2023). Compression of hydrogen gas for energy storage: a review. *Latv. J. Phys. Tech. Sci.* 60 (2), 4–16. doi:10.2478/lpts-2023-0007

Osman, A. I., Chen, L., Yang, M., Msigwa, G., Farghali, M., Fawzy, S., et al. (2023). Cost, environmental impact, and resilience of renewable energy under a changing climate: a review. *Environ. Chem. Lett.* 21 (2), 741–764. doi:10.1007/s10311-022-01532-8

Panchenko, V. A., Daus, Y. V., Kovalev, A. A., Yudaev, I. V., and Litti, Y. V. (2023). Prospects for the production of green hydrogen: review of countries with high potential. *Int. J. Hydrogen Energy* 48 (12), 4551–4571. doi:10.1016/j.ijhydene.2022.10.084

Pasini, G., Lutzemberger, G., and Ferrari, L. (2023). Renewable electricity for decarbonisation of road transport: batteries or E-fuels? *Batteries* 9 (2), 135. doi:10.3390/batteries9020135

Pastore, L. M., Lo Basso, G., Sforzini, M., Santoli, L., and de Santoli, L. (2022). Technical, economic and environmental issues related to electrolysers capacity targets according to the Italian Hydrogen Strategy: a critical analysis. *Renew. Sustain. Energy Rev.* 166, 112685. doi:10.1016/j.rser.2022.112685

Patel, M. (2020). Green hydrogen: a potential export commodity in a new global marketplace. *Trade and Industrial Policy Strategies (TIPS) Pretoria, S. Afr.*

Patonia, A., and Poudineh, R. (2022). Cost-competitive green hydrogen: how to lower the cost of electrolysers? *(No. 47)*. OIES Paper: EL.

Pinto, J., and Chege, K. (2024). Regulating green and low-carbon hydrogen in africa: a case study of South Africa. *Adv. Sci. Technol.* 142, 15–24.

Posso, F., Pulido, A., and Acevedo-Páez, J. C. (2023). Towards the hydrogen economy: estimation of green hydrogen production potential and the impact of its uses in Ecuador as a case study. *Int. J. Hydrogen Energy* 48 (32), 11922–11942. doi:10.1016/j.ijhydene.2022.05.128

Pourasl, H. H., Barenji, R. V., and Khojastehnezhad, V. M. (2023). Solar energy status in the world: a comprehensive review. *Energy Rep.* 10, 3474–3493. doi:10.1016/j.egyr.2023.10.022

Qian, Y., Yu, J., Lyu, Z., Zhang, Q., Lee, T. H., Pang, H., et al. (2023). Durable hierarchical phosphorus-doped biphase MoS2 electrocatalysts with enhanced H* adsorption. *Carbon Energy* 6, e376. doi:10.1002/cey2.376

Rai, A., and Pramanik, S. (2022). Fuel cell utilization for energy storage. *Renew. Energy Sustain. Growth Assess.*, 389–407. doi:10.1002/9781119785460.ch14

Raman, R., Kumar Nair, V., Prakash, V., Patwardhan, A., and Nedungadi, P. (2022). Green-hydrogen research: what have we achieved, and where are we going? Bibliometrics analysis. *Energy Rep.* 8, 9242–9260. doi:10.1016/j.egyr.2022.07.058

Razi, F., and Ibrahim, D. (2022). Renewable energy development and hydrogen economy in MENA region: a review. *Renew. Sustain. Energy Rev.* 168, 112763. doi:10.1016/j.rser.2022.112763

Roos, T., and Wright, J. (2020). *Powerfuels and green hydrogen (public version)*. The Council for Scientific and Industrial Research CSIR.

Roos, T. H. (2021). The cost of production and storage of renewable hydrogen in South Africa and transport to Japan and EU up to 2050 under different scenarios. *Int. J. hydrogen energy* 46 (72), 35814–35830. doi:10.1016/j.ijhydene.2021.08.193

Rufus, O. S., Olusola Edward, O., and Bamidele Abel, I. (2022). Unemployment among technical students: implication for managers of higher education. *Education* 4 (1), 1–7.

Runge, P., Sölch, C., Albert, J., Wasserscheid, P., Zöttl, G., and Grimm, V. (2023). Economic comparison of electric fuels for heavy duty mobility produced at excellent global sites-a 2035 scenario. *Appl. Energy* 347, 121379. doi:10.1016/j.apenergy.2023.121379

Ruseckas, L. (2022). *Europe and the Eastern Mediterranean: the potential for hydrogen partnership*. Germany: SWP Comment. No. 50/2022.

Sadik-Zada, E. R. (2021). Political economy of green hydrogen rollout: a global perspective. *Sustainability* 13 (23), 13464. doi:10.3390/su132313464

Sánchez-Bastardo, N., Schlogl, R., and Ruland, H. (2021). Methane pyrolysis for zero-emission hydrogen production: a potential bridge technology from fossil fuels to a renewable and sustainable hydrogen economy. *Industrial and Eng. Chem. Res.* 60 (32), 11855–11881. doi:10.1021/acs.iecr.1c01679

Santos, A. L., Cebola, M. J., and Santos, D. M. (2021). Towards the hydrogen economy—a review of the parameters that influence the efficiency of alkaline water electrolyzers. *Energies* 14 (11), 3193. doi:10.3390/en14113193

Sarker, A. K., Kalam Azad, A., Rasul, M. G., and Doppalapudi, A. T. (2023). Prospect of green hydrogen generation from hybrid renewable energy sources: a review. *Energies* 16 (3), 1556. doi:10.3390/en16031556

Schaffert, J. (2022). Progress in power-to-gas energy systems. *Energies* 16 (1), 135. doi:10.3390/en16010135

Schnuelle, C., Wassermann, T., and Stuehrmann, T. (2022). Mind the gap—a socio-economic analysis on price developments of green hydrogen, synthetic fuels, and conventional energy carriers in Germany. *Energies* 15 (10), 3541. doi:10.3390/en15103541

Singh, G., Ramadass, K., Dbc DasiReddy, V., Yuan, X., Ok, Y. S., Bolan, N., et al. (2023). Material-based generation, storage, and utilisation of hydrogen. *Prog. Mater. Sci.* 135, 101104. doi:10.1016/j.pmatsci.2023.101104

Sohani, A., Cornaro, C., Hassan Shahverdian, M., Pierro, M., Moser, D., Nižetić, S., et al. (2023). Building integrated photovoltaic/thermal technologies in Middle Eastern and North African countries: current trends and future perspectives. *Renew. Sustain. Energy Rev.* 182, 113370. doi:10.1016/j.rser.2023.113370

Sontakke, U., and Jaju, S. (2021) "Green hydrogen economy and opportunities for India," in IOP Conference Series: Materials Science and Engineering.

Statista (2024). Forecast of the total population of Africa 2020-2050. Available at: https://www.statista.com/statistics/1224205/forecast-of-the-total-population-of-africa/ (Accessed July 08, 2024).

Stavroulakis, P., Koutsouradi, M., Kyriakopoulou-Roussou, M.-C., Manologlou, E.-A., Tsioumas, V., and Papadimitriou, S. (2023). Decarbonization and sustainable shipping in a post COVID-19 world. *Sci. Afr.* 21, e01758. doi:10.1016/j.sciaf.2023.e01758

Sun, D., Guo, Di, and Xie, D. (2023). Using multicriteria decision making to evaluate the risk of hydrogen energy storage and transportation in cities. *Sustainability* 15 (2), 1088. doi:10.3390/su15021088

Szemat-Vielma, W., Scheibz, J., Kasraoui, N., and Al-Omar, F. (2023). "Sun powered green hydrogen-A comparative analysis from the kingdoms of Morocco and Saudi arabia," in SPE EuropEC-Europe Energy Conference featured at the 84th EAGE Annual Conference and Exhibition, Dhahran, Saudi Arabia, February 12, 2024.

Tang, D., Tan, G.-L., Li, G.-W., Liang, J.-G., Ahmad, S. M., Bahadur, A., et al. (2023). State-of-the-art hydrogen generation techniques and storage methods: a critical review. *J. Energy Storage* 64, 107196. doi:10.1016/j.est.2023.107196

Tarkowski, R., and Uliasz-Misiak, B. (2022). Towards underground hydrogen storage: a review of barriers. *Renew. Sustain. Energy Rev.* 162, 112451. doi:10.1016/j.rser.2022.112451

Tchouvelev, A. V., de Oliveira, S. P., and Neves, N. P. (2019). "Regulatory framework, safety aspects, and social acceptance of hydrogen energy technologies," in *Science and engineering of hydrogen-based energy technologies* (Academic Press), 303–356.

Teoh, Y. H., Geok How, H., Danh Le, T., Nguyen, H. T., Lin Loo, D., Rashid, T., et al. (2023). A review on production and implementation of hydrogen as a green fuel in internal combustion engines. *Fuel* 333, 126525. doi:10.1016/j.fuel.2022.126525

Terlouw, T., Bauer, C., McKenna, R., and Mazzotti, M. (2022). Large-scale hydrogen production via water electrolysis: a techno-economic and environmental assessment. *Energy Environ. Sci.* 15 (9), 3583–3602.

Tiar, B., Fadlallah, S. O., Serradj, D. E. B., Graham, P., and Aagela, H. (2024). Navigating Algeria towards a sustainable green hydrogen future to empower North Africa and Europe's clean hydrogen transition. *Int. J. Hydrogen Energy* 61, 783–802. doi:10.1016/j.ijhydene.2024.02.328

Tiruye, G. A., Besha, A. T., Mekonnen, Y. S., Benti, N. E., Gebreslase, G. A., and Tufa, R. A. (2021). Opportunities and challenges of renewable energy production in Ethiopia. *Sustainability* 13 (18), 10381. doi:10.3390/su131810381

Van Hoecke, L., Laffineur, L., Campe, R., Perreault, P., Verbruggen, S. W., and Lenaerts, S. (2021). Challenges in the use of hydrogen for maritime applications. *Energy and Environ. Sci.* 14 (2), 815–843. doi:10.1039/d0ee01545h

van Wijk, A., Wouters, F., Rachidi, S., and Ikken, B. (2019). A North africa—europe hydrogen manifesto. *Dii Desert Energy*.

Vardhan, R. V., Mahalakshmi, R., Anand, R., and Mohanty, A. (2022). "A review on green hydrogen: future of green hydrogen in India," in 2022 6th International Conference on Devices, Circuits and Systems (ICDCS), Coimbatore, India, 21-22 April 2022 (IEEE), 303–309.

Wappler, M., Unguder, D., Lu, X., Ohlmeyer, H., Teschke, H., and Lueke, W. (2022). Building the green hydrogen market–Current state and outlook on green hydrogen demand and electrolyzer manufacturing. *Int. J. Hydrogen Energy* 47 (79), 33551–33570. doi:10.1016/j.ijhydene.2022.07.253

Weko, S., Farrand, A., Fakoussa, D., and Quitzow, R. (2024). *The politics of green hydrogen cooperation*.

Yu, D., Duan, C., and Gu, B. (2023). Design and evaluation of a novel plan for thermochemical cycles and PEM fuel cells to produce hydrogen and power: application of environmental perspective. *Chemosphere* 334, 138935. doi:10.1016/j.chemosphere.2023.138935

Zachary, J. B., Diaz, L. L., Tatyana, K., and Zhou, Q. A. (2022). Materials research directions toward a green hydrogen economy: a review. *ACS Omega* 7 (37), 32908–32935. doi:10.1021/acsomega.2c03996

Zhang, K., Liang, X., Wang, L., Sun, K., Wang, Y., Xie, Z., et al. (2022). Status and perspectives of key materials for PEM electrolyzer. *Nano Res. Energy* 1 (3), e9120032. doi:10.26599/nre.2022.9120032

frontiers | Frontiers in Energy Research

TYPE Original Research
PUBLISHED 23 December 2024
DOI 10.3389/fenrg.2024.1471265

OPEN ACCESS

EDITED BY
Sunday Olayinka Oyedepo,
Bells University of Technology, Nigeria

REVIEWED BY
Elizabeth Oses Amuta,
Covenant University, Nigeria
Sirote Khunkitti,
Chiang Mai University, Thailand

*CORRESPONDENCE
A. Sharmila,
asharmila@vit.ac.in

RECEIVED 27 July 2024
ACCEPTED 22 November 2024
PUBLISHED 23 December 2024

CITATION
Shanmugam S and Sharmila A (2024) An intelligent adaptive neuro-fuzzy based control for multiport DC-AC converter with differential power processing converter for hybrid renewable power generation systems.
Front. Energy Res. 12:1471265.
doi: 10.3389/fenrg.2024.1471265

An intelligent adaptive neuro-fuzzy based control for multiport DC-AC converter with differential power processing converter for hybrid renewable power generation systems

S. Shanmugam and A. Sharmila*

School of Electrical Engineering, Vellore Institute of Technology, Vellore, Tamil Nadu, India

The increasing demand for renewable energy sources necessitates the development of sophisticated control systems that can seamlessly integrate and manage multiple power sources. This research introduces an advanced intelligent adaptive neuro fuzzy-based control (IANFC) for multiport DC-AC converters with differential power processing (DPP) converters, tailored for customized hybrid renewable power generation systems (HRPGS). The system aims to optimize HRPGS performance and efficiency through neuro-fuzzy control techniques. When integrating different DC power sources, such solar panels and wind turbines, into AC loads or the grid, multiport DC-AC converters are essential. These converters reduce the amount of power conversion steps, which improves the system's overall efficiency and scalability. Complementary DPP converters process only the differential power, thereby significantly reducing total power consumption and conversion losses. The IANFC framework combines fuzzy logic reasoning, based on rules, with neural network adaptive learning capabilities. This hybrid control method effectively manages the nonlinear and dynamic behavior of HRPGS, ensuring reliable performance under varying load demands and environmental conditions. The controller dynamically adjusts the converter's operating point to ensure optimal power flow and system stability. Simulation findings using MATLAB/Simulink verify the efficacy of the suggested IANFC system. Under various operational situations, key performance measures like response time, stability, and system efficiency are examined. As evidenced by the data, system performance has significantly improved as compared to traditional control techniques. The proposed system demonstrates an efficiency of 99.45% and achieves stability in just 0.02 s. Compared to conventional algorithms, this approach shows superior performance across multiple metrics.

KEYWORDS

hybrid energy systems, intelligent adaptive neuro-fuzzy based control (IANFC), SES, BESS, MPC, MSVPWM and ANFIS, DPC

1 Introduction

The growing need for renewable energy means that creative control systems are needed to efficiently integrate and manage multiple power sources. Hybrid renewable energy producing systems (HRPGS) combine many renewable energy sources, including solar and wind power, to deliver a consistent and reliable power supply. A multiport DC-AC converter is a crucial part of these systems, since it facilitates the integration of various DC inputs into a single AC output. By processing only differential power, DPP (Differential Power Processing) converters further improve efficiency and lower losses. This research suggests using intelligent adaptive neuro fuzzy control (IANFC) to maximize HRPGS performance. In order to manage the nonlinear and dynamic behavior of HRPGS, this advanced control technique makes use of rule-based fuzzy logic reasoning and neural networks' adaptive learning capabilities. Real-time dynamic adjustment of the converter operating point is made by the IANFC system to guarantee stable and effective energy management. The suggested system performs well in terms of efficiency, stability, and response time under a range of operating situations, according to thorough simulations conducted in MATLAB/Simulink. Future developments and commercialization are made possible by the integration of IANFC with multiport DC-AC and DPP converters, which offers a strong, effective, and flexible response to the problems that contemporary renewable energy systems face.

The current electrical transmission system cannot handle the exponential growth in demand for electricity. In order to satisfy consumer demand, distributed generation must be generated locally or funds must be allocated to expand the transmission infrastructure's capacity. Comparing renewable energy sources like solar and wind requires the usage of both large and local networks. If the effect on system voltage, frequency stability, and interference levels is not taken into consideration, the inclusion of an unconventional energy source may result in interruptions, power outages, and vulnerabilities in the network. Furthermore, during consumption, the voltage and frequency will fluctuate if the installed capacity of non-conventional energy is equal to that of conventional energy. Since unconventional energy is irregular and unpredictable, it is challenging to predict how much electricity will be produced.

Numerous experts have observed the possible effects of increasing small-scale power production technologies' integration and deployment on grid efficiency. It is imperative to address the significant issue of microgrid electricity output's unpredictability. The variability of the cargo supply can be mitigated in a number of methods, such as demand-side management, generation dispatch, and storage device integration. Engineers are never able to come up with a good solution when they have too many possibilities.

The global fight against global warming requires a significant increase in renewable energy in the electricity industry. This requires considering power quality, grid stability, and reliability. Utilizing renewable energy near the load centre can optimize operational efficiency and reduce transmission losses. Microgrids, small-scale grids, concentrate power generation resources in a small geographic region, using natural renewable energy as the primary energy source. Renewable energy systems' intermittency needs to be managed in order to meet load requirements as shown in Supplementary Figure S1.

One of the key advantages of hybrid solar power systems over traditional solar power systems is continuous power delivery. The battery of a hybrid solar system can hold energy to deliver power continually. Batteries serve as inverters during blackouts, providing backup power for your home and important appliances. The battery provides backup power to keep the device operational during a blackout or power loss. This system's long-term cost effectiveness is another benefit. The consumer ultimately saves money even though the initial cost of these systems may be higher because they require less maintenance and do not require the purchase of fuel, unlike generators. Conventional generators have a limited initial energy output as shown in Supplementary Figure S2. On the other hand, hybrid solar energy systems disperse energy at night after storing it during the day. Technology can be utilized to automatically modify a hybrid solar system's energy intake according to the power requirements of particular appliances, including air conditioners and fans.

Multiport converters (MPCs) are a way to reduce the number of converters required in these power systems by combining many converters into a single unit. MPCs can be classified as partially insulated, insulated, or non-insulated. You can expand the number of input/output ports by using inverter bridges and windings. Power and storage components in DC microgrids are usually connected by means of separate power electronic converters (DCMGs), which can be single- or multi-stage. However, voltage fluctuations, complicated protection requirements, high system costs owing to switch activation, and decreased efficiency due to more conversion steps are the main drawbacks of these configurations (particularly for intermediate energy and energy storage devices). Multiport converter (MPC) technology is a great choice for different voltage levels since it enables bidirectional power flow between different energy storage devices (batteries, supercapacitors, etc.) and power sources (solar energy, fuel cells, etc.). Conventional DCMG architectures with their complex communication specifications and superfluous conversion steps are eliminated. The use of multiport converters (MPCs) is becoming increasingly popular in non-logic power supplies, satellite communications, microgrids, and hybrid vehicles. Transformer-isolated MPC topologies are particularly advantageous for applications requiring high voltage conversion rates, as they allow for the achievement of the desired voltage gain by adjusting the transformer's turns ratio.

The energy demand boom is primarily driven by industrialization and population growth, along with a shortage of traditional energy sources like coal, oil, and natural gas. Self-renewable energy sources like geothermal, biomass, solar, wind, and water are crucial for environmental protection and energy security, with solar and wind being the most promising (Arani et al., 2019).

In renewable energy systems, static power converters are utilized to enhance power tracking, adjust the power supply according to load demands, and improve both static and dynamic characteristics (Mihai, 2015; Gunasekaran and Chakraborty, 2023), as noted by Mihai. Power electronic converters, either single- or multi-stage, are needed based on the output characteristics when connecting batteries and hybrid renewable energy sources to the load or

grid. It is perfect to link several renewable energy sources to a load using multiport converters, which are more economical and efficient than standard converters, as shown in (Dobbs and Chapman, 2003; Jiang and Fahimi, 2011; Wu et al., 2015; Madhana and Geetha, 2022; Alargt et al., 2019a; Shanmugam and Sharmila, 2022; Benavides and Chapman, 2005). In addition to comparing the benefits and drawbacks of different multiport converter topologies, A.K. Bhattacharjee and associates (Bhattacharjee et al., 2018) give an overview of multiport converters used for combining solar energy generation with energy storage systems.

Multiport converter topologies fall into three categories: partially isolated, non-isolated, and isolated. DC link or electrical coupling is used in non-isolated arrangements, and transformers are used in fully and partially isolated topologies to connect various sources or loads via magnetic coupling (Madhana and Mani, 2022). The high power density and compact design are the result of a non-isolated topology, in which ports are not split but are instead directly connected to one another. You may find a report in (Tao et al., 2008; Krishnaswami and Mohan, 2009; Ajami and Shayan, 2015; Tao et al., 2005; Zeng et al., 2013; Zeng et al., 2014; Wu et al., 2014; Savitha and Kanakasabapathy, 2016) on discrete MICs with buck-boost topology. This design is more expensive since it requires multi-winding magnetically coupled transformers and larger energy storage coils. This makes it possible for the design to include elements like turns ratio and leakage inductance that are pertinent to transformers. Consequently, it is possible to achieve great efficiency under various operating conditions.

A new soft-switching non-isolated high-boost multiport DC-DC converter that can simultaneously charge and output ESS was proposed in Rasoul Faraji's research (Matsuo et al., 2004). It considers several aspects, including minimal converter component count, independence of every power flow line, strong boost voltage gain, and smooth switching conditions. Numerous suggested topologies for more effective voltage rise have been published in scholarly journals. One notable achievement highlighted by the authors of (Wu et al., 2011; Iannone et al., 2005) involves the integration of fuzzy logic control into dual-input DC-DC converters. This fuzzy logic control approach aims to enhance the parameters of the PID controller and modify the duty cycle of the dual-input DC-DC converter by introducing an additional nonlinear characteristic source. A modular integrated converter with DPP capabilities that was built on cascading quasi-Z source inverters was introduced in (Chakraborty et al., 2015). (Faraji and Farzanehfard, 2020) published a distributed control technique based on DPP for tracking a solar cell system's submodule maximum power point. It is common to connect DPP designs in parallel or series. The current differential between PV cells at the module, sub-module, or cell level is mainly provided by DPP converters. Thus, features of DPP designs include module or device level, bidirectional or unidirectional, isolated or non-isolated, shared between modules or between strings. A study that using a built pulsed current source cell in (Alargt et al., 2019b) synthesized a cascade structure from two input interleaved boost converters. In (Zhang et al., 2016; Alargt et al., 2019a; Chu et al., 2019; Uno and Shinohara, 2019; R and Mani, 2023; Chu et al., 2017), developed a MPC with centralized controller using various algorithm has been discussed.

This design, which comprises of a multiport DC-AC converter (MPC) and a DC-DC converter (DPPC), is recommended to be integrated with a solar PV system that is connected to a battery energy storage system (ESS). Only a tiny portion of the power, referred to as the differential power, needs to be controlled by the DPPC; the MPC efficiently controls the remainder of the active power distribution between the PV, battery, and AC grid. This suggested strategy offers better efficacy and affordability. While prior DPP techniques primarily addressed the DC-DC stage of PV systems, our research focuses on the DC-DC and DC-AC phases of the battery ESS-integrated PV system.

An altered SVPWM approach is used in the construction of the MPC to compensate variations in PV and battery voltages. Battery-ESS integrated solar cell systems are studied, and multi-port and partial current conversion techniques are used, drawing on the literature review. The major work is focused on creating highly integrated, economical, and efficient designs by utilizing latest technical developments.

Wang et al. (2021) introduced a differential power processing (DPPC) and multi-port DC-AC converter (MPC) to integrate battery ESS and solar PV systems. The MPC regulates active power flow, while DPPC handles the differential power component. The architecture offers high integration, efficiency, and cost-effectiveness.

Elkeiy et al. (2023) developed a multi-port DC-DC converter for EV rapid charging stations, improving efficiency and reducing costs. The architecture consists of two current flow paths: outer loop and inner loop, with a primary DPPC controlling the loop's current and an auxiliary DC-DC converter managing fractional power. This configuration offers fault tolerance and cost-effectiveness.

Perera et al. (2021) propose a bidirectional multiport converter with twin inverters, allowing a single power unit to power DC/AC converters using solid-state and magnetic drives. This configuration offers more power limit and efficiency than traditional methods due to inverter multitasking and single-stage DC/DC and DC/AC power transmission techniques. Independent inverter control ensures uninterrupted power transfer even in case of failure.

Madana et al. developed an energy-efficient multiport converter using predictive energy correction algorithms. The converter maintains high power, transmission efficiency, and reliability while enhancing energy extraction from multiple ports. The dynamic duty cycle controls gate voltages, reducing fluctuations and improving system dependability. The converter's performance was tested using MATLAB/SIMULINK, outperforming conventional PID controllers by 6.88%.

The major contribution of this paper in the differential power processing of MPC DC-AC converter is to manage power processing between various ports of MPC and grid. Additionally, the paper introduces the IANFC scheme for effectively controlling the nonlinear and dynamic behavior of MPC.

The Crayfish Optimization Algorithm (COA) is proposed for optimal optimization of multiple BESS sites and sizes, enhancing peak demand, power loss, and voltage deviation performance (Pompern et al., 2023). The study identifies optimal BESS locations and dimensions for distribution networks, aiming to reduce power loss and voltage variation expenses, comparing particle swarm optimization and genetic algorithms (Boonluk et al., 2020). BESS capacity, PV and EV integration improve

distribution system efficiency, reduce expenses, and enhance voltage profile. Metaheuristic methods optimize setup, maintenance, transmission losses, and voltage profile (Wichitkrailat et al., 2024).

This is how the rest of the article is organized. In Section 2, the basic idea of the MPC with DPPC is provided, followed by the related topologies. A detailed discussion of the various control and modulation approaches is provided in Section 3. After a quantitative analysis of the MPC's active power regulation, Section 4 presents the results of the suggested system's simulation. Ultimately, significant conclusions are established in Section 5.

2 Multiport converter

In the context of this study, the Multiport Converter (MPC) is a crucial part that makes it easier for HRPGS to manage and integrate different renewable energy sources efficiently. An energy storage device, wind turbine, solar panel, or other DC source can be interfaced with an AC demand or grid through the use of an MPC. This allows for smooth power distribution while reducing the energy losses that occur during conversion operations. Because of its flexible, scalable, and efficient design, it can accommodate a wide range of energy sources and load needs. The MPC ensures optimal resource use by providing adaptability to changing system requirements through its modular architecture. Furthermore, the application of complex techniques like Differential Power Processing (DPP), which further improve system stability and efficiency, is made possible by the MPC's sophisticated control capabilities. The performance of the MPC is examined in detail throughout this work, with the goal of enhancing its functioning under various operating conditions and load profiles using simulations and experimental validations. The MPC, a key component of HRPGS, not only makes it easier to integrate renewable energy sources smoothly, but it also makes a major contribution to the advancement of sustainable power generating techniques.

2.1 Configuration of the MPC with DPPC for different modes of operation

It has been researched that DPPC systems can function quite well under unfavorable and partial shadowing scenarios. While they are connected to each PV panel in a similar manner as Full Power Processing Converters (FPPCs), DPP converters are built differently. The DPP converters transfer very little power to keep the MPP operating in the case of a PV panel mismatch. Stated differently, DPP systems require less electricity processing than FPP systems. The main current flow of the DPP and FPP systems is depicted in Supplementary Figure S3. It is evident that the FPPC consumes all of the PV power after receiving the principal power in the FPPC system. Only a fraction of the electricity from the PV panels is processed by the DPP converters in the DPPC system. This implies that converter loss and component costs can be reduced because the DPP converter's power rating is lower than the FPP converter's. Since the DPP converters might not always receive full power, reducing wear on them also improves reliability.

Voltage equalizers and DPPC are being actively pursued as effective partial shading solutions. Different classes of DPP converters are categorized based on potential power redistribution scenarios. DPP converters can be made using single-input, multiple-output, bidirectional, and isolated converters. This is accomplished by using a Differential Electricity Processing (DPPC) converter, which transfers electricity to the battery by processing only a fraction of the power flowing from a generator (in this case, a PV string). In comparison, Supplementary Figure S4 illustrates a more conventional complete power processing method in which the converter processes all of the power a DPP converter operating in boost and buck modes is shown in Supplementary Figure S4. This DPP converter's operating mode is determined by the relative voltages, which are boost mode for $V_{PV} > V_{BATT}$ and buck mode for $V_{PV} < V_{BATT}$.

3 Control of MPC and PWM method

In the field of MPC control, pulse width modulation (PWM) techniques are essential for managing power flow between the converter's ports and the load or grid. By altering the pulse widths of the signals, PWM approaches regulate the average voltage or current applied to the converter's output. This provides accurate control over power transfer and improves system stability and efficiency. PWM control of MPC requires a number of important factors. First, the system topology, switching frequency, and required performance criteria all play a role in choosing the best PWM approach, be it space vector PWM or sinusoidal PWM. Space vector PWM, which offers improved efficiency and harmonic performance, and sinusoidal PWM, which is well-known for its simplicity and compatibility with grid-tied applications, are popular options. Furthermore, key factors in PWM control that affect the waveform and harmonic content of the converter's output voltage are modulation index, duty cycle, and switching frequency. The MPC can minimize distortion and losses while meeting voltage and current requirements by precisely adjusting these parameters.

Along with PWM approaches, the control algorithm selection also has a big impact on MPC performance. Examples of sophisticated control systems that provide precise regulation of converter operation, enhancing dynamic response and stability under a variety of operating conditions, include hysteresis control, model predictive control and proportional-integral-derivative (PID) control. By combining advanced control algorithms and PWM approaches, MPCs in HRPGS are essentially given the ability to efficiently manage power flow between renewable energy sources and the grid. By combining robust control algorithms with PWM approaches, MPCs help to construct sustainable energy systems that facilitate dependable and efficient power conversion, contributing to the creation of a more ecologically friendly future.

A Dual-Port Power Converter is used in Figure 1 to integrate a photovoltaic (PV) system with a battery storage unit and a power grid through a complex control architecture. A control algorithm is used to maximize the PV system's output of electricity. The battery stores extra energy, which is then released when needed. Energy

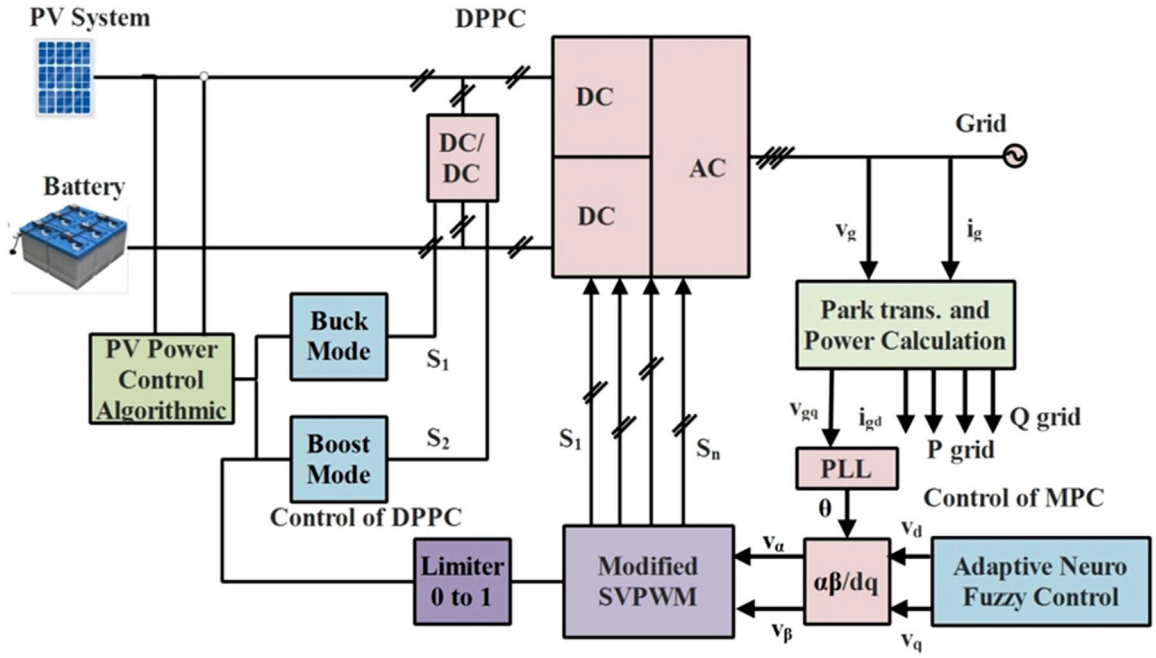

FIGURE 1
Control strategy of overall system.

transfer between the PV system, battery, and grid is managed by the DPPC, which has stages for DC/DC and DC/AC conversion. It can function in either the Boost or Buck modes, depending on the situation. A limiter controls control signals, and modified space vector pulse width modulation, or SVPWM, enables effective inverter management.

The flexibility and resilience of an Adaptive Neuro-Fuzzy Control system are enhanced. Park transformation is utilized for power computation, phase-locked loops (PLLs) are used for grid synchronization, and dq coordinate transformation is employed for efficient inverter control. This integrated system ensures efficient power conversion, storage, and distribution while maintaining peak performance and stability. The output of the PV power control loop is indicated by the parameter k, and the ratio of positive to negative tiny vectors is controlled by the control parameter kc ($0 \leq kc < 1$). The driving signal for switch S1 is obtained by comparing k to a triangle carrier ranging from −1 to 0, and the driving signal for switch S2 is obtained by comparing k to a triangular carrier ranging from 1 to 2. Figure 1 demonstrates how the system exhibits varied behavior based on different values of k.

Case 1. where the k lies between 0 and 1 where k = kc where switches S1 and S2 are both turned off and DPPC is in non-operative condition where MPC regulates the SES and grid.

Case 2. where the $k < 0$ switch is When the solar energy power supply is low, S1 turns on and the DPPC operates in a buck fashion. The battery empties and powers the converter.

Case 3. where the DPPC operates in boost mode, charging the battery with solar energy and powering the converter, and the $k > 1$ switch S2 begins to turn on.

Figure 2 shows the flowchart of power flow management of HRPGS using differential power processing converter for the above-mentioned cases.

3.1 Modified space vector modulation PWM (MSVPWM)

In the traditional SVPWM system, the number of switching sequences vary across subregions, changing the switching frequency and ultimately increasing the switching loss. Due to these drawbacks, improved space vector modulation PWM techniques have been published in a number of scholarly journals in an effort to reduce losses and maximize the DC link capacity. In this work, the voltages of the DC link capacitors are compared and incorporated into the control logic alongside a carrier signal. This combination of inputs is utilized to determine the necessary switching sequence for the Space Vector Modulation (SVM) approach.

The control system shown in Figure 3 combines a three-level Neutral Point Clamped (NPC) inverter with a load consisting of a solar panel and battery storage. The DC power produced by the solar panel is controlled by a bidirectional switch that is connected to the battery, allowing for flexible energy supply and energy storage. The DC power (V_dc) is received by the NPC inverter, which uses switches (V1, V2) and capacitors (C1, C2) to generate a three-level voltage output. The inverter converts DC power into AC power to service a load connected at points A, B, and C. Current transformers (CT) measure the current flowing to the load and supply the Vector Control Block with this information. This block computes the direct (V_d) and quadrature (V_q) voltage components in order to precisely control the inverter output.

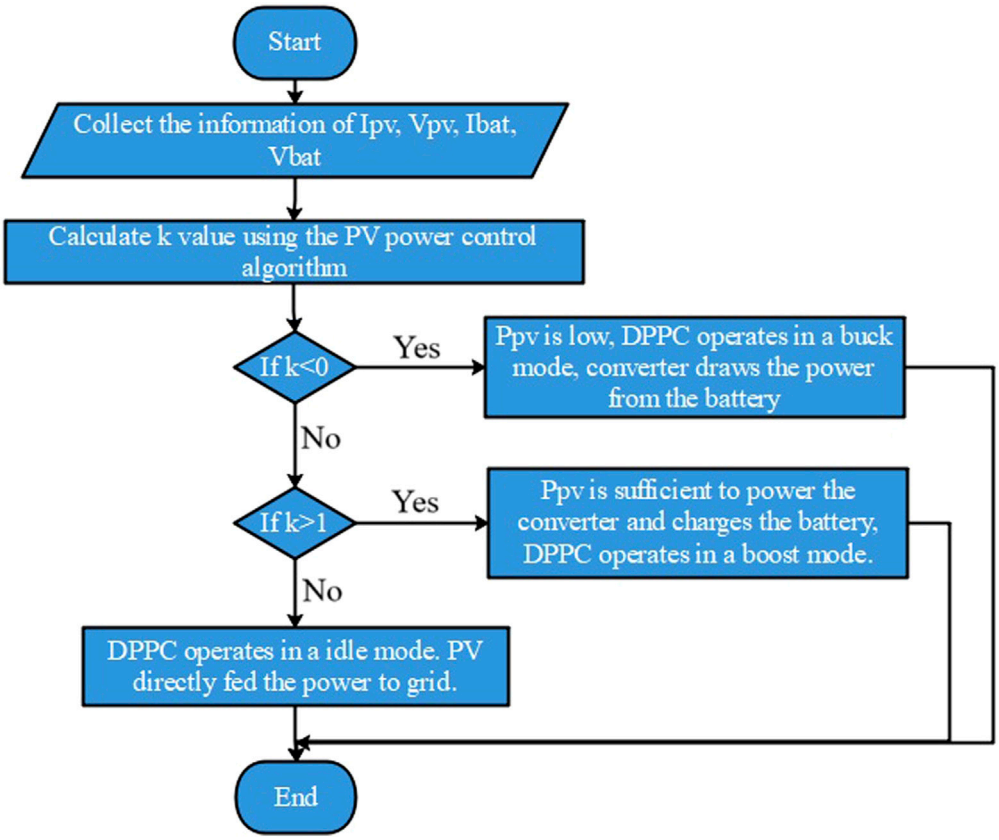

FIGURE 2
Flowchart of power processing in HRPGS.

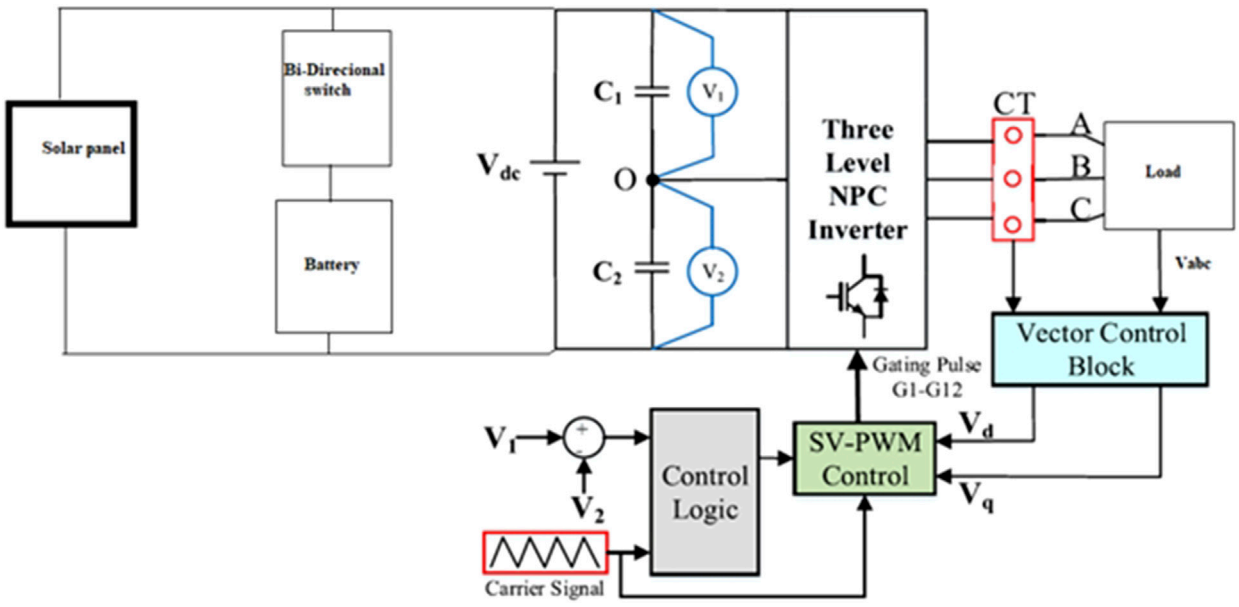

FIGURE 3
Inverter with DC link balancing.

The control logic receives the carrier signal (Vcarrier) and reference signals (V1, V2), and then creates the appropriate gating pulses (G1-G12) for the inverter switches. The SVPWM control optimizes the inverter switching to produce a stable AC output. This integrated system ensures the efficient conversion of solar and battery storage energy into the load, maintaining performance and stability through the application of cutting-edge control techniques.

When Vdc1 is greater than Vdc2, the switching sequence is selected to discharge Vdc1. In a similar vein, when Vdc2 surpasses Vdc1, the switching sequence is selected to permit Vdc2 to be discharged. The corresponding switching sequence is given in Supplementary Table S1. The DC link capacitance's voltage is balanced using this arrangement. The control logic will only update the voltage difference information at the beginning of each switching cycle in order to prevent duty cycle alterations in between switching cycles. It generates PWM with a constant switching frequency and an equal switching sequence under all conditions as shown in Supplementary Figure S5. A consistent switching frequency leads to a decrease in the switching frequency.

3.2 Adaptive neuro-fuzzy inference system (ANFIS)

The ANFIS is a hybrid intelligent framework that combines the learning capabilities of neural networks with the reasoning abilities of fuzzy logic. This amalgamation effectively models complex, nonlinear systems by capitalizing on the strengths of both methodologies. The ANFIS utilizes a structured architecture that consists of a neural network training algorithm that optimizes the fuzzy if-then rules and membership functions using input-output data, and a fuzzy inference system that includes fuzzy rules. Five layers typically make up an architecture: the first layer handles input variables and their fuzzy membership functions; the second layer evaluates the strength of the rules using fuzzy logic operators; the third layer normalizes these strengths; the fourth layer establishes the rules' consequent parameters; and the fifth layer aggregates the results to produce the final output. ANFIS modifies the parameters of the membership functions and rules during the learning process, frequently using techniques like backpropagation or hybrid learning integrating least squares and gradient descent. Improving forecast accuracy and reducing error are the main goals.

Due to its versatility in handling uncertainties, modeling nonlinear relationships, and adapting to varying conditions, ANFIS finds extensive application across various domains, including signal processing, control systems, pattern recognition, and decision-making processes. Its precision and adaptability enable the successful resolution of intricate problems in engineering, finance, and other fields. ANFIS controllers, resulting from the fusion of Fuzzy Logic Control (FLC) and artificial neural networks, are preferred for their capability to perform effectively across diverse scenarios and their automatic real-time parameter adjustments ensuring optimal control.

The architecture of an ANFIS is depicted in Supplementary Figure S6, illustrating the fusion of fuzzy logic reasoning and neural network learning. The process begins with the Fuzzification block, where an error signal is transformed into fuzzy inputs using predefined membership functions. The Decision Making block then analyzes these fuzzy inputs using a Knowledge Base containing membership functions and fuzzy rules. The system's adaptability to changing input conditions is enhanced by the NN-based Rule Update block, which utilizes neural network training techniques to continually refine these rules and membership functions. This neural network approach maintains a knowledge base that enhances fuzzy inference, leading to more precise decision-making. Despite the decision-making process, the outcome remains uncertain. The Defuzzification block converts this fuzzy output into a crisp value, which is then utilized in real-world applications by control systems such as digital-to-analog converters (DAC). This transformation is crucial for the fuzzy logic system to produce actionable insights.

For a variety of intricate, nonlinear applications, our ANFIS architecture offers resilient and flexible control overall. By merging the advantages of neural networks and fuzzy systems, it achieves this. NN receives different inputs according to inputs; NN has a standard output, thus training NN depends on both input and output; the FL receives the NN output and uses MATLAB to create the IF THEN rules and membership functions.

FL and ANN have emerged as prominent areas of study for addressing control problems. This trend can be attributed to the limitations of classical control theory, which often necessitates statistical controller designs. Control performance is frequently hindered by the imprecision in the mathematical modeling of the plant, particularly in complex and nonlinear control scenarios. The advancement of neural controllers based on multi-layered neural networks (NNs) and fuzzy logic controllers (FLCs) holds promise for enhancing control efficacy and expanding knowledge in this field. The integration of FL and NN has led to the development of FNN, commonly referred to as ANFIS. Unlike a FL network, which typically has multiple inputs and a single output, a neural network features multiple inputs and multiple outputs. The fusion of these two approaches is proposed to yield ANFIS for nonlinear applications.

The ANFIS controllers are designed using FLC and artificial neural networks. These controllers are used because they can operate efficiently in a variety of settings and dynamically modify their settings in real time to attain the best possible control.

To model complex, nonlinear systems, the ANFIS combines the linguistic representation capacity of fuzzy logic with the adaptability of neural networks. Fuzzy sets, language variables, and inference methods like Sugeno and Mamdani are some of the tools that ANFIS, which is founded on the ideas of fuzzy logic, employs to manage uncertainty in control systems. Layers for fuzzification, rule assessment, aggregation, and defuzzification are included in ANFIS structures. These layers are complemented by neural networks, which are superior at approximating complex functions and learning from data, leading to precise outputs, as seen in Supplementary Figure S7. By fine-tuning its parameters—which are usually a combination of least squares estimation and backpropagation—the hybrid learning algorithm maximizes ANFIS performance. Real-world applications in robotics, process control, finance, and healthcare show how flexible ANFIS is when handling stochastic and nonlinear systems. Evaluation metrics like as mean squared error and correlation coefficient are used to quantify ANFIS performance, and these metrics often outperform

traditional control techniques. Future research directions promise to advance ANFIS control further; these include integrating deep learning, enhancing scalability, and addressing real-time implementation challenges.

The ANFIS architecture is built upon the Sugeno Model, which consists of five layers, one output, and two inputs. Initially, the inputs undergo fuzzification, followed by de-fuzzification using an internal rule knowledge base. Each rule within the hierarchy is assigned a weight indicating its relative importance. These rules and weights can be adjusted during training to minimize errors and achieve the desired controller response. The first-order Sugeno model can be represented as follows:

u1 is the result if inputs e = A1 and Δe = B1.

u2 is the result if inputs e = A2 and Δe = B2.

Consequently, output u = w1u1 + w2u2.

The inputs that have been fuzzified are A and B, and the chosen weight is denoted by w. Supplementary Figure S8 shows the ANFIS controller's structural layout. The following layers make up the ANFIS structure.

3.2.1 Layer 1 (input or fuzzification layer)

Membership grades are generated for the input vectors Ai = 1, 2. n for each adaptive node in this layer.

A membership function, also known as the degree of membership, is a curve ranging from 0 to 1, illustrating how input data points are transformed into membership values. The parameters within the equation aij, bij, and cij correspond to the membership functions. In this study, the crossover slope value, bij, for the Gaussian membership function is typically set to 1. The curve's midpoint, denoted by the parameter cij, and its inflection point, represented by aij, collectively determine the curve's width as per Equations 1–3.

$$\varphi A_i(e,\Delta e) = \frac{1}{1+\left[\left(\frac{(e,\Delta e)-c_{ij}}{a_{ij}}\right)^2\right]^{b_{ij}}} \quad (1)$$

$$\varphi A_i(e,\Delta e) = e^{-\left[\left(\frac{(e,\Delta e)-c_{ij}}{a_{ij}}\right)^2\right]^{b_{ij}}} \quad (2)$$

$$\varphi A_i(e,\Delta e;\ a_i,b_i,c_i) = \max\left(\min\left(\min\left(e^{-\left[\left(\frac{(e,\Delta e)-c_{ij}}{a_{ij}}\right)^2\right]^{b_{ij}}}\right)\right)\right) \quad (3)$$

3.2.2 Layer 2 (rule inference layer)

Each node's output in this layer represents the level of activation of each rule.

$$out_i^2 = w_1 = min\left(\varphi A_i(e), \varphi AB_i(\Delta e)\right) \quad (4)$$

3.2.3 Layer 3 (normalization layer)

The fixed node I of this layer determines the ratio of the degree of activation of the *i*th rule to the sum of all degrees of activation:

$$out_i^3 = \frac{p}{\sum_{i=1}^{2} W_i} \quad (5)$$

3.2.4 Layer 4 (consequent layer)

This layer's adaptive node I calculates the contribution of the *i*th rule to the overall output using the node function below.

$$out_i^4 = \underline{wl}\ \left(P_i\, e + q_i \Delta e + r_i\right) \quad (6)$$

3.2.5 Layer 5 (output layer)

This layer's lone fixed node computes the overall output, which is a summary of the contributions made by each rule.

$$out_i^5 = \frac{w_1 z_1 + w_2 z_2}{w_1 + w_2} \quad (7)$$

Equations 3–7, which produce the result z, are simplified as in Equation 8.

$$z = (\bar{\bar{w}}_1 x)p_1 + \left(\bar{\bar{w}}_1 y\right)q_1 + \left(\bar{\bar{w}}_1\right)r_1 + \left(\bar{\bar{w}}_2 x\right)p_2 + \left(\bar{\bar{w}}_2 y\right)p_2 + \left(\bar{\bar{w}}_2\right)r_2 \quad (8)$$

4 Simulation results

The design and assessment of a simulation setup is done using MATLAB/Simulink software to confirm that the suggested configuration, control, and modulation strategies work as intended. Supplementary Tables S2, S3 present an illustration of the simulation parameters. Supplementary Table S2 contains the solar system's parameters, while Supplementary Table S3 lists the battery system's specifications. Using Vbat = 90 V in the experiments, the improved SVPWM scheme for the MPC is validated. The steady-state waveforms of the switching sequence are shown in Supplementary Figure S5. The reference voltage vector Vref rotates anticlockwise via S2, S3, S6, S5, and S6 when Vbat = 90 V or 100 V. It also rotates between S1 and S6 counterclockwise when Vbat = 150 V. For example, as Fiure. 4 shows, the switching sequences when Vref spins about S6 are (l,l,0)→(h,l,0)→(h,l,l)→(h,h,l)→(h,l,l)→(h,l,0)→(l,l,0). Moreover, it is observed that the halfway point of phase voltages, vxn, have been asymmetrically distributed in all other instances, with the exception of those in which the battery voltage, Vbat, is equal to half of the PV voltage, Vpv (i.e., Vbat = 100 V).

Supplementary Table S4 describes the performance of proposed IANFIS converter for different irradiation. Figure 4 depicts the IV and PV characteristics, which provide valuable insights into the behavior of electrical devices. Regarding photovoltaic systems, the I-V curve demonstrates the correlation between the current generated by a solar panel and the voltage across its terminals, thereby illustrating the panel's response to variations in temperature and irradiance. At the short circuit current (Isc), there is no voltage across the terminals, while at the open circuit voltage (Voc), no current flows. The shape of the I-V curve can be utilized to estimate the efficiency and condition of the solar panel. Conversely, the P-V curve illustrates the relationship between the power output and the voltage across the panel, highlighting the MPP at which the solar panel operates optimally. To ensure maximum energy harvesting in a range of operating scenarios and to improve solar system efficiency and design, it is imperative to get an understanding of these qualities. A visual representation of these curves can provide valuable insights

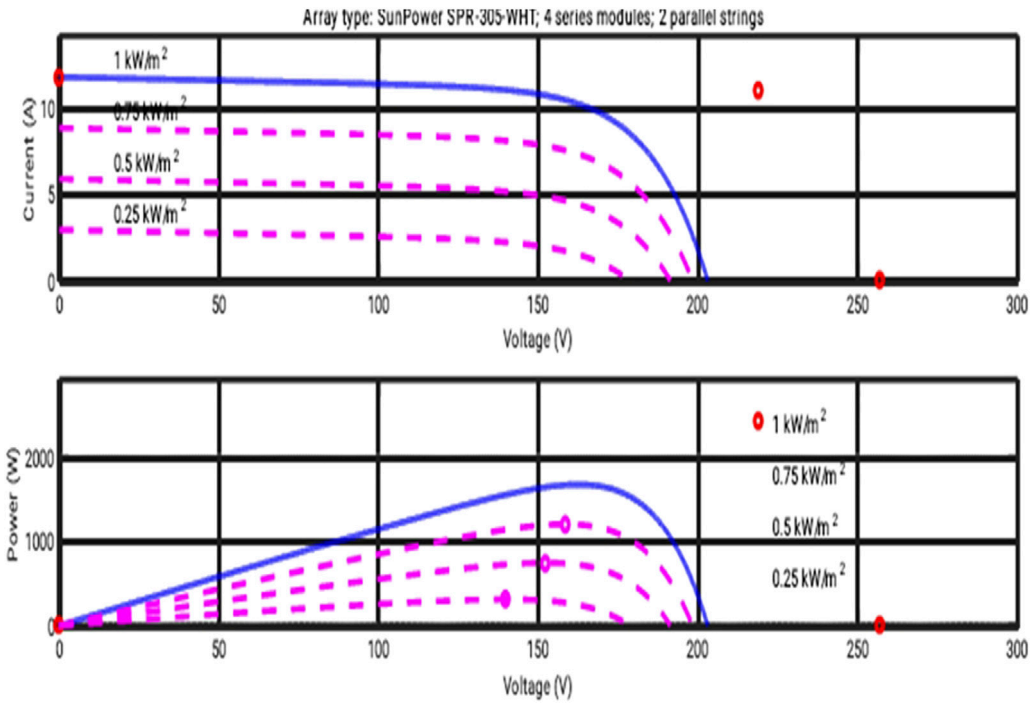

FIGURE 4
I-V and P-V characteristics.

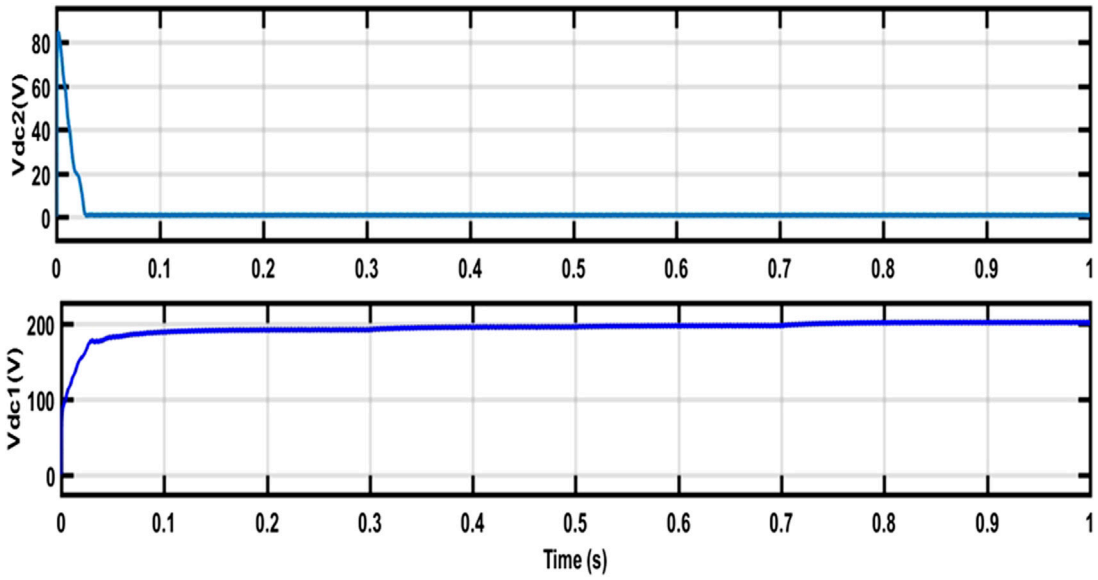

FIGURE 5
Capacitor voltage (vdc1 and vdc2).

for engineers and academics in optimizing solar energy consumption and system efficiency.

The function of capacitor voltages (Vdc1 and Vdc2) in energy storage and regulation in electrical circuits is demonstrated in Supplementary Figure S4. When shown visually, these voltages demonstrate the dynamic behavior of capacitors over time. Generally speaking, one capacitor's voltage is indicated by Vdc1, while another capacitor's voltage is indicated by Vdc2, usually when they are linked in series or parallel.

As the conditions of the circuit vary, capacitors charge and discharge, causing these voltage values to fluctuate. It is essential to comprehend capacitor voltage fluctuations to guarantee the stability,

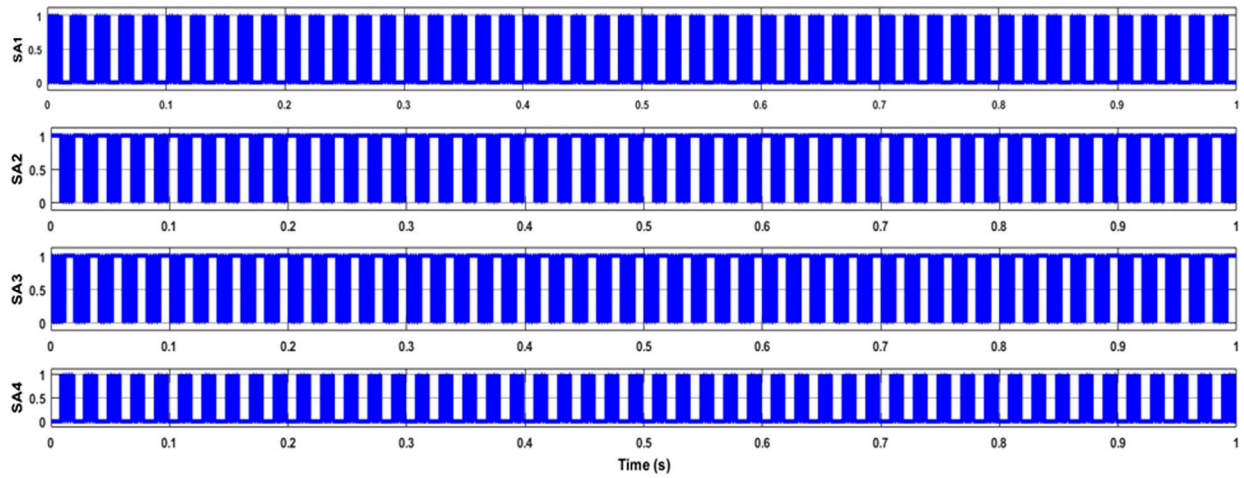

FIGURE 6
Pulses to the MPC phase A.

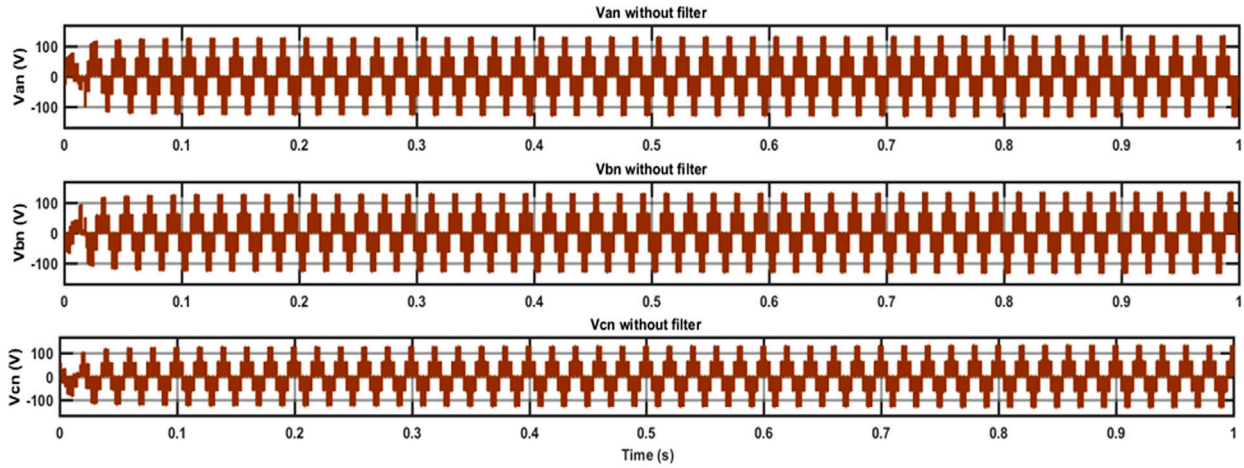

FIGURE 7
Phase Voltage without filter.

effectiveness, and appropriate operation of electronic systems. These voltage profiles are used by designers and engineers to maintain ideal operating conditions, avoid voltage spikes, and maximize circuit performance. Capacitor voltage visualization aids in the investigation, debugging, and optimization of electrical circuits, advancing a range of technologies from telecommunications to power electronics.

The revised SVPWM scheme for the MPC is validated through simulations using Vbat = 150 V. Figure 5 displays the switching sequence's steady-state waveforms. When Vbat is less than the rated voltage, the reference voltage vector Vref spins through S2, S3, S6, S5, and S6 in an anticlockwise manner. When Vbat = 150 V, it also rotates counterclockwise between S1 and S6. For instance, as Vref rotates around S6, the switching sequences are as follows: (l,l,0)→(h,l,0)→(h,l,l)→(h,h,l)→(h,l,l)→(h,l,0)→(l,l,0).
Moreover, it is observed that the halfway point of phase voltages, vxn, have been asymmetrically distributed in all other circumstances, except in those where the Vbat, is equal to half of the PV voltage.

The voltage and current waveforms with and without filters are shown in graphs 6 through 10. The system's phase and line voltages without the filter connected are displayed in Figures 6, 7, respectively. The phase and line voltage waveforms following the filter's connection are shown in Figures 8, 9, respectively. It is evident that once the filter is connected to the circuit, the ripple content is significantly decreased. After the filter is connected, the current waveform is seen in Figure 10.

By comparing the simulation results in different scenarios, the functioning of the suggested setup is tested. Pulse signal production for various instances is shown in Figure 11. In case 1, power control is handled only by the MPC; the DPPC is not used. It drains the battery to give the remaining power needed by the grid-side power because it operates on a buck cycle. This example has a lower PV

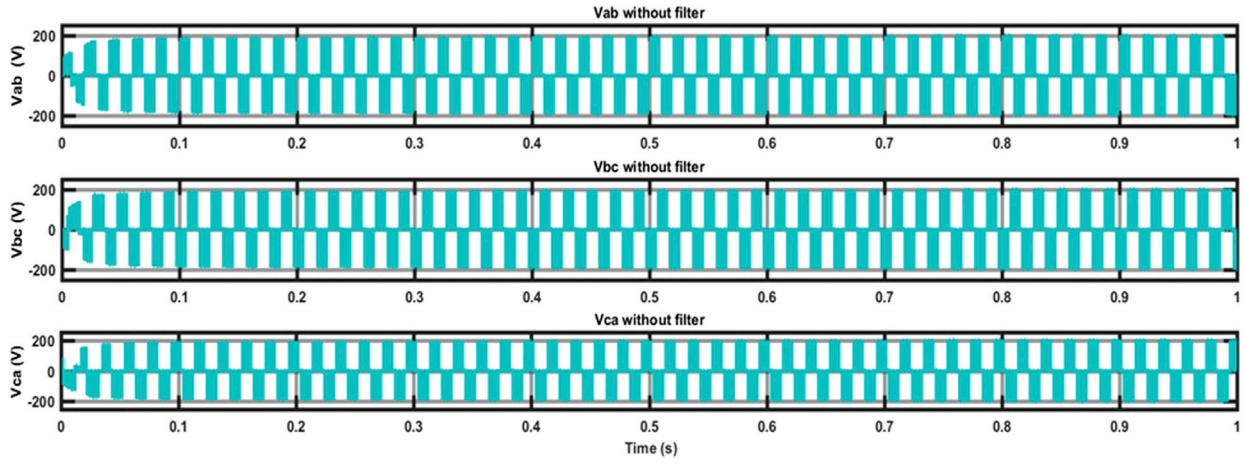

FIGURE 8
Line Voltage without filter.

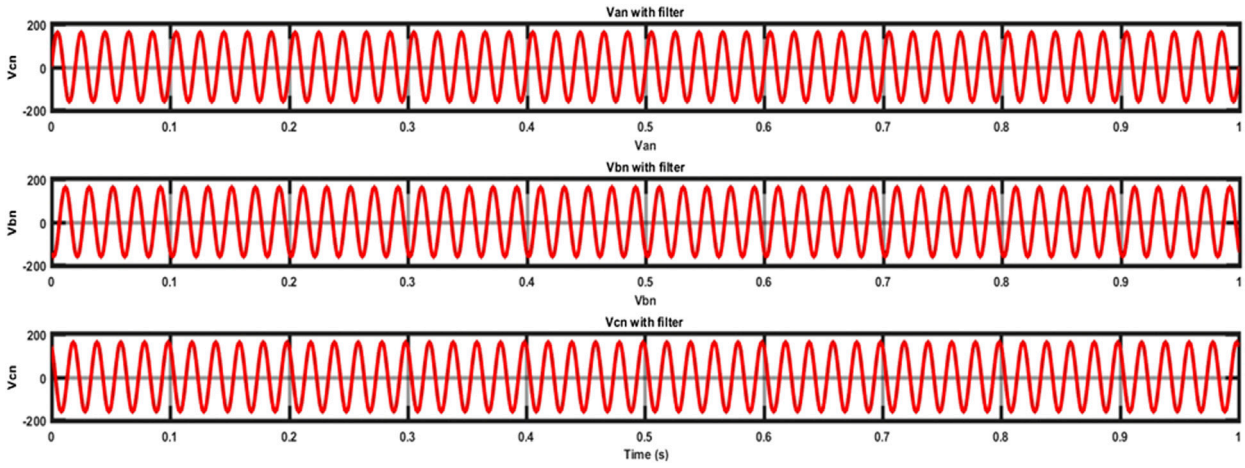

FIGURE 9
Phase Voltage with filter.

power output (Ppv) than grid-side power Battery charging or discharging is not required because photovoltaic (PV) energy supplies the ac grid with active power by matching grid-side power. In this instance, when PV power exceeds grid-side power, some of it is transferred to the ac grid and the rest is used to charge the battery. Within a certain Ppv range, it is evident that the MPC can accomplish active power regulation between the PV, battery, and ac grid.

Switch S1 on the DPPC goes on while switch S2 stays off in the following example, demonstrating how the DPPC enters the buck mode of operation when Ppv reaches its maximum value. In this case, half of the PV power that charges the battery is processed by the DPPC and the other half by the MPC. The final conceivable state is reached when Ppv reaches zero. The DPPC is using boost mode in this instance, with switch S1 off and switch S2 on. In this case, the DPPC and the MPC each supply a percentage of the battery's active power to the ac grid. In conclusion, Figure 11 shows how the suggested configuration modifies the k value to offer appropriate performance in various scenarios depending on the fluctuating PV power.

In the following example, it is evident that the DPPC enters the buck mode of operation when Ppv reaches its maximum value, since switch S1 on the DPPC turns on while switch S2 remains off. The MPC processes a portion of the PV power used to charge the battery in this instance, while the DPPC processes the remaining portion. When Ppv is zero, that is the last case. In this instance, switch S1 is off and switch S2 is on, meaning that the DPPC is operating in boost mode. Both the DPPC and the MPC contribute a portion of the battery's active power to the ac grid in this instance. To summarize, the recommended arrangement based on changing PV power modifies the k value to give good performance in various conditions, as shown in Figure 11.

The solar input and battery system's current, voltage, and power waveforms are shown in Supplementary Figure S9. Figure 12 shows

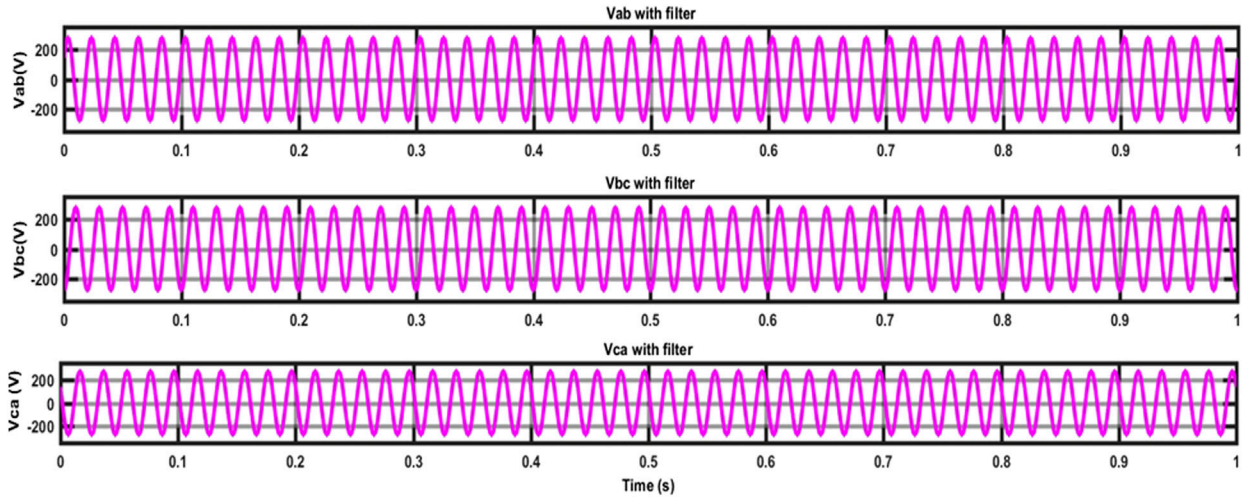

FIGURE 10
Line Voltage with filter.

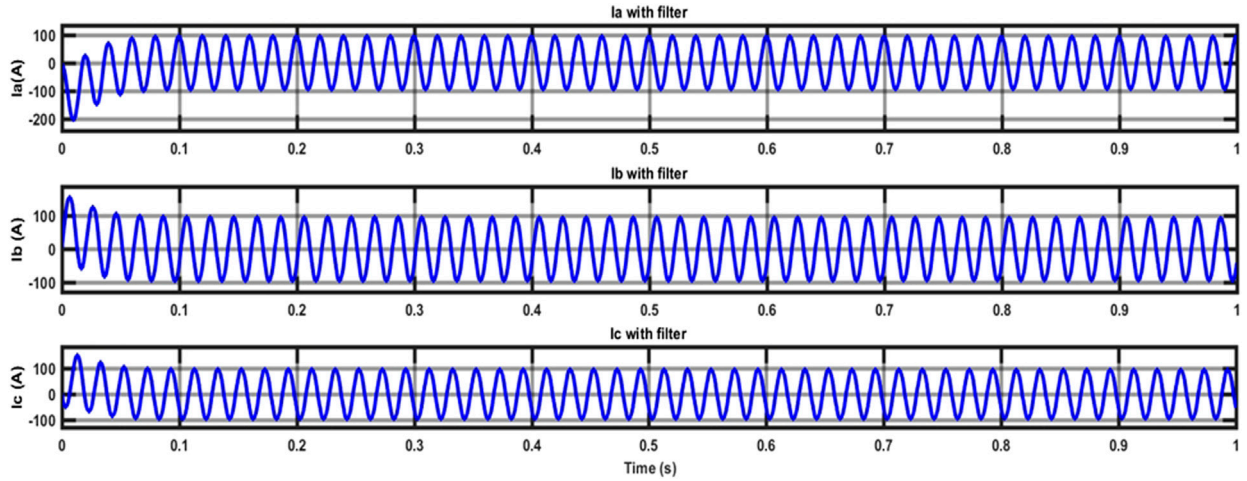

FIGURE 11
Line current with filter.

display the fluctuation of the k value and the solar irradiance curve. Figures 13A–C, 14 shows the source power, load power, and the system's overall efficiency in relation to each other. At the points k = 1 and k = 0, the proposed method offers a higher system efficiency. Efficiency is almost constant in the region where only MPC functions exist. Efficiency decreases as DPPC processes additional power outside of this range. Table 1 describes the comparison of different algorithms with proposed technique. The proposed IANFIS approach provided the better efficiency (99.45%) and minimum stability period (0.02s) and minimum distortion.

5 Conclusion

A reliable method for enhancing hybrid renewable power generation systems (HRPGS) is the Intelligent Adaptive Neuro-fuzzy based Control (IANFC) suggested for Multiport DC-AC converters with Differential Power Processing (DPP). This strategy provides a thorough framework for handling the challenges of integrating renewable energy sources and improving system performance by fusing cutting-edge converter technologies with sophisticated control approaches. The results of simulations and experimental validations demonstrate the efficacy of the proposed control system, underscoring its potential to significantly improve HRPGS's efficiency, adaptability, and stability. The proposed IANFIS approach provided the better efficiency (99.45%) and minimum stability period (0.02s) and minimum distortion loss. The IANFC guarantees effective power management and distribution by dynamically modifying converter operating points in real-time, hence making a positive impact on the energy landscape. Subsequent investigations pertaining to this study may concentrate on the realistic application of the

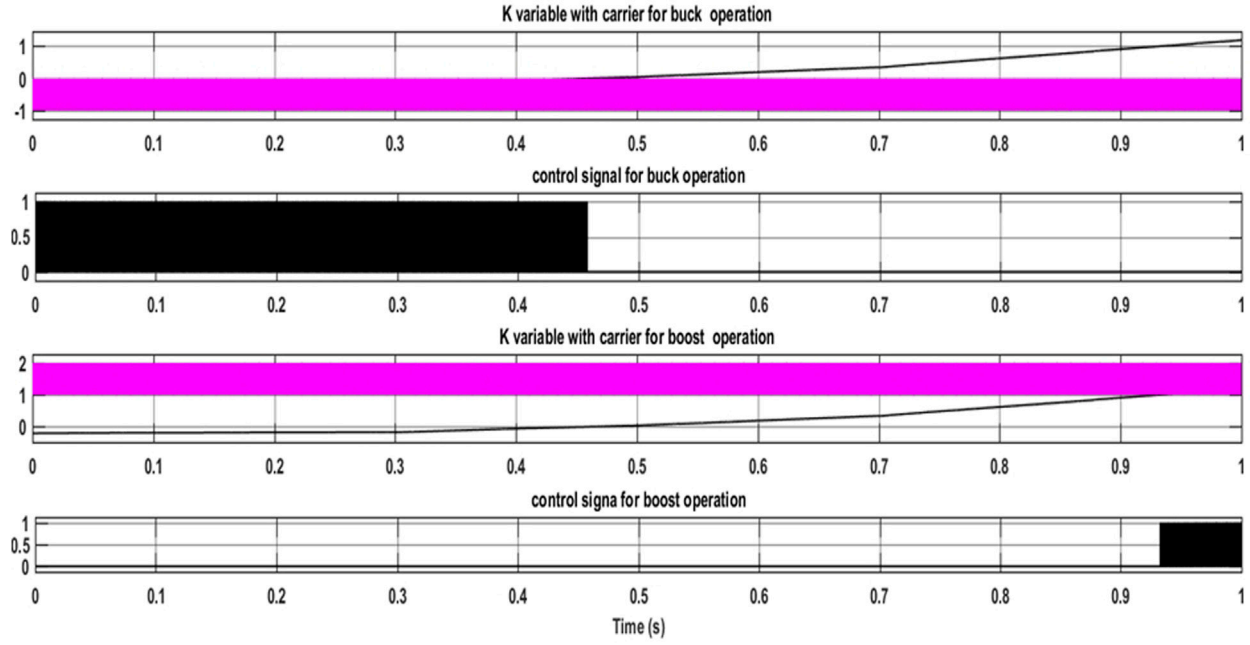

FIGURE 12
Pulse generation for buck and boost operation.

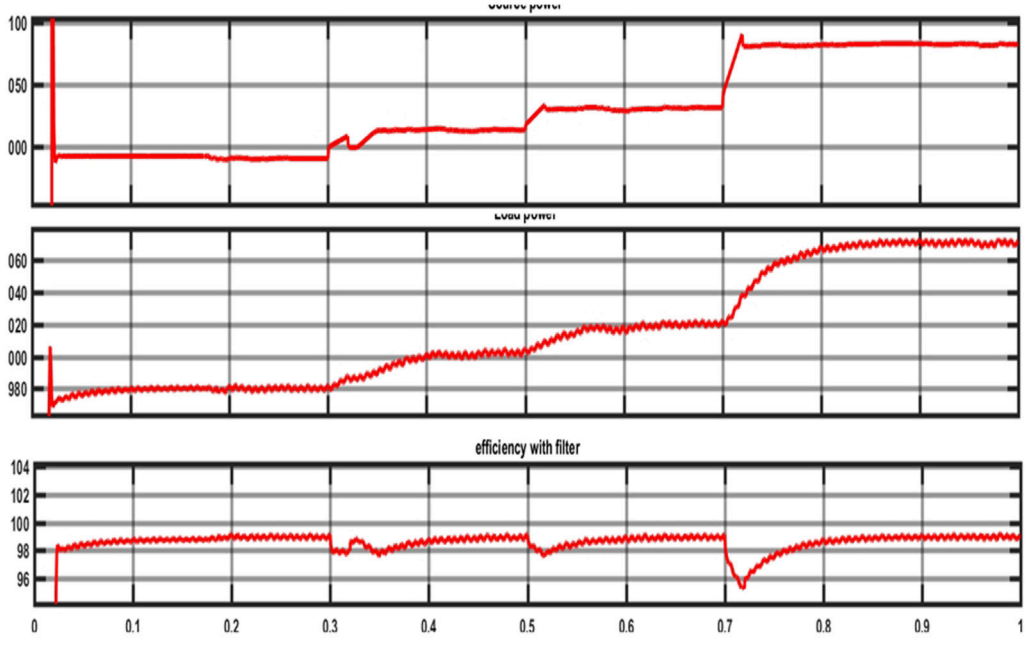

FIGURE 13
(A) Source power **(B)** load power **(C)** Efficiency.

suggested control system in actual HRPGS installations, permitting additional verification and improvement. Furthermore, continuous efforts to create optimization algorithms specific to HRPGS control systems may open up new possibilities for enhancing resource usage and system efficiency. Additionally, investigating sophisticated converter topologies and incorporating smart grid technologies have the potential to improve system resilience and make the grid integration of renewable energy sources easier. The goal of a future powered by HRPGS for greener, more sustainable energy

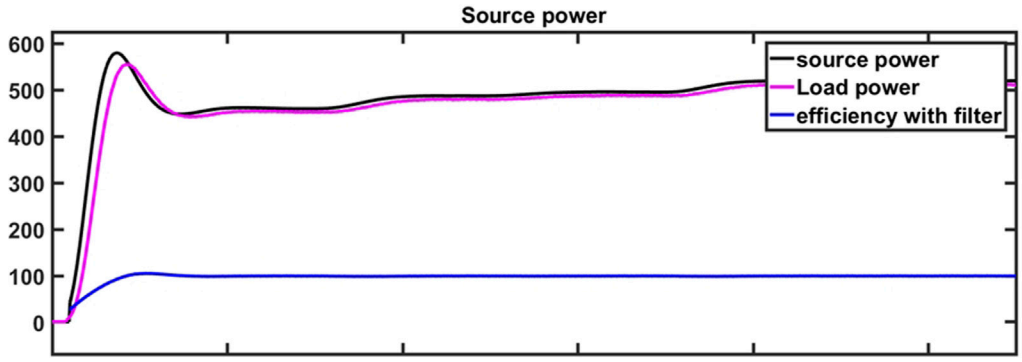

FIGURE 14
Output characteristics of proposed system.

TABLE 1 Performance analysis of proposed work with conventional algorithms.

Algorithms	Efficiency	Stability period	Distortion loss	Complexity in design
Adaptive SAR	93.6%	0.28s	High	High
GA	95.4%	0.21s	Moderate	Moderate
ANN	96.8%	0.15s	Moderate	Moderate
Conventional ANFIS	97.3%	0.09s	LOW	Less
Proposed IANFIS	99.45%	0.02s	LOW	Less

can be achieved by carrying out more innovation and advancement in these fields.

Data availability statement

The original contributions presented in the study are included in the article/Supplementary Material, further inquiries can be directed to the corresponding author.

Author contributions

SS: Conceptualization, Data curation, Investigation, Methodology, Validation, Writing–original draft, Writing–review and editing. AS: Supervision, Validation, Writing–review and editing.

Funding

The author(s) declare that no financial support was received for the research, authorship, and/or publication of this article.

Conflict of interest

The authors declare that the research was conducted in the absence of any commercial or financial relationships that could be construed as a potential conflict of interest.

Publisher's note

All claims expressed in this article are solely those of the authors and do not necessarily represent those of their affiliated organizations, or those of the publisher, the editors and the reviewers. Any product that may be evaluated in this article, or claim that may be made by its manufacturer, is not guaranteed or endorsed by the publisher.

Supplementary material

The Supplementary Material for this article can be found online at: https://www.frontiersin.org/articles/10.3389/fenrg.2024.1471265/full#supplementary-material

References

Ajami, A., and Shayan, P. A. (2015). Soft-switching method for multiport DC/DC converters applicable in grid-connected clean energy sources. *IET Power Electron.* 8 (7), 1246–1254. doi:10.1049/iet-pel.2014.0592

Alargt, F. S., Ashur, A. S., and Kharaz, A. H. (2019a). "Parallel interleaved multi-input DC-DC converter for hybrid renewable energy systems," in *54th international universities power engineering conference (UPEC)*. Bucharest, Romania, 1–5.

Alargt, F. S., Ashur, A. S., and Kharaz, A. H. (2019b). "Analysis, simulation, and comparison of multi-module interleaved DC-DC converter for hybrid renewable energy systems," in *54th international universities power engineering conference (UPEC)*. Bucharest, Romania, 1–6.

Arani, A. K., Gharehpetian, G., and Abedi, M. (2019). Review on energy storage systems control methods in microgrids. *Int. J. Electr. Power Energy Syst.* 107, 745–757. doi:10.1016/j.ijepes.2018.12.040

Benavides, N. D., and Chapman, P. L. (2005). Power Budgeting of a multiple-input buck-boost converter. *IEEE Trans. Power Electron.* 20 (No.6), 1303–1309. doi:10.1109/tpel.2005.857531

Bhattacharjee, A. K., Kutkut, N., and Batarseh, I. (2018). Review of multiport converters for solar and energy storage integration. *IEEE Trans. Power Electron.* 34, 1431–1445. doi:10.1109/tpel.2018.2830788

Boonluk, P., Siritaratiwat, A., Fuangfoo, P., and Khunkitti, S. (2020). Optimal siting and sizing of battery energy storage systems for distribution network of distribution system operators. *Batteries* 6 (4), 56. doi:10.3390/batteries6040056

Chakraborty, S., Simões, M. G., and Kramer, W. E. (2015). *Power electronics for renewable and distributed energy systems*. Berlin, Germany: Springer, 1–620.

Chu, G., Wen, H., Jiang, L., Hu, Y., and Li, X. (2017). Bidirectional flyback based isolated-port submodule differential power processing optimizer for photovoltaic applications. *Sol. Energy* 158, 929–940. doi:10.1016/j.solener.2017.10.053

Chu, G., Wen, H., Yang, Y., and Wang, Y. (2019). Elimination of photovoltaic mismatching with improved submodule differential power processing. *IEEE Trans. Industrial Electron.* 67, 2822–2833. doi:10.1109/tie.2019.2908612

Dobbs, B. G., and Chapman, P. L. (2003). A multiple-input DC-DC converter topology. *IEEE Power Electron. Lett.* 1 (No.1), 6–9. doi:10.1109/lpel.2003.813481

Elkeiy, M. A., Abdelaziz, Y. N., Hamad, M. S., Abdel-Khalik, A. S., and Abdelrahem, M. (2023). Multiport DC-DC converter with differential power processing for fast EV charging stations. *Sustainability* 15 (4), 3026. doi:10.3390/su15043026

Faraji, R., and Farzanehfard, H. (2020). "Fully soft switched multi-port DC-DC converter with high integration," in *IEEETransactions on power electronics*.

Gunasekaran, V., and Chakraborty, S. (2023). Technical and environmental aspects of solar photo-voltaic water pumping systems: a comprehensive survey. *Water Supply* 23 (7), 2676–2710. doi:10.2166/ws.2023.165

Iannone, F., Leva, S., and Zaninelli, D. (2005). "Hybrid photovoltaic and hybrid photovoltaic-fuel cell system: economic and environmental analysis," in *Proceedings of the IEEE power engineering society general meeting* (San Francisco, CA, USA), 1503–1509.

Jiang, W., and Fahimi, B. (2011). Multiport power electronic interface—concept, modeling, and design. *IEEE Trans. Power Electron.* 26 (7), 1890–1900. doi:10.1109/tpel.2010.2093583

Krishnaswami, H., and Mohan, N. (2009). Three-port series-resonant DC-DC converter to interface renewable energy sources with bidirectional load and energy storage ports. *IEEE Trans. Power Electron.* 24 (No.10), 2289–2297. doi:10.1109/tpel.2009.2022756

Madhana, R., and Geetha, M. (2022). Power enhancement methods of renewable energy resources using multiport DC-DC converter: a technical review. *Sustain. Comput. Inf. Syst.* 35, 100689. doi:10.1016/j.suscom.2022.100689

Madhana, R., and Mani, G. (2022). Design and analysis of the multi-port converter based power enhancement for an integrated power generation system using predictive energy amendment algorithm. *Front. Energy Res.* 10, 1000242. doi:10.3389/fenrg.2022.1000242

Matsuo, H., Lin, W., Kurokawa, F., Shigemizu, T., and Watanabe, N. (2004). Characteristics of the multiple-input DC-DC converter. *IEEE Trans. Industrial Electron.* 51 (3), 625–631. doi:10.1109/tie.2004.825362

Mihai, M. (2015). "Multiport converters - a brief review," in *7th international conference on electronics, computers and artificial intelligence (ECAI)*, 27–30.

Perera, C., Salmon, J., and Kish, G. J. (2021). Multiport converter with enhanced port utilization using multitasking dual inverters. *IEEE Open J. Power Electron.* 2, 511–522. doi:10.1109/ojpel.2021.3109098

Pompern, N., Premrudeepreechacharn, S., Siritaratiwat, A., and Khunkitti, S. (2023). Optimal placement and capacity of battery energy storage system in distribution networks integrated with pv and evs using metaheuristic algorithms. *IEEE Access* 11, 68379–68394. doi:10.1109/access.2023.3291590

R, M., and Mani, G. (2023). A novel assimilate power flow control technique based multi port converter for hybrid power generation system with grid connected application. *Authorea Prepr.* doi:10.22541/au.167710239.95236779/v1

Savitha, K. P., and Kanakasabapathy, P. (2016). "Multi-port DC-DC converter for DC microgrid applications," in *IEEE 6th international conference on power systems (ICPS)-New Delhi*, 1–6.

Shanmugam, S., and Sharmila, A. (2022). Multiport converters for incorporating solar photovoltaic system with battery storage: a pilot survey towards modern influences, challenges and future scenarios. *Front. Energy Res.* 10, 947424. doi:10.3389/fenrg.2022.947424

Tao, H., Duarte, J. L., and Hendrix, M. A. M. (2008). Three-port triple-half-bridge bidirectional converter with zero-voltage switching. *IEEE Trans. Power Electron.* 23 (2), 782–792. doi:10.1109/tpel.2007.915023

Tao, H., Kotsopoulos, A., Duarte, J. L., and Hendrix, M. A. M. (2005). Multi-input bidirectional DC-DC converter combining DC-link and magnetic-coupling for fuel cell systems. *Fourtieth IAS Annu. Meet. Conf. Rec. Industry Appl. Conf.* 3, 2021–2028. doi:10.1109/ias.2005.1518725

Uno, M., and Shinohara, T. (2019). Module-integrated converter based on cascaded quasi-Z-source inverter with differential power processing capability for photovoltaic panels under partial shading. *IEEE Trans. Power Electron.* 34, 11553–11565. doi:10.1109/tpel.2019.2906259

Wang, J., Sun, K., Xue, C., Liu, T., and Li, Y. (2021). Multi-port DC-AC converter with differential power processing DC-DC converter and flexible power control for battery ESS integrated PV systems. *IEEE Trans. Industrial Electron.* 69 (5), 4879–4889. doi:10.1109/tie.2021.3080198

Wichitkrailat, K., Premrudeepreechacharn, S., Siritaratiwat, A., and Khunkitti, S. (2024). Optimal sizing and locations of multiple BESSs in distribution systems using crayfish optimization algorithm. *IEEE Access* 12, 94733–94752. doi:10.1109/access.2024.3425963

Wu, H., Xing, Y., Xia, Y., and Sun, K. (2011). "A family of non-isolated three-port converters for the stand-alone renewable power system," in *IECON 37th annual conference of the*. Melbourne: IEEE Industrial Electronics Society, 1030–1035.

Wu, H., Xu, P., Hu, H., Zhou, Z., and Xing, Y. (2014). Multiport converters based on integration of full-bridge and bidirectional DC-DC topologies for renewable generation systems. *IEEE Trans. Industrial Electron.* 61 (2), 856–869. doi:10.1109/tie.2013.2254096

Wu, H., Zhang, J., and Xing, Y. (2015). A family of multiport buck-boost converters based on DC-link-inductors (DLIs). *IEEE Trans. Power Electron.* 30 (No.2), 735–746. doi:10.1109/tpel.2014.2307883

Zeng, J., Qiao, W., and Qu, L. (2014). An isolated multiport bidirectional DC-DC converter for PV-battery-DC microgrid applications. *IEEE Energy Convers. Congr. Expo. (ECCE)*, 4978–4984. doi:10.1109/ecce.2014.6954084

Zeng, J., Qiao, W., and Qu, L. (2013). An isolated three-port bidirectional DC-DC converter for photovoltaic systems with energy storage. *IEEE Ind. Appl. Soc. Annu. Meet.*, 1–8. doi:10.1109/ias.2013.6682520

Zhang, N., Sutanto, D., and Muttaqi, K. M. (2016). A review of topologies of three-port DC-DC converters for the integration of renewable energy and energy storage system. *Renew. Sustain. Energy Rev.* 56, 388–401. doi:10.1016/j.rser.2015.11.079

frontiers | Frontiers in Energy Research

TYPE Review
PUBLISHED 03 January 2025
DOI 10.3389/fenrg.2024.1417453

OPEN ACCESS

EDITED BY
Michael Carbajales-Dale,
Clemson University, United States

REVIEWED BY
Moses Omolayo Petinrin,
University of Ibadan, Nigeria
Debabrata Barik,
Karpagam Academy of Higher Education, India

*CORRESPONDENCE
Sunday O. Oyedepo,
sooyedepo@bellsuniversity.edu.ng

RECEIVED 14 April 2024
ACCEPTED 25 October 2024
PUBLISHED 03 January 2025

CITATION
Oyedepo SO, Waheed MA, Abam FI, Dirisu JO, Samuel OD, Ajayi OO, Somorin T, Popoola API, Kilanko O and Babalola PO (2025) A critical review on enhancement and sustainability of energy systems: perspectives on thermo-economic and thermo-environmental analysis.
Front. Energy Res. 12:1417453.
doi: 10.3389/fenrg.2024.1417453

A critical review on enhancement and sustainability of energy systems: perspectives on thermo-economic and thermo-environmental analysis

Sunday O. Oyedepo[1]*, Mufutau A. Waheed[2], Fidelis I. Abam[3], Joseph O. Dirisu[4], Olusegun D. Samuel[5,6], Oluseyi O. Ajayi[4], Tosin Somorin[7], Abimbola P. I. Popoola[8], Oluwaseun Kilanko[4] and Philip O. Babalola[4]

[1]Department of Mechanical/Biomedical Engineering, Bells University of Technology, Ota, Nigeria, [2]Department of Mechanical Engineering, Federal University of Agriculture, Abeokuta, Nigeria, [3]Department of Mechanical Engineering, University of Calabar, Calabar, Nigeria, [4]Department of Mechanical Engineering, Covenant University, Ota, Nigeria, [5]Department of Mechanical Engineering, Federal University of Petroleum Resources, Effurun, Nigeria, [6]Department of Mechanical Engineering, University of South Africa, Science Campus, Florida, South Africa, [7]Department of Chemical Engineering, University of Strathclyde, Glasgow, United Kingdom, [8]Department of Chemical and Metallurgical Engineering, Tshwane University of Technology, Pretoria, South Africa

Given the increased natural resource consumption of contemporary energy conversion systems, as well as the emissions, waste disposal, and climate changes that accompany them, a critical review of new techniques - known as thermo-economic and thermo-environmental analyses - has been carried out for the evaluation and optimization of energy conversion processes, from the perspectives of thermodynamics, economics, and the environment. Such a review study is essential because of the energy system's impacts on sustainability and performance management requirements, and more importantly, it is crucial to understand the whole picture of performance evaluation of energy systems from the sustainability perspective. The study evaluated the performance and optimization of energy systems and examined the different approaches that integrate the economic, environmental, and second law of thermodynamics for sustainable development. Moreover, to assess the technical, economic, and environmental worth of energy systems and guarantee that the chosen designs are well-suited to a sustainable development framework, a mix of thermodynamic, economic, and environmental indicators is taken into consideration. In this regard, thirteen sustainability indicators for the design, analysis, and performance improvement of energy systems from the viewpoints of thermodynamics, economics, and the environment are presented and discussed. The outcome of this study shows that (i) the sustainability of energy conversion systems can be enhanced with the use of exergy techniques assessment; (ii) by reducing energy losses, exergy efficiency initiatives can lessen their adverse effects on the environment; (iii) the best methods for efficient use of energy resources, low energy production costs, and less environmental impact can be provided by hybrid energy systems; and (iv) use of a single performance metric to

optimize the energy process results in improbable outcomes. Hence, multi-criteria techniques should be utilized, allowing for a more comprehensive optimization and planning of sustainable energy systems. Researchers and field engineers working on energy systems' design, modeling, assessment, and performance optimization would find great value in this comprehensive review study.

KEYWORDS

thermodynamics, sustainability indices, thermo-economic, thermoenvironmental, energy systems, sustainable development

1 Introduction

Today, scientists and engineers are developing new technologies and more effective energy-harvesting systems to maximize the use of available energy resources. Because of this, studying and improving energy conversion systems is important from a scientific standpoint and is also necessary for the effective use of available energy resources (Oyedepo, 2014a). Any country's ability to grow economically depends on its supply of energy. Social developments impact the energy system in various ways, but society is also affected by the energy system (Oyedepo, 2014b). The production and availability of energy significantly influence global economic and political development. A strong energy sector is essential for success in other socioeconomic domains. The link between natural resource availability and security for energy consumption is known as energy security. These days, having access to economically priced energy is crucial to the functioning of modern economies. The attainment of the Sustainable Development Goals (SDGs) is contingent upon every individual having access to modern, adequate, and efficient energy (Bishoge et al., 2020). Since then, a vast array of technical applications for energy have been created, making energy availability a crucial concern for civilization (Huggins, 2016).

Sustainable development has recently been recognised as the utmost task of this new age (Annamalai et al., 2018). The latter leads to several transnational consequences, particularly environmental contamination, climate change, reduction of natural deposits, natural decimation, and international injustice (Akbari et al., 2020). Human activities have added undesirably to sustainable growth. Additionally, it is known that a transformation to economic sustainability requires substantial variations in energy demands and resources (Mulvihill et al., 2011). However, in recent times, the lack of adequate energy supply and limited capital, followed by efforts to alleviate the hazard posed by contamination of the environment, has resulted in the growth of feasible engineering science (Das et al., 2019).

The prime objective of sustainable technology is to attain economic feasibility for scenic surroundings. Sustainable technology has a principal goal in environmental disciplines and the development of worldwide economies, generally linked alongside the design layout and breakdown of multifaceted, unified energy processes and economic sustainability. Lessening material and energy supply and minimising misuse is a significant environmental objective (Srebrenkoska et al., 2013). Sustainable energy is necessary for any strategies for global sustainability due to (i) the generality of energy usage, (ii) its demand in economic growth and standards of living, and (iii) the significant effects of energy processes and systems on the environment and its continued influence (Oyedepo, 2012). Increasing environmental issues and limited available non-renewable conventional energy resources have engendered new impulses in modern sustainable energy technologies. This is because resources for energy and their utilisation closely have to do with sustainable developments. The development of cleaner energy systems is one of the significant advances of this advanced century. Most forecasts demonstrate that combustion type of energy conversion systems remains the prime method for most energy consumption (Lieuwen and Yang, 2013). Hence, to accomplish sustainable progress, it is crucial to increase the efficiencies of energy processes that utilize sustainable energy (Hepbasli, 2008).

In the next 20 years, energy use worldwide is projected to rise considerably worldwide, with developing countries having the highest growth rates. Fossil fuels are anticipated to deliver a big part of the world's energy, up to 75% of overall energy utilization in 2040 (Rao, 2015). Following the massive expansion in petroleum derivative use around the world, the ozone-depleting substance CO_2 emanations to the environment are relied upon to increment by an average yearly development of 1.29% within the range of the years 2010–2040 or by as far as 45.8% by 2040 from 2010. Notwithstanding this ozone-harming substance, the tackling of the energy trapped inside a fuel by incineration generates contaminations like oxides of sulphur, nitrogen, and partly combusted fossil fuels that are brought into the air, the quantity dependent upon the effectiveness and efficiency of the technology utilized for transformation. A challenge emanates between raising the quality of life (assessed by gross national product *per capita*), and energy use *per capita* that can directly influence the surroundings provided sustainable energy conversion systems and operations are followed up.

Research in generating alternative energy sources has made more energy available to consumers. Different equipment and processes convert energy into different forms, as shown in Table 1. An IC engine converts the chemical energy from gasoline into heat, which in turn creates mechanical energy that moves a vehicle. The energy passes through a device that converts it, which produces another energy source. The output energy is always less than the input energy. However, the quantity of energy is conserved (Demirel, 2012). Figure 1 depicts a representation of the energy use and its conversion process.

The different forms of energy are grouped into three general categories: (i) primary energy (hydropower, fossil fuel, hydraulic energy, wind energy and solar energy), (ii) secondary energy (gasoline, diesel, and kerosene. Others are, ethanol fuel and biodiesel derived from biomass, thermal energy from solar collectors, and

TABLE 1 Processes/devices for energy conversion (Demirel, 2012).

Process and device	Energy input	Suitable energy output
Fuel Cell	Chemical Energy	Energy by electricity
Photosynthesis	Solar Energy	Energy by electricity
Electric Bulb	Electrical Energy	Heat and Light
Thermoelectric	Heat	Energy by electricity
Piezoelectric	Strain	Energy by electricity
Battery	Chemical Energy	Energy by electricity
Solar Cell	Solar Energy	Energy by electricity

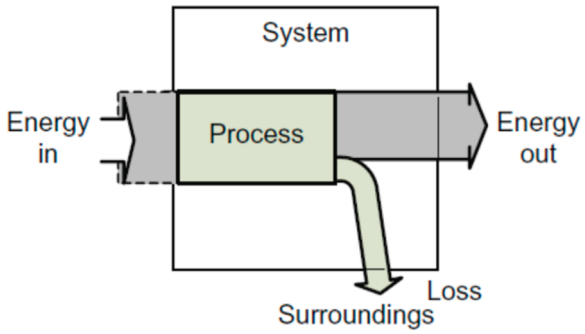

FIGURE 1
Diagram of energy use and its conversion process (Demirel, 2012).

district heating from geothermal fluids), (iii) tertiary energy (electric energy, nuclear energy, gas, coal, and most of the different renewable energy source of energy, which are categorised as primary energy sources, contribute to the supply of tertiary energy when they are used to produce electricity). The processing and transformations that produce secondary and tertiary energy forms always involve energy losses, which are often significant for tertiary energy (Khartchenko and Kharchenko, 2014). The first two laws of thermodynamics control the energy dissipation during such transformations. The efficiency of the transformation process indicates how well the primary resource's original energy can be converted to the secondary form (Michaelides, 2018).

Thermal efficiencies of energy transformation are typically far less than 100% because of inefficiencies caused by friction, heat loss, and other factors. For example, in a steam power station, only 35%–40% of the thermal energy can be transformed into electrical current. A typical gasoline automobile engine operates at about 25% efficiency. Energy is always conserved, according to the first law of thermodynamics. But some of the energy that was initially available is lost during energy transformations as waste heat that is not needed or used by human society.

Due to different energy conversion technologies based on differences in economic and environmental factors, energy utilization should be guided by principles whose validity has been proven beyond doubt (Giovanni, 2014). Hence, analysis and optimisation of energy systems are logical and vital for humanity from the socio-economic and environmental points of view.

Furthermore, the past 2 decades have witnessed tremendous transformation in energy technology, now a focal field for research and development studies. Extensive studies were carried out in energy system research to optimize energy conversion efficiency and advance the technologies that promote other energy sources. The main objective of such studies was to determine the degradation effect of exergy resources. To complement this drive, the research area of thermo-economic and thermo-environmental involves combining thermodynamic, economic and environmental issues in design, assessment and enhanced optimal performance of energy conversion systems and industrial process efficiencies without jeopardizing an energy system's financial feasibility. The resulting improvement in efficiency has further decreased environmental impact due to improved system efficiency (von Spakovsky and Frangopoulos, 2011).

The sustainable utilization of energy is inherently connected to the systems' effectiveness in transforming crude materials into useful products. The technology of these energy converters straightforwardly impacts the value and amount of their energy consumption, services, and the effluent dispersed to the atmosphere. In this regard, the consumption of sources of fuel, paying little mind to fossil fuel or the supposed renewable energy, should be led by utilizing an effective conversion system during its final use as well as in the entire process of energy transformation measures starting from the fuel source, through the energy conversion process till the waste disposal stage. Assessing each stage of energy usage is imperative in determining the extent of energy quality (de Oliveira, 2013).

In view of the above, the energy conversion system is recognised as a device that consumes fuel and other scarce natural resources. Consequently, it has an adverse effect on the atmosphere in the course of operation. Hence, the study on assessing and optimising energy systems must consider sustainability matters quantifiably. Accordingly, this paper focuses on the critical review of the enhancement and sustainability of energy systems from thermodynamic, thermo-economic and thermo-environmental perspectives, considering selected performance indicators as signposts of sustainability for energy conversion systems.

2 Thermodynamics assessment of energy conversion systems

Thermodynamics plays a vital role in dissecting frameworks and equipment where energy transformation occurs. Thermodynamics' significance is across the board of human initiative (Dincer and Cengel, 2001). Thermodynamics science follows two central natural laws, the first and second (Oyedepo, 2014a). The thermodynamic first law emphasizes that energy as a thermodynamic property interacts and can transform from state to state. However, the energy is conserved. The first law is conventionally used to analyze energy consumption and plant operation. Unfortunately, it does not consider the energy quality, which is now remedied by the second law of thermodynamics. The thermodynamic second law affirms

that energy has quantity and quality and that real processes exist in the path of reducing the quality of energy called exergy.

The energy system is designed to provide energy services to consumers by continuously evaluating its exergy performance (Granet and Bluestein, 2000). Exergy studies have been used to extract the maximum amount of useful work or performance of an operation as it moves from one equilibrium state to another (Ahmadi et al., 2011a). It is also considered the elementary notion by which the thermodynamic cycle is modelled and analyzed by the applications of the laws of thermodynamics (Zare and Hasanzadeh, 2016). Moreover, it thoroughly analyzed energy systems' efficiencies, optimal performance and irreversibility sources (Saidur et al., 2007).

Surprisingly, the various means of generating and supplying power are unsustainable and costly, leading to an upsurge in energy demand; if appropriate actions are not taken, this increase in energy demand will be truncated with more energy waste, resulting in environmental pollution. Therefore, if carried out sustainably, increased energy demand, efficient energy systems, improved technologies, and environmental preservation dictate improvement in a nation's industrial development (Saidur et al., 2010).

2.1 Analysis of energy and exergy of an energy systems

Presently, humankind faces incredible economic, environmental, and energy difficulties. A solid essential exists to more readily configure, investigate, evaluate and enhance energy measures, systems and utilization (Dincer et al., 2014). Accordingly, energy and exergy analysis are the two essential tools for designing and optimising energy systems to use effectively resource-constrained fossil fuels (Oyedepo et al., 2018). Researchers have delved into using exergy analysis to overcome the shortcomings of the first and foremost law of thermodynamics.

Moreover, studies reveal a correlation between sustainable development and exergy. Both will establish that the energy system is cost-effective, steady and non-threat to the environment. Hence, exergy analysis is broadly employed in the design of our energy equipment (Hepbasli, 2008). The exergy idea is dependent on the first two thermodynamic laws. Exergy assessment shows the positions of energy deterioration in a procedure and can result in enhanced technology. Exergy analysis mainly detects energy losses in a system and the magnitude of such loss. It also identifies energy efficiency to optimize the system (Zare, 2020).

With the exergy analysis concept, it is possible to gauge energy transformation operation processes on a thermodynamics aspect and the eco-environmental impact of the process in the study. This inclusive approach to energy conversion is essential for sustainable energy resource utilization (de Oliveira, 2013). Exergy methods can help improve the sustainability of energy systems. Studies have indicated that enhancing the exergy efficiency of energy systems can reduce environmental impacts by cutting down on energy wastage (Oyedepo, 2014a; Rao, 2015; Ahmadi et al., 2011a; Zare and Hasanzadeh, 2016). A measure to assess the relationship between exergy efficiency and environmental sustainability is the Exergetic Sustainability Index (ESI). This indicator helps to determine the capacity and effective utilization and preservation of energy resources (Dincer et al., 2014; Oyedepo et al., 2018; Rosen, 2021). Figure 2 illustrates this qualitatively by demonstrating how, as exergy efficiency increases, sustainability increases and environmental impact decreases. Exergy efficiency becomes closer to 100%, sustainability approaches infinity since the process approaches reversibility, while environmental impact approaches zero because exergy is converted from one form to another without any loss. Exergy efficiency approaches 0% since exergy resources are used to accomplish nothing, hence, sustainability approaches zero. On the other hand, environmental impact approaches infinity because increasing resources must be used and increasing exergy wastes are emitted for a fixed service (Rosen, 2021).

Environmental pollution from fossil fuels has led to numerous studies on energy-efficient conversion and eco-friendly renewable energy sources (Rosen, 2021). An energy-efficient system assures sustainable development. A deliberate improved system as a function of exergy analysis will usher in reliability, sustainability and cost-effectiveness (Hepbasli, 2008). A correlation exists among exergy analysis, sustainable development, and ecological and environmental management (Rosen, 2009). The analysis of exergy aids in projecting thermodynamics into ecological and environmental impact on devices in consideration. The essence of exergy analysis investigates the useful energy that does work on the system. It looks into the primary source of irreversibility in the cycle and improves it to prevent exergy destruction.

Another essential feature of the second law of thermodynamic (exergy) concept is its capability to be integrated with economic and environmental constraints. These integrated methods, called "thermo-economic and thermo-environmental" approaches, are powerful tools to identify, quantify, and interpret economic losses and environmental burdens of energy systems at the component level. Precisely, the thermo-economic method can effectively address the shortcomings of techno-economic analysis by accounting for thermodynamic losses (Al-Qayim, 2019). In addition, the thermo-environmental method can reliably cope with the drawbacks of Life Cycle Assessment (LCA) analysis in the sustainability assessment of energy systems by allocating the environmental burdens at the component level and measuring the environmental burdens of intermediate products. This unique combination of exergy, economy, and environment can reliably assess the thermodynamic productivity, economic viability, environmental safety, and overall sustainability of energy and material conversion processes (Figure 3) (Aghbashlo et al., 2022).

Additionally, numerous studies on the exergy assessment of energy operations have been carried out to study the variability of energy systems for power generation or industrial processes. Among the explored studies are gas turbines (Rosen, 2021; Aghbashlo et al., 2022), steam power plants, combined cycle power plants, refrigeration systems, ORC and Kalina cycles, wind energy and solar energy systems, among others (Ahmadi et al., 2011a; Saidur et al., 2010; Rosen, 2021; Aghbashlo et al., 2022; Waheed et al., 2018).

2.1.1 Gas turbine engine

The demand for gas turbine engines is increasing due to their low cost, high flexibility, high reliability without complexity, short delivery time, and fast starting and loading but low efficiency. Several analyses have therefore been conducted to improve the low thermal efficiency in Simple Gas Turbine (SGT) (Rosen, 2009). In recent times, efforts to improve the power generation efficiency of SGTs

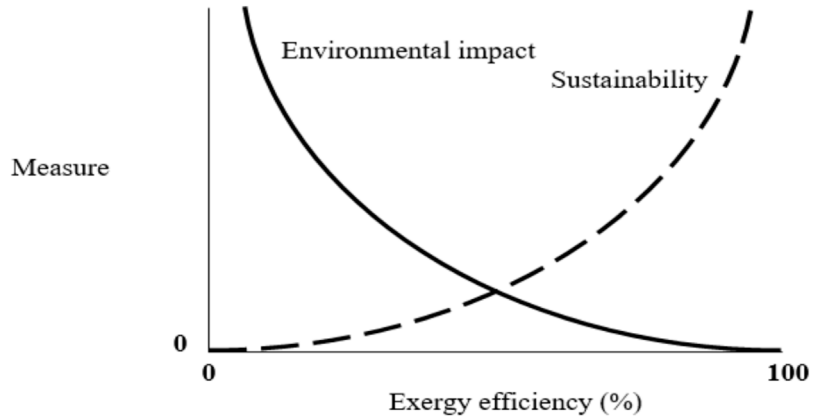

FIGURE 2
Qualitative depiction of relation of environmental impact and sustainability with exergy efficiency (Rosen, 2021).

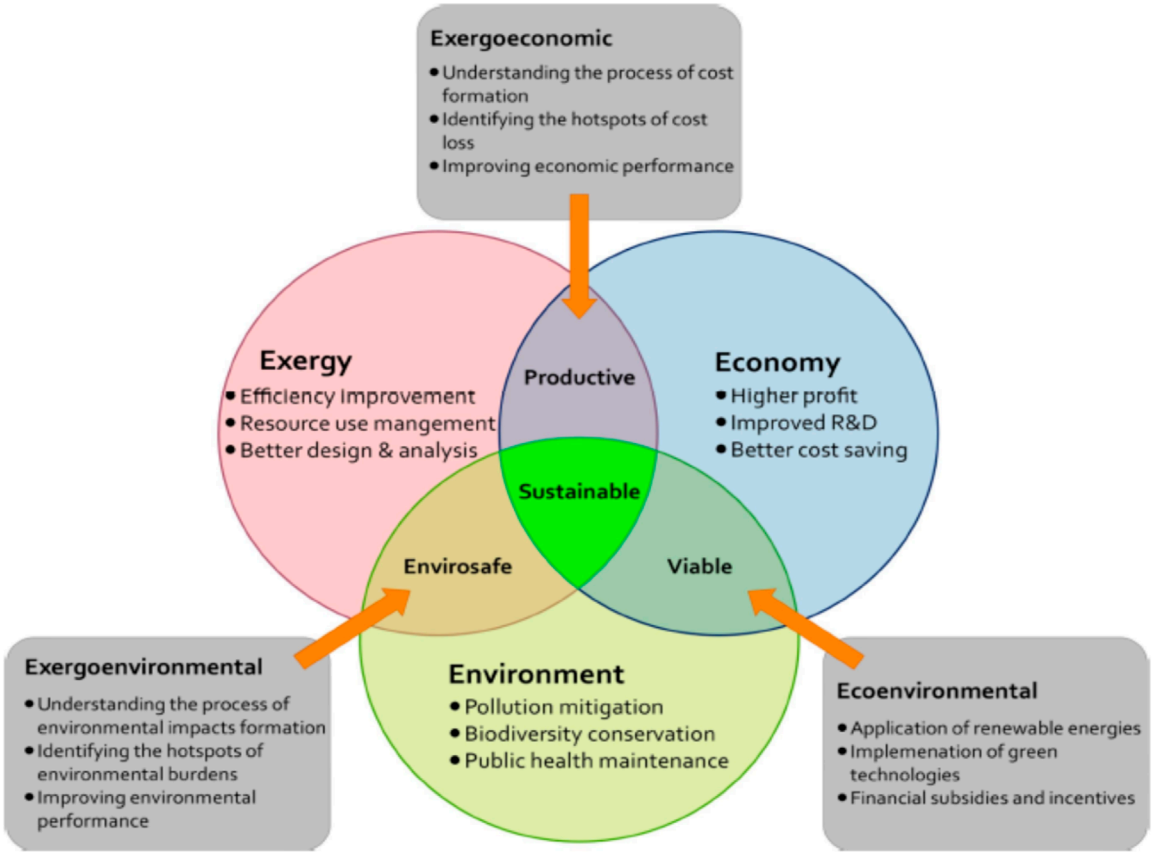

FIGURE 3
Opportunity interactions among exergy, economy, and environment (Aghbashlo et al., 2022).

have been through gas-to-gas recuperation, steam injection (STI), evaporation cycle, chemical recuperation, inlet air cooling (IAC) and combined cycle. These efforts have led to an increase in output power, thermal efficiency and work-back ratio (Waheed et al., 2018).

A typical gas turbine unit comprises a low-pressure turbine (LPT) and a high-pressure turbine (HPT). The LPT consist of four segments with an effectual blade for cooling and negligible leak. The HPT is positioned within two combustors possessing a single stage. During the initial expansion, most of the exhaust gases diffuse to the second combustor (Aghbashlo et al., 2022). Numerous researchers have worked on the thermodynamic assessment of different gas turbines (Wang and Chiou, 2004; Farzaneh-Gord and

Deymi-Dashtebayaz, 2009). The thermodynamic investigation of gas turbines revealed that ambient temperature, humidity, pressure ratio, turbine inlet temperature (TIT) (around 500°C) and nature of fuel are the essential factors affecting gas turbine performance. The enormous exhaust temperature shows that energy is being flared uncontrollably into the environment. In the work of Sulaiman et al. (2017), the effect of decreasing entry air cooling of the compressor with energy wasted in the gas pressure drop station on a basic gas turbine power plant was studied. They proposed recuperating misused energy within exhaust through the heat-regaining steam generator and adding steam into the combustion compartment. The least specific fuel consumption of 0.15 kg/kWh, the highest energetic efficiency of 47.35%, and high-enhanced capacity in thermal efficiency along with power output were reported. Fagbenle et al. (2014) applied an exergy study to numerous gas turbine power equipment in Nigeria. They stated that the energetic efficiency improved as the turbine inlet temperature increased.

Oyedepo et al. (2015c) evaluated a selection of gas turbine performance in Nigeria utilizing energy and exergy analyses. The study revealed that the maximum proportion of energy loss happened in the combustion channel, ranging from 33.30% to 39.94%. The exergy investigation additionally confirmed the combustion compartment as the utmost exergy critical part contrasted with other cycle constituents. The exergy ruin in the fire chamber ranged from 86.04% to 94.66%. Its energetic proficiency is lesser than other workings. A rise in the entry turbine temperature increased the exergetic effectiveness in response to an upsurge in the turbine's outlet power and losses in the combustion chamber.

Zhang et al. (2018) suggested eight arrangements of gas turbines fuelled by biomass gasification and simulated their performance. They described that exergy effectiveness ranged between 22.2% and 37.2%. De Souza-Santos also investigated the functioning of a gas turbine fuelled by syngas from the environment and the pressurized gasifying of sugarcane bagasse (De Souza-Santos, 1999). They reported that the syngas obtained from pressurised vaporization produce greater effectiveness than the climatic one. Gümüş (Gümüş and Atmaca, 2013) investigated the exergy effect on mixed fuel and diesel in a diesel engine. Exergy, energy and irreversibility increase as engine speeds increase for both energy sources. Mixed fuel proved to possess a higher exergy efficiency than diesel fuel. The operation of some gas turbine devices was studied by Almutairi et al. (Granet and Bluestein, 2000) on diverse load requirements and weather circumstances applying two configurations. The reheat systems boosted output power and reduced exergy efficiency compared to the elementary gas turbo. Athari et al. (2015a) conducted an exergy analysis on a simple gas turbine. It was observed that the combustor's improved exergy efficiency was achieved once the compressor pressure ratio was increased. The compressor pressure ratio is seen as a focal factor determining both energy and exergy efficiencies of both steam injection gas turbines alone and steam injection gas turbines with inlet fogging cooler.

Ahmadi et al. (2013) performed an all-inclusive thermodynamic simulation and multipurpose optimisation of a multi-operational system comprising an absorption chiller, ejector refrigeration system, heat regain steam generator, and an electrolyser that gives numerous products: energy, hot water boiler, refrigeration, and hydrogen (Figure 4). Exergy and environmental studies were performed. A multipurpose optimisation method based on a rapid and elite non-dominant categorization genomic process was applied to assess the system's optimal design factors. The two goals tasks used across the streamlining study were the framework's complete expense rate, which shaped the expense related to fuel, part procuring and environmental effect, and the system's exergy effectiveness. The framework's all-out expense rate was scaled down while the cycle exergy effectiveness was expanded utilizing a developmental calculation (evolutionary algorithm). A shut structure condition about the connection amid exergy proficiency and the overall cost was inferred. A sensitivity investigation was also accomplished to evaluate the impacts of a few plan boundaries' total exergy destruction rate on the system, carbon dioxide discharge, and exergy effectiveness. The major conclusions made were that an increase in heat recovery steam generator pressures increased exergy efficiency of the system and decreased the system's rate of total cost. In contrast, a rise in heat recovery steam generator throttle point temperatures reduced the exergy efficiency of the system.

Ahmadi et al. (2012) executed an all-inclusive thermodynamic modelling of a trigeneration operation for heating system, chilling, and energy generation. The trigeneration operation comprises a gas turbine cycle, an ORC, a single-effect absorption chiller and a native water boiler (Figure 5). An exercise-based environmental analysis was undertaken, and parameters that assessed ecological effect and sustainability were gauged. The trigeneration system's exergy efficiency was discovered to be greater than classic mixed heating and power systems. The outcome also shows that the trigeneration system's CO_2 emissions are less than those mentioned above. The exergy results revealed that the exergy obliteration was most elevated in the combustion chamber because of the temperature contrast between the working fluid and combustion temperature. The study concludes that the entry temperature of the turbine, the pressure proportion of the compressor, and the turbine's isentropic efficiency significantly affect the system's performance. Moreover, raising the inlet temperature of the turbine diminishes the expense of the surrounding effect, basically by lessening the concentration transfer rate of the combustion chamber.

2.1.2 Steam power plant

Steam injection technology enhances the functioning of a basic gas turbine. Ghazikhani et al. (2005) studied the impact of steam injection at the Mashhad Power Plant with a gas turbine, GE-F5. They observed an increase of 10% in the system's thermal efficiency while the back-work ratio improved by 15%. Bouam et al. (2008) enhanced a gas turbine under Sahara conditions by injecting steam into the combustion chamber when the efficiency of the steam gas turbine was held constant at 50% while the ambient temperature was varied from ISO conditions to 50°C. This study shows that steam injection makes it possible to achieve high efficiency. Ziółkowski et al. (2012) also investigated the effects of steam injection on a gas turbine performance at the PGE Gorzow power plant using COM-GAS code and Aspen plus software. Agarwal and Mishra, (2011) reviewed current and future sustainable gas turbine technologies by comparing their thermodynamic characteristic and concluded that mixed air steam technologies offered superior performances compared to other technologies. Comparative exergoeconomic analysis of a steam injection gas turbine fuelled with biomass gasification was also studied to assess

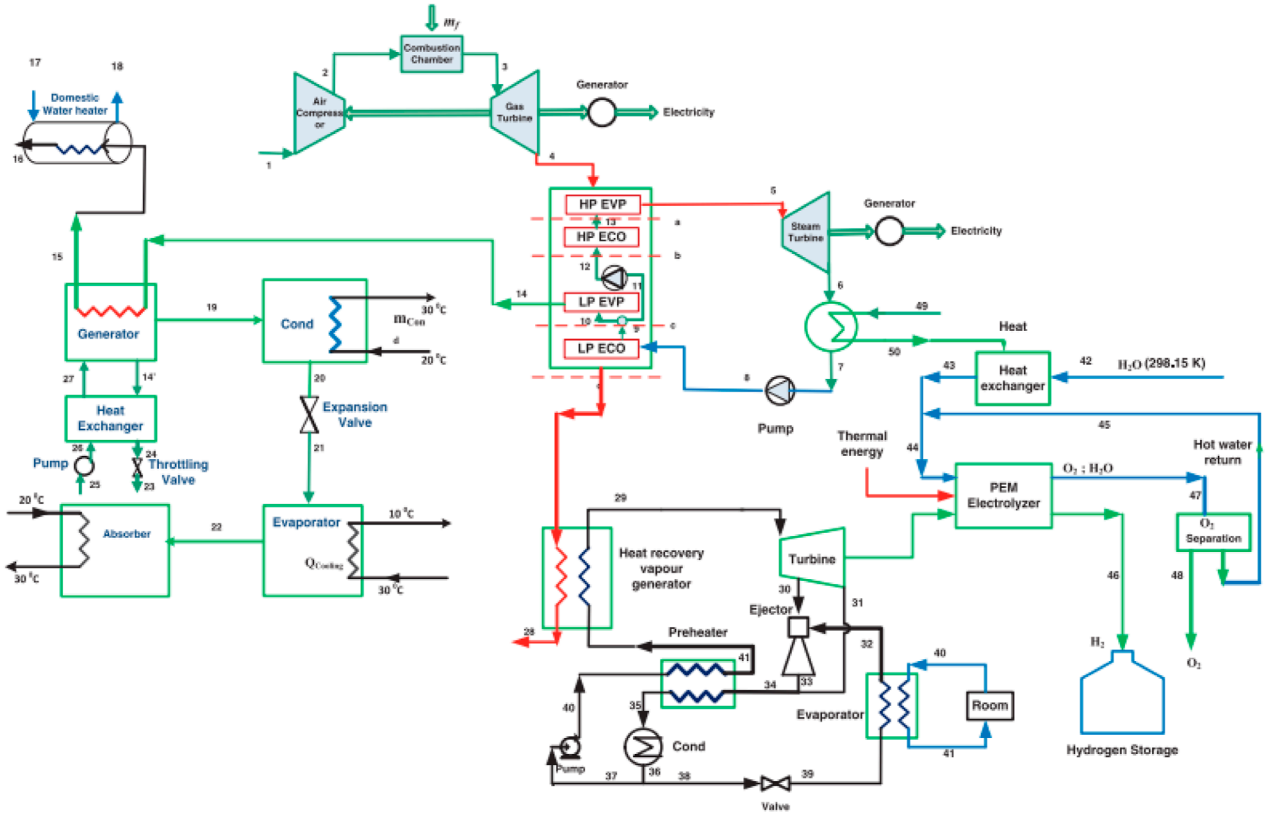

FIGURE 4
Multigeneration energy system (Ahmadi et al., 2013).

the influences and performance of operating variables with and without fogging inlet cooling (Jana and De, 2014).

Keçebaş and Gokgedik (2015) performed conventional and advanced exergy analyses of an existing geothermal binary power system for power generation (Figure 6). Details about the exergy destruction in the system and its parts were analysed through advanced analysis to investigate the interactions between the system components and the actual performance of the reasonable improvements. The obtained results showed that the primary improved components were in the order of CON 1, TURB 1 and VAP 2 for the conventional analysis, as shown in the schematic, while for the advanced exergy analysis, the order of improvement was CON 1, CON 2 and PRE-HE 1. From the study, the conventional exergy analysis results were found to be more qualified than the conventional exergy analysis. Following the improvements made to the system, the modified exergy efficiency increased to 18.26%. However, the total system efficiency was found to be about 9.60% in the real conditions.

2.1.3 Combined cycle power plant

Recently, attempts to advance the capacity and effectiveness of simple gas turbine power generators were carried out through different combined heat and power cycle (CHP) methods (Ahmadi et al., 2011b). For instance, Boonnasa et al. (2006) improved a mixed cycle power plant in Bangkok using a steam absorption chiller to chill inlet air to 16°C and 100% humidity. This gives a 14% increase in the plant's power output. Traverso and Massardo (2002) evaluated the function of four diverse combined cycle types of machinery. Humid air-water injection turbine was found to be more attractive than other technologies.

Moreover, some studies were focused on biomass-fuelled gas turbine systems for improved performance. For instance, Vera et al. (2011a) studied a CHP-gas turbine system with a capacity of 70 kWe and 150 kWth for an olive mill. Vera et al. (2011b) reported that there is higher thermal efficiency for the externally fuel gas turbine (EFGT) in comparison to the internally fuel gas turbine (IFGT) on a 30 kWe CHP system due to the extra required work for syngas compression in IFGT. Iora and Silva (2013) studied a biomass-fuelled 50 kWe CHP-EFGT and obtained an efficiency of 21%. Also, the CHP-EFGT system is fuelled by wastes from poultry, with a part at the turbine exit planned to dry the fuel and another for steam generation (Bianchi et al., 2006). For instance, biomass gasification fuelled on EFGT-Rankine combined cycle with steam injection and fog inlet cooling was investigated by (Athari et al. (2016a), Athari et al. (2016b). Besides, Gholamian et al. (2016) used a biomass-fuelled mutual cycle involving a conventional EFGT and a supercritical CO_2 cycle. They reported an increase from 26.95% to 38.18% for exergy efficiency through EFGT combined with a supercritical CO_2 cycle. Almutairi et al. (2015) observed the combustion chamber in a mixed-cycle power plant as the primary source of irreversibility due to poor air-fuel mixing and fuel oxidation. Therefore, adding an air preheater and reducing

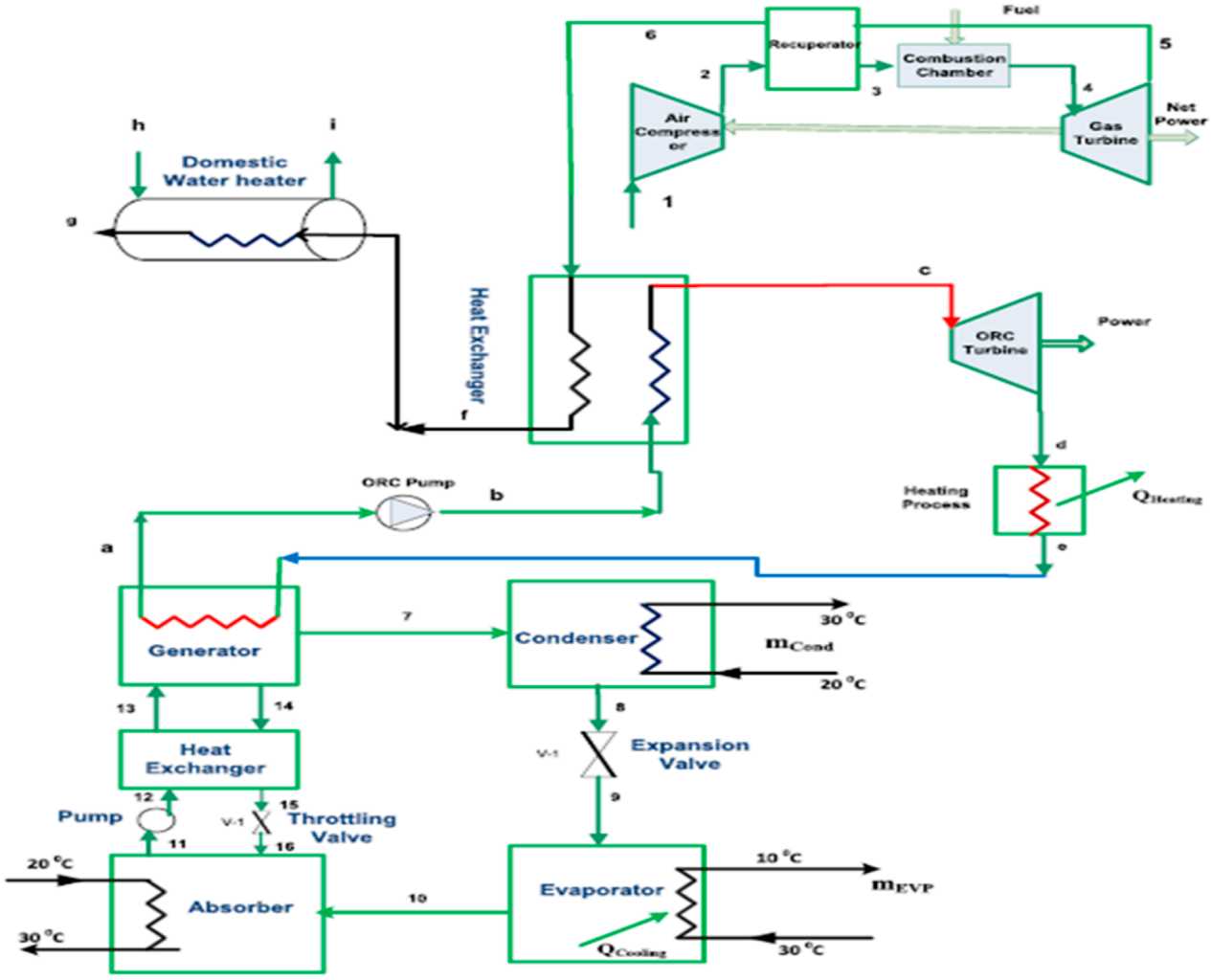

FIGURE 5
Representation of a Multigeneration system for steaming, refrigeration plus power generation (Ahmadi et al., 2012).

the air-fuel ratio were recommended to solve the cycle's high exergy destruction. Doseva and Chakyrova, (2015) investigated the cogeneration system's exergy efficiency of an internal combustion engine for use with biogas from a wastewater treatment plant. It was observed that the focal cause of irreversibility in the cogeneration plant emanated from the combustion chamber due to friction, temperature variation and chemical reaction.

Oko and Njoku (2017) explored the thermodynamic viability of upgrading an existing 650 MW combined thermal power plant (Figure 7) by adding an organic Rankine cycle unit. Energy and exergy methods were utilised to thermodynamically analyse the performance of the integrated gas, steam, and organic fluid-cycle power plant. The choice of organic refrigerant greatly enhanced the system's performance.

Manente, (2016) built a detailed off-design model of a 390 MW three-pressure level natural gas combined cycle (Figure 8) to assess the different integration schemes of solar energy, which keep the equipment of the combined cycle unchanged or include new equipment which comprises the steam turbine and heat recovery steam generator. Power-boosting and fuel-saving operation strategies were analysed to search for the highest annual efficiency and solar share. The results showed that without modifying the existing equipment, the maximum incremental power output from solar at design solar irradiance is limited to 19 MW. Depending on solar share and extension of tube banks in the heat recovery steam generator, high solar radiation-to-electrical efficiencies in the 24%–29% range were achievable in the integrated solar combined cycle. Compared to power-boosting, the fuel-saving strategy shows lower thermal efficiencies of the integrated solar combined cycle due to the efficiency drop of the gas turbine at reduced loads.

Another form of integrated combined cycle is a biomass integrated gasification combined cycle (BIGCC). The BIGCC, as a power generation process, incorporates a biomass gasification system with a combined cycle power plant. This process is an attractive alternative for power generation compared to the conventional CHP processes due to high thermal efficiency and energy output, smaller production of greenhouse gases, and reduced generation of solid wastes. Moreover, A BIGCC process without

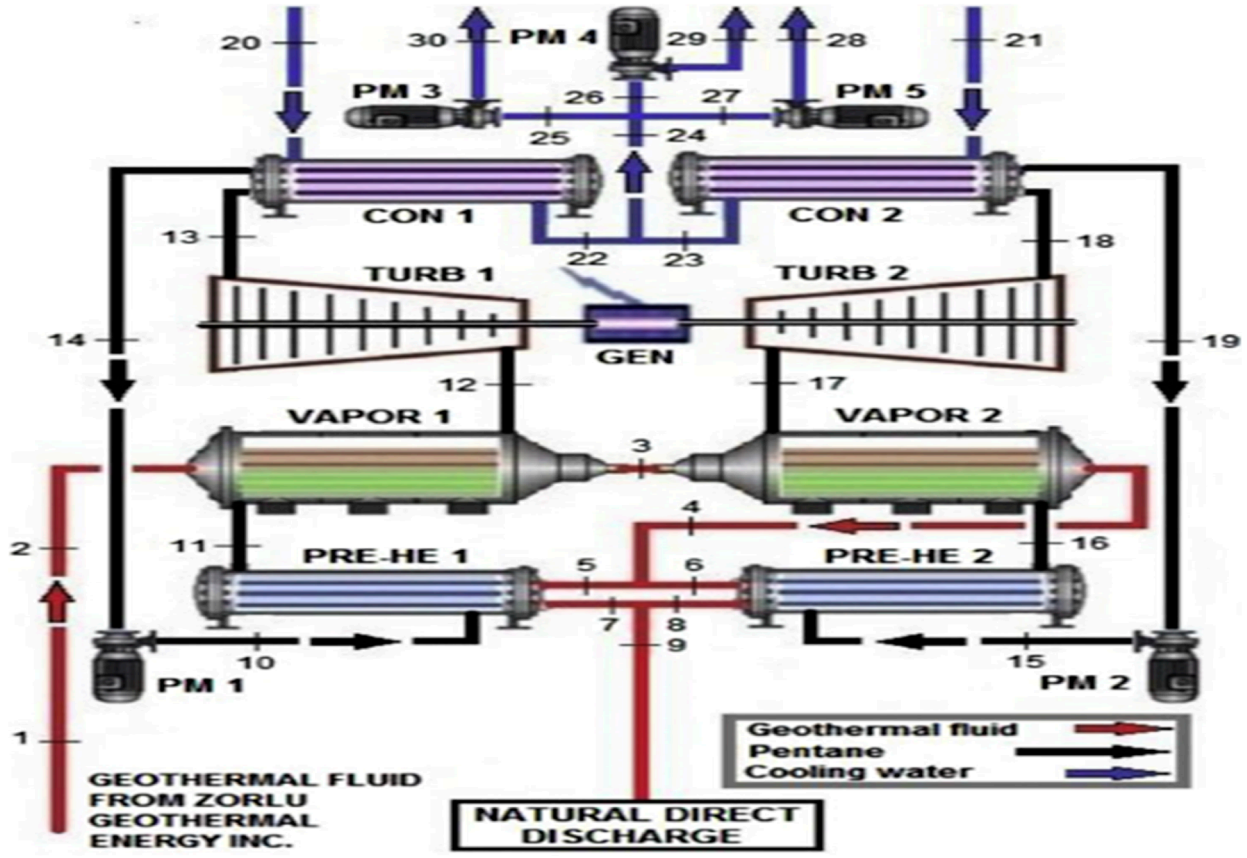

FIGURE 6
Geothermal binary power system for power generation (Keçebas and Gokgedik, 2015).

carbon capture and storage (CCS) may contain four central operating units: an air separation unit (ASU), a gasifier, a syngas cooling and clean-up system, and a combined cycle power plant (Santos et al. (2016)]. Figure 9 shows a simplified scheme of a BIGCC process without CCS. Due to the promising benefits of BIGCC over the firing-based conventional power plants and coal-firing-based IGCC plants, several types of research from the second law of thermodynamics perspectives have been conducted to improve its performance. Bhattacharya et al. (Santos et al., 2016) investigated a 50 MWe BIGCC system integrated to supplement biomass firing. The study showed Second law (exergetic) efficiency of 36.86% for the entire power plant. Khanmohammadi et al. (Bhattacharya et al., 2011) studied integrating combined EFGT, ORC and biomass gasifier for CHP applications. Zhang et al. (Oyedepo et al., 2015c) used an IFGT-based CHP combined cycle powered by biomass gasification and coupled with a ground source heat pump. A Second law (exergetic) efficiency of 13.6% was obtained. A novel BIGCC based on IFGT, and oxy-fuel combustion was proposed by Xiang et al. (Khanmohammadi et al., 2019).

2.1.4 Refrigeration systems

Refrigeration systems are widely used for cooling purposes in industrial and residential sectors. These systems have been recognised to consume a high proportion of energy. Because of climate change resulting from the greenhouse effect and depletion of the ozone layer many world unions have recommended decreasing climate effects by improving the system's efficiency and changing the existing refrigerants with ozone-friendly and eco-friendly ones (Xiang et al., 2019; Bolaji, 2010; Gill and Singh, 2018).

Lugo-Leyte et al. (Borokinni et al., 2018) studied the refrigeration cycle's energy and exergetic analysis via R134a as the operating fluid. The equipment's irreversibilities, the temperature of the refrigerated spaced and the exergetic operation cost in function of the environmental temperature were reported. The energy and exergy analysis of R502, R404A and R507 was also investigated by Arora and Kaushik (Lugo-Leyte et al., 2013). They computed the exergy destruction, exergetic efficiency, coefficient of performance and efficiency defects in the system. Based on exergy concept, Ahamed et al. (Keçebas and Gokgedik, 2015) stated that the major parameters that affect a vapour compression system are evaporating and condensation temperatures, undercooling and compressor pressure. Kizilkan et al. (Arora and Kaushik, 2008) presented that major irreversibility happened in the compressor and then the condenser, the evaporator, and the throttling valve for diverse compressor frequencies. Similarly, the exergy study of plant refrigeration with R407C, R507 and R417A as the working fluids by varying the compressor speed was examined by Aprea et al. (Kizilkan et al., 2010). The result obtained indicated that the compressor contributed better to the overall irreversibility, while R407C performed better than R507 and R417A. The total

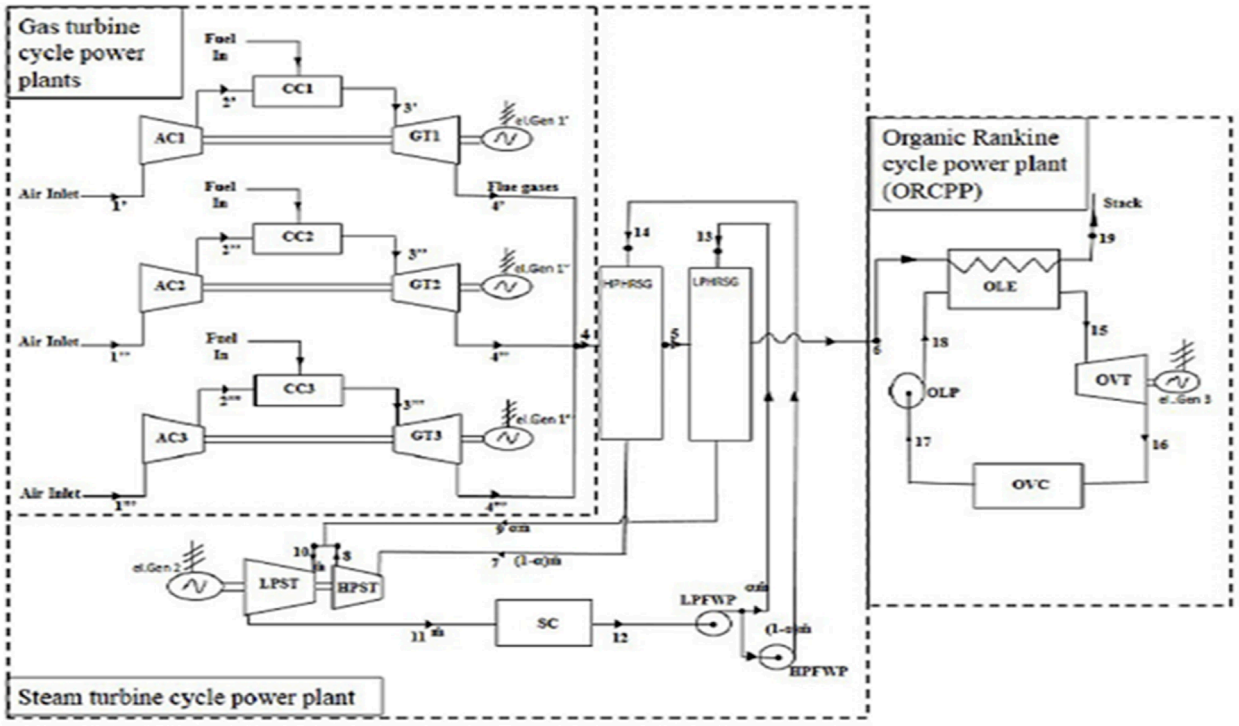

FIGURE 7
Schematic layout of Integrated Combined Thermal Power Plant with Organic Rankine Cycle (Oko and Njoku, 2017).

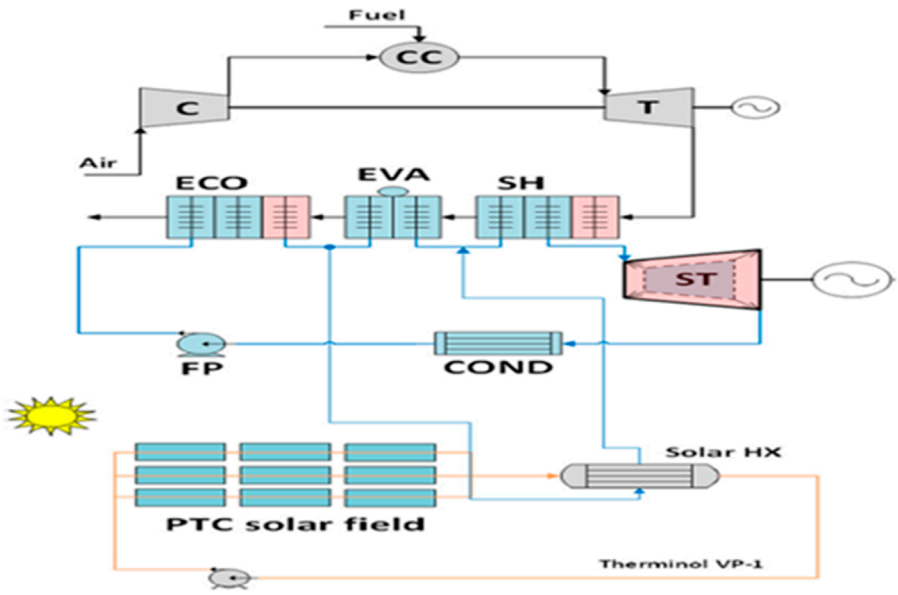

FIGURE 8
Schematic layout of integrated solar combine cycle (Manente, 2016).

energy and exergy performance of a domestic refrigeration cycle working with R413A is consistently better than that of R12 when the performance of R413A in an unmodified R12 system was evaluated by Padilla et al. (Aprea et al., 2003).

Kalaiselvam and Saravan (Padilla et al., 2010) also investigated the total exergy losses on different scroll compressors using R22, R417A and R407C as the working fluid. They suggested that R417A, being eco-friendly, can be used as an alternative to

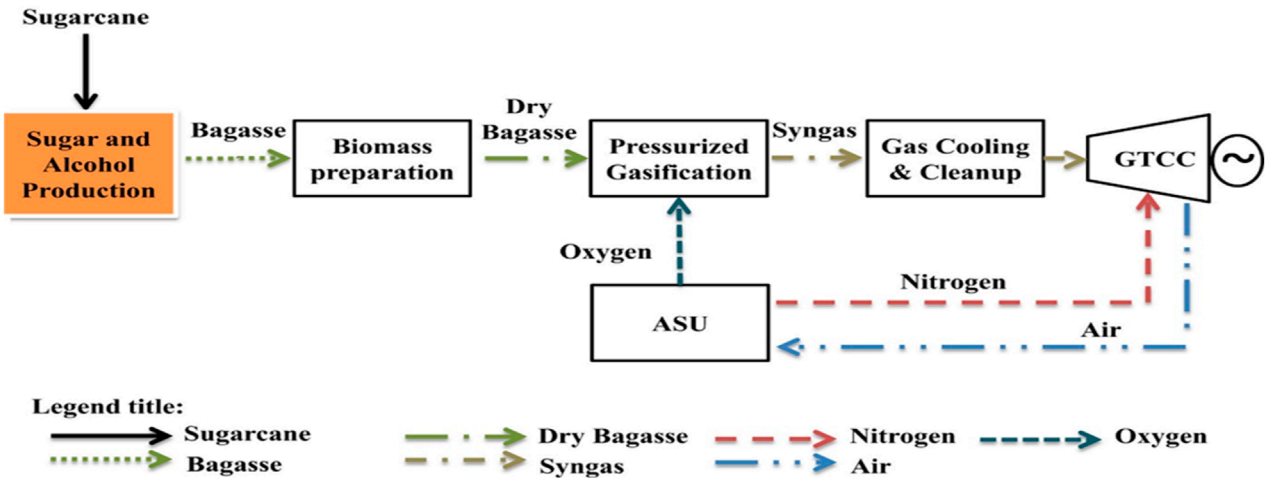

FIGURE 9
Simplified diagram of the Biomass Integrated Gasification Combined Cycle (B-IGCC) [Santos et al. (2016)].

other refrigerants. Agarwal et al. (Kalaiselvam and Saravan, 2009) investigated the performance of mechanically subcooled simple vapour compression refrigeration systems based on energy and exergy analysis. Compatibility of alternative low GWP and zero ODP HFOs R1234yf and R1234ze were investigated to replace the HFC 134a. Results of the study revealed that R1234ze was the best alternate refrigerant considered in the analysis and can replace R134a as the COP and exergetic efficiency of R1234ze were 1.87% and 1.88% higher than that of R134a for 30°C of sub-cooling. On the other hand, R1234yf offered lower performance than R134a. According to the study, the condenser and evaporator components had the highest and lowest exergy destruction sites, respectively (Agarwal et al., 2021).

Al-Sayyab and Abdulwahid (Yataganbaba et al., 2015) used R1234yf, R1234ze, R245fa, and R227ea as alternative refrigerants to R134a for exergy study of ten vapour compression cycles. The study results revealed that the maximum no-reversibility among the system mechanisms happened in the compressor, followed by the throttling valve, flash tank, and condenser. At the same time, the evaporator possessed the least no-reversibility. R245fa possessed the least exergy destruction with high exergetic efficiency and high COP with respect to other refrigerants. Hence, this refrigerant has the potential to serve as an alternative refrigerant to R134a. From the study by (Al-Sayyab and Abdulwahid, 2019), R454B was found to be the satisfactory fluid for use in the ground source heat pump. Menlik et al. (Bobbo et al., 2019) presented the second law of thermodynamic analysis, the potential of R22, and its alternatives, R407C and R410A, in a VCRS. Results of the study revealed that R407C was a better alternative to R22 than R410A. The highest exergy-destroyer component of VCRS was the condenser. Gill and Singh (Menlik et al., 2013) experimentally inspected a vapour compression refrigeration framework's thermodynamic performance utilizing a combination of R134a and LPG refrigerant as a swap for R134a. From the investigation, the proposed combination of R134a and LPG performed in a way that is better than R134a from insightful exergy and energy examinations.

2.1.5 Organic Rankine Cycle (ORC) and Kalina Cycle (KC)

Organic Rankine Cycle (ORC) and Kalina Cycle (KC) are new energy conversion technologies. These technologies convert low-temperature waste heat from industries (or solar energy sources) into useful energy (heat or power) (Kim et al., 2013). Based on the desire for effective energy utilization and preservation of the environment from pollution, various researchers have worked on performance improvement and economic assessment of ORC and KC.

Gill and Singh, (2017) and Kim et al. (2012) investigated the energy and exergy system performance characteristics of the ammonia-water Rankine cycle using low-temperature heat sources and ammonia-water mixture heat exchangers with and without regenerator. Similarly, Kim et al. (2012) reported the pinch point characteristics in heat exchangers and ammonia-water-based power cycle condensers. Moreover, studies on integrating ORC/KC with other heat sources were studied. For instance, (Lolos and Rogdakis, 2009; Kim et al., 2014) studied a Kalina cycle's performance with solar energy as a heat source. Ogriseck, (2009) analysed the integration of Kalina power in a combined heat and power plant in Germany.

Ogriseck, (2009) compared and analysed the Kalina Cycle's performance and bottoming transcritical organic Rankine cycle in the cryogenic cogeneration system for engine exhaust heat recovery. Yue, et al. (2015) and Sun et al. (2012) carried out energy, and exergetic analysis for solar-boosted KC with an auxiliary superheater to utilise low-grade heat sources. Sun et al. (2014) investigated a 150 kWe EFGT system fuelled by a downdraft gasifier and combined with an ORC to maximise the electrical energy generation. They reported an electrical efficiency, generated power and biomass consumption of 20.7%, 200 kWe and 217 kg/h. Vera and Jurado, (2018) compared ORC and KC's low-temperature waste heat recovery performance. At the expense of higher pressure, KC generated more power with higher efficiency.

Furthermore, an investigation on KC driven by low-grade geothermal energy integrated with thermoelectric generators

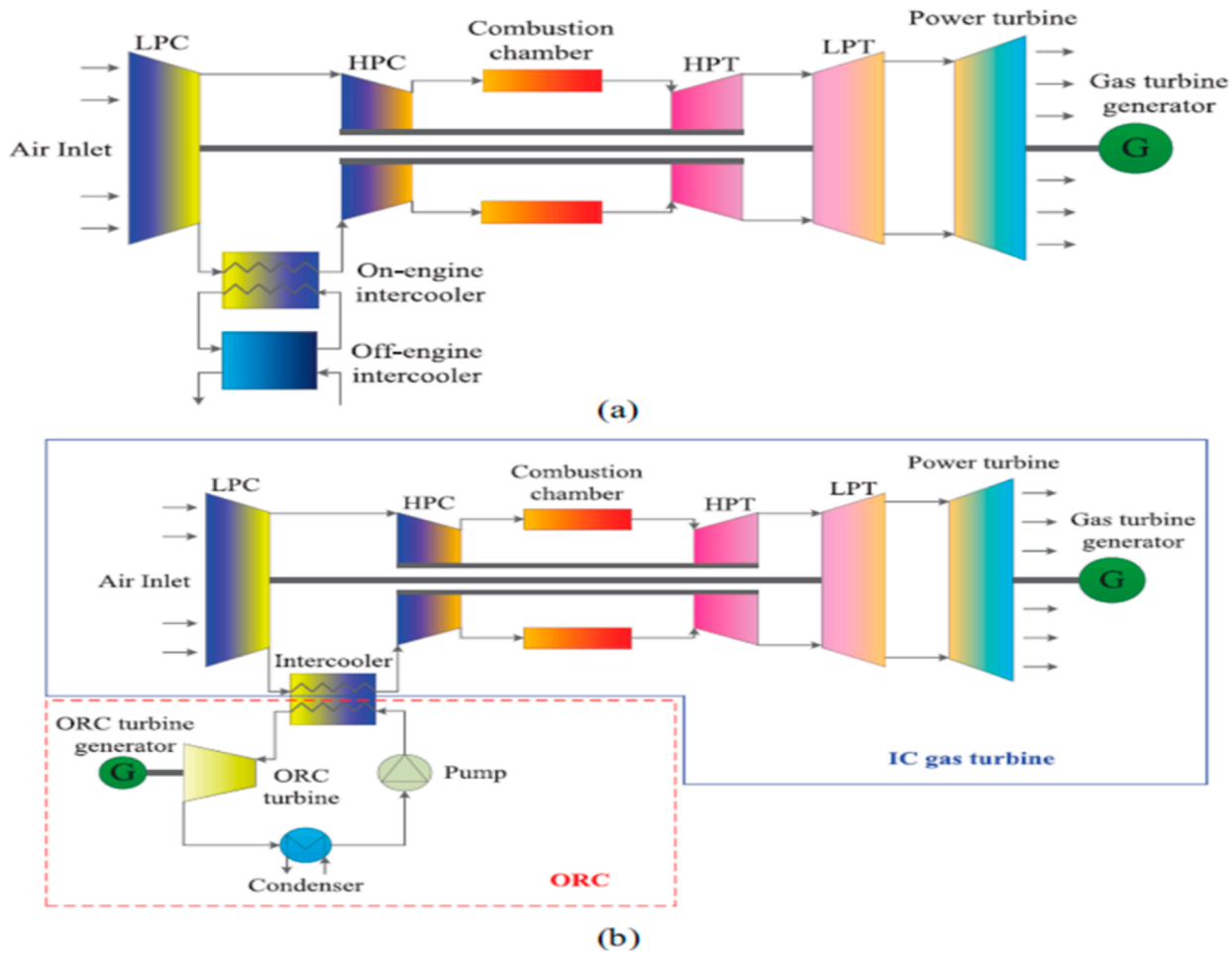

FIGURE 10
Schematic diagram of the IC gas turbine **(A)** without and **(B)** with ORC power generation system (Zare and Palideh, 2018).

to convert heat into electricity directly has been carried out (Varga and Palotai, 2017). The study enhanced the net power by 7.3%, with efficiencies comparable to the conventional KCs. Zare and Palideh, (2018) developed a novel Organic Rankine cycle (ORC) (see Figure 10). The ORC system's thermodynamic performance was investigated to study the system's operational improvement. The study results indicated that ORC integration and intercooled cycle gas turbines could recover waste heat. From the study, the maximum enhancements of output power and thermal efficiency were 6.08% and 2.14%, respectively. Based on the outcome of the investigation, it was established that both room temperature and operating conditions of gas turbines are principal factors influencing the operating performances of the ORC system. Koç et al. (Liu et al., 2018) performed energy, exergy, and parametric analysis on the Organic Rankine Cycle (ORC) with a simple and recuperative ORC case study using a gas turbine-based combined cycle. The study showed high power output at quasi 9 MW for simple ORCs that employed methanol and recuperative ORCs using trans-2-butane as working fluids. Recuperative ORC was observed to have the potential for reduction in CO_2 emission.

2.1.6 Renewable energy systems

Renewable energy systems are gaining users' attention as an incomplete or total substitution of fossil fuel-based sources. Numerous studies have been conducted on using renewable sources to replace fossil fuels. The superior substitutes are solar and biomass energy, which replace power generation's thermal energy because of their carbon-neutral nature and environmental beneficence (Koç et al., 2020). Moreover, these renewable energy resources are easily accessible to humanity worldwide and also available in abundance (Seyam et al., 2020). In his study, Hepbasli, (2008) presented a comprehensive review of exergetic analysis and performance evaluation of different renewable energy resources (RERs). The RERs studied are solar, wind, geothermal, and biomass energy systems. The paper concluded that such a study is of great importance and relevant to engineers and scientists applying the second law of thermodynamics in the design, simulation and performance improvement of RERs.

This section presents a thermodynamic performance assessment of the selected renewable energy systems based on energy and exergy analyses. The focus is on integrated renewable energy sources with the conventional energy system.

2.1.6.1 Integrated solar energy system

Solar energy is a form of renewable energy that converts the sun entering the earth's surface into heat or electricity. Integrated solar-assisted polygeneration systems have emerged as an effective and sustainable alternative for meeting thermal, cooling, power and freshwater demands (Khani et al., 2022). Because of this, numerous studies on integrated solar-assisted plants with conventional thermal power plants have been carried out (Alta et al., 2010; Oztop et al., 2013; Akyuz et al., 2012). Assareh et al. (2023) proposed an innovative power generation system based on solar and biomass energy resources. The system consists of a biomass unit, a solar unit, a waste heat recovery unit, and a hydrogen liquefaction unit. The power was generated by two gas turbines and two Rankine cycles. Results of the study showed that solar energy with waste-heat recovery reduces CO_2 emissions by 30.5% while increasing the system's electrical power output by 44%. Roshanzadeh et al. (2023) conducted a study focusing on utilizing solar cooling systems to achieve low inlet air temperature and generate high electricity yields. The study simulated the thermodynamic behavior of a combined cycle power plant with integrated solar-driven inlet air cooling for Tehran, Phoenix, and Houston during warm-hot seasons. Results of the study revealed that a considerable reduction in the output power was realized during hot ambient conditions due to the lower density of the air and lower mass flow rate to the turbines. The output power decreased from 306.6 to 260.8 MW as the ambient temperature increased from 15 to 45°C.

Moreover, Ghorbani et al. (Ratlamwala et al., 2011) developed and analysed an integrated system capable of producing 65.2 MW of heating, 1.87 MW of power and 83.2 kg/s of freshwater. Servam et al. (Koç et al., 2020) assessed the performance of a novel integrated large-scale combined cycle power plant (CCPP). This system depends on renewable sources such as solar radiation and seawater from the Atlantic Ocean to provide clean and sustainable energy. The integrated power plant consists of six subsystems: solar farm, Gas turbine cycle, Rankine cycle, multi-effect desalination, electrolyser, and hydrogen liquefaction subsystem. The combined cycle was studied thermodynamically to investigate thermal and exergy performance. The integrated system's overall thermal efficiency was 88.12%, while the exergetic efficiency was 23.05%. The combined system has the energy cost of 14.59 $/MWh, which was found to be economical due to the system's multiple services. Also, the emissions were significantly low, making this power plant environmentally benign. Alibaba et al. (Ghorbania et al., 2018) developed an optimal thermodynamic, exergo-economic and exergo-environmental design for the geothermal power plant used as a complement to concentrated solar power (CSP) and then combined energy-exergy-economic-environmental analysis was conducted. In the study, a standalone geothermal cycle and hybrid Geothermal-Solar cycle were investigated to generate the heating/cooling power. The study revealed that the exergo-economic analysis of the hybrid power plant has the highest investment cost when related to the solar power plant. It also had the lowest exergy degradation cost with zero environmental impact. The highest environmental rate was associated with the solar power plant. However, its environmental destruction rate was minimal because it does not consume fuel. Sarhaddi et al. (Alibaba et al., 2020) did an exhaustive energy and exergy investigation to assess a commonplace PV cluster's electrical performance, componentwise exergy destruction, and exergy efficiency. The consequences of the investigation demonstrated that the PV exhibit temperature greatly affects the exergy efficiency. The investigation reasoned that a PV cluster's exergy proficiency could be improved if the heat could be eliminated from the PV array surface.

Yuanyuan and Yongping (Sarhaddi et al., 2009) presented a thermodynamic and economic analysis for an integrated solar combined cycle (ISCC) system with two pressure-level DSG solar fields (ISCC–2DSG) (Figure 11). The impacts of solar multiples on the system's performance with or without consideration of thermal storage were studied. In that order, the solar thermal energy produced from two solar fields in the ISCC–2DSG system was only used to supply latent heat for low and high-pressure water vaporisation. The analysis characterised several such ISCC–2DSG systems' annual thermodynamic performances, using different solar multiple values but identical design parameters in the power subsystem. The results showed that the capacity factor increases with a more significant solar multiple due to more outstanding electricity production for ISCC–2DSG systems without thermal storage. The capacity factors were more substantial than those without thermal storage for the systems with thermal storage, following the effective utilisation of the surplus solar thermal energy generated. The results concluded that the system's levelized electricity cost with thermal storage was considerably higher for a given solar multiple than without thermal storage.

Al-Ali and Dincer (Yuanyuan and Yongping, 2015) proposed a thermodynamic analysis of a multi-generation integrated geothermal-solar (GS) system that consists of the geothermal-solar cycle, organic Rankine cycle 1, organic Rankine cycle 2 and a single absorption chiller that produces electricity, space heating, hot water, industrial process heat and cooling. Results obtained show the energy efficiencies for single-generation and multi-generation systems were 16.4% and 78%, respectively. The exergy efficiencies yield 26.2% and 36.6%, respectively. Adibhatla and Kaushik (Al-Ali and Dincer, 2014) performed energy, exergy and economic analyses of a conceptual power plant cycle formed by adding solar energy to the steam cycle of a natural gas-based combined cycle power plant (Figure 12). The solar integration idea was made at a moderate temperature level using a direct steam generation technique with parabolic trough collectors. The simulated results showed that the solar field's energy and exergy efficiencies were 53.79% and 27.39%, respectively. The results have indicated that the plant output was increased by 7.84%, with the solar field operating at the design point for a 50 MW nominal solar field-rated capacity. The results showed that the levelized cost of electricity generation decreased from 7.4 to 6.7 cents/kW.

2.1.6.2 Integrated biomass energy system

Reducing natural resources for fossil fuel has shifted attention to sustainable renewable energy integrated systems (Gholamian et al., 2016). The economic policy international bodies support research into utilizing renewable energy to minimize environmental pollution posed by fossil fuel. Biomass is being explored as renewable energy. With the increase in the depletion of fossil fuels and greenhouse gas (GHG) emissions, highly efficient energy utilisation systems have drawn increasing attention, especially renewable and sustainable energy integration systems (Gholamian et al., 2016). The current global

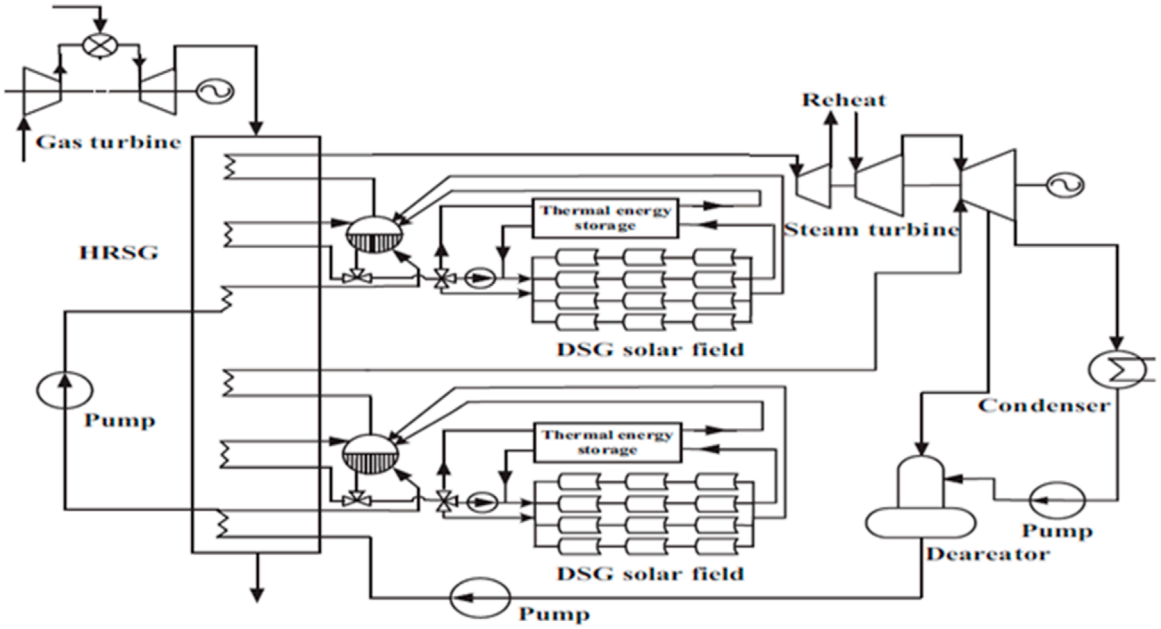

FIGURE 11
Schematic diagram of an ISCC system with two DSG solar fields with thermal storage (Sarhaddi et al., 2009).

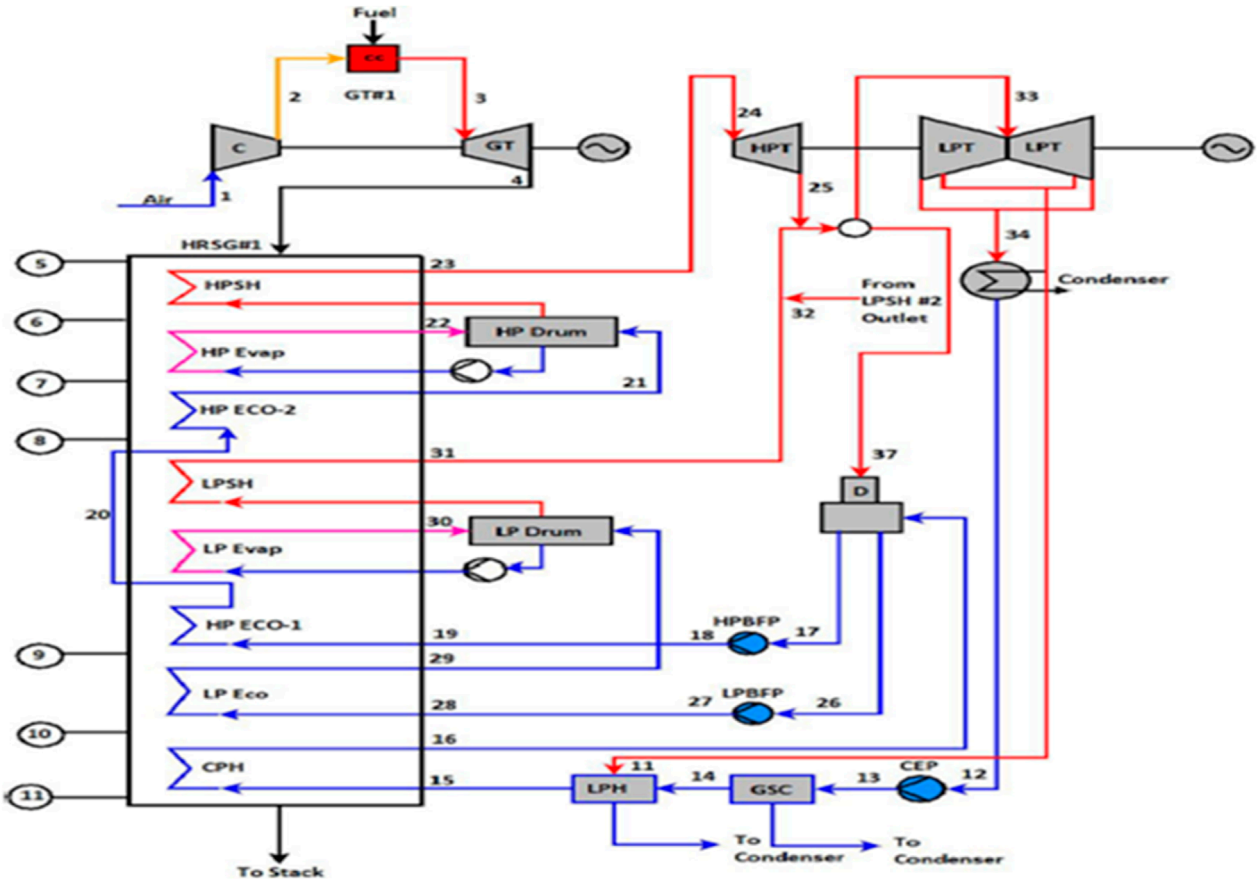

FIGURE 12
Integrated solar direct steam generation combined cycle power plant (Al-Ali and Dincer, 2014).

energy policies promote research to enhance the utilisation of renewable energy sources, largely to minimise environmental problems and improve the national energy security of countries dependent on the use of imported fossil fuels. Biomass is currently one of the most popular renewable energy sources. This is because biomass has great potential as a clean, renewable feedstock for producing modern energy carriers (Adibhatla and Kaushik, 2017).

Buentello-Montoya and Zhang (2019) analysed the thermodynamic efficiencies of biomass gasification from char-activated char catalysts. The work introduced an equilibrium model for the thermodynamic analysis and assessed the effect of the reactor temperature, reaction time and equivalence ratio based on the gas quality. The result showed that there is a thermodynamic advantage and reduction in exergy destruction due to high reforming temperature. The result is in tandem with Echegaray et al. (Adibhatla and Kaushik, 2017) as the exergetic efficiency of the gasification process lessened when all measured working parameters were increased.

There was also the attempt to generate electricity through a combination of solar heat and biomass-fired power systems (Khalid et al., 2015). Thermodynamic performance of the hybrid solar heat–biomass-fired plant was carried out, which resulted in an improved efficiency of 20%. The exergetic conversion efficiency of the combined heat power plant was estimated to attain 21% (Buentello-Montoya and Zhang, 2019) (Figure 13). A cost assessment of the system was investigated for a case study considering a typical apartment block on a Greek Island, assuming Parabolic Trough Collector (PTC) area of 50 m^2. The savings in fuel oil and electricity consumption accounted for an Internal Rate of Return (IRR) of around 12%, with a payback period of 7 years (Asim et al., 2020).

A thermodynamic evaluation and optimisation of a hybrid solar-biomass (HSB) system in a polygeneration process for combined power, cooling and desalination (Figure 14) was investigated by Sahoo et al. (2017) purposely to identify the effects of various operating parameters. Primary energy savings (PES) of the polygeneration process in the HSB system was achieved to 50.5%. The energy output from this system was increased to 78.12% compared to that of simple power plants (Chen et al., 2020).

2.2 Thermodynamic optimisation of energy systems

In order to improve the performance of an energy conversion system, thermodynamic analysis of energy systems offers a comprehensive, systems-based approach that offers a methodological scientific framework for arriving at realistic, integrated solutions to complex energy systems problems. Modern energy systems are evolving quickly and exhibit increasingly complex features. This is mostly because modern energy systems have other purposes in addition to energy conversion and supply. Aside from providing energy, energy systems should also secure their resources to ensure long-term operation, minimize their effects on the environment and ecology during construction and operation, provide energy at a reasonable cost to maximize benefits to a larger population, and help mitigate carbon emissions that contribute to global warming. In an effort to meet some of the aforementioned goals, new energy technologies are always developing. With the implementation of these technologies, renewable energy has been increasingly exploited and used, the energy efficiency of conventional power generation has been continuously improved, and energy end-consumers have become more energy-efficient and environmentally benign (Sahoo et al., 2017). According to Benja et al. (Kopanos et al., 2017), a thermodynamic optimization aims to minimise the thermodynamic inefficiencies: exergy destruction and loss in energy system components.

Many researchers have contributed valuable publications on the thermodynamic optimisation of a variety of energy systems via hybrid systems or waste heat recovery technology. These endless sustainable energy technologies can reduce fossil fuel consumption and decrease carbon emissions when its operations are optimised and controlled. Vera et al. (Sun et al., 2014) reported a value of 15.6% for exergy efficiency at base case operating conditions, which was increased to 18% by optimisation. They also reported a parametric optimisation result for a pilot system that generates power, exergy and energy efficiencies reaching up to 491 kW, 35.6% and 6.48%, respectively. Not too long ago, Prananto et al. (Bejan et al., 1996) investigated the electricity-generating performance of a KC by recovering the heat of the unused brine discharged from a geothermal power plant. In an optimised condition, 48 kg/s of unused brine was reported to generate up to 1.66 MW of electricity. In addition, Ghaebi et al. (Prananto et al., 2018) proposed and assessed geothermal power by combining KC with an ejector refrigeration cycle. In optimised conditions, the cycle has the potential to produce 2.3 MW of net power and 1.1 MW of refrigeration. Ahmadi et al. (Ghaebi et al., 2018; Ahmadi et al., 2015) optimised a transcritical CO_2 power cycle operated by a geothermal energy source with LNG as its heat sink and an irreversible Carnot refrigerator. Ahmadi et al. (2016a) also studied the exergetic and sustainable multi-objective optimisation on a nano-scale Braysson cycle operating with Maxwell–Boltzmann gas. A solar-geothermal combined cooling, heating and power plant, becoming more popular as an efficient alternative to fossils, was optimised using multiple criteria by Boyaghchi and Chavoshi (Ahmadi et al., 2016b). Boyaghchi and Sabaghian, (2017) also wrote a similar work optimising the Kalina power cycle on a parabolic trough solar collector. Ahmadi and Dincer (Boyaghchi and Sabaghian, 2016) also optimised the cogeneration of a combined cooling, heating and power plant using exergo environmental principles through a Multimodal Genetic Algorithm. Ahmadi and Dincer, (2010) made significant contributions to the multi-objective optimisation of gas turbine power plants for increased efficiency of the thermodynamic system. Further studies by Barzeger et al. (Ahmadi and Dincer, 2011) focused on a closely related study investigating the multi-objective optimisation of a gas turbine power plant with a preheater using evolutionary algorithms. Shamoushaki et al. (Barzegar- Avval et al., 2011) built on this work by applying multiple objective optimisations of gas turbine power plants in Aliabad Katoul by evolutionary algorithms to improve efficiency.

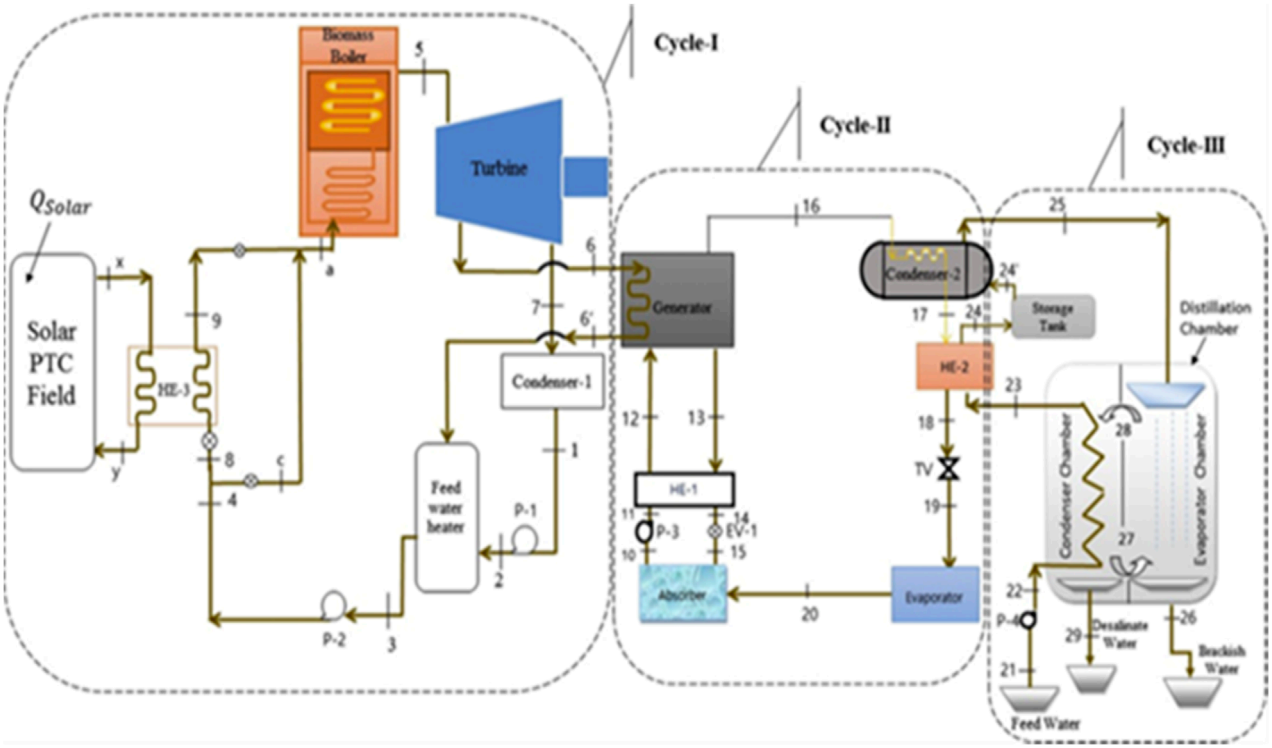

FIGURE 13
The combined ORC–VCC cycle and biomass boiler and PTC heating water circuits (Buentello-Montoya and Zhang, 2019).

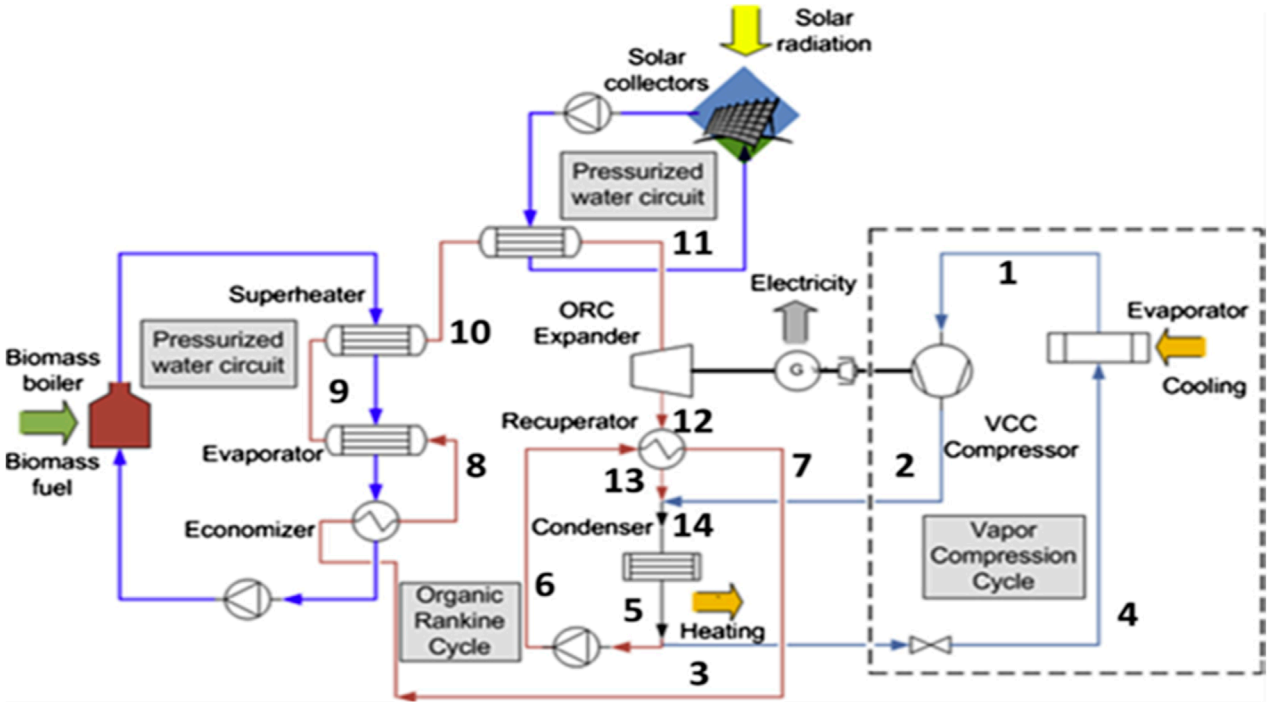

FIGURE 14
Schematic diagram of hybrid solar-biomass power plant with cooling and desalination in polygeneration process (Karellas and Braimakis, 2016).

3 Thermoeconomic assessment of energy systems

Economic studies of an energy system allow using costing equations, elaboration of estimation and optimisation algorithms, cost optimisation and low-cost energy systems and operations for thermoeconomic evaluation (Ahmadi and Dincer, 2011; Shamoushaki et al., 2017; Palazzo, 2013). Thermoeconomic studies, on the other hand, provide a balance between system efficiency and cost. Therefore, in designing and evaluating an energy system, the oil price, yearly equipment purchase cost (EPC), and functioning and management are valuable indicators for economic benefit analysis of energy systems by assessing several energy generation devices (Khanmohammadi et al., 2019; Goncalves and Arrieta, 2010; Boukelia et al., 2016). Hence, thermoeconomics is the art of saving natural resources that connects engineering and costing accounts through the Second Law of Thermodynamics. Energy systems are obtained from a set of sub-assemblies that network with one another environment and consume external resources that are transformed into products (Bakhshmand et al., 2015). Almutairi et al. (Valero and Cuadra, 2002) stated that the thermos-economic impact analysis of some power plants shows that the cost of destroying exergy is reduced. The suitability of thermo-economic study ranges to alternative energy areas of usefulness, such as heat engines, dewatering plants, refrigeration systems, etc. (Almutairi et al., 2016; Esen et al., 2007).

3.1 Thermoeconomic analysis and optimisation of energy systems

Thermoeconomics combines thermodynamics with principles of analytical accounting, and the main aim is minimising cost. In contrast to typical fiscal study, thermoeconomic provides a choice to examine and advance the operation of individual parts in the energy system (Taner, 2015). Hence, thermoeconomic appeared as a vital instrument to optimise the work of energy systems from both thermodynamic and economic perspectives. In thermoeconomics, the individual cost of part and stream is connected to its exergy subject. Capital expenditure of the mechanisms and the ecological influence are considered methodically for thermoeconomic optimisation of energy systems (Jamil et al., 2020). For energy transformation operations, accounting as a practice studies unit costs as it relates to energy. In view of this, several authors have suggested that budgets are preferably spread amid turnouts if management accounting is built on the thermodynamic exergy quantity. This is justified because exergy, but not energy, is often assigned economic value (Kopanos et al., 2017).

Numerous research studies on the relationship between thermodynamic (exergy) and economics analysis to evaluate quality output and optimisation of energy systems are stated in the literature. Pellegri (Dincer and Rosen, 2007) carried out a thermoeconomic and environmental study on sugarcane and ethanol for electricity generation in cogeneration plants. It was observed that a reduction in entropy resulted in a more efficient cogeneration operation, a reduction in exergy destruction and a better thermoeconomic and environmental operation. Oyedepo et al. (Pellegrini and de Oliveira Junior, 2011) conducted exergy estimation and quality assessment of carefully chosen gas turbine energy stations in Nigeria. From the study, the unit cost of electricity produced in the carefully chosen power plants varied from cents 1.98/kWh to cents 5.66/kWh. The result confirms that the combustion chamber had the highest exergy destruction cost in comparison to other components, as further confirmed by (Oyedepo et al., 2015a). Imran et al. (Athari et al., 2015b) introduced the thermo-economic improvement of fundamental ORC and regenerative ORC for waste heat recovery systems at consistent heat source conditions. In the examination, optimization was performed for five distinctive working fluids. The after-effects of the examination demonstrated that R245fa was the best working fluid under considered conditions, and basic ORC has a low explicit investment cost and thermal efficiency, which is in contrast to regenerative ORC. The sensitivity analysis revealed that evaporation pressure has promising effects on thermal efficiency and specific investment costs (Imran et al., 2014).

Bakhshmand et al. (Singh and Kaushik, 2014) investigated the thermos-economic analysis and optimisation of a triple-pressure combined cycle power station with one reheat stage (Figure 15). The total cost rate of the plate formed the optimisation objective function. The results showed that the optimisation process brought an increase of about 2.9% in energetic and exergetic efficiencies and a reduction of about 8.9% in the total thermos-economic cost.

4 Thermo-environmental analysis of energy systems

Recently, the environmental effects of unsustainable ways of energy consumption have been a serious concern, and the Second Law of thermodynamic analysis has been employed as an improvement method to (i) reduce atmospheric discharges and increase the life span of natural means through improving effectiveness and (ii) evaluate the probable influences of emissions. Thermo-environmental analysis combines the first two laws of thermodynamic examination and environment estimation to analyse thermodynamic efficiency and environmental impacts of energy systems components [Oyedepo et al. (Bakhshmand et al., 2015)]. The amalgamation of exergy and environmental studies unveils the interconnections among thermodynamic actions and environmental influences amid energy systems' constituents (Oyedepo et al., 2018).

Environmental impact for energy utilisation results in climate change, acid rain and ozone depletion. Carbon dioxide emissions cause harmful environmental effects when the resources are used. In this regard, estimating carbon dioxide emissions is a substantial part of making an environmental assessment. At the point when the exergy efficiency, overall cost of the equipment and CO_2 emissions are utilized for the improvement of mixed cycle power generation station with accompanying burning, the outcomes show that the cost of exergy destruction and losses diminished as the turbine inlet temperature expanded alongside burning compartment, the significant source of irreversibility (Keçebas and Gokgedik, 2015). The CO_2 discharge could be limited by upgrading the efficiency of the components and bringing down the fuel rate of flow. Almutairi et al. (Granet and Bluestein, 2000) also stated that variation in ambient temperature demonstrates climatic

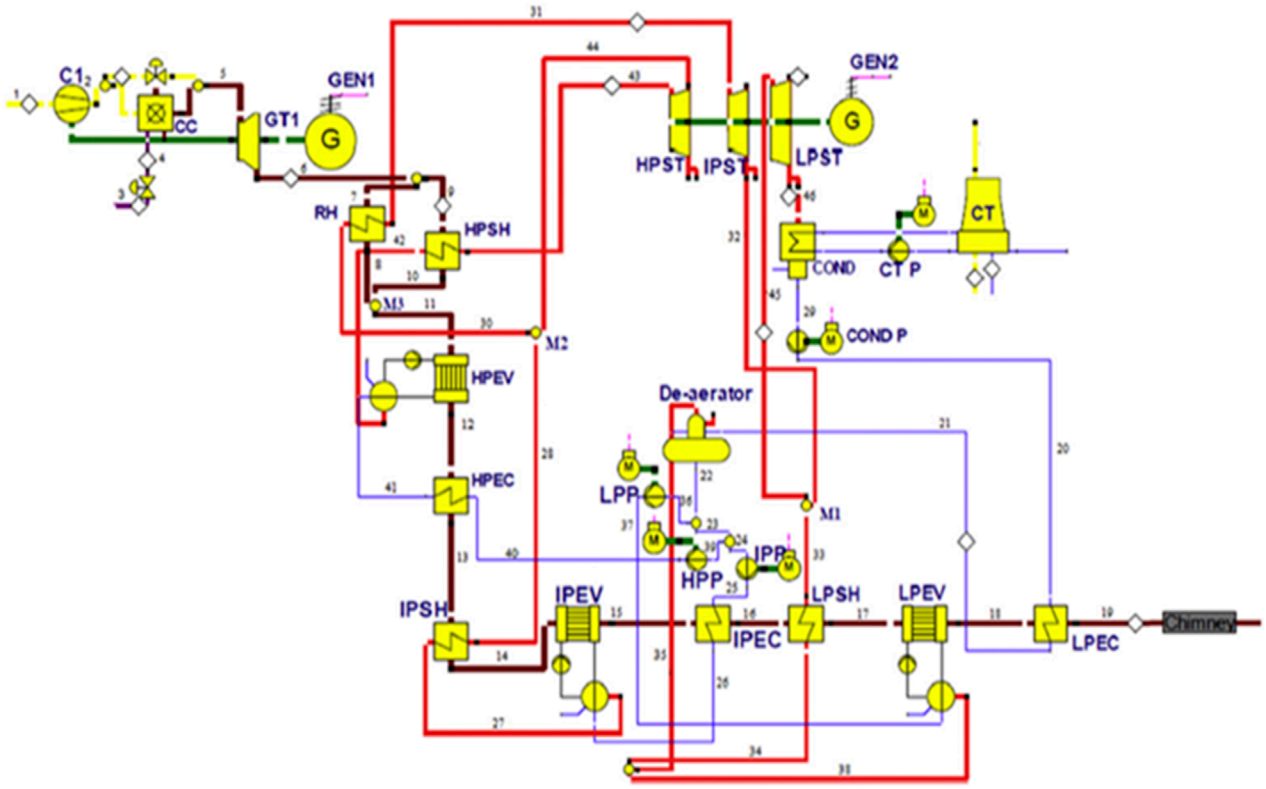

FIGURE 15
Schematic diagram of combined power plant with triple-pressure levels and one reheating stage (Singh and Kaushik, 2014).

circumstances about the location of a gas turbine. They further noted that the rise in ambient temperature reduces both exergetic efficiency and overall power outflow.

4.1 Thermo-environmental analysis and optimisation of energy systems

Research has shown that global warming is the utmost ecological task confronting the globe these days. Energy systems play a chief part in the emission of greenhouse gases. For example, about 21.2% of greenhouse gases are solely released by power stations (Oyedepo et al., 2015b). The need to understand the linkages between the first two laws of thermodynamics (energy and exergy) analysis and the ecological effect becomes more noteworthy due to the relations between exergy and the environment revealing the causal forms impacting environmental transformation. Recently, it has been shown that raising the exergy efficiency will reduce conditions for energy capacity and emissions. Moreover, exergy has been linked to ecological influence, as such a proportion from departing from the condition of a framework from the surrounding (Oyedepo et al., 2016; Baumgärtner and Arons, 2003).

The environmental analysis looks into the costs related to the movements of contaminants as well as the exergetic and economic costs of mass concentration and energy flows in energy devices (Jørgensen and Svirezhev, 2004). The rise of the exergy efficiency of these developments can decrease the environmental effect of energy transformation progressions. An increase in exergy efficiency will lessen the consumption of resources and consequently reduce the waste and the noxious discharge to the environment. This infers an enhancement in the ecological efficiency of these operations (de Oliveira, 2013).

Numerous studies related to the linkages between the first and second laws of thermodynamic analysis (exergy), and environmental impacts to assess the performance and optimisation of energy systems are reported (Pellegrini and de Oliveira Junior, 2011; Oyedepo et al., 2015b; Ahmadi and Dincer, 2010; Ahmadi and Dincer, 2011; Ameri et al., 2016). Owebor et al. (Amrollahi et al., 2011) carried out an energy, thermo-environmental and fiscal study for a projected municipal waste-propelled power station. The projected plant consisted of vaporization, solid oxide fuel cells, gas and steam turbines, absorption refrigeration, and organic Rankine cycles (Figure 16). Results of the study revealed that the fuel noxious release factor, explicit CO_2 discharge and sustainability exponent were 0.00097, 148.23 kg_{CO2}/MWh and 6.56, correspondingly. Moreover, the energy-economic sustainability exponent was shown, which considered the efficiency of the energy change progressions and its commercial effect on the people in terms of cost and social, economic state. Oyedepo et al. (2015b) presented an all-inclusive thermodynamic simulation and exergoenvironomic performance analysis for Nigeria's designated gas turbine power station. In the study, the exergo-environomic parameters computed were carbon (IV) oxide emission in kg per MWh of power generated, sustainability index, consumption number, price flow rate of

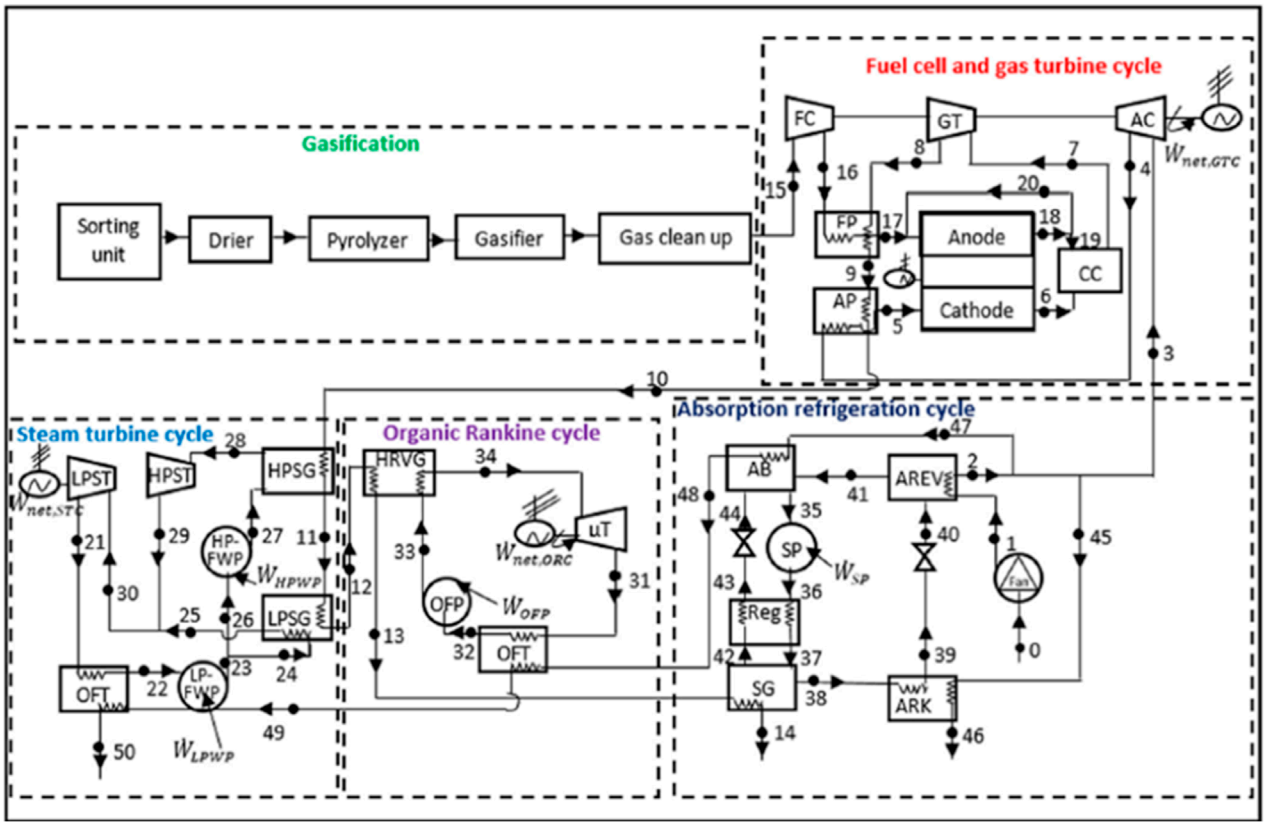

FIGURE 16
Schematics of an integrated gasification, SOFC, GT, ST, ORC and AR cycles (Amrollahi et al., 2011).

environmental effects in $/h and overall rate of cost of products in $/hr. Results of the study revealed that the combustion chamber was the utmost exergy-damaging section linked to other cycle components. However, the exergy ruin of this module is lessened by the growing gas turbine inlet temperature (GTIT). Moreover, it was observed that the thermodynamic inefficiency was responsible for the environmental power of gas turbine components. Hence, the study showed that CO_2 discharges and the cost of environmental impact decreased with increasing GTIT.

Ameri et al. (Jørgensen and Svirezhev, 2004) presented the exergoeconomic and ecological maximization of a selected huge steam generating station. The impact of additional air on exergy efficiency and noxious emissions were studied. Furthermore, the optimization process was presented by exergetic efficiency, standardized CO_2 emissions of the plant, and three diverse cost functions, including electricity costs, environmental impacts, and total plant costs. Aftereffects of the study revealed that the cost of electricity generation and the cost of environmental impacts diminished by 20.25% and 49.6%, respectively, at the optimum operating conditions of the plant. A thorough thermoeconomic and thermoenvironomic modeling and analysis of selected gas turbine power plants in Nigeria were presented by Oyedepo et al. (Pellegrini and de Oliveira Junior, 2011) utilizing the first and second laws of thermodynamics (exergy) principle. The consequences of the study uncovered that CO_2 emissions varied somewhere in the range of 100.18 and 408.78 kg CO_2/MWh for the selected power plants, while the cost rate of the green effect varied from 40.18 $/h to 276.97 $/h. It was additionally shown that CO_2 discharges and the consequence of environment influence diminished with growing GTIT. Meanwhile, the sustainability index of the plants increased with increasing GTIT.

Maraver et al., (2014) showed the thermodynamic streamlining of ORCs, combined alongside absorption or adsorption refrigeration components, for consolidated CCHP production from biomass burning. In the study, system modelling with the prime objective of proffering optimization procedures with the condition of operation of such systems was carried out. Furthermore, the energy and ecological execution of the distinctive ideal CCHP machine were explored. The study established that the trigeneration plant is capable of being designed in an energy-environmentally effective route with an n-pentane restorative ORC and a volumetric sort expander. Ahmadi et al. (Keçebas and Gokgedik, 2015) investigated exergoeconomic and environmental analyses for a mixed cycle and examined the impacts of additional burning on the effectiveness of bottoming cycle and CO_2 discharges. Memon et al. (2015) performed parametric-based thermoenvironmental and exergoeconomic analyses of a combined cycle power plant. Abam et al. (Memon et al., 2015) proposed an in-service turbine gas device, burned by gas to be modified with a steam turbine (ST), organic Rankine cycle (ORC), gas turbine (GT) for refrigeration and electricity generation, an adapted Kalina cycle (KC) for electricity development and refrigeration, and a vapour absorption system (VAS) for refrigeration (Figure 17). The integrated multi-generation

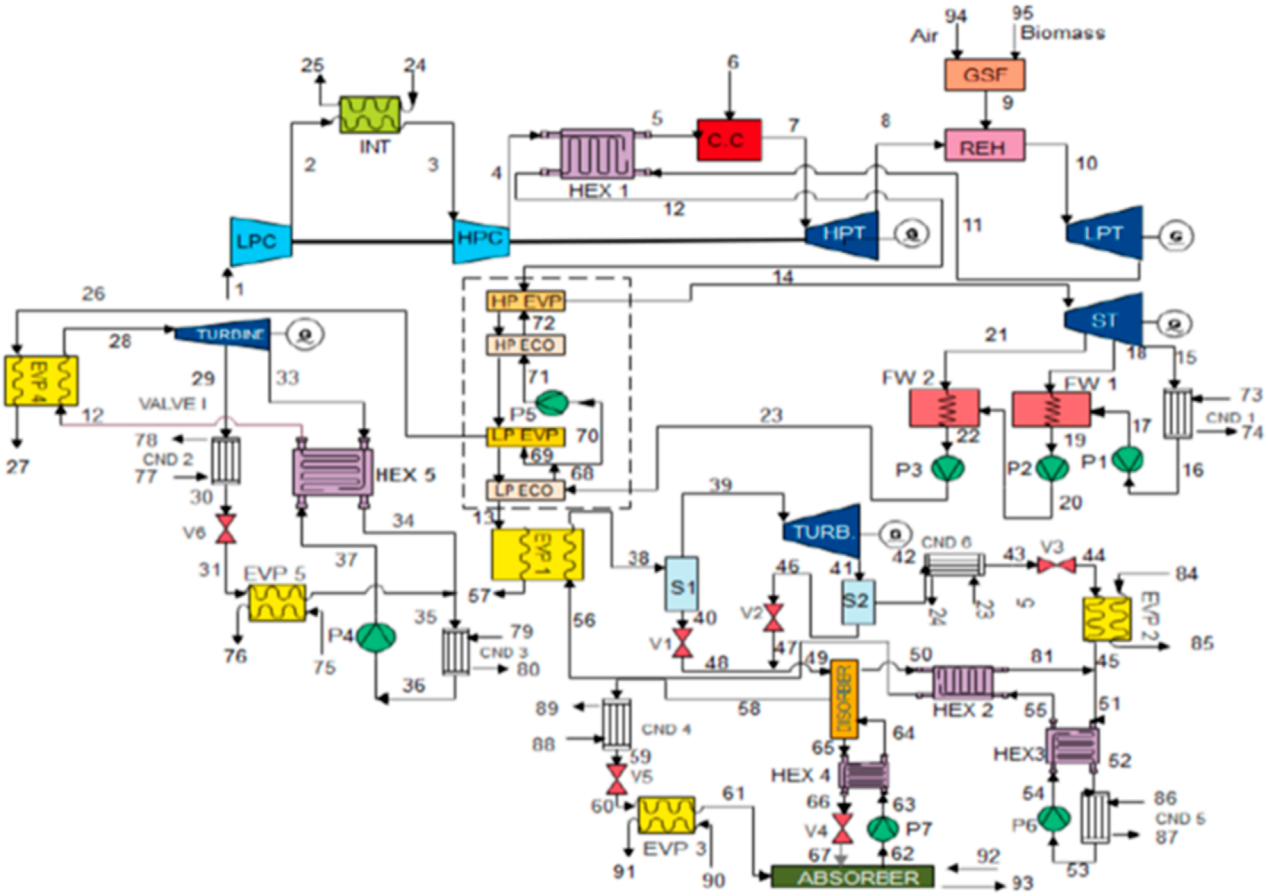

FIGURE 17
The proposed integrated multi-generation plant (Memon et al., 2015).

plant (IMP) was to be burned by biomass-based syngas as a supplementary firing source. Exergoeconomic and environmental analysis was carried out on the IMP. The after-effects of the study demonstrated that the planned system could propel the existing energy evolution predicament in the energy sector of Nigeria and workable energy approach to match the Agreement of Paris and Sustainable Development Goals (SDGs) strategy.

5 Assessment of sustainability indices (indicators) of energy systems

One of the fundamental ideas of sustainable development is sustainable energy development (SED). It ensures affordable, accessible energy for all while adhering to social and economic development requirements and the environment. Increasing the share of alternative energy sources in the energy mix, such as renewables, improving energy efficiency, and lowering greenhouse gas and air pollution emissions, are some of the actions that help implement the SED (Abam et al., 2020a). The evaluation criteria for the energy system's sustainability must consider the resource, environmental, social, and economic facets.

The process of converting energy from sources like fossil fuels and renewables into easily utilised forms, like electrical energy, propulsive energy, heating, and cooling, is known as energy conversion. The primary goal of the energy conversion systems sustainability evaluation is to ensure that options have been thoroughly considered and assessed for their potential short- and long-term impacts on the environment, economy, society, and other factors (Deng et al., 2022). In other words, when new and innovative energy systems are introduced for transportation, electric power generation, or industrial operations, it is prudent and essential to conduct a thorough sustainability assessment before moving forward with the execution of these innovative concepts. This is so because sustainability refers to an energy supply that is affordable, readily available, and likely has little to no impact on the environment (Chamchine et al., 2022).

Establishing a strong and comprehensive set of indicators to track the advancement of sustainable energy development is now essential, as sustainable development has made sustainable energy development a key goal of international policy. United Nations Sustainable Development Goal (SDG 7) calls for support in ensuring everyone can access affordable, clean energy (UN, 2015). This demonstrates the dedication to clean energy and sustainability. Affordable and sustainable electricity is essential for the growth of

business, communications, agriculture, healthcare, education, and transportation. Energy constraints impede human development and economic growth, especially in developing countries.

Setting up various suitable performance indicators is a prerequisite for measuring the effectiveness of energy conversion systems. A mix of thermodynamic, economic, and environmental indicators is considered to assess the technical, financial, and societal worth of the energy systems and guarantee that the chosen designs are well-suited to a sustainable development framework. Numerous general energy system performance indicators and new ones are included in the performance indicators below (Spelling, 2013). The sustainability indices of the energy systems listed below are examined based on the economic, environmental, and first and second laws of thermodynamics.

5.1 Enthalpic efficiency indicator (thermal efficiency)

Enthalpic change values (ΔH) are used to quantify "heat content," which is how the indicator gauges the efficiency of the process inputs and outputs. For every process, the enthalpic efficiency ratio can be calculated by dividing the ΔH value of the process's useable output by its inputs' ΔH value. Equation 1 can be used to compute enthalpic efficiency (Patterson, 1996):

$$\eta_{\Delta H} = \frac{\Delta H_{out}}{\Delta H_{in}} \tag{1}$$

where,

$\eta_{\Delta H}$ = enthalpic efficiency

ΔH_{out} = sum of the useful energy outputs of a process

ΔH_{in} = sum of the energy inputs into a process

For instance, a basic gas turbine has an enthalpic efficiency of roughly 33%. The enthalpic efficiency indicator evaluates the "useful" output. The conversion rate of chemical energy (ΔH) into electricity in this process is only 33%; the remaining 67% is lost as "waste" heat to the environment. When computing energy in enthalpic terms, the total output equals the total inputs if each activity's "waste" output is combined with the "useful" output from all processes. This is essentially another way of saying the first law of thermodynamics, which states that energy cannot be generated or destroyed during any type of conversion. Because of this, enthalpic efficiency is frequently referred to as first-law efficiency.

5.2 Thermal discharge index (TDI)

The number of thermal energy units released into the environment for every unit of electrical energy generated by a plant is known as the thermal discharge index of the power system. The following can be used to express it in power units (Ofodu and Abam, 2002).

$$TDI = \frac{Thermal\ energy\ discharged\ in\ to\ the\ environment(MW)}{Electrical\ output\ of\ the\ power\ plant(MW)} \tag{2a}$$

Every thermal power plant must have an index that is not zero to comply with the second law of thermodynamics; however, the index should be as low as feasible to maximize plant efficiency and maintain low pollution levels (Rajput, 2003; Labele-Alawa and Asuo, 2011; Abam et al., 2012). The thermal discharge index can be described as follows in terms of thermal efficiency, a crucial determinant of the index (Ofodu and Abam, 2002).

$$TDI = \frac{P_{th}(1-\eta_{th})}{P_{th}\eta_{th}} = \frac{1}{\eta_{th}} - 1 \tag{2b}$$

where Pth is the thermal energy input and η_{th} is the thermal efficiency.

5.3 Overall exergetic efficiency (OEE)

Exergy plays a significant role in identifying efficiency improvements and decreases in thermodynamic losses related to energy conversion processes. By lowering energy losses, exergy efficiency initiatives can lessen their adverse effects on the environment. Naturally, minimizing irreversibility or exergy loss results in an energy conversion process's most significant increase in exergy efficiency (Inoussah et al., 2017).

The overall exergy efficiency of an energy system can be calculated as the ratio of the total useful exergy output to the total exergy input. Equation 3 gives the expression for overall exergetic efficiency:

$$\dot{E}_{xoverall} = \left(\frac{\dot{E}_{xout}}{\dot{E}_{xin}}\right) \tag{3}$$

5.4 Exergy improvement potential (EIP)

An energy conversion system's exergy improvement potential measures how much and how quickly the system could be optimized. It is a thermodynamic method that combines effectiveness and exergy losses to provide a more comprehensive parameter of the system's performance (Rivero et al., 2004). By creating a hierarchy of the system's components and identifying its essential points, the exergy improvement potential enables the application of measures where they will be most effective.

The system's efficiency and exergy losses yield the exergetic improvement potential. Equation 4 is used to compute it (Hammond, 2004):

$$ExIP = (1-\varepsilon)I \tag{4}$$

where ExIP is the exergetic improvement potential, ε is the exergetic efficiency (%), and I is the exergy loss or irreversibility rate. This is computed by using Equation 5

$$I = \Delta E_{lost} = E_{in} - E_{out} > 0 \tag{5}$$

For a control volume at a steady state Equation 6 is used to compute, the exergetic efficiency

$$\varepsilon = \frac{\dot{E}_P}{\dot{E}_F} = 1 - \frac{\dot{E}_D + \dot{E}_L}{\dot{E}_F} \tag{6}$$

where the rates at which the fuel is supplied and the product is generated are denoted by $\dot{E}_F$ and $\dot{E}_P$, respectively. $\dot{E}_D$ and $\dot{E}_L$ denote the exergy destruction and loss rates, respectively.

In any real energy conversion process (irreversible), exergy is degraded, and the exergy efficiency is consequently less than unity. According to Van Gool, (1992), the maximum improvement in the exergy efficiency for a process or system is achieved when ΔE_{lost} is minimized.

5.5 Environmental effect factor (EEF)

An indicator of the extent of environmental harm caused by waste exergy destruction is termed the environmental effect factor (EEF). The EEF is a crucial thermo-sustainability indicator as it indicates whether environmental damage results from the destruction of waste exergy. According to Equation 7, the EEF is defined as (Aydin, 2013; Abam et al., 2018):

$$EEF = \frac{Waste\ exergy\ ratio}{Exergy\ efficiency} \tag{7}$$

5.6 Exergetic sustainability index (ESI)

When evaluating the energy system's sustainability, the exergetic sustainability index (ESI) is a crucial objective parameter among the sustainability indicators. This index has values between the intervals of 0 and ∞. The higher efficiency of the energy system means a low waste-exergy ratio and low environmental effect factor; as a result, there is a higher ESI. Studies have indicated that enhancing exergy efficiency can reduce environmental impacts by reducing energy wastage. These procedures result in higher exergy efficiency and lower exergy losses within the bounds of exergy methods (Midilli and Dincer, 2009). For example, an excellent fuel economy enables the energy conversion process to support exergy-based sustainability since it lowers resource requirements and environmental implications. Hence, ESI helps to assess the capacity and effective utilization and preservation of energy resources.

The relation between exergy efficiency and exergetic sustainability index is given by Equation 8:

$$ESI = \frac{\eta_{ex}}{1 - \eta_{ex}} \tag{8}$$

Where,

η_{ex} is the exergy efficiency, and it is defined as the ratio of useful, final, value and input value, i.e.,

$$\eta_{ex} = \frac{Ex_i}{Ex_p}$$

ESI is also defined as the extent of sustainability and can also be calculated as a reciprocal of the EEF and it is given by Equation 9 (Abam et al., 2018):

$$ESI = \frac{1}{Environmental\ Effect\ Factor} = \frac{1}{EFF} \tag{9}$$

5.7 Depletion number

Reducing the damaging emissions into the environment from energy conversion systems (which burn fossil fuels) has been shown to improve system efficiency, extending the life span of the fuel resources and boosting sustainability. Researchers have established the links among sustainability, exergy efficiency, and environmental effects (Connelly and Koshland, 1997).

Studies have shown that efficient fuel consumption is characterized by a depletion number defined and computed by using Equation 10:

$$D_p = \frac{\dot{E}_{dest}}{\dot{E}_{xin}} \tag{10}$$

Where $\dot{E}_{dest}$ is the exergy destruction, and $\dot{E}_{xin}$ is the exergy input by fuel consumption. The relationship between the depletion number and the exergy efficiency is given by Equation 11:

$$\eta_{ex} = 1 - D_p \tag{11}$$

According to Altayib, (2011), the sustainability of the fuel resource can be expressed by a sustainability index (SI) as the inverse of the depletion number and is computed by using Equation 12:

$$SI = \frac{1}{D_p} \tag{12}$$

5.8 Environmental impact factor (EIF)

This factor indicates whether the exergy losses damage the environment. The environmental impact factor is defined as the inverse of the exergetic sustainability index and computed by using Equation 13:

$$EIF = \frac{1}{SI} \tag{13}$$

A high environmental effect factor translates into a low exergetic sustainability index, while a low environmental impact factor translates into a high exergetic sustainability index. When evaluating the environmental impact and sustainability of energy processes, the exergy technique of study is a useful tool. According to research, combustion is a highly irreversible process with a small exergy sustainability index and low exergy efficiency when directly producing heat at a low temperature. As a result, it greatly impacts the environment and raises CO_2 emissions (Gojak and Bajc, 2019).

5.9 Waste exergy ratio (WER)

The energy conversion system transforms energy from primary sources into conveniently used forms. During the conversion processes, some exergy is destroyed in the engine components, and some exergy is lost by hot exhaust gases that are discharged into the environment. Hence, the total waste exergy is calculated as the sum of both the destructed exergy and loss exergy of the system. For a given energy system, total waste exergy (WE) is evaluated using Equation 14, while waste exergy ratio (WER) is expressed as the ratio of the total WE to the overall exergy input, and it is shown in Equation 15 (Aydin, 2013):

$$\sum \dot{E}x_{we,out} = \sum \dot{E}x_{dest,out} + \sum \dot{E}x_{loss,out} \tag{14}$$

$$WER = \frac{Total\ exergy\ waste}{Overall\ exergy\ input} \quad (15)$$

5.10 Exergetic utility index (EUI)

The exergetic utility index (EUI) measures the extent of exergy resource utilization in an energy system regarding the same system's net output. It is a function of combustion chamber efficiency, η_{CC}, net output, W_{net}, exergy input, E_{xin} and the exergy efflux to the environment, E_{xout}. EUI shows the degree to which exergy of the resource input is used for work production. EUI is calculated using Equation 16 (Abam et al., 2020b):

$$EUI = \frac{\eta_{CC}\dot{W}_{net\cdot}}{\dot{E}_{xin} - \dot{E}_{xout}} \quad (16)$$

The small values of EUI presaged poor process conversion, especially for multi-generation energy systems.

5.11 Exergo-thermal index (ETI)

The thermal effect of an energy system on the environment while converting energy is measured by the exergo-thermal index (ETI). Low ETI values can be attained by continually powering other low-heat bottoming cycles with high-temperature flue gas from energy conversion systems. The expression for ETI is given by using Equation 17 (Aydin, 2013; Abam et al., 2018):

$$ETI = \frac{EUI}{\beta} = \frac{\eta_{CC} x \dot{W}_{net}}{(\dot{E}_{xin} - \dot{E}_{xout})} X \frac{1}{\beta} \quad (17)$$

where β is the thermal pollution factor (enviro-thermal conservation factor) and can be computed by using Equation 18:

$$\beta = \frac{T_{Ref}}{T_{Fg}} \quad (18)$$

T_{ref} is the environmental temperature, and T_{Fg} is the temperature of the exhaust stream (fluid gases). Research has shown that the ETI increases with an increase in T_{Fg}; the low values of ETI are desired and connote less environmental impact (Abam et al., 2020b).

5.12 The *specific energy costs* (C′)

This is an economic–thermodynamic indicator, and it is defined as the ratio of total energy system costs (including all costs for investment and operation) *C* and the final energy demand FE (Klemm and Wiese, 2022). It is computed using Equation 19:

$$\dot{C}_E = \frac{C}{FE} \quad (19)$$

When the absolute cost of an energy system is considered for optimization purposes, the specific energy cost (ce) is expressed as the ratio of the average annual cost of energy produced (TC_{av}) to the average annual supplied energy amount (E_{av}) during the life cycle of the energy system, expressed by Equation 20 (Su, 2020):

$$\dot{C}_E = \frac{TC_{av}}{E_{av}} \quad (20)$$

5.13 Consistency indicators for energy systems

By replacing non-renewable resources with renewable ones, energy consistency seeks to transform the energy production and use paradigm. Using renewable energy sources rather than fossil fuels is one well-known example. Moving from fossil fuels to renewable energy sources is the most common definition of energy consistency. Therefore, it is possible to view the share of renewables (SoR) as a suitable metric of energy consistency (Samadi et al., 2017). This is computed by using Equation 21 :

$$SoR = \frac{FE_{Ren}}{FE_T} \quad (21)$$

An energy source cannot be used more than its rate of regeneration in order to be considered sustainable. In this case, the usable life t_{use} of materials utilized in an energy system in proportion to its regeneration time t_{reg} could be used to evaluate the system's consistency. This can be obtained by using Equation 22:

$$t = \sum_{1}^{n} \frac{t_{use,n}}{t_{reg,n}} \quad (22)$$

In order to obtain a meaningful value of consistency energy indicator, all materials used within an energy system, for example, from the concrete in the foundation of a power plant up to the fuel consumption, must be taken into account.

6 Conclusions

This paper extensively appraises the thermodynamics, thermo-economic and thermo-environmental analysis and enhancement of energy conversion systems for sustainable development. Also discussed are several appropriate performance indicators applied by researchers for assessing the performance of energy systems. A combination of thermodynamic, economic and environmental indicators was considered to evaluate the technical, financial and societal value of energy systems and thus ensure that the selected designs fit well within a sustainable development framework. Based on the outcome of this review study, it can be concluded that:

- The sustainability of the energy conversion system can be enhanced by assessing exergy techniques. Based on the exergetic approach, as exergy efficiency is getting closer to 100%, sustainability is getting closer to infinity because the process is getting closer to reversibility, and the environmental effect is getting closer to zero as energy is transformed without any loss.
- By reducing energy losses, exergy efficiency initiatives can lessen their adverse environmental effects. These techniques result in lower exergy losses and higher exergy efficiency within the context of exergy approaches.

- It is evident that when exergy loss or irreversibility is kept to a minimum, a process or system will increase its exergy efficiency to the greatest extent possible.
- By presenting a hierarchy of the energy system's components, the exergy improvement potential indicator allows for determining the system's crucial points and applying measures where they will have the most significant impact.
- Sustainable energy development depends on the availability of affordable, reliable energy from environmentally friendly sources.
- The best methods for efficient use of energy resources, low energy production costs, and less environmental impact are provided by hybrid energy systems (i.e., integrating conventional and renewable energy systems) and adopting multi-generation technologies.
- Maintaining the current conventional energy systems, which rely on fossil fuels and thermal energy conversion, seriously impacts climate change and global warming. As such, if we are to fulfil and surpass sustainable development goals worldwide, a paradigm shift in the energy-producing sector is needed.
- While some performance indicators are appropriate for assessing different facets of energy sustainability, none can capture the total energy sustainability of energy systems. Therefore, using a single performance metric to optimize the energy process results in improbable outcomes. Multi-criteria techniques, which allow for a more comprehensive optimization and planning of sustainable energy systems, should be utilized to prevent this.
- Direct low-temperature heat production through combustion has a low exergy sustainability index and low exergy efficiency and is irreversible. As a result, it has a significant environmental impact and produces considerable CO_2 emissions. If at all possible, such combustion processes ought to be reduced or prevented.

An energy-efficient system assures sustainable development. A deliberate improved system as a function of exergy analysis will usher in energy systems' reliability, sustainability and cost-effectiveness. Hence, a study like this aids in evaluating the exhibition of energy transformation measures on a thermodynamics premise and by adding fiscal and ecological perspectives and effects of the studied procedures. This comprehensive review of energy system performance and optimization would not only assist in effective energy properties use but also be one of the utmost characteristics in the establishment of justifiable methods of energy resource utilization.

Author contributions

SO: Writing–review and editing, Writing–original draft, Resources, Project administration, Methodology, Conceptualization. MW: Writing–review and editing, Writing–original draft, Validation, Methodology, Investigation. FA: Writing–review and editing, Project administration, Methodology, Investigation. JD: Writing–original draft, Validation, Methodology. OS: Writing–review and editing, Validation, Methodology, Investigation. OA: Writing–review and editing, Validation, Investigation. TS: Writing–review and editing, Validation. AP: Writing–review and editing, Validation, Methodology. OK: Writing–review and editing, Validation. PB: Writing–review and editing, Validation.

Funding

The author(s) declare that no financial support was received for the research, authorship, and/or publication of this article.

Conflict of interest

The authors declare that the research was conducted in the absence of any commercial or financial relationships that could be construed as a potential conflict of interest.

Publisher's note

References

Abam, F. I., Diemuodeke, O. E., Ekwe, E. B., Alghassab, M., Samuel, O. D., Khan, Z. A., et al. (2020a). Exergoeconomic and environmental modeling of integrated polygeneration power plant with biomass-based syngas supplemental firing. *Energies* 13, 6018–6027. doi:10.3390/en13226018

Abam, F. I., Diemuodeke, O. E., Ekwe, E. B., Alghassab, M., Samuel, O. D., Khan, Z. A., et al. (2020b). Exergoeconomic and environmental modeling of integrated polygeneration power plant with biomass-based syngas supplemental firing. *Energies* 13, 6018. doi:10.3390/en13226018

Abam, F. I., Ekwe, B. E., Samuel, O., Effiom, S. O., and Afangideh, C. B. (2018). Performance and thermo-sustainability analysis of non-hybrid organic Rankine cycles (ORCs) at varying heat source and evaporator conditions. *Aust. J. Mech. Eng.*, 1–14. doi:10.1080/14484846.2017.1373585

Abam, F. I., Ugot, I. U., and Igbong, D. I. (2012). Performance analysis and components irreversiblities of a (25 MW) gas turbine power plant modeled with a spray cooler. *Am. J. Eng. Appl. Sci.* 5 (1), 35–41. doi:10.3844/ajeassp.2012.35.41

Adibhatla, A., and Kaushik, S. C. (2017). Energy, exergy and economic (3E) analysis of integrated solar direct steam generation combined cycle power plant. *Sustain. Energy Technol. Assessments* 20, 88–97. doi:10.1016/j.seta.2017.01.002

Agarwal, S., Arora, A., and Arora, B. B. (2021). Energy and exergy investigations of r1234YF and r1234ZE as r134A replacements in mechanically subcooled vapour compression refrigeration cycle. *J. Therm. Eng.* 7 (1), 109–132. doi:10.18186/thermal.846561

Agarwal, S. K. S. S., and Mishra, R. S. (2011). Performance improvement of a simple gas turbine cycle through integration of inlet air evaporative cooling and steam injection. *J. Sci. industrial Res.* 70, 544–533.

Aghbashlo, M., Hosseinzadeh-Bandbafha, H., Shahbeik, H., and Tabatabaei, M. (2022). The role of sustainability assessment tools in realizing bioenergy and bioproduct systems. *Biofuel Res. J.* 35, 1697–1706. doi:10.18331/brj2022.9.3.5

Ahmadi, M. H., Ahmadi, M. A., Pourfayaz, F., Bidi, M., and Açıkkalp, E. (2016b). Multi-objective optimization and exergetic-sustainability of an irreversible nano scale Braysson cycle operating with Maxwell–Boltzmann gas. *Alex. Eng. J.* 55, 1785–1798. doi:10.1016/j.aej.2016.03.034

Ahmadi, M. H., Ahmadi, M. A., and Sadatsakkak, S. A. (2015). Thermodynamic analysis and performance optimization of irreversible Carnot refrigerator by using multi-objective evolutionary algorithms (MOEAs). *Renew. Sustain. Energy Rev.* 51, 1055–1070. doi:10.1016/j.rser.2015.07.006

Ahmadi, M. H., Mehrpooya, M., and Pourfayaz, F. (2016a). Thermodynamic and exergy analysis and optimization of a transcritical CO2 power cycle driven by geothermal energy with liquefied natural gas as its heat sink. *Appl. Therm. Eng.* 109, 640–652. doi:10.1016/j.applthermaleng.2016.08.141

Ahmadi, P., and Dincer, I. (2010). Exergoenvironmental analysis and optimization of a cogeneration plant system using Multimodal Genetic Algorithm (MGA). *Energy* 35, 5161–5172. doi:10.1016/j.energy.2010.07.050

Ahmadi, P., and Dincer, I. (2011). Thermodynamic and exergoenvironmental analyses, and multi-objective optimization of a gas turbine power plant. *Appl. Therm. Eng.* 31, 2529–2540. doi:10.1016/j.applthermaleng.2011.04.018

Ahmadi, P., Dincer, I., and Rosen, M. (2011b). Exergy, exergoeconomic and environmental analyses and evolutionary algorithm based multi-objective optimization of combined cycle power plants. *Energy* 36 (10), 5886–5898. doi:10.1016/j.energy.2011.08.034

Ahmadi, P., Dincer, I., and Rosen, M. A. (2012). Exergo-environmental analysis of an integrated organic Rankine cycle for trigeneration. *Energy Convers. Manage* 64, 447–453. doi:10.1016/j.enconman.2012.06.001

Ahmadi, P., Dincer, I., and Rosen, M. A. (2013). Thermodynamic modeling and multi-objective evolutionary-based optimization of a new multigeneration energy system. *Energy Convers. Manag.* 76, 282–300. doi:10.1016/j.enconman.2013.07.049

Ahmadi, P., Rosen, M. A., and Dincer, I. (2011a). Greenhouse gas emission and exergo-environmental analyses of a trigeneration energy system. *Int. J. Greenh. Gas. Control* 5, 1540–1549. doi:10.1016/j.ijggc.2011.08.011

Akbari, M., Khodayari, M., Danesh, M., Davari, A., and Padash, H. (2020). A bibliometric study of sustainable technology research, *Cogent Bus. and Manag.* 7:1751906. doi:10.1080/23311975.2020.1751906

Akyuz, E., Coskun, C., Oktay, Z., and Dincer, I. (2012). A novel approach for estimation of photovoltaic exergy efficiency. *Energy* 44 (1), 1059–1066. doi:10.1016/j.energy.2012.04.036

Al-Ali, M., and Dincer, I. (2014). Energetic and exergetic studies of a multigenerational solar geothermal system. *Appl. Therm. Eng.*, 71, 16–23. doi:10.1016/j.applthermaleng.2014.06.033

Alibaba, M., Pourdarbani, R., Manesh, M. H. K., Ochoa, G. V., and Forero, J. D. (2020). Thermodynamic, exergo-economic and exergo-environmental analysis of hybrid geothermal-solar power plant based on ORC cycle using emergy concept. *Heliyon* 6, 037588–e3812. doi:10.1016/j.heliyon.2020.e03758

Almutairi, A., Pilidis, P., and Al-Mutawa, N. (2015). Energetic and exergetic analysis of combined cycle power plant: Part-1 operation and performance. *Energies* 8 (12), 14118–14135. doi:10.3390/en81212418

Almutairi, A., Pilidis, P., and Al-Mutawa, N. (2016). Exergoeconomic and sustainability analysis of reheat gas turbine engine. *Am. J. Energy Res.* 4, 1–10. doi:10.12691/ajer-4-1-1

Al-Qayim, K. A. Integrated solar thermal combined cycle for power generation in Iraq (2019), *IOP Conf. Ser. Mater. Sci. Eng.*, 518, 4. 042002. doi:10.1088/1757-899x/518/4/042002

Al-Sayyab, A. K. S., and Abdulwahid, M. A. (2019). Energy-exergy analysis of multistage refrigeration system and flash gas intercooler working with ozone-friendly alternative refrigerants to R134a. *J. Adv. Res. Fluid Mech. Therm. Sci.* 63 (2), 188–198.

Alta, D., Bilgili, E., Ertekin, C., and Yaldiz, O. (2010). Experimental investigation of three different solar air heaters: energy and exergy analyses. *Appl. Energy* 87, 2953–2973. doi:10.1016/j.apenergy.2010.04.016

Altayib, K. (2011). *Energy, exergy and exergoeconomic analyses of gas-turbine based systems*. Canada: University of Ontario Institute of Technology. MSc Thesis.

Ameri, M., Mokhtari, H., and Bahrami, M. (2016). Energy, exergy, exergoeconomic and environmental (4E) optimization of a large steam power plant: a case study. *J. Sci. Technol. Trans. Mech. Eng.* 40, 11–20. doi:10.1007/s40997-016-0002-z

Amrollahi, Z., Ertesvag, I., and Bolland, O. (2011). Thermodynamic analysis on post-combustion CO2 capture of natural-gas fired power plant. *Int. J. Greenh. Gas. Control* 5, 422–426. doi:10.1016/j.ijggc.2010.09.004

Annamalai, S., Santhanam, M., Selvaraj, S., Sundaram, M., Pandian, K., and Pazos, M. (2018). "Green technology": bio-stimulation by an electric field for textile reactive dye contaminated agricultural soil. *Sci. Total Environ.* 624, 1649–1657. doi:10.1016/j.scitotenv.2017.10.047

Aprea, C., de Rossi, F., Greco, A., and Renno, C. (2003). Refrigeration plant exergetic analysis varying the compressor capacity. *Int. J. Energy Res.* 27, 653–669. doi:10.1002/er.903

Arora, A., and Kaushik, S. (2008). Theoretical analysis of a vapour compression refrigeration system with R502, R404A and R507A. *Int. J. Refrig.* 31, 998–1005. doi:10.1016/j.ijrefrig.2007.12.015

Asim, M., Saleem, S., Imran, M., Leung, M. K. H., Hussain, S. S. A., Miró, L. S., et al. (2020). Thermo-economic and environmental analysis of integrating renewable energy sources in a district heating and cooling network. *Energy Effic.* 13, 79–100. doi:10.1007/s12053-019-09832-9

Assareh, E., Agarwal, N., Paul, M. C., Ahmadi, P., Ghodrat, M., and Lee, M. (2023). Investigation and development of a novel solar-biomass integrated energy system for clean electricity and liquid hydrogen production. *Therm. Sci. Eng. Prog.* 42 (1), 101925. doi:10.1016/j.tsep.2023.101925

Athari, H., Soltani, S., B¨olükbas¸i, A., Rosen, M. A., and Morosuk, T. (2015a). Comparative exergoeconomic analyses of the integration of biomass gasification and a gas turbine power plant with and without fogging inlet cooling. *Renew. Energy* 76, 394–400. doi:10.1016/j.renene.2014.11.064

Athari, H., Soltani, S., Rosen, M. A., Gavifekr, M. K., and Morosuk, T. (2016a). Exergoeconomic study of gas turbine steam injection and combined power cycles using fog inlet cooling and biomass fuel. *Renew. Energy* 96, 715–726. doi:10.1016/j.renene.2016.05.010

Athari, H., Soltani, S., Rosen, M. A., Mahmoudi, S. M. S., and Morosuk, T. (2015b). Comparative exergoeconomic analyses of gas turbine steam injection cycles with and without fogging inlet cooling. *Sustainability* 7, 12236–12257. doi:10.3390/su70912236

Athari, H., Soltani, S., Rosen, M. A., Mohammad, S., Mahmoudi, S., and Morosuk, T. (2016b). Gas turbine steam injection and combined power cycles using fog inlet cooling and biomass fuel: a thermodynamic assessment. *Renew. Energy* 92, 95–103. doi:10.1016/j.renene.2016.01.097

Aydin, H. (2013). Exergetic sustainability analysis of LM6000 gas turbine power plant with steam cycle. *Energy* 57, 766–774. doi:10.1016/j.energy.2013.05.018

Bakhshmand, S., Saray, R., Bahlouli, K., Eftekhari, H., and Ebrahimi, A. (2015). Exergoeconomic analysis and optimization of a triple-pressure combined cycle plant using evolutionary algorithm. *Energy* 93, 555–567. doi:10.1016/j.energy.2015.09.073

Barzegar- Avval, H., Ahmadi, P., Ghaffarizadeh, A., and Saidi, M. (2011). Thermo-economic-environmental multiobjective optimization of a gas turbine power plant with preheater using evolutionary algorithm. *Int. J. Energy Res.* 35, 389–403. doi:10.1002/er.1696

Baumgärtner, S., and Arons, J. D. S. (2003). Necessity and inefficiency in the generation of waste: a thermodynamic analysis. *J. Industrial Ecol.* 7 (2), 113–123. doi:10.1162/108819803322564389

Bejan, A., Tsatsaronis, G., and Moran, M. (1996). *Thermal design and optimization*. Canada: John Wiley and Sons, Inc, 558.

Bhattacharya, A., Manna, D., Paul, B., and Datta, A. (2011). Biomass integrated gasification combined cycle power generation with supplementary biomass firing: energy and exergy based performance analysis. *Energy* 36, 2599–2610. doi:10.1016/j.energy.2011.01.054

Bianchi, M., Cherubini, F., Pascale, A. De, Peretto, A., and Elmegaard, B. (2006) *Cogeneration from poultry industry wastes: indirectly fired gas turbine application*, 31, 1417–1436.

Bishoge, O. K., Kombe, G. G., and Mvile, B. N. (2020). Renewable energy for sustainable development in sub-Saharan African countries: challenges and way forward. *J. Renew. Sustain. Energy* 12, 052702. doi:10.1063/5.0009297

Bobbo, S., Fedele, L., Curcio, M., Bet, A., De Carli, M., Emmi, G., et al. (2019). Energetic and exergetic analysis of low global warming potential refrigerants as substitutes for R410A in ground source heat pumps. *Energies* 12 (3538), 3538–3616. doi:10.3390/en12183538

Bolaji, B. O. (2010). Exergetic performance of a domestic refrigerator using R12 and its alternative refrigerants. *J. Eng. Sci. Technol.* 5 (4), 435–446.

Boonnasa, S., Namprakai, P., and Muangnapo, T. (2006). Performance improvement of the combined cycle power plant by intake air cooling using an absorption chiller. *Energy* 31, 2036–2046. doi:10.1016/j.energy.2005.09.010

Borokinni, F. O., Bolaji, B. O., and Ismail, A. A. (2018). Eksperimentalna analiza svojstava ekološki prihvatljivih radnih tvari R510A i R600a u modificiranome parnome kompresorskome rashladnom sustavu. *NASE MORE* 65 (1), 11–17. doi:10.17818/nm/2018/1.2

Bouam, A., Aïssani, S., and Kadi, R. (2008). Gas turbine performances improvement using steam injection in the combustion chamber under Sahara conditions. *Oil and Gas Sci. Technology– Rev. IFP* 63 (2), 251–261. doi:10.2516/ogst:2007076

Boukelia, T. E., Arslan, O., and Mecibah, M. S. (2016). ANN-based optimization of a parabolic trough solar thermal power plant. *Appl. Therm. Eng.* 107, 1210–1218. doi:10.1016/j.applthermaleng.2016.07.084

Boyaghchi, F. A., and Chavoshi, M. (2017). Multi-criteria optimization of a micro solar-geothermal CCHP system applying water/CuO nanofluid based on exergy,

exergoeconomic and exergoenvironmental concepts. *Appl. Therm. Eng.* 112, 660–675. doi:10.1016/j.applthermaleng.2016.10.139

Boyaghchi, F. A., and Sabaghian, M. (2016). Multi objective optimisation of a Kalina power cycle integrated with parabolic trough solar collectors based on exergy and exergoeconomic concept. *Int. J. Energy Technol. Policy* 12, 154–180. doi:10.1504/ijetp.2016.075673

Buentello-Montoya, D., and Zhang, X. (2019). An energy and exergy analysis of biomass gasification integrated with a char-catalytic tar reforming system. *Energy fuels.* 33 (9), 8746–8757. doi:10.1021/acs.energyfuels.9b01808

Chamchine, A. V., Makhviladze, G. M., and Vorobyev, O. G. (2022). Thermodynamic indicators for integrated assessment of sustainable energy Technologies. *Int. J. Low Carbon Technol.* 1 (1), 69–78. doi:10.1093/ijlct/1.1.69

Chen, H., Xue, K., Wu, Y., Xu, G., Jin, X., and Liu, W. (2020). Thermodynamic and economic analyses of a solar-aided biomass-fired combined heat and power system. *Energy* 214, 119023. doi:10.1016/j.energy.2020.119023

Connelly, L., and Koshland, C. P. (1997). Two aspects of consumption: using an exergy-based measure of degradation to advance the theory and implementation of industrial ecology. *Resour. Conservation Recycl.* 19 (3), 199–217. doi:10.1016/s0921-3449(96)01180-9

Das, P., Dutta, S., Singh, K. K. K. K., and Maity, S. (2019). Energy saving integrated membrane crystallization: a sustainable technology solution. *Sep. Purif. Technol.* 228, 115722. doi:10.1016/j.seppur.2019.115722

Demirel, Y. (2012). *Energy production, conversion, storage, conservation, and coupling*. Springer-Verlag London Limited, 180–190.

Deng, D., Li, C., Zu, Y., Liu, L. Y. J., Zhang, J., and Wen, S. (2022). A systematic literature review on performance evaluation of power system from the perspective of sustainability. *Front. Environ. Sci.* 10 (10), 1–20. doi:10.3389/fenvs.2022.925332

de Oliveira, S. (2013). *Exergy production, cost and renewability*. Springer-Verlag London, 130–135.

De Souza-Santos, M. L. (1999). A feasibility study of an alternative power generation system based on biomass gasification/gas turbine concept. *Fuel* 78 (5), 529–538. doi:10.1016/s0016-2361(98)00181-1

Dincer, I., and Cengel, Y. A. (2001). Energy, entropy and exergy concepts and their roles in thermal engineering. *Entropy* 3, 116–149. doi:10.3390/e3030116

Dincer, I., Midilli, A., and Kucuk, H. (2014). *Progress in exergy, energy, and the environment*. Springer International Publishing Switzerland, 850–870.

Dincer, I., and Rosen, M. A. (2007). *Exergy: energy, environment and sustainable development*. Oxford OX2 8DP, UK: Elsevier, Linacre House, Jordan Hill, 473.

Doseva, N., and Chakyrova, D. (2015). Energy and exergy analysis of cogeration system with biogas engines. *J. Therm. Eng.* 1 (3), 391–401. doi:10.18186/jte.75021

Echegaray, M. E., Castro, M. R., Mazza, M. G. D., and Rodriguez, G. I. R. A. (2016). Exergy analysis of syngas production via biomass thermal gasification. *Int. J. Thermo.* 19 (3), 178–184. doi:10.5541/ijot.5000182576

Esen, H., Inalli, M., Esen, M., and Pihtili, K. (2007). Energy and exergy analysis of a ground-coupled heat pump system with two horizontal ground heat exchangers. *Build. Environ.* 42 (10), 3606–3615. doi:10.1016/j.buildenv.2006.10.014

Fagbenle, R. O., Adefila, S. S., Oyedepo, S. O., and Exergy, O. M. (2014). Exergoeconomic and exergoenvironomic analyses of selected gas turbine power plants in Nigeria. *ASME Int. Mech. Eng. Congr. Expo.*, 1–13. doi:10.1115/IMECE2014-40311

Farzaneh-Gord, M., and Deymi-Dashtebayaz, M. (2009). A new approach for enhancing performance of a gas turbine (case study: khangiran refinery). *Appl. Energy* 86, 2750–2759. doi:10.1016/j.apenergy.2009.04.017

Ghaebi, H., Parikhani, T., Rostamzadeh, H., and Farhang, B. (2018). Proposal and assessment of a novel geothermal combined cooling and power cycle based on Kalina and ejector refrigeration cycles. *Appl. Therm. Eng.* 130, 767–781. doi:10.1016/j.applthermaleng.2017.11.067

Ghazikhani, M., Manshoori, N., and Tafazoli, D. (2005). "Experimental investigation of steam injection in Ge-F5 gas turbine nox reduction applying vodoley system," in *Second international conference on applied thermodynamics*. Istanbul, Turkey, 18–20.

Gholamian, E., Mahmoudi, S. M. S., and Zare, V. (2016). Proposal, exergy analysis and optimization of a new biomass-based cogeneration system. *Appl. Therm. Eng.* 93, 223–235. doi:10.1016/j.applthermaleng.2015.09.095

Ghorbania, B., Mehrpooya, M., and Sadeghzadeh, M. (2018). Developing a tri-generation system of power, heating, and freshwater (for an industrial town) by using solar flat plate collectors, multi-stage desalination unit, and Kalina power generation cycle. *Energy Convers. Manag.* 165, 113–126. doi:10.1016/j.enconman.2018.03.040

Gill, J., and Singh, J. (2017). Energy analysis of vapor compression refrigeration system using mixture of R134a and LPG as refrigerant. *Int. J. Refrig.* 84, 287–299. doi:10.1016/j.ijrefrig.2017.08.001

Gill, J., and Singh, J. (2018). Component-wise exergy and energy analysis of vapor compression refrigeration system using mixture of R134a and LPG as refrigerant. *Heat Mass Transf.* 54 (5), 1367–1380. doi:10.1007/s00231-017-2242-x

Giovanni, P. (2014). *Energy conversion and management: principles and applications*. Cham Heidelberg New York Dordrecht London: Springer, 150–178.

Gojak, M., and Bajc, T. (2019). Thermodynamic sustainability assessment for heating of residential building. *E3S Web Conf.* 111 04028, 04028–4036. CLIMA 2019. doi:10.1051/e3sconf/201911104028

Goncalves, L. P., and Arrieta, F. R. P. (2010). An exergy cost analysis of a cogeneration plant. *Rev. Eng. Térmica* 9 (1-2), 28–34. doi:10.5380/reterm.v9i1-2.61927

Granet, I., and Bluestein, M. (2000). *Thermodynamics and heat power*. 6th Ed. Upper Saddle River: Prentice Hall, 838.

Gümüş, M., and Atmaca, M. (2013). Energy and exergy analyses applied to a CI engine fueled with diesel and natural gas. *Energy Sources, Part A Recovery, Util. Environ. Eff.* 35 (11), 1017–1027. doi:10.1080/15567036.2010.516312

Hammond, G. P. (2004). Engineering sustainability: thermodynamics, energy systems, and the environment. *Int. J. Energy Res.* 28, 613–639. doi:10.1002/er.988

Hepbasli, A. (2008). A key review on exergetic analysis and assessment of renewable energy resources for a sustainable future. *Renew. Sustain. energy Rev.* 12 (3), 593–661. doi:10.1016/j.rser.2006.10.001

Huggins, R. A. (2016). *Energy storage - fundamentals, materials and applications*. 2nd Edition. Springer International Publishing Switzerland, 30–50.

Imran, M., Park, B. S., Kim, H. J., Lee, D. H., Usman, M., and Heo, M. (2014). Thermo-economic optimization of Regenerative Organic Rankine Cycle for waste heat recovery applications. *Energy Convers. Manag.* 87, 107–118. doi:10.1016/j.enconman.2014.06.091

Inoussah, M. M., Adolphe, M. I., and Daniel, L. (2017). Assessment of sustainability indicators of thermoelectric power generation in Cameroon using exergetic analysis tools. *Energy Power Eng.* 9, 22–39. doi:10.4236/epe.2017.91003

Iora, P., and Silva, P. (2013). Innovative combined heat and power system based on a double shaft intercooled externally fired gas cycle. *Appl. Energy* 105, 108–115. doi:10.1016/j.apenergy.2012.11.059

Jamil, M. A., Shahzad, M. W., and Zubair, S. M. (2020). A comprehensive framework for thermoeconomic analysis of desalination Systems. *Energy Convers. Manag.* 222, 113188–113220. doi:10.1016/j.enconman.2020.113188

Jana, K., and De, S. (2014). Biomass integrated gasification combined cogeneration with or without CO2 capture-a comparative thermodynamic study. *Renew. Energy* 72, 243–252. doi:10.1016/j.renene.2014.07.027

Jørgensen, S. E., and Svirezhev, Y. M. (2004). *Towards a thermodynamic theory for ecological systems*. Amsterdam: Elsevier, 380.

Kalaiselvam, S., and Saravan, R. (2009). Exergy Analysis of scroll compressors working with R22, R407C, and R417A as refrigerant for HVAC system. *Therm. Sci.* 13, 175–184. doi:10.2298/tsci0901175k

Karellas, S., and Braimakis, K. (2016). Energy–exergy analysis and economic investigation of a cogeneration and trigeneration ORC–VCC hybrid system utilizing biomass fuel and solar power. *Energy Convers. Manag.* 107, 103–113. doi:10.1016/j.enconman.2015.06.080

Keçebas, A., and Gokgedik, H. (2015). Thermodynamic evaluation of a geothermal power plant for advanced exergy analysis, *Energy*. 88, 746–755. doi:10.1016/j.energy.2015.05.094

Khalid, F., Dincer, I., and Rosen, M. A. (2015). Energy and exergy analyses of a solar-biomass integrated cycle for multi-generation. *Sol. Energy* 112, 290–299. doi:10.1016/j.solener.2014.11.027

Khani, N., Manesh, M. H. K., and Onishi, V. C. (2022). 6E analyses of a new solar energy-driven polygeneration system integrating CO_2 capture, organic Rankine cycle, and humidification-dehumidification desalination. *J. Clean. Prod.* 379, 1–29. doi:10.1016/j.jclepro.2022.134478

Khanmohammadi, S., Saadat-Targhi, M., Al-Rashed, AAAA, and Afrand, M. (2019). Thermodynamic and economic analyses and multi-objective optimization of harvesting waste heat from a biomass gasifier integrated system by thermoelectric generator. *Energy Convers. Manage* 195, 1022–1034. doi:10.1016/j.enconman.2019.05.075

Khartchenko, N. V., and Kharchenko, V. M. (2014). "6000 broken sound parkway NW, suite 300," in *Advanced energy systems*. 2nd edition (Boca Raton: CRC Press Taylor and Francis Group), 215–230.

Kim, K. H., Han, C. H., and Kim, K. (2012). Effects of ammonia concentration on the thermodynamic performances of ammonia-water based power cycles. *Thermochim. Acta* 530, 7–16. doi:10.1016/j.tca.2011.11.028

Kim, K. H., Han, C. H., and Kim, K. (2013). Comparative exergy analysis of ammonia-water based Rankine cycles with and without regeneration. *Int. J. Exergy.* 12, 344–361. doi:10.1504/ijex.2013.054117

Kim, K. H., Ko, H. J., and Kim, K. (2014). Assessment of pinch point characteristics in heat exchangers and condensers of ammonia-water based power cycles. *Appl. Energy* 113, 970–981. doi:10.1016/j.apenergy.2013.08.055

Kizilkan, O., Kabul, A., and Yakut, A. K. (2010). Exergetic performance assessment of a variable speed R404a refrigeration system. *Int. J. Energy Res.* 34, 463–475. doi:10.1002/er.1553

Klemm, C., and Wiese, F. (2022). Indicators for the optimization of sustainable urban energy systems based on energy system modeling. *Energy, Sustain. Soc.* 12 (3), 3–20. doi:10.1186/s13705-021-00323-3

Koç, Y., Yağlı, H., and Kalay, I. (2020). Energy, exergy, and parametric analysis of simple and recuperative organic Rankine cycles using a gas turbine–based combined cycle. *J. Energy Eng.* 146 (5), 1–20. doi:10.1061/(asce)ey.1943-7897.0000693

Kopanos, G. M., Liu, P., Michael, C., and Georgiadis, M. C. (2017). *Advances in energy systems engineering*. Springer International Publishing Switzerland, 837.

Labele-Alawa, B. T., and Asuo, J. M. (2011). Optimization of the system performance of a gas turbine plant. *Int. J. Appl. Sci. Technol.* 1 (6), 250–255.

Lieuwen, T. C., and Yang, V. (2013). *Gas turbine emissions*. New York, NY: Cambridge University Press 32 Avenue of the Americas, 150–210. 10013-2473, USA.

Liu, W., Zhang, X., Zhao, N., Shu, C., Zhang, S., Ma, Z., et al. (2018). Performance analysis of organic Rankine cycle power generation system for intercooled cycle gas turbine. *Adv. Mech. Eng.* 10 (8), 1–12. doi:10.1177/1687814018794074

Lolos, P. A., and Rogdakis, E. D. (2009). A Kalina power cycle driven by renewable energy sources. *Energy* 34, 457–464. doi:10.1016/j.energy.2008.12.011

Lugo-Leyte, R., Salazar-Pereyra, M., Ru´ız-Ram´ırez, O. A., Zamora-Mata, J. M., and Torres-Gonz´alez, E. V. (2013) *Exergoeconomic operation cost analysis to theoretical compression refrigeration cycle of HFC-134a*, 12. Mexico: Revista Mexicana de Ingenier´ıa Qu´ımica, 361–370.

Manente, G. (2016). High performance integrated solar combined cycles with minimum modifications to the combined cycle power plant design. *Energy Convers. Manag.* 111, 186–197. doi:10.1016/j.enconman.2015.12.079

Maraver, D., Quoilin, S., and Royo, J. (2014). Optimization of biomass-fuelled combined cooling, heating and power (CCHP) systems integrated with subcritical or transcritical organic rankine cycles (ORCs). *Entropy* 16, 2433–2453. doi:10.3390/e16052433

Memon, A. G., Memon, R. A., Harijan, K., and Uqaili, M. (2015). Parametric based thermo-environmental and exergoeconomic analyses of a combined cycle power plant with regression analysis and optimization. *Energy Convers. Manag.* 92, 19–35. doi:10.1016/j.enconman.2014.12.033

Menlik, T., Demircioğlu, A., and Özkaya, M. G. (2013). Energy and exergy analysis of R22 and its alternatives in a vapour compression refrigeration system, *Int. J. Exergy*. 12 1, 11–30. doi:10.1504/ijex.2013.052568

Michaelides, E. E. (2018). Energy, the environment, and sustainability, in *6000 broken sound parkway NW, suite 300*. Boca Raton: CRC Press Taylor and Francis Group, 230–245.

Midilli, A., and Dincer, I. (2009). Development of some exergetic parameters for PEM fuel cells for measuring environmental impact and sustainability. *Int. J. Hydrogen Energy* 34, 3858–3872. doi:10.1016/j.ijhydene.2009.02.066

Mulvihill, M. J., Beach, E. S., Zimmerman, J. B., and Anastas, P. T. (2011). "Green chemistry and green engineering: a framework for sustainable technology development,". Editors A. Gadgil, and D. M. Liverman, 36, 271–293. doi:10.1146/annurevenviron-032009-095500*Annu. Rev. Environ. Resour.*

Ofodu, J. C., and Abam, D. P. S. (2002). Exergy analysis of afam thermal power plant. *NSE Tech. Trans.* 37 (3), 14–28.

Ogriseck, S. (2009). Integration of Kalina cycle in a combined heat and power plant, a case study. *Appl. Ther. Eng.* 29, 2843–2848. doi:10.1016/j.applthermaleng.2009.02.006

Oko, C. C., and Njoku, I. H. (2017). Performance analysis of an integrated gas-steam- and organic fluid-cycle thermal power plant, *Energy*. 122: 431–443. doi:10.1016/j.energy.2017.01.107

Owebor, K., Oko, C. O. C., Diemuodeke, E. O., and Ogorure, O. J. (2019). Thermo-environmental and economic analysis of an integrated municipal waste-to-energy solid oxide fuel cell, gas, steam, organic fluid- and absorption refrigeration cycle thermal power plants. *Appl. Energy* 239, 1385–1401. doi:10.1016/j.apenergy.2019.02.032

Oyedepo, S. O. (2012). On energy for sustainable development in Nigeria. *Renew. Sustain. Energy Rev.* 16, 2583–2598. doi:10.1016/j.rser.2012.02.010

Oyedepo, S. O. (2014a). *Thermodynamic performance analysis of selected gas turbine power plants in Nigeria*. Ota, Nigeria: Covenant University, 1–282. Ph.D Thesis.

Oyedepo, S. O. (2014b). Towards achieving energy for sustainable development in Nigeria. *Renew. Sustain. Energy Rev.* 34, 255–272. doi:10.1016/j.rser.2014.03.019

Oyedepo, S. O., Fagbenle, R. O., Adefila, S. S., and Alam, M. M. (2015a). Exergy costing analysis and performance evaluation of selected gas turbine power. *Plants Cogent Eng.* 2, 2–21. doi:10.1080/23311916.2015.1101048

Oyedepo, S. O., Fagbenle, R. O., Adefila, S. S., and Alam, M. M. (2015b). Thermoeconomic and thermoenvironomic modeling and analysis of selected gas turbine power plants in Nigeria. *Energy Sci. Eng.* 3 (5), 423–442. doi:10.1002/ese3.79

Oyedepo, S. O., Fagbenle, R. O., Adefila, S. S., and Alam, M. M. (2016). Exergoenvironomic modelling and performance assessment of selected gas turbine power plants. *World J. Eng.* 13 (2), 149–162. doi:10.1108/wje-04-2016-020

Oyedepo, S. O., Fagbenle, R. O., Adefila, S. S., Alam, M. M., and Dunmade, I. S. (2018). Thermo-economic and environmental assessment of selected gas turbine power plants in Nigeria. *Prog. Industrial Ecol. – An Int. J.* 12 (4), 361–384. doi:10.1504/pie.2018.097164

Oyedepo, S. O., Fagbenle, R. O., Adefila, S. S. and M. M., and Alam, M. M. (2015c). Performance evaluation of selected gas turbine power plants in Nigeria using energy and exergy methods. *World J. Eng.* 12 (2), 161–176. doi:10.1260/1708-5284.12.2.161

Oztop, H. F., Bayrak, F., and Hepbasli, A. (2013). Energetic and exergetic aspects of solar air heating (solar collector) systems. *Renew. Sustain. Energy Rev.* 21, 59–83. doi:10.1016/j.rser.2012.12.019

Padilla, M., Revellin, R., and Bonjour, J. (2010). Exergy analysis of R413A as replacement of R12 in a domestic refrigeration system. *Energy Convers. Manag.* 51, 2195–2201. doi:10.1016/j.enconman.2010.03.013

Palazzo, P. (2013). Thermoeconomics and exergy method in environmental engineering. J civil. *Environ. Eng.* 3, e110. doi:10.4172/2165-784X.1000e110

Patterson, M. G. (1996). What is energy efficiency? *Energy Policy* 24 (5), 377–390. doi:10.1016/0301-4215(96)00017-1

Pellegrini, L. F. ., and de Oliveira Junior, S. (2011). Combined production of sugar, ethanol and electricity: thermoeconomic and environmental analysis and optimization. *Energy*. 36(6), 3704–3715. doi:10.1016/j.energy.2010.08.011

Prananto, L. A., Zaini, I. N., Mahendranata, B. I., Juangsa, F. B., and Aziz, M. (2018). Use of the Kalina cycle as a bottoming cycle in a geothermal power plant: case study of the Wayang Windu geothermal power plant. *Appl. Therm. Eng.* 132, 686–696. doi:10.1016/j.applthermaleng.2018.01.003

Rajput, R. K. (2003). *A textbook of power plant engineering*. LAMI Publications. New Delhi: Ltd.

Rao, A. (2015). *Sustainable energy conversion for electricity and coproducts: principles, technologies, and equipment*. Hoboken, New Jersey, Canada: John Wiley and Sons, Inc., 130–137.

Ratlamwala, T. A. H., Gadalla, M. A., and Dincer, I. (2011). Performance assessment of an integrated PV/T and triple effect cooling system for hydrogen and cooling production. *Int. J. Hydrogen Energy* 36, 11282–11291. doi:10.1016/j.ijhydene.2010.11.121

Rivero, R., Garcia, M., and Urquiza, J. (2004). Simulation, exergy analysis and application of diabatic distillation to a tertiary amyl methyl ether production unit of a crude oil refinery. *Energy* 29, 467–489. doi:10.1016/j.energy.2003.10.007

Rosen, M. A. (2009). "Applications of exergy to enhance ecological and environmental understanding and stewardship," in *Proceedings of the 4th IASME/WSEAS international conference on energy and environment* (Stevens Point Wisconsin United States: World Scientific and Engineering Academy and Society (WSEAS)), 146–152.

Rosen, M. A. (2021). Exergy analysis as a tool for addressing climate change. *Eur. J. Sustain. Dev. Res.* 5 (2), em0148–10. doi:10.21601/ejosdr/9346

Roshanzadeh, B., Asadi, A., and Mohan, G. (2023). Technical and economic feasibility analysis of solar inlet air cooling systems for combined cycle power plants. *Energies* 16, 5352–5423. doi:10.3390/en16145352

Sahoo, U., Kumar, R., Pant, P. C., and Chaudhary, R. (2017). Development of an innovative polygeneration process in hybrid solar-biomass system for combined power, cooling and desalination. *Appl. Therm. Eng.* 120, 560–567. doi:10.1016/j.applthermaleng.2017.04.034

Saidur, R., Ahamed, J. U., and Masjuki, H. H. (2010). Energy, exergy and economic analysis of industrial boilers. *Energy Policy* 38, 2188–2197. doi:10.1016/j.enpol.2009.11.087

Saidur, R., Sattar, M. A., Masjuki, H. H., Ahmed, S., and Hashim, U. (2007). An estimation of the energy and exergy efficiencies for the energy resources consumption in the transportation sector in Malaysia. *Energy Policy* 35 (8), 4018–4026. doi:10.1016/j.enpol.2007.02.008

Samadi, S., Gröne, M.-C., Schneidewind, U., Luhmann, H.-J., Venjakob, J., and Best, B. (2017). Sufficiency in energy scenario studies: taking the potential benefits of lifestyle changes into account. *Technol. Forecast. Soc. Change* 124, 126–134. doi:10.1016/j.techfore.2016.09.013

Santos, V. E. N., Ely, R. N., Szklo, A. S., and Magrini, A. (2016). Chemicals, electricity and fuels from biorefineries processing Brazil´s sugarcane bagasse: production recipes and minimum selling prices. *Renew. Sustain. Energy Rev.* 53, 1443–1458. doi:10.1016/j.rser.2015.09.069

Sarhaddi, F., Farahat, S., Ajam, H., and Behzadmehr, A. (2009). Exergetic optimization of a solar photovoltaic array. *J. Thermodyn.* 2009. Article ID 313561, 1 – 12. doi:10.1155/2009/313561

Seyam, S., Dincer, I., and Agelin-Chaab, M. (2020). Development of a clean power plant integrated with a solar farm for a sustainable community. *Energy Convers. Manag.* 225, 113434–113520. doi:10.1016/j.enconman.2020.113434

Shamoushaki, M., Ghanatir, F., Ehyaei, M., and Ahmadi, A. (2017). Exergy and exergoeconomic analysis and multi-objective optimisation of gas turbine power plant by evolutionary algorithms. Case study: Aliabad Katoul power plant. *Int. J. Exergy* 22, 279–307. doi:10.1504/ijex.2017.083160

Singh, O. K., and Kaushik, S. C. (2014). Exergoeconomic analysis of a Kalina cycle coupled coal-fired steam power plant. *Int. J. Exergy* 14 (1), 38–59. doi:10.1504/ijex.2014.059512

Spelling, J. D. (2013). *Hybrid solar gas-turbine power plants - a thermoeconomic analysis*. Stockholm, Sweden: KTH Royal Institute of Technology School of Industrial Engineering and Management Department of Energy Technology, 100 44. PhD Thesis.

Srebrenkoska, V., Fidancevska, E., Jovanov, V., and Angusheva, B. (2013). "Sustainable technology and natural environment," in *Proceedings of XXI international scientific and professional meeting "ecological truth" ECO-IST'13*. Serbia: University of Belgrade, 238–242. Technical Faculty. Serbia, 2013.

Su, Y. (2020). Smart energy for smart built environment: a review for combined objectives of affordable sustainable green. *Sustain. Cities Soc.* 53, 101954–102015. doi:10.1016/j.scs.2019.101954

Sulaiman, M. A., Waheed, M. A., Adesope, W. A., and Noike, A. (2017). Techno-economic investigation of different alternatives of improving simple gas turbine integration options. *Niger. J. Technol.* 36, 849–857. doi:10.4314/njt.v36i3.27

Sun, F., Ikegami, Y., and Jia, B. (2012). A study on Kalina solar system with an auxiliary superheater. *Renew. Energy* 41, 210–219. doi:10.1016/j.renene.2011.10.026

Sun, F., Zhou, W., Ikegami, Y., Nakagami, K., and Su, X. (2014). Energy-exergy analysis and optimization of the solar-boosted Kalina cycle system 11 (KCS-11). *Renew. Energy* 66, 268–279. doi:10.1016/j.renene.2013.12.015

Taner, T. (2015). Optimisation processes of energy efficiency for a drying plant: a case of study for Turkey. *Appl. Therm. Eng.* 80, 247–260. doi:10.1016/j.applthermaleng.2015.01.076

Traverso, A., and Massardo, A. F. (2002). Thermoeconomic analysis of mixed gas-steam cycles. *Appl. Therm. Eng.* 22: 1–21. doi:10.1016/s1359-4311(01)00064-3

UN (2015). *Transforming our world: the 2030 agenda for sustainable development. Report A/RES/70/1*. United State of America: United Nations. Available at: https://sustainabledevelopment.un.org/post2015/transformingourworld/publication.

Valero, A., and Cuadra, C. T. (2002) "Thermoeconomic analysis, exergy, energy system analysis and optimization – vol. II - thermoeconomic analysis," in *Encyclopedia of life support systems*. Paris, France: EOLSS, 1–15.

Van Gool, W. (1992). Exergy analysis of industrial processes. *Energy* 17 (8), 791–803. doi:10.1016/0360-5442(92)90123-h

Varga, Z., and Palotai, B. (2017). Comparison of low temperature waste heat recovery methods. *Energy* 137, 1286–1292. doi:10.1016/j.energy.2017.07.003

Vera, D., and Jurado, F. (2018). *Biomass gasification coupled to an EFGT-ORC combined system to maximize the electrical energy generation: a case applied to the olive oil industry*, 144, 41–53.

Vera, D., Jurado, F., and Carpio, J. (2011a). Study of a downdraft gasifier and externally fired gas turbine for olive industry wastes. *Fuel Process Technol.* 92 (10), 1970–1979. doi:10.1016/j.fuproc.2011.05.017

Vera, D., Jurado, F., de Mena, B., and Schories, G. (2011b). Comparison between externally fired gas turbine and gasifier-gas turbine system for the olive oil industry. *Energy* 36 (12), 6720–6730. doi:10.1016/j.energy.2011.10.036

von Spakovsky, M. R., and Frangopoulos, C. A. (2011). Exergy, energy system analysis and optimization – vol. III - analysis and optimization of energy systems with sustainability considerations. *Encycl. Life Support Syst. (EOLSS)*.

Waheed, M. A., Ajayi, O. O., and Ohijeagbon, O. D. (2018). Techno-economic analysis of NERC's feed-in tariff for sustained grid-connected renewable power supply: case of 3 selected sites of northern Nigeria. *Proc. World Congr. Eng.*

Wang, F. J., and Chiou, J. (2004). Integration of steam injection and inlet air cooling for a gas turbine generation system. *Energy Convers. Manag.* 45, 15–26. doi:10.1016/s0196-8904(03)00125-0

Xiang, Y., Cai, L., Guan, Y., Liu, W., He, T., and Li, J. (2019). Study on the biomass-based integrated gasification combined cycle with negative CO2 emissions under different temperatures and pressures. *Energy* 179, 571–580. doi:10.1016/j.energy.2019.05.011

Yataganbaba, A., Kilicarslan, A., and Kurtbas, I. (2015). Exergy analysis of R1234yf and R1234ze as R134a replacements in a two evaporator vapour compression refrigeration system. *Int. J. Refrig.* 60, 26–37. doi:10.1016/j.ijrefrig.2015.08.010

Yuanyuan, L., and Yongping, Y. (2015). Impacts of solar multiples on the performance of integrated solar combined cycle systems with two direct steam generation fields. *Appl. Energy* 160, 673–680. doi:10.1016/j.apenergy.2015.08.094

Yue, C., Han, D., Pu, W., and He, W. (2015). Comparative analysis of a bottoming transcritical ORC and a Kalina cycle for engine exhaust heat recovery. *Energy Convers. Manage* 89, 764–774. doi:10.1016/j.enconman.2014.10.029

Zare, V. (2020). Role of modeling approach on the results of thermodynamic analysis: concept presentation via thermoeconomic comparison of biomass gasification-fueled open and closed cycle gas turbines. *Energy Convers. Manag.* 225, 113479. doi:10.1016/j.enconman.2020.113479

Zare, V., and Hasanzadeh, M. (2016). Energy and exergy analysis of a closed Brayton cycle-based combined cycle for solar power tower plants. *Energy Convers. Manage* 128, 227–237. doi:10.1016/j.enconman.2016.09.080

Zare, V., and Palideh, V. (2018). Employing thermoelectric generator for power generation enhancement in a Kalina cycle driven by low-grade geothermal energy. *Appl. Therm. Eng.* 130, 418–428. doi:10.1016/j.applthermaleng.2017.10.160

Zhang, X., Li, H., Liu, L., Bai, C., Wang, S., Song, Q., et al. (2018). Exergetic and exergoeconomic assessment of a novel CHP system integrating biomass partial gasification with ground source heat pump. *Energy Convers. Manage* 156, 666–679. doi:10.1016/j.enconman.2017.11.075

Ziółkowski, P., Lemański, M., Badur, J., and Nastałek, L. (2012). Power augmentation of PGE gorzow's gas turbine by steam injection – thermodynamic overview. *Rynek Energii* 1 (98), 161–167.

Nomenclature

Abbreviated terms

ASU	Air Separation Unit
BIGCC	Biomass Integrated Gasification Combined Cycle
CC	Combustion Chamber
CCPP	Combined Cycle Power Plant
CCS	Carbon Capture Storage
CHP	Combined Heat and Power
CON	Condenser
COP	Coefficient of Performance
CSP	Concentrated Solar Power
DSG	Direct Steam Generation
EEF	Environmental Effect Factor
EFGT	Extended Fuel Gas Turbine
EIF	Environmental Impact Factor
EIP	Exergy Improvement Potential
ESI	Exergetic Sustainability Index
ETI	Exergo-Thermal Index
EUI	Exergetic Utility Index
GHG	Green House Gas
GT	Gas Turbine
GWP	Global Warming Potential
HFC	Hydrofluorocarbon
HSB	Hybrid Solar- Biomass
HPT	High Pressure Turbine
IAC	Inlet Air Cooling
IGCC	Integrated Gas Combined Cycle
IFGT	Internally Fuel Gas Turbine
IRR	Internal Rate of Return
ISCC	Integrated Solar Combined Cycle
ISO	International Standards Organisation
KC	Kalina Cycle
LCA	Life Cycle Assessment
LPT	Low Pressure Turbine
MW	Mega Watts
ODP	Ozone Depletion Potential
ORC	Organic Rankine Cycle
PES	Primary Energy Saving
PRE-HE	Pre- Heater
PTC	Parabolic Trough Collector
PV	Photovoltaic
RERs	Renewable Energy Resources
SED	Sustainable Energy Development
SGT	Simple Gas Turbine
SoR	Share of Renewables
STI	Steam Injection
TDI	Thermal Discharge Index
TIT	Turbine Inlet Temperature
Turb	Turbine
VAP	Vapour
VCC	Vapour Compression Cycle
WER	Waste Exergy Ratio

Greek letters

$\eta_{\Delta H}$	Enthalpic Efficiency
ΔH_{out}	Sum of the useful energy outputs of a process
ΔH_{in}	Sum of the energy inputs into a process
P**th**	Thermal energy input
η_{th}	Thermal efficiency
$\dot{E}_{xoverall}$	Over all Exergy
η_{ex}	Exergetic Efficiency
D_p	Depletion Number
β	Thermal pollution factor
C′	Specific Energy Costs

frontiers | Frontiers in Energy Research

TYPE Original Research
PUBLISHED 28 April 2025
DOI 10.3389/fenrg.2025.1500515

OPEN ACCESS

EDITED BY
Mufutau Adekojo Waheed,
Federal University of Agriculture,
Abeokuta, Nigeria

REVIEWED BY
Dimitrios Nalmpantis,
Aristotle University of Thessaloniki, Greece
Olasunkanmi Ismaila,
Federal University of Agriculture,
Abeokuta, Nigeria
Adekunle Oyelami,
Federal University of Agriculture,
Abeokuta, Nigeria

*CORRESPONDENCE
Ezhilmaran Devarasan,
ezhil.devarasan@yahoo.com

RECEIVED 23 September 2024
ACCEPTED 03 February 2025
PUBLISHED 28 April 2025

CITATION
Devarasan E, Nagarajan D and Rachel J (2025) Advancing sustainable mobility in India with electric vehicles: market trends and machine learning insights.
Front. Energy Res. 13:1500515.
doi: 10.3389/fenrg.2025.1500515

Advancing sustainable mobility in India with electric vehicles: market trends and machine learning insights

Ezhilmaran Devarasan[1]*, Deepikaa Nagarajan[2] and Jenisha Rachel[1]

[1]Department of Mathematics, Vellore Institute of Technology, Vellore, Tamilnadu, India, [2]P.G. Student in Business Statistics, Vellore Institute of Technology, Vellore, Tamilnadu, India

India, as a rapidly growing country facing significant pollution challenges, sees a major opportunity for sustainable mobility through the adoption of electric vehicles. Since a large amount of India's crude oil is imported, the country is vulnerable to changes in the price of crude oil globally. India may improve its energy security and lessen its reliance on imported fossil fuels by switching to electric vehicles (EVs) that are powered by electricity generated domestically. Air pollution from internal combustion engine vehicles is a contributing factor to several health issues, such as heart disease and respiratory disorders. Making the switch to EVs can result in better public health outcomes and cleaner air. This study offers an in-depth analysis of India's Electric Vehicle (EV) market dynamics from FY 2014 to February 2024, utilizing machine learning techniques to identify sales trends, regional disparities, and adoption drivers. Through meticulous examination, the research aims to elucidate sales trends, regional variations, and underlying factors influencing EV adoption across the nation. Objectives include analysing sales trajectories over the past decade, estimating EV sales across states, exploring category-specific trends, identifying drivers of regional disparities, investigating EV adoption patterns in the Tamil Nadu, evaluating the advantages and disadvantages of EVs. With a particular interest in analyzing the complex dynamics of charging infrastructure in cities, this study extensively examines EV adoption in India. By using data-driven insights, this research aims to contribute to a deeper understanding of the dynamics shaping the EV landscape in India and provide valuable guidance for stakeholders, industry participants and policymakers on how to promote the country's electric mobility sector's sustainable growth.

KEYWORDS

electric vehicles, energy efficiency, energy storage, machine learning, energy security, sales trends, charging infrastructure, sustainable growth

1 Introduction

Electric Vehicles (EVs) represent a major shift in the automotive industry, providing cleaner, more efficient, and sustainable transportation. Unlike traditional internal combustion engine vehicles that rely on fossil fuels, EVs are powered by electricity, either from onboard batteries or through external charging sources. The shift toward

EV adoption is driven by growing concerns over climate change, air pollution, and fossil fuel depletion. EVs come in various forms, including electric cars, electric buses, electric scooters, electric bicycles, and so on··· They utilize advanced technologies such as lithium-ion batteries, electric motors, regenerative braking systems, and sophisticated power electronics to deliver performance comparable to or even better than conventional vehicles. EVs produce zero emissions, contributing to improved air quality and reduced greenhouse gas emissions, thus mitigating the impacts of climate change. It has lower operating costs compared to traditional vehicles, as electricity is generally cheaper than gasoline or diesel fuel. Electric motors operate more quietly and smoothly than internal combustion engines, providing a more comfortable and serene driving experience for occupants and reducing noise pollution in urban environments. EVs are inherently more energy-efficient than conventional vehicles, with electric motors converting a higher percentage of energy from the battery into motion. This efficiency contributed to extended driving ranges on a single charge and reduces overall energy consumption. EVs offer the potential for integration with renewable energy sources such as solar and wind power. Through smart charging and vehicle-to-grid technology, EVs can serve as energy storage devices and help balance the grid further enhancing sustainability and resilience.

Research on electric vehicle (EV) adoption highlights several key factors across various regions. In Korea, consumer attitudes towards EVs are significantly influenced by familiarity with EV driving, household vehicle count, educational attainment, parking availability, and perceptions of government incentives (Kim et al., 2019). In India, financial, societal, technological, and environmental factors play a role in shaping EV adoption. The focus is on expanding charging infrastructure and educating the public about EV benefits, with predictions indicating market growth despite challenges (Kalita and Hussain, 2021). A deeper examination of the Indian EV market using machine learning identifies key influences such as demographics, financial considerations, and environmental awareness, while also stressing the importance of government policies for boosting adoption (Dixit and Singh, 2022). In Europe, the expansion of EV markets hinges on technological advancements, policy support, and collaboration between governments and businesses, with an emphasis on improving battery technology and charging infrastructure to further market growth (Razmjoo et al., 2022). In India, financial incentives, charging infrastructure, environmental concerns, and social reinforcement are key determinants of EV adoption, with pricing emerging as the most significant driver, as shown through SEM and CFA analyses (Ali and Naushad, 2022). Further studies into consumer perspectives in India highlight cost and charging infrastructure as primary barriers to widespread adoption, recommending that policymakers focus on overcoming these challenges to foster a sustainable transportation network (Singh, 2023). Addressing air pollution and emissions reduction through EV adoption is critical for India, with rising fossil fuel prices, consumer awareness, and government initiatives expected to drive increased EV sales, contributing to achieving net-zero emissions by 2070 (Infanto et al., 2023).

The literature also reviews the adoption of EVs, identifying air pollution reduction as a key motivator, while high purchase costs and limited driving range remain significant barriers. Rapid charging and battery improvements are proposed as solutions to accelerate EV adoption (Pamidimukkala et al., 2024). Surveys conducted in Europe, particularly in Finland, Austria, Spain, and Italy, show positive attitudes towards light-duty electric vehicles (LEVs) among users, with recommendations for increasing awareness among non-users to further drive adoption (Mesimäki and Lehtonen, 2023). In Maharashtra, India, strategic placement of EV chargers is critical for promoting sustainable mobility. Researchers identified prime locations like Mumbai, Thane, and Pune through predictive models, contributing to the development of EV infrastructure in densely populated urban areas (Chandra et al., 2023). Similarly, research from Spain developed a model to optimize charging stations on highways by analyzing factors like road slope and weather, thereby facilitating long-distance EV travel (Saldarini et al., 2023). Accurate power usage prediction for charging stations is also essential for infrastructure planning, with models like SARIMA providing valuable insights into energy consumption patterns, supporting sustainable EV network development (Akshay et al., 2024).

Innovations in battery technologies and hybrid energy storage systems (HESS) are crucial for improving electric vehicle (EV) efficiency and sustainability. HESS, combined with machine learning (ML) control, optimizes energy use from renewable sources, ensuring stable performance under varying conditions (Punyavathi et al., 2024). Vehicle-to-grid (V2G) systems, coupled with power management strategies, enhance EV integration into sustainable transit networks (Agarwal et al., 2024). Machine learning models like Random Forest and Lasso Regression effectively predict EV sales and market trends, enabling manufacturers to tailor strategies to consumer needs (Khusanboev et al., 2023; Yeh and Wang, 2023). Research shows factors such as CO2 emissions and renewable energy availability significantly influence EV sales, linking environmental policies to market dynamics (Yeh and Wang, 2023). Additionally, marketing strategies targeting psychographic and behavioral market segments, especially in regions with sustainability-conscious consumers, are vital for boosting EV adoption (Tripathy et al., 2023; Kautish et al., 2024). Machine learning frameworks like Light GBM help predict household EV adoption, enabling manufacturers to target potential buyers effectively (Dai and Zhang, 2023). The shift to EVs is critical for achieving global climate targets and reducing dependence on fossil fuels, with research increasingly focused on key areas such as charging infrastructure, EV adoption, thermal management, and routing problems. The development of wireless charging systems, advancements in AI-driven sustainable transportation solutions, and predictive maintenance models for EV batteries further illustrate the breadth of technological progress aimed at enhancing EV performance and market adoption (Miconi and Dimitri, 2023; Obrador Rey et al., 2024). Lastly, studies on consumer behavior, charging infrastructure, and emerging technologies such as autonomous EVs and flying vehicles highlight the multifaceted challenges and opportunities in the transition to a low-carbon transportation future (Dai and Zhang, 2023; Tripathy et al., 2023).

The EV adoption is widely recognized as crucial for achieving global climate change targets and advancing sustainable transport (Haghani et al., 2023). Recent research trends in electric vehicles

(EVs) highlight key areas such as charging infrastructure (Fescioglu-Unver and Aktas, 2023), adoption rates (Moreno Rocha et al., 2024), thermal management systems, and routing problems (Singh et al., 2024), with a noticeable decline in hybrid EV research across subfields. Addressing global challenges like urban congestion and environmental degradation, renewable energy-powered EVs and flying automobiles are being explored to reduce fossil fuel dependence and carbon emissions. Studies emphasize the need for integrating flying vehicles into existing infrastructures through dynamic modeling and a mixed-methods approach, analyzing drivers and challenges, such as infrastructure, safety, and airspace management. The importance of wireless charging, particularly inductive and capacitive power transfer (Govathoti, 2024), is also highlighted, while policies like the European Union's 2035 ban on internal combustion engine vehicle registrations aim to boost EV adoption (Menyhart, 2024). Transforming public transportation requires machine learning-driven predictions of energy economy for electric buses, with studies indicating that predictive maintenance and consumer-centric policies can enhance EV adoption. Research also points to growing consumer interest in EVs in the Nordic countries (de Rubens, 2019), where vehicle-to-grid technologies and pricing strategies drive market adoption. Furthermore, machine learning models have proven effective in predicting market dynamics (Ahmadi et al., 2020), identifying charging infrastructure needs, and forecasting individual consumer behavior, aiding manufacturers and policymakers (Dixit and Singh, 2022; Neeraja et al., 2023). Studies highlight the significant potential of AI, blockchain, and autonomous EVs in achieving a sustainable future for urban mobility, while also identifying challenges related to infrastructure and emissions (Kavcic et al., 2022; Jin et al., 2024). Finally, the environmental footprint of EVs, including indirect emissions and recyclability, remains a critical focus, with recommendations for further technological advancements and sustainable policy frameworks (Vajsz et al., 2022).

The paper is organized as follows: The complete methodology is explained in Section "Materials and methods." To demonstrate the application of the suggested problem, a numerical example is given in Section "Analysis and Interpretation." Section "Conclusion" of the paper provides concluding remarks, an analysis of the study's shortcomings, and implications.

2 Materials and methods

The study's methodology is illustrated in Figure 1. It starts by gathering both primary and secondary data, which involves obtaining responses from surveys and information from sources. Data was sourced from the Vahan dashboard and district distance matrices for Tamil Nadu, including survey responses for consumer perception analysis. Once data collection is complete, thorough cleaning and preprocessing procedures are undertaken to ensure the data quality, including addressing missing values and standardizing data format. Following this, relevant features are identified, and the target variable (the year of EV sales) is established, leading to the consolidation of datasets for a comprehensive analysis. Machine learning models such as Linear Regression, Support Vector Regressor, K Nearest Neighbours, Random Forest Regressor, Decision Tree Regressor, Gradient Boosting Regressor, AdaBoost Regressor, Ridge Regression, and Lasso Regression were used. The dataset is subsequently divided into training and testing sets for the purpose of model training and evaluation. The performance of the chosen model is assessed using appropriate metrics, and adjustments to hyperparameters may be made for optimization if necessary. The interpretation of results involves analysing insights into the dynamics of the EV market and regional disparities. Ultimately, actionable recommendations are formulated to promote sustainable growth in India's electric mobility sector based on the study's findings.

3 Analysis and interpretation

A thorough analysis of India's EV market dynamics from FY 2014 to 2024 up to February is presented by using the steps in Figure 2. Using ML methods, it examines sales patterns, regional differences, and factors impacting EV adoption across the country. Key points include insights into sales trends, regional adoption patterns, category-specific dynamics, and performance disparities among states. Moreover, a specific focus on Tamil Nadu provides localized insights, while an evaluation of EV advantages and disadvantages offers clarity on their overall feasibility. Additionally, spatial analysis of charging infrastructure expansion assists in strategic planning for infrastructure development.

3.1 Total sales of EV in India FY 2014–2024 (Feb)

Figure 3 illustrates a steady increase in EV sales from 2014 to 2023, reflecting growing adoption across India. This upward trend can be attributed to several factors, including government incentives, increased environmental awareness, rising fuel prices, and advancements in EV technology. Despite this growth, the rate of increase may vary over time due to shifts in consumer preferences, economic conditions, and government policies.

The Indian government has played a crucial role in promoting EV adoption through initiatives such as the Faster Adoption and Manufacturing of Electric Vehicles (FAME) scheme, which offers subsidies and incentives for both consumers and manufacturers. Additionally, state governments have implemented localized policies to further encourage the use of EVs. Although EV sales have been rising, they still represent a small fraction of the total vehicle sales in India. Nevertheless, the continued emphasis on reducing emissions and dependence on fossil fuels is expected to drive substantial growth in EV sales in the coming years.

Year-to-year fluctuations in EV sales are also evident. For instance, in 2020, the global automotive industry faced a significant downturn due to the COVID-19 pandemic, which led to lockdowns, supply chain disruptions, and reduced consumer spending. This resulted in a temporary dip in EV sales, reflecting the broader impact on the automotive sector.

Overall, the bar plot underscores the growth and potential of the EV market in India, highlighting the progress achieved thus far and the opportunities for further expansion in the future.

FIGURE 1
Methodology of the study.

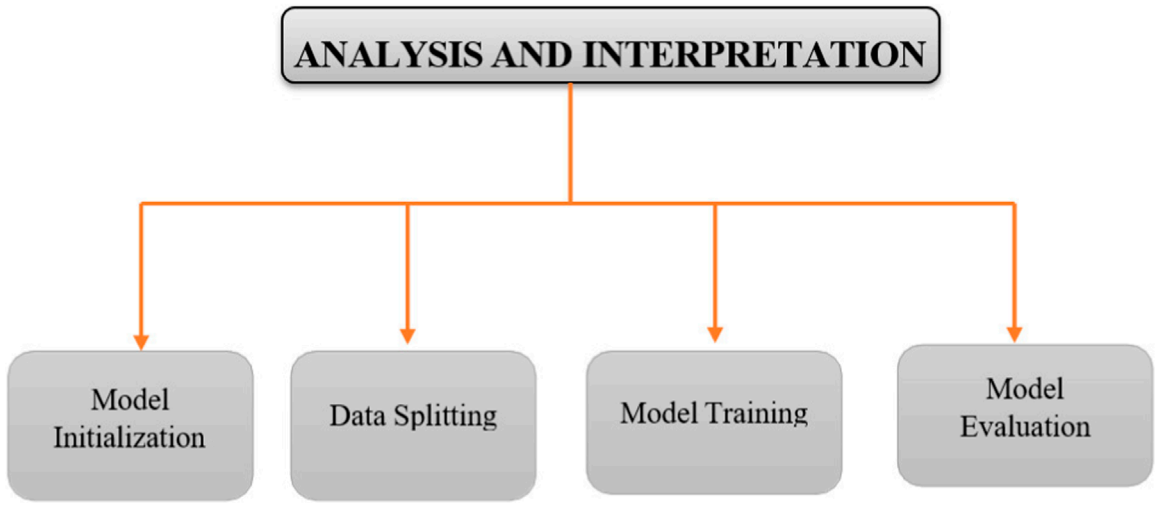

FIGURE 2
Analysis and interpretation.

3.2 State-wise EV sales in India (2021–2024)

India is witnessing a steady rise in EV sales; however, challenges such as high upfront costs and a lack of accessible charging infrastructure persist. State governments play a pivotal role in addressing these issues by implementing supportive policies, investing in infrastructure, and promoting awareness of the benefits of electric vehicles. For a cleaner and more sustainable future, all Indian states must work towards increasing EV adoption.

Uttar Pradesh has consistently emerged as the top-performing state in EV sales across multiple years (up to 2023), reflecting strong market demand and widespread adoption in the region. Maharashtra and Karnataka ranked second and third in terms of EV sales in 2022 and 2023, respectively, maintaining their prominent positions in the rankings. In 2024, Gujarat has taken the lead as the top-selling state based on data available up to February. This notable shift in rankings highlights Gujarat's expanding EV market, driven by factors such as favorable policies, well-developed charging infrastructure, growing consumer awareness, and interest in electric vehicles.

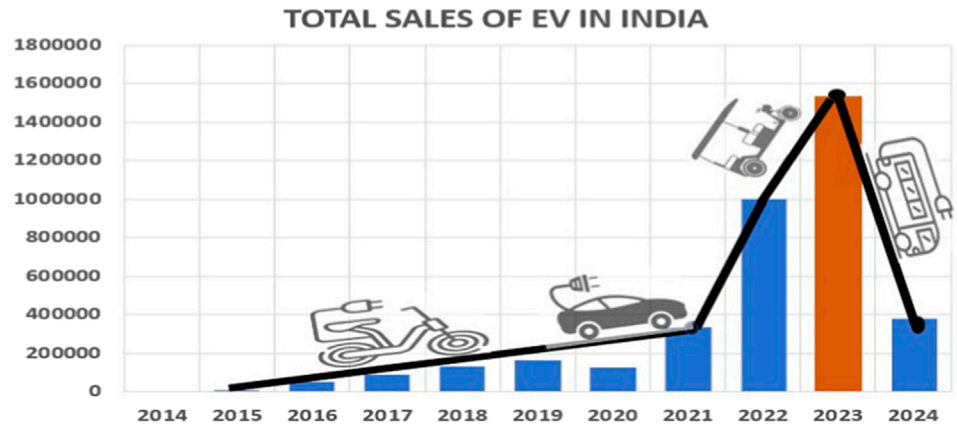

FIGURE 3
Total sales of EV in India (2024 is not a full year).

TABLE 1 Output of ML models.

Models	MSE	MAE
Linear Regression	**0.6381**	**0.6832**
Decision Tree Regressor	0.9048	0.7143
Random Forest Regressor	0.7380	0.7539
SVR	0.7099	0.7268
KNN	0.8400	0.8095
Ridge Regression	**0.6381**	**0.6832**
Lasso Regression	0.6431	0.6856
Gradient Boosting Regressor	0.8252	0.8032
Ada Boost Regressor	0.8865	0.7976

Best prediction models are found to be Ridge Regression and Linear Regression based on the category-wise EV sales data in India.

Tamil Nadu has also positioned itself among the leading states in EV sales. Projections for 2024 suggest that Tamil Nadu is expected to become the top-selling state for electric vehicles across India (refer Supplementary Figure S1). These developments underscore the dynamic nature of the EV market in India and the importance of continued efforts to promote EV adoption nationwide.

3.3 Category-wise EV sales in India

The category-wise EV sales chart (see Supplementary Figure S2) for the years 2021, 2022, and 2023 in India provides valuable insights into the trends and dynamics of the electric vehicle market. The data illustrates that the 2W and 3W segments consistently outperform other categories, such as 4W, Buses, and Others, across all 3 years, indicating a strong consumer preference for electric 2Ws and 3Ws in India.

The year 2022 stands out as the period with the highest overall EV sales, driven primarily by a remarkable surge in the 2W segment. This highlights 2022 as a pivotal year for the EV market in India, marked by widespread adoption and increased consumer confidence in EV technology. Although overall sales in 2023 did not surpass the peak achieved in 2022, the 2W segment maintained its dominance, achieving the second-highest sales volume within this category.

This sustained growth reflects a maturing market, with consumers continuing to adopt electric 2Ws as a viable mode of transportation. The high demand for 2W and 3W EVs highlights the need for tailored policies and incentives to promote the adoption of these categories. Policymakers and industry stakeholders should prioritize enhancing charging infrastructure, incentivizing manufacturing, and implementing supportive measures to further accelerate growth in the 2W and 3W segments.

While the 2W and 3W segments currently dominate the market, there is significant potential for growth and diversification in other categories, such as electric 4Ws, Buses, and specialized vehicles. Strategic investments in research and development, along with targeted marketing efforts, can unlock the full potential of these segments and contribute to the overall expansion of India's EV market.

4 Analysis & interpretation: initializing models

Dependent variable: EV category-wise sales data (2W,3W, 4W, BUS, OTHERS) Independent variable: Year.

4.1 Linear regression

Linear regression models the relationship between a dependent variable and one or more independent variables by fitting a linear

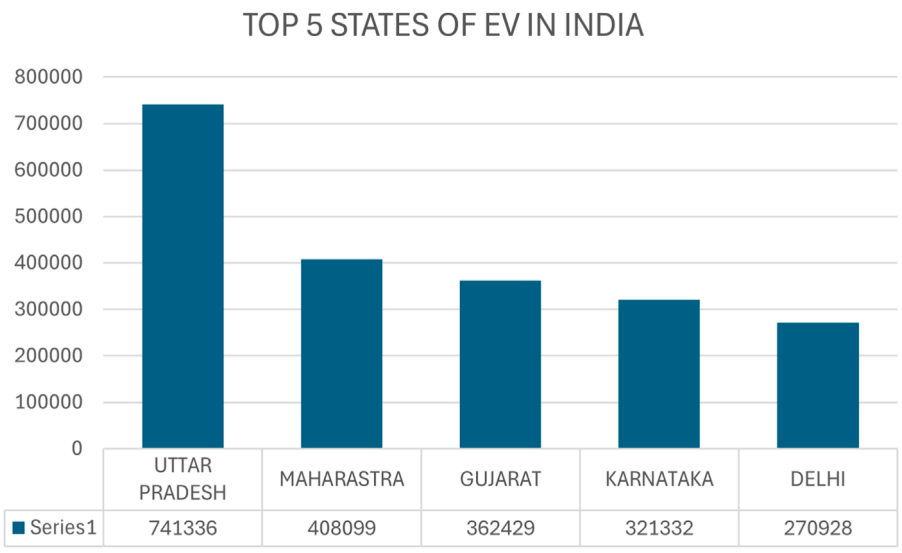

FIGURE 4
Top 5 states of EV in India.

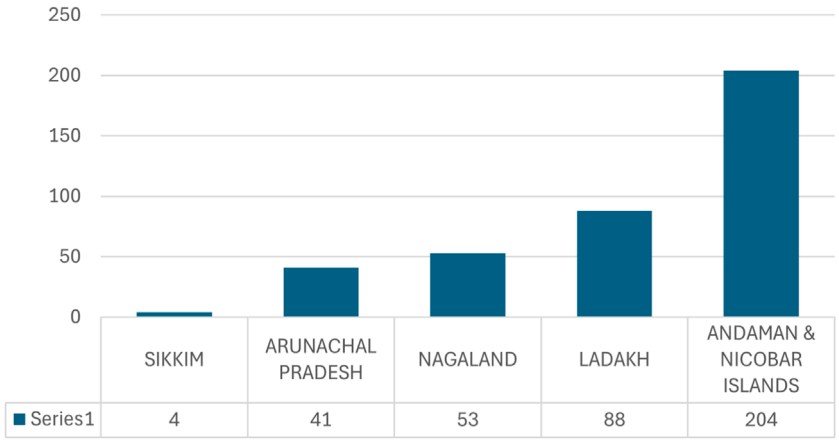

FIGURE 5
Least 5 states of EV in India.

equation to observed data. To put it simply, it clarifies how changing one or more independent variables affects the value of the dependent variable.

4.2 Support vector regressor

For regression tasks, the supervised learning algorithm known as the support vector regressor is employed. The way it operates is by projecting the input data onto a high-dimensional feature space, then identifying the ideal hyperplane to minimize error and effectively divide the data into distinct classes. These metrics show the degree to which the model's predictions agree with the actual target values.

4.3 K-nearest neighbour

For classification and regression tasks, K Nearest Neighbors (KNN) is an easy to understand, accessible supervised learning algorithm. It uses the majority class (classification) or average value (regression) of their K nearest neighbors to forecast new points while storing the training set in storage.

4.4 Random forest regressor

With the use of multiple decision trees built during training, the random forest regressor is an ensemble learning technique that produces the mean prediction of each individual tree for regression tasks. By combining the

TABLE 2 Cross tabulation b/w gender & awareness of EV.

Gender	Are you aware of EV		Total
	1	2	
1	60	0	60
2	74	13	87
Total	134	13	147

TABLE 3 Cross tabulation b/w education & awareness of govt. schemes.

Education	Awareness of government schemes		Total
	1	2	
1	7	14	21
2	28	41	69
3	25	32	57
Total	60	87	147

predictions of several trees, it decreases overfitting and increases prediction accuracy.

4.5 Decision tree regressor

For regression tasks, a supervised learning algorithm called a decision tree regressor is employed. With the training set, it constructs a decision tree, with each leaf node denoting the expected output value, each branch representing a decision, and each node representing a feature.

4.6 Gradient boosting regressor

Gradient Boosting Regressor is a machine learning technique for regression that builds an ensemble of weak prediction models, focusing on minimizing errors in a sequential manner. It's used for accurate regression tasks, especially in complex datasets with nonlinear relationships, and is favoured in competitions for its high performance and versatility.

4.7 Ada boost regressor

AdaBoost Regressor is a machine learning algorithm that sequentially trains weak learners to correct errors made by previous models, emphasizing difficult-to-predict instances. It's used for regression tasks, particularly when dealing with noisy data or complex relationships, and excels in scenarios where robustness to outliers is crucial.

4.8 Ridge regression

Ridge regression, or L2 regularization, is a linear regression technique that adds a penalty term to the loss function, penalizing large coefficient values. It helps to prevent overfitting and improve the generalization performance of the model.

4.9 Lasso regression

Lasso regression, or L1 regularization, is a linear regression technique that adds a penalty term to the loss function, forcing some of the coefficient values to be exactly zero. It helps to select a subset of the most relevant features and reduce model complexity.

4.10 Output of machine learning models & interpretation

The best prediction models are found to be Ridge Regression and Linear Regression based on the category-wise EV sales data (refer Table 1) in India. Compared to the other regression procedures examined, these models show the lowest Mean Squared Error (MSE) and Mean Absolute Error (MAE). Their predictability, ease of interpretation, and effective computing power make them the ideal options for analyzing and predicting EV sales trends across various categories. Their usefulness for stakeholders seeking actionable insights in the rapidly expanding EV industry is further enhanced by their capacity to offer insights into the relative contributions of specific characteristics. Since Ridge Regression and Linear Regression balance predictive accuracy, interpretability, and computational efficiency, they are recommended for estimating category-wise EV sales in India.

5 Top 5 states of EV in India

The bar chart (see Figure 4) illustrates the distribution of EV sales in India, with Uttar Pradesh (UP), Maharashtra, Gujarat, Karnataka, and Delhi leading the transition towards electric vehicles. Uttar Pradesh emerges as the largest contributor, indicating a growing market for EVs, particularly in cities such as Lucknow and Noida. Maharashtra, recognized for its industrial and commercial significance, also plays a significant role in EV sales, while Gujarat leverages its strong industrial base and government initiatives to support EV growth. Karnataka and Delhi, although contributing slightly less, demonstrate substantial participation in EV sales, supported by favorable policies and increased consumer awareness, including incentives such as 100.

TABLE 4 Chi-Square b/w gender & awareness of EV.

	Value	df	Asymp. Sig. (2-sided)	Exact Sig. (2-sided)	Exact Sig. (1-sided)
Pearson Chi-Square	9.835[a]	1	0.002		
Continuity Correction[b]	8.069	1	0.005		
Likelihood Ratio	14.500	1	0.000		
Fisher's Exact Test				0.001	0.001
Linear-by-Linear Association	9.768	1	0.002		
N of Valid Cases	147				

[a] 0 cells (0.0%) have expected count less than 5.
The minimum expected count is 5.31.
[b] Computed only for a 2 × 2 table.

TABLE 5 Chi-square b/w education & awareness of EV.

	Value	df	Asymp. Sig. (2-Sided)
Pearson Chi-Square	5.178[a]	2	0.075
Likelihood Ratio	5.403	2	0.067
Linear-by-Linear Association	0.849	1	0.357
N of Valid Cases	147		

[a] 1 cells (16.7%) have expected count less than 5.
The minimum expected count is 1.86.

TABLE 7 Chi-square b/w age & awareness of EV.

	Value	df	Asymp. Sig. (2-Sided)
Pearson Chi-Square	8.281[a]	4	0.082
Likelihood Ratio	12.627	4	0.082
Linear-by-Linear Association	5.724	1	0.013
N of Valid Cases	147		

[a] 4 cells (40.0%) have expected count less than 5.
The minimum expected count is 0.62.

TABLE 6 Cross tabulation b/w age & awareness of EV.

Age	Are you aware of EV		Total
	1	2	
1	80	13	93
2	23	0	23
3	13	0	13
4	11	0	11
5	7	0	7
Total	134	13	147

5.1 What makes EV sales go up in UP?

Uttar Pradesh (UP) emerges as a frontrunner in electric vehicle (EV) sales due to its proactive governmental strategies, exemplified by the UP Electric Vehicle Manufacturing and Mobility Policy 2022 and the establishment of 582 operational public charging stations. Despite grappling with a poverty rate of 22.93%, UP showcases robust economic indicators, with a GDP *per capita* of 79,396 rupees and a minimal unemployment rate of 2.9%. With a dense population density of 1,001/km^2, UP represents a lucrative market for EV adoption, signifying significant strides in sustainable transportation.

From 2014 to February 2024, UP maintains a consistent upward trajectory in EV sales (refer Supplementary Figure S3), peaking notably in 2023 with 278,017 units sold. The state further incentivizes EV adoption by offering a full waiver on road tax, though it does not impose any maximum subsidy provisions.

6 Least 5 states of EV in India

The bar chart (refer Figure 5) indicates that Sikkim, Arunachal Pradesh, Nagaland, Ladakh, and the Andaman and Nicobar Islands have lower rates of EV adoption compared to other parts of India. This is likely due to factors such as insufficient charging infrastructure, limited awareness of the benefits of EVs, absence of government incentives, and geographical challenges. Among these regions, Sikkim demonstrates the smallest share of EV sales, followed by Arunachal Pradesh, Nagaland, Ladakh, and the Andaman and Nicobar Islands. While Ladakh and the Andaman and Nicobar Islands show slightly higher proportions of EV sales, they still fall short of national averages, highlighting the need for targeted

TABLE 8 Chi-square b/w gender & awareness of govt. schemes.

	Value	df	Asymp. Sig. (2-Sided)	Exact sig. (2-Sided)	Exact sig. (1-Sided)
Pearson Chi-Square	0.028[a]	1	0.867		
Continuity Correction[b]	0.000	1	1.000		
Likelihood Ratio	0.028	1	0.867		
Fisher's Exact Test				1.000	0.502
Linear-by-Linear Association	0.028	1	0.868		
N of Valid Cases	147				

[a] 0 cells (0.0%) have expected count less than 5.
The minimum expected count is 24.49.
[b] Computed only for a 2 × 2 table.

TABLE 9 Chi-Square b/w age & awareness of govt. schemes.

	Value	df	Asymp. Sig. (2-Sided)
Pearson Chi-Square	7.947[a]	4	0.094
Likelihood Ratio	9.401	4	0.052
Linear-by-Linear Association	2.397	1	0.122
N of Valid Cases	147		

[a] 4 cells (40.0%) have expected count less than 5.
The minimum expected count is 0.62.

TABLE 10 Chi square b/w education & awareness of govt. schemes.

	Value	df	Asymp. Sig. (2-Sided)
Pearson Chi-Square	0.707[a]	2	0.702
Likelihood Ratio	0.717	2	0.699
Linear-by-Linear Association	0.650	1	0.420
N of Valid Cases	147		

[a] 0 cells (0.0%) have expected count less than 5.
The minimum expected count is 8.57.

TABLE 11 Chi-square b/w gender & intention to purchase EV in future.

	Value	df	Asymp. Sig. (2-Tailed)
Pearson Chi-Square	8.31	2	0.016
Likelihood Ratio	8.38	2	0.015
Linear-by-Linear Association	3.82	1	0.051
N of Valid Cases	150		

TABLE 12 Chi-square b/w age & intention to purchase EV in future.

	Value	df	Asymp. Sig. (2-Tailed)
Pearson Chi-Square	29.50	8	0.000
Likelihood Ratio	24.61	8	0.002
Linear-by-Linear Association	2.31	1	0.129
N of Valid Cases	150		

efforts to enhance EV adoption in line with India's sustainable transportation objectives.

6.1 Why are EV sales lower in Sikkim?

Several factors contribute to the slow sales of electric vehicles (EVs) in Sikkim (refer Supplementary Figure S4). The potential EV market in the region is limited by its small population, which is further impacted by unfavorable climatic conditions and security concerns.

Census data shows a population of 610,577, with only slight growth over time. With just two EV charging stations in East Sikkim, limited infrastructure hampers widespread EV adoption. Economic dynamics also play a role, as Sikkim's agrarian economy, despite a notable GDP *per capita*, restricts consumer spending on EVs. The emerging EV market in Sikkim faces challenges such as restricted model availability and limited services, which hinder consumer acceptance. Furthermore, given the region's reliance on agriculture as the predominant occupation, the lack of diverse economic activities also impacts the potential for EV sales.

TABLE 13 Chi-square b/w Age & intention to purchase EV in future.

	Value	df	Asymp. Sig. (2-Tailed)
Pearson Chi-Square	8.39	4	0.078
Likelihood Ratio	7.74	4	0.101
Linear-by-Linear Association	0.03	1	0.872
N of Valid Cases	150		

TABLE 14 Top 10 optimal locations based on single mode analysis.

District1	District 2	Distance
Chennai	Kanniyakumari	705
Kanniyakumari	Thiruvallur	700
Kanniyakumari	Ranipet	662
Kancheepuram	Kanniyakumari	654
Chennai	Tenkasi	652
Kanniyakumari	Vellore	644
Chengalpattu	Kanniyakumari	644
Tenkasi	Thiruvallur	638
Chennai	Tirunelveli	629
Chennai	Thiruvallur	617

7 EV sales trend in the Tamil Nadu region

The Tamil Nadu EV sales data from 2021 to 2023 indicates a steady rise (refer Supplementary Figure S5 in supplementary material), with notable peaks in March each year, possibly due to increased demand or promotional activities. In 2022, sales surged, particularly from April to August, with March recording the highest sales at 8,179 units. This trend continues in 2023, with March remaining a top-selling month. Notably, May 2023 sees a significant spike in sales at 11,484 units, potentially influenced by seasonal factors or specific market events. Cultural preferences and societal norms also play a role in shaping consumer behavior and perceptions toward EVs. Factors such as the status symbols associated with traditional vehicles or cultural attitudes toward technology adoption may impact EV sales.

8 Public perceptions of EVs

The examination of Electric Vehicles (EVs) advantages and disadvantages is essential in gauging their potential influence on transportation and the environment. A structured questionnaire has been devised to gather insights from respondents, evaluating aspects such as EV awareness, government incentive awareness, and future EV purchase intentions. This survey aims to collect valuable data for comprehensive assessment of perceptions, preferences, and considerations regarding EV adoption. Statistical analysis, including chi-square analysis were performed using SPSS to further explore the relationships between variables and derive meaningful insights.

8.1 Gender vs. are you aware of EV

A Chi-square analysis revealed a statistically significant association between gender and EV awareness, with males reporting higher levels of awareness than females ($\chi^2 = 9.835, df = 1, p < 0.005$). This suggests that awareness of EVs and gender are significantly correlated. The connection was further validated by additional analysis using Fisher's exact test ($p < 0.001$). More specifically, compared to females (13 out of 87), a greater percentage of males (60 out of 134) claimed to be aware of EVs. As an outcome, it seems that gender affects EV awareness, with men exhibiting higher degrees of awareness than women.

The bar chart (refer Supplementary Figure S6) depicts the relationship between gender and awareness of EVs among respondents. The x-axis represents gender, where "1" corresponds to males and "2" to females. The y-axis indicates the count of respondents, with light blue bars representing those who are aware of EVs and dark violet bars representing those who are not aware.

8.2 Education vs. are you aware of EV

The chi-square tests were conducted to examine the relationship between variables. The results indicate no significant association between the variables at the conventional significance level of 0.05. Additionally, there is no significant linear trend observed. However, it is important to note that a portion of the cells have low expected counts, which may impact the reliability of the test results (refer Supplementary Figure S7).

8.3 Age vs. are you aware of EV

The chi-square tests were conducted to explore the relationship between variables. The results indicate that while there is no significant association between the variables at the conventional significance level of 0.05 based on the Pearson and likelihood ratio tests, a significant linear trend is observed according to the linear-by linear association test. It's important to note that a considerable portion of cells have low expected counts.

The bar chart (refer Supplementary Figure S8) displays how different age groups relate to knowing about EVs. The x-axis represents Age where "1" corresponds to Less than 25 years, "2" corresponds to 26–35 years, "3" corresponds to 36–45 years, "4" corresponds to 46–55 years, and "5" corresponds to Above 55 years. Notably, the youngest age group (Less than 25 years) exhibits the highest level of awareness, followed by the other age groups.

8.4 Gender vs. are you aware of any government schemes or policies related to EV

The chi-square tests conducted to explore the relationship between variables reveal no significant association based on various measures. For example, Pearson's chi-square value is 0.028 with a p-value of 0.867, continuity correction yields a value of 0.000 with a p-value of 1.000, and likelihood ratio chi-square value is 0.028 with a p-value of 0.867. Fisher's exact test shows a two-sided p-value of 1.000 and a one-sided p-value of 0.502. The linear-by-linear association chi-square value is 0.028 with a p-value of 0.868. All cells have expected counts greater than 5.

8.5 Age vs. are you aware of any government schemes or policies related to EV

The chi-square show no significant association between variables. Pearson's chi-square value is 7.947 with 4 (df), yielding a p-value of 0.094. Likelihood ratio chi-square is 9.401 with 4 df, resulting in a p-value of 0.052. However, 30.0% of cells have expected counts less than 5, with a minimum expected count of 2.86, potentially impacting reliability.

9 Education vs. are you aware of any government schemes or policies related to EV

The chi-square examination assessed the connection between education levels and awareness of government programs concerning EVs. The findings, such as the Pearson Chi-square value of 0.707 with 2 degrees of freedom and a significance level of 0.702, upheld the null hypothesis. Likewise, both the Likelihood Ratio and Linear-by-Linear Association analyses produced non-significant outcomes, affirming that there's no statistically meaningful link between education levels and awareness of EV-related governmental policies among the participants.

The bar chart presents the relationship between education levels and awareness of government schemes or policies related to EVs. Across different education categories, there is notable variation in awareness levels. Graduates exhibit the highest awareness, followed by those with postgraduate and above education, Conversely, individuals with Up to 12th grade education show the lowest awareness.

9.1 Gender vs. would you like to purchase EV in future

The outcomes of the chi-square tests indicate a potential link between demographic variables and the inclination to purchase an EV. Both the Pearson Chi-square and Likelihood Ratio tests showed p-values of 0.016 and 0.015, suggesting a plausible association. Furthermore, the Linear-by-Linear Association test approached significance with a p-value of 0.051, indicating a possible linear trend in the relationship. These findings suggest that demographic factors may influence individuals' intentions to buy EVs.

9.2 Age vs. would you like to purchase EV in future

The chi-square tests highlight substantial correlations between demographic variables and whether someone wants to buy and EV. The results of two tests, Pearson Chi-Square and Likelihood Ratio, had really low p-values-0.000 and 0.002. These low p-values mean they give strong evidence that there is a connection. However, the Linear-by-Linear Association test yielded a p-value of 0.129, suggesting a potential linear trend, albeit less conclusively than the other test.

9.3 Education vs. would you like to purchase EV in future

The Pearson Chi-Square and Likelihood Ratio tests produced p-values are 0.078 and 0.101, indicating they are not statistically significant at the common significance level of 0.05. This suggests there might not be a significant link between the variables being examined. However, the Linear-by-Linear Association test showed a minimal chi-square value of 0.03 with 1 degree of freedom and a high p-value of 0.872, indicating no noticeable linear trend in the relationship. Based on these tests, there is not strong evidence of a connection between the variables being studied. Tables 2, 3 gives the cross tabulation between gender and awareness of EV and education and awareness of govt. schemes respectively. Tables 4–13 calculates the chi- square of different parameters. Table 14 gives the top 10 optimal locations based on single mode analysis. Table 15 represents the district wise data for income, road density, EV sames, and population in TN.

9.4 Advantages

Based on the responses from the 147 participants regarding the advantages of EVs, the majority highlighted saving fuel costs (118 respondents), followed by reducing emissions (81 respondents), and mitigating noise pollution (86 respondents). Notably, several participants also cited additional benefits, including addressing air pollution, facilitating easy adaptation for current and future generations, the convenience of home charging, and the ease of handling due to lower weight and robust design. This comprehensive range of responses underscores the multifaceted appeal and perceived advantages of EVs beyond the conventional benefits typically associated with them.

9.5 Disadvantages

Based on the responses from the 147 participants regarding the advantages of EVs, the majority highlighted saving fuel costs (118 respondents), followed by reducing emissions (81 respondents), and mitigating noise pollution (86 respondents). Notably, several participants also cited additional benefits, including addressing

10.3389/fenrg.2025.1500515

TABLE 15 District-wise data for income, road density, EV sales, and population in TN.

Districts	Average income	Road density	Total sales of EV	Population
Ariyalur	139,000	218.78	560	754,894
Chengalpattu	158,000	167.64	10,910	2,556,244
Chennai	266,000	85.32	56,283	4,681,087
Coimbatore	335,000	264.89	26,034	1,601,864
Cuddalore	155,000	25.43	2,589	2,605,943
Dharmapuri	176,000	172.45	3,487	1,504,311
Dindigul	163,000	163.87	2,813	2,159,775
Erode	317,000	184.65	5,167	2,270,856
Kallakurichi	98,467	18.23	1747	1,347,204
Kancheepuram	137,000	163.43	5,517	3,963,252
Karur	252,000	238.48	3,737	1,064,493
Krishnagiri	290,000	151.2	7,883	1,879,890
Madurai	188,000	183.87	6,893	3,038,252
Mayiladuthurai	268,900	268.6	1,047	918,356
Nagapattinam	154,000	199.8	8,147	1,616,450
Kanniyakumari	214,000	373.5	4,472	330,572
Namakkal	270,000	276.31	9,079	1,726,601
Perambalur	89,529	183.78	630	468,060
Pudukkottai	124,000	272.64	2,771	3,101,991
Ramanathapuram	130,000	171.53	3,213	942,746
Ranipet	108,700	135.4	2070	264,330
Salem	192,000	245.09	8,385	3,482,055
Sivagangai	119,000	177.84	3,314	926,256
Tenkasi	157,000	147.69	1738	714,245
Thanjavur	162,000	344.49	5,185	1,554,531
Theni	134,000	136.58	1,380	1,545,531
Thiruvallur	384,000	243.87	13,527	1,299,709
Thiruvarur	110,000	405.34	1,624	1,006,482
Thoothukudi	113,000	134.46	2,278	1,750,176
Tiruchirappalli	244,000	221.24	7,344	1,384,257
Tirunelveli	179,000	154.28	1,581	1,614,242
Tirupathur	218,090	233.54	2,624	83,612

(Continued on the following page)

TABLE 15 (*Continued*) District-wise data for income, road density, EV sales, and population in TN.

Districts	Average income	Road density	Total sales of EV	Population
Tiruppur	222,000	256.26	13,201	2,479,052
Tiruvannamalai	106,000	153.76	4,699	1,969,930
The Nilgiris	203,000	121.01	277	299,739
Vellore	205,000	175.85	4,499	1,614,242
Villupuram	115,000	115.45	2,731	96,253
Virudhunagar	228,000	127.06	4,206	962,062

air pollution, facilitating easy adaptation for current and future generations, the convenience of home charging, and the ease of handling due to lower weight and robust design. This comprehensive range of responses underscores the multifaceted appeal and perceived advantages of EVs beyond the conventional benefits typically associated with them.

9.6 Interpretation

The analysis presented a comprehensive examination of various factors related to EVs, including demographic influences on awareness, perceptions regarding government initiatives, purchase intentions, and perceived advantages and disadvantages. The study found that factors like age and whether someone is a man or woman affect how much they know about EVs. Younger people and mean usually know more about them. Being educated does not always mean you know more about EVs, but it does mean you might know more about government plans for them. Even though people have different levels of knowledge, many are interested in EVs because they can save money and help the environment. But, problems like not enough places to charge them and how expensive they are can make it hard for more people to use them.

10 Strategic placement of charging infrastructure in TN

Tamil Nadu's greenhouse gas (GHG) emissions surged by an astonishing 84% from 2005 to 2019, reaching 184 million tons of Carbon dioxide Equivalent (MtCO2eq). This increase was predominantly driven by the energy sector, contributing 77% of the total emissions, equivalent to 141 MtCO2eq in 2019. The substantial rise underscores the urgent need for measures to curb emissions, particularly focusing on the energy sector. Transitioning to sustainable energy sources like EVs is crucial. However, TN faces challenges in its EV infrastructure, including poor road conditions and gaps in power distribution, hindering the deployment of charging stations. Addressing these challenges and optimizing charger placement are essential steps toward facilitating smoother journeys with reduced environmental impact, thus advancing TN towards a more sustainable future.

10.1 Data collection

For data collection, the initial step involved utilizing a distance calculator to compile a matrix detailing the distances between districts within Tamil Nadu. Preprocessing was omitted prior to analysis. This distance matrix served as pivotal data for strategically positioning charging stations. It facilitated an understanding of district proximity and guided decisions regarding optimal placement. The raw data derived from the distance calculator formed the cornerstone for subsequent analyses and determinations concerning charger placement.

10.2 Algorithm used

10.2.1 MST

It is a subset of the edges of a connected, undirected graph that connects all the vertices together without any cycles and with the minimum possible total edge weight. Essentially, it's a tree that covers all the graph's vertices with the least total edge weight. MSTs find applications in diverse fields like network planning, clustering, and optimization.

10.2.2 MST-K

It is a greedy approach to finding the MST of a connected, weighted graph. It selects edges based on their weights, ensuring no cycles are formed, until all vertices are included in the tree. With a time complexity of O (E log V), it efficiently constructs the MST.

11 Execution & outcome

The graphs show how TN districts are connected geographically, aiding in planning. The first graph (Figure 6) displays distances between districts, while the optimized MST graph (Figure 7) highlights efficient connections. Central districts play key roles in linking others, while peripheral districts may need better infrastructure. Analyzing these graphs informs decisions, including where to place charging stations for EVs.

After conducting a detailed analysis of edge weight in a single-mode examination. I've identified the top 10 optimal sites [refer (Table 14)] for installing charging stations throughout

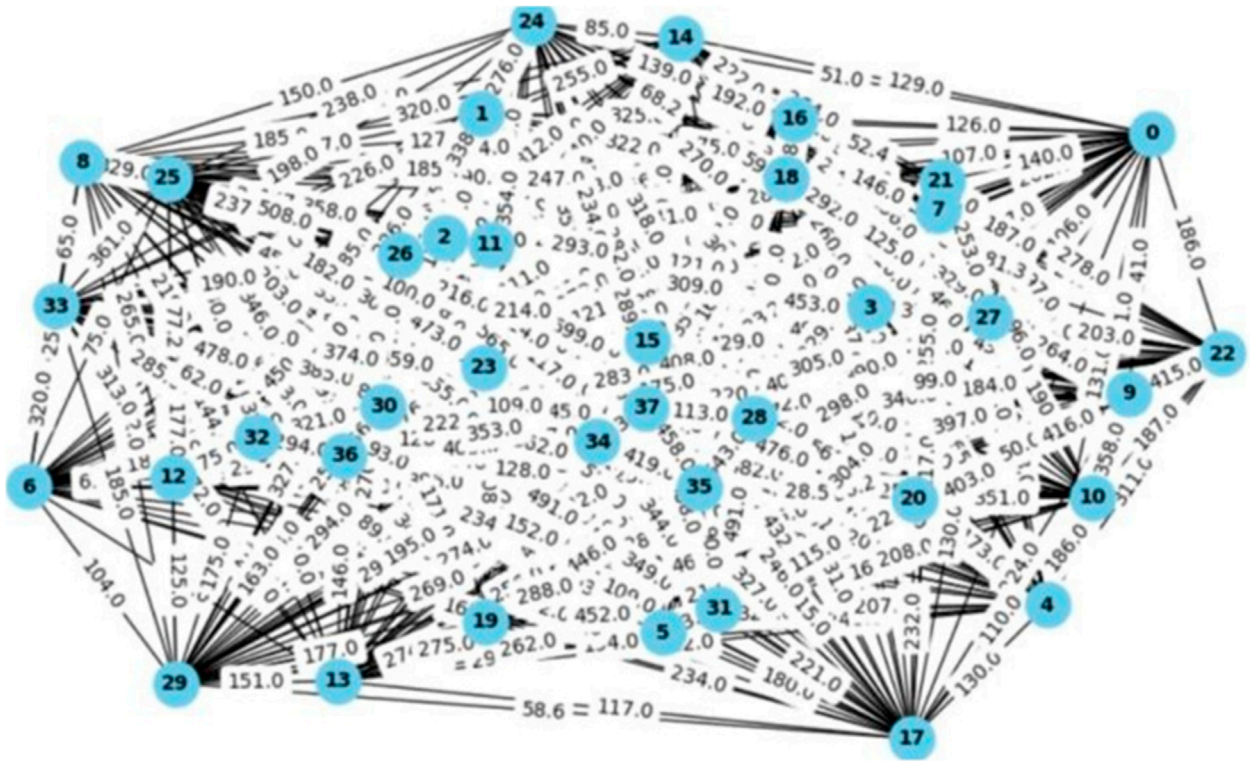

FIGURE 6
MST of TN Districts.

TN. These locations were selected meticulously to ensure effective coverage and accessibility, encouraging the adoption of EVs and supporting sustainable transportation infrastructure. The selection criteria focused on edge weights in the connectivity graph, prioritizing areas with longer distances between districts. This strategic approach aims to minimize travel distances for EVs, marking a substantial step towards establishing a strong EV infrastructure network in TN.

A histogram graph [see (Figure 8)] has been created to depict the total distance for each district in Tamil Nadu. This histogram offers insights into distance distribution across the state, revealing connectivity and transportation dynamics. Shorter distances suggest efficient transportation networks and proximity to key hubs. Longer distances signal connectivity issues, necessitating targeted interventions like improved infrastructure. Optimizing charging station placement can enhance transportation efficiency and very useful for the EV users. Figure 9 displays the raw graph, which was generated using multi-modal edge weights with the assistance of Python programming.

12 Results & discussion

The recent data collected for district-wise population, income, road density, and electric vehicle (EV) sales across Tamil Nadu are tabulated in Table 15. Figure 10 illustrates the resulting Minimal Spanning Tree, generated with Chennai as the central hub. Strategically placing charging stations along main roads is crucial for encouraging greater EV adoption in Tamil Nadu.

After analyzing the top 10 edge weights derived from the MST multi-modal analysis, several critical pathways emerge. These corridors connect major urban centers like Chennai, Coimbatore, and Madurai, along with key junctions such as Salem and Tirupur. Establishing charging stations along these routes facilitates long-distance travel, supports inter-city commuting, and promotes the use of eco-friendly transportation options for both residents and visitors.

Additionally, focusing on areas with significant commuter activity, industrial presence, and tourist influx, such as Chengalpattu and Thanjavur, ensures widespread access to EV charging infrastructure. In conclusion, strategically placing charging stations on these key routes enhances transportation efficiency, boosts the local economy, and contributes to environmental sustainability in the region.

13 Limitations

The success of the project relies on the availability of sufficient and high-quality data. Incomplete or poor-quality data can impede the progress of the project, potentially leading to inaccurate conclusions. A significant limitation stems from regional variations in data, as variations in reporting standards, data collection methods, and regional focus can introduce biases. These variations in lifestyle, infrastructure, and socioeconomic factors limit the generalizability of the findings across diverse areas within India. As a result, the conclusions drawn may not fully reflect the experiences or conditions of all regions, thus potentially skewing the understanding of EV adoption trends.

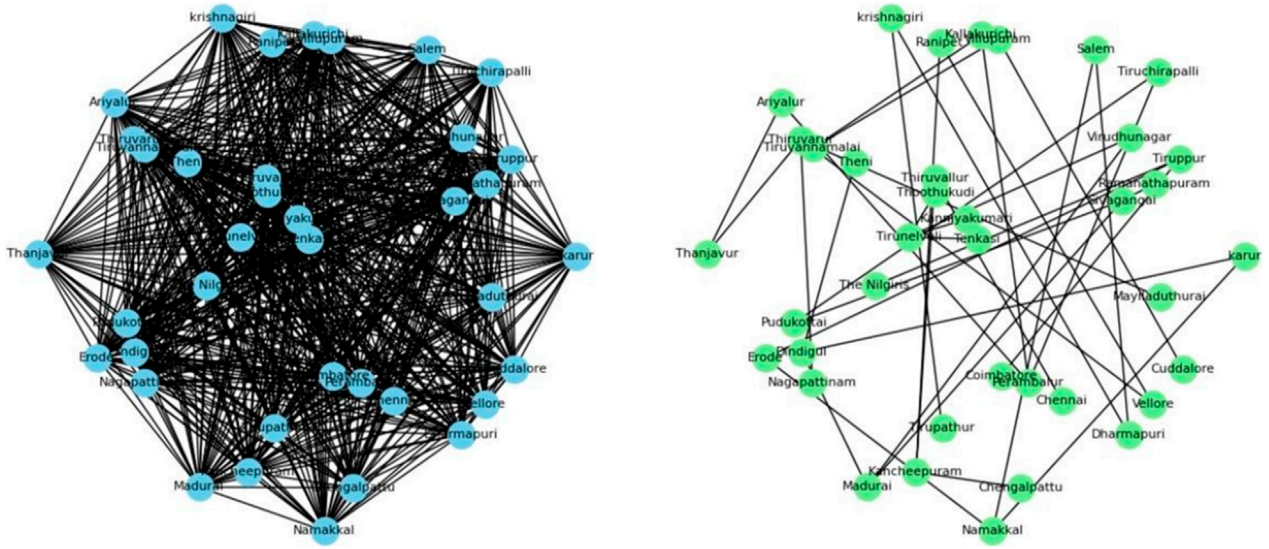

FIGURE 7
Initial and optimized MST.

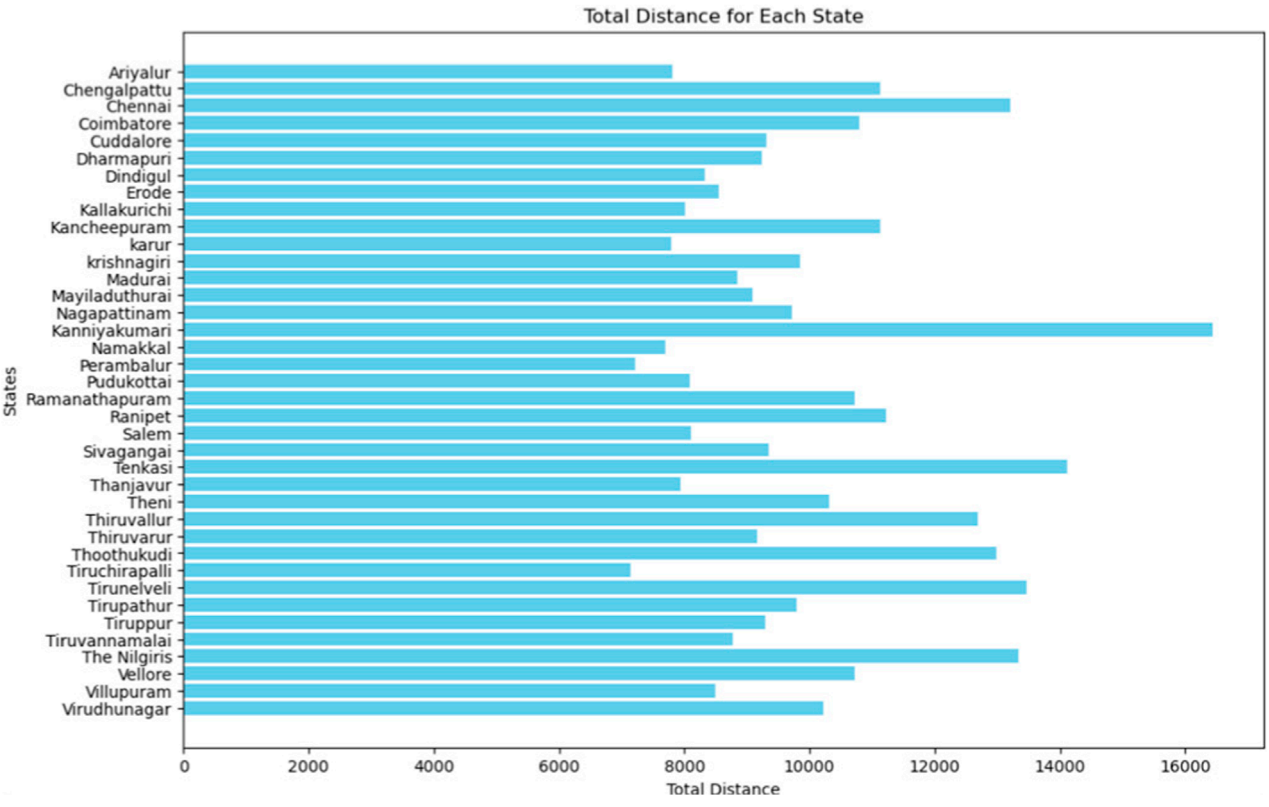

FIGURE 8
Total distance for each state (Histogram).

Another limitation concerns the machine learning models employed in the study. These models rely on historical data and assumptions about future trends, which may not always hold true, especially in a rapidly evolving market like electric vehicles. Unexpected shifts in consumer behavior, technological advancements, or policy changes could lead to inaccuracies in predictions. Furthermore, the models' accuracy is constrained by the quality and completeness of the available data, and they may struggle

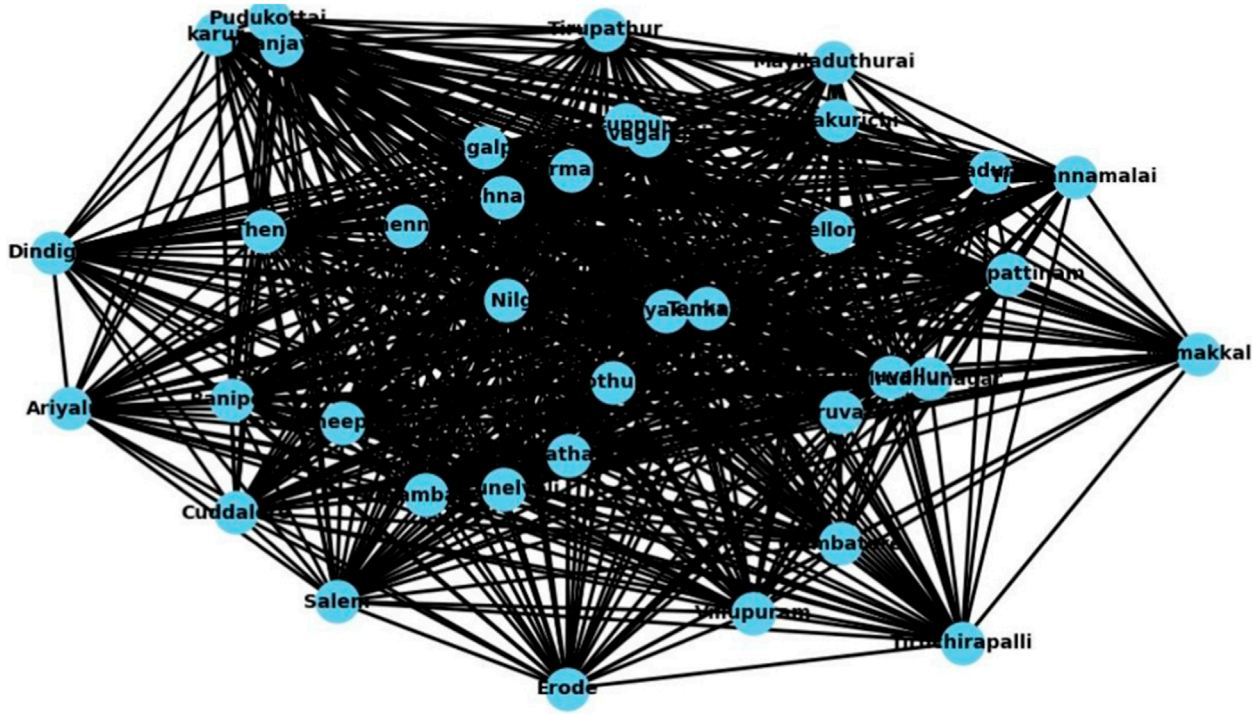

FIGURE 9
Raw graph using multi-modal edge weights.

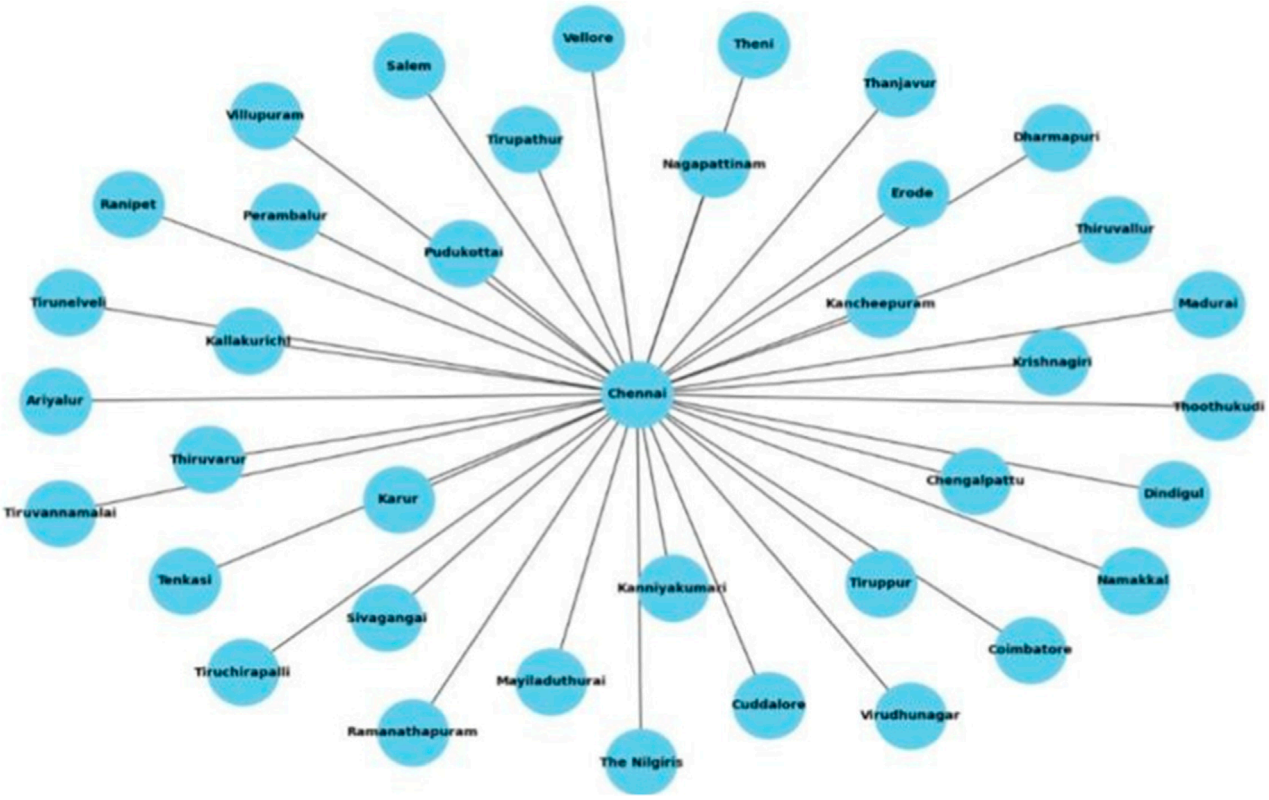

FIGURE 10
Resulting MST generated (central hub-Chennai).

to capture the full complexity of real-world dynamics, limiting the reliability of the predictions.

The study's focus on car sales trends during a specific period also introduces limitations. While these trends offer valuable insights, they overlook the broader global changes and external factors that could influence the EV market. Additionally, the study does not fully address consumer sentiment beyond surveys, which is a crucial aspect of EV adoption. Consumer attitudes, preferences, and psychological factors play a significant role in purchasing decisions and may not be adequately captured by sales data alone. Moreover, the research does not account for variations in the placement of EV chargers across different locations. The distribution and availability of charging infrastructure significantly impact the adoption of EVs, and differences in this regard can greatly affect sales trends, which this study does not comprehensively capture.

14 Conclusion

The analysis indicates a consistent rise in EV sales in India from FY 2014 to 2024, driven by factors like environmental awareness, technological advancements in EV, and government incentives. UP leads in EV sales due to proactive government strategies and strong economic indicators. Other states like Maharashtra, Karnataka, Gujarat, and Tamil Nadu also show promising growth, highlighting the importance of supportive policies and charging infrastructure. Electric 2Ws and 3Ws dominate the market, reflecting strong consumer preferences. While these segments have been supported by strategic policies, there's potential for growth in other categories like electric 4Ws and buses, requiring targeted investments. Despite growth, challenges such as high costs and limited charging stations persist. However, these challenges present opportunities for state governments to implement supportive policies and infrastructure development to promote EV adoption.

Predictive Analysis the use of Ridge Regression and Linear Regression models offers valuable insights for predicting EV sales trends, aiding strategic planning for infrastructure development and ensuring widespread access to charging facilities. Strategically placing EV charging stations along major roads in TN, connecting urban centres and essential junctions, supports long-distance travel, inter-city commuting, and eco-friendly transportation. Focusing on high-traffic areas ensures widespread access, improving transportation, boosting the economy, and promoting environmental sustainability.

Addressing key challenges, such as high initial costs and limited charging infrastructure, is essential to drive broader EV adoption across India. We can do this by making helpful rules, investing in charging spots wisely, and telling people about the good factors about EVs. Tailoring EV adoption strategies to meet the unique needs of different regions will be crucial in making EVs a popular choice nationwide. By dealing with these challenges well, we can make it easier for people to pick EVs for cleaner and better transportation, which will help everyone and the environment too.

Future research should focus on integrating real-time data on consumer sentiment and behavior to better understand the factors influencing EV adoption. Expanding the scope to include diverse regions and considering socio-economic dynamics will enhance the generalizability of findings. Additionally, exploring the impact of charging infrastructure density and accessibility on EV sales is essential. Long-term studies can track how evolving policies and technological advancements shape the market. Lastly, incorporating advanced machine learning models that account for unforeseen market shifts would improve prediction accuracy.

Data availability statement

The datasets presented in this study can be found in online repositories. The names of the repository/repositories and accession number(s) can be found below: https://vahan.parivahan.gov.in/vahan4dashboard/.

Ethics statement

Ethical review and approval was not required for the study on human participants in accordance with the local legislation and institutional requirements. Written informed consent from the [patients/ participants OR patients/participants legal guardian/next of kin] was not required to participate in this study in accordance with the national legislation and the institutional requirements.

Author contributions

ED: Conceptualization, Formal Analysis, Methodology, Writing–review and editing. DN: Methodology, Software, Writing–original draft. JR: Data curation, Formal Analysis, Writing–review and editing.

Funding

The author(s) declare that no financial support was received for the research, authorship, and/or publication of this article.

Acknowledgments

We thank the reviewers for their careful reading of our manuscript and their many insightful comments and suggestions.

Conflict of interest

The authors declare that the research was conducted in the absence of any commercial or financial relationships that could be construed as a potential conflict of interest.

Publisher's note

All claims expressed in this article are solely those of the authors and do not necessarily represent those of

their affiliated organizations, or those of the publisher, the editors and the reviewers. Any product that may be evaluated in this article, or claim that may be made by its manufacturer, is not guaranteed or endorsed by the publisher.

Supplementary material

The Supplementary Material for this article can be found online at: https://www.frontiersin.org/articles/10.3389/fenrg.2025.1500515/full#supplementary-material

References

Agarwal, B., Pathak, V., Nagar, B., and Chauhan, B. (2024). Driving towards sustainability: a comprehensive review of electric vehicles. *Int. J. Marit. Eng.* 1, 19–26. doi:10.5750/ijme.v1i1.1333

Ahmadi, S., Anam, K., and Saleh, A. (2020). "Steering system of electric vehicle using extreme learning machine," in *2020 7th international conference on electrical engineering, computer sciences and informatics (EECSI)* (IEEE), 105–108.

Akshay, K., Grace, G., Gunasekaran, K., and Samikannu, R. (2024). Power consumption prediction for electric vehicle charging stations and forecasting income. *Sci. Rep.* 14, 6497. doi:10.1038/s41598-024-56507-2

Ali, I., and Naushad, M. (2022). A study to investigate what tempts consumers to adopt electric vehicles. *World Electr. Veh. J.* 13, 26. doi:10.3390/wevj13020026

Chandra, A., Srivastava, A., and Devarasan, E. (2023). Strategic placement of electric vehicle charging infrastructure for sustainable mobility in Maharashtra. *Int. J. Recent Innovations Trends Comput. Commun.* 11, 4295–4299.

Dai, Z., and Zhang, B. (2023). Electric vehicles as a sustainable energy technology: observations from travel survey data and evaluation of adoption with machine learning method. *Sustain. Energy Technol. Assessments* 57, 103267. doi:10.1016/j.seta.2023.103267

de Rubens, G. (2019). Who will buy electric vehicles after early adopters? using machine learning to identify the electric vehicle mainstream market. *Energy* 172, 243–254. doi:10.1016/j.energy.2019.01.114

Dixit, S., and Singh, A. (2022). Predicting electric vehicle (ev) buyers in India: a machine learning approach. *Rev. Socionetwork Strateg.* 16, 221–238. doi:10.1007/s12626-022-00109-9

Fescioglu-Unver, N., and Aktas, M. (2023). Electric vehicle charging service operations: a review of machine learning applications for infrastructure planning, control, pricing, and routing. *Renew. Sustain. Energy Rev.* 188, 113873. doi:10.1016/j.rser.2023.113873

Govathoti, S. (2024). V2g nonlinear connection in ev's for wireless and sustainable mobility with support of machine learning. *Commun. Appl. Nonlinear Analysis* 31, 214–233. doi:10.52783/cana.v31.637

Haghani, M., Sprei, F., Kazemzadeh, K., Shahhoseini, Z., and Aghaei, J. (2023). Trends in electric vehicles research. *Transp. Res. Part D Transp. Environ.* 123, 103881. doi:10.1016/j.trd.2023.103881

Infanto, V., and Pandiaraj, S. (2023). A study on demand side incentives offered to consumers for purchase of electric vehicles in Tamil nadu. *South India J. Soc. Sci.* 25, 1–10.

Jin, W., Li, C., and Zheng, M. (2024). Sustainable energy management in electric vehicle secure monitoring and blockchain machine learning model. *Comput. Electr. Eng.* 115, 109093. doi:10.1016/j.compeleceng.2024.109093

Kalita, M., and Hussain, G. (2021). Opportunities and challenges of electric vehicles in India. *IJERT* 10, 33.

Kautish, P., Lavuri, R., Roubaud, D., and Grebinevych, O. (2024). Electric vehicles' choice behaviour: an emerging market scenario. *J. Environ. Manag.* 354, 120250. doi:10.1016/j.jenvman.2024.120250

Kavcic, M., Mutavdzija, M., and Buntak, K. (2022). New paradigm of sustainable urban mobility: electric and autonomous vehicles—a review and bibliometric analysis. *Sustainability* 14, 9525. doi:10.3390/su14159525

Khusanboev, I., Yodgorov, I., and Karimov, B. (2023). "Advancing electric vehicle adoption: insights from predictive analytics and market trends in sustainable transportation," in *Proceedings of the 7th international conference on future networks and distributed systems*, 314–320.

Kim, J. H., Lee, G., Park, J. Y., Hong, J., and Park, J. (2019). Consumer intentions to purchase battery electric vehicles in korea. *Energy Policy* 132, 736–743. doi:10.1016/j.enpol.2019.06.028

Menyhart, J. (2024). Overview of sustainable mobility: the role of electric vehicles in energy communities. *World Electr. Veh. J.* 15, 275. doi:10.3390/wevj15060275

Mesimäki, J., and Lehtonen, E. (2023). Light electric vehicles: the views of users and non-users. *Eur. Transp. Res. Rev.* 15, 33. doi:10.1186/s12544-023-00611-3

Miconi, F., and Dimitri, G. (2023). A machine learning approach to analyse and predict the electric cars scenario: the Italian case. *PLoS One* 18, e0279040. doi:10.1371/journal.pone.0279040

Moreno Rocha, C., Ospino, M., Ramos, I., and Guzman, A. (2024). Enhancing sustainable mobility: multi-criteria analysis for electric vehicle integration and policy implementation. *Int. J. Energy Econ. Policy* 14, 205–218. doi:10.32479/ijeep.15021

Neeraja, B., Singh, R., Panda, S., Kumar, S., and Singh, P. (2023). "A machine learning model develops the electrical energy consumption and costs for charging evs through the grid," in *2023 international conference on advances in computing, communication and applied informatics (ACCAI)* (IEEE), 1–6.

Obrador Rey, S., Canals Casals, L., Gevorkov, L., Cremades Oliver, L., and Trilla, L. (2024). Critical review on the sustainability of electric vehicles: addressing challenges without interfering in market trends. *Electronics* 13, 860. doi:10.3390/electronics13050860

Pamidimukkala, A., Kermanshachi, S., Rosenberger, J., and Hladik, G. (2024). Barriers and motivators to the adoption of electric vehicles: a global review. *Green Energy Intell. Transp.* 3, 100153. doi:10.1016/j.geits.2024.100153

Punyavathi, R., Pandian, A., Singh, A., Bajaj, M., Tuka, M., and Blazek, V. (2024). Sustainable power management in light electric vehicles with hybrid energy storage and machine learning control. *Sci. Rep.* 14, 5661. doi:10.1038/s41598-024-55988-5

Razmjoo, A., Ghazanfari, A., Jahangiri, M., Franklin, E., Denai, M., Marzband, M., et al. (2022). A comprehensive study on the expansion of electric vehicles in europe. *Appl. Sci.* 12, 11656. doi:10.3390/app122211656

Saldarini, A., Miraftabzadeh, S., Brenna, M., and Longo, M. (2023). Strategic approach for electric vehicle charging infrastructure for efficient mobility along highways: a real case study in Spain. *Vehicles* 5, 761–779. doi:10.3390/vehicles5030042

Singh, A., Sharma, K., Rengarajan, A., and Gautam, A. (2024). Promoting sustainable transportation solutions through electric vehicles in smart cities. *E3S Web Conf. EDP Sci.* 540, 02021. doi:10.1051/e3sconf/202454002021

Singh, P. (2023). Consumer perception towards electric cars in India.

Tripathy, N., Hota, S., Satapathy, P., Nayak, S., and Prusty, S. (2023). "An empirical analysis of electric vehicle in urban transportation market using deep-learning techniques," in *2023 IEEE 3rd international conference on sustainable energy and future electric transportation (SEFET)* (IEEE), 1–5.

Vajsz, T., Horváth, C., Geleta, A., Wendler, V., Bálint, R., Neumayer, M., et al. (2022). "An investigation of sustainable technologies in the field of electric mobility," in *2022 IEEE 1st international conference on cognitive mobility (CogMob)* (IEEE).

Yeh, J., and Wang, Y. (2023). A prediction model for electric vehicle sales using machine learning approaches. *J. Glob. Inf. Manag. (JGIM)* 31, 1–21. doi:10.4018/jgim.327277

Frontiers in Energy Research

Advances and innovation in sustainable, reliable and affordable energy

Explores sustainable and environmental developments in energy. It focuses on technological advances supporting Sustainable Development Goal 7: access to affordable, reliable, sustainable and modern energy for all.

Discover the latest Research Topics

See more →

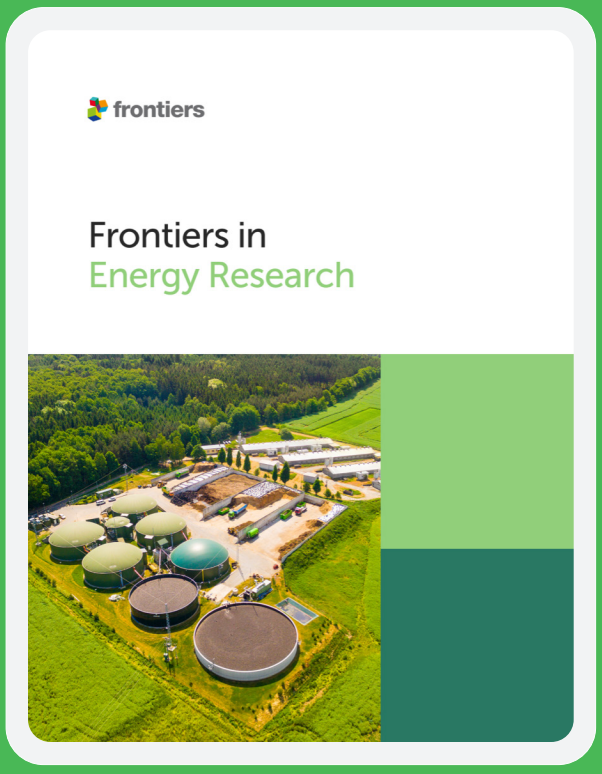

Frontiers

Avenue du Tribunal-Fédéral 34
1005 Lausanne, Switzerland
frontiersin.org

Contact us

+41 (0)21 510 17 00
frontiersin.org/about/contact